Universitat Autònoma de Barcelona

Role of SSAO/VAP-1 expression on the effect of soluble amyloidbeta forms on synapses in a neurovascular environment

Cristina Fábregas Ordóñez

Institut de Neurociències
Departament de Bioquímica i Biologia Molecular
Unitat de Bioquímica, Facultat de Medicina
Universitat Autònoma de Barcelona

Role of SSAO/VAP-1 expression on the effect of soluble amyloid-beta forms on synapses in a neurovascular environment

Cristina Fábregas Ordóñez

Tesis doctoral. Programa de Neurociencias.

Bellaterra, 2022

Institut de Neurociències
Departament de Bioquímica i Biologia Molecular
Unitat de Bioquímica, Facultat de Medicina
Universitat Autònoma de Barcelona

Role of SSAO/VAP-1 expression on the effect of soluble amyloid-beta forms on synapses in a neurovascular environment

Implicación de la expresión de SSAO/VAP-1 en el efecto de las formas solubles de beta-amiloide sobre las sinapsis en un entorno neurovascular

Memoria de tesis doctoral presentada por Cristina Fábregas Ordóñez para optar al grado de Doctora en Neurociencias por la Universidad Autónoma de Barcelona.

Trabajo realizado en la Departamento de bioquímica y biología molecular de la Facultad de medicina y en el Instituto de neurociencias de la Universidad Autónoma de Barcelona, bajo la dirección de los doctores Montserrat Solé Piñol, Alfredo J. Miñano Molina y José Rodríguez Álvarez.

El trabajo realizado en esta tesis doctoral ha estado parcialmente financiado por los siguientes proyectos de investigación: Ministerio de Ciencia e Innovación (SAF2017-89271-R and PID2020-11751ORB-100), FEDER (Regional European Development Fund), CIBERNED (CB06/05/0042) y Generalitat de Catalunya (SGR2017-0749).

Bellaterra, 15 de junio de 2022

Doctoranda	Director de tesis	Director de tesis	Director de tesis
Cristina Fábregas Ordóñez	Montserrat Solé Piñol	Alfredo J. Miñano Molina	José Rodríguez Álvarez

"No haver-te conegut
seria terrible.
Però terrible terrible.
I no ho sabria.
A sobre, no ho sabría".

Enric Casasses*, del llibre «El nus la flor»* (*Edicions Poncianes*)

CONTENTS

I ABSTRACT 11

II ABBREVIATIONS 15

III INTRODUCTION 21

1 Neurodegeneration and dementia 23

1.1 Dementia and pathological vascular alterations 23

2 Alzheimer's disease and cerebral amyloid angiopathy 25

2.1 Alzheimer's disease 25

2.1.1 General features and statistics data 25

2.1.2 Diagnostic criteria and neuropathological hallmarks 25

2.2 Cerebral Amyloid Angiopathy 31

2.2.1 Pathological hallmarks 31

3 The Neurovascular unit 32

3.1 The neurovascular unit components 34

3.1.1 Cells of the nervous system 34

3.1.2 Cells of the vascular system 44

3.2 Neurovascular unit failure as a key element on Alzheimer's disease and cerebral amyloid angiopathy 49

3.2.1 Synaptic dysfunction and neuronal loss 50

3.2.2. Glial cell alterations within NVU pathologic failure 53

3.2.3. Vascular cells in pathologic conditions related with NVU failure in Alzheimer's disease and CAA 54

3.3 Molecular communication between the integrators of the NVU 60

3.3.1 Neurotrophins: BDNF 61

3.3.2 Neurotrophins in neurodegeneration 63

3.4 Neurovascular unit in vitro models 65

3.4.1 Microfluidic systems 65

3.4.2. Conditioned mediums 67

3.4.3. Cell lines co-culture 69

4 The two-hit hypothesis of AD 72

IV AIMS 77

V MATERIALS AND METHODS 81

1 Cell cultures 83

1.1 Primary mouse cortical mixed neuron-glia culture 83

1.1.1 Reagents and mediums 83

1.1.2 Dissection, tissue disaggregation and cell culture maintenance 83
1.2 Human cerebral microvascular endothelial cells culture 84
1.2.1 Reagents and mediums 84
1.2.2. Maintenance, sub-culturing, seeding and cell storage 85
1.3 Co-culture 86
1.3.1 Co-culture establishment and in vitro maintenance 86
2 Cell treatments 88
2.1 Conditioned medium treatment 88
2.2 BDNF treatment 88
2.2.1 BDNF treatment in conditioned medium experiments 88
2.2.2 BDNF in co-culture experiments 88
2.3 α-BDNF antibody treatment 89
2.4 Aβ1-40-D treatment 89
3 Cell viability assessment 89
3.1 MTT 89
3.2 LDH cytotoxicity assay 90
4 Samples obtainment 90
4.1 Cell lysis 90
4.1.1 Neuron-glia mixed culture 90
4.1.2 hCMEC/D3 91
4.2 Cell medium collection 91
4.3 Cellular fractionation 91
4.3.1 Buffers and solutions 91
4.3.2. Procedure 91
4.4 Cellular fixation 92
5 Protein analysis 92
5.1 Western Blot 92
5.1.1 Tris-Glycine SDS-PAGE 93
5.1.2 Tris-Bicine SDS-PAGE 94
5.2 Immunocytochemistry and image acquisition 95
5.2.1 Reagents and solutions 95
5.2.2. Procedure 96
5.2.3. Image acquisition and quantification analysis 96
5.3 Enzyme-linked immunosorbent assay (ELISA) 99
5.4 Multiplex 99
6 Statistical analysis 99

VI RESULTS 101

1 Study of hSSAO/VAP-1 hCMEC/D3 cells conditioned medium treatment on neuron-glia mixed culture 103

2 Establishment and characterization of the Neurovascular unit in vitro co-culture model 106

3 $A\beta_{1-40}$-D flux in the co-culture system 113

4 Analysis of endothelial-secreted angioneurins within NVU: BDNF 116

5 Analysis of the effects induced by SSAO/VAP-1-expressing endothelial cells on neurons from mixed culture 118

6 Evaluation of the role of BDNF in SSAO/VAP-1- and Amyloid-β-mediated effects on co-cultured neurons 131

7 Exploring BDNF-TrkB signaling pathway in our NVU in vitro model 140

VII DISCUSSION 145

1 Establishing a new neurovascular unit in vitro model 148

2 Brain-derived neurotrophic factor secretion by cerebral microvascular endothelial cells 150

3 On the value of these results 151

VIII CONCLUSSIONS 159

IX REFERENCES 163

X ANNEX: contribution to previous publications 217

1 Solé, Montse, María Esteban-Lopez, Biel Taltavull, Cristina Fábregas, Rut Fadó, Núria Casals, Jose Rodríguez-Álvarez, Alfredo J. Miñano-Molina, and Mercedes Unzeta. 2019. "Blood-Brain Barrier Dysfunction Underlying Alzheimer's Disease Is Induced by an SSAO/VAP-1-Dependent Cerebrovascular Activation with Enhanced Aβ Deposition." *Biochimica et Biophysica Acta - Molecular Basis of Disease* 1865 (9): 2189–2202. https://doi.org/10.1016/j.bbadis.2019.04.016. 219

2 Siedlecki-Wullich, Dolores, Judit Català-Solsona, Cristina Fábregas, Isabel Hernández, Jordi Clarimon, Alberto Lleó, Merce Boada, Carlos A. Saura, José Rodríguez-Álvarez, and Alfredo J. Miñano-Molina. 2019. "Altered MicroRNAs Related to Synaptic Function as Potential Plasma Biomarkers for Alzheimer's Disease." *Alzheimer's Research and Therapy* 11 (1): 1–11. https://doi.org/10.1186/s13195-019-0501-4 235

3 Cheng, Wenwen, Dolores Siedlecki-Wullich, Judit Català-Solsona, Cristina Fábregas, Rut Fadó, Núria Casals, Montse Solé, et al. 2020. "Proteasomal-Mediated Degradation of Akap150 Accompanies Ampar Endocytosis during Cltd." *ENeuro* 7 (2): 1–19. https://doi.org/10.1523/ENEURO.0218-19.2020. 249

I. Abstract

Alzheimer's disease (AD) is rapidly becoming one of the most lethal, expensive and burdening diseases of this century representing up to 60 – 70 % of dementia cases. During many years, multiple drugs developed to treat this pathology have been designed assuming that amyloid β-peptide (Aβ) drives the disease. However, this approach has not yielded therapeutics that cure or produce significant improvements. In this regard, a broader outlook considering alternative mechanisms driving AD may be required. Different kinds of dementia, including AD, are related with several risk factors such as pathological vascular alterations (i.e. diabetes, atherosclerosis and malignant hypertension) and disturbances in brain microcirculation (i.e. defective blood-brain barrier functions and breakdown). This relationship evidences an intercellular communication between the cerebrovasculature and neurons, which is mainly mediated by multiple messenger molecules known as angioneurins. To study this interrelation and the role of these signaling factors, we decided to focus on the neurovascular unit (NVU) and we established a new *in vitro* system constituted by microvascular endothelial cells, neurons and astrocytes. We took advantage of the human cerebral microvascular endothelial cell line (hCMEC/D3) expressing the human semicarbazide-sensitive amine oxidase, also known as vascular adhesion protein-1 (hSSAO/VAP-1) as a model of vascular alteration in AD. SSAO/VAP-1 was described to be increased in plasma and cerebrovascular tissue from AD patients. Analyzing endothelial-secreted angioneurins in these cells we observed that hSSAO/VAP-1 expression induced an activity-independent significant decrease in its brain-derived neurotrophic factor (BDNF) releasing levels. Assessing the impact of such BDNF reduction on neurons we found that, co-culturing with hSSAO/VAP-1 endothelial cells in a context mimicking Aβ pathological presence induced a decrease of PSD95 and GluA1 synaptic protein levels. Moreover, we determined the relevance of having the appropriate endothelial-secreted BDNF levels for neuronal network maintenance. In summary, our results revealed for the first time that hSSAO/VAP-1 enzyme alters endothelial BDNF secretion and that this neurotrophin is a critical mediator between endothelial cells and neurons within our NVU *in vitro* system. In fact our results suggest that hSSAO/VAP-1 induces a sensitization, due to endothelial-secreted BDNF reduction, of co-cultured neurons to face an aversive stimulus such as Aβ. On one hand, BDNF is a key factor involved in AD pathology as its depletion has been associated with the main pathological hallmarks of the disease. On the other hand, the SSAO/VAP-1 is increased in several systemic vascular pathologies, also considered risk factors for AD. Therefore, although more experiments are required, we suggest that designing a potential therapeutic strategy based on BDNF and/or decreasing the SSAO/VAP-1 expression may result extremely powerful.

II. List of abbreviations

Aβ – Amyloid β-peptide

$A\beta_{1\text{-}40}D$ – Dutch mutation (E22Q) of amyloid β-peptide (1-40)

α-BDNF – Anti-BDNF mouse monoclonal antibody

AD – Alzheimer's Disease

AGEs – Advanced Glycation End Products

AJ – Adherens Junction

AKAP – A-Kinase Anchoring Protein (AKAP)

AMPA – α-amino-3-hydroxy-5-methyl-4-isoxazole propionic acid

AMPAR – AMPA Receptors

APP – Amyloid Precursor Protein

Ara-C – Cytosine-β-arabinofuranoside

BBB – Blood-Brain Barrier

BDNF – Brain-Derived Neurotrophic Factor

bFGF – human Fibroblast Growth Factor-basic

BME – Basal Medium Eagle's

BSA – Bovine Serum Albumin

CAA – Cerebral Amyloid Angiopathy

CaN – Calcineurin phosphatase

CBF – Cerebral Blood Flow

CNS – Central Nervous System

COX-2 – cyclooxygenase-2

CREB – cAMP-Response Element-Binding

DiV – Days *in Vitro*

DAC – Days After Confluence

DiV-CC – Days in Vitro of the co-culture

DMSO – Dimethyl sulfoxide

DNase I – Deoxyribonuclease I

EBM-2 – Endothelial cell Basal Medium-2

EDTA – Ethylenediaminetetraacetic acid

ELISA – Enzyme-Linked Immunosorbent Assay

FBS – Fetal Bovine Serum

FDA – Food and Drug Administration

G418 – Geneticin

GFAP – Glial Fibrillary Acidic Protein

HBSS – Hanks' Balanced Salt Solution

HCHWA-D – Hereditary Cerebral Hemorrhage With Amyloidosis Dutch type

HBMECs – Human Brain Microvascular Endothelial Cells

hCMEC/D3 – human Cerebral Microvascular Endothelial Cell lines/D3

HFIP – Hexafluoro-2-propanol

HRP – Horseradish Peroxidase

hSSAO – human Semicarbazide-Sensitive Amine Oxidase

HS – Horse Serum

iGluR – Ionotropic Glutamate Receptors

JNK – c-Jun amino-terminal kinase

LDH – Lactate dehydrogenase

LRP-1 – Lipoprotein Receptor-related Protein-1

MAGUK – Membrane-Associated Guanylate Kinase

MAPK – Mitogen-Activated Protein Kinase

MPTP – 1-methyl-4-phenyl-1,2,3,6-tetrahydropyridine

MTT – 3-(4,5-dimethylthiazol-2-yl)-2,5-diphenyltetrazolium bromide

NGF – Nerve Growth Factor

NFT – Neurofibrillary Tangles

NMDA – N-methyl-D-aspartate

NMDAR – NMDA Receptors

nNOS – neuronal Nitric Oxide Synthase

NO – Nitric Oxide

NTs – Neurotrophins

NT-3 – neurotrophin-3

NVU – Neurovascular Unit

oAβ – Amyloid β-peptide oligomers

PAGE – Polyacrylamide gel electrophoresis

PBS – Phosphate Buffered Saline

PET– Positron Emission Tomography

PI3K – phosphoinositide 3-kinases

PIP2 – acidic phospholipid phosphatidylinositol-4,5-bisphosphate

PKA– Protein Kinase A

PKC– Protein Kinase C

PLC-1– Phospholipase C1

PrAO – Primary Amine Oxidase

PSD – Post-Synaptic Density

RAGE – Receptor for Advanced Glycation End products

Ras-MAPK – Ras-Mitogen-Activated Protein Kinase

ROS – Reactive Oxygen Species

SAMP8 – Senescence-Accelerated Mouse-Prone 8

SDS – Sodium Dodecyl Sulfate

sPBS – supplemented Phosphate Buffered Saline

SPM –Synaptic Plasma Membrane

SSAO – Semicarbazide-Sensitive Amine Oxidase

SV2A – Synaptic Vesicle Glycoprotein 2

TARPS – Transmembrane AMPAR Regulatory Proteins

TJ – Tight junctions

TNF-α – Tumor Necrosis Factor-α

Trk – Tropomyosin-related kinase receptor

TrkA – Tropomyosin-related kinase receptor type A

TrkB – Tropomyosin-related kinase receptor type B

TrkC – Tropomyosin-related kinase receptor type C

Tw – Transwell insert

VAP-1 – Vascular Adhesion Protein-1

VEGF-A – Vascular Endothelial Growth Factor A

VSMC – Vascular Smooth Muscle Cells

WT – Wild Type

ZO-1 – Zona Occludens-1

III. Introduction

1. Neurodegeneration and dementia

Neurodegeneration consists on the gradual loss of structure or function of especially vulnerable neuronal populations. Neurodegenerative disorders can be sorted out attending to principal molecular abnormality, anatomic distribution of neurodegeneration (frontotemporal degenerations, spinocerebellar degenerations or extrapyramidal disorders) or to primary clinical hallmarks (dementia, parkinsonism or motor neuron disease) (Dugger and Dickson, 2017).

Dementia involves syndromes or pathologies that are characterized by a crescent loss of social, emotional and cognitive abilities (Cunningham *et al.*, 2015). This process is related with an atypical level of cellular decline within the brain that surpasses normal aging (Šimić *et al.*, 1997). It must be emphasized that dementia is not a normal feature of aging although it mostly affects older people. Pursuant to the World Health Organization, around 55 million people have dementia, with nearly 60 % living in low- and middle-income countries. The amount of new cases diagnosed rises by 10 million each year while estimations suggest that these figures will reach 78 million people affected by 2030, increasing up to 139 million in 2050 (World health organization, 2021). Dementia has acquired importance over the past years up to be considered as one of the major causes of death nowadays. Among other causes, this can be linked to demographic changes due to an increase in life expectancy in industrial and also in developing countries (Noe *et al.*, 2020). The consequences derived from this disease affect the physical, psychological, social and economic circumstances of the patients. Thereby, this pathology involves more than just people suffering dementia as it also affects their careers, families and society at large.

Heterogeneous mechanisms can be underlying neurodegeneration. Different types of dementia superpose between them, further complicating the diagnostic process (Iadecola, 2010). Leading causes have been determined in some cases. However, regarding the etiology of neurodegeneration there are many relevant gaps that need to be filled.

1.1. Dementia and pathological vascular alterations

Diverse types of dementia are related with pathological vascular alterations (O'Brien and Thomas, 2015), which allows linking neurodegeneration and cardiovascular diseases. Hypercholesterolemia, obesity, hypertension, diabetes mellitus, hyperhomocysteinemia and metabolic syndrome are risk factors associated with developing dementia (Fillit *et al.*, 2008). Besides, several cardiovascular diseases like peripheral artery disease, coronary artery disease, atrial fibrillation, carotid artery atherosclerosis, heart failure and stroke are also linked with a higher prevalence of dementia (De La Torre, 2006).

The principal pathways of vascular dysfunction that are related with neurodegenerative diseases include endothelial metabolic dysfunction, hypoperfusion and blood-brain barrier (BBB) breakdown (Zlokovic, 2011). Consequently, the BBB has lately become an attractive element by the role that it can play in neurodegeneration (Yamazaki and Kanekiyo, 2017). Because of its function in active transport, the BBB supplies a bunch of potentially dysfunctional receptors and transporters that might be critical for the course of neurodegeneration (Baumgart *et al.*, 2015). Moreover, brain microvascular deficits reduce cerebral blood flow (CBF) and this affects the supply of oxygen, substrates, nutrients and energy to the brain. Apart from this, the clearance of neurotoxic molecules is also impaired and, thereby, they accumulate and/or are deposited in neurons, interstitial fluid and non-neuronal cells. Failures in CBF as consequence of heart-brain vascular-related risk factors are found in the early stages of several neurological disorders including Alzheimer's disease (AD), stroke and amyotrophic lateral sclerosis (Iadecola, 2004, 2013; Zlokovic, 2011).

There are several examples of dementia-causing diseases that are associated with alterations in brain microcirculation such as defective BBB functions and breakdown. Also, CBF reductions have been reported in people with mild cognitive impairment with memory loss (Zhang *et al.*, 2021). Therefore, CBF reductions and dysregulation, impaired cerebrovascular reactivity and BBB breakdown are considered early events within the pathophysiological cascade of AD (Kisler *et al.*, 2017). Previous findings have also proved that patients with amyotrophic lateral sclerosis present BBB breakdown in the motor cortex along with blood–spinal cord barrier breakdown, which occurs prior to motor neuron degeneration or brain atrophy (Zhong *et al.*, 2008; Miyazaki *et al.*, 2011). As well, murine models of Parkinson's disease induced by the administration of 1-methyl-4-phenyl-1,2,3,6-tetrahydropyridine (MPTP) exhibit BBB breakdown in the substantia nigra and the striatum (Zhao *et al.*, 2007; Chen *et al.*, 2008; Chao, He and Tay, 2009). Moreover, BBB breakdown has also been reported in a rat model of Huntington's disease induced with 3-nitropropionic acid (Duran-Vilaregut *et al.*, 2009). Cerebral amyloid angiopathy (CAA) is another example linking neurodegenerative and vascular processes. In CAA the accumulation of vascular amyloid-β peptide (Aβ), due to reduced perivascular clearance and cerebral hypoperfusion, contributes to cognitive impairment through cortical microinfarcts (Okamoto *et al.*, 2012).

All these evidences support that vascular dysfunction induces neuronal dysfunction and neurodegeneration as it might promote the development of proteinaceous brain and cerebrovascular storage disorders (Zlokovic, 2011). In this thesis, we focus on AD, as it is the most common form of dementia, and also on CAA as it is a relevant vascular alteration that most of the times it coexists as one of the AD histopathological hallmarks.

2. Alzheimer's disease and cerebral amyloid angiopathy

2.1. Alzheimer's disease

2.1.1. General features and statistics data

Alzheimer's disease is the main cause of dementia representing up to 60 – 70 % of cases (World health organization, 2021). It is rapidly becoming one of the most lethal, expensive and burdening diseases of this century (Alzheimer Europe, 2019). In 2019, the latest year for which data are available, AD became the sixth leading cause of death in the United States ('Alzheimer's association report', 2021). A European study performed with a memory clinic-based cohort determined that the average survival time after the diagnosis was 6 years (Rhodius-Meester *et al.*, 2019). Recently published data indicate that in Europe there are approximately 10 million AD patients and that this figure may rise to 14 million by the end of this decade (Report, 2021). However, the prevalence at any age is higher when AD is defined by biological, rather than clinical, hallmarks (Jack *et al.*, 2019). The difference is mainly due to asymptomatic individuals with biological AD, which highlights the need for good biomarkers and the design of disease-specific treatments to prevent symptom onset.

2.1.2. Diagnostic criteria and neuropathological hallmarks

The criteria for the clinical diagnosis of AD were defined in 1984 (McKhann *et al.*, 1984). These guidelines were universally adopted and survived intact without modification for over a quarter of a century until 2011 when they were revised (Jack *et al.*, 2011).

The updated diagnostic criteria establish three stages of the disease; preclinical, mild cognitive impairment and Alzheimer's dementia. The preclinical is defined as a stage in which brain changes, including amyloid build-up, may already be in progress but significant clinical symptoms are not yet evident. Mild cognitive impairment is marked by symptoms of memory that are greater than normal for a person's age and education, but that do not interfere with his or her independence. People with MCI may or may not progress to Alzheimer's dementia. Finally, Alzheimer's dementia is the last stage of the disease in which symptoms, such as memory loss, word-finding difficulties, and visual/spatial problems, are significant enough to impair a person's ability to function independently.

Until 2012, the neuropathological evaluation of AD consisted mainly on clinical diagnosis, but it changed when it was shown that pathophysiological processes underlying AD already start decades before any clinical symptoms appear. Since then, neuropathological assessment of AD changed and thereafter was based on the presence and extent of Amyloid-beta (Aβ) extra-neuronal plaques and intracellular neurofibrillary tangles distribution as well as neuritic plaque

density (Montine *et al.*, 2012). Each of these three pathological hallmarks is individually scored in a three-tiered scoring system, and these data are used to determine the probability that the observed changes underlie the clinically observed symptoms (Montine *et al.*, 2012).

2.1.2.1. Amyloid beta: APP processing and amyloid cascade hypothesis

Amyloid-beta (Aβ) is the main component of extracellular plaques (Glenner and Wong, 1984). Multiple kinds of Aβ deposits can be identified in the AD brain including neuritic, diffuse, dense-cored, or classic and compact type plaques. Proteolytic cleavage enzymes such as β-secretase and γ-secretase are responsible for the biosynthesis of Aβ, from the transmembrane amyloid precursor protein (APP), which afterwards deposit (Serrano-Pozo *et al.*, 2011).

APP is a type 1 membrane glycoprotein that is involved in several biological functions including signalling, neuronal development and intracellular transport among other neuronal homeostasis activities. It consists of a single membrane-spanning domain, a larger extracellular glycosylated N-terminus and a shorter cytoplasmic C-terminus (Chen *et al.*, 2017). APP is synthesized in the endoplasmic reticulum and then it is transported to the Golgi complex. In the Golgi complex, it maturates before it is finally transported to the plasma membrane. Mature APP can be processed through two alternative pathways each one occurring in different cellular compartments **(figure 1)**. The non-amyloidogenic pathway takes place at the cell surface where APP is cleaved by the α-secretase. Alternatively, APP can undergo the amyloidogenic pathway when it is internalized in endosomal compartments where it is first processed by the β-secretase (Campion *et al.*, 2016). Each pathway generates membrane-tethered α- or β-C terminal fragments respectively. Further processing implies the intra-membrane proteolysis of α- and β-C terminal fragments by the γ-secretase, liberating the P3 and Aβ peptides respectively (Kahle and De Strooper, 2003; Iwatsubo, 2004). In case of the 99-amino acid C-terminal fragment of APP produced by the β-secretase, it is further processed by the γ-secretase at multiple sites. This produces 43, 45, 46, 48, 49 and 51 amino acids cleavage fragments that are additionally proteolyzed to obtain the main final Aβ forms; the 40-amino acid ($A\beta_{1-40}$) and the 42-amino acid ($A\beta_{1-42}$) (Takami *et al.*, 2009; Olsson *et al.*, 2014).

$A\beta_{1-40/42}$ monomers are removed to the extracellular space where they can aggregate into different forms of oligomers. Aβ oligomers (oAβ) can form regular fibrils and plaques. Insoluble amyloid plaque cores are poor neurotoxic but soluble oAβ, especially dimers, are the synaptotoxical species (Shankar *et al.*, 2008). In fact, plaques present a penumbra of soluble oAβ in which synaptic density is low. The farther someone measures from the rim of the plaque core, the more the number of synapses rises toward normal (Koffie *et al.*, 2009).

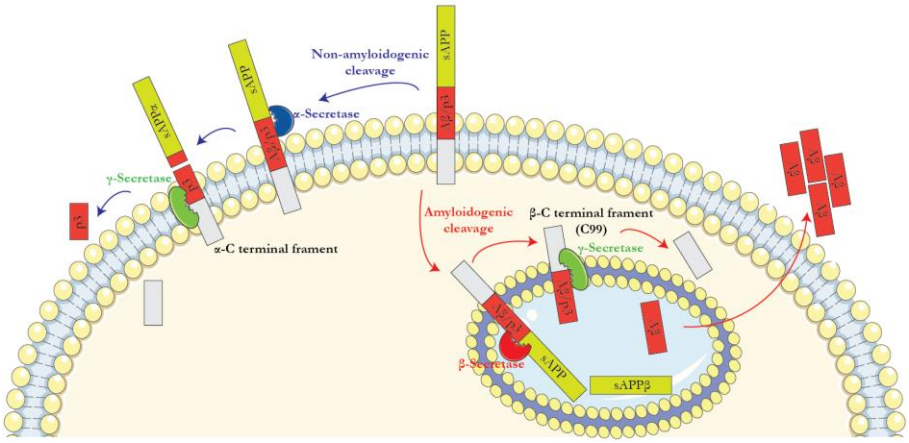

Figure 1: Schematic representation of APP trafficking and processing (adapted from: (Campion *et al.*, 2016; Arbor, 2017)). APP can be processed through the non-amyloidogenic pathway when it is proteolyzed at the cell surface by the α-secretase before being cleavaged by the γ-secretase. On the other hand, APP can be reinternalized in endosomal compartment and then be processed by the β-secretase prior the γ-secretase, leading to the production and secretion of Aβ peptide.

Aβ plaques propagate through the brain following a predictable pattern described in five distinct phases by Thal and colleagues **(figure 2)** (Thal *et al.*, 2002). Early deposits emerge in the neocortex (phase 1). Then Aβ plaques can be seen in in limbic regions including entorhinal cortex, subiculum, amygdala, and cingulate gyrus (phase 2). Afterwards, Aβ deposits appear in subcortical areas including basal ganglia and thalamus (phase 3). In later disease stages the progression affects structures of the brainstem including midbrain, pons, and medulla oblongata (phase 4). Finally in end stage cases, Aβ plaques can also be detected in the cerebellar cortex (phase 5). Whilst phases 1 and 2 are mainly observed in asymptomatic individuals, phases 4 and 5 are associated with dementia. Regarding the current neuropathology criteria, the original phases were condensed into a three stages system; early stage often seen in asymptomatic individuals (phases 1 and 2), intermediate stage (phase 3) and end stage (phases 4 and 5) (Hyman *et al.*, 2012; Montine *et al.*, 2012).

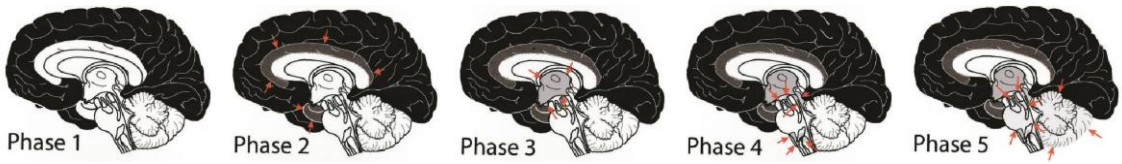

Figure 2: Phases of β-amyloidosis (from: (Thal *et al.*, 2002)). Phase 1 is characterized by exclusively neocortical Aβ deposits (Neocortex: black). Phase 2 shows additional allocortical Aβ deposits (red arrows), phase 3 additional Aβ deposits in diencephalic nuclei (red arrows) and the striatum (not shown), phase 4 additional Aβ deposits in distinct brainstem nuclei (substantia nigra, red nucleus, central gray, superior and inferior collicle, inferior olivary nucleus, and intermediate reticular zone) (red arrows), and phase 5 in the cerebellum and additional brainstem nuclei (pontine nuclei, locus coeruleus, parabrachial nuclei, reticulo-tegmental nucleus, dorsal tegmental nucleus, and oral and central raphe nuclei) (red arrows).

However, Aβ not only accumulates in the brain parenchyma but also prominent deposits can be observed in cerebral blood vessels, triggering CAA. Actually, the composition of vascular amyloid deposits differs from parenchymal plaques. Whilst $A\beta_{1-42}$ is the prevalent form present in the brain parenchyma, $A\beta_{1-40}$ peptides are the predominant ones deposited in the walls of

leptomeningeal and cortical arteries and, occasionally, veins (Miller *et al.*, 1993). Nevertheless, although $A\beta_{1-42}$ peptides are also present in vascular deposits, the $A\beta_{1-40}$:$A\beta_{1-42}$ ratio is higher than that in plaques (Roher *et al.*, 1993). Regarding capillary deposits, the $A\beta_{1-40}$:$A\beta_{1-42}$ ratio is lower than in arteries and veins and it is comparable to that in parenchymal plaques (Attems, Lintner and Jellinger, 2004).

Altogether, identifying Aβ as the main component of extracellular plaques (Glenner and Wong, 1984) and the genetic evidence linking the processing of APP to autosomal-dominant forms of AD (Citron *et al.*, 1992) led to the formulation of the amyloid cascade hypothesis (Hardy and Higgins, 1992; Hardy and Selkoe, 2002). It was suggested that an imbalance between Aβ production and degradation triggers the accumulation of Aβ peptides ($A\beta_{1-40}$ and $A\beta_{1-42}$) into amyloid plaques, which were considered the primary cause of AD.

However, the poor correlation between amyloid plaque load and cognitive functions in AD induced the modification of the amyloid hypothesis over the years (Roth, Tomlinson and Blessed, 1966; Terry, 1996). Consequently, the original hypothesis switched to the oligomer hypothesis of AD, which specifically highlights the oAβ as the neurotoxic forms causing synaptic toxicity and leading to synaptic dysfunction and eventual neuronal loss **(figure 3)** (Selkoe and Hardy, 2016).

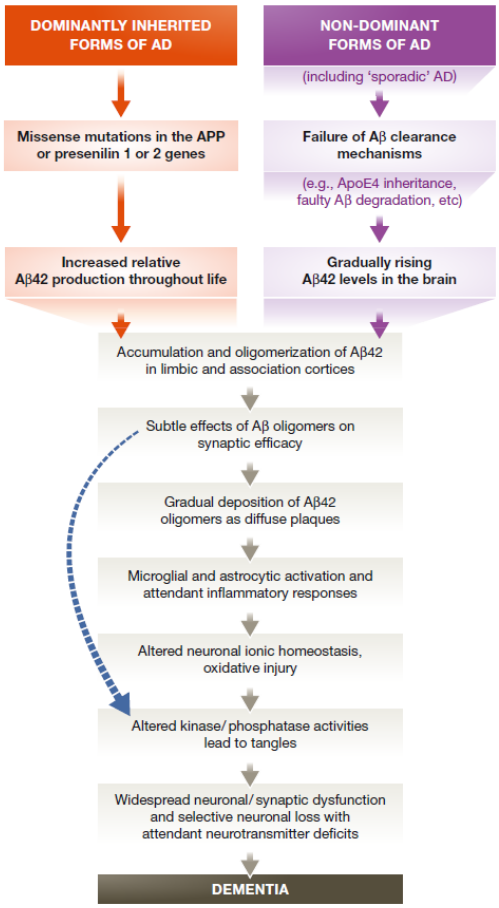

Figure 3: Sequence of principal pathogenic events leading to AD proposed by the amyloid cascade hypothesis (from: (Selkoe and Hardy, 2016). Aβ oligomers may directly injure the synapses and neurites of brain neurons (curved blue arrow) as well as they can activate microglia and astrocytes.

2.1.2.2. Tau and Tau hypothesis

As aforementioned, NFT is the second principal pathological hallmark in AD. They are constituted by aggregates of the microtubule associated protein tau (Wood *et al.*, 1986) with abnormal phosphorylation pattern that redistribute from the axonal compartment to the somato-dendritic space (Mandelkow and Mandelkow, 2012).

The NFTs were identified to follow a stereotypic spreading pattern (Braak and Braak, 1991) **(figure 4)**. As reported, the initial NFTs were detected in the transentorhinal region of the hippocampal formation (stage I). Then, the density of aggregates expanded an also involved the Subiculum region of the hippocampal pyramidal cell layer (stage II). This early NFT accumulation was described as "transentorhinal stages". As the disease continues, the NFTs start affecting the entorhinal cortex and the hippocampal pyramidal cell layer, including CA1 sector (stage III). Further progression of NFT pathology impacts other neocortical areas such as superior temporal cortex and frontal cortex (stage IV). Both intermediate (III and IV) stages are often known as "limbic stages" due to the hippocampal formation is most critically affected. Finally, in later phases also called "isocortical stages", the alterations affect other neocortical areas including secondary association areas and primary cortical areas, apart of continue increasing in the hippocampal formation. Specifically, these isocortical stages involve accumulation in the peristrate area (stage V) and intraneuronal aggregates in the striate area (stage VI).

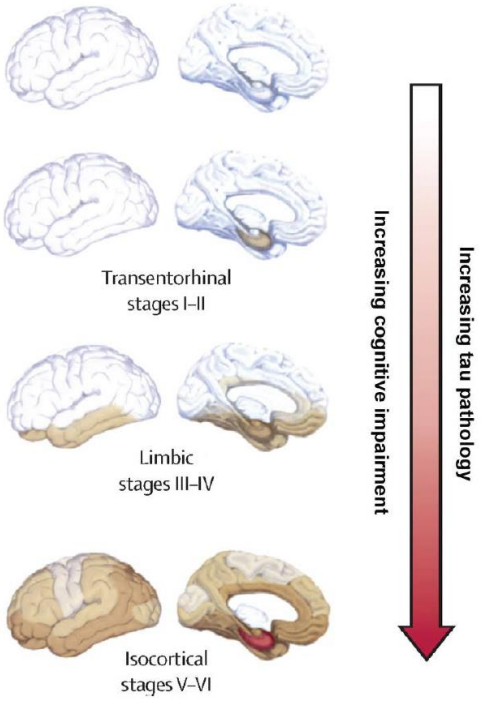

Figure 4: Progression of tau deposition in Alzheimer's disease according to Braak and Braak staging (adapted from (Villemagne *et al.*, 2015)). Stereotypical regional tau deposition in the brain according to the six stages described by Braak and Braak.

As happened for Aβ spreading pattern described by Thal et al, the described NFT stages also correlates somehow with observed clinical symptoms. While stages I and II are usually related with asymptomatic individuals, the strongest association with clinically observed dementia corresponds with V and VI Braak stages.

Altogether took to the formulation of tau hypothesis which postulates that tau tangle pathology precedes Aβ plaque formation and that tau phosphorylation and aggregation is the main cause of neurodegeneration in AD (Lansdall, 2014).

The tau propagation hypothesis was introduced in 2009 (Frost, Jacks and Diamond, 2009). According to the tau propagation hypothesis, abnormally phosphorylated tau proteins depolymerize microtubules and affect signal transmission within and between neurons (Grundke-Iqbal, Iqbal, Quinlan, *et al.*, 1986; Grundke-Iqbal, Iqbal, Tung, *et al.*, 1986; Arriagada, Marzloff and Hyman, 1992).

Noteworthy, protein levels of total tau, hyperphosphorylated Tau, along with $A\beta_{1-42}$, are the three classical cerebrospinal fluid biomarkers for the diagnosis of AD (Janeiro *et al.*, 2021). When they are measured together, they show better specificity and sensitivity than when measured alone (Olsson *et al.*, 2016). Although they are also able to predict the conversion of mild cognitive impairment to AD, they are tricky to use as there is a lack of consensus regarding limits to consider "low Aβ42 levels" and "high t-Tau levels", due to the inter-laboratory variability (Robinson, Amin and Guest, 2017). Moreover, their diagnostic use is limited due to invasive harvest by lumbar puncture with potential side effects. Alternatively, both Aβ and tau, can be visualized using neuroimaging techniques, such as positron emission tomography.

2.1.2.3. Other neuropathological hallmarks

Regarding the current criteria for neuropathological assessment of AD, neuritic plaques density is also a remarkable hallmark along with Aβ plaques and NFT. Neuritic plaques are a specific type of plaques containing degenerating neural processes (dystrophic neurites) with tau filaments, reactive astrocytes, and microglia (Naha, 2021; Trejo-Lopez, Yachnis and Prokop, 2022). The density of neuritic plaque pathology is defined by criteria described by the Consortium to establish a registry for Alzheimer's diseases (CERAD) (Mirra *et al.*, 1991). Specifically, the present guidelines for the neuropathological evaluation of AD highlight the relevance of identifying as "neuritic" only plaques surrounded by dystrophic neurites (Hyman *et al.*, 2012).

While AD is mainly neuropathologically defined by the presence and extent of Aβ plaques, NFT distribution and the neuritic plaque density, it is increasingly becoming more apparent that the majority of patients present a multitude of additional pathological changes, which are possible contributing factors to the clinical presentation and disease progression. Synaptic and neuronal loss, inflammation, BBB breakdown, cerebral hypoperfusion, atherosclerosis, microinfarcts and CAA (Wirths and Bayer, 2012) are examples of these alterations that are also related with AD pathology. Cerebral hypoperfusion consists on the pathological reduction in cerebral blood flow (CBF). As previously reported, there is a spatial-temporal pattern of decreased CBF that correlates with the progression of AD (Zhang *et al.*, 2021). Regarding CAA, although it can be identified in approximately 85 – 95 % of AD brains, it is usually less considered than Aβ plaques and neurofibrillary tangles, in part due to its variable in severity among the patients (Vinters, 2015).

2.2. Cerebral Amyloid Angiopathy

Cerebral amyloid angiopathy (CAA) consists on the deposition of Aβ in the walls of cerebrovascular capillaries and arteries. It is a surprisingly common finding within elderhood, considered not only to be a leading cause of spontaneous intracerebral hemorrhage, but also to be a remarkable contributor to age-related cognitive decline (Viswanathan and Greenberg, 2011; Boulouis *et al.*, 2016). Its prevalence is about 20 – 40 % in non-demented and 50 – 60 % in demented elderly populations, in an age range among 80 – 90 years (Keage *et al.*, 2009).

It is remarkable that CAA remains clinically different from AD, although the near molecular relationship that both entities share. Nevertheless, CAA has the potential to relate cerebrovascular and neurodegenerative pathways in the ageing brain (Cordonnier and Van Der Flier, 2011).

2.2.1. Pathological hallmarks

The main pathological hallmark in CAA is a preferential implication of capillaries and small arterioles of the leptomeninges and cerebral cortex without the necessity of implicate the adjacent parenchyma. It is also characteristic a topographical distribution involving posterior lobar brain regions. Moreover, there is a lack of implication of white matter small vessels, along with the absence of any connection with systemic amyloidosis (Charidimou *et al.*, 2017). Furthermore, there are sentinel clinical presentations like sudden lobar intracerebral haemorrhage, transient focal neurological episodes and cognitive impairment and dementia.

More severe CAA pathological features might be presented by patients carrying different kind of APP mutations within or just outside the Aβ coding region, which could modify Aβ properties and effects.

Focusing on one of these mutations, the one causing a nucleotide change at APP codon 693 results in a single amino acid substitution (glutamic acid by a glutamine) at Aβ position 22 (Levy *et al.*, 1990). As described, it consequently produces an autosomal dominant disease known as hereditary cerebral hemorrhage with amyloidosis Dutch type (HCHWA-D) which is clinically characterized by precocious repetitive haemorrhagic strokes and dementia (Wattendorff *et al.*, 1995). HCHWA-D patients present severe CAA affectation of leptomeningeal and cortical blood vessels with diffuse parenchymal Aβ deposits and almost absent dense-core plaques (Maat-Schieman *et al.*, 1996). Results about pathogenic mechanisms showed that Aβ peptide containing the Dutch substitution (Aβ-Dutch) presents different fibril formation kinetics. In fact, this mutation produces an increase in the velocity of amyloid fibril formation (Miravalle *et al.*, 2000). Besides, due to the abnormal charge of the mutant peptide, its assembly occurs on the surface of cerebrovascular smooth muscle cells, where it induces a pathological response (Melchor, McVoy and Van Nostrand, 2000). Related to its elimination, it has been shown that Aβ-Dutch is more resistant to proteolytic degradation and also less efficiently cleared across the BBB than wild type Aβ (Monro *et al.*, 2002). Additionally, it has been suggested that the Dutch mutation enhances Aβ deposition in the cerebral vasculature, probably increasing the $A\beta_{1\text{-}40}$:$A\beta_{1\text{-}42}$ ratio (Herzig *et al.*, 2004).

Furthermore other mutations have been described at Aβ position 22 such as the Artic mutation (Glu693Gly) (Kamino *et al.*, 1992) and the Italian (Glu693Lys) (Bugiani *et al.*, 2010) mutation. Moreover there are others that have been identified to alter Aβ at 21th (the Flemish (Ala692Gly) (Cras *et al.*, 1998), 23th (Iowa (Asp694Asn)27 (Grabowski *et al.*, 2001), and 34th (Piedmont (Leu705Val) (Obici *et al.*, 2005) position. Whilst all of them cause severe CAA, specifically the Arctic and the Flemish mutations also produce parenchymal fibrillar Aβ deposits (Kumar-Singh *et al.*, 2002; Basun *et al.*, 2008). Remarkably, patients carrying these familiar variants present a predominant deposition of $A\beta_{1\text{-}40}$ forms without an overall increase in Aβ production (Greenberg *et al.*, 2020).

3. The Neurovascular unit

As reviewed above, there are many evidences supporting the link between vascular dysfunction and neurodegeneration **(figure 5)** (Scheffer *et al.*, 2021). More precisely, there are also numerous reports demonstrating the relationship between cerebrovascular alterations and AD (Zlokovic, 2011). Regarding altogether there is a concept that interestingly arises; the neurovascular unit (NVU).

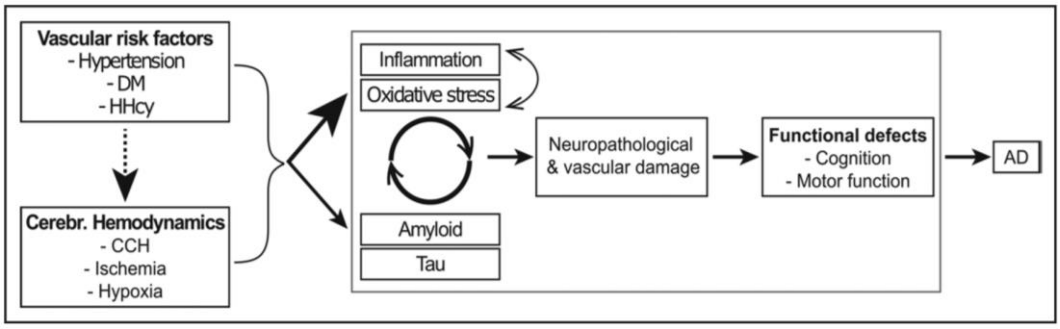

Figure 5: The link between cardiovascular disease and Alzheimer's disease (from (Scheffer *et al.*, 2021)). Vascular risk factors, such as hypertension, diabetes (DM), and hyperhomocysteinemia (HHcy) can disrupt normal cerebral hemodynamics, causing, for example, chronic cerebral hypoperfusion (CCH), ischemia, or hypoxia. All are known to cause oxidative stress intimately linked to neuroinflammation, which can chronically lead to abnormal amyloid and tau protein aggregation. Inherent predisposition to aberrant amyloid processing and tau phosphorylation, enhanced by cardiovascular disease, has an additive effect. These combined factors can then impair neurovascular function, ultimately resulting in functional defects typical for advanced AD.

The NVU is a group of different cell types that are closely interrelated and work functionally integrated to maintain the homeostasis of the cerebral microenvironment (Iadecola, 2010). The cellular composition of the NVU varies along the vascular tree **(figure 6)**; however the main components are vascular cells (endothelial cells, pericytes and vascular smooth muscle cells (vSMCs)), glia (astrocytes, microglia and oligodendrocytes) and neurons (Zlokovic, 2011).

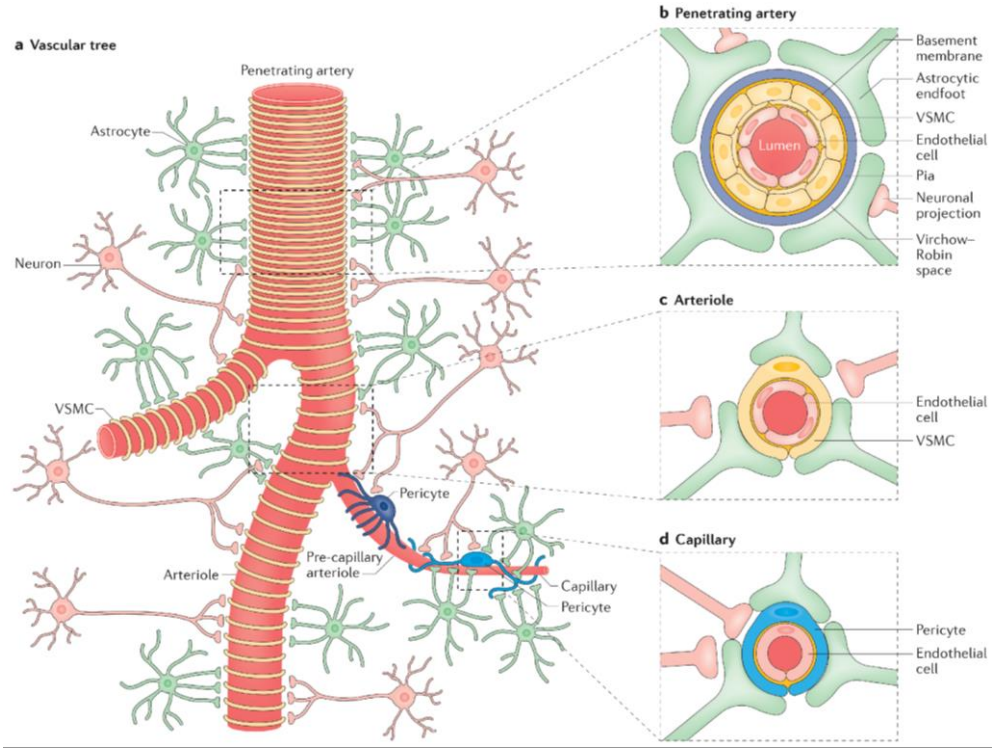

Figure 6: The neurovascular unit schematic representation (from (Kisler *et al.*, 2017)). Different cell types integrate the neurovascular unit along the vascular tree **(A)**. Endothelial cells always constitute the inner layer of the vessel wall. At the level of penetrating arteries **(B)**, endothelial cells are covered by a thin extracellular basement membrane and surrounded by one to three layers of VSMC, altogether ringed by Pia. The Pia and the astrocytic endfeet limit the Virchow-Robin space that contains the cerebrospinal fluid. Local neurons innervate both VSMC and astrocytes. In arterioles segment **(C)**, endothelial inner layer is only ensheathed by one layer of VSMC. At the capillary level **(D)**, the NVU is integrated by endothelial cells that are surrounded by pericytes, both sharing a common basement membrane between them. Astrocytes endfeet cover both pericytes and endothelial cells. Local neurons innervate astrocytes and pericytes.

The near proximity between all the neighboring cell types enables for effective cell-to-cell cross-communications. These interactions are essential for normal functions in the healthy central nervous system. Moreover, they are increasingly recognized as critical in the pathological process in multiple neurological disorders (Boillée *et al.*, 2006; Zhong *et al.*, 2008; Zlokovic, 2008).

The NVU functions in the healthy brain include control of cerebral blood flow, matrix interactions and BBB permeability, inactivation of neurotransmitters and signaling through angioneurins. It also contributes to immune surveillance in the brain and toxins clearance (Sagare, Bell and Zlokovic, 2012).

3.1. The neurovascular unit components

3.1.1. Cells of the nervous system

The nervous system is a complex communication network that enables an organism to interact with its surroundings. It comprises the central nervous system (CNS; the brain and spinal cord) and the peripheral nervous system (the autonomic and somatic nervous systems). Different cell types constitute the central nervous system including neurons, glial cells (astrocytes, microglia, oligodendrocytes and ependymal cells), choroid plexus cells, and cells related to blood vessels and coverings (leptomeninges and dura mater) (Kovacs, 2018). It was reported that the human brain contains about 86 billion neurons (NeuN-positive cells), which are distributed non-uniformly across the cerebral cortex, cerebellum and subcortical nuclei, and 85 billion non-neuronal cells (NeuN-negative) (Azevedo *et al.*, 2009).

During development of brain architecture and functions, the neurovascular interaction plays decisive roles (Andreone, Lacoste and Gu, 2015). CNS-derived axonal guidance molecules were reported also to guide the blood vessel outgrowth (Tam and Watts, 2010) and vascular-derived signals were shown to be involved in axonal guidance (Makita *et al.*, 2008). In addition, local neural activity has been described to affect vascular branching and density in the cortex (Lacoste *et al.*, 2014) and cerebral vascularization impairment inhibited neuronal proliferation (Haigh *et al.*, 2003). Altogether contribute with the concept that since CNS development, neuronal and vascular cells form a functionally integrated network.

Within the human brain, the cerebral cortex is crucial not only for perception, cognition, volitional movement, memory and emotion, but also for capabilities such as language and tool use (Van Essen, Donahue and Glasser, 2018). The remarkable diversity of adult cortical cell types appears gradually along development and it can be traced back to only a few neural stem and progenitor cell types at the beginning of neurogenesis. Accordingly, all cortical neurons

and glia derive from neuroepithelial cells that form the rostral neural tube after neurulation (Nikolopoulou *et al.*, 2017). Briefly, neocortical neurogenesis starts when neuroepithelial cells coating the ventricles begin to generate nascent neurons and progressively change into radial glia that constitutes a proliferative ventricular zone. This ventricular radial glia produces both neurons and astrocytes (Silbereis *et al.*, 2016).

3.1.1.1. Neurons

Neurons are the basic unit of the nervous system. They are the most highly specialized cells that are able to process and transmit complex cellular signals. They consist of a large cell body, called soma, and two types of filament that extrude from it; the dendrites and the axon. The dendrites typically branch profusely as they are the cell compartment where the majority of the electrical impulses are received via the dendritic spines. The axon is a long fiber that projects from the soma, precisely from the axon hillock, to contact another cell at the axon terminal. On the other hand, the term neurites is used for both dendrites and axon when referring to developing or immature neurons and especially for cultured ones (Flynn, 2013).

Neurons have different morphological, molecular, connectional and functional properties. In order to manage this complexity, they are grouped into types, which can be later analyzed systematically and reproducibly. However, neuronal classification has been challenging both conceptually and technically (Zeng and Sanes, 2017). Focusing on cortical neurons, they are classified in two groups; the glutamatergic excitatory neurons and the GABAergic inhibitory neurons **(figure 7)**. Each one has multiple subclasses, five for excitatory neurons (locally projecting layer 4 neurons, cortico-cortical projection neurons (also known as callosal projection neurons or intratelencephalic neurons), subcerebral projection neurons (also named pyramidal tract neurons), cortico-thalamic projection neurons, and layer 6b subplate neurons) (Molyneaux *et al.*, 2007; Harris and Shepherd, 2015) and four within inhibitory neurons (parvalbumin-expressing cells, somatostatin-expressing cells, vasoactive intestinal peptide-expressing cells and cells that express 5-hydroxytryptamine receptor 3A but lack vasoactive intestinal peptide expression) (Tremblay, Lee and Rudy, 2016). Regarding the five subclasses of excitatory neurons, it is unclear how many types of neurons constitute each one. The few studies in which types have been defined by projection targets suggest that great variations exist with respect to projection specificity between different neurons. As an example, the layer 4 neurons, which are the major postsynaptic targets of thalamic sensory nuclei, can be subdivided further into spiny stellate cells and star pyramidal cells, depending on whether they have an apical dendrite. Their axons and those of the layer 6b subplate neurons project locally or to nearby regions (Zeng and Sanes, 2017). The inhibitory neurons subclasses can also be divided into types such as basket cells and chandelier cells (for parvalbumin-expressing cells),

Martinotti cells and non-Martinotti cells (for somatostatin-expressing cells somatostatin-expressing cells), bipolar and multipolar cells (for vasoactive intestinal peptide-expressing cells) and neurogliaform cells and single bouquet cells (for cells that express 5-hydroxytryptamine receptor 3A but lack vasoactive intestinal peptide expression).

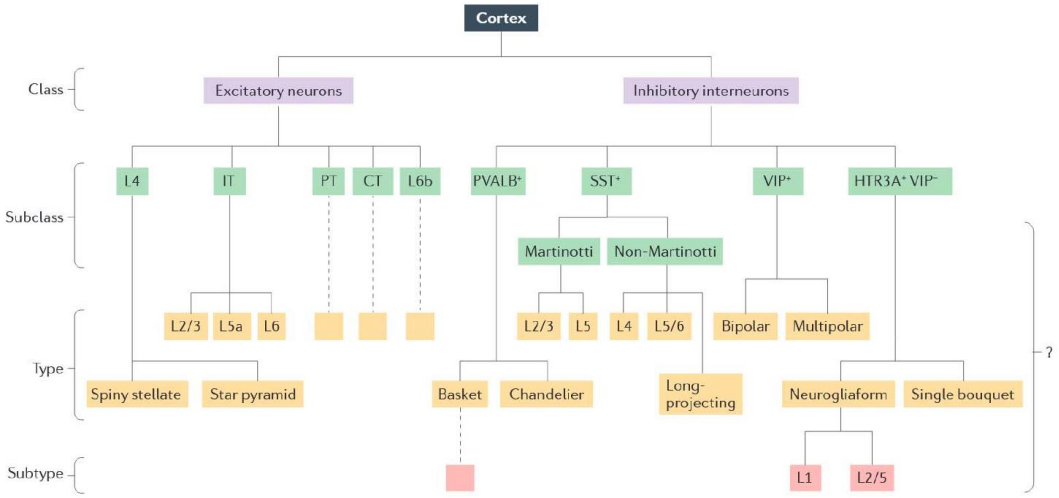

Figure 7: Hierarchical classification of cerebral cortex neurons (from (Zeng and Sanes, 2017)). Individual cell types can be grouped into classes and intermediate levels of subclasses can be determined based on distinct morphological, physiological and molecular features. Types are the commonly validated terminal branches in the current hierarchical arrangement of cell types. Lower-order groupings into subclasses may largely be provisional until additional data are collected that could determine if they could constitute new types or should be merged into other types. Dashed lines indicate the presence of additional types that cannot be labeled due to lack of space. The question mark indicates that the status of the cortical cell groups indicated may be either subclasses, types or subtypes. CT: cortico-thalamic neurons; HTR3A: 5-hydroxytryptamine receptor 3A; IT: intratelencephalic neurons; L4: layer 4; L6b: layer 6b subplate neurons; PT: pyramidal tract neurons; PVALB: parvalbumin; SST: somatostatin; VIP: vasoactive intestinal peptide.

Regarding neuron's communication, it takes place through specialized intercellular junctions named synapses (Südhof, 2018). Synaptic transmission consists on the presynaptic exocytosis of neurotransmitters contained on synaptic vesicles, followed by the detection of these molecules by postsynaptic receptors. The depolarizing electrical signal received at the presynaptic terminal is converted into a chemical signal by the releasing of the neurotransmitters to the synaptic cleft. The neurotransmitters diffuse across this space and bind to their corresponding juxtaposed postsynaptic receptors (Batool *et al.*, 2019). After the interaction between the appropriate neurotransmitter and its receptor, the channels coupled to it open and trigger either depolarization or hyperpolarization of the postsynaptic membrane, thereby reconverting the chemical signal back into an electrical one. Consequently, it is required a spatial and temporal restriction of neurotransmitters release and reception together with the precise alignment of pre- and postsynaptic structures at a synaptic junction (Biederer, Kaeser and Blanpied, 2017).

The dynamic gain and loss of synapses is crucial for healthy brain function (Jackson *et al.*, 2019). Modification of synaptic transmission is a relevant mechanism by which the neural activity generated by an experience modifies brain function. This process is defined as synaptic

plasticity and over a century has been proposed to play a main role in the brain capacity for incorporating transient experiences into persistent memories (Citri and Malenka, 2007). Synaptic plasticity is also proposed to be critically involved in early development of the neural circuitry (Lohmann and Kessels, 2014). Moreover, there are numerous evidences indicating that impairments in synaptic plasticity mechanisms contribute to several prominent neuropsychiatric disorders (Martella *et al.*, 2018). Synaptic plasticity is generally regulated by the release of various neurotransmitters from the presynaptic membrane and/or by varying the density, types, and properties of neurotransmitter receptors at the postsynaptic membrane (Sumi and Harada, 2020). While synaptic plasticity describes persistent and activity-dependent changes in synaptic strength, structural plasticity refers to the physical morphology and number of synapses. An essential concept relating synaptic and structural plasticity is Hebbian learning (Attneave, B. and Hebb, 1950) where a threshold of coincident activity at synapses between cells will result in relative strengthening of these connections, potentially balanced by the relative weakening of other connections. Hebbian plasticity is a fundamental substrate of multiple learning events and it is complemented by processes of homeostatic plasticity which consist on rescaling synaptic numbers and efficiencies to maintain an overall stable synapse density (Jackson *et al.*, 2019). The most actively studied forms of Hebbian plasticity are long-term potentiation (LTP) and long-term depression (LTD). Both are considered to represent cellular correlates of particular types of learning and memory (Citri and Malenka, 2007). LTP results after persistent enhancement of synaptic transmission and LTD when the efficacy of synaptic transmission is reduced (Bliss and Cooke, 2011). The specific cellular and molecular mechanisms mediating these processes depend on the synapses and circuit that are being activated and the specific pattern of activity.

Synaptic structure

The huge number of synapses, their plasticity and the molecular and functional diversity across them are the responsible of the computational power and cognitive capacity of the brain (Tao *et al.*, 2018). Synapses may present different properties considering the neurotransmitter types that are involved, the release probability, the postsynaptic receptor composition and the short- and long-term potentiation. In terms of presynaptic components, all synapses contain similar elements although the specific isoforms of various proteins, like neurotransmitter transporters or calcium channels, can vary. Conversely, the postsynaptic integrators of excitatory and inhibitory synapses exhibit no homology, neither considering the participating receptors nor at the level of postsynaptic scaffolding proteins (Südhof, 2018). Indeed, the two main types of central synapses, glutamatergic and GABAergic, have been shown by biochemical and electrophysiological methods to contain different combination of cellular and molecular

components and to present distinct plasticity rules and functional characteristics (Tao *et al.*, 2018). On the other hand, in terms of location, excitatory synapses are found mainly on dendrites and dendritic spines, while inhibitory ones mostly locate on cell soma and axonal initial segment (Harris and Weinberg, 2012).

Focusing on excitatory synapses, the involved presynaptic boutons contain round, clear vesicles loaded with glutamate neurotransmitter (Qu *et al.*, 2009). Regarding postsynaptic elements of this kind of synapses, the postsynaptic density (PSD) is the most notable one. The PSD is a diffuse electron-dense structure situated beneath the plasma membrane and expanding 35 – 50 nm approximately into the cytoplasm (Gulley and Reese, 1981; Landis and Reese, 1983). The surface area of the PSD corresponds almost perfectly with spine head volume and the total number of presynaptic vesicles (Harris and Weinberg, 2012). The PSD contains a variety of receptors, scaffold and adaptor proteins, signaling complexes, cell-adhesion molecules and components of the cytoskeleton implicated in synaptic transmission and plasticity **(figure 8)** (Feng and Zhang, 2009).

Integrated within the plasma membrane, neurotransmitter receptors and trans-synaptic adhesion molecules accumulate at the external face of the PSD. In glutamatergic synapses from the mammalian brain, the α-amino-3-hydroxy-5-methyl-4-isoxazole propionic acid (AMPA)-sensitive ionotropic receptors accomplish the major part of fast excitatory neurotransmission (Traynelis *et al.*, 2010). Ionotropic glutamate receptors (iGluR) are assembled as tetramers that form a central non-selective cation channel. Studies with iGluR agonists revealed the existence of three main subfamilies: N-methyl-D-aspartate (NMDA), kainate and the aforementioned AMPA. The σ-receptors, although poorly understood, are another subfamily which is important for trans-synaptic organization and plasticity despite they are not directly activated by ligands (Reiner and Levitz, 2018). AMPA receptors (AMPAR) assemble as dimers of dimers by different combinations of four subunits (GluA1 to GluA4) forming homo- or heterotetrameric receptors. Expression of all subunits is region and cell-type specific, developmentally regulated and activity-dependent (Ashby, Daw and Isaac, 2008). GluA1 and GluA2 are the predominant subunits present in the principal neurons from adult forebrain, including cortex and hippocampus. GluA2/3 receptors play a secondary minor role (Lu *et al.*, 2009). Both AMPAR and NMDA receptors (NMDAR) have pivotal roles in excitatory synaptic plasticity. Activity-dependent changes in AMPAR trafficking regulates the expression of LTP or LTD increasing or decreasing, respectively, the number of AMPAR present in the plasma membrane at synapses (Watson, Ho and Greger, 2017). In case of NMDAR, their activation can induce either LTP or LTD depending on the downstream activation of specific intracellular

cascades in response to the extent of intracellular calcium rise in the dendritic spines (Kasai *et al.*, 2010).

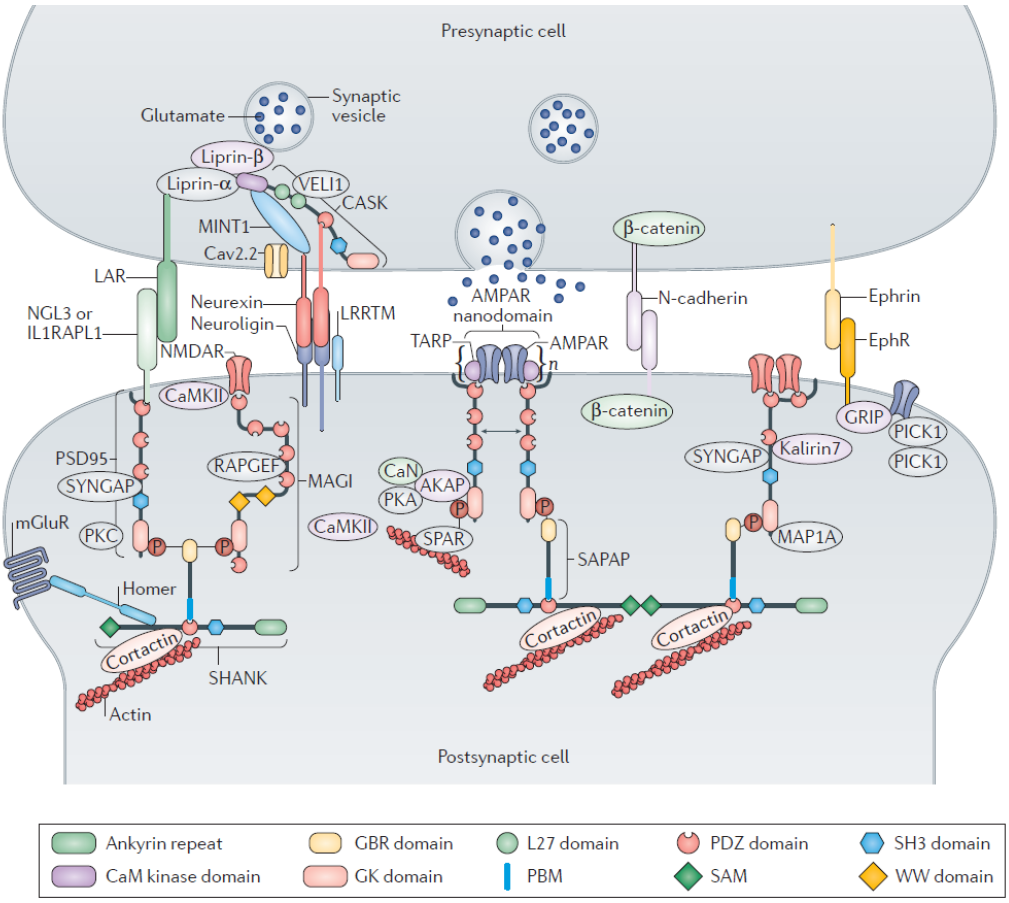

Figure 8: A schematic diagram showing synaptic complex organization in both pre- and post-synaptic sides of excitatory synapses (from (Zhu, Shang and Zhang, 2016)). The presynaptic boutons contain round, clear vesicles loaded with glutamate neurotransmitter. The PSD contains a variety of receptors, scaffold and adaptor proteins, signalling complexes, cell-adhesion molecules and components of the cytoskeleton implicated in synaptic transmission and plasticity. NMDA, KAR and AMPA are the main subfamilies of iGluR. AMPAR are anchored to PSD95 scaffold protein through TARP. PSD95 also interacts, by the domains near its carboxyl terminus, with the postsynaptic master scaffolding protein AKAP. AKAP as well binds to kinases and phosphatases. AKAP: A-kinase anchor protein; CaMKII: calcium/calmodulin-dependent protein kinase II; CaN: calcineurin; Cav2.2: voltage-gated calcium channel subunit-α Cav2.2; EphR: ephrin receptor; GBR: GK-binding region; GK: guanylate kinase-like; GRIP: glutamate receptor-interacting protein; L27: LIN2–LIN7; LAR: leukocyte common antigen related; LRRTM: leucine-rich repeat transmembrane protein; MAGI: membrane-associated guanylate kinase inverted; MAP1A: microtubule-associated protein 1A; mGluR: metabotropic glutamate receptor; NGL-3: netrin-G3 ligand; NMDAR: NMDA-type glutamate receptor; PBM: PDZ-binding motif; PDZ: PSD95–DLG1–Zonula occludens 1; PKA: protein kinase A; PKC: protein kinase C; PICK1: protein interacting with C kinase 1; SAM: sterile α-motif; TARP: transmembrane AMPAR regulatory protein; VELI1: vertebrate lin-7 homologue 1.

In the PSD, underneath the receptors, it is also found a dense matrix of proteins constituted by scaffold, actin-binding and downstream signaling molecules. In excitatory neuronal synapses, the main components of this PSD complex are PDZ-domain-containing scaffold proteins. They regulate the clustering of surface glutamate receptors and participate in the dynamic trafficking. Moreover, they also organize synaptic signaling complexes and coordinate cytoskeletal dynamics (Feng and Zhang, 2009). The most abundant scaffold protein is the PSD95 family of membrane-associated guanylate kinase (MAGUK) proteins. PSD95 family

members adopt an extended conformation to form vertical filaments with the amino terminus located at the postsynaptic membrane and the carboxyl terminus protruding into the cytosol (Chen *et al.*, 2015). Moreover, PSD95 synaptic anchoring also requires the binding of its amino terminus to α-actinin (Matt *et al.*, 2018).

PSD95 plays crucial role in regulating the surface location of AMPA receptors via the binding to transmembrane AMPAR regulatory proteins (TARPS) (Ehrlich and Malinow, 2004). AMPAR localization is functionally important due to their affinity for glutamate is fairly low, so only receptors that are exactly aligned to presynaptic release sites might be effectively activated (Franks, Stevens and Sejnowski, 2003; Lisman and Raghavachari, 2006). Molecular manipulations have demonstrated a correlation between changes in the levels of PSD95 and the synaptic AMPAR content (El-Husseini *et al.*, 2000). On the other hand, biochemical modifications to induce PSD95 loss from synapses have been reported to be critically involved in the agonist-induced endocytosis of AMPARs in cultured neurons (Bhattacharyya *et al.*, 2009).

PSD95 also interacts, by the domains near its carboxyl terminus, with numerous proteins including A-kinase-anchoring protein (AKAP) family scaffold proteins (Colledge *et al.*, 2000). AKAP79/150 (human 79/rodent 150) is a postsynaptic master scaffolding protein that acts as an integrator binding numerous signaling, scaffolding, receptor and ion channel proteins to coordinate signal transduction (Sanderson and Dell'Acqua, 2011). In particular, AKAP79/150 links cortical F-actin, the acidic phospholipid phosphatidylinositol-4,5-bisphosphate (PIP2), MAGUKs, cadherins, kinases and phosphatases, along with glutamate receptors and ion channels to regulate activity dependent signaling processes at synapses. AKAP79/150 regulates AMPAR activity in neurons as it forms a complex that dually anchors and poises the two enzymes protein kinase A (PKA) and Calcineurin (CaN) phosphatase.

Neurovascular coupling

Related also with neuronal communication through synaptic signaling but in a neurovascular context, the communication between neurons and vessels was defined as neurovascular coupling. It consists on regulating temporal and spatial increases of CBF in response to neuronal activity (Iadecola, 2004). In this regard, neurons generate signals that act on local blood vessels directly or through intermediary cells (Iadecola, 2017). Postsynaptic AMPA and NMDA receptors activation in glutamatergic synapses increase the intracellular calcium concentration. In this environment, calcium-dependent enzymes, such as neuronal nitric oxide synthase (nNOS) and cyclooxygenase-2 (COX-2), are activated and produce potent vasodilators; nitric oxide (NO) and prostanoid, respectively (Attwell *et al.*, 2010; Lecrux and Hamel, 2016).

3.1.1.2. Glial cells

The nervous system is also integrated by non-neuronal cells called glial cells. In particular, glia within the central nervous system comprises astrocytes, oligodendrocytes, ependymal cells and microglia. On the other hand, Schwann cells and satellite cells are the glial cells that constitute the peripheral nervous system. The term neuroglia was used for the first time in 1858 to report what was described as a kind of connective tissue constituted by several cell types within the brain (Virchow, 1858). Later, the name astrocyte was introduced due to the stellate morphology observed (Lenhossek 1893).

Astrocytes

The criteria to identify astrocytes have been recurrently debated (Barres, 2003, 2008; H. K. Kimelberg, 2004; Harold K. Kimelberg, 2004; Kimelberg, 2010). Although astrocytes are able to response to excitability and can communicate between them through calcium signaling, they are mainly defined as non-excitable cells because they do not generate action potentials or depolarizations as neurons, which are considered excitable cells, do. Astrocytes present a negative membrane potential determined by a transmembrane potassium gradient. Despite these features are the more accepted ones, they are necessary but not sufficient for astrocytes identification. Other several traits like the presence of intermediate filament bundles and glycogen granules, specific transporters to uptake glutamate and GABA, processes surrounding synapses and blood vessels and gap junctions between cells are astrocyte-specific but not absolute (Kimelberg, 2010). In astrocytes, the principal intermediate filament protein is the glial fibrillary acidic protein (GFAP) (Liem and Messing, 2009) and its up-regulation is considered a sensitive and reliable marker of reactivity (Sofroniew, 2009). Nevertheless, it has been reported that GFAP is not a sensitive marker since many mature astrocytes in healthy tissue or remote from lesions can also express it although at very low levels. Moreover, there are evidences that GFAP is not exclusive to astrocytes as other cell types in the central nervous system, such as Bergmann glia of the cerebellum, tanycytes at the base of the third ventricle, pituicytes in the neurohypophysis and cribrosocytes at the optic nerve head, can also express it (Hol *et al.*, 2003; Sofroniew and Vinters, 2010).

Astrocytes are involved in the maintenance of cellular, metabolic and molecular homeostasis. They play a crucial role as integrators of the neurovascular unit because they can act as a bridge between microvasculature and neurons (Zonta *et al.*, 2002). They participate in the aforementioned neurovascular coupling as they can sense synaptic activity and through their multiple end-feet **(figure 9)**, providing almost total coverage of cerebral microvessels, they participate in the coordination between the delivery of oxygen and glucose and the metabolic requirements of the nervous tissue (Bélanger, Allaman and Magistretti, 2011; Howarth, 2014).

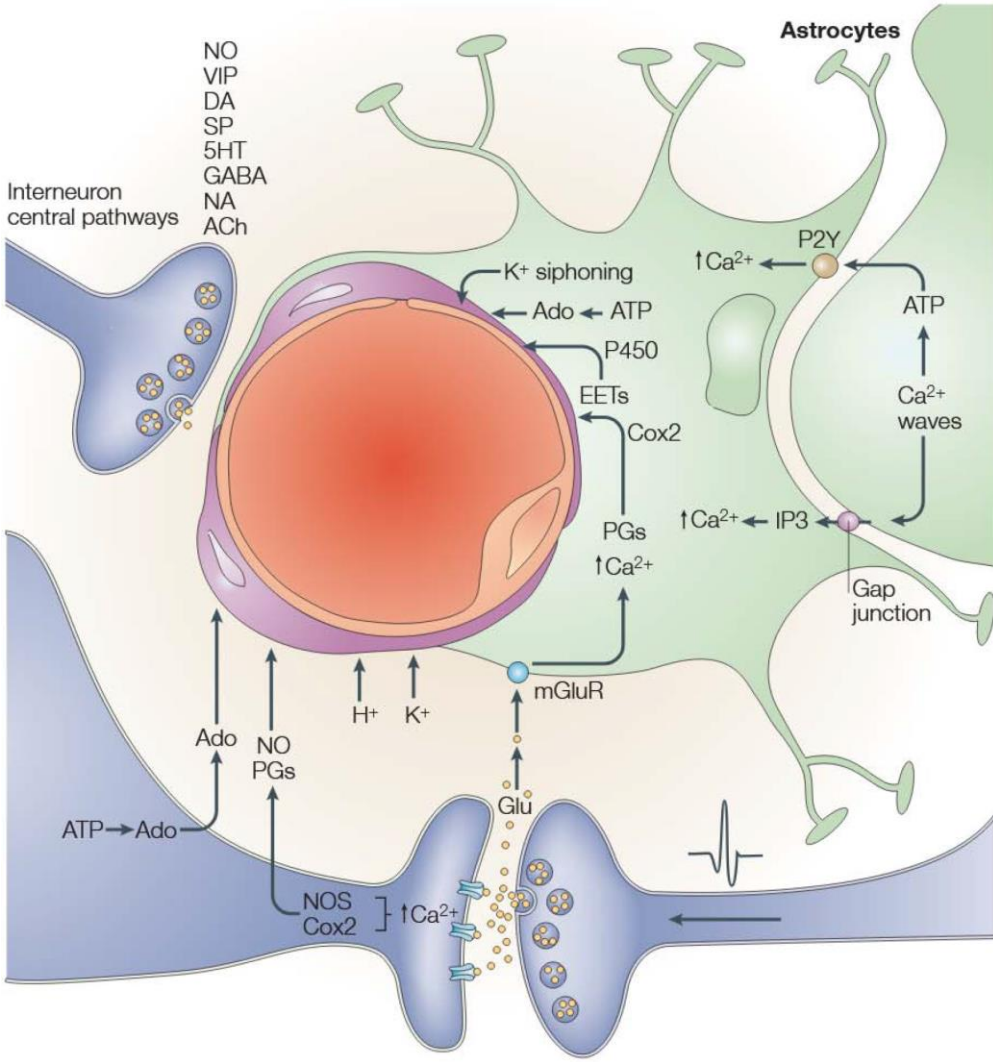

Figure 9: Astrocytes as a bridge between neurons and microvasculature (from (Iadecola, 2004)). Vasoactive mediators are released from neurons and astrocytes by neuronal activity. Glutamate induces an increase in intracellular calcium concentration both in neurons and glia. The activated signaling pathway triggers the synthesis of NO, prostaglandins and epoxyeicosatrienoic acids. In astrocytes, metabotropic glutamate receptors are the ones mediating calcium response to glutamate.

Astrocytes are also taking part of the synapse constituting what is known as tripartite complexes (Araque *et al.*, 1999; Hillen, Burbach and Hol, 2018). Astrocytic peri-synaptic processes can modulate the dynamics, maturation and stabilization of dendritic spines. Besides, they can participate in the modulation of synaptic transmission and plasticity (Ullian *et al.*, 2001; Haber, Zhou and Murai, 2006; Nishida and Okabe, 2007). Astrocytes express ionotropic and metabotropic membrane receptors that can be activated by several neurotransmitters, such as glutamate, released to the synaptic cleft. Thus, astrocytes can sense the intensity of the synaptic activity and modulate synaptic function in turn (Verkhratsky and Nedergaard, 2014). Astrocytes in the tripartite synapse can also regulate the signal transmission, controlling the homeostasis of transmitters (Sofroniew and Vinters, 2010). Astrocyte processes are rich in transporters through which the released neurotransmitters can be taken into them. These removed neurotransmitters are later converted by enzymes into precursors, recycling back to synapses

and reconverting into active transmitters. In case of glutamate, this astrocytic function also prevents excitotoxicity as it cooperates in maintaining sufficient extra-synaptic low levels (Schousboe *et al.*, 2004).

Astrocytes also participate in CBF regulation (Takano *et al.*, 2006). In addition to the NO released by neurons during neuronal activity, astrocytes can release vasoactive substances in a calcium-dependent manner to induce vasodilation or vasoconstriction (Attwell *et al.*, 2010).

As well, astrocytes are key elements for the BBB integrity and the homeostasis of ionic and water due to the tight relationship between their end-feet and the microvasculature. They are able to up-regulate physical, transport and metabolic barrier features (Abbott, Rönnbäck and Hansson, 2006). Astrocytes have been involved in the induction and maintenance of the BBB integrity as they play a primary role in the expression, in the mature brain vasculature, of several tight junction proteins like Claudin-5 and ZO-1 (Willis *et al.*, 2004).

Furthermore, another way to introduce potent and persistent impact on synapse is by releasing growth factors and related molecules, including tumor necrosis factor-α (TNF-α) and brain-derived neurotrophic factor (BDNF) (Sofroniew and Vinters, 2010). TNF-α has been shown to influence homeostatic synaptic scaling by inducing the insertion of AMPA receptors at post-synaptic membranes (Stellwagen and Malenka, 2006). BDNF influences both structural and functional aspects of synaptic transmission, enhancing activity-induced changes, which leads to increased efficiency of signal transfer (Lynch, 2004).

Microglia

Microglia are the resident immune cells of the brain (Bilbo and Stevens, 2017). These embryonic mesoderm-derived cells constantly surveil the CNS and respond to insult, accomplishing roles in phagocytosis and inflammation, thus ensuring CNS maintenance and health (Nimmerjahn, Kirchhoff and Helmchen, 2005). They express both pro-inflammatory (e.g., IL-1β) and anti-inflammatory (e.g., IL-10) molecules, with subsequent up-regulation of factors such as GFAP.

As additional functions, the described microglia-to-astrocyte crosstalk in response to glutamate plays a role in neuro-immune-interactions (Macht, 2016) and microglia is also required for normal neurogenesis, mainly by nerve growth factor (NGF) and tumor necrosis factor (TNF) (Matejuk and Ransohoff, 2020).

However, their dynamic phagocytic activity and active release of immune signals, playing critical roles in brain homeostasis and repair processes (Hanisch and Kettenmann, 2007), can be disturbed during pathology, causing their shift toward a reactive phenotype. As

consequence, these reactive microglia respond with exacerbated secretion of proinflammatory mediators (Vinuesa *et al.*, 2019) and altered phagocytotic properties (Baik *et al.*, 2019; Zhang *et al.*, 2020). Moreover, weakened microglia is highlighted as important mediators in AD pathology, as it has been recently published that microglia coverage within the NVU was significantly lower in AD patients compared to non-demented controls in the hippocampus and cortex (Kirabali *et al.*, 2020).

Oligodendrocytes

During the CNS developmental myelination, oligodendrocyte progenitor cells proliferate and migrate to their final destination, where they definitively differentiate into mature oligodendrocytes and myelinate axons (Elbaz and Popko, 2019). Moreover, myelinating oligodendrocytes are also newly generated in adult brain; derived from adult oligodendrocyte progenitor cells (Franklin and Ffrench-Constant, 2017).

It has recently become increasingly evident that those adult-born oligodendrocytes and myelin are crucial for motor-skill learning (McKenzie *et al.*, 2014; Xiao *et al.*, 2016). In addition, it was reported that myelin is a fairly dynamic structure that undergoes changes and remodelling in adulthood (Hughes *et al.*, 2018). These changes occur at least in part in response to neuronal activity, and are observed in behavioural settings such as skilled learning and social isolation (Jensen and Yong, 2016). The unique molecular cues that govern non-developmental CNS myelination remain largely unknown, however if the capacity to produce myelinating oligodendrocytes diminishes, then remyelination failure appear and consequently demyelinating diseases (Chang *et al.*, 2002).

3.1.2. Cells of the vascular system

In the human brain, cerebral blood vessels represent a total length of approximately 650 km. Within this network, cerebral arteries, arterioles and capillaries deliver energy metabolites, nutrients and oxygen to the brain by the CBF and transport across the BBB. The cerebral venous return removes metabolic waste products and carbon dioxide from brain into systemic circulation for clearance by kidney, liver and lungs, respectively (Kisler *et al.*, 2017). Capillaries contribute to 85 % of the vessel length, so it means that they provide about 12 m^2 of endothelial surface area (Abbott *et al.*, 2010). Accordingly, the vasculature present in the CNS is a primary barrier that acts as an interface between the brain and peripheral influences (Segarra, Aburto and Acker-Palmer, 2021). As an interface it mainly contributes to the preservation of the cerebral parenchyma. However it may also be affected due to these aforementioned peripheral pressures and consequently transmit them to the parenchyma, altering the brain homeostasis.

Focusing on the brain microvasculature, it is constituted by endothelial cells surrounded by mural cells. Mural cells are located in the basement membrane shared with endothelial cells. Mural cells are critically implicated in vascular development and maintenance (Gaengel *et al.*, 2009). They are also involved in BBB physiology and control CBF by regulating vasodilatation and constriction (Armulik *et al.*, 2010; Tong *et al.*, 2021). Furthermore, they have been reported to be disrupted in numerous brain pathological processes (Winkler, Bell and Zlokovic, 2011). Mural cells can be usually classified into two groups: vascular smooth muscle cells (vSMCs) and pericytes.

3.1.2.1. Vascular smooth muscle cells

Vascular smooth muscle cells (vSMCs) present a ring-like morphology around the vascular lumen and express the contractile protein known as smooth muscle actin (Hill *et al.*, 2015). These cells are highly plastic and are situated in the medium part of a blood vessel forming several layers. In case of capillaries, they are replaced by pericytes. vSMCs play relevant roles physiological functions including vasoconstriction, vasodilatation and extracellular matrix production (Bacakova *et al.*, 2018).

3.1.2.2. Pericytes

Pericytes extend along the abluminal surface of brain capillaries. They present longitudinal processes that encompass multiple vessel branches and lack expression of smooth muscle actin protein (Armulik, Genové and Betsholtz, 2011; Bell *et al.*, 2019). These cells share the inner basement membrane with brain endothelial cells to which they are directly connected via peg-socket junctions. Through this kind of junctions there is a direct exchange of metabolites, ions and other small molecules (Kisler *et al.*, 2017; Zarekiani *et al.*, 2022). Broadly regarding pericytes functions, they are involved in the development, maturation and functionality of microvascular networks (Balabanov and Dore-Duffy, 1998). However, their main function has been described in relation with BBB development and function (Sá-Pereira, Brites and Brito, 2012). Pericytes at the BBB regulate on one hand, endothelial cells gene expression via upregulation of the production of several markers associated with BBB function. On the other hand, pericytes mediate the polarization and fastening of astrocyte end-feet to blood vessels (Armulik *et al.*, 2010). In addition to their importance in barrier function, pericytes are also involved in the regulation of the vessel diameter, which in turn regulates the CBF (Hall *et al.*, 2014).

3.1.2.3. Endothelial cells

Endothelial cells that constitute the microvasculature of the CNS differ mainly from other vascular tissues in their capacity to regulate the crossing of molecules and cells to and from the neural parenchyma (Weksler *et al.*, 2005).

Endothelial cells comprising the capillaries are surrounded by the basement membrane, also known as the basal lamina. Briefly, the basement membrane represents a highly organized structure that is constituted by extracellular matrix molecules such as laminins, integrins, fibronectin and collagen (Reed, Damodarasamy and Banks, 2019). These anchoring proteins define the relevant role that the basement membrane plays in vascular integrity and in the maintenance of BBB stability and properties (Persidsky *et al.*, 2006); providing attaching support to vessels and surrounding cells (Yurchenco and Patton, 2009) and therefore promoting close associations and structural connections.

It is worthy to highlight that cerebral endothelial cells are unique due to the special features that they present. They constitute a monolayer tightly-sealed by highly specialized intercellular junctional structures to restrict paracellular flow. Moreover brain endothelial cells are not fenestrated and they have lost pinocytosis activity to restrict transcelular flow. Furthermore, they display highly selective transport systems to eliminate toxic substances along with exchanging nutrients and metabolites between circulation and brain (Sweeney *et al.*, 2019). As a consequence of all these characteristics, they constitute a high selective barrier known as the BBB.

The BBB is centrally positioned within the NVU and, as aforementioned, it is fortified by perivascular structures like pericytes and the basement membrane that are ensheathing endothelial capillary wall (Persidsky *et al.*, 2006; Armulik *et al.*, 2010). The BBB prevents neurotoxic plasma components and pathogens from entering the brain. It also controls the entry of leukocytes and red blood cells. At the same time, the BBB effectively regulates the passive exchange of solutes, transporter-mediated substances (like ions, amino acids or glucose), signaling molecules and the trafficking of macromolecules (like peptides or proteins), maintaining the chemical composition of the neuronal milieu tightly controlled (Kadry, Noorani and Cucullo, 2020).

The integrity of the BBB relies in part on the establishment and maintenance of the aforementioned junctional molecules that seal endothelial cells between them. There are different kinds of molecules involved in this junctional structure and altogether contribute to keep BBB endothelium polarity (Abbott *et al.*, 2010). In fact, this apicobasal polarity is more considerable than those in other organs in terms of polarized distributions of receptors, lipids, glycoproteins and transporters between apical and basal membranes (Worzfeld and Schwaninger, 2016).

The main kind of junctional molecules include adherens junctions, gap junctions and tight junctions **(figure 10)**. Adherens junction (AJ) proteins (like VE-cadherin) are localized nearest

to the basolateral membrane and form homophilic cell-to-cell contacts. AJs are linked to cytoskeleton and modulate receptor-signaling processes along with transendothelial migration of lymphocytes, neutrophils, monocytes and leukocytes (Vorbrodt and Dobrogowska, 2003). Gap junctions (like CX30 and CX43) form hemichannels between endothelial cells allowing intercellular communications, thus intracellular responses can be transmitted to adjacent cells (Zhao *et al.*, 2015). Tight junctions (TJ) proteins (like Zonula occludens (ZO-1) and Claudin-5) are located closest to the apical membrane and they limit paracellular diffusion of solutes and ions across the BBB (Nitta *et al.*, 2003). Deficiency of TJ proteins leads to microbleeds and BBB breakdown in human neurodegenerative disorders (Sweeney *et al.*, 2019). In summary, all these junctional molecules contribute to the BBB functions and as well as maintaining its structure as a restrictive barrier. Moreover it is worthy to remark that they are also involved in processes that require physiopathological opening of the BBB as happens when immune cells need to move into the brain parenchyma. It was reported that the BBB enables for immune cells entering the CNS in the absence of neuroinflammation but strictly limits this trafficking to immune cells subsets involved in immune surveillance and detected in the cerebrospinal fluid (Marchetti and Engelhardt, 2020). In this situation **(figure 11)**, among the dynamic mechanisms implicated in the transmission of immune cells across the BBB, there is also a disruption in TJ proteins during paracellular migration events (Kadry, Noorani and Cucullo, 2020).

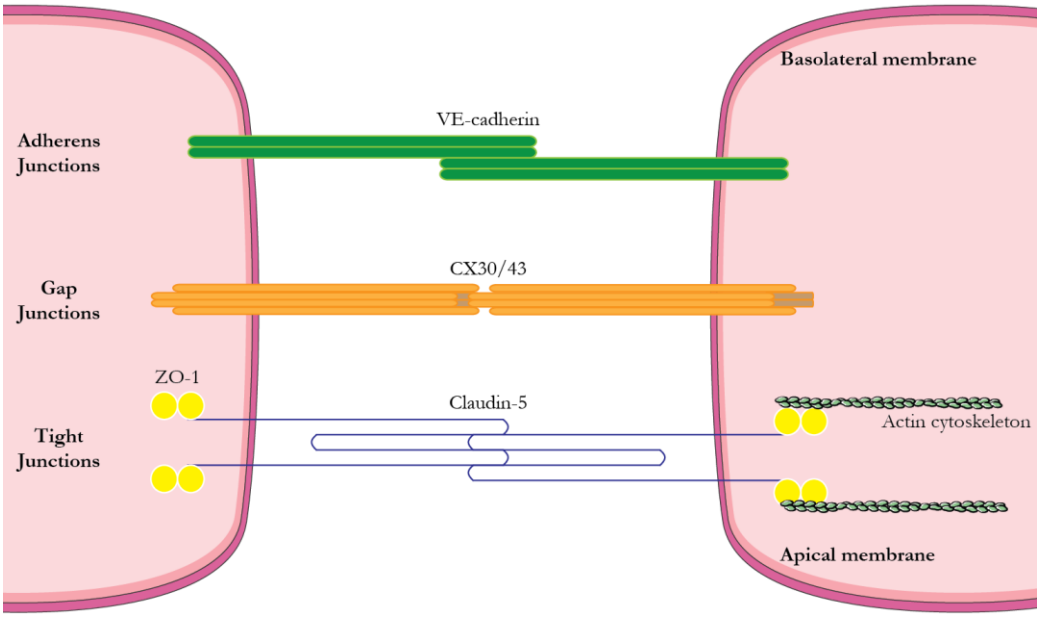

Figure 10: Simplified scheme of the main junctional molecules sealing cerebral microvascular endothelial cells (adapted from (Sweeney *et al.*, 2019)). Different types of junctional molecules contribute to maintain the BBB structure. Nearest to basolateral membrane Adherens junction proteins (VE-cadherin) form homophilic cell-to-cell contacts. Gap junctions (CX30 and CX43) form hemichannels between endothelial cells enabling intercellular communications. Tight junction proteins (Claudin-5 and ZO-1) locate closets to apical membrane limiting paracellular diffusion of solutes and ions.

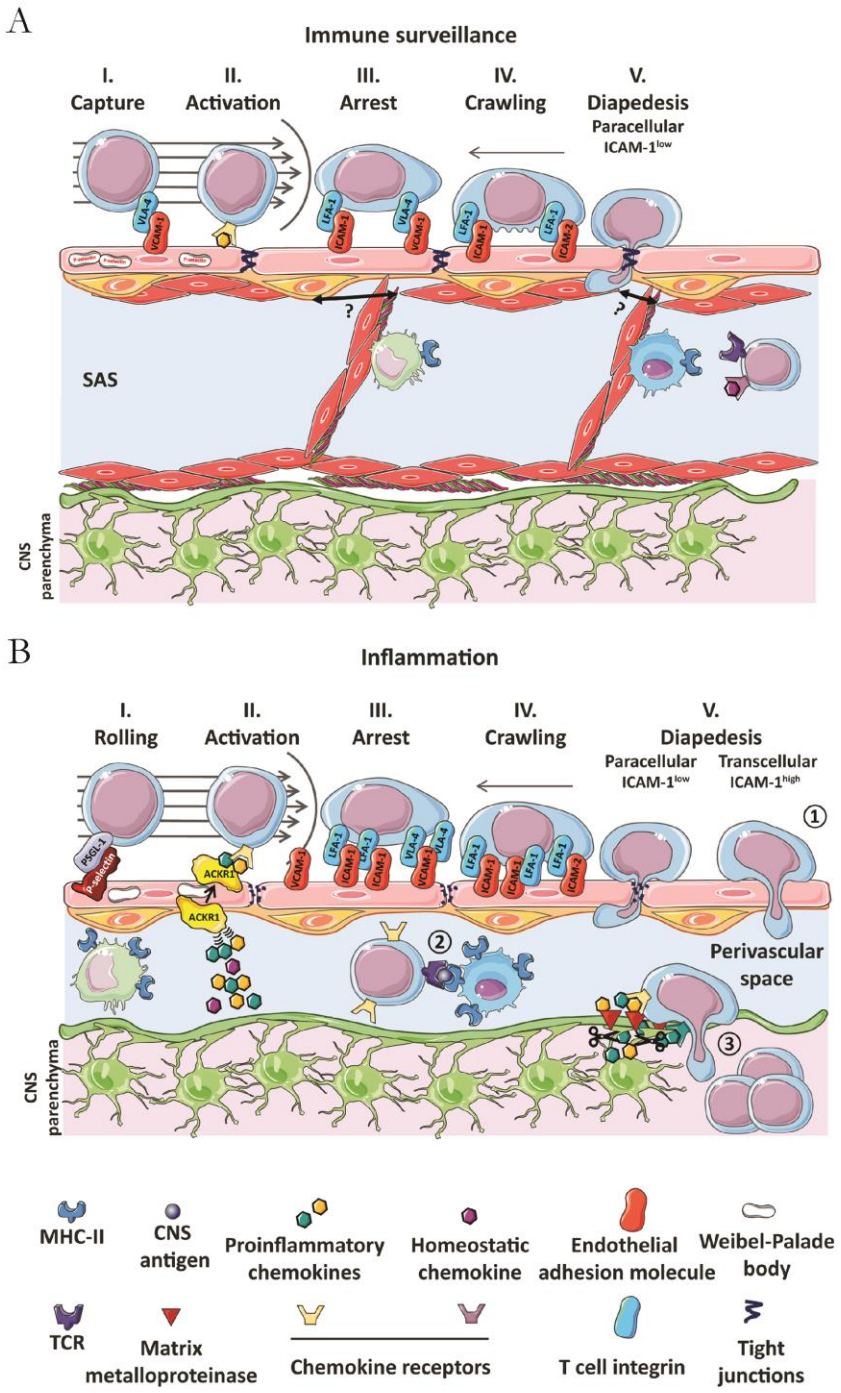

Figure 11: Multi-step T-cell extravasation across the BBB during heath and neuroinflammation (from (Marchetti and Engelhardt, 2020)). T-cell extravasation across subarachnoid venules during immune surveillance **(A)** or across BBB postcapillary venules during inflammation **(B)** is depicted. After GPCR-mediated shear resistant arrest, T cells crawl against the direction of the flow and cross the BBB endothelium preferentially via the paracellular pathway. Pial cells are reported to partially cover the venular wall in the SAS (highlighted by the question mark), but do not seem to establish a barrier for T cell extravasation. In the absence of CNS antigens presented by subarachnoid macrophages and dendric cells on MHC-II molecules, T cells will not cross the glia limitans and may rather be flushed away with the CSF. During inflammation, leptomeningeal but also parenchymal BBB endothelial cells **(B)** allow for activated T-cell rolling, mediated by P-selectin which is de novo expressed as it is not stored in Weibel-Palade bodies. Inflammatory chemokines produced by astrocytes are transported from the abluminal to the luminal side of the BBB by ACKR1. After their GPCR-dependent arrest, T cells crawl on endothelial ICAM-1 and ICAM-2 against the direction of the flow with increased levels of endothelial ICAM-1 leading to increased transcellular T cell diapedesis. Once T cells have crossed the BBB endothelium **(1)**, CNS-antigen-specific T cells may recognize their cognate antigens on perivascular APCs **(2)** and become reactivated behind the BBB. Matrix metalloproteinases produced by infiltrating and perivascular-activated myeloid cells as well as astrocytes cleave the astrocytic endfeet from the parenchymal basement membrane, allowing for T-cell passage, a process guided by proinflammatory chemokines produced by astrocytes. Once in the CNS parenchyma, T cells induce CNS damage and manifestation of clinical disease symptoms **(3)**. Subarachnoid space (SAS).

Brain endothelial cells are more than just the cells coating the blood vessels. Actually, they are active players controlling the blood flow and the intravascular blood coagulation. Besides, they also communicate with surrounding glia thus monitoring brain parenchymal health (Martinez-Lozada and Robinson, 2020; Menaceur *et al.*, 2021). On the other hand, the ion channels present on their membrane enable the propagation of information about neuronal activity from the capillaries in near proximity to each neuron, to bigger vessels to regulate vasodilatation or vasoconstriction and so intervening in neurovascular coupling (Harraz *et al.*, 2018).

In summary, suitable functioning of homeostatic mechanisms requires dynamic crosstalk among cells of the NVU, many of which present complementary functions. Altogether call for a combined strategy for addressing the functional status of the NVU and its vulnerability under disease conditions.

3.2. Neurovascular unit failure as a key element on Alzheimer's disease and cerebral amyloid angiopathy

According to the reviewed physiological functions of the main NVU integrators and considering the relevance of an appropriate dynamic communication between them, the failure of any of these factors would compromise the whole NVU functions and consequently induce brain damage and neurodegeneration (de la Torre, 2017). Dysfunction of the NVU is characterized by dysregulation of neurovascular coupling, neuronal death, gliosis, microglia activation, mural cell transmigration, and BBB breakdown (Zlokovic, 2005; Willis, 2011).

Almost all neurodegenerative conditions involve oxidative stress and inflammation (Ransohoff, 2016), and both situations can arise after NVU dysfunction. In diseases like AD, the coexistence of cerebrovascular lesions with neurodegeneration is well documented.

In an AD context, vascular lesions increase the whole lesion load of the brain and it may lower the threshold for cognitive deficits. Alternatively, both processes may act synergistically, amplifying each other (Iadecola, 2017). Any cell type within the NVU could initiate the pathogenic disease cascade if its function is impaired. As an example, brain endothelial cells functioning may be affected due intrinsic genetic dysfunction and/or AD-specific molecular and cellular phenotype. Moreover, peripheral pathologies, such as hypercholesterolemia, hypertension or diabetes mellitus, may also influence endothelial cells constituting the BBB and as previously mentioned, although the main BBB function is to preserve the brain homeostasis, it may be affected under critical peripheral alterations and afterwards, transfer them to the parenchyma. Anyhow, the BBB alteration would lead to ionic imbalance and toxic metabolic products accumulation in neuronal environments and consequently induce synaptic and neuronal dysfunction (Iadecola, 2017).

3.2.1. Synaptic dysfunction and neuronal loss

Synapse dysfunction and loss is a typical feature of many neurodegenerative diseases associated with dementia and particularly in AD. In accordance with both, the amyloid hypothesis and the tau hypothesis of AD, the concept that AD is principally a disorder of synaptic function (synaptopathy) is by no means new (Hardy and Selkoe, 2002). An undeniable and considerable loss of synapses and neurons was described in late stage of AD (Jack *et al.*, 2010). In fact, mice models expressing familial AD-associated mutations in genes coding for APP (increasing Aβ levels) or for mutated tau (leading to NFT) provide an entry point to study mechanisms of synapse loss associated with prominent AD-related pathologies (Jankowsky and Zheng, 2017).

However, more interesting is the possibility that synaptic dysfunction can occur early in prodromal stages of the disease and may robustly present before frank atrophy (Scheff *et al.*, 2006). Traditionally, synapses can only be observed by electron microscopic and immunohistochemical examinations in biopsy and autopsy tissue samples (Bao *et al.*, 2021). Recently a series of novel positron emission tomography (PET) radiotracers selectively targeting synaptic vesicle glycoprotein 2 (SV2A) have been developed (Mercier *et al.*, 2014; Estrada *et al.*, 2016; Nabulsi *et al.*, 2016; Li *et al.*, 2019; Cai *et al.*, 2020), enabling non-invasive observation and quantification of synaptic density in humans (Finnema *et al.*, 2016; Bahri *et al.*, 2017; Naganawa *et al.*, 2021). Recently, it was reported that there is a significant reduction in SV2A binding in AD patients compared to healthy controls (Chen *et al.*, 2018). Moreover, these authors also found a relationship between overall SV2A binding and episodic memory scores.

Synaptic dysfunction in AD is mainly characterized by excitotoxicity, glutamate receptors desensitization, LTP inhibition, and triggering of LTD (Forner *et al.*, 2017). The spines collapse has been related with the depolymerization of fibrillar actin into globular form due to the exposure to Aβ (Kommaddi *et al.*, 2018). Synapse loss close to plaques may be caused by increased levels of soluble oligomeric species rather than the plaques themselves (Koffie *et al.*, 2009). Moreover, high oAβ levels also correlate with the extent of synaptic loss and cognitive impairment (Lesné *et al.*, 2006). Altogether lead to a re-evaluation of Aβ roles in synaptic dysfunction.

During the disease progression, Aβ aggregation starts to be enriched at synapses. However, this happens quite before amyloid plaques formation (Klementieva *et al.*, 2017). Synapses can be contacted by a mixture of Aβ species that might induce diverse biological reactions. On one hand, high-molecular-weight oligomers cause a temporary decline of cognitive functions without evident synaptic pathology. On the other hand, low-molecular-weight oligomers lead

to a faster and more persistent cognitive impairment along with the significant reduction of pre- and postsynaptic proteins (Figueiredo *et al.*, 2013).

At high concentrations, Aβ peptides affect glutamatergic neurotransmission interfering with both, pre- and postsynaptic mechanisms **(figure 12)**. Aβ oligomers can be easily internalized and accumulate at presynaptic terminals of glutamatergic neurons (Russell *et al.*, 2012). Aβ-induced presynaptic dysfunction involves deficits in critical functions including axonal transport, synaptic vesicle trafficking and neurotransmitter recycling (Chen, Fu and Ip, 2019). Subsequently, the abnormal glutamate release may significantly contribute to the widespread synaptic dysfunction in AD (Marsh and Alifragis, 2018).

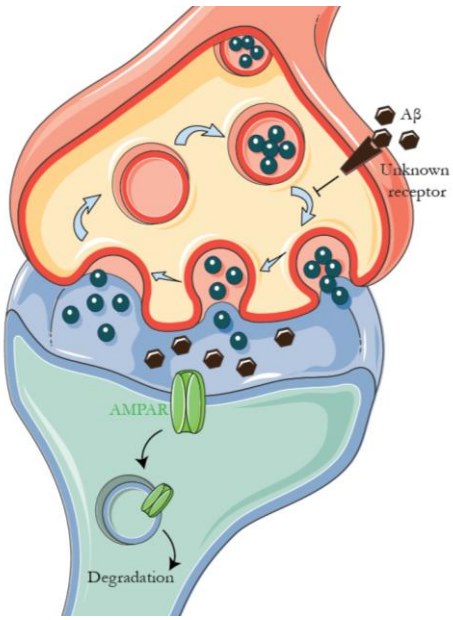

Figure 12: Abbreviated scheme representing the main Aβ-induced alterations on synaptic failure. Presynaptically, Aβ oligomers impair the key processes in synaptic vesicle cycling, including trafficking, release, and recycling. Postsynaptically, Aβ induces the removal of AMPA receptors from the synaptic membrane, leading to synaptic depression.

Aβ oligomers also present high affinity for targeting the postsynaptic compartment of excitatory synapses. Aβ-induced postsynaptic dysfunction involves structural and functional disturbance of synapses (Koffie *et al.*, 2009). Aβ oligomers can bind to different cell surface molecules, constituting putative Aβ receptor complexes that potentiate synaptoptoxicity. Ionotropic glutamate receptors are one of these cell surface molecules for which Aβ present attaching affinity (Texidó *et al.*, 2011; Miller *et al.*, 2014).

Early reports described that AD patients presented decreased AMPA receptor expression in the entorhinal cortex and hippocampus (Dewar *et al.*, 1991). Moreover, it was also described that Aβ levels can induce AMPA receptors removal from excitatory synapses, leading to dendritic spinal loss and synaptic depression (Hsieh *et al.*, 2006). Aβ oligomers decrease basal levels of GluA1 phosphorylation at Ser-845 thus affecting the composition of heteromeric AMPARs at the cell surface (Miñano-Molina *et al.*, 2011).

GluA1 trafficking is activity-dependent. Its insertion into the membrane is regulated by two phosphorylation sites, at serine-845 and serine-831, in the intracellular carboxyl terminal tail (Song and Huganir, 2002). Phosphorylation of GluA1 at serine-845 specifically promotes the recruitment of new AMPA receptors into extrasynaptic sites, preventing GluA1 homomers endocytosis and lysosomal degradation (Oh *et al.*, 2006). This mechanism has been proposed to be related with LTP establishment because with synaptic activity, AMPAR stored at extrasynaptic sites will be delivered into the synapses. On the other hand, dephosphorylation of this residue is critical for NMDA receptor-dependent LTD. Regarding serine-831 residue; its phosphorylation seems to increase the apparent single-channel conductance of GluA1. This suggests that serine-831 phosphorylation might mediate synaptic transmission potentiation during long-term potentiation (Song and Huganir, 2002). Nevertheless, previous data described that serine-831 phosphorylation was not affected by Aβ oligomers, at least in the experimental conditions applied (Lee *et al.*, 2010; Miñano-Molina *et al.*, 2011).

Therefore, synaptic dysfunction during early stages of AD could be the result, as least in part, of the effect that Aβ oligomers induce as a synaptic depressor affecting the mechanisms involved in AMPAR targeting to synapses. However, considering other contributors the glutamate excitotoxicity may come to mind.

Glutamate excitotoxicity is a mechanism that most neuroinflammatory diseases have in common. Interestingly, glutamate is an essential component of physiological CNS activities, not only mediating neuronal signaling, but also by mediating communication between neurons and other compartments. In this regard, glutamate is involved in the coupling of neuronal activity with the activity of their glial support infrastructure, the vasculature as well as the immune system (Fairless, Bading and Diem, 2021). Nevertheless, under pathophysiological conditions glutamate is also a mediator of neurodegeneration. Since long time ago, glutamate has been recognized as a key activator of excitotoxicity whereby excessive glutamate receptor stimulation can result in neuronal death (Lucas and Newhouse, 1957). This excitotoxic death has been described for most diseases affecting the CNS (Doble, 1999; Dong, Wang and Qin, 2009) like neurodegenerative diseases such as AD (Wang and Reddy, 2017).

According to the pivotal role of glutamate signaling between neurons, glia and vasculature (altogether constituting the NVU), under pathophysiological conditions, glutamate alterations will adversely affect not only neurons but also glia and endothelial cells. Reviewing glutamate regulation of cellular function in glial cells, it is remarkable that both astrocytes (Chen, Liao and Kuo, 2000) and oligodendrocytes (Yoshioka *et al.*, 1995; Matute *et al.*, 1997) present vulnerability to glutamate excitotoxicity. Cerebrovascular endothelial cells have also been

reported to be vulnerable to glutamate toxicity (Parfenova *et al.*, 2006), as treatment with glutamate caused a reduction in the brain endothelial barrier integrity *in vitro* (Sharp *et al.*, 2003) and a reorganization of their cell tight-junction proteins (András *et al.*, 2007).

Overall, synaptic dysfunction in AD not only involves neuronal affectation and cognitive failure, but also it may have an impact on other NVU cells through aberrant glutamate signaling.

3.2.2. Glial cell alterations within NVU pathologic failure

Due to their location within the NVU, glial cells are in direct physical contact with neurons and vascular cells and consequently, they act as interface between these cellular components, contributing to modulate the overall crosstalk (Kugler, Greenwood and MacDonald, 2021).

Beyond their respective roles in physiological conditions, astrocytes and microglia contribute to neuroinflammation in response to stroke and other neurological diseases (Cekanaviciute and Buckwalter, 2016), where they act as primary initiators of the inflammation cascade by increasing reactivity and secreting signalling factors such as chemokines (Sofroniew and Vinters, 2010; Karve, Taylor and Crack, 2016).

Increasing evidences consider astrocytes as a link between vascular and neurological contributions in AD (Edison, Donat and Sastre, 2018; Price *et al.*, 2018). In AD, reactive astrocytes participate in shifting the excitation-inhibition balance through secretions of GABA. While in the healthy brain, astrocytes do not contribute much to GABA production, in AD GABA starts to be synthesised by astrocytes through putrescine-MAO-B pathway (Jo *et al.*, 2014). In this way, reactive astrocytes start to secrete GABA thus increasing inhibition, likely to be a defensive response against neuronal hyperexcitability that seems to be a universal result of AD progression (Garaschuk and Verkhratsky, 2019; Ghatak *et al.*, 2019).

Moreover, it is broadly acknowledged that AD involves inflammatory responses, initiated, or mediated via astrocytes and microglia that lead to BBB breakdown (Akiyama *et al.*, 2000; Nagele *et al.*, 2004). Aβ can activate the NF-κB pathway in astrocytes, which leads the releasing of the complement protein C3. The C3 binding to its microglial receptor alters Aβ phagocytosis while the C3 binding to its neuronal receptor disrupts dendritic morphology and network function, both effects contributing to AD pathogenesis (Lian and Zheng, 2016). Recently, it was shown that activation of microglia leads to the conversion of resting astrocytes to reactive astrocytes via secretion of IL-1α, TNFα, and C1q in a variety of neurodegenerative disorders including AD (Liddelow *et al.*, 2017; Liddelow, 2019).

3.2.3. Vascular cells in pathologic conditions related with NVU failure in Alzheimer's disease and CAA

A relevant component of AD pathophysiology **(figure 13)** is the alteration and dysfunction of the cerebral vasculature, as it could contribute to the emergence and progression of the disease as well as promoting Aβ accumulation, tau phosphorylation, inflammation and neurodegeneration (Sagare, Bell and Zlokovic, 2012). Several reports support the vascular dysfunction in AD applying different methodologies such as neuroimaging techniques, analysis of postmortem brain samples and CSF biomarkers detection (Montagne, Zhao and Zlokovic, 2017; Sweeney, Sagare and Zlokovic, 2018).

Neuroimaging studies determined a reduction in glucose transporter-1 in the BBB, thus linking alterations in glucose transport to early AD (Bailly *et al.*, 2015). By neuroimaging technique it was also described that Aβ transport across the BBB is impaired in AD patients (Deo *et al.*, 2014). Moreover, through magnetic resonance imaging, it was shown that early AD patients presented BBB leakage in the grey matter and cortex, which is associated with cognitive impairment and a decreased CBF in grey matter (van de Haar *et al.*, 2016; Van De Haar *et al.*, 2016). It is highly interesting the fact that hippocampal BBB leakage appeared before brain atrophy or dementia occurred and, furthermore, it was independently of Aβ and/or tau changes (Nation *et al.*, 2019). The presence of microbleeds in the CNS in 40 % of patients at the initial stages of AD was also revealed by magnetic resonance images (Yates *et al.*, 2014). Collectively, these results corroborated the early endothelial dysfunction underlying the onset of AD.

BBB permeability was already described in AD postmortem tissue, where, specifically in the parenchyma, certain substances (such as fibrinogen, plasmin, immunoglobulins or albumin) were detected after their leakage from capillaries (Ryu and McLarnon, 2009). In addition, the extravasation of neutrophils, erythrocytes and peripheral macrophages was also observed (Fiala *et al.*, 2002; Cullen, Kócsi and Stone, 2005; Zenaro *et al.*, 2015).

Related with BBB alteration, it was determined that pericyte coverage of brain capillaries dropped in AD by around 30% (Sengillo *et al.*, 2013). As pericytes are considered key cells in the maintenance of the BBB, their loss may correlate with the increase in BBB permeability. Moreover, pericyte degeneration was also shown to influence Aβ plaque formation (Sagare *et al.*, 2013) as the over-expression of APP in pericyte-deficient mice resulted in accelerating the Aβ plaque-formation process. As well, they also described that pericytes contributed to Aβ clearing, so the decrease of pericytes number during AD leaded to the accumulation and reduced clearance of Aβ, which in turn reduces the pericytes population, thus initiating a

cascade effect. Besides, other report showed that pericytes and/or vSMCs loss may be also involved in the drop of CBF that has been shown to occur in AD (Roher *et al.*, 2012). This drop has also been previously hypothesized to reduce nutrient delivery and waste removal and increase oxidative stress and Aβ aggregation, altogether leading to an overall decline in neuronal cells (De la Torre and Mussivand, 1993; Tublin *et al.*, 2019).

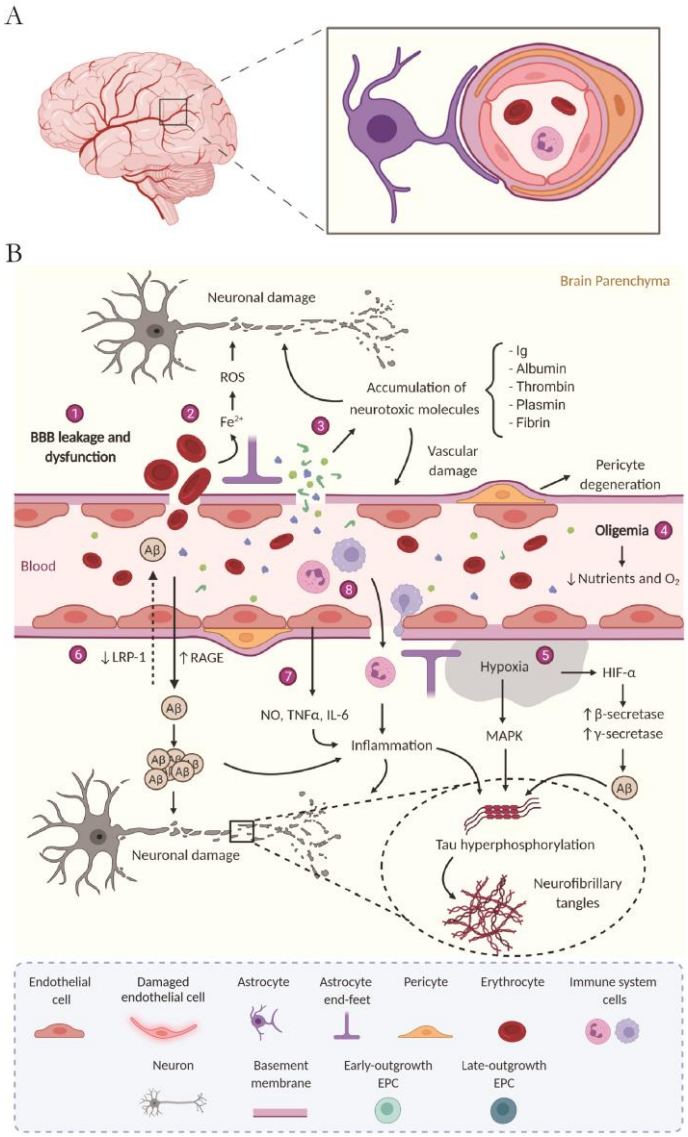

Figure 13: Vascular alterations related with neurovascular unit failure (adapted from (Custodia *et al.*, 2022)). **(A)** Healthy capillary; the BBB has TJ proteins between endothelial cells, pericytes enveloping endothelial cells, astrocytes, and normal blood flow. **(B)** AD capillary; Main vascular alterations occurring in AD: **(1)** the rupture and dysfunction of the BBB increase the permeability of different cells and molecules; **(2)** the accumulation of erythrocytes in the parenchyma generates neurotoxic products that damage brain cells through the production of ROS; **(3)** the extravasation and consequent accumulation of neurotoxic molecules induces neurodegeneration and vascular damage; **(4)** oligemia induces a reduction in nutrient and oxygen supply, **(5)** generating hypoxic zones increases Aβ production and tau phosphorylation; **(6)** Aβ flow through the BBB is impaired due to a lower expression of LRP-1 and a higher expression of RAGE, leading to Ab accumulation in the brain parenchyma; **(7)** blood vessels release a large amount of proinflammatory mediators (NO, TNFα, and IL-6) that together with **(8)** the extravasation of immune system cells generate inflammation. All together finally generate neuronal damage. ROS, reactive oxygen species; Ig, immunoglobulins; BBB, blood-brain barrier; Aβ, amyloid β protein; LRP-1, low-density lipoprotein receptor-related protein 1, RAGE, receptor for advanced glycation end products; NO, nitric oxide; TNF-α, tumor necrosis factor-alpha; IL-6, interleukin-6, HIF-1α, hypoxia-induced factor 1α; MAPK, mitogen-activated protein kinase.

Furthermore, the presence of endothelial degeneration, the reduced expression of TJ proteins in capillaries and the reduction in the length of such vessels have been described in AD patients (Baloyannis and Baloyannis, 2012). Remarkably, some molecular changes have been also observed in brain endothelial cells from AD patients, such as decreased expression of low-density lipoprotein receptor-related protein-1 (LRP-1), involved in Aβ removal from the brain, and the aforementioned glucose transporter-1 (Donahue *et al.*, 2006). Moreover, other molecular changes involved the increase of the receptor for advanced glycation end products (RAGE), which induces the uptake of circulatory Aβ to the parenchyma, and also the levels of the semicarbazide-sensitive amine oxidase (SSAO), also known as vascular adhesion protein-1 (VAP-1) or primary amine oxidase (PrAO) are increased (Ferrer *et al.*, 2002). Briefly, this SSAO/VAP-1 is a multifunctional enzyme that mediates the binding and promotes the transmigration of circulating leukocytes into inflamed tissue (Unzeta *et al.*, 2021). Regarding the inflammatory context, higher levels of inflammatory mediators like NO, TNF-α, interleukin-6, and 8 (IL-6 and IL-8), matrix metalloproteinases, prostaglandins and leukocyte adhesion molecules were determined in microvessels isolated from AD brains, compared with healthy controls (Grammas and Ovase, 2001).

3.2.3.1. The semicarbazide-sensitive amine oxidase / vascular adhesion protein-1

Semicarbazide-sensitive amine oxidase (SSAO; E.C. 1.4.3.21) belongs to the amine oxidase subgroup that contains topa-quinone or lysine tyrosyl quinone as attached cofactor. These cofactors are the responsible of making the enzymes being easily inhibited by carbonyl compounds like semicarbazide (Jalkanen and Salmi, 2001; Klinman and Mu, 2003). The cloning of endothelial vascular adhesion protein-1 (VAP-1) showed that it has SSAO activity and was significantly similar to copper-containing amine oxidases (Smith *et al.*, 1998). Thenceforth, SSAO/VAP-1 was defined as a new kind of adhesion molecule with both cell adhesion function and SSAO enzymatic activity.

SSAO/VAP-1 is present in a huge number of mammalian species (Lewinsohn, 1984). It can be located at the plasmatic cell membrane but also can be found as a soluble form in blood plasma (Lyles, 1996). High SSAO activity is associated with adipose tissue as well as with vascularized tissues (Lizcano *et al.*, 1990), where it is specifically linked with blood vessels, as it is expressed by endothelial cells and smooth muscle cells (Lyles and Singh, 1985; Salmi and Jalkanen, 1995). In humans, the presence of the SSAO enzyme was reported in those mentioned cell types extracted from different tissues such as heart, kidney, skin, liver and brain (Andrés *et al.*, 2001; Ramonet *et al.*, 2003).

Structure, catalytic activity and physiological functions

Molecular modeling assays revealed that human membrane-bound SSAO/VAP-1 is constituted by two identical 90 kDa monomer subunits, resulting in a 180 kDa homodimeric glycoprotein **(figure 14)**. It comprises a short membrane spinning domain and each monomer contains a catalytically active extracellular copper-containing amine oxidase domains (Jakobsson *et al.*, 2005).

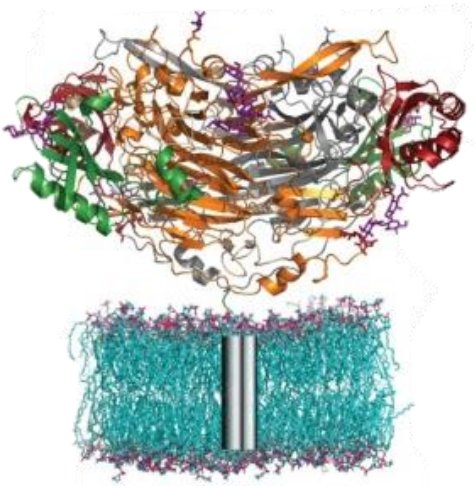

Figure 14: Putative position of SSAO/VAP-1 with respect to cell membrane (from (Jakobsson et al., 2005). The enzyme comprises short membrane-bound helices, represented by grey cylinders, and two copper-containing amine oxidase domains.

The SSAO/VAP-1 is able to catalyze the oxidative deamination of primary amines to aldehydes, ammonia and hydrogen peroxide, following the next reaction:

$$R\text{-}CH_2\text{-}NH_2 + O_2 + H_2O \rightarrow R\text{-}CHO + NH_3 + H_2O_2$$

Methylamine and aminoacetone are the physiological substrates that are exclusively metabolized by SSAO/VAP-1 (O'Sullivan *et al.*, 2004). When catalyzed, deamination of these primary amines produces formaldehyde and methylglyoxal respectively, along with ammonia and hydrogen peroxide.

All the obtained catalytic products present biological activities and may have relevant roles at physiological concentrations. Consequently, these products generated from its enzymatic activity contribute with several SSAO/VAP-1 functions. In fact, low concentrations of hydrogen peroxide can act as intracellular second messengers involved in several functions like cell growth or cell death regulation, ligand stimulation, or NF-κB signalling activation. NF-κB activation regulates the expression of many other genes like cytokines and vascular cell adhesion molecules (Kunsch and Medford, 1999; Jalkanen and Salmi, 2001). Furthermore, hydrogen peroxide signalling also mediates angiogenesis and cellular differentiation processes, as well as being involved in the activation of mitogen-activated protein kinase (MAPK) and the c-Jun amino-terminal kinase (JNK) (Finkel, 1998). Other physiological functions consist on protecting against endogenous and xenobiotic amines (Tipton and Strolin, 2002) and regulating

glucose transportation (Morin *et al.*, 2001). Moreover it is also implicated in blood pressure control and elastic fiber organization (Göktürk *et al.*, 2003), as well as in adipocyte differentiation (Morin *et al.*, 2001) and leukocyte trafficking under inflammation (Salmi, Kalimo and Jalkanen, 1993; Salmi *et al.*, 2001; Salmi and Jalkanen, 2005; Lalor *et al.*, 2007).

SSAO/VAP-1 in pathological conditions: Alzheimer's disease

Several pathological conditions increase soluble SSAO/VAP-1 form. Diabetes (Grönvall-Nordquist *et al.*, 2001), atherosclerosis (Karádi *et al.*, 2002), non-diabetic morbidity obesity (Weiss *et al.*, 2003) and congestive heart failure (Boomsma *et al.*, 1997), along with malignant hypertension (Boomsma *et al.*, 1997), retinopathies associated with diabetes mellitus (Yu and Zuo, 1993) and inflammatory diseases (Kurkijärvi *et al.*, 1998) are described to present increased plasma soluble SSAO/VAP-1 levels. However, the specific mechanisms controlling the pathologic increase of soluble levels and activity are still not fully elucidated. Probably, it might be due to an up-regulated expression of membrane-bound form in response to inflammation. Then, the membrane-bound form is processed by a matrix metalloproteinase and thus, the soluble form is released.

SSAO/VAP-1 levels have also been reported to be altered in CNS pathologies as it was shown to be actively involved in the development of inflammatory lesions such as multiple sclerosis, autoimmune encephalomyelitis, stroke and AD (Ferrer *et al.*, 2002; Airas *et al.*, 2006, 2008).

SSAO/VAP-1 alterations described in several AD cardiovascular and lifestyle-related risk factors suggest that this enzyme could be involved in AD onset, as well in the pathology progression. Meningeal and parenchymal blood vessels of AD patient's brains showed increased levels of SSAO/VAP-1 enzyme (Ferrer *et al.*, 2002; Unzeta *et al.*, 2007; Valente *et al.*, 2012). Endothelial SSAO/VAP-1 may play a role in promoting or aggravating AD pathology through its function related with the regulation of granulocytes binding and leukocyte trafficking into tissues. Accordingly, different peripheral inflammatory cells, such as monocytes, lymphocytes and neutrophils, have been detected in brains from AD patients and also in animal models (Rossi *et al.*, 2021). The SSAO/VAP-1 function related with adhesion is especially active for neutrophils which have been described to be able to infiltrate into the brain parenchyma in AD pathology and also to have the capacity to migrate towards Aβ deposits in experimental mouse model (Baik *et al.*, 2014). Nevertheless, although the precise participation of SSAO/VAP-1 has not been assessed in this model, it is reasonable to speculate about its intervention.

Besides, SSAO/VAP-1 increased levels have been reported to be associated with vascular Aβ deposits in patients with AD (Ferrer *et al.*, 2002) . Moreover, circulating SSAO/VAP-1 activity

evidenced a clear rise in the plasma of sporadic AD patients at moderate-severe and severe stages of the disease (Del Mar Hernandez *et al.*, 2005). This elevated plasmatic SSAO activity could promote oxidative stress and vascular damage.

All these pathological increments of the SSAO/VAP-1 levels involve the overproduction of potentially hazardous metabolites as consequence of its higher enzymatic activity. Methylglyoxal and formaldehyde are toxic at high concentrations, especially in blood vessels (Matyus *et al.*, 2004). In fact, the methylglyoxal obtained after aminoacetone SSAO processing has been linked with vascular alterations, inducing oxidative stress and apoptosis. Actually, it is a precursor of advanced glycation end products (AGEs) that are related with vascular degeneration and diabetic complications (Mathys *et al.*, 2002). On the other hand, formaldehyde obtained when treating vascular cells *in vitro* with methylamine induces time- and dose-dependent cytotoxic effect and also activates apoptotic cell death. In the senescence-accelerated mouse-prone 8 (SAMP8) mice model, high formaldehyde concentration due to increased SSAO activity, correlates with cognitive dysfunction (Qiang *et al.*, 2014). Moreover, the formaldehyde has been described to induce protein unfolding and to produce protein cross-linkages with lysine residues (Gubisne-Haberle *et al.*, 2004). Interestingly, it may interact with Aβ lysines thus promoting its misfolding, oligomerization and fibrillognesis (Chen, Kazachkov and Yu, 2007) and therefore be considered the responsible of the SSAO/VAP-1 stimulation of Aβ aggregation and deposition on the vascular walls *in vitro*. Furthermore, it has been reported that Aβ itself can stimulate SSAO/VAP-1 increasing levels, thus boosting its toxic action and inducing vascular dysfunction within AD context (Solé, Miñano-Molina and Unzeta, 2015). Summarizing, altogether support the role of SSAO/VAP-1 in vascular pathology related with AD.

Within the NVU context, it was reported that SSAO/VAP-1 induces BBB leakage and leukocyte adhesion. Moreover, it was also described to lead endothelial activation by modifying the releasing pattern of pro-inflammatory and pro-angiogenic angioneurins IL-6, IL-8 and VEGF (Solé *et al.*, 2019). Once more, as previously mentioned, all these alterations related with SSAO/VAP-1, which originally affecting endothelial cells, may impact the rest of the neighboring cells constituting the NVU.

Considering globally all the mentioned data about different alterations affecting the main NVU integrators, there are enough evidences, from multiple approaches, to suggest the existence of a neurovascular component in the onset of AD **(figure 15)**.

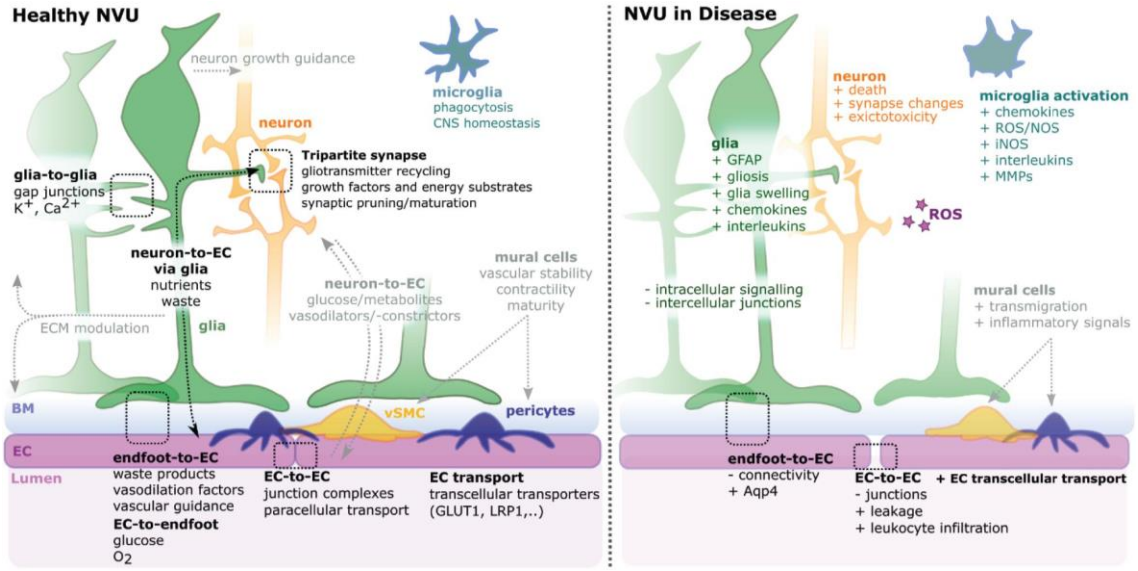

Figure 15: Schematic of the neurovascular unit (NVU) in health and disease (from (Kugler, Greenwood and MacDonald, 2021)). The NVU is a hetero-cellular complex formed by glia, neurons, vSMCs, pericytes, microglia, and blood vessels, which form the blood-brain barrier (BBB). Glial cells (green) impact neurons (orange), endothelial cells (ECs) (magenta), and each other. For NVU functionality, various direct (glia-to-glia, tripartite synapse, endfeet-to-EC, EC-to-endfeet) and indirect (neuron-to-EC via glia, neuron-to-EC via mural cells, microglia) pathways need to be considered. Upon disease multi-level changes are observed, including altered cell shapes, function, and interactions. NVU component changes include gliosis, neuron death, EC-connectivity changes, mural cell transmigration, and microglia activation.

3.3. Molecular communication between the integrators of the NVU

All the integrators constituting the complex structure of the NVU communicate between them through the secretion of molecular factors known as angioneurins. Angioneurins are described as signalling molecules that are able to influence simultaneously both vascular and neural network, either in the central or the peripheral nervous system, during development and also in adulthood (Zacchigna, Lambrechts and Carmeliet, 2008).

There are two requirements that these signalling molecules must accomplish to be considered as angioneurins. First, both vascular and neuronal structures express appropriate functional receptors for the factors. Second, the molecules must act as proliferating, maintaining or survival factors on neurons and vascular cells. Thereby, on one hand, angioneurins usually regulate angiogenesis, vascular perfusion and BBB integrity maintenance, and on the other hand they act as neurotrophic or neuroprotective factors also involved in synaptic plasticity (Zacchigna, Lambrechts and Carmeliet, 2008).

It has been reported that vascular and neural systems influence each other simultaneously through angioneurins communication during development (Adams and Eichmann, 2010). However, angioneurins also play crucial roles in adult tissue as maintenance or survival factors in physiology and pathology, so it means that they are important elements for CNS health and disease (Kunze and Marti, 2019).

Angioneurins can be classified into three main groups according to the definition above (Kunze and Marti, 2019). The first one includes factors, such as brain-derived neurotrophic factor (BDNF) that in the beginning were identified as neurotrophins and later on their angiogenic potential was discovered. The second group encompasses factors that were originally described attending to their angiogenic potential and then they were found to present neuronal activity. The most remarkable example is vascular endothelial growth factor (VEGF) as it regulates vessel growth in healthy and diseased tissues and also affects numerous neuronal and glial cell types. Finally, the third group contains molecules like the erythropoietin, which were first identified through their pleiotropic effects on different cell types and then were described as well by their neurotrophic and angiogenic effects.

3.3.1. Neurotrophins: BDNF

Neurotrophins (NTs) are growth factors that are important mediators in the development and survival of neurons from both central and peripheral nervous system (Thoenen, 1995). Neurotrophins signal via tropomyosin-related kinase (Trk) receptors and with low affinity through the pan-neurotrophin receptor $p75^{NTR}$. Nerve growth factor (NGF) is the associated ligand for Trk type A (TrkA), brain-derived neurotrophic factor (BDNF) for Trk type B (TrkB), and neurotrophin-3 (NT-3) for Trk type C (TrkC). NT-3 also binds TrkA and TrkB as a heterologous ligand. All neurotrophins bind p75, which regulates ligand affinity and Trk signals (Zaccaro *et al.*, 2001).

In the adult brain, BDNF is the predominant member of the neurotrophins family (Sasi *et al.*, 2017). BDNF synthesis begins with its gene transcription. The obtained mRNAs are processed by the endoplasmic reticulum into preproBDNF. Later, several enzymes cleave preproBDNF into proBDNF and BDNF. Both synthesis and secretion are proportional to neuronal activity (Greenberg *et al.*, 2009).

BDNF and its receptor TrkB are extensively distributed through numerous brain regions. The BDNF/TrkB pathway activity and also its dysfunction are related with several neurodegenerative diseases (Jin, 2020). BDNF/TrkB signaling **(figure 16)** contributes to neuronal survival, differentiation, growth and plasticity via activation of several downstream cascades. Once BDNF binds to TrkB, the receptor homodimerizes and triggers the activation of adaptor proteins. These activated adaptor proteins lead to the activation of phosphoinositide 3-kinases (PI3K)-AKT (PI3K-AKT), Ras-mitogen-activated protein kinase (Ras-MAPK), and phospholipase C1 (PLC-1)-protein kinase C (PKC) signaling pathways (Huang and Reichardt, 2003).

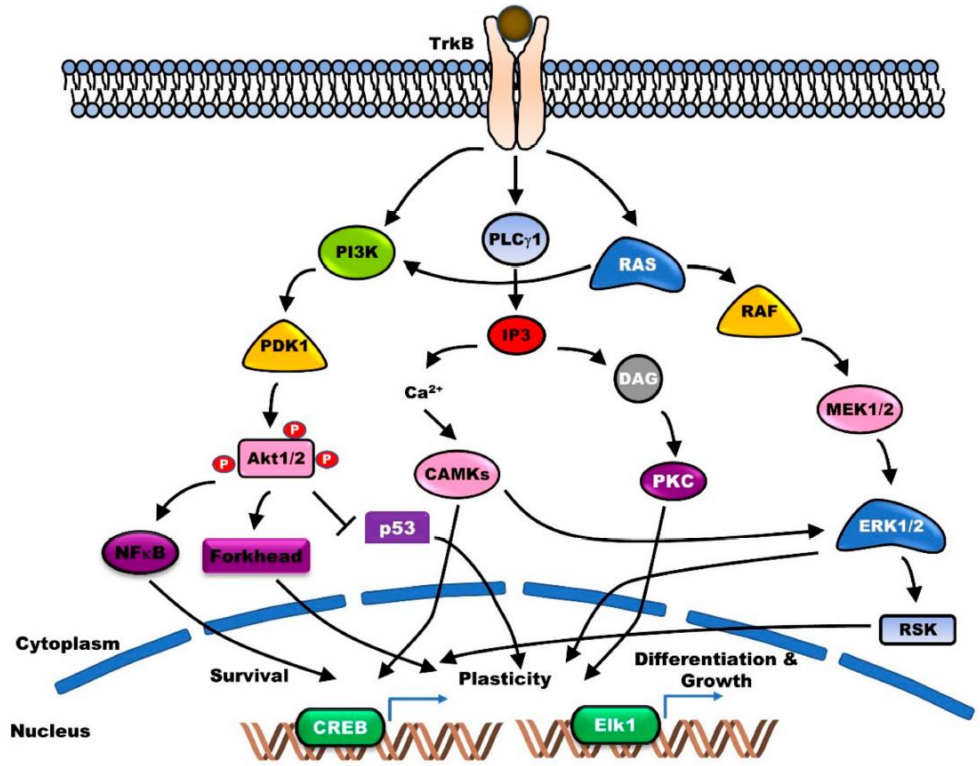

Figure 16: Schematic diagram of BDNF/TrkB signalling transduction pathways (from (Jin, 2020)). Binding of BDNF to TrkB triggers homodimerization and leads to the recruitment of adaptor proteins that interact with specific phosphotyrosine residues in the cytoplasmic domains of TrkB receptors. These interactions lead to the activation of signaling pathways, such as the Ras, phosphatidylinositol-3-kinase (PI3k), and phospholipase C (PLC)-*γ* pathways, and ultimately result in activation of gene expression, neuronal survival, and neurites outgrowth.

There is also a mutual and bidirectional link between the BDNF/TrkB signalling pathway and the glutamatergic system that plays an important role in neuroplasticity (Messaoudi *et al.*, 2002). In one hand, glutamate stimulates BDNF production. On the other hand, BDNF regulates neuronal glutamate sensitivity, calcium homeostasis and plasticity. BDNF can modify glutamate signaling indirectly by inducing the production of antioxidant enzymes, anti-apoptotic Bcl-2 family members and energy-regulating proteins. Moreover, BDNF can also alter glutamate signal transmission directly via modifying the expression of glutamate receptor subunits and calcium-regulating proteins (Mattson, 2008). As it was reported, BDNF up-regulates the protein levels of AMPA receptor subunits (GluA1, GluA2 and GluA3) in hippocampal neurons. Besides, BDNF promotes synaptic delivery of homomeric GluA1 AMPA receptors in cultured organotypic slices by a mechanism independent of NMDA receptor activation (Caldeira *et al.*, 2007).

Neurons are commonly considered the main cellular source of BDNF in the brain. This is due to the evidences that show that changes in neuronal activity translate into parallel changes in brain BDNF levels and that a decrease in BDNF levels is involved in neurodegeneration (Monnier *et al.*, 2017). However, brain BDNF is also obtained from other cell types.

Within the neurovascular unit, astrocytes are also another important source of BDNF (Miyamoto *et al.*, 2015). Astrocytes release BDNF through exocytosis and thus regulate neighboring neurons function as well as support them (Parpura and Zorec, 2010; Quesseveur *et al.*, 2013). Astrocytes restrict BDNF availability at neuron-astrocyte contacts. ProBDNF, secreted by neurons to extracellular medium after theta-burst stimulation, is fastly internalized into perineuronal astrocytes via endocytosis by the $p75^{NTR}$ receptor. After internalization, proBDNF can undergo a recycling process that provides astrocytes with the ability to re-secrete this neurotrophin upon their stimulation (Parpura and Zorec, 2010).

Cerebral endothelial cells also express and secrete BDNF as it was reported using *in vitro* culture twenty years ago (Leventhal *et al.*, 1999; Kallmann *et al.*, 2002). In fact, cerebral endothelial cells seem to produce BDNF at fifty time's higher rate than cortical neurons (Guo *et al.*, 2008). There are studies that reported a strong reduction in cortical and hippocampal BDNF levels after *in situ* removal of cerebral endothelial cells (Monnier *et al.*, 2017). As well, changes in cerebrovascular BDNF imply collateral changes in brain BDNF levels. Other assay demonstrated that cerebral endothelial cells-derived BDNF protects neurons from a wide range of neuronal insults including oxidative damage, oxygen and glucose deprivation, hypoxia, endoplasmic reticulum stress and amyloid toxicity (Guo *et al.*, 2008). BDNF/TrkB activity also promotes neuronal survival through angiogenesis stimulation. By means of PI3K-AKT signalling pathway, TrkB is involved in enhancing endothelial survival thus repairing the neurovasculature (Kermani and Hempstead, 2007; Espinera *et al.*, 2013). Altogether indicates that a large part of the BDNF found in the brain corresponds to which is produced by the brain microvessels. Therefore, this provides a paradigm shift in the cellular source of brain BDNF.

3.3.2. Neurotrophins in neurodegeneration

According to the contribution of neurotrophins on the innervation of target tissues and promoting the survival of several neuronal populations during the nervous system development, in case they become deficient it may induce dramatic neurodevelopmental defects (Zacchigna, Lambrechts and Carmeliet, 2008). Moreover as mentioned above, most of the neurotrophic factors, such as NGF, BDNF or NT3, also present angiogenic activity and are involved in postnatal neurodegeneration. For instance, NGF activity blockade induces progressive neuronal loss and results in cortical atrophy, amyloid deposits and memory and sensory deficits (Capsoni *et al.*, 2000). Besides, impairments affecting the neurotrophin receptors trkB and/or trkC also cause neurodegeneration. It was reported that their alteration induced signaling failure, leading to a phenotype that recapitulated two Parkinson's disease hallmarks in neurons from the substantia nigra (Bohlen und Halbach, Minichiello and

Unsicker, 2005). Furthermore, affectations on the BDNF-TrkB pathway have been reported to induce neuronal cell death, synaptic plasticity alterations and memory deficits observed in AD (von Bohlen und Halbach and von Bohlen und Halbach, 2018).

3.3.2.1. BDNF and Alzheimer's disease

BDNF plays critical roles in neuronal survival and synaptic plasticity (Lynch *et al.*, 2008). BDNF is involved within the natural ageing process as it was reported a negative correlation between serum BDNF levels and age in healthy aged humans (Ziegenhorn *et al.*, 2007). Moreover, the lack BDNF has also been implicated in the pathophysiology of different kind of dementia, such as AD, vascular dementia, frontotemporal dementia and Lewy body dementia (Ventriglia *et al.*, 2013).

Multiple evidences support the relationship between BDNF and AD. BDNF, as mentioned above, causes the activation of the Ras-MAPK signaling cascade leading to the phosphorylation of cAMP response element-binding protein (CREB). Although this pathway exerts a well-known trophic and protective role on neuronal cells both *in vitro* and *in vivo*, it has become clear that the Ras-MAPK pathway may also promote neurodegeneration or impede the action of neurotrophic factors when activated by noxious stimuli as occurs in AD (Colucci-D'Amato, Perrone-Capano and Di Porzio, 2003). Particularly, it was reported that APP and/or $A\beta_{1-42}$ oligomer induced the activation of Ras-MAPK and glycogen synthase kinase-3β (GSK3β) signaling, that, in turn, caused hyperphosphorylation of tau and APP. The implication of these molecular events in the pathogenesis AD was corroborated by the finding that activation of Ras-MAPK and GSK3β correlated with Aβ levels in the brain of AD patients (Nizzari *et al.*, 2012; Kirouac *et al.*, 2017). GSK3β mediates the inactivation of CREB, so Aβ activation of GSK3β decreases CREB activity (DaRocha-Souto *et al.*, 2012) therefore impairing BDNF expression (Tong *et al.*, 2001; DaRocha-Souto *et al.*, 2012). Moreover, it has been suggested that Aβ, due to axonal transport impairment, induces a reduction in BDNF signalling (Poon *et al.*, 2011). Regarding TrkB receptor, its deletion boosts and aggravates the phenotype associated to 5xFAD mouse model of AD, whilst TrkB agonists improve it (De Pins *et al.*, 2019). The dysregulation of associated downstream signalling pathways is able to modulate the amounts of essential synaptic proteins like PSD95 (Yoshii and Constantine-Paton, 2014) which at the same time are altered in AD models (Almeida *et al.*, 2005; Shao *et al.*, 2011) and also in AD patients (Gylys *et al.*, 2004). Furthermore, AD patients present diminished serum, plasma and cerebrospinal fluid BDNF concentrations compared to controls (Gezen-Ak *et al.*, 2013). A remarkably reduction in proBDNF was described in parietal post-mortem samples from AD terminal patients (Peng *et al.*, 2005).

Altogether led to a raising interest in BDNF as a potential therapeutic agent for AD. Several studies suggested that therapeutically increasing BDNF levels in brain regions important for memory and cognition may lead to improved clinical outcomes of AD patients (Blurton-Jones *et al.*, 2009; Xiang *et al.*, 2019). For instance, BDNF was described to induce neuroprotection against Aβ peptide neurotoxicity both *in vitro* and *in vivo* (Arancibia *et al.*, 2008). This protection involved the activation of TrkB receptor since the effect was totally inhibited by a potent tyrosine kinase inhibitor. Other report showed that in amyloid-transgenic mice, BDNF gene delivery improved cell signalling, reversed synapse loss, partially normalized abnormal gene expression and restored learning and memory (Nagahara *et al.*, 2009). Moreover these authors also reported that BDNF also induced the recovery of neuronal atrophy and reduced the age-related cognitive impairment in aged primates.

3.4. Neurovascular unit *in vitro* models

To deeply study the roles of different cell types involved in the neurovascular unit and their interactions, many *in vitro* models have been established in last decades. One of the methodologies applied involves microfluidic systems. However, other approximations consisted on transferring conditioned cell mediums or co-culturing different cell lines, directly or using transwell systems.

3.4.1. Microfluidic systems

Traditionally, cells are cultured using flasks, petri dishes or microtiter plates with solutions that maintain the biosamples alive during a determined period of time. With conventional devices, cells are cultured often in static conditions thus the dynamic physiological conditions cannot be reproduced. Furthermore, usually the cells are in presence of undesired temperature and CO_2 gradients (Coluccio *et al.*, 2019). To overcome these influences on cells functionalities, the microfluidic devices were created. Microfluidic technology tries to reproduce the environment as the cells are in nature. This is particularly relevant when culturing endothelial cells as physiologically they are in a circulatory environment.

Microfluidic-based cell cultures present several interesting characteristics like continuous nutrient supply, waste removal, liquid handling systems, flexibility of schedules and high automation capability.

There are different types of microfluidic devices available depending on the platform configuration. Moreover they can be designed in 2D or 3D. One of these 2D multi-compartment microfluidic platforms described in literature was proposed for neuron-glia co-culture (Park *et al.*, 2012). It consisted **(figure 17)** on one circular soma compartment and six square shaped satellite axon/glia compartments that were attached through radially positioned

array of microchannels. In this design, the compartments were open wells instead of channel-type close ones. This feature represented a considerable advantage for accurately controlling cell density. Another configuration, also designed for interaction between axons and glia, used a circular microfluidic platform to isolate soma from axons (Hosmane *et al.*, 2010). Two more devices **(figure 18),** one vertically-layered **(figure 18a)** and other constituted by four chambers separated by valve membranes **(figure 18b)**, were developed to overcome the limitations that the previously existing models presented to study the interactions within a neuron-glia co-culture (Shi *et al.*, 2013).

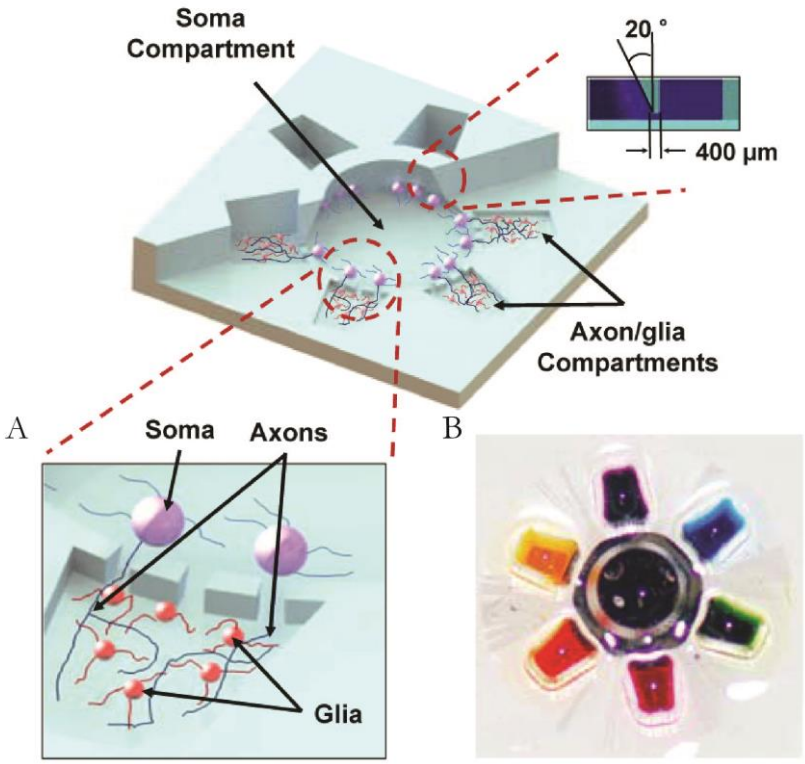

Figure 17: Scheme of the multi-compartment neuron-glia co-culture microsystem (from Multi-Compartment Neuron-Glia Co-culture Platform for Localized CNS Axon-glia Interaction Study. (Park *et al.*, 2012). **(A)** Diagram illustrating the isolation of axons from neuronal soma for localized axon-glia interaction studies. **(B)** Image of neuron-glia co-culture platform replenished with seven different color dyes for visualization.

Nevertheless, microfluidic culture chambers also have some drawbacks, although the advantages aforementioned compared with static platforms. Microfluidic devices mainly rely on laminar flow where diffusion is the mixing mechanism. Diffusion is a very slow process that represents a large restriction for applications where chemical gradients are strongly unwanted. Moreover, adaptation of biological protocols to microsystems is complicated due to scaling. In terms of arrangement, microfluidic systems involve complex devices to be handled and managed. Thereby the instruments needed to run them, or the integrated sensors required, represent a great cost. Furthermore, specialized staff is required to run the equipment so; in some cases it also affects the throughput of the produced data. Altogether imply that

comparing data obtained from microsystems with results from macroscopic experiments is a tricky exercise (Coluccio *et al.*, 2019).

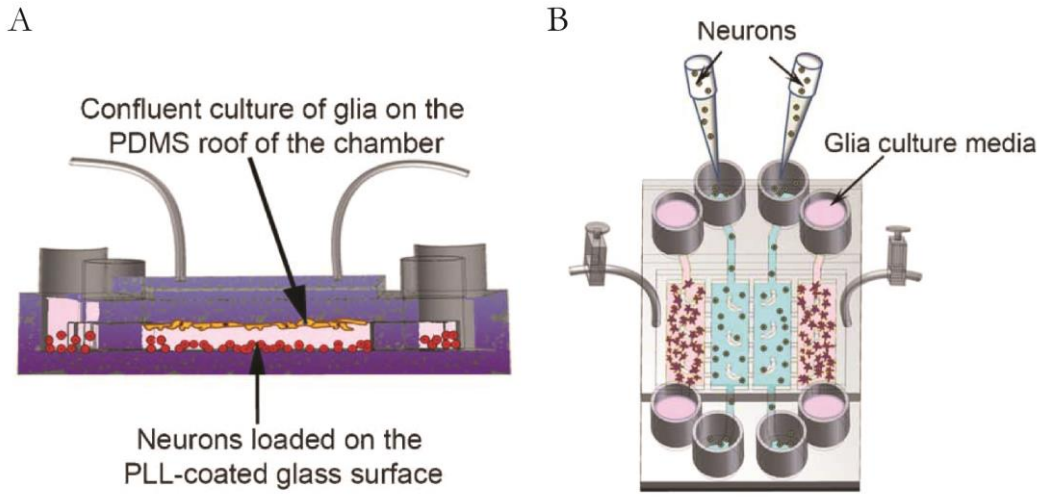

Figure 18: Illustrative diagram of two types of microfluidic devices (adapted from Glia co-culture with neurons in microfluidic platforms promote the formation and stabilization of synaptic contacts. (Shi *et al.*, 2013). **(A)** Vertically-layered microfluidic platform. A cross-section through a device is depicted with confluent glia (orange spheres) culture attached on the poly(dimethylsiloxane) roof of a cell culture chamber. Neurons (red spheres) suspended in neuron media are loaded into the devices and allowed to attach to the PLL-coated glass surfaces of the cell chambers. **(B)** Four chamber microfluidic device. The four cell chambers were separated by three valve-enabled poly(dimethylsiloxane) barriers. To facilitate cell loading, the valve barriers were activated to isolate the four cell chambers. Glia (purple spheres) were loaded into the glial chambers and incubated until they reached confluence. Then, neurons (grey spheres) were loaded into the neuronal chambers. After neurons attached, the chambers were connected by deactivating the valve barriers.

3.4.2. Conditioned mediums

Other approximation to study the interactions between the cells within the neurovascular unit is analyzing the molecules that constitute the secretome of each cell type. The cell secretome alludes to the collection of proteins released through different mechanisms such as classical secretion, non-classical secretory pathway and release by exosomes. These secreted proteins comprise numerous growth factors, enzymes, cytokines, hormones and other soluble mediators. They play a crucial role regulating cell-to-cell and cell-to-extracellular matrix interactions. Consequently, they are essential in the processes of cell growth, differentiation, invasion and angiogenesis (Dowling and Clynes, 2011).

Different combinations developing this methodology are described in literature. One of these reports used two types of glia-conditioned medium to study the effects that they could induce on microvascular endothelial cells **(figure 19)** (Brown *et al.*, 2003). Actually, the goal was to determine the impact of culturing with C6 glioma- or astrocyte-conditioned medium on microvascular endothelial cell permeability and tight-junction protein expression in normoxic and in hypoxic environment. Furthermore, this approximation was useful to analyze the glia-secreted factors that might be involved and their potential mechanisms of action.

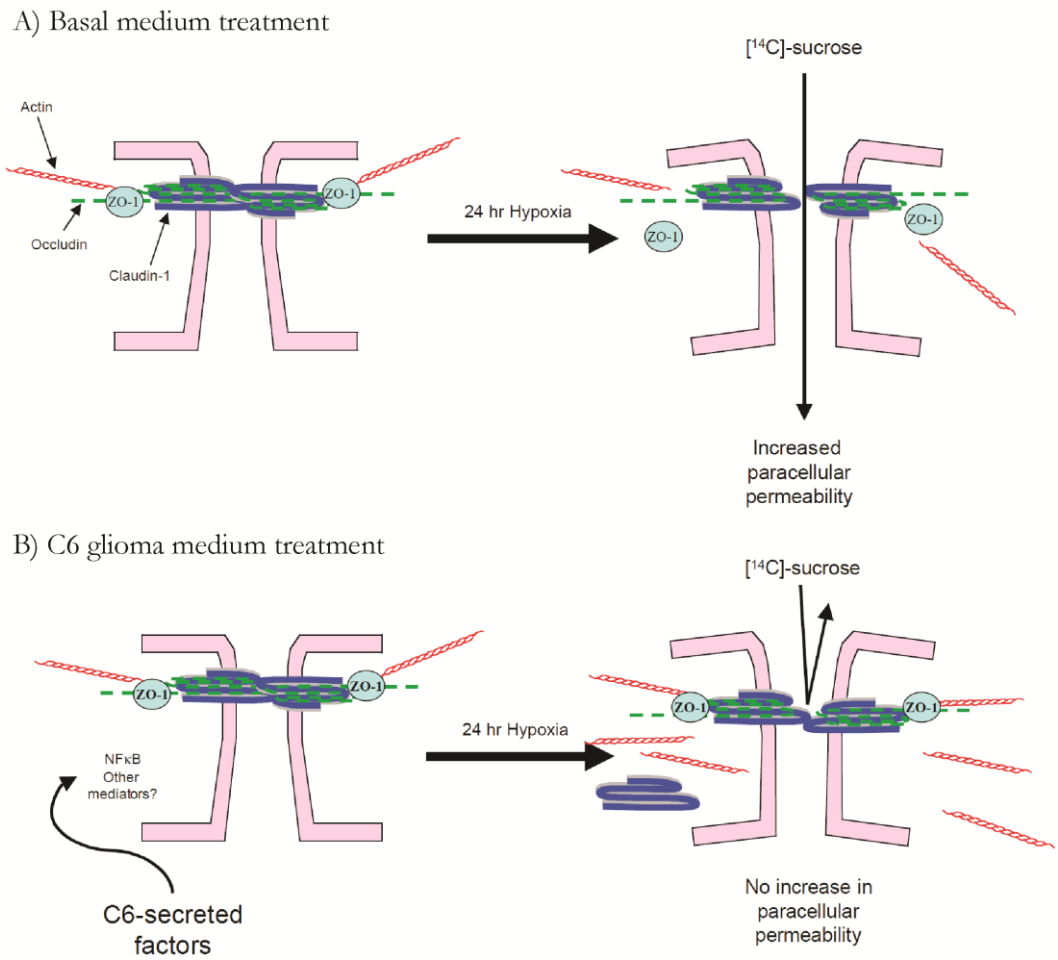

Figure 19: Scheme of the potential model for C6 glioma-conditioned medium protection to hypoxia-induced alterations in paracellular permeability (adapted from (Brown *et al.*, 2003). **(A)** Cells grown in basal medium and subjected to a 24-hour hypoxic stress undergo a breakdown of the TJ, with a resulting increase in paracellular permeability as measured by [^{14}C]-sucrose flux. **(B)** With C6 glioma-conditioned medium co-culture secreted factors trigger the activation of signal transduction mechanisms, linked to NFκB or other as yet unidentified pathways. This treatment allows for an adaptive response in the microvessels endothelial cells when they are exposed to 24 hours hypoxic stress and prevents the increase in paracellular permeability seen under basal condition.

Proteins released into conditioned medium by cultured cells are a rich source for biomarker research. Biomarkers are molecules used for screening the presence of disease or for monitoring therapeutic effectiveness. Over the last years, the analysis of conditioned medium under well-defined experimental conditions has been fundamental in the investigations for biomarker discovery. This technique represents a useful and less invasive alternative to direct clinical specimen analysis (Dowling and Clynes, 2011).

Analysis of conditioned medium presents many advantages apart from the non-invasive method of sample collection. There are numerous cell lines available representing several stages of different diseases that can be used in this approximation (Gunawardana *et al.*, 2009). Moreover, the identification and quantification of these secreted proteins are relatively simple without the drawbacks that are associated with high-abundance proteins or the dynamic range related with many biofluids.

However, this strategy also includes some limitations. The microenvironment where a cell type is developed and maintained is crucial. At the molecular level, an *in vitro* system is different from the *in vivo* situation. This can be reflected in the secretome and thereby it is tricky when directly comparing proteins expressed in the cell line culture conditioned medium and in the biofluid. Furthermore, disease-affected cells can trigger the release of secondary biomarkers in neighboring cell types. These secondary biomarkers are also a source of candidate molecules that is as well missing when analyzing the conditioned medium from cell cultures.

To overcome these limitations, advanced systems are described in the literature. Co-cultures involving two or more cell types to generate conditioned medium is an alternative approximation that may reflect the microenvironment to a greater extent.

3.4.3. Cell lines co-culture

Among the *in vitro* models described, co-cultures are the methodology that better mimics the *in vivo* anatomical conditions. They must involve at least two cell types to procure the spatiotemporal context and to reach a relevant level of similarity of the *in vivo* tissue. Several reports have demonstrated that co-culture systems react in a more realistic way and are more predictive of the *in vivo* response (U. *et al.*, 2017).

Different cell lines are used in co-culture systems and, particularly, they are fundamental in the development of human brain *in vitro* models. This approximation allows the establishment of biologically significant cell-to-cell interactions that sum up the tissue microenvironment. As well, these human brain *in vitro* models mimic in the best way the physiological conditions of this organ.

There are many reports in literature that take profit of this methodology. However, specific configurations are developed depending on the precise adaptations that are required attending to experimental conditions.

One of these reports adapted the methodology to set up a co-culture model constituted by neuronal cells (human neuroblastoma-SH-SY5Y cell line) and astrocytes (human astrocytoma-D384 cell line) in a transwell system (U. *et al.*, 2017). In the transwell system, the cell types are separated by a semi-permeable membrane. In this human neuron-astrocyte co-culture system, neuronal SH-SY5Y cells were seeded in the lower compartment of a 6-well transwell system and astrocytic D384 cells were cultured in the insert **(figure 20)**. The study consisted on evaluating if this co-culture system represents a more predictable cell model, compared to mono-culture, for analysing the cytotoxic impact on human CNS after chemical and new product exposure.

Other methodological adaptation described in literature established the co-culture model using glass bottom microwells and coverslips (Park, Zhang and Gibson, 2001). Precisely, the system was constituted by hippocampal neurons plated on poly-d-lysine coated MatTek glass bottom microwells and astrocytes or microglia from forebrains plated on poly-d-lysine coated coverslips. Then the coverslips were translocated to the edge of the MatTek dish. This model was developed to test neuronal-glia interactions and responses to *in vitro* thiamine deficiency. The main goal was to determine the role of these cell types in mechanisms underlying selective neurodegeneration.

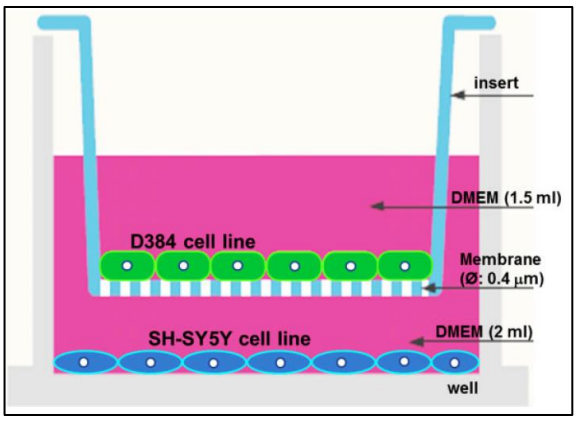

Figure 20: Schematic diagram of the developed co-culture system (from (U. *et al.*, 2017). The *in vitro* model consists on human neuroblastoma-SH-SY5Y cells seeded in the lower compartment of a 6-well transwell system and human astrocytoma-D384 cells cultured within the insert.

Although most of the co-culture models reported in literature are mainly limited to two cell types, there are also a few that have developed triple cell co-culture systems. These more complex *in vitro* systems may offer a more appropriate view of the neurovascular unit for further investigation of cerebral diseases and drug screening.

One of these triple cell co-culture model involved immortalized vascular endothelial cells along with primary astrocytic and neuronal cultures (Schiera *et al.*, 2005). However, immortalized cells are not much closer to cell *in vivo* phenotype than primary cells. To overcome this, other model was established using primary rat cultures of brain microvascular endothelial cells, astrocytes and pericytes (Nakagawa *et al.*, 2009). Nevertheless this new model did not include neurons.

Consequently, other approximation was established comprising the main three types of primary cells of the neurovascular unit. It involved primary cultures of neurons, brain microvascular endothelial cells and astrocytes (Xue *et al.*, 2013), thus exhibiting the basic structure, function and cell-to-tell interaction of the NVU. It was developed employing a transwell insert to distribute the cell types within the system **(figure 21)**. Neurons were seeded in the bottom of the well. Astrocytes were seeded in the outer side of the insert membrane and placed in the matching well. Brain microvascular endothelial cells were seeded in the inner side of the insert membrane. From the results obtained with this model the authors concluded that this system exhibited a better BBB function and significantly increased expression of ZO-1 and P-

glycoprotein compared with brain microvascular endothelial cells only or co-culture with astrocytes or neurons. Therefore, they considered that this model offered a more proper *in vitro* configuration of the NVU that could be used for further investigation of cerebral diseases and drug screening (Xue *et al.*, 2013).

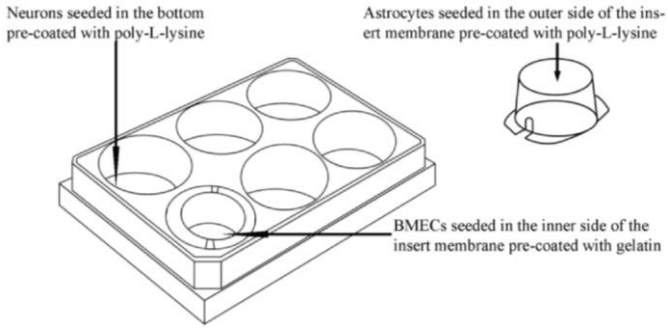

Figure 21: Schematic drawing of the triple cell co-culture model (from (Xue et al., 2013)). The three cell types are settled using a transwell system.

Other report also took advantage of the transwell system to create a BBB model within the NVU context where to study changes in permeability post oxygen-glucose deprivation and for using in *in vitro* pharmacology (Stone, England and O'Sullivan, 2019). That model only used primary human cells and included four of the key cells of the BBB (astrocytes, pericytes, brain microvascular endothelial cells (HBMECs) and neurons) in different combinations **(figure 22)**. From their obtained data they described the relevant role that neurons play in response to ischaemia, particularly how they contribute to BBB maintenance and breakdown.

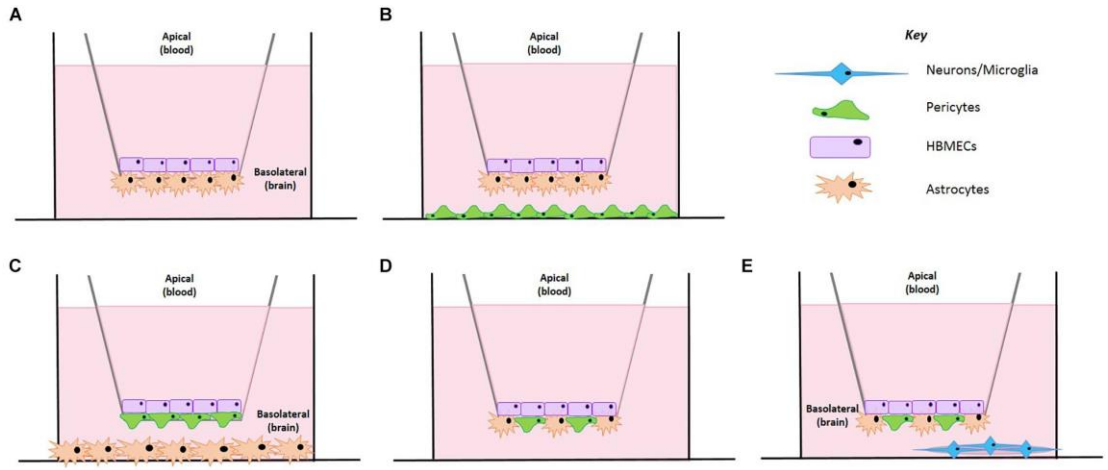

Figure 22: Schematic representation of the BBB model development (from (Stone, England and O'Sullivan, 2019)). **(A)** A co-culture cell model containing brain microvascular endothelial cells (HBMECs) and astrocytes. **(B)** HBMECs seeded on the apical side, astrocytes seeded on the underside of the insert and pericytes seeded on the plate bottom. **(C)** HBMECs seeded on the apical side of the insert, pericytes seeded on the underside of the insert and astrocytes seeded on the plate bottom. **(D)** HBMECs seeded on the apical side of the insert with mixed culture of astrocytes and pericytes on the underside of the insert. **(E)** HBMECs seeded on the apical side of the insert with mixed culture of astrocytes and pericytes on the underside of the insert and neurons seeded on a poly-L-lysine coated coverslip on the plate bottom.

Moreover, these authors also present a comparative table regarding different approaches to configure *in vitro* models of the BBB **(table 1)** and recapitulating their features, advantaged and disadvantages (Stone, England and O'Sullivan, 2019).

Regarding the multiple methodological adaptations, co-culture systems highlight as a useful tool to study the neurovascular unit. In terms of technical requirements, co-culture devices are easier to handle than microfluidic approximations. Besides, they do not require peripheral devices or integrated sensors like microfluidic systems, so co-cultures are a cheaper alternative. On the other hand, comparing with conditioned medium approach, co-cultures represent better the integrity of cerebral function as they reflect more physiologically the intercellular communications between the cell types.

Table 1: Different models of the blood brain barrier: their features, advantages, and disadvantages (from (Stone, England and O'Sullivan, 2019)).

Model type	Typical components	Advantages	Limitations	Representative of BBB phenotype	References
Single-cell transwell systems (non-co-culture)	A monolayer of HBMECs cultured in the apical compartment of the transwell insert.	Very easy to set up. Minimal cost. Low labor intensity. Useful if wanting to study endothelial cells alone.	TEER is typically low.	Cobblestone appearance of HBMECs, barrier formation. Little information on the impact of additional cell types.	Borges et al., 1994; Hartz et al., 2010
Co-culture /multicellular transwell systems	HBMECs cultured on the apical side of the transwell insert and astrocytes and/or pericytes cultured on the underside of the transwell insert.	Time and cost effective. Higher TEER. Greater barrier stability.	Some models are not fully in contact.	Closer representation of the BBB with the addition of important cell types. Able to study interactions between cell types and how they influence BBB phenotype.	Hind, 2014; Wang et al., 2015; Appelt-Menzel et al., 2017
Spheroid	3D organization of cells typically using matrigel. Typically consists of HBMECs and astrocytes and/or pericytes with some models containing neuronal cell types.	3D Cell model. No scaffold. Reduced de-differentiation.	Cannot measure permeability with this model. Expensive and greater skill required.	Microvessels wrap around endothelial cells and provide structural support. Helps to induce tight junction proteins. Closely represents the *in vivo* set up with cells in direct contact with each other. Applications include: cancer drug and neurotoxicity screening.	Cho et al., 2017; Nzou et al., 2018
Microfluidic systems/3D chip-style models	3D organization of cells with the added benefit of a "flow" system to mimic cerebral blood flow. Typically consists of HBMECs and astrocytes and/or pericytes with some models containing neuronal cell types.	Advantage of mimicking sheer stress which is essential for HBMECs optimum phenotype.	Difficult to set up and maintain adequate flow unless linked to a computer system.	Useful to assess the impact of blood flow on cell development and optimum phenotype. Also useful in studying cell migration and metastatic progression.	Yeon et al., 2012; Wang et al., 2017

HBMECs = human brain microvascular endothelial cells, TGFβ = transforming growth factor beta, TEER = transepithelial resistance, BBB = blood brain barrier.

Specifically considering transwell systems, they present all the aforementioned advantages as co-cultures without transwell insert and furthermore, they enable to create a system with two different compartments. This implies that cells can be maintained in an environment very similar to the in vivo and consequently multiple experiments may be performed. Moreover, as the insert remains suspended within the platewell, the cells co-cultured in the down chamber are perfectly preserved.

4. The two-hit hypothesis of AD

Over the past two decades, the so-called amyloid hypothesis dominated the field of AD research (Scheffer *et al.*, 2021). As previously commented, this hypothesis postulates that extracellular Aβ deposition initiates neurodegenerative processes, such as inflammation and

NFT formation, leading to cognitive impairment (Hardy and Higgins, 1992; Makin, 2018). Accordingly, it was initially believed that eliminating the Aβ plaques through targeting Aβ would enhance cognition. This was supported by encouraging results in transgenic mice overexpressing mutant human APP, where immunization with Aβ prevented plaque development and neurite damage (Schenk *et al.*, 1999). Moreover, other report showed that targeting Aβ peptide generation reduced plaques and NFT (Baik *et al.*, 2014). Further evidence in favour of this amyloid hypothesis was described when reporting that in Down's Syndrome an additional copy of Chromosome 21 produces an extra APP gene hence causing the individual to display AD-like neuropathology (Selkoe and Hardy, 2016).

As consequence, during many years, many drugs developed to treat AD have been designed on the assumption that Aβ drives the disease. However, this approach has not yielded therapeutics that cure the disease or produce significant improvements in long-term cognition through removal of plaques and Aβ oligomers. In this regard, although proponents of the amyloid hypothesis feel that anti-Aβ therapies may have been administered too late in the disease process, and that this hypothesis remains valid, other researchers propose alternate mechanisms that drive AD or act in conjunction with amyloid to promote neurodegeneration (Steinman, Sun and Feng, 2021). Nevertheless, understanding the myriad of factors altered in AD is needed to moving beyond traditional interpretation of the amyloid hypothesis.

There are various descriptive hypotheses regarding the causes of sporadic AD, including the aforementioned tau hypothesis (considering that phosphorylated tau induces cognitive deficits through decreasing the number of synapses and triggering cell death (Di *et al.*, 2016), the mitochondrial cascade hypothesis (genetically and environmentally determined decline in mitochondrial function triggers AD pathology (Swerdlow, Burns and Khan, 2014), the neuroangiogenesis hypothesis (a decline in growth factors and angiogenic cytokines leads to a reduction in vessel density and cognition (Ambrose, 2012) and the vascular hypothesis (reduced blood flow may increase amyloid pathology through activation of β/γ-secretases that induces APP cleavage (Cai *et al.*, 2017).

Reviewing the different AD hypothesis, it is difficult to determine the relevancy of each one considering that AD develops according to genetic, sex and environmental factors that differ for each subject (Frenkel, 2020). Therefore, due to the multifactorial nature of this disease, a hypothesis that considers multiple agents involved in the development of AD would better approach to the real scenario.

In line with this idea the two-hit vascular hypothesis summarizes this outlook **(figure 23)**. Briefly, it suggests that vascular damage (hit 1) can trigger a cascade of events leading to Aβ

accumulation in the brain, which precipitates the Aβ-dependent pathway of neurodegeneration (hit 2).

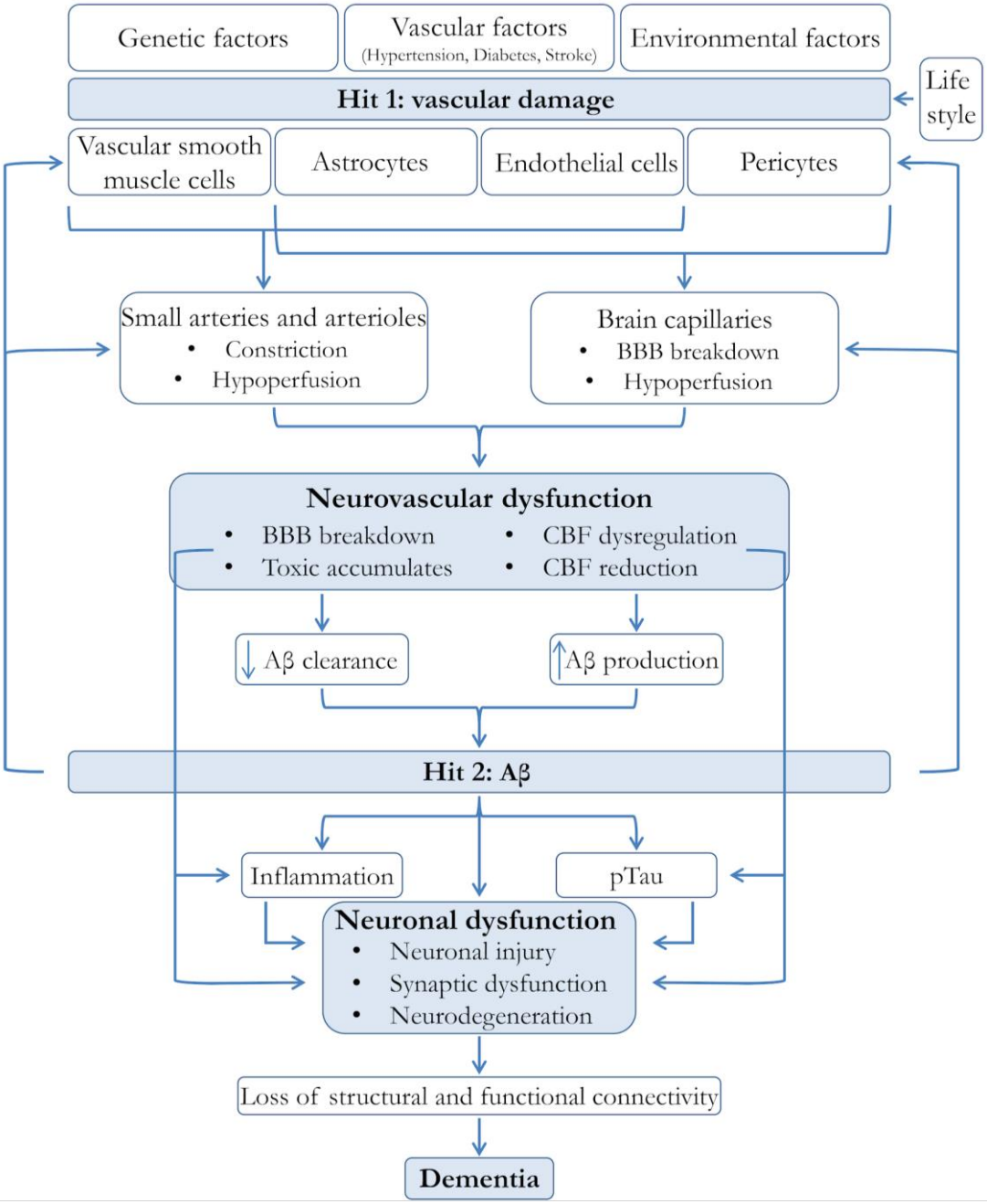

Figure 23: Two-hit vascular hypothesis scheme (adapted from (Kisler *et al.*, 2017)). Genetic, vascular and environmental factors contribute to small arteries, arterioles and brain capillaries damage and lead to neurovascular dysfunction by Aβ-independent (hit 1) and/or Aβ-dependent (hit 2) pathways. Lifestyle can modify the effects of these hits. Both pathways can independently or synergistically take to neuronal dysfunction and thereby to dementia.

More detailed, different genetic risk factors for developing AD, vascular factors such as hypertension or diabetes mellitus, and environmental factor like pollution lead to neurovascular dysfunction and impairment to small arteries, arterioles and brain capillaries via Aβ-independent (hit 1) and/or Aβ-dependent (hit 2) pathway. Both pathways interrelate and merge on blood vessels, and can independently or synergistically induce neuronal injury, synaptic

dysfunction and neurodegeneration contributing to dementia. Moreover, lifestyle can influence the effects of these hits as moderate exercise and diet have beneficial effects on cardiovascular and cerebrovascular system.

As previously reviewed, different integrators of the NVU are affected in AD. Summarily, vSMCs hypercontractility and degeneration leads to abnormal responses of small arteries and arterioles and dysregulation and reductions of CBF both, independently of Aβ or in Aβ-dependent manner. In the Aβ pathway, impairment to small arteries and arterioles are often related with amyloid angiopathy and disruption of the vessel wall with microhemorrhages. Regarding pericytes' degeneration, it takes to capillary dilation loss in response to neuronal simulation, hypoperfusion and BBB breakdown leading to the accumulation of blood-derived toxins and fluid in the perivascular spaces. Both, Aβ-independent, like ischemia or hypoxia, and Aβ-dependent mechanisms contribute to alterations in capillary circulation. Glial cell activation mediates the inflammatory response and release of vasoactive cytokines and chemokines, further compromising CBF regulation and BBB integrity. Endothelial impairment induces endothelial-dependent vasodilation loss and dysregulation and reductions of CBF. Afterwards, blood vessels damage can trigger a cascade of concatenating events leading to Aβ accumulation in brain (hit 1), which accelerates the Aβ-dependent pathway of neurodegeneration (hit 2). For instance, brain ischemic alterations (hit 1) induce an increase of Aβ production through enhancing the expression of enzymes mediating Aβ generation, while BBB dysfunction in Aβ clearance leads to Aβ retention in brain. Besides, CBF (hit 1) and increased Aβ (hit 2) can each independently or synergistically lead to tau phosphorylation and tau pathology in neurons, and worsen neuroinflammation. When mixed, they boost neuronal damage and injury (Kisler *et al.*, 2017).

IV. Aims

This doctoral thesis wants to increase our knowledge of the contribution of cerebral endothelium on the alteration of vascular and neuronal function in AD. Regarding the vascular alterations, we wanted to specifically focus on the SSAO/VAP-1, but also in the presence soluble forms of Aβ, to mimic an AD context. SSAO/VAP-1 was reported to be increased in plasma and cerebrovascular tissue from AD patients and to be involved in a crosstalk with Aβ. Moreover, the SSAO/VAP-1 is increased in several systemic vascular pathologies also considered among the aforementioned risk factors for AD. Therefore, we looked for determining whether, in AD-like conditions, endothelial SSAO/VAP-1 induces neuronal impairment within the neurovascular unit and if it is related with an alteration in angioneurins communication. Altogether is highly inspiring because identified angioneurins and/or the SSAO/VAP-1 may be considered likely therapeutic targets.

To achieve these aims, more specific objectives have been described:

1. To establish an *in vitro* co-culture model where to study the interactions between different neurovascular components.

2. To determine synaptic changes in mixed-culture cells co-cultured with WT or SSAO/VAP-1-expressing endothelial cells and in presence or absence of Aβ**.**

3. To assess whether SSAO/VAP-1 expression on endothelial cells alters their releasing levels of BDNF and the effect of Aβ on BDNF secretion from microvascular endothelial cells.

4. To determine if changes on endothelial release of BDNF affect synapses by modifications on synaptic structure such as spine number and morphology.

5. To study whether BDNF-related alteration in the communication between endothelial cells and neurons disturbs the expression of crucial synaptic proteins involved in glutamatergic neurotransmission.

V. Materials and methods

1 Cell cultures

1.1 Primary mouse cortical mixed neuron-glia culture

1.1.1 Reagents and mediums

Reagents used for cortical primary cultures. All the solutions were filtered prior to use.

- Solution 1: 50 ml Krebs-Ringer Buffer (120.98 mM NaCl, 4.83 mM KCl, 1.22 mM KH_2PO_4, 25.47 mM $NaHCO_3$ and 14.27 mM Glucose) pH 7.0 – 7.6 , with 0.3 % Bovine Serum Albumin (BSA; *Merck-Sigma*) and 0.03 % $MgSO_4$.

- Solution 2: 0.025 % Trypsin (*Merck-Sigma*) in 10 ml solution 1.

- Solution 3: 0.052 % Trypsin inhibitor (*Merck-Sigma*), 0.008 % DNase I (*Merck-Sigma*) and 0.04 % $MgSO_4$ in 10 ml solution 1.

- Solution 4: 8.4 ml solution 1 plus 1.6 ml solution 3.

- Solution 5: 0.03 % $MgSO_4$ and 0.0014 % $CaCl_2$ in 5 ml solution 1.

- Phosphate Buffered Saline (PBS 1X; *Merck-Sigma*): 136.89 mM NaCl, 2.68 mM KCl, 8.10 mM Na_2HPO_4 (anhydrous) and 1.47 mM KH_2PO_4; pH 7.4.

- sPBS: PBS 1X (*Merck-Sigma*) supplemented with 0.57 % Glucose, 10 000 u/ml Penicillin (*ThermoFisher Scientific*) and 0.01 g/ml Streptomycin (*ThermoFisher Scientific*).

- Poly-D-Lysine solution: 0.001 % poly-D-lysine in 0.1 M Sodium Borate Buffer pH 8.4.

Cell mediums used in mixed-cortical primary culture:

- BME 5 % HS/FBS: Basal Medium Eagle's (BME; *Merck-Sigma*) supplemented with 5 % Horse Serum (HS; *Thermo Fisher*), 5 % Fetal Bovine Serum (FBS; *Thermo Fisher*), 33.3 mM Glucose and 2 mM Glutamax (*Thermo Fisher*).

- BME 10 % HS: BME supplemented with 10 % Horse Serum (HS; *Thermo Fisher*), 33.3 mM Glucose and 2 mM Glutamax (*Thermo Fisher*).

- BME 5 % HS: BME supplemented with 5 % Horse Serum (HS; *Thermo Fisher*), 33.3 mM Glucose and 2 mM Glutamax (*Thermo Fisher*).

1.1.2 Dissection, tissue disaggregation and cell culture maintenance

Cells were extracted from E14.5-15.5 C57BL/6JRccHsd (*Envigo*) wild type (WT) mouse embryonic cortices. After brain extraction, cortex dissection was performed in cold sPBS. Isolated cortices were

transferred to a 50 ml tube containing solution 1. Then, solution 1 was removed via glass pipette before adding solution 2 containing trypsin. Solution 2 was incubated at 37 ºC within a H_2O bath for 10 minutes, shaking every 3 min, to allow enzymatic tissue disaggregation. After incubation, solution 4 was added to stop trypsin effect with trypsin inhibitor. Solution 4 also contains DNase I to degrade DNA from those cells that might be lysed by trypsin. Next, cells were centrifuged for 1min at 200 g. The pellet was resuspended in solution 3 and cells were mechanically disaggregated through a glass pipette and filtered through a 40 µm nylon mesh. Filtered cells were transferred into solution 5 and centrifuged for 5 min at 300 g. After removing supernatant, cells were resuspended in BME 5 % HS/FBS and a 20 µl aliquot was taken to be stained with 20 µl Trypan Blue to be counted in a Neubauer chamber.

Cells were seeded at 250 000 cel/cm^2 in culture plates (6-wells, 12-wells, 24-wells or 35-mm dishes) or on glass coverslips, both previously coated for 4 h with poly-D-Lysine solution. Cells were maintained in an incubator at 37 ºC with a humidified atmosphere with 5 % CO_2.

Culture maintenance implied several medium changes at different days *in vitro* (DiV) **(figure 24)** along the time until the end of the experiment. At 4 DiV, half of the medium was renewed with BME 5 % HS/FBS. At 7 DiV the entire medium was replaced by BME 10 % HS supplemented with 10 µM cytosine-β-arabinofuranoside (Ara-C; *Merck-Sigma*) to stop astrocyte proliferation. At 9 DiV half of the medium was renewed with BME 10 % HS. At 12 DiV half of the medium was superseded by BME 5 % HS. Since then, each 3 DiV half of the medium was renewed with BME 5% HS.

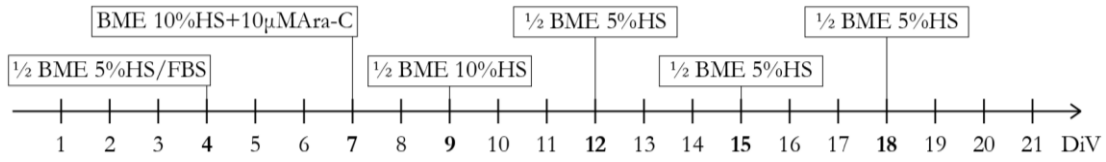

Figure 24: Mixed neuron-glia culture *in vitro* maintenance timeline. The different medium changes needed at each time point are indicated. DiV: days *in vitro*.

1.2 Human cerebral microvascular endothelial cells culture

1.2.1 Reagents and mediums

These were the reagents and the mediums used in maintaining, sub-culturing and storing the human cerebral microvascular endothelial cell line (hCMEC/D3):

- EBM-2 fully supplemented: Endothelial cell Basal Medium-2 (EBM-2; *Lonza*) enriched with: 5 % FBS (*Thermo Fisher*), 5 000 u/ml Penicillin (*Thermo Fisher*), 0.005 g/ml Streptomycin (*Thermo Fisher*), 1.4 µM Hydrocortisone (*Merck-Sigma*), 4 µg/ml Ascorbic Acid (*Merck-Sigma*), 1 % Chemically Defined Lipid Concentrate (*Thermo Fisher*), 10 mM HEPES (*Thermo Fisher*) and 1 ng/ml human Fibroblast Growth Factor-basic (bFGF; *Merck-Sigma*).

- EBM-2 partially supplemented. This medium was enriched as for the fully supplemented but without adding FBS neither Ascorbic acid nor bFGF.

- Freezing medium: EBM-2 fully supplemented medium further enriched with up to 20% FBS plus 10 % Dimethyl sulfoxide (DMSO).

- sPBS: PBS 1X (*Merck-Sigma*) supplemented with 0.57 % Glucose, 10 000 u/ml Penicillin (*Thermo Fisher*) and 0.01 g/ml Streptomycin (*Thermo Fisher*).

- Collagen type I solution: 150 µg/ml collagen type 1 from rat tail (*Corning*) in distilled H_2O.

- Fibronectin solution: 1% fibronectin (*Merck-Sigma*) in Hanks' Balanced Salt Solution (HBSS; *Thermo Fisher*).

1.2.2 Maintenance, sub-culturing, seeding and cell storage

The hCMEC/D3 cell line was obtained from Dr. Couraud's laboratory in Paris, France (Weksler *et al.*, 2005; Weksler, Romero and Couraud, 2013). These cells by default are considered as wild type (WT) ones. The hCMEC/D3 cell line expressing human Semicarbazide-Sensitive Amine Oxidase, also known as Vascular Adhesion Protein-1 (hSSAO/VAP-1), was generated as described previously (Sun *et al.*, 2015). hSSAO/VAP-1 cell line presents activity levels comparable to those observed in human brain tissue (Unzeta *et al.*, 2007) while WT hCMEC/D3 cells do not express SSAO/VAP-1 (Sun *et al.*, 2015).

Both hCMEC/D3 cell lines (WT and hSSAO/VAP-1) were maintained in EBM-2 fully supplemented medium. In case of hSSAO/VAP-1 cells, 100 µg/ml Geneticin (G418; *Thermo Fisher*) were added to the medium to ensure maintaining plasmidic DNA containing SSAO/VAP-1 sequence. Cells were kept in an incubator at 37 ºC with a humidified atmosphere with 5 % CO_2 and were used until passage 40.

Cells were sub-cultured once a week, when the confluence reached more than 95 % at a 1/10 dilution. The sub-culturing procedure started removing maintenance medium and washing the cells twice with sPBS. To harvest the cells, 20 µl/cm² Trypsin-Ethylenediaminetetraacetic acid (EDTA; *Merck-Sigma*) were added and incubated at 37 ºC for 2 minutes. After incubation, trypsin effect was stopped by adding 6 ml EBM-2 fully supplemented medium. Cells were resuspended and centrifuged for 5 min at 400 g. The pellet was resuspended in 5 ml EBM-2 fully supplemented medium and a 20 µl aliquot was taken to be stained with 20 µl Trypan Blue and counted in a Neubauer chamber to be seeded at the appropriate concentration.

Cell line stocks were stored in liquid nitrogen. Freezing protocol started similarly to sub-culturing protocol but the pellet was resuspended in freezing medium instead of EBM-2 fully supplemented

medium. Prior to freeze, cells were kept in freezing medium during 15 min at room temperature to let it permeate into the cells. Then, the cryotubes containing 1ml aliquot each were transferred to the cryo-freezing container (*Nalgene*) filled with isopropanol and stored at -80 ºC for at least 24 h. After 24 h, the cryotubes were eventually moved to the liquid nitrogen tank.

When needed, new cell line stocks were thawed. To do so, selected cryotubes were taken out of the liquid nitrogen tank and rapidly partially immersed in a 37 ºC H_2O bath. One ml EBM-2 fully supplemented medium was added to the vial and slightly resuspended. Cell suspension was transferred to a collagen-coated T75 flask containing proper EBM-2 fully supplemented medium. To remove DMSO present in the freezing medium from the thawed vial, the entire cell medium was renewed once the cells were properly attached, approximately 4 h later after seeding.

In case of using them for following experiments, cells were seeded at 200 000 cells/ml on plates previously coated for 2 h with collagen type 1 solution. When Transwell inserts (Tw: Transwell polyethylene terephthalate transparent membrane inserts, pore size 0.4 μm; *Sarstedt*) were used, after collagen coating and before cell seeding, they were further incubated for 1h with fibronectin solution. The medium was changed 3 days after seeding. At this concentration the cells reached confluence three days after seeding. At this moment, and prior to be used for experiments, their medium was replaced by EBM-2 partially supplemented medium.

1.3 Co-culture

Mature neuron-glia mixed primary culture was co-cultured with both hSSAO/VAP-1 and WT hCMEC/D3 cells to reproduce an *in vitro* model mimicking the neurovascular unit (NVU) environment.

1.3.1 Co-culture establishment and *in vitro* maintenance

Primary mouse cortical mixed neuron-glia culture and hCMEC/D3 cells were the components of the co-culture system. Each one had to be developed in synchrony **(figure 25)** until the moment of setting up the co-culture.

In one hand, neuron-glia mixed primary culture was seeded in 6-well or 12-well plates and maintained until 9 DiV as previously described. In the morning of the 9th DiV, half of the medium was replaced by BME 5 % HS.

On the other hand, hCMEC/D3 cells were seeded on collagen and fibronectin-coated 6-well or 12-well Transwell inserts as previously described. hCMEC/D3 cells were seeded in parallel to mixed primary culture development so they could reach confluence by the mixed primary culture 9th DiV. In the same 9th DiV morning, hCMEC/D3 cells were deprived by replacing their EBM-2 fully supplemented medium by EBM-2 partially supplemented one.

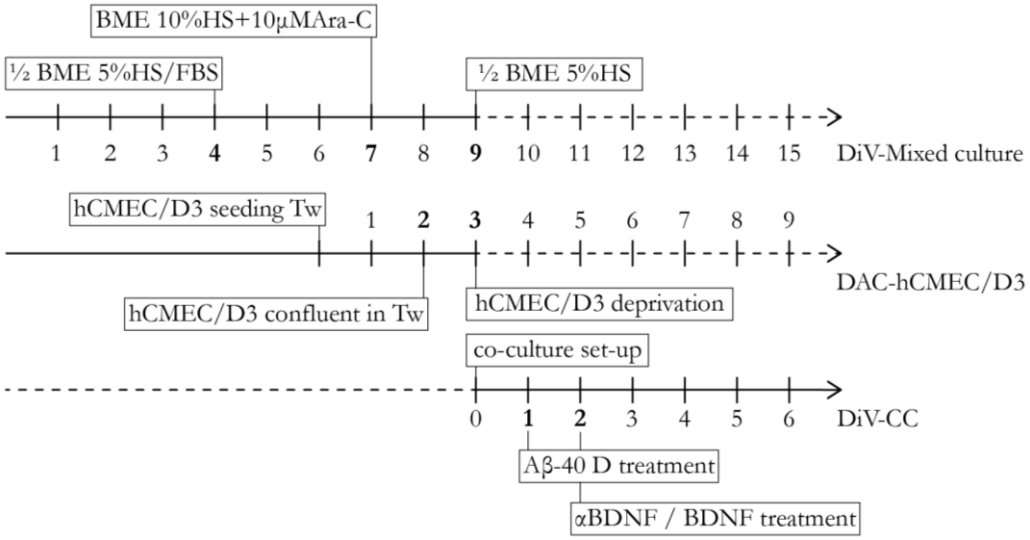

Figure 25: Timeline scheme for synchronizing both neuron-glia mixed culture development and hCMEC/D3 proliferation *in vitro*. The upper arrow represents neuron-glia mixed culture timeline. Medium changes needed at each time point are indicated. The middle arrow represents hCMEC/D3 timeline. Seeding, confluence reaching and deprivation moments are indicated in synchronicity to mixed culture development. The lower arrow represents the timeline since both parts of the co-culture are put together. Treatments are indicated by the day they are performed. DAC: days after confluence; DiV-CC: DiV of the co-culture; Tw: transwell insert.

hCMEC/D3 Transwell inserts were placed inside mixed primary culture wells **(figure 26)** 10 h after both cell mediums were changed. Coupling both co-culture components defined that day as 0 DiV of the co-culture (DiV-CC). Both parts of the system; the apical chamber (hCMEC/D3 cells) and the basolateral chamber (neuron-glia mixed culture cells) could communicate with each other through the semipermeable membrane of the Transwell insert.

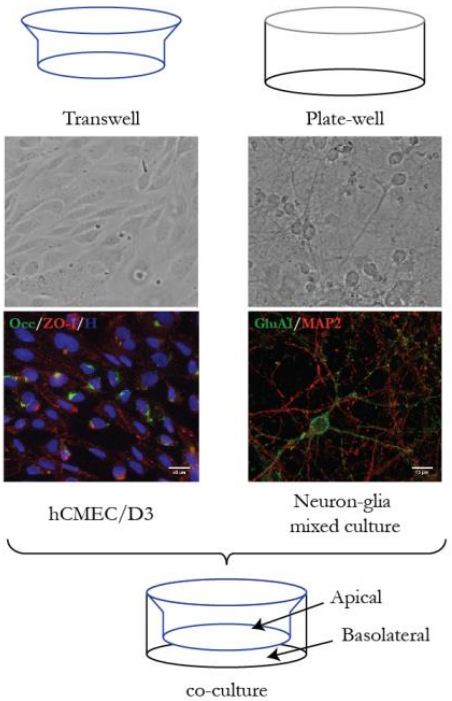

Figure 26: Co-culture experimental scheme with representative phase contrast and immunohistochemistry images from hCMEC/D3 cells (Occ: Occludin, ZO-1: Zonula Occludens, H: Hoechst) and neuron-glia mixed culture (GluA1, MAP2) before settling the co-culture. hCMEC/D3 cells seeded in the transwell device are placed inside the neuron-glia mixed culture well. Both parts can communicate through the semipermeable membrane in the bottom of the transwell.

2 Cell treatments

2.1 Conditioned medium treatment

To start assessing if hCMEC/D3 cells induce an impact on neurons from the mixed culture, neuron-glia mixed culture medium was half-replaced with hCMEC/D3 cells conditioned medium.

In order to obtain conditioned medium from endothelial cells, both hSSAO/VAP-1 and WT hCMEC/D3 cells were seeded in 24-wells plate in parallel to the mixed culture in development. At 9 DiV half of mixed culture medium was renewed with 5 days after confluence (DAC) conditioned hCMEC/D3 medium. Mixed culture cells were kept in this condition until 15 DiV, when the appropriate experiment was performed.

2.2 BDNF treatment

2.2.1 BDNF treatment in conditioned medium experiments

To further complete the experiments with conditioned medium, BDNF was added to the procedure previously described.

Lyophilized recombinant human brain-derived neurotrophic factor protein (BDNF; *R&D Systems*) was resuspended at 25 µg/ml in sterile PBS 1X supplemented with 0.1 % BSA. Reconstituted BDNF was aliquoted and stored at -80 ºC.

When needed, BDNF aliquots were thawed and further diluted in resuspending buffer to treat at a final concentration of 125 pg/ml or 1.25 ng/ml.

2.2.2 BDNF in co-culture experiments

Lyophilized recombinant human brain-derived neurotrophic factor protein (BDNF; *Merck-Sigma*) was resuspended at 500 µg/ml in sterile distilled H_2O, diluted in sterile PBS 1X at 4.5 pg/µl, aliquoted and stored at -20 ºC.

When needed, BDNF aliquots were thawed to treat at 45 pg/ml neuron-glia mixed cultures, co-cultured with $A\beta_{1-40}D$-treated SSAO/VAP-1-expressing endothelial cells **(figure 27)**.

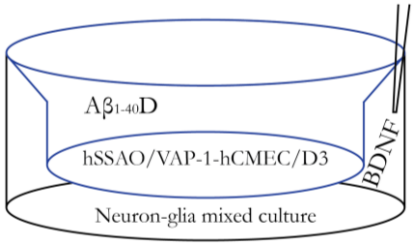

Figure 27: BDNF treatment scheme. BDNF (45 pg/ml) was added to neuron-glia mixed cultures co-cultured with Aβ-treated SSAO/VAP-1-expressing endothelial cells.

2.3 α-BDNF antibody treatment

Lyophilized anti-BDNF mouse monoclonal antibody (α-BDNF; clone 35928.11, Cat. No.GF35L, *Merck-Millipore*) was resuspended at 100 µg/ml in sterile PBS 1X, aliquoted and stored at -20 ºC.

When needed, α-BDNF aliquots were thawed to treat at 2 µg/ml neuron-glia mixed cultures, co-cultured with WT-hCMEC/D3 $A\beta_{1-40}D$-treated **(figure 28)**.

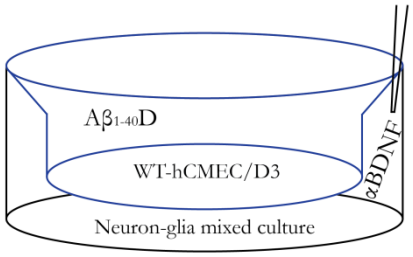

Figure 28: α-BDNF treatment scheme. Anti-BDNF neutralizing antibody (2 µg/ml) was added to neuron-glia mixed cultures co-cultured with Aβ-treated WT endothelial cells.

2.4 $A\beta_{1-40}$-D treatment

Lyophilized (Gln^{22})-Amyloid β-Protein (1-40) ($A\beta_{1-40}D$) trifluoroacetate salt (*Bachem*) was resuspended at 1 mg/ml in Hexafluoro-2-propanol (HFIP) to monomerize any possible aggregate. Once completely resuspended, it was aliquoted and re-lyophilized by evaporating using a speed vacuum concentrator. Aliquots were stored at -80 ºC.

When needed, $A\beta_{1-40}D$ aliquots were resuspended at 100 µM in PBS 1X supplemented with 0.1 % NH_4OH. hCMEC/D3 cells were treated with 5 µM $A\beta_{1-40}D$ at 1 DiV-CC. Previously to the treatment, endothelial cells medium was renewed with conditioned EBM-2 partially supplemented medium coming from a sister hCMEC/D3 cells plate maintained in parallel.

3 Cell viability assessment

3.1 MTT

Viable cells with active mitochondrial metabolism reduce 3-(4,5-dimethylthiazol-2-yl)-2,5-diphenyltetrazolium bromide (MTT) into a purple colored formazan product with a maximum absorbance near 570 nm. When mitochondrial metabolism fails, they lose the ability to convert MTT into formazan, thus color formation serves as an useful and convenient marker of only metabolic viable cells (Riss *et al.*, 2004).

Procedure consisted on adding MTT (*Merck-Sigma*) at a final concentration of 0.2 mg/ml to neuron-glia mixed culture and at 0.5 mg/ml to hCMEC/D3 cells and incubating for 45 min at 37 ºC in a humidified incubator with 5 % CO_2. For neuron-glia mixed culture, cell medium was replaced by PBS

1x supplemented with glucose and antibiotic prior to adding MTT. In case of hCMEC/D3, the cell medium was replaced by M199 medium (*Invitrogen*) supplemented with 1.2 mM glutamine (*Thermo Fisher*) and antibiotic prior to adding MTT as EBM-2 medium interferes with the assay and during absorbance measuring.

After MTT incubation, both PBS and M199 medium were removed and DMSO was added to solubilize the formazan product precipitate prior to recording absorbance readings. Dual wavelengths were measured at 560 and 620 nm in a microplate reader (*Synergy HT*) using KC4 data analyzer software (*Bio-tek instruments inc.*). Data was analyzed as the difference in absorbance between 560 and 620 nm and expressed as living cells percentage compared to basal condition.

3.2 LDH cytotoxicity assay

Cell mediums were collected as described in samples obtainment section (see 4.2 cell medium collection) and stored at -80 ºC until lactate dehydrogenase (LDH) cytotoxicity assay was performed.

LDH test consisted on determining the levels of LDH released to the medium as consequence of cell death. It was performed using Pierce LDH Cytotoxicity Assay Kit (*Thermo fisher*) and following manufacturer indications. In summary, plasma membrane damage releases LDH into the cell culture media. LDH levels in the media can be indirectly quantified determining its activity by a coupled enzymatic reaction, which involves LDH catalysing the conversion of lactate to pyruvate via NAD+ reduction to NADH. Diaphorase then uses NADH to reduce a tetrazolium salt into a red formazan product. This formazan was measured directly from the medium at 490 nm in a microplate reader (*Synergy HT*) using KC4 data analyzer software (*Bio-tek instruments inc.*). Cytotoxicity was inferred by the directly proportional relation between formazan formation and the amount of LDH released to the medium.

4 Samples obtainment

4.1 Cell lysis

4.1.1 Neuron-glia mixed culture

Neuron-glia mixed cultured cells were washed with PBS 1X and lysed by scrapping in cold NP-40 lysis buffer containing 20 mM Tris Base pH 7.4, 150 mM NaCl, 5mM EDTA, 1 % NP-40, 1 mM Na_3VO_4, 1mM PMSF, 1 % protease inhibitor cocktail (*Merck-Sigma*) and 1 % phosphatase inhibitor cocktail (*Merck-Sigma*). Samples were sonicated for 10 s using sonic dismembrator. Protein extracts were quantified using Bradford reaction kit (*Bio-rad*), based on a standard curve made with known albumin (*ThermoFisher Scientific*) concentrations.

4.1.2 hCMEC/D3

hCMEC/D3 cells were washed in PBS 1X and lysed by scrapping in cold Tris pH 9 buffer supplemented with 1 % protease inhibitor cocktail (*Merck-Sigma*). Samples were also sonicated and protein extracts were quantified as previously described.

4.2 Cell medium collection

When the experiment required, cell medium was collected. To discard possible floating death cells or debris, medium was centrifuged for 5 min at 3 000 g and 4 ºC. Supernatant was transferred to a new tube and stored at -20 ºC or -80 ºC depending on the maintenance requirements of the following experiment.

4.3 Cellular fractionation

The cellular fractionation procedure consisted on a synaptosomal membrane preparation with sucrose gradient for post-synaptic density (PSD) fraction isolation. Several centrifugations and ultracentrifugations took place and the different fractions were separated until the PSD was purified. The procedure and the required reagents are detailed as follows.

4.3.1 Buffers and solutions

- HEPES: 4 mM HEPES pH 7.4, 1 % protease inhibitor cocktail (*Merck-Sigma*), 1 % phosphatase inhibitor cocktail (*Merck-Sigma*), 1 mM NaF, 0.05 % NaPPi and 0.01 % glicerolphosphate.

- HEPES-sucrose: 4 mM HEPES pH 7.4, 0.32 M sucrose (*Acros*), 1 % protease inhibitor cocktail (*Merck-Sigma*), 1 % phosphatase inhibitor cocktail (*Merck-Sigma*), 1 mM Na_3VO_4, 1 mM NaF, 0.04 % NaPPi and 0.01 % glycerol phosphate.

- Discontinuous sucrose gradient: constituted by three sucrose phases (0.8 M, 1 M and 1.2 M) supplemented with 1 % protease and 1 % phosphatase inhibitors cocktails (*Merck-Sigma*).

- Triton-HEPES-EDTA: 0.5 % Triton X-100 (*Prolabo*), 50 mM HEPES pH 7.4, 2 mM EDTA, 1 % protease inhibitor cocktail (*Merck-Sigma*) and 1 % phosphatase inhibitor cocktail (*Merck-Sigma*).

4.3.2 Procedure

Neuron-glia mixed culture cells were washed with PBS 1X, scrapped in HEPES-sucrose buffer and homogenized using a motor-driven grinder with the 1.5 ml microtube pestle end (*Merck-Sigma*) for 25 s. To keep an aliquot of the whole homogenized sample, 37.5 µl were taken and stored at -20 ºC. The rest was centrifuged for 10 min at 1 000 g and 4 ºC. The supernatant (S1) was transferred to a new tube and was centrifuged for 15 min at 10 000 g and 4 ºC. After centrifugation, the pellet (P2) was washed with HEPES-sucrose buffer and re-centrifuged again for 15 min at 10 000 g and 4 ºC. From the P2 centrifugation, the pellet (P2') was resuspended in HEPES solution and homogenized with the

motor-driven grinder with the 1.5 ml microtube pestle end for 25 s. The homogenate was transferred to a mini-ultracentrifuge tube and ultracentrifuged for 20 min at 25 000 g and 4 ºC with a S120-AT2 rotor. After ultracentrifugation, the pellet (P3) was resuspended in HEPES-sucrose buffer and loaded to the discontinuous sucrose gradient. The gradient was ultracentrifuged in a S52-ST swinging rotor for 2 h at 150 000 g, 4 ºC and 1-1 acceleration/brake. After ultracentrifugation, desired fraction (between 1 M and 1.2 M sucrose phases) was isolated and diluted in HEPES solution. The dilution was ultracentrifuged again in a S52-ST swinging rotor for 30 min at 150 000 g, 4 ºC and 9-9 acceleration/brake. The pellet was resuspended in Triton-HEPES-EDTA solution to be lysated by vortex during 15 min. The lysate was transferred to a mini-ultracentrifuge tube and ultracentrifuged for 20 min at 32 000 g and 4 ºC using a S120-AT2 rotor. The supernatant synaptic plasma membrane (SPM) fraction was transferred to a new tube and stored at -20 ºC. The pellet (PSD fraction) was resuspended in Triton-HEPES-EDTA buffer and transferred to a new tube to be stored at -20 ºC.

Protein concentration was determined by BCA protein assay kit (*Pierce*). Samples were analyzed by Western blot assay, where Homogenate samples were loaded at 1 µg/µl and SPM and PSD samples were loaded both at 5 µg/µl.

4.4 Cellular fixation

Neuron-glia mixed culture was plated on poly-D-lysine-coated glass coverslips pretreated with HCl.

Briefly, coverslips pretreatment consisted on incubating them in 8 % Hydrochloric acid fuming 37% (*Merck*) solution gently shaking overnight. Next day, they were washed for three times, 15 min each one, with absolute ethanol also in soft shaking conditions. Finally, HCl-treated coverslips were stored in absolute ethanol in a sealed plate to prevent ethanol evaporation.

To fix the cells, the medium was removed and the cells were washed twice with PBS 1X. The cells were fixed in cold 4 % paraformaldehyde/4 % sucrose PBS 1x solution for 15 min on ice. Afterwards, the cells were washed twice with PBS 1X and immediately used or stored before immunocytochemistry protocol in PBS 1x supplemented with 0.1 % Azide to preserve them.

5 Protein analysis

5.1 Western Blot

Depending on the samples, two different western blot protocols were used. Most proteins were analyzed following Tris-Glycine Sodium Dodecyl Sulfate-polyacrylamide gel electrophoresis (SDS-PAGE) procedure. However, for amyloid β-peptide (Aβ) analysis, the Tris-Bicine SDS-PAGE protocol was used.

5.1.1 Tris-Glycine SDS-PAGE

5.1.1.1 Reagents and solutions

- Separating gel buffer: 1.5 M Tris pH 8.8 adjusted with HCl. Stored at 4 ºC.

- Stacking gel buffer: 1 M Tris pH 6.8 adjusted with HCl. Stored at 4 ºC.

- Electrophoresis buffer 10X: 1.92 M Glycine and 0.247 M Tris.

- Electrophoresis buffer 1X: 192 mM Glycine, 24.7 mM Tris and 0.1 % SDS.

- Sample buffer 4X: 277.8 mM Tris-HCl pH 6.8, 4.4 % SDS, 44.4 % Glycerol, 0.008 % w/v Bromophenol blue and 1.4 M β-mercaptoethanol.

- Transference buffer 1X: 192 mM Glycine, 24.7 mM Tris and 20 % Methanol.

- Ponceau S staining solution: 0.1 % w/v Ponceau S in 5 % v/v acetic acid.

- PBS 10X: 1.36 M NaCl, 26.83 mM KCl, 42.9 mM $Na_2HPO_4 \cdot 7\ H_2O$ and 14.7 mM KH_2PO_4. pH 6.9.

- PBS/Tween-20 (PBS-T): 0.05 % w/v Tween-20 in PBS 1X.

- Blocking solution: 10 % w/v non-fat dry milk and 0.1 % w/v BSA in PBS 1X pH 7.4, adjusted with NaOH.

- Antibody dilution buffer: 0.1 % w/v BSA and 0.02 % w/v Thimerosal in PBS 1X.

- Primary antibodies used and their concentrations:

Table 2: Primary antibodies used for Tris-Glycine SDS-PAGE Western Blot.

Antibody	Host	Source	Reference	Dilution
AKAP150	Rabbit	Merck-Millipore	07-210	1/1 000
GluA1	Rabbit	Merck-Millipore	1504	1/1 000
PSD95	Mouse	Abcam	2723	1/1 000
β-Tubulin	Mouse	BD Bioscience	556321	1/10 000
GFAP	Mouse	Merck-Millipore	3402	1/1 000
β-Actin	Mouse	Merck-Sigma	A1978	1/10 000
GAPDH	Mouse	ThermoFisher Scientific	4300	1/10 000
Synaptophysin	Mouse	Merck-Sigma	5768	1/40 000
ZO-1	Rabbit	ThermoFisher Scientific	40-2200	1/1 000
VE-Cadherin	Mouse	Santa Cruz	sc-9989	1/500
Claudin-5	Mouse	Santa Cruz	sc-374221	1/500

- Secondary antibodies used: horseradish peroxidase (HRP) enzyme-coupled polyclonal goat anti-mouse Ig (*BD Bioscience* 554002) and polyclonal HRP goat anti-rabbit IgG (*BD Bioscience* 554021) were diluted in blocking solution at the proper concentration depending on protein abundance, but mainly in a 1/2 000 dilution.

5.1.1.2 Procedure

After protein concentration determination, samples were prepared in sample buffer at 1 µg/µl if not specified a different concentration. Samples were boiled for 5 min at 95 ºC and then loaded, along with a molecular weight marker (Precision Plus Protein™ Standard All Blue; *Bio-Rad*), in 7.5 % or 10 % polyacrylamide (30 % acrylamide/Bis solution 37:5:1; *Bio-Rad*) gels in SDS-PAGE conditions. Electrophoresis was performed at 100-120 V in electrophoresis buffer 1X. Then, proteins were transferred onto nitrocellulose blotting membrane (Amersham Protran 0.2 NC; *Cytiva*) at 90 V for 1 h in transfer buffer 1X. To check if transference process elapsed correctly, membranes were stained with Ponceau S staining solution. To remove Ponceau S staining, membranes were washed several times with PBS-T and then were incubated for 1h at room temperature in blocking solution. Once blocked, membranes were washed twice for 5 min and twice more for 10 min with PBS-T and then were incubated overnight at 4 ºC with the appropriate primary antibody **(table 2)** diluted in antibody dilution buffer. Membranes were abundantly washed with PBS-T and incubated for 1 h at room temperature with HRP secondary antibody diluted in blocking solution. Finally, membranes were again abundantly washed with PBS-T (twice for 5 min and twice more for 10 min) and developed by chemoluminescent reaction using the ECL western blotting detection reagents (*Amersham, Cytiva*). Protein bands were detected on X-ray films (*Fuji Medical X-ray films*). Semi-quantitative analysis was performed by densitometry using ImageJ software (*National Institutes of Health, USA*). Alternatively, Odyssey Fc Imager was used and the analysis was done through Image Studio™ Lite software 5.x (*LI-COR Biosciences, USA*).

5.1.2 Tris-Bicine SDS-PAGE

5.1.2.1 Reagents and solutions

- Separating gel buffer 4X: 1.6 M Tris and 0.4 M H_2SO_4. pH 8.1 adjusted with 9.86 M H_2SO_4. Stored at 4 ºC.

- Stacking gel buffer 2X: 0.8 M BisTris and 0.2 M H_2SO_4. pH 6.7 adjusted with 9.86 M H_2SO_4. Stored at 4 ºC

- Cathode electrophoresis buffer: 0.2 M Bicine, 0.1 M NaOH and 0.25 % w/v SDS. pH 8.2 adjusted with HCl.

- Anode electrophoresis buffer: 0.2 M Tris and 50 mM H_2SO_4. pH 8.1 adjusted with 9.86 M H_2SO_4.

- Sample buffer 2X: 0.72 M BisTris, 0.32 M Bicine, 2 % w/v SDS, 25 % w/v Glycerol, 100 mM Dithiothreitol and 0.008 % w/v Bromophenol blue. Stored at -20 ºC.

- Transference buffer: 10 mM CAPS pH 11 and 10 % v/v methanol.

5.1.2.2 Procedure

Cell medium and cell lysates samples, both from neuron-glia mixed culture and hCMEC/D3 cells, were prepared in sample buffer and loaded in 12 % polyacrylamide (30 % acrylamide/Bis solution 19:1; *Bio-Rad*) gels in SDS-PAGE conditions. Electrophoresis was performed at 100 V in cathode electrophoresis buffer, in the inner tank between gels, and anode electrophoresis buffer in the external tank outside gels. Then, proteins were transferred to previously methanol-activated PVDF blotting membrane (Amersham Hybond P 0.45; *Cytiva*) at 90 V for 1 h in transfer buffer. After transference, membranes were washed and incubated for 7 min in boiling PBS 1X to uncover the antigen. Afterwards, the membranes were incubated for 1h at room temperature in blocking solution prepared as in the previous procedure. Once blocked, membranes were washed several times with PBS-T and then were incubated overnight at 4 ºC with mouse anti-APP 20.1 primary antibody (generated from 20.1 hybridoma cells; *W.E. Van Nostrand*) diluted in PBS-T supplemented with 0.1 % BSA. From here the procedure continued similarly to the previous described but membranes were washed four times for 5 min and three times more for 10 min with PBS-T. In summary, membranes were generously washed with PBS-T and incubated for 1 h at room temperature with HRP secondary antibody diluted in blocking solution. Finally, the membranes were washed four times during 5 min and three times for 10 min with PBS-T and revealed by chemoluminescent reaction using the ECL western blotting detection reagents (*Amersham, Cytiva*). Proteins bands were detected on X-ray films (*Fuji Medical X-ray films*). Semi-quantitative analysis was performed by densitometry using ImageJ software (*National Institutes of Health, USA*). Alternatively, Odyssey Fc Imager was used and the analysis was done through Image Studio™ Lite software 5.x (*LI-COR Biosciences, USA*).

5.2 Immunocytochemistry and image acquisition

5.2.1 Reagents and solutions

- PBS 1X (*Thermo Fisher*): 136.89 mM NaCl, 2.68 mM KCl, 8.10 mM $Na_2HPO_4 \cdot 7\ H_2O$ and 1.47 mM KH_2PO_4.

- Permeabilizing solution: PBS 1X supplemented with 0.1 % Triton X-100.

- Blocking solution: PBS 1X supplemented with 5 % normal Goat Serum (*Merck-Sigma*).

- Antibody solution: PBS 1X supplemented with 2 % normal Goat Serum (*Merck-Sigma*). Some primary antibodies required 5 % normal Goat Serum to minimize better background signal.

Table 3: Primary and secondary antibodies used for immunocytochemistry.

Antibody	Host	Source	Reference	1ary Ab Dil.	2ary Ab Dil.
AKAP150	Rabbit	Santa Cruz	10765	1/500	1/500
GluA1	Rabbit	Merck-Millipore	1504	1/250	1/500
PSD95	Mouse	Abcam	2723	1/500	1/1 000
Synaptophysin1	Rabbit	Synaptic Systems	101 002	1/1 000	1/2 000
MAP2	Mouse	Merck-Sigma	M1406	1/500	1/500
MAP2	Rabbit	Synaptic Systems	188 002	1/1 000	1/500
VGlut1	Guinea Pig	Merck-Millipore	5905	1/500	1/500
GFAP	Rabbit	DAKO	Z0334	1/500	1/1000
OX42	Rat	ThemoFisher Scientific	12-0110-82	1/250	1/500

5.2.2 Procedure

After previously described fixation procedure, cells were incubated with permeabilizing solution for 20 min at room temperature. Then, the cells were washed twice with PBS 1X previous being blocked with blocking solution for 1 h at 37 ºC in shaking conditions. After blocking, cells were incubated in humidified chamber overnight at 4 ºC with primary antibodies **(table 3)** diluted in antibody solution. Next day, cells were washed twice with PBS 1X and were incubated in humidified chamber for 1 h at 37 ºC with the proper secondary antibodies (Alexa Fluor 568 Goat anti-Mouse IgG, Alexa Fluor 488 Goat anti-Rabbit IgG and Alexa Fluor 568 Goat anti-Guinea Pig IgG; *Thermo Fisher*) diluted in antibody solution. Afterwards, cells were washed twice and incubated for 5 min with 1 µg/ml Hoechst (*Invitrogen, ThemoFisher Scientific*) to visualize nuclei. Finally, cells were washed twice with PBS 1X and mounted on glass slides with Fluoromount-G (*Southern biotech*).

5.2.3 Image acquisition and quantification analysis

Images were acquired by confocal laser scanning microscopy ZEISS LSM 700 with 40X oil objective for most of the experiments or 63X oil objective to get neuritic crops. Sequential frame acquisition was set to acquire planes in 1.0 µm interval per stack at 16 bits, in zoom 1, a minimum of 1024 × 1024 resolution and with a laser speed value of 6. These acquisition settings were modified in case of getting images from the selected neuritic crops with zoom 3, 1024 x 350 resolution and with a laser speed value of 7. Lasers conditions were optically adapted for each antibody condition to minimize saturation of punctae and maintained between replicates of each experiment. Unmodified images were used for all analyses, which were done in blind manner. Linear scaling was applied on images only for presentation purposes using ImageJ software (*National Institutes of Health, USA*). Fluorescent signal was analyzed from the maximum intensity projection of each stack to quantify mean intensity of punctae over the defined region of interest (ROI). Specifically for crops analysis, the PSD particles to define the PSD zone were defined by the PSD95-labeling punctae.

5.2.3.1 Image quantification for intensity subpopulations classification

Neurons from neuron-glia mixed culture population were blind-classified depending on the mean intensity values registered for the different immunolabeled markers (GluA1, PSD95, and AKAP150). Firstly, we defined the non-treated WT-CC as the basal condition. Then, in case of GluA1-labeling, positive cells were identified **(figure 29a, left part)** for all the conditions of each independent experiment, and the mean intensity value from each cell was calculated using ImageJ software by measuring within ROI drawn surrounding the soma of each GluA1-positive cell. To describe the classifying criteria **(figure 29b)**, percentile value 25th and 75th were calculated from the intensity values of the basal condition using Graph-Pad Prism 6.0 software (San Diego, CA, USA). Both percentiles were considered the thresholds to limit the subpopulation types as Type I (low intensity; below percentile 25th), Type II (intermediate intensity; between 25th and 75th percentile), and Type III (high intensity; higher than 75th percentile). Defined thresholds were applied to previously identified GluA1-positive cells **(figure 29a, left part)** from basal and the rest of experimental conditions. In case of PSD95 and AKAP150 labeling, the same procedure was performed to define the thresholds and to classify the cells. Specifically for PSD95 staining, it was difficult to extend the previous study due to the network complexity of mixed culture along with the labeling pattern that this structural marker presents. Therefore, considering the high percentage of co-localization of GluA1 with PSD95 (Nair *et al.*, 2013), we decided that the somatic ROIs we would apply in case of PSD95 would be those previously described for GluA1 labeling, meaning that PSD95 data were obtained from GluA1-positive cells.

A

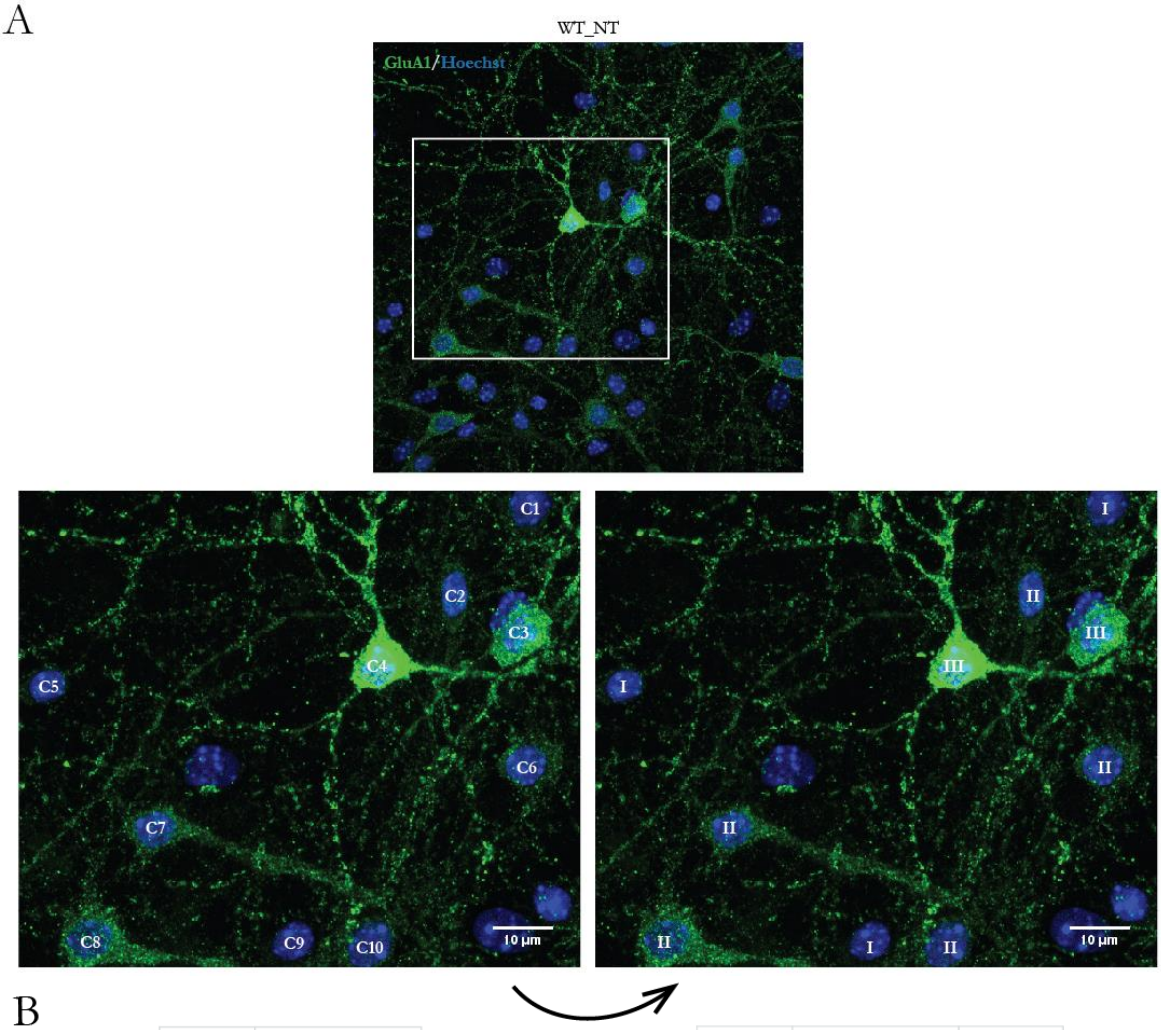

B

Cell	Mean Intensity
C1	X1
C2	X2
C3	X3
C4	X4
C5	X5
C6	X6
C7	X7
C8	X8
C9	X9
C10	X10
Cn	Xn

Cell	Mean Intensity	Type
C1	X1	I
C2	X2	II
C3	X3	III
C4	X4	III
C5	X5	I
C6	X6	II
C7	X7	II
C8	X8	II
C9	X9	I
C10	X10	II
Cn	Xn	I/II/III

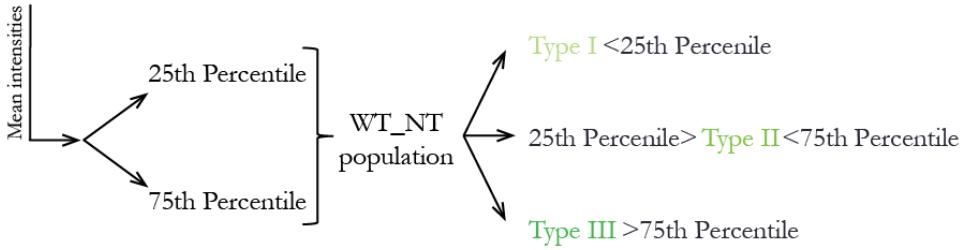

Figure 29: Classification process in subpopulation types according to GluA1-labeling mean intensity values. (A) Representative images and tables from classifying process. GluA1-positive cells were identified (C1, C2, … Cn) and the mean intensity of each one (X1, X2, … Xn) was registered. Mixed primary cells co-cultured with non-treated WT hCMEC/D3 were the control condition. Scale bar: 10 µm. **(B)** Mean intensity values from control condition were used to establish the thresholds (25th and 75th percentile intensity values) between subpopulation types (Type I, Type II, Type III). This determined threshold values were applied to the rest of the conditions to classify their cells into the proper subpopulation types.

5.3 Enzyme-linked immunosorbent assay (ELISA)

Human Aβ40 ELISA kit (KHB3481; *Invitrogen*) was used to detect and quantify the levels of human $A\beta_{1-40}$ in medium and cell lysates samples from both parts of the co-culture. Manufacturer instructions were followed. Briefly, washing and standard reconstitution buffers were prepared as indicated as well as standard samples. Samples were pre-diluted (apical medium: 1/10 000, apical lysate: 1/2 000, basolateral medium: 1/1 000 and basolateral lysate: 1/500). The procedure started binding the antigen and adding the detector. Then the IgG HRP freshly-prepared solution was added. Next the stabilized chromogen was added and finally the stop solution was added. The absorbance was read at 450 nm in a microplate reader (*Synergy HT*) within 30 minutes after adding the stop solution using KC4 data analyzer software (*Bio-tek instruments inc.*). To quantify, the curve-fitting software was used to generate the standard curve through a four parameter algorithm. The background absorbance was subtracted from all data points, including standards, samples and controls, prior to plotting. The sample values were inferred from the standard curve and the obtained data were multiplied by the appropriate factor to correct for the sample dilution.

5.4 Multiplex

Cell medium from neuron-glia mixed culture and hCMEC/D3 cells, both in non-co-culture and in co-culture conditions and after being treated with $A\beta_{1-40}$-D or not, were collected as described previously and stored at -80 ºC.

Magnetic milliplex kit (HNDG3MAG-36K; *Merck-Millipore*) for BDNF detection was used following the manufacturer instructions. Quantification was performed with a Magpix analytical test instrument xPONENT (*Luminex*) and xPONENT 4.2 software (*Luminex*).

6 Statistical analysis

Results are given as mean ± SEM of independent experiments. Number of independent experiments is indicated in each figure legend. Statistical analyses were performed by one-way ANOVA tests followed by a Bonferroni multiple comparison tests when comparing more than two conditions. Statistical differences between 2 conditions were evaluated by unpaired Student's t-test. A two-way ANOVA test was performed when the influence of 2 independent variables on one independent variable was analyzed. A $p < 0.05$ was considered to be statistically significant, according to the following significance levels: $***p < 0.001$, $**p < 0.01$ and $*p < 0.05$. Statistical analyses and graphic representations were obtained with Graph-Pad Prism 6.0 software (San Diego, CA, USA).

VI. Results

1 Study of hSSAO/VAP-1 hCMEC/D3 cells conditioned medium treatment on neuron-glia mixed culture

The interactions between the different cells types constituting the NVU are crucial for normal brain function in physiological conditions. In case these cell-to-cell cross-communications are altered, they have been reported to represent a critical impact in the pathological development of several neurological diseases (Zlokovic, 2008). In multifactorial neurodegenerative disorders like AD, deciphering these alterations amongst the NVU integrators would be extremely useful on assessing how neuronal function gets affected. Besides, in case of AD, the coexistence of vascular risk factors and cerebrovascular lesions with neurodegeneration is well documented, although the molecular mechanisms underlying AD-related vascular alterations and how they affect brain functionality are still not well defined.

In order to undertake this approach, we decided to study how cerebrovascular alterations affect neurons within the NVU in an AD-like pathological environment. Specifically, we regarded to focus on if and how the mediator molecules between the NVU integrators, known as angioneurins, and more precisely those secreted by endothelial cells, are able to affect neurons.

In addition, as a model of cerebrovascular alteration, we worked with endothelial cells expressing the vascular-adhesion protein (VAP-1), a homodimeric glycoprotein with semicarbazide-sensitive amine oxidase (SSAO, E.C 1.4.3.21) enzymatic activity and leukocyte-adhesion pro-inflammatory action. SSAO/VAP-1 has been previously reported to be involved not only in cerebrovascular dysfunction and vascular Aβ aggregation (Solé *et al.*, 2019) but also to be overexpressed in vascular pathologies considered AD-related chronic risk factors, as well as in AD, both in cerebrovascular tissue (Ferrer *et al.*, 2002) and released into blood plasma (Del Mar Hernandez *et al.*, 2005) from AD patients. Furthermore, SSAO/VAP-1 expression has also been reported to alter several angioneurins-releasing pattern by endothelial cells (Solé et al., 2019).

For this work we used the hCMEC/D3 cell line as it is a specific endothelial model from human cerebral origin from which to analyze angioneurins. Nevertheless, immortalized cell lines do not present SSAO expression or activity and primary cultures progressively lose its expression (Salmi and Jalkanen, 1995). To study this enzyme, former group members stably transfected the hCMEC/D3 cell line to permanent express the human SSAO/VAP-1 (Sun, Solé and Unzeta, 2014). On the other side, to study the effect of these endothelial angioneurins on neurons, we used primary mouse cortical mixed neuron-glia cultures to represent these NVU components. Working with mixed cultures mimics the existing physiological interactions between neurons and glial cells.

We first wanted to elucidate whether the hCMEC/D3 cells conditioned mediums, containing endothelial-secreted angioneurins, were able to produce any impact on neurons from the mixed culture. To evaluate this, we focused on analyzing the protein levels of two crucial synaptic markers relevant for glutamatergic neurotransmission. PSD95 protein is the most abundant scaffolding protein within the PSD structure and its loss from synapses is linked with synaptic depression. On the other hand GluA1 is a subunit constituting the AMPA subfamily of ionotropic glutamate receptors that are involved in the major part of fast excitatory neurotransmission and whose failure is critical during AD pathology. An affectation of their levels may be relevant as it would indicate that endothelial cells are able to directly modulate neuronal function.

We used conditioned mediums obtained 5 days after confluence (DAC) of endothelial cells expressing or not (WT) the hSSAO/VAP-1 (WT hCMEC/D3 cells as EBM_WT; and hSSAO/VAP-1 hCMEC/D3 cells as EBM_SSAO). With these mediums, we treated neuron-glia mixed cultures from 9 DiV to 15 DiV to collect mixed culture lysates **(figure 30a)**, a timeframe enough to detect possible protein levels alteration. Immunoblotting quantification from whole cell lysates **(Figure 30b)** showed that hSSAO/VAP-1 conditioned medium did not affect PSD95 protein levels (EBM_SSAO: 1.053±0.111). However, AMPA receptor subunit GluA1 protein levels tended to decrease in presence of hSSAO/VAP-1 conditioned medium (EBM_SSAO: 0.765±0.116).

The obtained results revealed a putative alteration of neuronal AMPA receptors function due to the angioneurins secreted by SSAO/VAP-1-expressing endothelial cells. However, as synaptic proteins only represent a small fraction within the whole lysate, and considering the tendency observed in the results, we decided to perform cellular fractionation protocol when we collected neuron-glia mixed samples. Thus we might directly detect changes within synapses and moreover to dismiss possible covering up effect by the rest of proteins present in the total lysate.

As expected, dissecting the results specifically in the PSD fraction showed that SSAO-expressing cells conditioned medium not only induced a significant reduction in the amount of the scaffolding protein PSD95 **(Figure 31a)**, which is critical for the synaptic structure maintenance, but also a dramatic decrease in GluA1 protein levels **(Figure 31b)**.

According to these results we could conclude that the levels of synaptic proteins PSD95 and GluA1 decreased when treating mixed-cultured neurons with hSSAO/VAP-1 conditioned medium. These data indicate that the expression of hSSAO/VAP-1 in endothelial cells may alter cell medium composition, probably by inducing a differential release of angioneurins, which are able to affect synaptic structure.

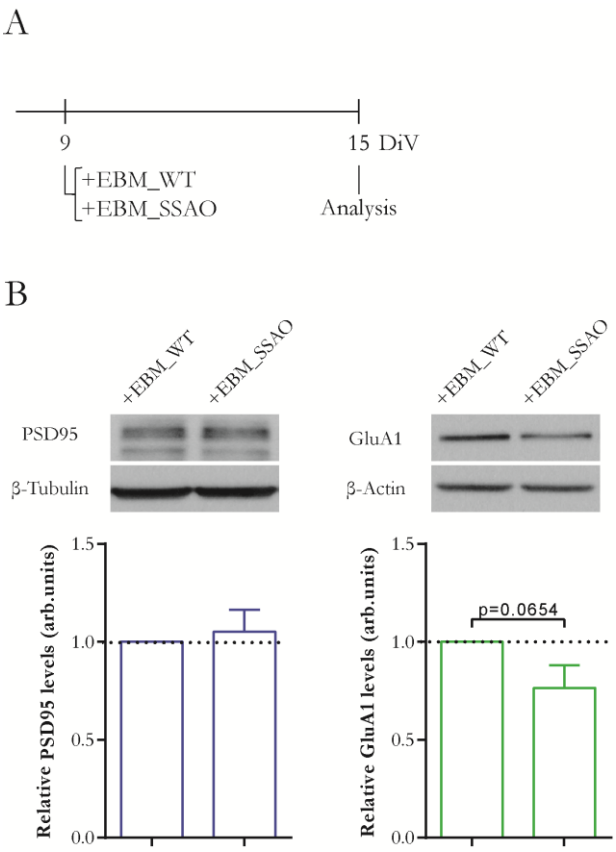

Figure 30: Conditioned mediums obtained from hSSAO/VAP-1-endothelial cells tend to reduce GluA1 protein levels in neuron-glia mixed cultures. (A) Experimental scheme. Neuron-glia mixed cultures at 9 DiV were treated with conditioned medium from WT hCMEC/D3 cells (EBM_WT) or hSSAO/VAP-1 hCMEC/D3 cells (EBM_SSAO) cultured for 5 DAC. The system was maintained until mixed culture achieved 15 DiV when the cell lysates were collected for immunoblotting. **(B)** Representative images and quantifications from immunoblotting analysis of PSD95 and GluA1 proteins. β-Tubulin and β actin were blotted as loading control proteins and were used for normalization. n=7. Mean ± SEM, unpaired Student's t-test.

However, we observed that neurons from mixed cultures were not in their optimal culture conditions after being treated by endothelial-conditioned media **(figure 32)**. We hypothesize that adding hCMEC/D3 cells conditioned medium might be altering their medium requirements, inducing impairment of the neuritic structure and increasing the debris as consequence of cell death, altogether making it not possible to further study in depth the effect of endothelial function on synapsis. Therefore, we needed to find a better system allowing the interaction between both endothelial cells and mixed cultures and assuring the best culturing conditions for each one.

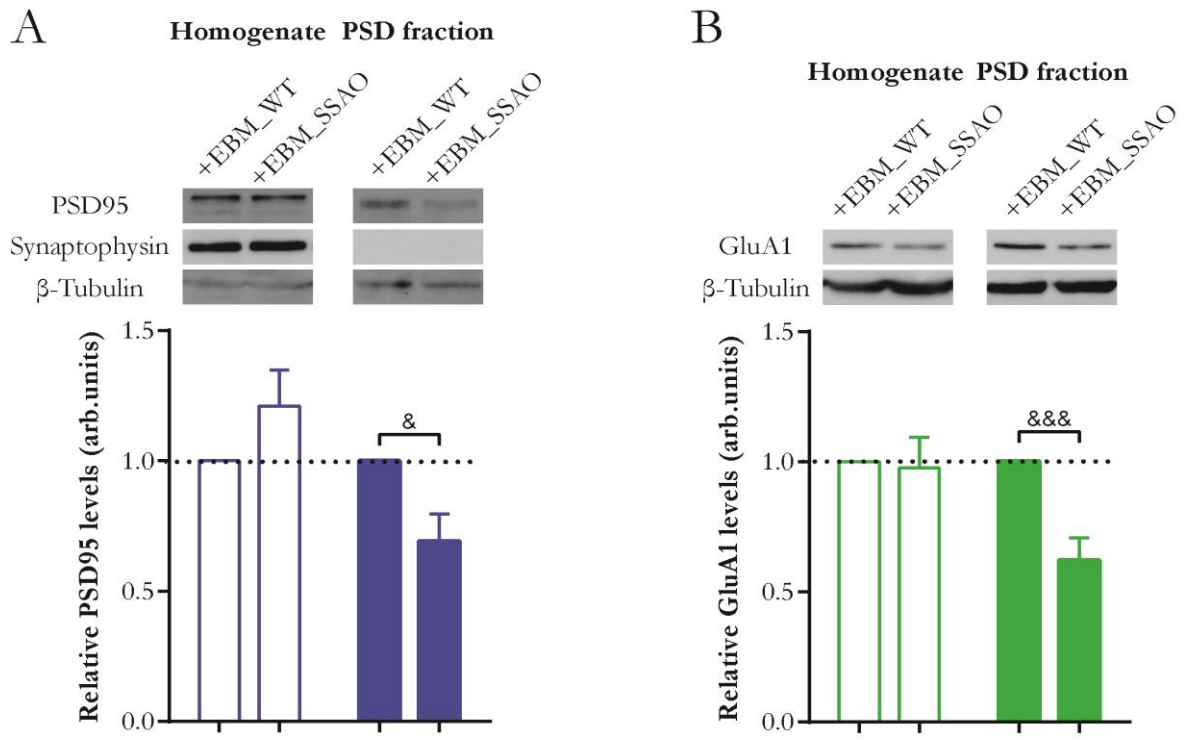

Figure 31: Reduction of synaptic protein levels in PSD fractions after treatment with conditioned medium from hSSAO/VAP-1-expressing endothelial cells. Neuron-glia mixed cultures at 9DiV were treated with 5 DAC conditioned medium from WT (EBM_WT) or hSSAO/VAP-1 hCMEC/D3 cells (EBM_SSAO). The system was maintained until mixed culture achieved 15 DiV, when the cell lysates were collected to perform PSD purification. Representative images and quantifications from immunoblotting analysis of **(A)** PSD95 in homogenate (EBM_SSAO: 1.212±0.137) and PSD (EBM_SSAO: 0.692±0.105; unpaired T-test: p= 0.0127) and **(B)** GluA1 protein levels in homogenate (EBM_SSAO: 0.977±0.117) and PSD (EBM_SSAO: 0.620±0.087; unpaired T-test: p= 0.0009) fractions. Synaptophysin was blotted to check the correct purification of PSD fraction. β-Tubulin was blotted as loading control protein and was used for normalization. n=7. Mean ± SEM. $^{\&}p \leq 0.05$, $^{\&\&\&}p \leq 0.001$, unpaired Student's t-test. PSD: post-synaptic density.

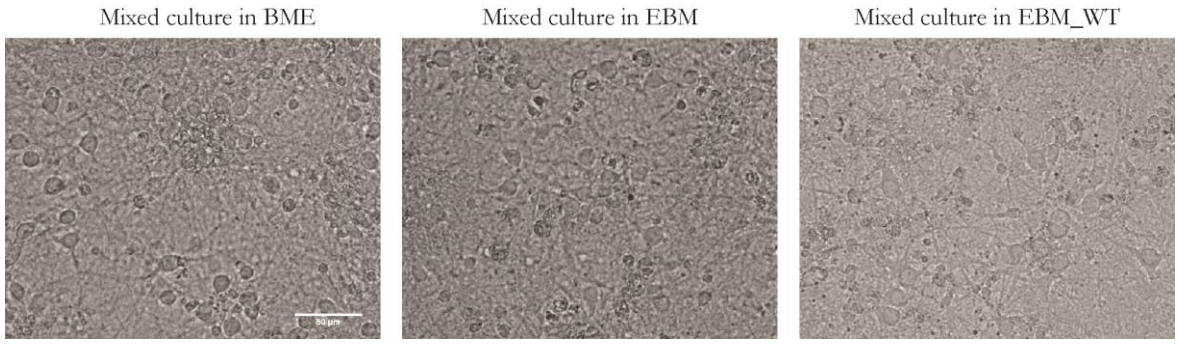

Figure 32: Representative phase contrast images of 15 DiV neuron-glia mixed cultures in different medium conditions. Left: basal condition where cells were maintained in their corresponding culture medium (BME 7.5 % HS medium). Middle: half of cells medium was replaced by fresh endothelial basal medium (EBM-2 medium). Right: half of cells medium was replaced by conditioned medium from WT endothelial cells at 5 DAC. Scale bar: 50 µm.

2 Establishment and characterization of the Neurovascular unit *in vitro* co-culture model

To address the necessity of a system that recapitulated the cell types of our interest involved in the neurovascular unit, we developed a novel *in vitro* model. It consisted on the co-culture of i) previously used hCMEC/D3 cells with ii) primary mouse cortical mixed neuron-glia culture (see materials & methods for details about co-culture procedure). We chose this co-culture system regarding the

results obtained from the conditioned medium experiments; as having confluent endothelial cells within the transwell insert would avoid severe affectation of neurons from the mixed culture due to direct contact with endothelial medium.

As a first step, to determine the optimal conditions to establish the co-culture system, we initially characterized both components to study the *in vitro* development of each one and therefore adjust the experimental variables to establish a viable model.

To assess the development of the endothelial component, we focused on its capacity to establish BBB properties attending to the amounts of two tight-junctions proteins (ZO-1 and Claudin 5) and one adherens-junction protein (VE-Cadherin). Particularly these proteins are critical for maintaining the narrowed sealing between cells that restricts paracellular flow and their alteration has been linked with increased BBB permeability. WT and hSSAO/VAP-1-expressing endothelial cells were monitored until they reached confluence and then the protein levels of the aforementioned BBB markers were analyzed at different DAC **(figure 33)**. The obtained results showed that since the first day after confluence SSAO/VAP-1-expressing cells presented significantly lower junctional protein levels compared to WT cells **(figure 33b)**. In fact, Claudin 5 levels were maintained significantly reduced in SSAO/VAP-1 cells along the rest of the study, compared to each corresponding DAC for WT cells **(figure 33c)**. Moreover, considering the results obtained from all junctional proteins analyzed revealed that, in general, levels of junctional proteins in WT cells increased from basal levels, achieving a peak around the 2nd and 3rd DAC, to progressively decrease after it **(figure 33c)**. Specifically at 2 DAC, ZO-1 protein levels were significantly higher than at 4 DAC in WT endothelial cells. Neither such increasing pattern nor any kind of peak of expression was observed for any of those analyzed proteins in SSAO/VAP-1-expressing endothelial cells. Consequently, comparing protein levels between WT and SSAO/VAP-1 at 2 DAC, the time at which WT cells show the maximum expression levels of junctional proteins, there was a significant reduction of ZO-1 in SSAO/VAP-1 cells, and also a tendency for VE-cadherin and ZO-1 at 3 DAC. Furthermore the analysis applying a two-way ANOVA statistic revealed significant effect in terms of genotype, meaning SSAO/VAP-1, for the levels of all junctional proteins analyzed.

Altogether, these results confirmed previously reported data (Solé *et al.*, 2019) showing that hSSAO/VAP-1-expressing cells are not able to properly establish the BBB as they present not only delocalization from tight-junction structure but also lower transendothelial electrical resistance measurements, both necessaries for achieving a tight BBB. Accordingly we can postulate that hSSAO/VAP-1 expression impairs the suitable BBB establishment within its features as a model of cerebrovascular alterations.

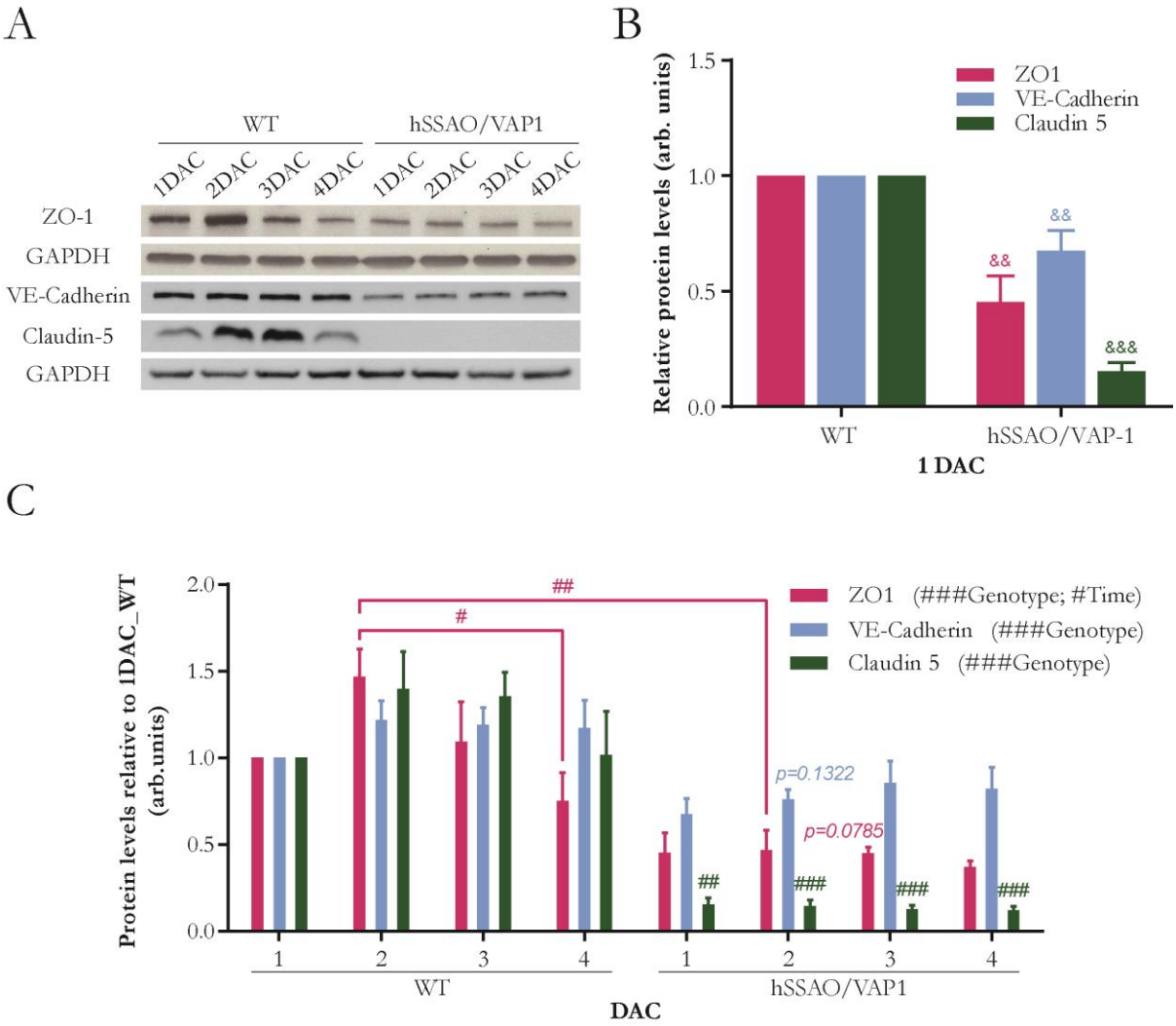

Figure 33: Human cerebral microvascular endothelial cells characterization. hSSAO/VAP-1-expressing cells present lower levels of proteins involved in BBB establishment. **(A)** Representative images from immunoblotting of tight-junction (ZO-1: Zonula Ocludens and Claudin-5) and adherens-junction (VE-Cadherin) protein levels at different days after confluence (DAC) in WT and hSSAO/VAP-1 endothelial cells. **(B)** Quantification at 1 DAC of ZO-1 (hSSAO/VAP-1 cells: 0.4536 ± 0.1134; unpaired T-test: p= 0.0085), VE-Cadherin (hSSAO/VAP-1 cells: 0.6754 ± 0.08871; unpaired T-test: p= 0.0064) and Claudin 5 (hSSAO/VAP-1 cells: 0.1542 ± 0.03740; unpaired T-test: p< 0.0001) protein levels versus WT cells. **(C)** Two-way ANOVA analysis from ZO-1 (significant effect of genotype [F (1, 16) = 49.60, p < 0.0001] and time [F (3, 16) = 3.367, p= 0.0448] but not for genotype x time interaction), VE-Cadherin (significant main effect of genotype [F (1, 32) = 23.80, p< 0.0001] with no-significant main effect of time, nor genotype x time interaction) and Claudin 5 (significant main effect of genotype [F (1, 32) = 134.6, p< 0.0001] with no-significant main effect of time, nor genotype x time interaction) protein levels quantification along 4 DAC in WT and hSSAO/VAP-1 endothelial cells. GAPDH was blotted as loading control protein and was used for normalization. n=3-5. Mean ±SEM. $^{\&}p \leq 0.05$, $^{\&\&}p \leq 0.01$, $^{\&\&\&}p \leq 0.001$, unpaired Student's t-test in (B). Mean ±SEM. $^{\#}p \leq 0.05$, $^{\#\#}p \leq 0.01$, $^{\#\#\#}p \leq 0.001$, two-way ANOVA analysis with Bonferroni's post-hoc test in (C).

Next, to characterize the neuron-glia mixed culture we firstly determined the proportion of astrocytes (GFAP-positive cells) and neurons (MAP2-positive cells) present in the mixed culture by immunocytochemistry. Results showed that astrocytes represented the 42.938±1.962 % of labelled nuclei whilst 57.062±1.962 % corresponded to neurons **(figure 34a)**. We also looked for microglia cells labelling with anti-OX42 but we did not detect almost any positive cell within all the analyzed images. According to these results we concluded that our mixed culture was mainly constituted by neurons and astrocytes with a despicable microglia percentage.

A

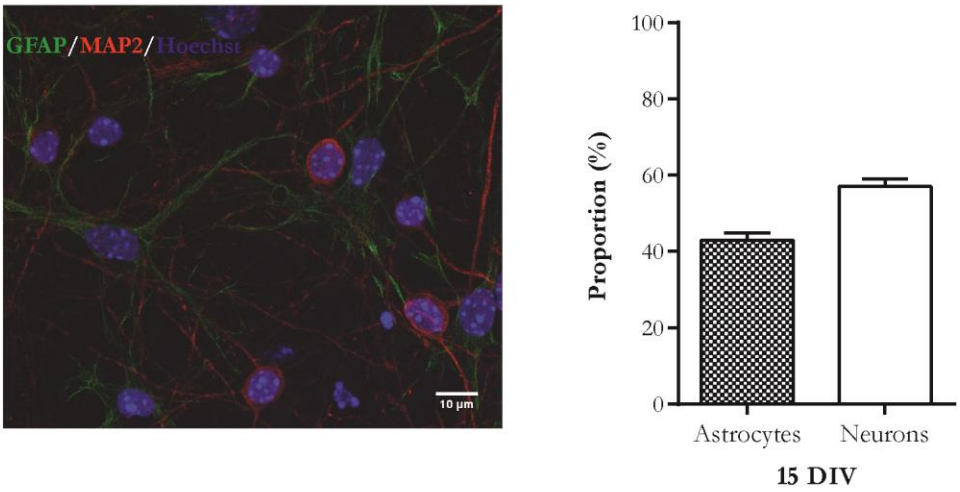
GFAP/MAP2/Hoechst
10 µm
Proportion (%)
100
80
60
40
20
0
Astrocytes
Neurons
15 DIV

B

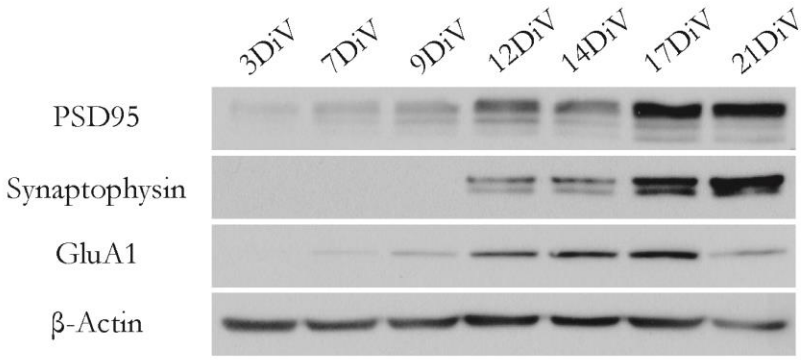
3DiV
7DiV
9DiV
12DiV
14DiV
17DiV
21DiV
PSD95
Synaptophysin
GluA1
β-Actin

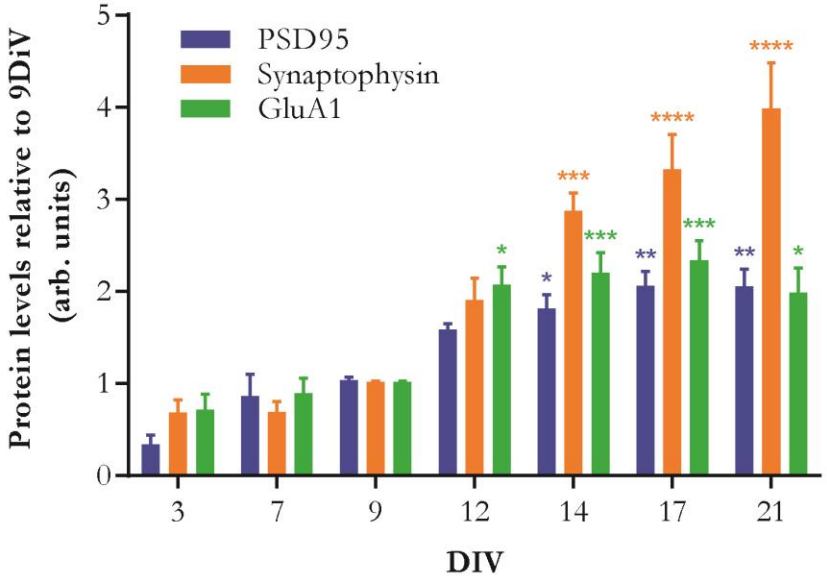
PSD95
Synaptophysin
GluA1
Protein levels relative to 9DiV (arb. units)
DIV
3
7
9
12
14
17
21

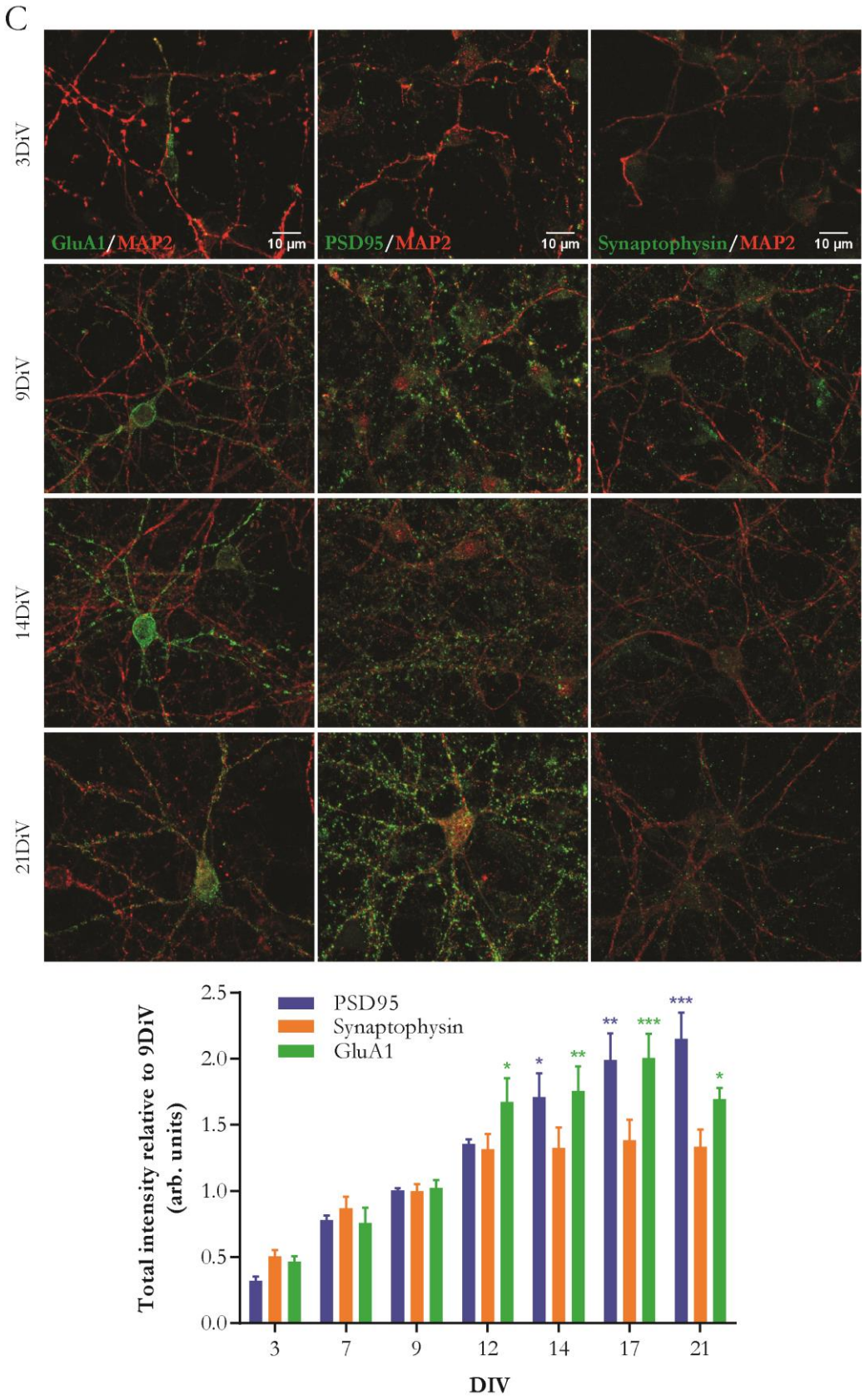

Figure 34: Neuron-glia mixed culture characterization. (A) Astrocytes (GFAP) and neurons (MAP2) proportion quantification within mixed culture, with corresponding representative immunofluorescence images. n=2. **(B)** Representative images and quantifications from immunoblot analysis of neurons' maturity focusing on PSD95, Synaptophysin and GluA1 protein levels at different DiV. Actin was blotted as loading control. **(C)** Representative images and quantifications from immunocytochemistry analysis of neurons' maturity focusing on neurites development by PSD95-, Synaptophysin- and GluA1-

immunolabeling at different DiV. MAP2-labeling was used as a reference of neurites structure. n=3-8. Scale bar: 10 μm. Mean ± SEM. *p ≤ 0.05, **p ≤ 0.01, ***p ≤ 0.001, ****p ≤ 0.0001, one-way ANOVA analysis with Bonferroni's post-hoc test.

Moreover, we followed the maturation of neural network analyzing the evolution of a pre-synaptic (synaptophysin) and post-synaptic protein marker (PSD95), together with AMPA receptor subunit GluA1 at different days in vitro by immunoblot and immunocytochemistry. Increments in their expressing levels are directly proportional to the development of cultured neurons in terms of neuritic maturity. Results showed expected increasing protein levels of the expression of these proteins as neurons developed **(figure 34b-c)**. Interestingly, there was an inflection point between 9th and 12th DiV when the protein levels increased strikingly, and since that moment they were mainly maintained, indicating they had achieved a mature stage. This observation let us conclude that by in between these timepoints neurons achieved a suitable maturational state.

Recapitulating the conclusions acquired from characterizing endothelial cells and mixed culture development, we could define the optimum day to put both parts in contact using a transwell system (see materials & methods for details). For neuron-glia mixed culture that moment would be at 9 DiV, since from that moment neurons are considered mature enough and thus we can maintain them in culture for longer. In case of microvascular endothelial cells it would be at 3 DAC because it is when the BBB is properly established attending to the pick observed for tight-junction and adherens-junction protein levels in WT endothelial cells. From this moment, each component will communicate with the other as the transwell system used has a semipermeable membrane through which molecules (angioneurins among them) would cross, mimicking *in vivo* communication processes.

In addition, to properly establish the co-culture system, serum concentration arrangements were needed to adjust on mixed culture medium, which was reduced. This adaptation was necessary to partially maintain endothelial cells conditions, as they are normally serum-deprived since they reach confluence. To corroborate that this adjustment did not alter mixed culture viability, LDH cytotoxicity assay was performed. As described in methodology section, released levels of LDH to the media are proportional to plasma membrane damage and cell death. Results showed that compared to a cytotoxic insult (1 mM glutamate: 9.251±1.289; *p<0.0001), all the conditions (+T.Ø: empty transwell, +T.WT: WT hCMEC/D3 seeded transwell and +T.SSAO: hSSAO/VAP-1 hCMEC/D3 seeded transwell) induced marginal levels of released LDH to the medium by mixed culture. Thus, we can assure that mixed culture viability was maintained despite reducing the serum concentration and besides, contrary to what we observed using conditioned mediums, implementing co-culture system did not alter neuronal viability **(figure 35a)**.

Once the system was established, we defined the treatment conditions to reproduce a CAA-AD pathological environment, which consisted in applying Aβ treatment. During the pathology, Aβ

deposits steadily accumulate in and around blood vessels triggering the degeneration of vascular wall that through different mechanisms contributes to cognitive decline. Moreover, according to the oligomer hypothesis of AD, soluble Aβ forms present synaptotoxical properties as they are able to directly damage synapses and to induce neuroinflammation and oxidative stress, eventually leading to neuronal loss and dementia (Selkoe and Hardy, 2016).

The aim of our Aβ treatment was to mimic this scenario and therefore we decided to treat endothelial cells with the vasculotropic Dutch-mutated $A\beta_{1–40}$ ($A\beta_{1\text{-}40}D$) in a manner that would make them react as in those aforementioned initial stages but without causing their death. Briefly, the $A\beta_{1\text{-}40}D$ presents an increased velocity of amyloid fibril formation (Miravalle *et al.*, 2000) and has been suggested to enhance Aβ deposition in the cerebral vasculature (Herzig *et al.*, 2004). To determine the required minimum concentration of $A\beta_{1\text{-}40}D$ allowing endothelial survival, we performed cell viability analysis. After confluence, endothelial cells were treated with increasing concentrations (0.5, 2.5, and 5 μM) of $A\beta_{1\text{-}40}D$. LDH cytotoxicity assay was carried out with medium from one day and three days after treatment and co-culture maintenance. The results showed that cell viability, for both mixed culture and endothelial cells, was not compromised **(figure 35b)**. As all three concentrations preserved cell viability, we decided to use $A\beta_{1\text{-}40}D$ 5 μM in our treatments to make sure we were able to challenge the system.

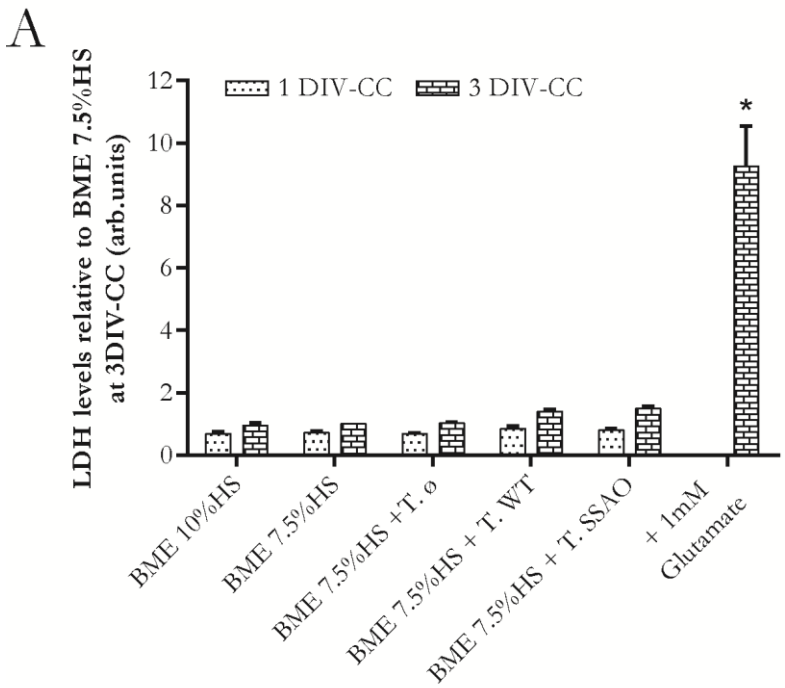

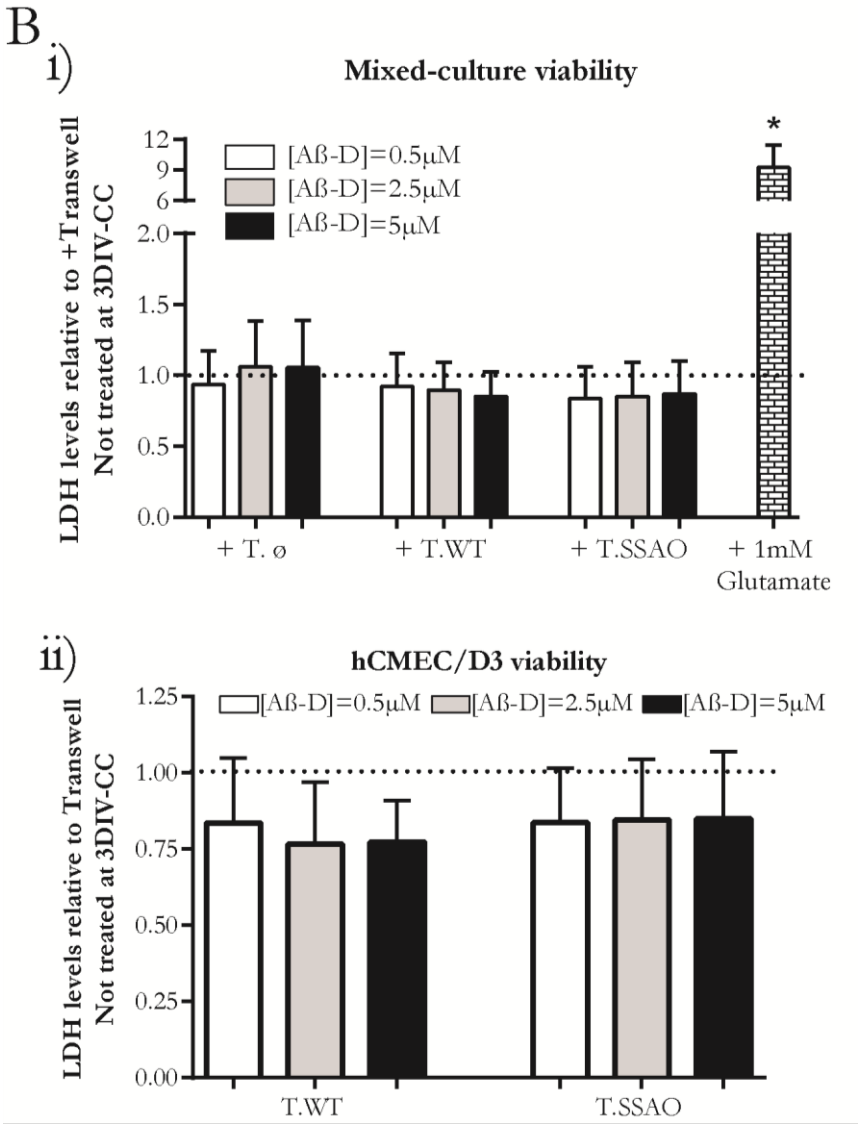

Figure 35: Viability analysis of neurovascular unit *in vitro* model. (A) LDH levels released to mixed culture medium in different medium serum percentage and co-culture conditions (T.Ø: empty transwell, T.WT: transwell seeded with WT hCMEC/D3 cells, T.SSAO: transwell seeded with hSSAO/VAP-1 hCMEC/D3 cells). n=3-8. **(B)** Determination of $A\beta_{1-40}$-D hCMEC/D3 cells-treatment concentration depending on viability impact. LDH levels released to (i) mixed culture and (ii) hCMEC/D3 cells medium from $A\beta_{1-40}$-D (0.5 µM, 2.5 µM and µM)-treatment applied into the upper chamber of co-culture system. n=5. Neuron-glia mixed culture viability was tested compared with an excitotoxic insult (1mM Glutamate). Mean ±SEM. *p ≤ 0.05, one-way ANOVA analysis with Bonferroni's post-hoc test. HS: Horse serum.

3 $A\beta_{1-40}$-D flux in the co-culture system

It was already reported that $A\beta_{1-40}$D aggregates more on SSAO/VAP-1-expressing endothelial cells than on WT ones (Solé, Miñano-Molina and Unzeta, 2015). Nevertheless this was observed in non-co-culturing conditions. Therefore we aimed to assess how $A\beta_{1-40}$D distributes between the two compartments of our co-culture *in vitro* model to determine its accumulative pattern not only in endothelial cells but also in the mixed culture.

To approach this study we first collected cell mediums and lysates from both parts of the co-culture. As an initial strategy we performed immunoblots to detect Aβ **(figure 36a)**. We quantified small Aβ

forms, such as monomer and dimer signals, together. The obtained results showed that there were no significant differences comparing $A\beta_{1-40}D$ levels between SSAO/VAP-1-expressing endothelial cells and WT ones in any of the system compartments. Remarkably, we could not detect any signal from basolateral lysates. This fact could be due to the $A\beta_{1-40}D$ elimination by cells from mixed culture through different mechanisms, like phagocytosis. Indeed, as it was described by Lee and colleagues, astrocytes can phagocytize both monomeric and oligomeric Aβ forms (Lee, Seo and Koh, 2015). Besides, comparing apical and basolateral medium samples representative images, a trend to lower $A\beta_{1-40}D$ levels was observed in apical medium from SSAO/VAP-1 cells, which could fit with higher amount in basolateral medium. This could be due to the higher BBB permeability that these cells present compared with WT ones, speculating that as tight-junctions proteins levels are decreased in hSSAO/VAP-1-expressing cells, $A\beta_{1-40}D$ could pass easily through the barrier, crossing through the semipermeable transwell insert, to the basolateral medium. Nevertheless, these observations were not ratified by their corresponding quantifications

In an attempt to clarify immunoblotting results, we decided to apply another technique to detect Aβ. We performed ELISA assay also from medium and lysate samples from both parts of the *in vitro* system **(figure 36b)**. Results from the apical lysates showed higher amount of Aβ in hSSAO/VAP-1 endothelial cells although it was not significant. In basolateral lysates, the values obtained were near the detection limit and there were no differences between conditions. On the other hand, apical medium values showed non-significant differences between WT and hSSAO/VAP-1-expressing endothelial cells, meanwhile basolateral medium quantifications showed the opposite tendency that it was obtained by immunoblot, but again it was not statistically significant.

The obtained results do not enable us to determine a precise Aβ dynamic through the endothelial cells within the co-culture system. However, this assertion implies that the effects that we could eventually observe after $A\beta_{1-40}D$ treatment in the co-culture system would probably not be related to its abundance in the lower compartment, but to the effect induced on Aβ-treated endothelial cells. Otherwise, regarding the different result obtained from that previously published (Solé, Miñano-Molina and Unzeta, 2015), they might not be comparable as those were obtained from endothelial cultures alone, without co-culture, and without using transwell inserts. In our hands, the flux between apical and basolateral compartments may be crucial to determine the distribution of Aβ within the system.

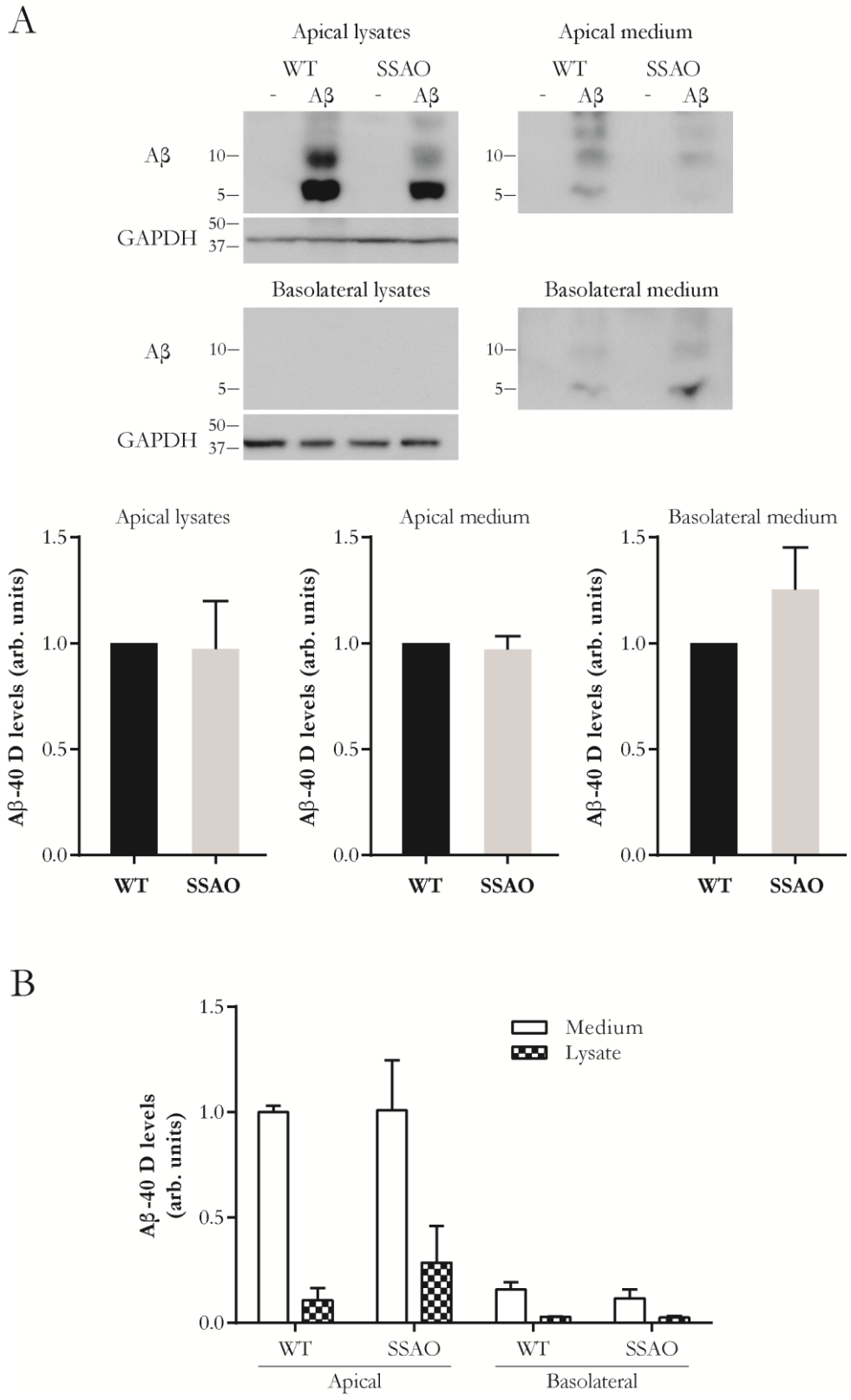

Figure 36: $A\beta_{1-40}$-D flux in the co-culture system. (A) Representative images and immunoblotting quantifications versus WT from lysates (Apical: $A\beta_{1-40}$D-treated hSSAO/VAP-1: 0.973±0.226; Basolateral: non-detected) and mediums (Apical: $A\beta_{1-40}$D-treated hSSAO/VAP-1: 0.970±0.063; Basolateral: 1.255±0.197. p=0.2078). GAPDH was blotted as loading protein control and was used for normalization. n=10-13. **(B)** ELISA quantification of $A\beta_{1-40}$-D levels in SSAO/VAP-1-expressing cells, versus WT cells apical medium, from lysates (Apical: WT: 0.106±0.059 and hSSAO/VAP-1: 0.286±0.175; Basolateral: WT: 0.029±0.001 and hSSAO/VAP-1: 0.026±0.006) and mediums (Apical: WT: 1.000±0.030 and hSSAO/VAP-1: 1.009±0.237; Basolateral: WT: 0.159±0.035 and hSSAO/VAP-1: 0.116±0.041). n=3. Apical chamber corresponds to endothelial cell seeded within the transwell insert while basolateral chamber represent the mixed culture cells seeded inside the plate well.

4 Analysis of endothelial-secreted angioneurins within NVU: BDNF

Once we established and characterized the new *in vitro* co-culture system, we used it to figure out whether angioneurins communication was affected between the NVU integrators. Angioneurins are signalling molecules that are able to simultaneously influence both vascular and neuronal network. They are angiogenic factors released at the nervous system and also neurotrophic factors with angiogenic attributes (Zacchigna, Lambrechts and Carmeliet, 2008). Among them, brain-derived neurotrophic factor (BDNF) is a crucial angioneurin for neuronal functions, including neuronal survival and synaptic maturation and plasticity (Lynch *et al.*, 2008). Although neurons are usually considered the main cell type secreting it, the fact is that large part of the BDNF found in the brain is produced by cerebral endothelial cells (Guo *et al.*, 2008; Monnier *et al.*, 2017). Data about the altered release of other endothelial-secreted trophic factors (VEGF, TGFβ-1 and NGF), molecules related with inflammatory processes (IL-6 and IL-8) and the adhesion protein VCAM1 were previously reported in hSSAO/VAP-1-expressing endothelial cells (Solé *et al.*, 2019). However, BDNF release alterations were not reported so far. Accordingly, and due to its importance for the neuronal function, we focused on determining the levels of BDNF within our NVU co-culture system to assess an eventual alteration in the regulation of its secretion by hSSAO/VAP-1 presence in vascular endothelial cells.

To quantify released amounts of human (endothelial) and mouse (mixed neuronal culture) BDNF to both apical and basolateral medium we performed multiplex assay. Results revealed that most of the BDNF present in the co-culture was released by endothelial cells, as the quantification of mouse BDNF, released by the mixed culture, was not detectable (data not shown). In addition, it was observed that the levels of BDNF released by hSSAO/VAP-1-expressing endothelial cells, in both apical and basolateral media, were significantly lower compared to those released by WT endothelial cells, either in non-co-culture **(figure 37a)** or in co-culture conditions **(figure 37b)**.

Previous studies have reported a crosstalk between SSAO/VAP-1 and Aβ (Solé, Miñano-Molina and Unzeta, 2015; Solé *et al.*, 2019). It was described due to the finding that, on one hand, the $A\beta_{1\text{-}40}D$ increased the SSAO levels and toxicity, and on the other hand, the SSAO enhanced $A\beta_{1\text{-}40}D$ deposition via activity-dependent and -independent mechanism (Solé, Miñano-Molina and Unzeta, 2015). Regarding this, to determine if reproducing such crosstalk has an effect on BDNF secretion, we treated the endothelial cells in the apical compartment with $A\beta_{1\text{-}40}D$.

The obtained results were similar to those observed in non-treated cells. Aβ-treated endothelial cells expressing hSSAO/VAP-1 released lower levels of BDNF compared to WT Aβ-treated endothelial cells, in both apical and basolateral medium either in non-co-culture **(figure 37a)** or in co-culture conditions **(figure 37b)**. Moreover, the Aβ treatment only show changes in BDNF secreted levels in

WT cells without co-culture (p=0.012*). Although not statistically significant, we also observed a decrease in BDNF release due to Aβ treatment in the apical medium of WT cells in co-culture conditions. On the other hand, treating with $A\beta_{1-40}D$ did not cause significant changes in the basolateral compartment in any of the conditions analyzed nor on the cell types. Regarding the levels of BDNF released by hSSAO/VAP-1-expressing endothelial cells we can conclude that Aβ treatment did not significantly change them, probably because they were already very low in basal conditions.

In summary, these results confirm that the presence of hSSAO/VAP-1 induces a significant decrease in BDNF release by these brain microvascular endothelial cells. Besides, through these experiments we were able to validate our NVU co-culture model and thereby, hereafter we continued the rest of the studies using this *in vitro* system.

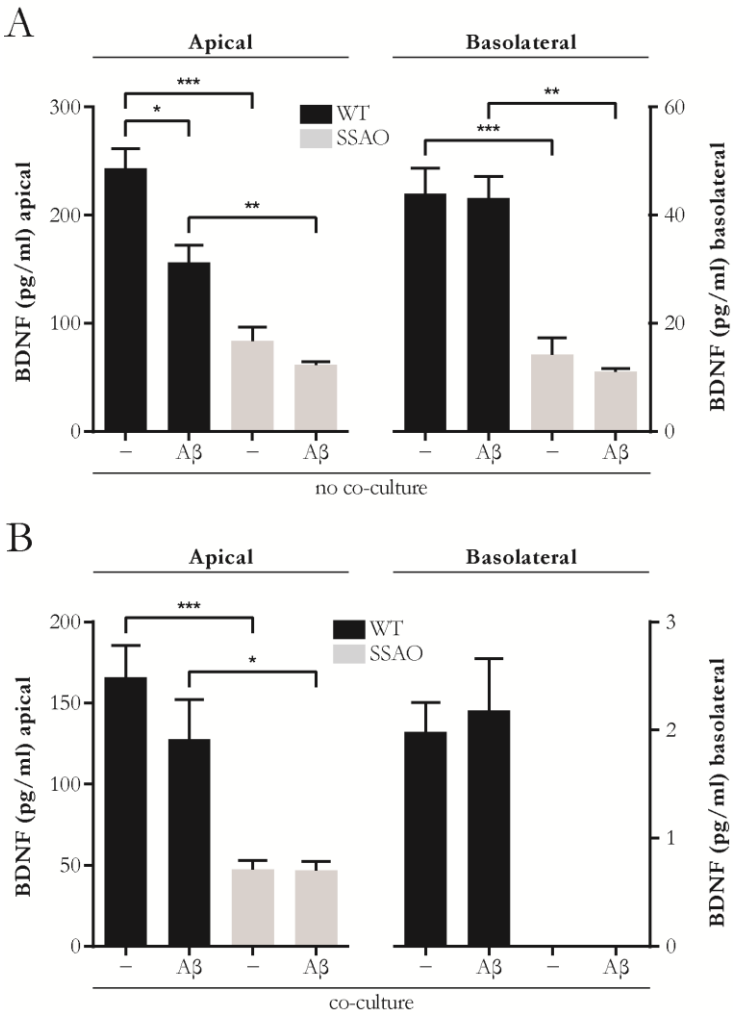

Figure 37: Reduction of BDNF release in apical and basolateral medium from hSSAO/VAP-1 hCMEC/D3 cells. (A) in no co-culture (Apical: WT, 243.318±17.997 pg/ml; Aβ-treated WT, 156.033±15.993 pg/ml; hSSAO/VAP-1, 83.616±12.861 pg/ml; Aβ-treated hSSAO/VAP-1, 61.340±3.179 pg/m and Basolateral: WT, 43.989±4.756 pg/ml; Aβ-treated WT, 43.133±4.016 pg/ml; hSSAO/VAP-1, 14.231±3.028 pg/ml; Aβ-treated hSSAO/VAP-1, 11.060±0.628 pg/ml) and **(B)** in co-culture conditions (Apical: WT, 165.857±19.630 pg/ml; Aβ-treated WT, 127.508±24.650 pg/ml; hSSAO/VAP-1, 47.373±5.653 pg/ml; Aβ-treated hSSAO/VAP-1, 46.902±5.586 pg/ml and Basolateral: WT, 1.982±0.274 pg/ml, Aβ-treated WT, 2.180±0.482 pg/ml; hSSAO/VAP-1: not detected; Aβ-treated hSSAO/VAP-1, not detected) both in basal conditions and in presence of 5μM $A\beta_{1-40}D$. n=3-9. Mean ± SEM. *p ≤ 0.05, **p ≤ 0.01, ***p ≤ 0.001, one-way ANOVA analysis with Bonferroni's post-hoc test.

5 Analysis of the effects induced by SSAO/VAP-1-expressing endothelial cells on neurons from mixed culture

The BDNF-TrkB signalling pathway contributes to critical neuronal functions and it is especially remarkable the link between the BDNF-TrkB activity and the glutamatergic system. BDNF was reported to locally control the translation of GluA1 subunits, and to promote the insertion of GluA1-containing AMPA receptors to the synaptic membrane (Leal, Comprido and Duarte, 2014). Recent reports have related the BDNF-TrkB signalling activity, and also its dysfunction in several neurodegenerative diseases such as Huntington disease, Alzheimer disease and Parkinson disease (Jin, 2020). Lately it has been also demonstrated that BDNF-TrkB pathway deficiency increases σ-secretase expression, triggering the cleavage of both APP and tau, thus boosting AD pathology (Xiang *et al.*, 2019). Moreover, dysregulation of BDNF-TrkB-associated downstream molecular pathways has been described to modulate the levels of key synaptic proteins, such as PSD95 (Yoshii and Constantine-Paton, 2014).

In this regard, since our results obtained so far showed that hSSAO/VAP-1-expressing brain microvascular endothelial cells released lower BDNF levels, we then aimed to determine the impact that this downregulation could induce on neurons within our NVU co-culture model. Furthermore, to reproduce AD-like environment, we added the Aβ-treatment condition to our experimental design to additionally study the effect of reduction of BDNF secreted levels in the presence of this vascular pathological insult. WT and hSSAO/VAP-1 co-cultures were established and endothelial cells compartments were treated with 5 μM $A\beta_{1-40}D$. Five days after treatment, co-cultures were disassembled and mixed culture cells were processed following a cellular fractionation protocol **(figure 38a)**. Total homogenate and PSD fractions were isolated to quantify PSD95 **(figure 38b)** and GluA1 protein levels **(figure 38c)**.

Analyses of PSD95 protein levels showed a significant decrease in PSD fractions only when co-cultured with $A\beta_{1-40}D$-treated hSSAO/VAP-1-expressing cells but not with WT endothelial cells neither treated or not. As previously observed, PSD95 protein levels in total homogenate fraction were not significantly altered in any condition or cell type. Regarding GluA1 results, homogenate fractions showed a significant reduction of GluA1 protein levels in $A\beta_{1-40}D$-treated hSSAO/VAP-1 endothelial cells co-culture condition compared to not treated conditions, both WT and hSSAO/VAP-1. In PSD fractions, results showed a trend but not significant decrease in GluA1 protein levels in co-cultures with $A\beta_{1-40}D$-treated hSSAO/VAP-1-expressing cells compared to $A\beta_{1-40}D$-treated WT endothelial cells co-cultures.

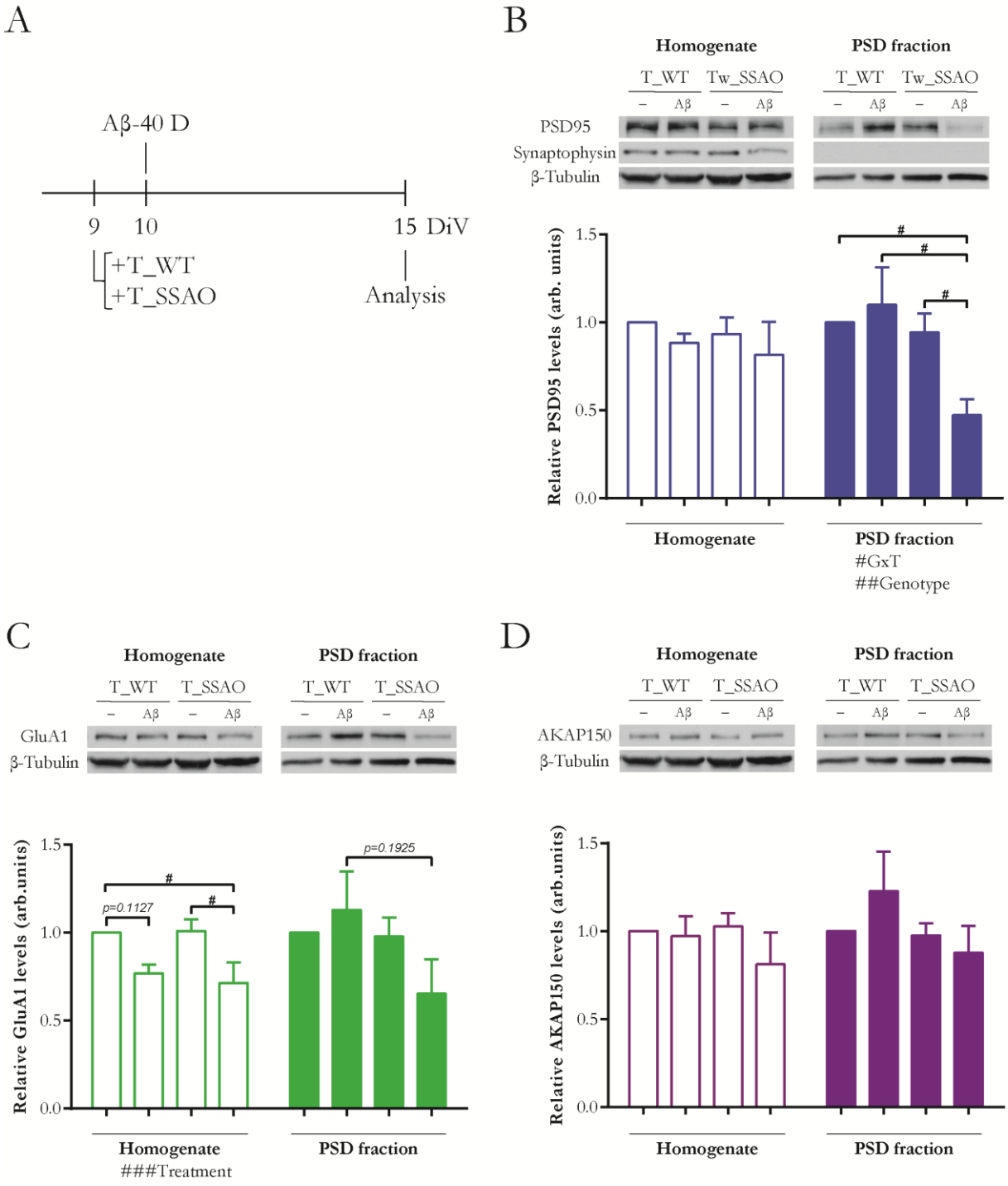

Figure 38: Synaptic protein levels reduction in Aβ-treated co-cultures with hSSAO/VAP-1 hCMEC/D3 endothelial cells. (A) Experimental scheme. Co-culture was set up when neuron-glia mixed culture was at 9DiV. Next day 5μM $Aβ_{1-40}D$ treatment was introduced and the system was maintained until 15 DiV when cell lysates were collected to perform cellular subfractionation. (B-D) Representative images and quantifications from immunoblotting analysis to determine protein levels in homogenate and PSD (post-synaptic density) fractions after cellular subfractionation of **(B)** PSD95 (Homogenate: $Aβ_{1-40}D$-treated WT-CC, 0.884±0.051; not-treated hSSAO/VAP-1-CC, 0.934±0.096 and $Aβ_{1-40}D$-treated hSSAO/VAP-1-CC: 0.817±0.188. PSD fraction: $Aβ_{1-40}D$-treated WT-CC, 1.101±0.213; not-treated hSSAO/VAP-1-CC, 0.943±0.108 and $Aβ_{1-40}D$-treated hSSAO/VAP-1-CC: 0.473±0.091. Also in PSD fraction, a two-way ANOVA of genotype and treatment revealed significant main effect of genotype [F (1, 22)=9.603, p= 0.0052] and genotype x treatment interaction [F (1, 22)=6.671, p=0.0170], with no-significant main effect of treatment [F (1, 22)=2.788, p=0.1092]). **(C)** GluA1 (Homogenate: $Aβ_{1-40}D$-treated WT-CC, 0.769±0.050; not-treated hSSAO/VAP-1-CC, 1.010±0.066 and $Aβ_{1-40}D$-treated hSSAO/VAP-1-CC, 0.714±0.118. Also in homogenate, a two-way ANOVA of genotype and treatment revealed significant main effect of treatment [F (1, 22)=16.70, p=0.0005] with no-significant main effect of treatment, nor genotype x treatment interaction. PSD fraction: $Aβ_{1-40}D$-treated WT-CC, 1.129±0.220; not-treated hSSAO/VAP-1-CC, 0.978±0.109 and $Aβ_{1-40}D$-treated hSSAO/VAP-1-CC, 0.654±0.195). **(D)** AKAP150 (Homogenate: $Aβ_{1-40}D$-treated WT-CC, 0.971±0.113: not-treated hSSAO/VAP-1-CC, 1.029±0.075 and $Aβ_{1-40}D$-

treated hSSAO/VAP-1-CC, 0.811±0.180. PSD fraction: $A\beta_{1-40}D$-treated WT-CC, 1.228±0.225; not-treated hSSAO/VAP-1-CC, 0.976±0.068 and $A\beta_{1-40}D$-treated hSSAO/VAP-1-CC: 0.877±0.152). Synaptophysin was blotted to verify the correct purification of PSD fraction. β-Tubulin was blotted as loading control protein and was used for normalization. n=4-9. Mean ± SEM. $^{\#}p \leq 0.05$, two-way ANOVA analysis with Bonferroni's post-hoc test.

Previous work from our group showed that Aβ oligomers induce the removal of AMPA receptors from cell surface of cultured neurons (Miñano-Molina *et al.*, 2011). Interestingly, recent data indicates that Aβ oligomers induce also the degradation of the scaffolding protein A-kinase anchoring protein (AKAP) 150 (AKAP150) in hippocampal-cultured neurons, altering AMPAR trafficking by affecting its endocytosis (Miñano-Molina, Cheng and Rodríguez-Alvarez; unpublished). As the interaction between AKAP150 and AMPA receptors is mediated by PSD95 (Bhattacharyya *et al.*, 2009) and considering our obtained results, we decided to examine AKAP150 protein levels to assess if they could become also affected in our experimental conditions **(figure 38d)**. According to the aforementioned previous data, we initially expected to find a reduction in AKAP150 protein levels as observed for PSD95 and GluA1. However, AKAP150 protein levels were not significantly reduced in either total homogenate fractions or PSD fractions in any assayed condition.

To further explore structural changes, we further performed immunocytochemistry assays from co-cultured neuron-glia mixed cells to analyze neurites and synapses. We studied the same experimental conditions, using the co-culture *in vitro* model treated on its endothelial compartment with 5μM $A\beta_{1-40}D$ for 5 days prior fixation.

We determined GluA1 and PSD95 levels by confocal microscopy. The obtained results for GluA1 immunoreactivity at neurites **(figure 39a)** showed significant changes for treatment condition, meanwhile PSD95 labeling at neurites was not significantly altered **(figure 39d)**. To assess whether their levels were specifically altered at PSD zone (PSD particles) we analyzed their labeling in PSD95 clusters. However, we neither observed changes between experimental conditions **(figure 39b and e)**. Finally we also quantified PSD95 cluster area and PSD95 punctae number at neurites to find out whether the PSD zone area and its abundance were altered. The obtained results did not show significant differences between co-culture or any treatment condition for neither of them **(figure 39c and f, respectively)**.

Regarding the obtained results, we hypothesize that results might be biased because all the images were taken from the most intense kind of cells of each condition. Due to the needed laser setting to get the images, only the neurons with higher intensities resisted such laser requirements and were those used for following quantification. Consequently, we cannot conclude whether there were significant synaptic structural changes in neurons from mixed cultures as we just analyzed a subpopulation of cells.

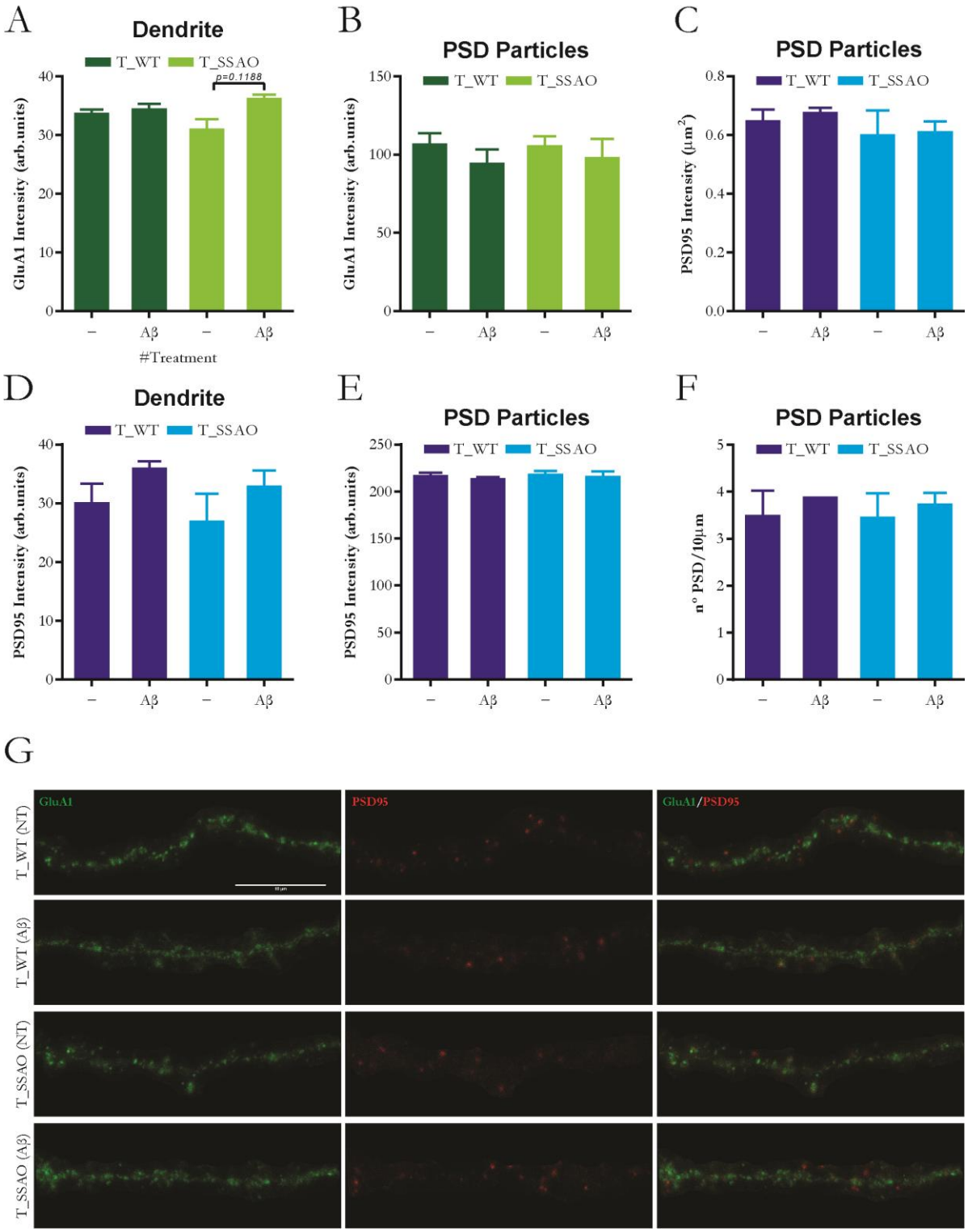

Figure 39: GluA1 and PSD95 immunocytochemical analysis from neurites crops did not show significant synaptic alterations due to co-culture or in 5µM $A\beta_{1-40}$D treatment conditions. (A) GluA1 quantification from whole neurite-signalling. **(B)** GluA1 quantification from PSD particles-signalling. **(C)** PSD particles area defined by PSD95-labelling. **(D)** PSD95 quantification from whole dendrite-signalling. **(E)** PSD95 quantification from PSD particles-signalling. **(F)** Number of PSD particles per 10 µm dendrite, defined by PSD95-labelling. **(G)** Representative images. Scale bar: 10 µm. n=29-48 dendrites per condition from three independent experiments. Mean ± SEM. $^{\#}p \leq 0.05$, by two-way ANOVA analysis with post-hoc Bonferroni's test.

Based on this experiment, from acquired confocal microscopy images we observed different types of neurons according to their GluA1-labeling intensity. Accordingly, we started to study these

differences within the mixed culture population to check whether there were changes between our experimental conditions that we were missing if we focused only on the shiniest neurons subpopulation.

To address this, we first defined non-treated WT co-culture (WT-CC) as the basal condition. Then, after measuring the intensity of all GluA1-labeled neurons from the basal condition we established the intensity criteria for classifying subpopulations (see materials & methods for details). Basically, classified neurons into three subpopulations (Type I: low intensity, Type II: medium intensity and Type III: high intensity), being thresholds between them the 25th and the 75th percentile values from the basal condition. Afterwards, we measured and classified the intensities of GluA1-positive cells from all experimental conditions. Finally, we performed mathematical analyses to assess whether changes in response to our treatment conditions were observed in different parameters as i) the cell percentage of each intensity type, ii) the intensity contribution of each subpopulation to the global population intensity, and iii) the mean intensity of each subpopulation. Initially we performed these analyses for GluA1 staining and then we extended them for PSD95 and AKAP150.

As we can see from our results, the analysis of cellular percentage of each intensity type showed that co-cultures containing Aβ-treated SSAO/VAP-1-expressing cells displayed a reduction in the number of Type III neurons, compared to basal condition, that was significant for GluA1 **(figure 40a)** and PSD95 **(figure 41a)** but not for AKAP150 **(figure 42a)**, probably due to the deviation. Specifically for GluA1, the number of Type III neurons was also reduced as consequence of Aβ treatment independently. Moreover, the percentage analysis showed as well that Aβ-treated SSAO/VAP-1-expressing cells co-cultures also induced a tendency to increase the number of Type I neurons that was significant only for PSD95 protein. This increase in Type I fits with the decrease in Type III, suggesting that co-cultures constituted by Aβ-treated SSAO/VAP-1-expressing cells induce the redistribution of types of neurons in detriment to the Type III cells.

On the other hand, the intensity contribution of each subpopulation to the global population intensity is an important parameter because it represents how the amount of labeling is affected. It means that changes would indicate that the affected subpopulations present altered levels (higher or lower) of immunolabeled markers. Regarding the obtained results from intensity contribution analysis we could observe that, compared with basal condition, co-culturing with Aβ-treated hSSAO/VAP-1-expressing cells significantly decreased the intensity contribution of Type III neurons for GluA1 **(figure 40b)** and PSD95 **(figure 41b)**. For AKAP150 **(figure 42b)**, there was also a reduction but not statistically significant. In parallel, we observed that Aβ-treated SSAO/VAP-1-expressing cells co-cultures showed a tendency to increase Type I neurons intensity contribution that was significant just for PSD95 protein.

Besides, with respect to the results from the analysis of the mean intensity of each subpopulation, we observed that there were no differences between conditions for any of the analyzed markers (GluA1, **figure 40c**; PSD95 **figure 41c**; AKAP150 **figure 42c**). This means that the mean value of all the neurons classified as each type was maintained for all the co-culture conditions. This result is particularly interesting as it indicates that there is not a general reduction in intensity labeling, but an affectation of a precise group of cells.

Altogether, considering the relationship between intensity and abundance of the immunolabeled marker, we could suggest that Aβ-treated SSAO/VAP-1-expressing cells induce a significant decrease in the number of the co-cultured neurons presenting a higher abundance of GluA1 and PSD95. Furthermore, those neurons with higher amounts that remained, contributed with less intensity to the total intensity of the culture, therefore we could speculate the loss of the immunolabeled markers on those cells.

In relation to the obtained results, and considering that AKAP protein is not only present in excitatory synapses (Sanderson and Dell'Acqua, 2011), but also it plays a role in inhibitory ones (Dacher *et al.*, 2013), we performed vGlut1 and AKAP150 co-labeling immunocytochemistry to analyze the percentage of vGlut1-positive neurons within AKAP150 population. Consequently, we would assess the number of AKAP150 neurons involved on excitatory synapses. We measured vGlut1 intensity values applying ROIs from AKAP-positive cells. Although obtained results did not show significant differences, there was a tendency for Aβ-treated SSAO/VAP-1-expressing cells to reduce the amount of Type II and Type III vGlut1-positive AKAP150-labeled neurons **(figure 43)**, compared with the basal condition. This result suggests that Aβ-treated SSAO/VAP-1-expressing cells might induce a reduction in Type II and III AKAP cells, particularly in excitatory ones.

Collectively, all these results let us conclude that, as we previously observed in cellular fractionation experiments, there is a significant reduction in PSD95 and GluA1 levels in neurons co-cultured with Aβ-treated SSAO/VAP-1-expressing cells. This lead us hypothesize that SSAO/VAP-1-expressing endothelial cells could induce some sensitization to co-cultured neurons that would became critical in front of an aversive stimulus such as Aβ presence. This sensitization could be due to the reduction in levels of BDNF release observed in SSAO/VAP-1-expressing endothelial cells.

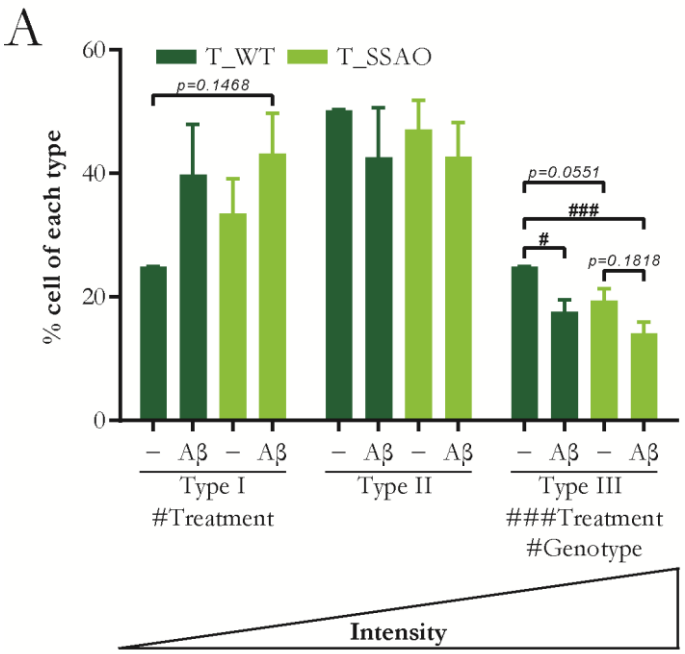
A
T_WT
T_SSAO
% cell of each type
60
40
20
0
p=0.1468
p=0.0551
###
#
p=0.1818
– Aβ – Aβ
Type I
#Treatment
– Aβ – Aβ
Type II
– Aβ – Aβ
Type III
###Treatment
#Genotype
Intensity

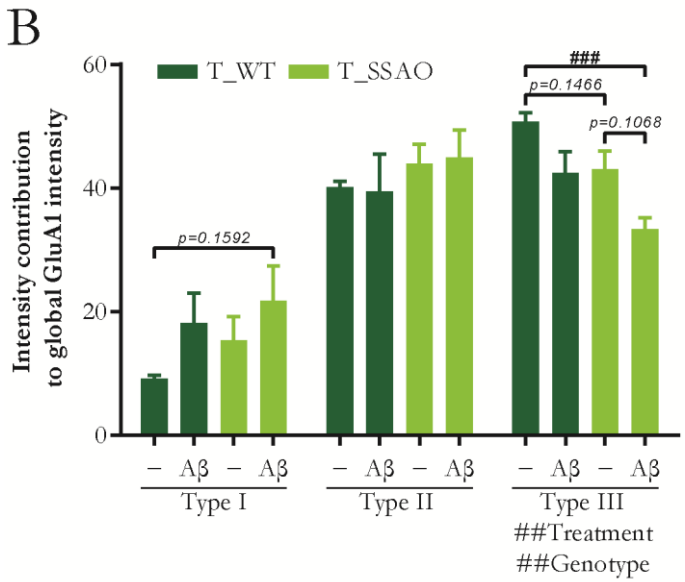
B
T_WT
T_SSAO
Intensity contribution
to global GluA1 intensity
60
40
20
0
###
p=0.1466
p=0.1068
p=0.1592
– Aβ – Aβ
Type I
– Aβ – Aβ
Type II
– Aβ – Aβ
Type III
##Treatment
##Genotype

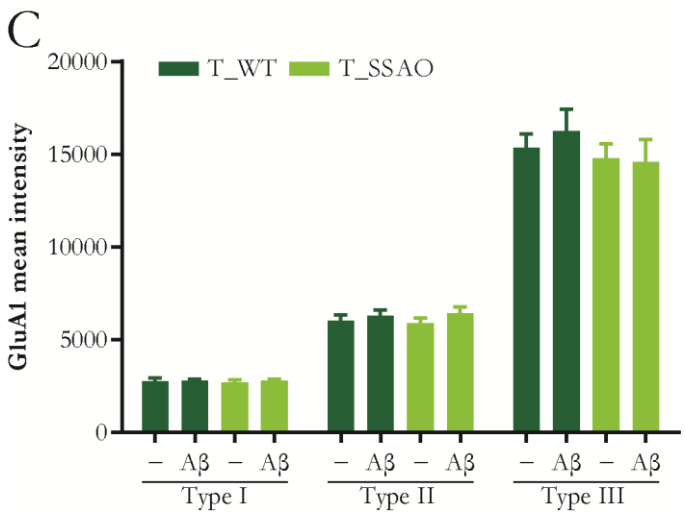
C
T_WT
T_SSAO
GluA1 mean intensity
20000
15000
10000
5000
0
– Aβ – Aβ
Type I
– Aβ – Aβ
Type II
– Aβ – Aβ
Type III

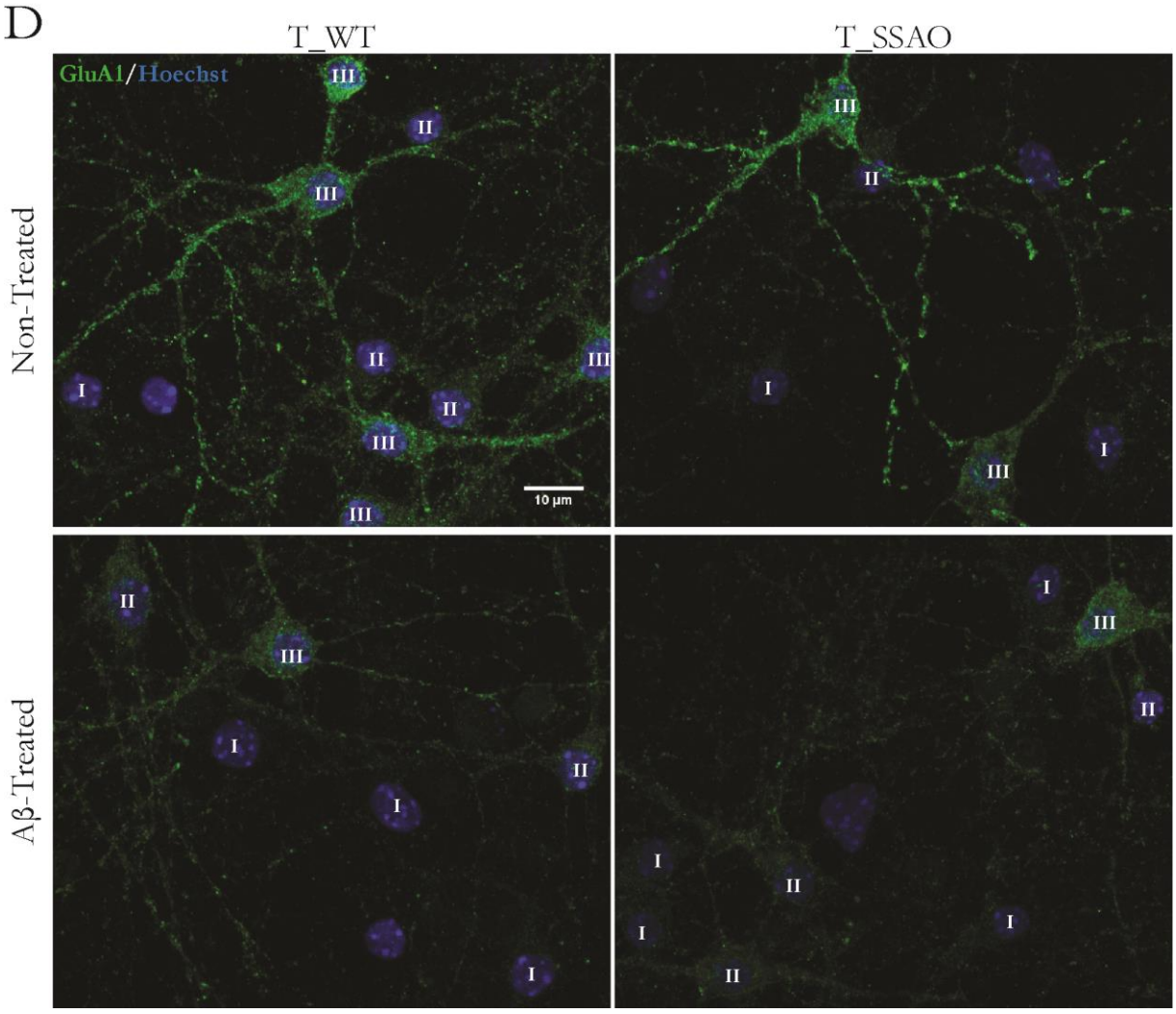

Figure 40: The amount and the intensity of GluA1-labeled neurons classified as high intensity cells is reduced in hSSAO/VAP-1 hCMEC/D3 5µM Aβ-treated co-cultures. (A) Cellular percentage of each intensity type, from low (Type I: non-treated WT-CC, 24.889±0.059 %; $A\beta_{1\text{-}40}$D-treated WT-CC, 39.783±8.187 %; non-treated hSSAO/VAP-1-CC, 33.490±5.628 % and $A\beta_{1\text{-}40}$D-treated hSSAO/VAP-1-CC, 43.187±6.556 %. A two-way ANOVA of genotype and treatment revealed significant main effect of treatment [F (1, 24)=5.205, p=0.0317] with non-significant main effect of genotype, nor genotype x treatment interaction) to high (Type III: non-treated WT-CC, 24.889±0.059 %; $A\beta_{1\text{-}40}$D-treated WT-CC, 17.615±1.964 %; non-treated hSSAO/VAP-1-CC, 19.400±1.912 % and $A\beta_{1\text{-}40}$D-treated hSSAO/VAP-1-CC, 14.123±1.798 %. A two-way ANOVA of genotype (co-culture with WT or hSSAO/VAP-1) and treatment (not treated or $A\beta_{1\text{-}40}$D-treated) revealed significant main effect of treatment [F (1, 24)=14.99, p=0.0007] and genotype [F (1, 24)=7.675, p=0.0106] with non-significant main effect of genotype x treatment interaction [F (1, 24)=0.3796, p=0.5436]). **(B)** Intensity contribution of each type to the total population intensity (Type I: non-treated WT-CC, 9.152±0.582 %; $A\beta_{1\text{-}40}$D-treated WT-CC, 18.152±4.858 %; non-treated hSSAO/VAP-1-CC, 15.373±3.838 % and $A\beta_{1\text{-}40}$D-treated hSSAO/VAP-1-CC; 21.754±5.642 %. Type III: non-treated WT-CC, 50.725±1.433 %; $A\beta_{1\text{-}40}$D-treated WT-CC, 42.425±3.466 %; non-treated hSSAO/VAP-1-CC, 43.001±3.026 % and $A\beta_{1\text{-}40}$D-treated hSSAO/VAP-1-CC, 33.320±1.872 %. Also in Type III, a two-way ANOVA of genotype (co-culture with WT or hSSAO/VAP-1) and treatment (not treated or $A\beta_{1\text{-}40}$D-treated) revealed significant main effect of treatment [F (1, 24)=11.16, p=0.0027] and genotype [F (1, 24)=9.778, p=0.0046] with non-significant main effect of genotype x treatment interaction [F (1, 24)=0.06592, p=0.7996]). **(C)** Mean intensity of each type. **(D)** Representative images. Scale bar: 10 µm. n=5-9. Mean ± SEM. $^{\#}p \leq 0.05$, $^{\#\#}p \leq 0.01$, $^{\#\#\#}p \leq 0.001$, by two-way ANOVA analysis with Bonferroni's post-hoc test.

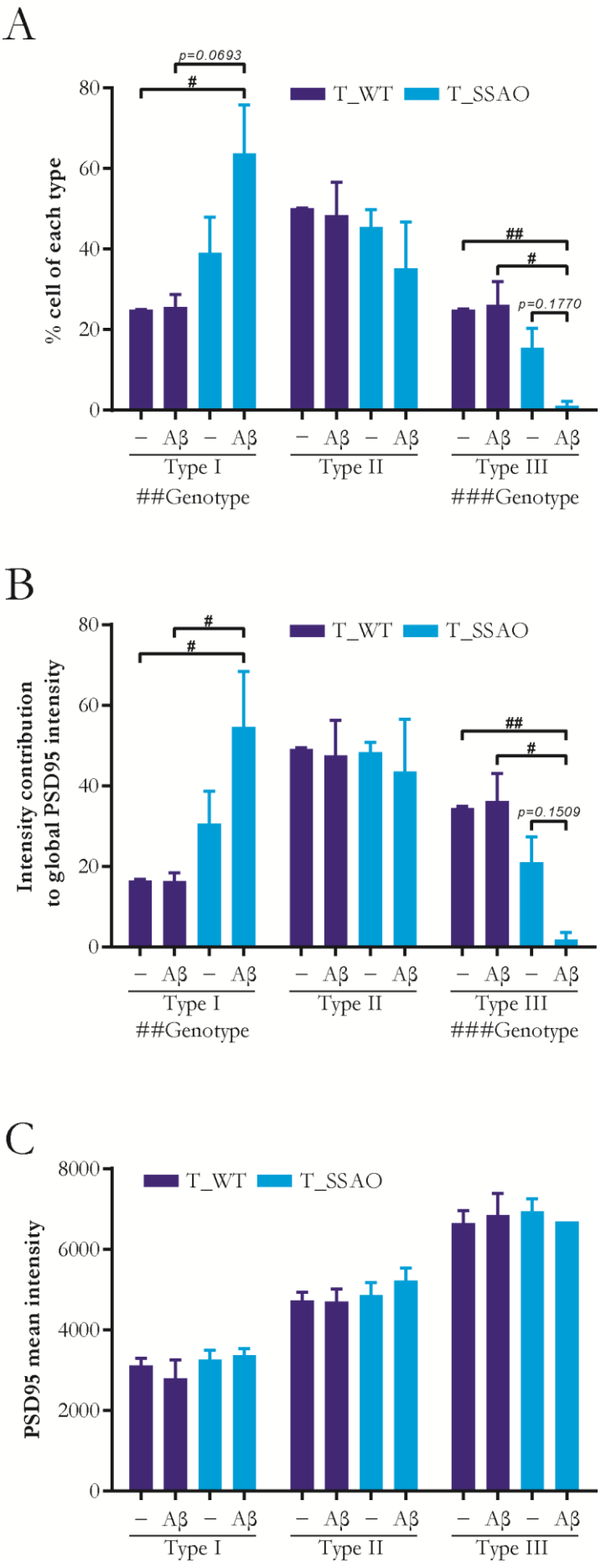
A
p=0.0693
#
T_WT
T_SSAO
% cell of each type
80
60
40
20
0
##
#
p=0.1770
– Aβ – Aβ
Type I
##Genotype
– Aβ – Aβ
Type II
– Aβ – Aβ
Type III
###Genotype
B
#
#
T_WT
T_SSAO
Intensity contribution to global PSD95 intensity
80
60
40
20
0
##
#
p=0.1509
– Aβ – Aβ
Type I
##Genotype
– Aβ – Aβ
Type II
– Aβ – Aβ
Type III
###Genotype
C
T_WT
T_SSAO
PSD95 mean intensity
8000
6000
4000
2000
0
– Aβ – Aβ
Type I
– Aβ – Aβ
Type II
– Aβ – Aβ
Type III

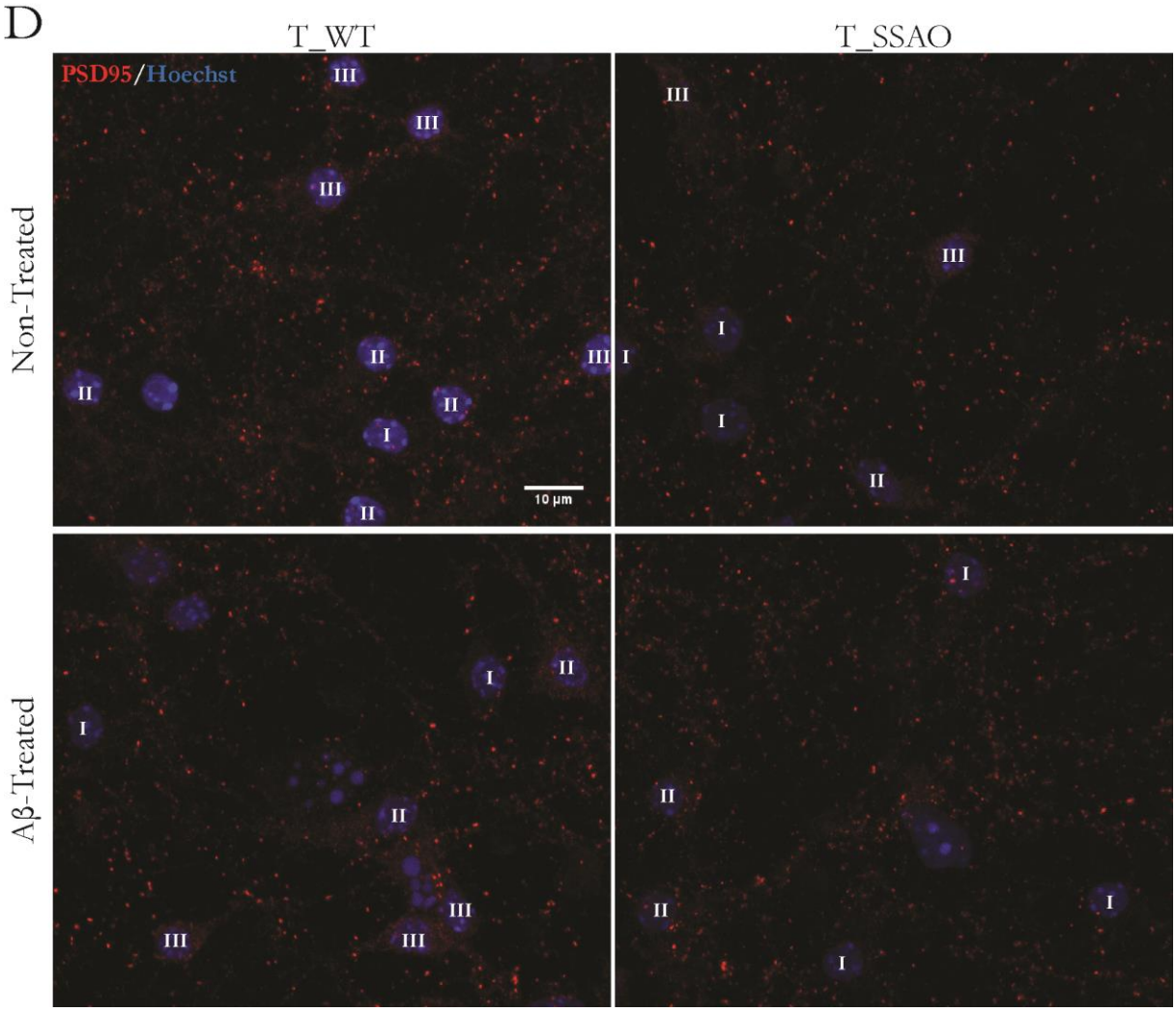

Figure 41: hSSAO/VAP-1 hCMEC/D3 5µM Aβ-treated co-culture reduces the amount and the intensity of PSD95-labeled neurons classified as high intensity cells. (A) Cellular percentage of each intensity type, from low (Type I: non-treated WT-CC, 24.920±0.093 %; $A\beta_{1-40}$D-treated WT-CC, 25.549±3.185 %; non-treated hSSAO/VAP-1-CC, 39.049±8.936 % and $A\beta_{1-40}$D-treated hSSAO/VAP-1-CC, 63.711±12.141 %. A two-way ANOVA of genotype and treatment revealed significant main effect of genotype [F (1, 16)= 10.68, p=0.0048] with no-significant main effect of treatment, nor genotype x treatment interaction) to high (Type III: non-treated WT-CC, 24.988±0.083 %; $A\beta_{1-40}$D-treated WT-CC, 26.096±5.826 %; non-treated hSSAO/VAP-1-CC, 15.456±4.885 % and $A\beta_{1-40}$D-treated hSSAO/VAP-1-CC, 1.093±1.093 %. A two-way ANOVA of genotype (co-culture with WT or hSSAO/VAP-1) and treatment (not treated or $A\beta_{1-40}$D-treated) revealed significant main effect of genotype [F (1, 16)=16.51, p=0.0009] with non-significant main effect of treatment [F (1,16)=2.432, p=0.1384], nor genotype x treatment interaction [F (1, 16)=3.314, p=0.0874]). **(B)** Intensity contribution of each type to the total population intensity (Type I: non-treated WT-CC, 16.431±0.374 %; $A\beta_{1-40}$D-treated WT-CC, 16.292±2.144 %; non-treated hSSAO/VAP-1-CC, 30.654±8.013 % and $A\beta_{1-40}$D-treated hSSAO/VAP-1-CC, 54.655±13.713 %. Also in Type I, a two-way ANOVA of genotype (co-culture with WT or hSSAO/VAP-1) and treatment (not treated or $A\beta_{1-40}$D-treated) revealed significant main effect of genotype [F (1, 16)=12.04, p=0.0032] with non-significant main effect of treatment nor genotype x treatment interaction. Type III: non-treated WT-CC, 34.424±0.524 %; $A\beta_{1-40}$D-treated WT-CC, 36.158±6.941 %; non-treated hSSAO/VAP-1-CC, 20.975±6.382 % and $A\beta_{1-40}$D-treated hSSAO/VAP-1-CC, 1.777±1.777 %. Also in Type III, a two-way ANOVA of genotype (co-culture with WT or hSSAO/VAP-1) and treatment (not treated or $A\beta_{1-40}$D-treated) revealed significant main effect of genotype [F (1, 16)=18.93, p=0.0005] with non-significant main effect of treatment [F (1,16)=2.524, p=0.1317], nor genotype x treatment interaction [F (1, 16)=3.626, p=0.0750]). **(C)** Mean intensity of each type. **(D)** Representative images. Scale bar: 10 µm. n=3-7. Mean ± SEM. $^{\#}p \leq 0.05$, $^{\#\#}p \leq 0.01$, by two-way ANOVA analysis with Bonferroni's post-hoc test.

A

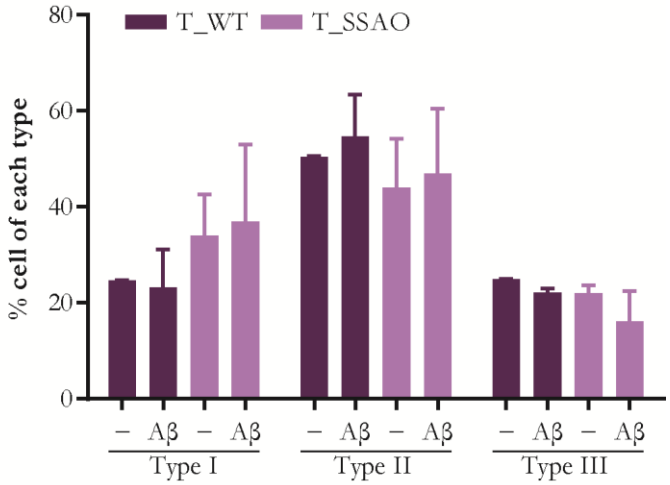
T_WT
T_SSAO
% cell of each type
80
60
40
20
0
– Aβ – Aβ
Type I
– Aβ – Aβ
Type II
– Aβ – Aβ
Type III

B

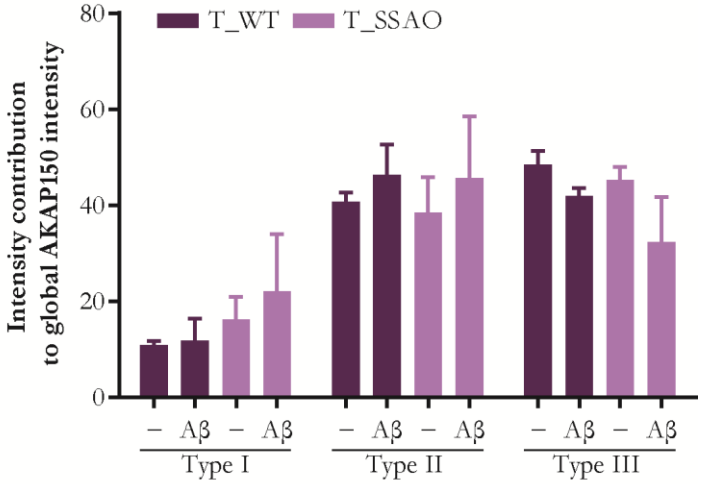
T_WT
T_SSAO
Intensity contribution to global AKAP150 intensity
80
60
40
20
0
– Aβ – Aβ
Type I
– Aβ – Aβ
Type II
– Aβ – Aβ
Type III

C

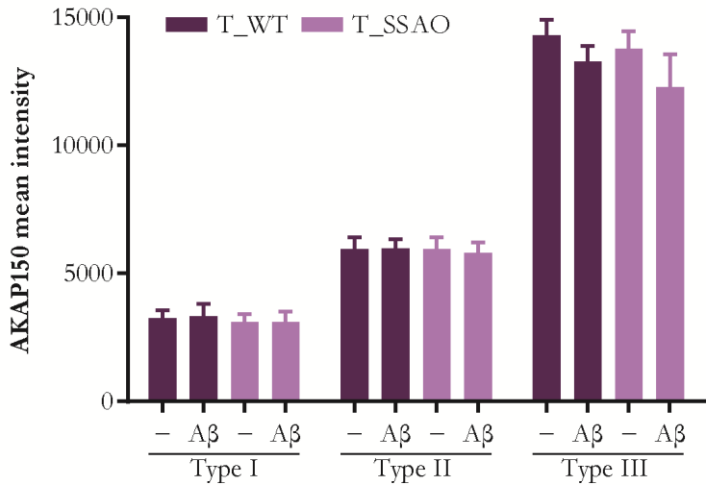
T_WT
T_SSAO
AKAP150 mean intensity
15000
10000
5000
0
– Aβ – Aβ
Type I
– Aβ – Aβ
Type II
– Aβ – Aβ
Type III

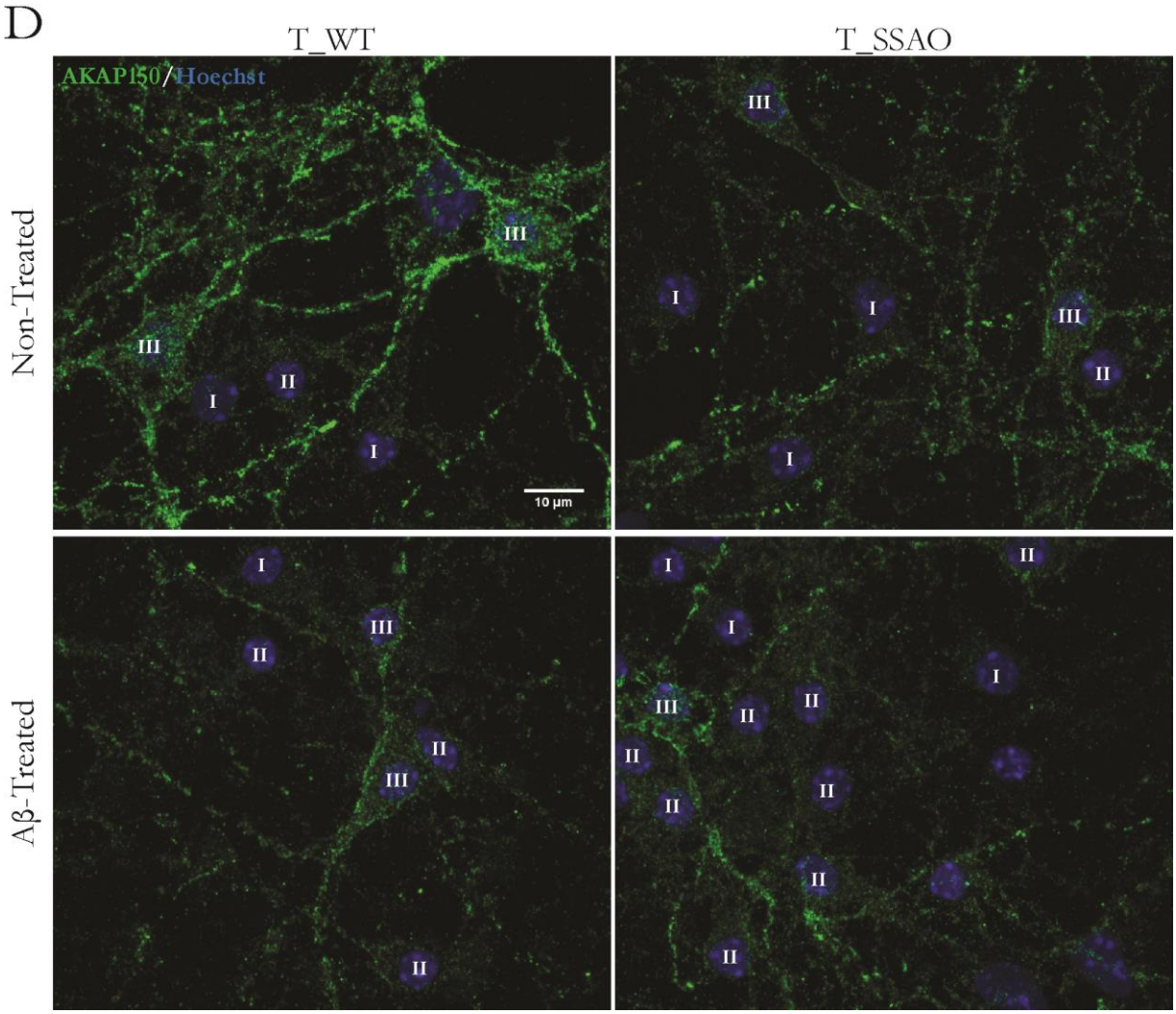

Figure 42: hSSAO/VAP-1 hCMEC/D3 5µM Aβ-treated co-culture trends to reduce the amount and the intensity of AKAP150-labeled neurons classified as high intensity cells. (A) Cellular percentage of each intensity type, from low (Type I: non-treated WT-CC, 24.677±0.075 %; $A\beta_{1\text{-}40}$D-treated WT-CC, 23.173±7.983 %; non-treated hSSAO/VAP-1-CC, 34.035±8.624 % and $A\beta_{1\text{-}40}$D-treated hSSAO/VAP-1-CC, 36.989±16.025 %) to high (Type III: not-treated WT-CC, 24.868±0.148 %; $A\beta_{1\text{-}40}$D-treated WT-CC, 22.155±0.873 %; non-treated hSSAO/VAP-1-CC, 21.998±1.631 % and $A\beta_{1\text{-}40}$D-treated hSSAO/VAP-1-CC, 16.139±6.377 %). **(B)** Intensity contribution of each type to the total population intensity (Type I: non-treated WT-CC, 10.895±0.779 %; $A\beta_{1\text{-}40}$D-treated WT-CC, 11.748±4.712%; non-treated hSSAO/VAP-1-CC, 16.233±4.757 % and $A\beta_{1\text{-}40}$D-treated hSSAO/VAP-1-CC, 22.028±12.023 %. Type III: non-treated WT-CC, 48.437±2.834 %; $A\beta_{1\text{-}40}$D-treated WT-CC, 41.940±1.676 %; non-treated hSSAO/VAP-1-CC, 45.313±2.694 % and $A\beta_{1\text{-}40}$D-treated hSSAO/VAP-1-CC, 32.279±9.436 %). **(C)** Mean intensity of each type. **(D)** Representative images. Scale bar: 10 µm. n=3. Mean ± SEM, by two-way ANOVA analysis with Bonferroni's post-hoc test.

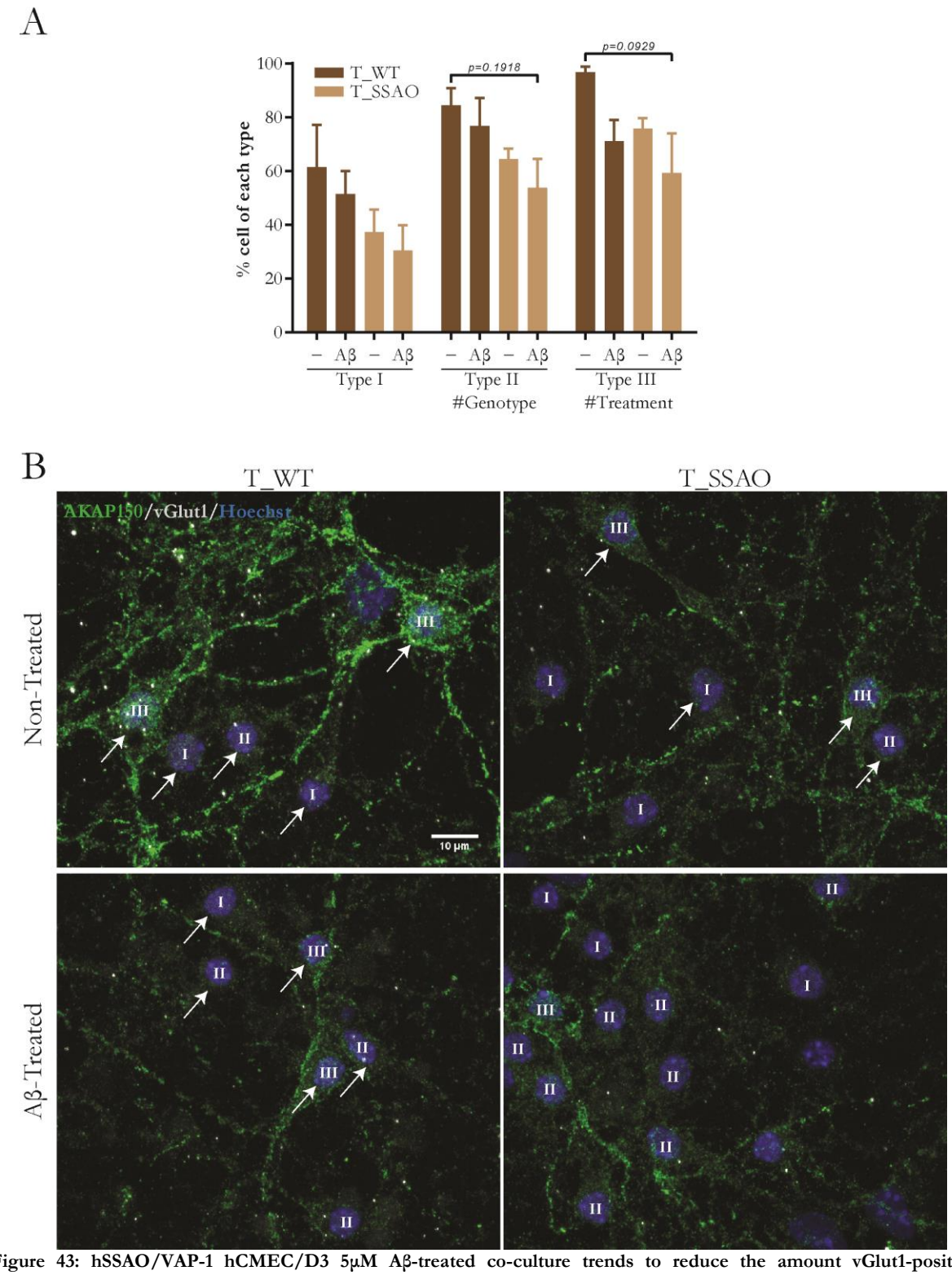

Figure 43: hSSAO/VAP-1 hCMEC/D3 5µM Aβ-treated co-culture trends to reduce the amount vGlut1-positive AKAP150-labeled neurons classified as intermediate and high intensity cells. (A) Cellular percentage of each intensity type (Type II: non-treated WT-CC, 84.373±6.515 %; $A\beta_{1\text{-}40}$D-treated WT-CC, 76.793±10.312 %; non-treated hSSAO/VAP-1-CC, 64.337±3.988 % and $A\beta_{1\text{-}40}$D-treated hSSAO/VAP-1-CC, 53.807±10.640 %. A two-way ANOVA of genotype (co-culture with WT or hSSAO/VAP-1) and treatment (not treated or $A\beta_{1\text{-}40}$D-treated) revealed significant main effect of genotype [F (1, 8)=6.661, p=0.0326] with non-significant main effect of treatment, nor genotype x treatment interaction. Type III: non-treated WT-CC, 96.775±1.977 %; $A\beta_{1\text{-}40}$D-treated WT-CC, 71.016±7.975 %; non-treated hSSAO/VAP-1-CC, 75.676±3.967 % and $A\beta_{1\text{-}40}$D-treated hSSAO/VAP-1-CC, 59.213±14.739 %. A two-way ANOVA of genotype and treatment from neurons classified as high intensity group revealed significant main effect of treatment [F (1, 8)=5.933, p=0.0408] and a tendency for genotype [F (1, 8)=3.603, p=0.0943], but non-significant main effect of genotype x treatment interaction). **(B)** Representative images. Roman numbers indicate AKAP150-labeled neurons intensity type. Arrowheads indicate vGlut1-positive cells. Scale bar: 10 µm. n=3. Mean ± SEM. $^{\#}p \leq 0.05$, by two-way ANOVA analysis with Bonferroni's post-hoc test.

6 Evaluation of the role of BDNF in SSAO/VAP-1- and Amyloid-β-mediated effects on co-cultured neurons

Among the different molecules and signaling factors classified as angioneurins, BDNF has a special relevance for neurons, as it is involved in plasticity, neuronal survival, growth and differentiation (Jin, 2020). Alterations in the BDNF-TrkB downstream molecular pathways have been previously reported to affect the levels of critical synaptic proteins like PSD95 and GluA1 (Leal, Comprido and Duarte, 2014; Yoshii and Constantine-Paton, 2014). Considering this along with our previous results showing a decrease in BDNF levels due to the presence of SSAO/VAP-1 **(figure 37)**, we wondered if such BDNF reduction is the responsible of the effects observed on synaptic proteins.

The first approach to assess the role of BDNF on the neuronal affectation consisted on reproducing the decrease on its levels. From our obtained results, the condition involving co-culture with Aβ-treated SSAO/VAP-1 cells was the one that induced more relevant changes in synaptic protein levels. Therefore, to determine if the BDNF levels are critical in this experimental condition we decided to mimic this environment by reducing its abundance but in Aβ-treated WT endothelial cells. To do so, we used an anti-BDNF neutralizing antibody (αBDNF), added at 12DIV into the basolateral compartment. Consequently it would involve lowering the concentration of BDNF on the medium which is directly in contact with neurons from the mixed culture **(figures 44 and 45)**. The experimental procedure **(figure 44a)** was the same previously followed. In general, our results showed that the neutralized BDNF levels had an impact on the number of neurons and the labeling intensity within GluA1- and PSD95-immunolabeled population.

Notably the results showed that compared to basal conditions, co-culturing neurons with $A\beta_{1-40}D$+αBDNF-treated WT endothelial cells significantly reduced the number of Type III neurons for GluA1- **(figure 44b)** and PSD95- **(figure 45a)** positive cells. Moreover, for PSD95 labeling, this condition also significantly reduced the number of Type II neurons. Remarkably for both markers, there is an increase in the amount of Type I neurons in parallel to the decrease in Type III cells.

According to the results obtained after intensity contribution analysis we could observe that, compared with basal condition, co-culturing neurons with $A\beta_{1-40}D$+αBDNF-treated WT endothelial cells significantly decreased the intensity contribution of Type III neurons for GluA1 **(figure 44c)** and PSD95 **(figure 45b)**. The results as well indicated a significant increase of Type I neurons intensity contribution for PSD95, which was a trend for GluA1 protein. Furthermore, from PSD95-immunolabeling images, a significant reduction in Type II neurons intensity contribution was observed with the condition of $A\beta_{1-40}D$+αBDNF-treated WT endothelial cells co-culture. These results are comparable to those obtained about the amount of cells of each intensity type.

Collectively, the data obtained from this first approximation are remarkable as they let us elucidate how critical are the levels of endothelial-secreted BDNF within the system, particularly meaning a relevant impact on the co-cultured neurons within the mixed culture.

The second approach to assess the importance of having the appropriate BDNF released levels, on neuronal network maintenance, was to restore the lower secreted amounts by SSAO/VAP-1 cells to the levels measured for WT cells. To achieve so, we added, at 12 DIV, fresh BDNF to mixed cultures co-cultured with Aβ-treated SSAO/VAP-1 endothelial cells to compensate the reduced levels present in their medium. Thus, we may see whether we restore the observed effects on synaptic protein **(figure 46 and 47)**. The experimental scheme is shown in **(figure 46a)**.

Notably, neurons co-cultured with Aβ-treated SSAO/VAP-1-expressing cells and in presence of BDNF restored levels presented a higher number of Type III neurons for GluA1 labeling **(figure 46b)**, similar to those in non-treated WT endothelial cells co-cultures. In case of PSD95, we observed only a partial recovery of the number on Type III neurons **(figure 47a)** with Aβ+BDNF-treated SSAO/VAP-1 cells co-culture condition. For both GluA1 and PSD95, the number of Type I neurons was partially reduced.

In terms of intensity contribution, co-culturing neurons with Aβ-treated SSAO/VAP-1-expressing cells and in presence of BDNF restored levels showed a clear tendency to recover Type III neurons intensity contribution for GluA1 **(figure 46c)**, comparable to the levels registered for non-treated WT cells co-cultures. As observed before, for PSD95 the Aβ+BDNF-treated SSAO/VAP-1 cells co-culture condition partially recovered the intensity contribution of neurons classified as Type III **(figure 47b)**. In parallel, for both GluA1 and PSD95, the intensity contribution of Type I cells was decreased as consequence of restoring BDNF levels in Aβ-treated SSAO/VAP-1-expressing cells co-culture condition.

Altogether, these results were very interesting evidences supporting that restoring BDNF levels is enough to improve GluA1 protein levels at neuronal cultures in $A\beta_{1\text{-}40}$D-treated SSAO/VAP-1 co-culture condition, reaching similar levels to those observed in neuronal cells with WT co-culture. In case of PSD95 quantification, the obtained results were also remarkable, although the recovery effect was not complete.

Furthermore, reviewing the obtained results from both approaches we could conclude that BDNF can be considered a key element in the sensitization that SSAO/VAP-1 induces to neuron-glia mixed culture.

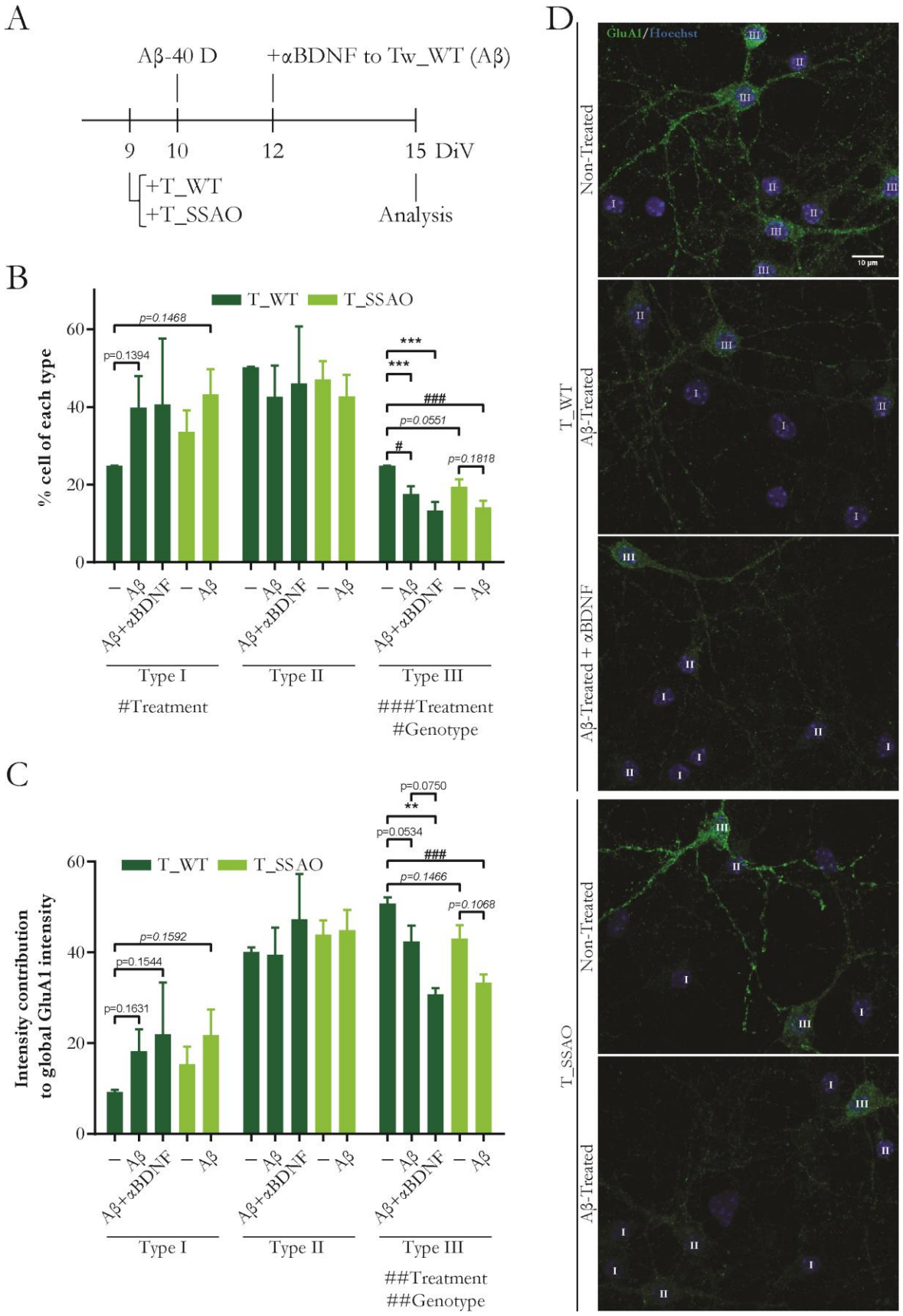

Figure 44: Reduction of BDNF levels in Aβ-treated WT hCMEC/D3 co-culture mimics the decrease observed in hSSAO/VAP-1 hCMEC/D3 Aβ-treated co-cultures. (A) Experimental scheme. Co-culture was set up when neuron-glia mixed culture was at 9DiV. Next day, 5µM $A\beta_{1-40}D$ treatment was introduced. At 12DiV, 2 µg/ml BDNF neutralizing antibody (αBDNF) was added to neuron-glia mixed cells co-cultured with Aβ-treated WT hCMEC/D3. The system was maintained until

15 DiV, when mixed cultured cells were fixated to perform immunocytochemistry procedure. **(B)** Cellular percentage of each intensity type, from low (Type I) to high (Type III: non-treated WT-CC, 24.889±0.059 %; $A\beta_{1-40}$D-treated WT-CC, 17.615±1.964 %; $A\beta_{1-40}$D+αBDNF-treated WT-CC, 13.334±2.223 %; non-treated hSSAO/VAP-1-CC, 19.400±1.912 % and $A\beta_{1-40}$D-treated hSSAO/VAP-1-CC, 14.123±1.798 %.). **(C)** Intensity contribution of each type to the total population intensity (Type I: non-treated WT-CC, 9.152±0.582 %; $A\beta_{1-40}$D-treated WT-CC, 18.152±4.858 %; $A\beta_{1-40}$D+αBDNF-treated WT-CC, 21.946±11.422 %; non-treated hSSAO/VAP-1-CC, 15.373±3.838 % and $A\beta_{1-40}$D-treated hSSAO/VAP-1-CC, 21.754±5.642 %. Type III: non-treated WT-CC, 50.725±1.433 %; $A\beta_{1-40}$D-treated WT-CC, 42.425±3.466 %; $A\beta_{1-40}$D+αBDNF-treated WT-CC, 30.793±1.347 %; non-treated hSSAO/VAP-1-CC, 43.001±3.026 % and $A\beta_{1-40}$D-treated hSSAO/VAP-1-CC, 33.320±1.872 %). **(D)** Representative images. Scale bar: 10 μm. n=2-9. Mean ± SEM. **p ≤ 0.01, ***p ≤ 0.001, one-way ANOVA analysis with Bonferroni's post-hoc test. $^{\#}p \leq 0.05$, $^{\#\#\#}p \leq 0.01$, $^{\#\#\#}p \leq 0.001$, two-way ANOVA analysis with Bonferroni's post-hoc test.

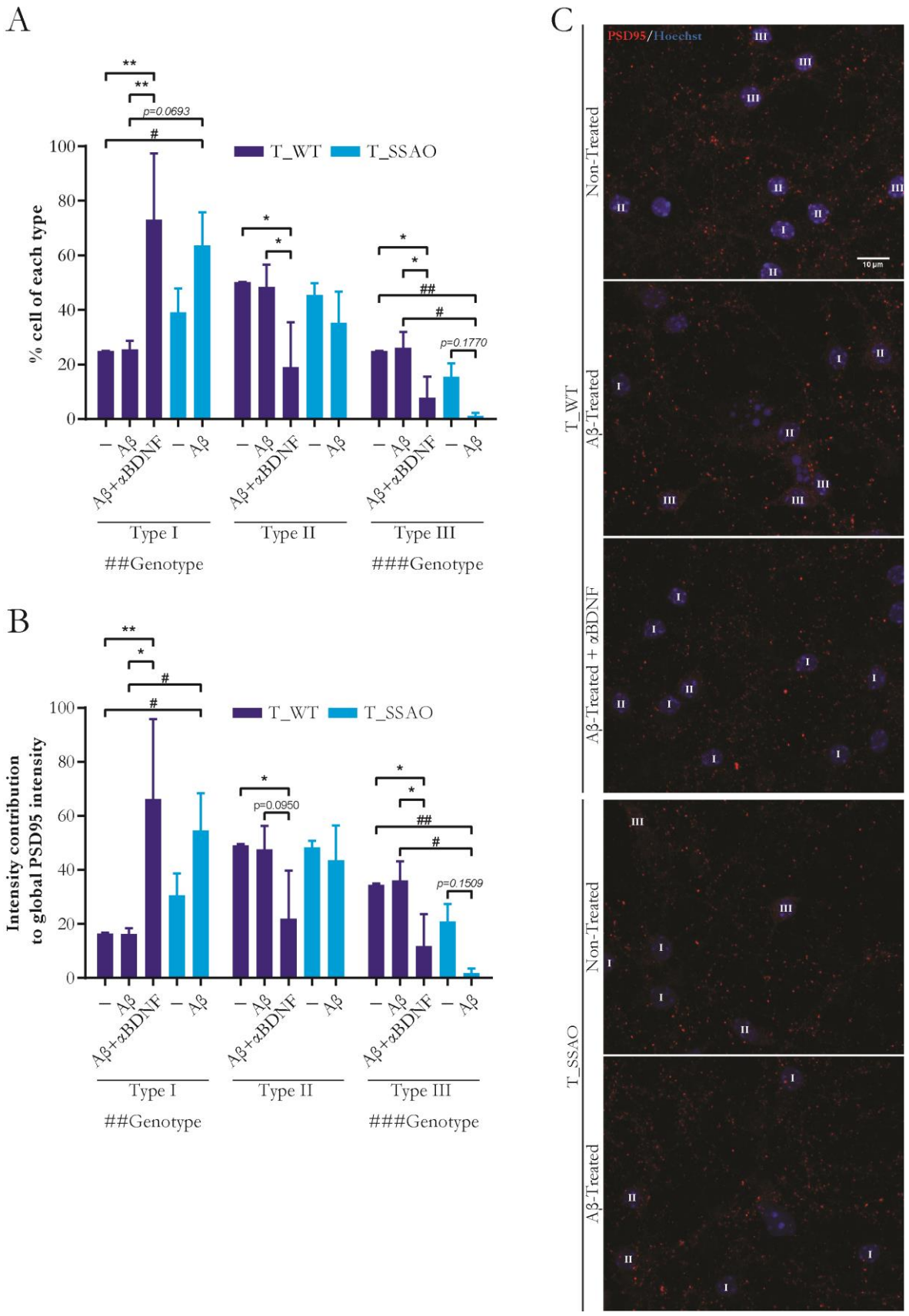

Figure 45: The decrease observed in hSSAO/VAP-1 hCMEC/D3 Aβ-treated co-cultures is reproduced when reducing BDNF levels in Aβ-treated WT hCMEC/D3 co-culture. (A) Cellular percentage of each intensity type (Type I: non-treated WT-CC, 24.920±0.093 %; $Aβ_{1-40}$D-treated WT-CC, 25.549±3.185 %; $Aβ_{1-40}$D+αBDNF-treated WT-CC, 73.149±24.260 %; non-treated hSSAO/VAP-1-CC, 39.049±8.936 % and $Aβ_{1-40}$D-treated hSSAO/VAP-1-CC, 63.711±12.141 %. Type II: non-treated WT-CC, 50.093±0.163 %; $Aβ_{1-40}$D-treated WT-CC, 48.355±8.285%; $Aβ_{1-40}$D+αBDNF-treated WT-CC, 19.074±16.483 %; non-

treated hSSAO/VAP-1-CC, 45.495±4.367 % and $A\beta_{1-40}D$-treated hSSAO/VAP-1-CC, 35.196±11.598 %. Type III: non-treated WT-CC, 24.987±0.083 %; $A\beta_{1-40}D$-treated WT-CC, 26.096±5.826 %; $A\beta_{1-40}D$+αBDNF-treated WT-CC, 7.778±7.778 %; non-treated hSSAO/VAP-1-CC, 15.456±4.885 % and $A\beta_{1-40}D$-treated hSSAO/VAP-1-CC, 1.093±1.093 %). **(B)** Intensity contribution of each type to the total population intensity (Type I: non-treated WT-CC, 16.431±0.374 %; $A\beta_{1-40}D$-treated WT-CC, 16.292±2.144 %; $A\beta_{1-40}D$+αBDNF-treated WT-CC, 66.187±29.668 %; non-treated hSSAO/VAP-1-CC, 30.655±8.013 % and $A\beta_{1-40}D$-treated hSSAO/VAP-1-CC, 54.655±13.713 %. Type II: non-treated WT-CC, 49.145±0.383 %; $A\beta_{1-40}D$-treated WT-CC, 47.549±8.725 %; $A\beta_{1-40}D$+αBDNF-treated WT-CC, 21.948±17.802 %; non-treated hSSAO/VAP-1-CC, 48.371±2.456 % and $A\beta_{1-40}D$-treated hSSAO/VAP-1-CC, 43.568±12.921 %. Type III: non-treated WT-CC, 34.424±0.524 %; $A\beta_{1-40}D$-treated WT-CC, 36.158±6.941 %; $A\beta_{1-40}D$+αBDNF-treated WT-CC, 11.866±11.866 %; non-treated hSSAO/VAP-1-CC, 20.975±6.382 % and $A\beta_{1-40}D$-treated hSSAO/VAP-1-CC, 1.777±1.777%). **(C)** Representative images. Scale bar: 10 μm. n=2-7. Mean ± SEM. *$p \leq 0.05$, **$p \leq 0.01$, one-way ANOVA analysis with Bonferroni's post-hoc test. $^{\#}p \leq 0.05$, $^{\#\#}p \leq 0.01$, $^{\#\#\#}p \leq 0.001$ two-way ANOVA analysis with Bonferroni's post-hoc test.

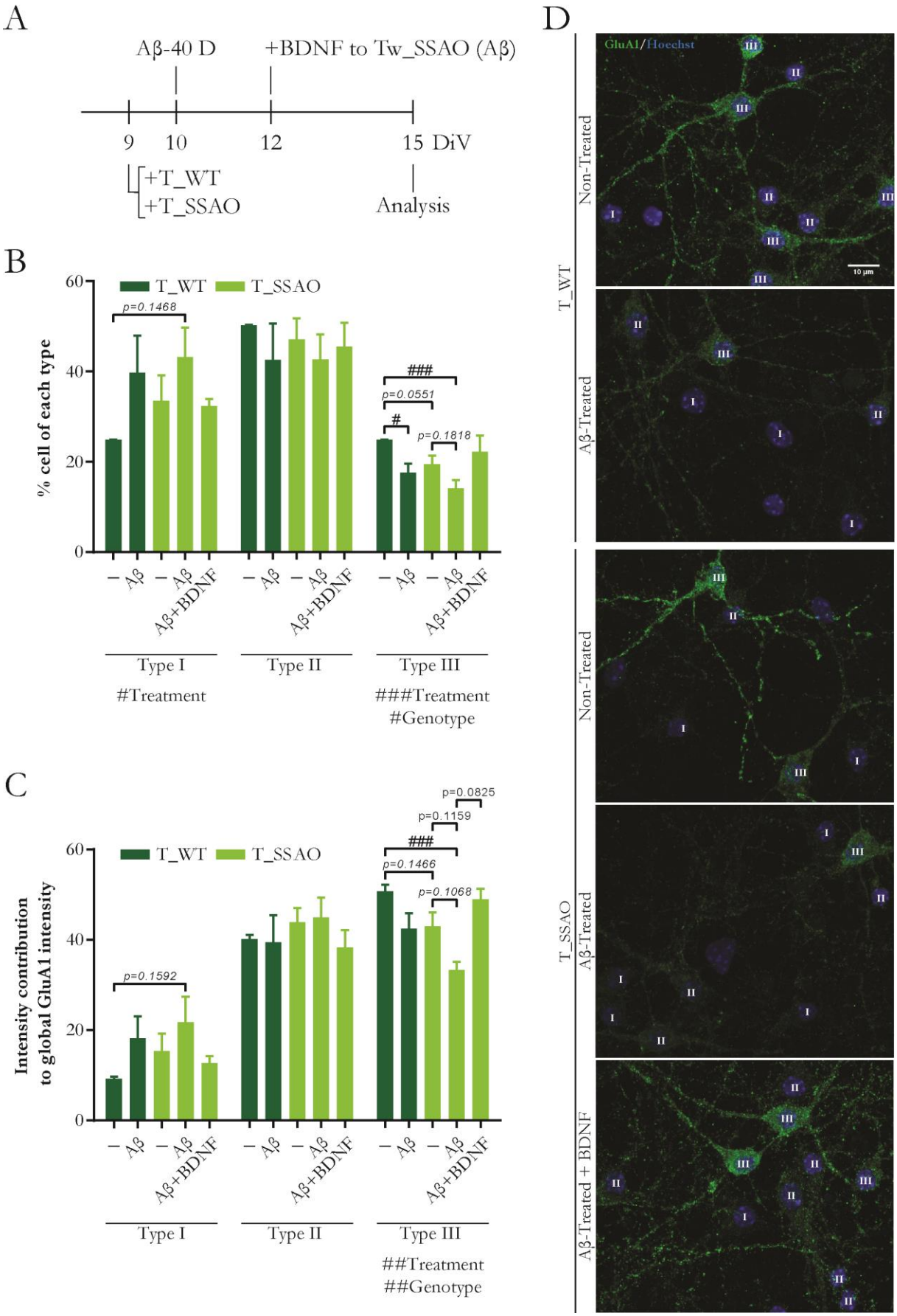

Figure 46: Restoring BDNF levels in Aβ-treated hSSAO/VAP-1 hCMEC/D3 co-culture prevents the reduction observed in this experimental condition. (A) Experimental scheme. Co-culture was set up when neuron-glia mixed culture was

at 9DiV. Next day 5μM $A\beta_{1-40}D$ was introduced. At 12DiV, 45 pg/ml BDNF was added to neuron-glia mixed cells co-cultured with Aβ-treated hSSAO/VAP-1 hCMEC/D3. The system was maintained until 15 DiV when mixed cultured cells were fixated to perform immunocytochemistry procedure. **(B)** Cellular percentage of each intensity type, from low (type I) to high (Type III: non-treated WT-CC, 24.889±0.059 %; $A\beta_{1-40}D$-treated WT-CC; 17.615±1.964 %; non-treated hSSAO/VAP-1-CC, 19.400±1.912 %; $A\beta_{1-40}D$-treated hSSAO/VAP-1-CC, 14.123±1.798 % and hSSAO/VAP-1 hCMEC/D3 Aβ+BDNF-CC, 22.155±3.693 %). **(C)** Intensity contribution of each type to the total population intensity (Type I: non-treated WT-CC, 9.152±0.582 %; Aβ1-40D-treated WT-CC, 18.152±4.858 %; non-treated hSSAO/VAP-1-CC, 15.373±3.838 %; Aβ1-40D-treated hSSAO/VAP-1-CC, 21.754±5.642 % and hSSAO/VAP-1 hCMEC/D3 Aβ+BDNF-CC, 12.740±1.554 %. Type III: non-treated WT-CC, 50.725±1.433 %; $A\beta_{1-40}D$-treated WT-CC, 42.425±3.466 %; non-treated hSSAO/VAP-1-CC, 43.001±3.026 %; $A\beta_{1-40}D$-treated hSSAO/VAP-1-CC, 33.320±1.872 % and hSSAO/VAP-1 hCMEC/D3 Aβ+BDNF-CC, 48.990±2.358 %). **(D)** Representative images. Scale bar: 10 μm. n=2-9. Mean ± SEM. *p ≤ 0.05, one-way ANOVA analysis with Bonferroni's post-hoc test. $^{\#}p \leq 0.05$, $^{\#\#}p \leq 0.01$, $^{\#\#\#}p \leq 0.001$, two-way ANOVA analysis with Bonferroni's post-hoc test.

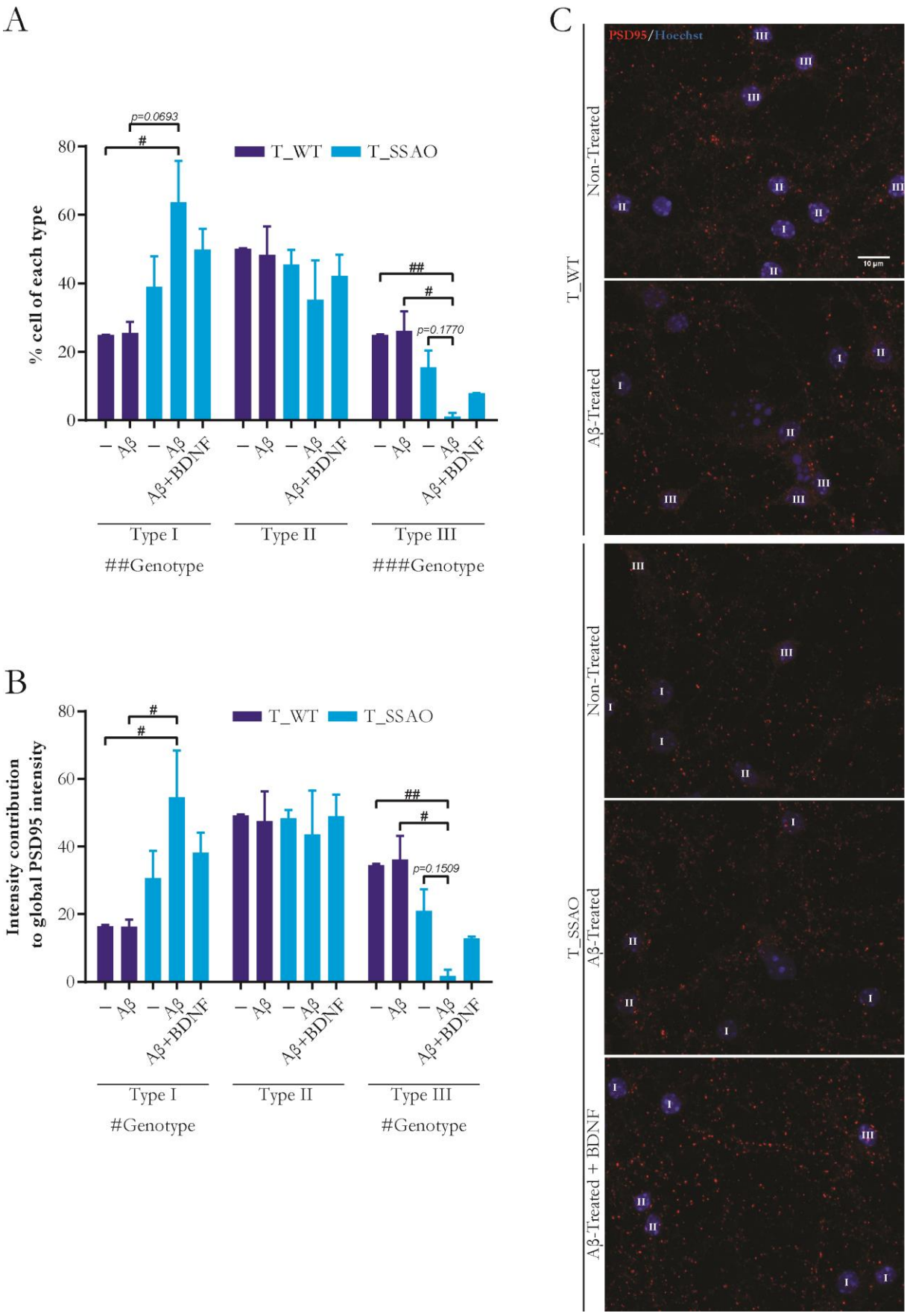

Figure 47: Prevention of the reduction observed in Aβ-treated hSSAO/VAP-1 hCMEC/D3 co-culture by restoring BDNF levels in mixed culture medium. (A) Cellular percentage of each intensity type, from low (type I) to high (Type III: non-treated WT-CC, 24.987±0.083 %; $Aβ_{1-40}$D-treated WT-CC, 26.096±5.826 %; non-treated hSSAO/VAP-1-CC, 15.456±4.885

%; $A\beta_{1-40}$D-treated hSSAO/VAP-1-CC, 1.093±1.093 % and hSSAO/VAP-1 hCMEC/D3 Aβ+BDNF-CC, 7.872±0.179 %). **(B)** Intensity contribution of each type to the total population intensity (Type III: non-treated WT-CC, 34.424±0.524 %; $A\beta_{1-40}$D-treated WT-CC, 36.158±6.941 %; non-treated hSSAO/VAP-1-CC, 20.975±6.382 %; $A\beta_{1-40}$D-treated hSSAO/VAP-1-CC, 1.777±1.777 % and hSSAO/VAP-1 hCMEC/D3 Aβ+BDNF-CC, 12.838±0.522 %). **(C)** Representative images. Scale bar: 10 μm. n=2-7. Mean ± SEM. $^{\#}p \leq 0.05$, $^{\#\#}p \leq 0.01$, two-way ANOVA analysis with Bonferroni's post-hoc test.

7 Exploring BDNF-TrkB signaling pathway in our NVU in vitro model

Disruptions in BDNF-TrkB system have been associated to synaptic plasticity affectations and neuronal cell death observed in AD (von Bohlen und Halbach and von Bohlen und Halbach, 2018). Previous publications described that TrkB collaborated, by activating the PI3K-AKT signalling pathway, in the neurovasculature reparation through improving endothelial survival (Espinera *et al.*, 2013). Moreover, it has been reported that BDNF-TrkB signalling, through the PI3K-AKT and the Ras-MAPK pathways, preserves neurons from reactive oxygen species (ROS)-induced cell death (Jin, 2020). Regarding the transcriptional autoregulation of BDNF, the cAMP-response element-binding (CREB) family of transcription factors are the principal regulators of BDNF gene expression after TrkB signalling (Esvald *et al.*, 2020). CREB is phosphorylated in response to BDNF-TrkB signalling and then, it binds to BDNF promoter IV and activates its transcription after recruiting CREB binding proteins. According to the relationship between the BDNF-TrkB signalling pathway and the glutamatergic system, critical for neuroplasticity, it was reported that BDNF up-regulates the AMPAR cellular levels by modulating GluA1 transport to the synapse (Caldeira *et al.*, 2007). Within the intracellular C-terminal of GluA1, both residues Ser831 and Ser845 are crucial in GluA1 trafficking process (Wang *et al.*, 2005). Specifically, increasing phosphorylation of Ser831 and Ser845 sites facilitates the transference of GluA1 to the synapses and enhances its conductivity (Kessels and Malinow, 2009). Considering how important are BDNF levels to be in the appropriate concentration and the significant impact that it has on the preservation of critical proteins involved in synaptic structure and function, we decided to check also the state of BDNF-TrkB signaling pathway in our system.

We firstly decided to use pure neuronal primary cultures, instead of mixed cultures, to eliminate the buffering role that astrocytes may do within the system. Thus, we treated neurons at 13 DiV with microvascular endothelial cells conditioned medium and before lysing and analyzing at indicated times. To develop this study we decided to explore phosphorylated and total levels of Akt, Erk, cAMP-response element-binding (CREB) and GluA1 (Ser845 and Ser831) by immunoblot **(figure 48)**. However, we did not observe significant differences between the treatments (WT or hSSAO/VAP-1 endothelial cells conditioned medium) along the time in any of the analyzed proteins or in their total or phosphorylated forms. Noteworthy, pure neuronal cultures did not tolerate well altering their medium requirements by adding endothelial-conditioned mediums. As happened previously for mixed cultures, these treatments modified the optimal culturing conditions.

Consequently, the main conclusion we could get from these results was that, although we could not observe significant differences, we got again another reason supporting our completed in vitro system in which cells viability was well preserved.

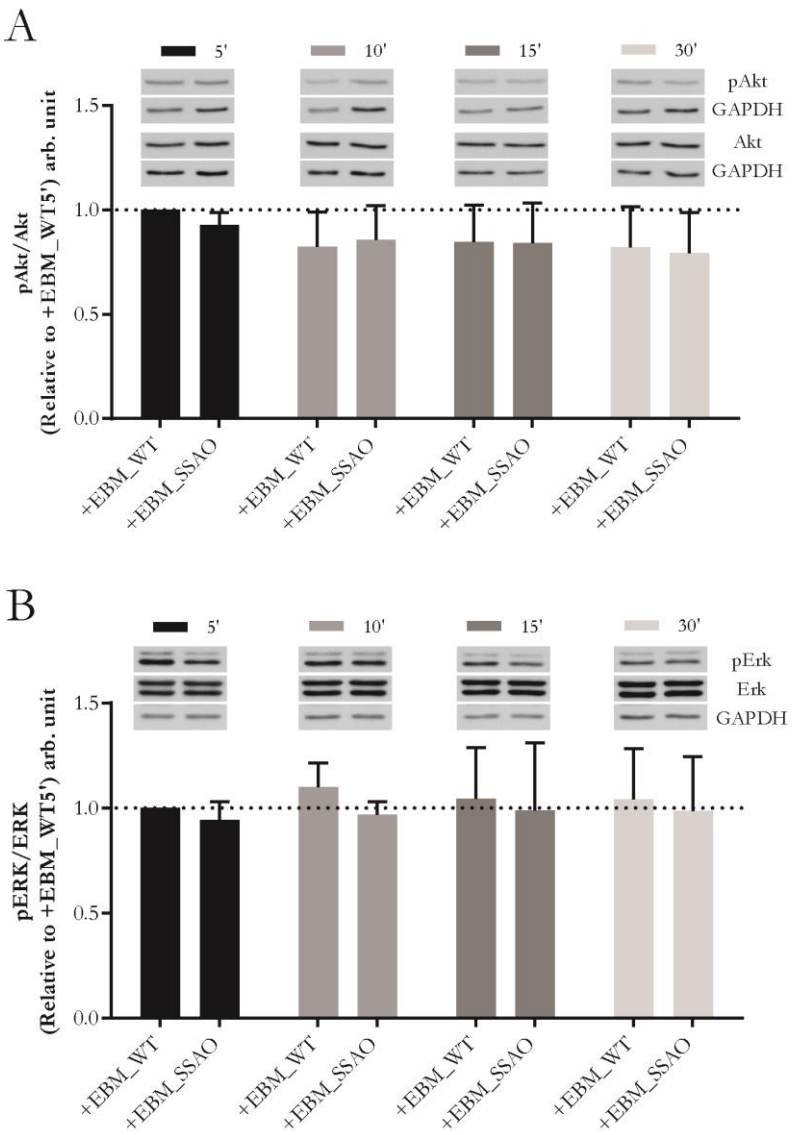

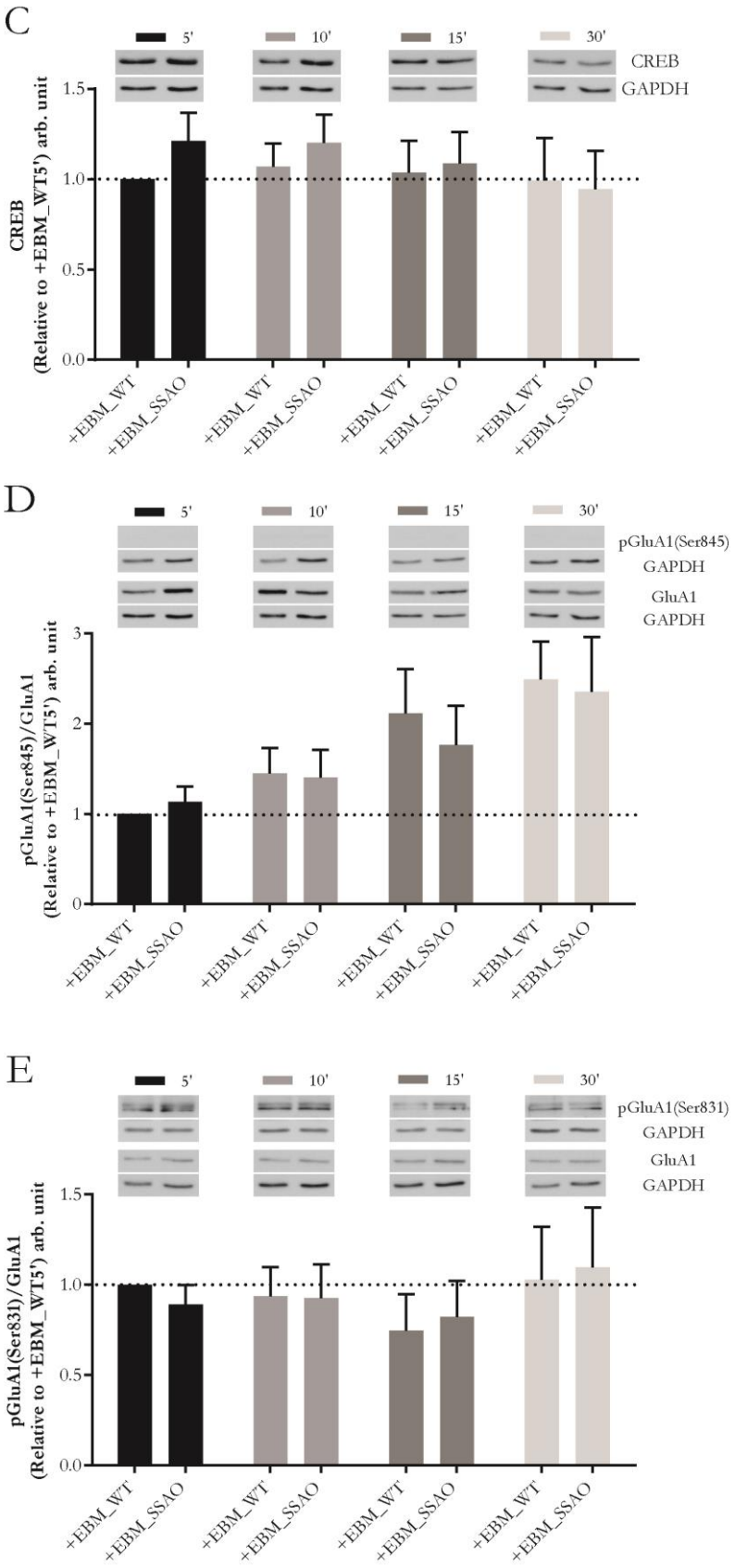

Figure 48: Representative images and quantifications from immunoblotting analysis of BDNF-TrkB signalling pathway from pure cultured neurons treated with hCMEC/D3 conditioned mediums. (A-B) Phosphorylated and total Akt and Erk protein levels, respectively. **(C)** CREB total protein levels. **(D-E)** Serine845 and Serine831, respectively, phosphorylated levels compared to total GluA1 protein levels. GAPDH was blotted as loading control protein and was used for normalization. n=4. Mean ± SEM.

Afterwards, we decided to check BDNF-TrkB signaling pathway using the same samples previously used for the study of immunolabeling intensity types **(figures 44-47)**. Our goal was to determine its activation focusing on the degree of phosphorylation of TrkB receptor **(figure 49a)**, along with two relevant downstream elements as Akt **(figure 49b)** and Erk **(figure 49c)**. Obtained results showed that $A\beta_{1\text{-}40}D$+αBDNF-treated WT cells co-culture condition trended to reduce the amount of phosphorylated TrkB compared to $A\beta_{1\text{-}40}D$-treated WT cells. However, a supposedly expected decrease in non-treated or $A\beta_{1\text{-}40}D$-treated SSAO/VAP-1 cells was not observed, neither the likely increased in $A\beta_{1\text{-}40}D$+BDNF-treated SSAO/VAP-1 cells co-culture condition where we saw a further reduction. Total TrkB levels did not change between conditions, except for the condition involving $A\beta_{1\text{-}40}D$+BDNF-treated SSAO/VAP-1 cells where we saw an increase but with a huge deviation bar. While we did not determine changes from pAkt quantification results, total Akt levels showed a slight trend to reduce its levels both in $A\beta_{1\text{-}40}D$+αBDNF-treated WT cells co-culture condition and when co-culturing with Aβ-treated hSSAO/VAP-1-expressing cells. Nevertheless, none of these observations were statistically significant. Finally, only for $A\beta_{1\text{-}40}D$-treated SSAO/VAP-1 cells there was a tendency to reduce the levels of pErk, with no changes for its total protein levels.

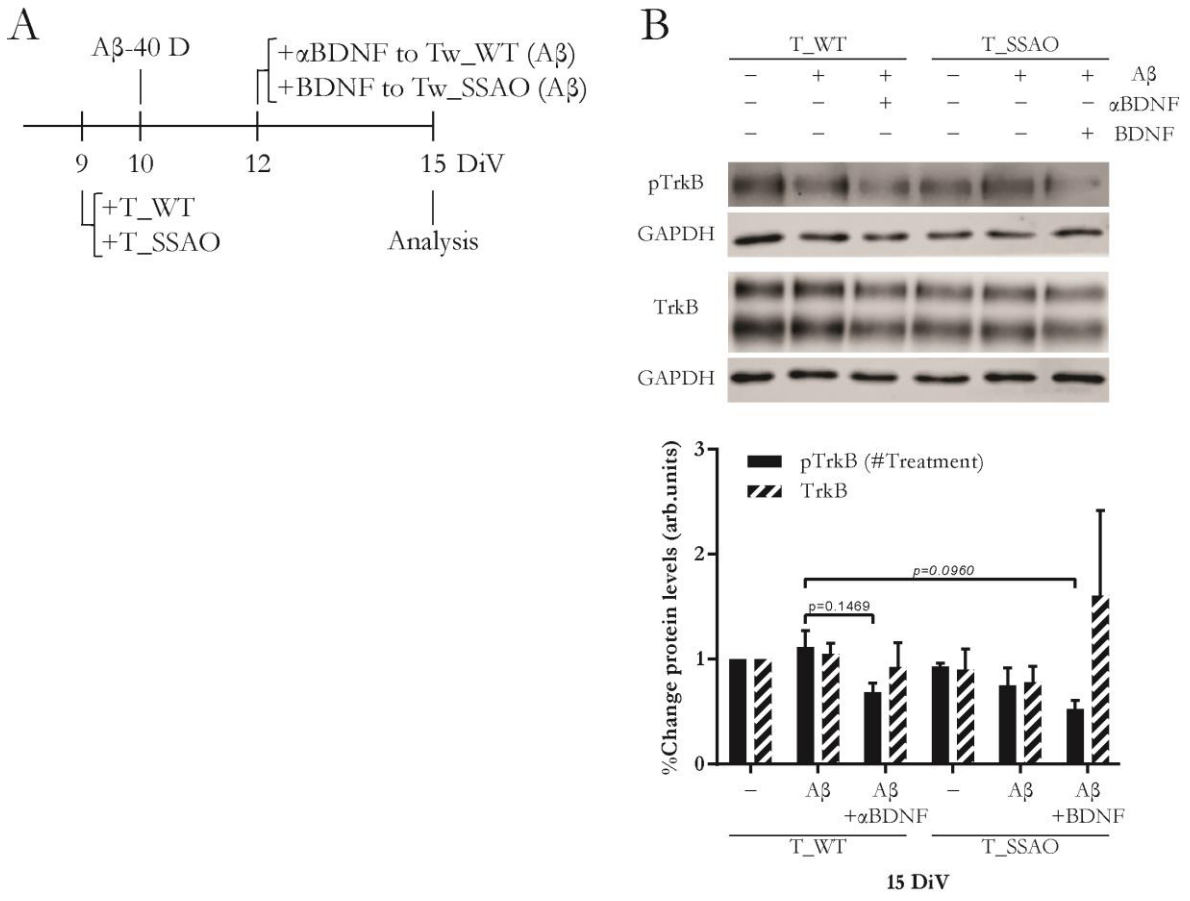

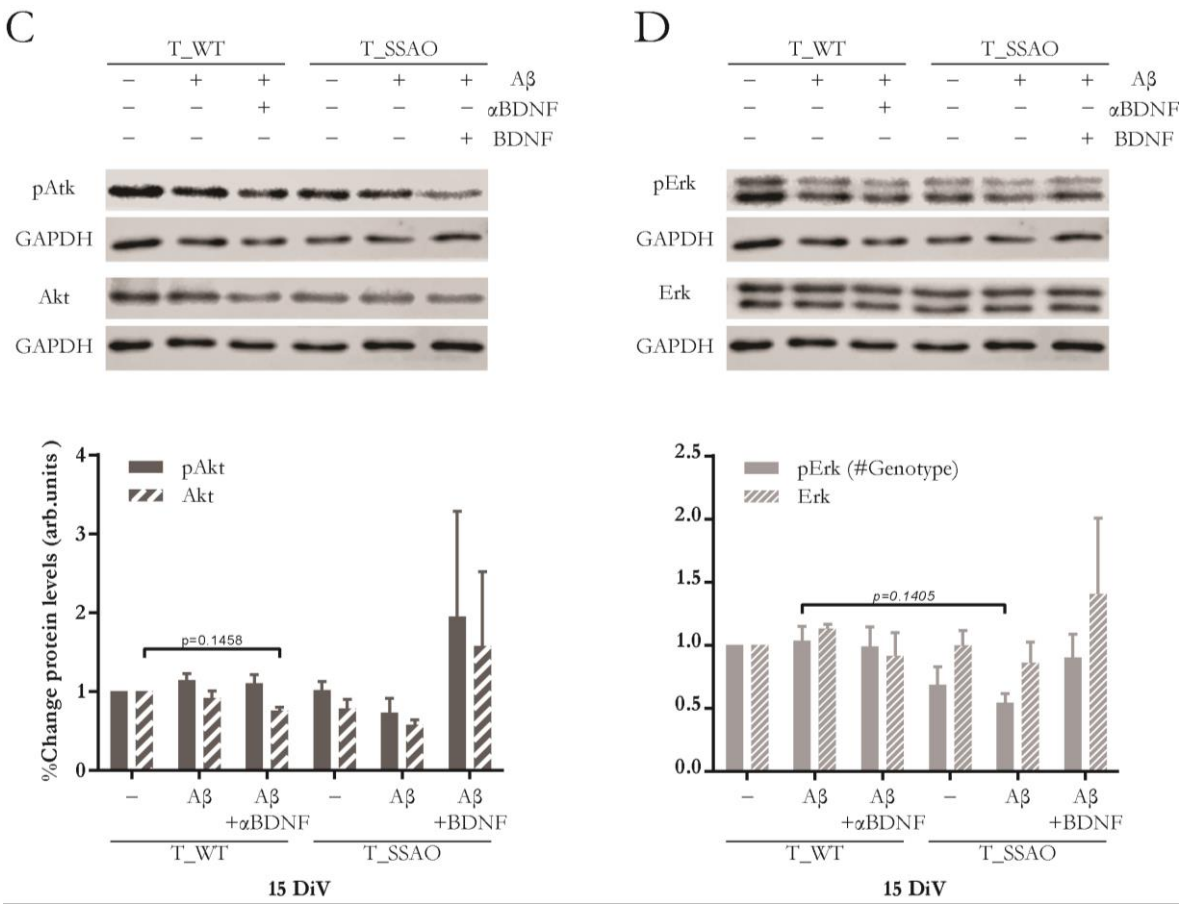

Figure 49: Immunoblotting analysis of BDNF-TrkB signalling pathway proteins from mixed-cultured neurons in different treatment and co-culture conditions. (A) Experimental scheme. Co-culture was set up when neuron-glia mixed culture was at 9DiV. Next day 5μM $A\beta_{1-40}D$ was introduced. At 12DiV, 2 μg/ml BDNF neutralizing antibody (αBDNF) were added to neuron-glia mixed cells co-cultured with Aβ-treated WT hCMEC/D3, and 45 pg/ml BDNF were added to neuron-glia mixed cells co-cultured with Aβ-treated hSSAO/VAP-1 hCMEC/D3. The system was maintained until 15 DiV, when cell lysates were collected. **(B-D)** Representative images and quantifications of phosphorylated and total forms of **(B)** TrkB, **(C)** Akt and **(D)** Erk. GAPDH was blotted as loading control protein and was used for normalization. n=2-3. Mean ± SEM. *p ≤ 0.05, one-way ANOVA analysis with Bonferroni's post-hoc test. $^{\#}p \leq 0.05$, two-way ANOVA analysis with Bonferroni's post-hoc test.

Otherwise, regarding the obtained results, one possible inconvenient of using these same samples might be that, indeed, the lysates were collected later than required for this kind of analysis, as cellular lysates were performed at the same time as we fixated the samples for aforementioned experiments **(figures 44-47)**. In order to study the activation of a signaling pathway, samples should be harvested sooner since applying the treatments. Anyhow our results are useful to know about the pathway at longer times.

Altogether, we could consider these results as preliminary data and therefore more experiments are required. These new experiments must be performed reproducing the second approach but harvesting the cellular lysates at shorter times after treatments. Thus we could detect more subtle changes in phosphorylation states in case they occurred.

VIII. Discussion

In last decades, numerous research projects have been focused on studying the mechanisms underlying Alzheimer's pathology, making huge efforts to find a disease-modifying treatment. In this regard, most of the developed drugs for treating AD have been designed on the premise that Aβ induces the disease. However, nowadays there is no therapy that effectively heals this disease and the currently food and drug administration (FDA)-approved medications such as glutamate blockers or cholinesterase inhibitors only treat AD symptoms (Steinman, Sun and Feng, 2021a). Consequently, before developing new therapies, it is necessary to consider other aspects of the disease beyond Aβ.

The 2020 Lancet Commission on dementia prevention, intervention, and care reported that at least twelve potentially modifiable risk factors account for around 40 % of worldwide dementias, including AD (Livingston *et al.*, 2020). It is remarkable that four of these established risk factors, such as hypertension, diabetes, obesity and physical inactivity, are also considered among cardiovascular disease risk factors (Francula-Zaninovic and Nola, 2018). Based on this publication, each factor contributes a cumulative 6 % to increase dementia risk, which is likely even higher when multiple cardiovascular risk factors converge in individual people (Livingston *et al.*, 2020). In line with this, although often overlooked in AD research, recent studies have suggested a critical role of the microvasculature impairment in disease progression (Cruz Hernández *et al.*, 2019; Nortley *et al.*, 2019). Therefore, among the different proposed hypothesis for AD onset, the two-hit vascular hypothesis comprises on one hand the multifactorial nature of the disease along with its relation with several cardiovascular diseases (Sagare, Bell and Zlokovic, 2012).

Briefly, the two-hit vascular hypothesis postulates that vascular risk factors and vascular damage are the "first hit" which initiates Aβ deposition, the "second hit". This is contextualized in a complex structure named the neurovascular unit, which is constituted by vascular cells (endothelial cells, pericytes and vascular smooth muscle cells (vSMCs)), glia (astrocytes, microglia and oligodendrocytes) and neurons (Zlokovic, 2011). The correct function of the NVU requires a dynamic crosstalk among its integrators and such communication is mediated by the signalling molecules known as angioneurins (Zacchigna, Lambrechts and Carmeliet, 2008). In consequence, the failure of any component of the NVU and/or the impairment in the angioneurins system would compromise the whole NVU functions and consequently induce brain damage and neurodegeneration (de la Torre, 2017). Among the angioneurins, the Brain-derived neurotrophic factor (BDNF) can be released by several integrators of the NVU and highlights due to its role in neuronal and synaptic plasticity.

From this background, through the present doctoral thesis we wanted to assess whether a cerebrovascular alteration, in special reproducing an inflammatory situation through the SSAO/VAP-1 expression, may have an impact on neurons within a NVU context. Our goal was to determine if the communication mediated by angioneurins secreted by endothelial cells, specifically focusing on

the BDNF, might be compromised under these conditions. Moreover, this study would be extended to an environment reproducing AD-like pathology, by the presence of soluble forms of amyloid-beta (Aβ). Particularly, we used the vasculotropic Dutch-mutated $A\beta_{1-40}$ ($A\beta_{1-40}D$) peptide, to reproduce the pathology *in vitro*. We decided to use this Aβ form as it has been postulated that the Dutch mutation boosts the Aβ deposition in the cerebral vasculature, probably increasing the $A\beta_{1-40}$:$A\beta_{1-42}$ ratio (Herzig *et al.*, 2004).

1. Establishing a new neurovascular unit *in vitro* model

In recent times, many *in vitro* models have been established to study the roles of different cell types involved in the neurovascular unit and their interactions. Among the approximations already described in the literature, we started our study taking advantage of the conditioned medium strategy, as this approach was already used to evaluate the communication through soluble secreted factors between pericytes and microvascular endothelial cells (Kurmann *et al.*, 2021). Although using microvascular endothelial cells-conditioned medium was useful to determine that SSAO/VAP-1-expressing cells' angioneurins altered the amounts of PSD95 and GluA1 protein levels in neurons, this system was not appropriate for our purposes, as neuronal medium requirements were altered when adding endothelial conditioned medium, resulting in an impairment of neuritic structure and neuronal viability. Consequently, to confirm and extend our results, we implemented another model inspired on that already described by Xue and colleagues (Xue *et al.*, 2013). They developed a NVU co-culture model composed of neurons, brain microvascular endothelial cells and astrocytes; all three obtained from rat primary cultures and distributed within the system employing transwell insert methodology (neurons inside the plate well, endothelial cells inside the transwell insert and astrocytes in the outer side of the insert, facing neurons but without physical contact). We took this transwell system and their cellular composition as a reference, and we modified the distribution and cellular sources according to our specific requirements.

For our experimental conditions we decided to work with the human cerebral microvascular endothelial cell line, as it is an accepted *in vitro* BBB model due to its human cerebral origin, which besides, was modified to stably express the hSSAO/VAP-1 (Solé and Unzeta, 2011; Sun *et al.*, 2015). For neuronal and astrocytes composition, we used mouse primary mixed culture, instead of two isolated rat primary cultures like Xue and colleagues (Xue *et al.*, 2013), in order to better mimic the physiological interactions between these cell types. Besides, their mouse origin would enable to design future experiments with transgenic animals, for further complement the already reported *in vivo* studies performed with such animal models.

The heterogenic cellular origin (human endothelial cells and mouse neuron-glia) of our system could be considered as a limitation in terms of intercellular communication specificity. However, using a multiple alignment tool (Altschul *et al.*, 1997), there is a 97 % of identity comparing human and mouse BDNF protein sequence. This 3 % of difference is enough to be detected by any methodology able to discriminate proteins between species, which in our hands it is an extra-value, as this angioneurin secreted by endothelial cells could be distinguished from that secreted by neuron-glia. Moreover, attending to the criteria to consider significant homology (Pearson, 2013), a 97% is enough to save its heterogenic source. To support this we could rely on the eventually performed experiments to determine the impact on neurons of co-cultures with SSAO/VAP-1-expressing endothelial cells due to its secretion of BDNF. From our obtained results, we observed that the reduction of human BDNF, from SSAO/VAP-1-expressing endothelial cells secretion, is able to affect mouse co-cultured neurons, which is not observed with WT endothelial cells co-cultures. Therefore, we assumed that BDNF released by WT endothelial cells is active for mouse neurons.

Furthermore, as pointed out by Stone and colleagues, one possible disadvantage of using the transwell system could be that cell types are not fully in contact, as it is our case (Stone, England and O'Sullivan, 2019). However for our goal this is not an inconvenient at all because we do not need microvascular endothelial cells to be in direct contact with the other components. In fact, we just require that all the cell types share a medium through which the angioneurins could travel. In relation with this requirement, other co-culture methodologies, like the microfluidic system, could be considered. The most remarkable feature of microfluidic technology is that it tries to mimic the dynamic physiological conditions in terms of continuous nutrient supply, waste removal and sheer stress (Coluccio *et al.*, 2019). Besides, compared to static systems, they prevent undesired temperature and CO_2 gradients. Nevertheless, microfluidic approach is quite complex in terms of set up and the specific knowledge to run it. Altogether, along with its higher economical expenses, took us to reject it in favor to the transwell system.

The SSAO/VAP-1 has been previously studied in several animal models *in vivo* (rat (Awasthi and Boor, 1993) and mouse (Göktürk *et al.*, 2003; Qiang *et al.*, 2014)), and *in vitro* (rat: intestinal microvascular endothelial cells (Zhang *et al.*, 2021), aortic smooth muscle cells A7r5 (Hernandez *et al.*, 2006; Solé, Miñano-Molina and Unzeta, 2015b), hearts smooth-muscle cells (Langford, Trent and Boor, 2002); mice: small intestine (Gubisne-Haberle *et al.*, 2004) and monkey: brain (Obata and Yamanaka, 2000)). Besides, it has also been investigated from human tissue or plasma samples (human microvessels and meningeal vessels (Castillo *et al.*, 1998; Lizcano, Tipton and Unzeta, 1998), post-mortem brain of AD patients (Jiang, Richardson and Yu, 2008), and arterial tissues (Nunes *et al.*, 2010) and plasma (Del Mar Hernandez *et al.*, 2005)), and *in vitro* (blood vessel model using sections of human umbilical cord (Jiang, Richardson and Yu, 2008), human umbilical vein endothelial cells (Solé,

Miñano-Molina and Unzeta, 2015), human aortic smooth muscle cells (Hernandez *et al.*, 2006), human umbilical arterial endothelial cell (Ullah *et al.*, 2013) and human brain meninges (Gubisne-Haberle *et al.*, 2004)). Nevertheless, it has never been studied in a NVU co-culture model except for the report published by our group Solé and colleagues (Solé *et al.*, 2019). Therefore our model, and the results obtained from it, might be considered as the starting point for future research projects in this issue.

During the characterization of our NVU *in vitro* model, we corroborated the previously reported impaired capacity that SSAO/VAP-1-expressing cells present for properly establishing a tight BBB (Solé *et al.*, 2019). Furthermore, our data about the composition of the mixed neuron-glia cell culture confirmed the already published *in vivo* percentages (Herculano-Houzel, Mota and Lent, 2006). These authors also described that the ratio between total neuronal and total non-neuronal mass for the whole brain is constant among species, regardless of brain size. Therefore, this let us suggest that our mixed culture composition would be comparable to the expected in case of human brain. Maintaining this ratio may be relevant as it may affect the angioneurins secretion and their communication between the NVU integrators.

2. Brain-derived neurotrophic factor secretion by cerebral microvascular endothelial cells

Since its discovery, several reports have described the relevant role that BDNF plays in neuronal and synaptic plasticity (Barde, Edgar and Thoenen, 1982; Zagrebelsky and Korte, 2014). It is involved in LTP both during developing and in mature brain. It may mediate learning and memory, and it is remarkable for rehabilitation approaches for neurodegenerative diseases (Binder and Scharfman, 2004; Park and Poo, 2013). BDNF is expressed in both central and peripheral nervous systems. It is found in different brain regions, neural and non-neural cells, cerebrospinal fluid, blood and peripheral tissue, such as in platelets, lymphocytes, and skeletal and smooth muscle cells (Barde, Edgar and Thoenen, 1982; Donovan *et al.*, 1995; Rosenfeld *et al.*, 1995; Radka *et al.*, 1996; Nakahashi *et al.*, 2000; Di Lazzaro *et al.*, 2007; Matthews *et al.*, 2009).

Particularly, cerebral endothelial cells also express and secrete a bioactive form of BDNF as it was originally reported by Leventhal et al. (Leventhal *et al.*, 1999) and lately confirmed by *in vivo* studies (Navaratna *et al.*, 2011; Quirié *et al.*, 2012). It is especially exciting the finding that the rate of BDNF production by mouse cerebral endothelial cells, cultured in static conditions, was estimated to be 50 times higher than that by cultured unstimulated neurons (Guo *et al.*, 2008). Our multiplex results agree with this as BDNF levels secreted by mouse neuronal source were despicable compared to the human endothelial-released amount. Besides, previous reports were also in this line, as showed that

BDNF levels measured in brain homogenates correspond for a large part to BDNF present in cerebral endothelial cells (Monnier *et al.*, 2017).

From our results, we have not only confirmed that the human cerebral microvascular endothelial cells expressed and secreted BDNF, but also revealed for the first time that SSAO/VAP-1 enzyme expression alters this BDNF secretion. Previous reports have indicated interplay between oxidative stress and BDNF levels (Wu, Ying and Gomez-Pinilla, 2004; Kapczinski *et al.*, 2008). Despite the mechanisms by which oxidative damage induces the reduction in BDNF expression are complex, it has been suggested the involvement of several factors such as the decrease of DNA-binding activities of activator protein-1 and CREB (Iwata *et al.*, 1997; Vellucci, Parrott and Mimmack, 2001). In our context, the products obtained due to SSAO/VAP-1 enzymatic activity (aldehydes, ammonia and hydrogen peroxide) are directly involved in oxidative stress (Yu *et al.*, 2003). Therefore, it might be suggested that the toxic products obtained after SSAO deamination activity could be one possible link between SSAO/VAP-1 presence and BDNF reduction. However, it must be highlighted that, as previous experiments performed in the group, adding the endogenous substrate of SSAO (methylamine) did not alter/modify BDNF secretion, and on the other hand, our determination of BDNF levels was performed without adding this substrate in excess, so theoretically this effect might be activity-independent. Nevertheless, we cannot rule out that low amounts of other possible substrates were present in culture medium, or secreted by mixed culture, and they could be processed by SSAO and then the obtained products could act triggering BDNF decrease. Anyhow, the observed reduction is so remarkable to be attributed to an unknown substrate and its processing, and we believe it may be driven by a mechanism not already described. It would be exciting to uncover such molecular mechanisms relating SSAO/VAP-1 and BDNF secretion, so it might be addressed by future projects.

3. On the value of these results

This result showing BDNF secretion reduction by SSAO/VAP-1-expressing endothelial cells highly motivated us to follow determining its consequences on co-cultured neurons within our NVU system, not only in basal conditions but also with Aβ-treatment to reproduce an AD-like environment. Previous reports showed that dysregulation of BDNF-TrkB-associated downstream molecular pathways modulates the levels of key synaptic proteins, such as PSD95 (Yoshii and Constantine-Paton, 2014) and GluA1-containing AMPA receptors (Caldeira *et al.*, 2007; Nakata and Nakamura, 2007; Leal, Comprido and Duarte, 2014). Consistent with these findings, our cellular fractionation results showed that co-culturing with $A\beta_{1\text{-}40}$D-treated hSSAO/VAP-1 expressing cells induced substantial alterations in both PSD95 and GluA1 protein levels. These results were further confirmed by the analysis of labeling intensity from immunocytochemistry images. Interestingly,

related with immunocytochemistry images we described three neuronal subpopulations attending to their intensity labeling for several synaptic markers (GluA1, PSD95 and AKAP150). To our best knowledge, we have not found references in the literature reporting anything similar. Although we do not know what this pattern means, we could speculate that, considering the direct relation between labeling and the amount of protein, the differential intensity may be linked with the function that each cell has within the neuronal network. Besides, for instance for GluA1 labeling, we could also relate the amount of protein with neuronal activity, in terms of glutamatergic signaling. According to this, we may hypothesize whether alterations in its labeling pattern may be related with synaptic weakening prior synaptic dysfunction and loss and eventually dementia. Altogether might be deeply studied by future electrophysiological assays and it would be interesting to establish a likely correlation between the described labeling patterns and neuronal activity.

According to former publications, BDNF regulates the location of PSD95 within the PSD zone through its TrkB receptor downstream signalling pathways (Yoshii and Constantine-Paton, 2014) by inducing PSD95 palmitoylation (Yoshii *et al.*, 2011). Moreover, related with AD, it has been recently reported that high levels of PSD95 protects synapses from Aβ toxicity, so it has been suggested that low levels of synaptic PSD95 might be considered as a molecular marker pointing out synapse susceptibility to Aβ (Dore *et al.*, 2021). In this regard, it was shown that pharmacological inhibition of PSD95 depalmitoylation increased its amount at synapses and restored the effects caused by Aβ (Dore *et al.*, 2021). From our results, it would be fascinating to assess the levels of PSD95 palmitoylation from our samples and eventually determine the mechanisms underlying. Furthermore it was described that PSD95 reduction, due to Aβ, also involved a reduction in surface expression of GluA1-containing AMPARs (Almeida *et al.*, 2005). The AMPA receptor comprises of four subunits (GluA1 to GluA4), but it was reported that GluA1 is a key factor involved in long-term synaptic plasticity (Jung *et al.*, 2020). The disruption of AMPAR trafficking by soluble forms of Aβ has been proposed a major contributor to synaptic dysfunction in AD (Walsh and Selkoe, 2007; Reiss *et al.*, 2018). In fact it has been recently demonstrated that oAβ primarily inhibited the increase in the number of GluA1 homomers and suppressed hippocampal LTP expression (Tanaka, Sakaguchi and Hirano, 2019). As well it is already known that Aβ can disrupt phosphorylation-dependent AMPAR trafficking and causing subsequent deficits in LTP/LTD (Gu, Liu and Yan, 2009). Otherwise, BDNF up-regulates the protein levels of GluA1 AMPA receptor subunits and induces the delivery of AMPARs to the synapse (Caldeira *et al.*, 2007).

Altogether, these data contribute to reinforce our results, where we observed a reduction in PSD95 and GluA1 protein levels when co-culturing with $A\beta_{1-40}D$-treated hSSAO/VAP-1 expressing cells. Particularly, we may relate our data with the relation described by Almeida and colleagues, between PSD95 reduction and the levels of GluA1-containg AMPARs. In our hands we observed more

significant affectation of PSD95 than GluA1 levels. Therefore, we could suggest that our results confirm what Almeida and colleagues reported. However, our results are not only relevant by the information they shed, but also because they corroborate the existing communication between endothelial cells and co-cultured neurons from mixed culture. Particularly, they led us to hypothesize whether SSAO/VAP-1 cells could induce some sensitization to co-cultured neurons that became critical in front of an aversive stimulus as Aβ treatment. In this respect we wondered if such sensitization could be due to the reduction observed in BDNF releasing levels by SSAO/VAP-1 cells. Interestingly, this consideration would fit with the proposed two-hit vascular hypothesis (Zlokovic, 2011), highlighting even more the repercussion of our results. In our hands, the SSAO/VAP-1-increased expression would represent the first hit. Actually, reviewing multiple available reports, the SSAO/VAP-1 has been reported to be up-regulated in several vascular peripheral pathologies which are also considered not only as risk factors for AD, but also as "hit 1" within the two-hit vascular hypothesis. Moreover, such pathological situations like diabetes (Boomsma *et al.*, 1999; Mathys *et al.*, 2002), atherosclerosis (Mészáros *et al.*, 1999; Karádi *et al.*, 2002; Wang *et al.*, 2018; Li *et al.*, 2021), congestive heart failure (Boomsma *et al.*, 1997), malignant hypertension (Boomsma *et al.*, 2003), non-diabetic morbidity obesity (Weiss *et al.*, 2003), stroke (Håkan Garpenstrand *et al.*, 1999; Hernandez-Guillamon *et al.*, 2012), AD (Ferrer *et al.*, 2002) and inflammatory liver diseases (Kurkijärvi *et al.*, 1998) among others, are broadly related with cardiovascular alterations and/or chronic inflammatory diseases, representing evident examples of peripheral pathologies that, through SSAO/VAP-1 activity and its role in cerebral microvascular endothelial cells, may finally affect brain parenchyma (Unzeta *et al.*, 2021).

Reviewing previous reports, we formerly described that other angioneurins related to inflammation (IL-6, IL-8, ICAM, and VCAM) and trophic factors (VEGF, TGF-β1 and NGF) are over-released due to SSAO/VAP-1 expression on endothelial cells (Solé *et al.*, 2019). It might be expected that each of them, as well as other molecules also altered but not described yet, may have an impact on the NVU communication. For instance, a recent publication has reported that VEGF signalling at the luminal side of the brain microvasculature plays an integral role in the capillary blood flow alteration in the APP/PS1 mouse model (Ali *et al.*, 2022). The relation between VEGF and BDNF has been previously studied in different models such as diabetic retinopathy (Zhang *et al.*, 2017). Particularly, it was found that diabetic retinopathy patients presented inversely proportional blood serum BDNF and VEGF levels (Zhu *et al.*, 2022). Diabetic retinopathy is one of the most common microvascular complications associated with diabetes mellitus, and both are considered among vascular risk factors for AD (Pedersen *et al.*, 2022). Moreover, the SSAO/VAP-1 has been related with retinopathy associated to diabetes Type 2 (Garpenstrand *et al.*, 1999; Grönvall-Nordquist *et al.*, 2001; Noda *et al.*, 2009). Related with diabetic retinopathy, regulating the VEGF/BDNF/NF-ϰB signaling pathway has

been recently proposed as a significant therapeutic strategy (Zhu *et al.*, 2022). Interestingly, in these reports the authors found that BDNF was increased after treatments with anti-VEGF or VEGF siRNA. Besides, they described a BDNF decrease from VEGF-overexpressing mice. Considering this regarding our results, it might be interesting for future experiments to treat SSAO/VAP-1 expressing cells with an anti-VEGF neutralizing antibody to try to rescue their BDNF secreted levels.

Reviewing this along with our obtained results, it is encouraging to determine the role that BDNF could be playing in the aforementioned sensitization induced by SSAO/VAP-1 cells. Besides, regarding the importance of having the appropriate BDNF-released levels, as it is involved in plasticity, neuronal survival, growth and differentiation (Jin, 2020), we applied two complementary strategies to address such study. Previously, other authors used anti-BDNF neutralizing antibodies to assess the role of BDNF on their hypothesis (Wang *et al.*, 2011, 2021; Ghosal *et al.*, 2018; Fukumoto *et al.*, 2019). Therefore, we decided to take advantage of this approach to reproduce the reduction of BDNF released levels observed in SSAO/VAP-1 cells but in co-cultures constituted by Aβ-treated WT endothelial cells. As a second strategy we followed previous reports describing exogenous BDNF exposure (Nigam *et al.*, 2017; Rauti *et al.*, 2020; Braschi *et al.*, 2021), thus we added fresh BDNF to mixed cultures co-cultured with Aβ-treated SSAO/VAP-1 endothelial cells to restore their BDNF levels. Noteworthy, we just added BDNF to recover the levels to those secreted by WT cells. Theoretically, the rest of angioneurins previously described to be altered (Solé *et al.*, 2019) should be maintained, although we did not check it. Results obtained from both strategies revealed that indeed, BDNF is crucial within the NVU *in vitro* system. Briefly on one hand, reducing the BDNF levels in the co-culture with Aβ-treated WT endothelial cells, using the anti-BDNF neutralizing antibody, mimicked the reductions of GluA1 and PSD95 expression pattern when co-culturing neurons with Aβ-treated SSAO/VAP-1 endothelial cells. On the other hand, restoring the BDNF levels on co-cultured with Aβ-treated SSAO/VAP-1 endothelial cells prevented the previously observed decreases in the expression pattern of the aforementioned synaptic markers. In this regard, we can claim the involvement of this critical angioneurin in the sensitivity to an aversive stimulus, like soluble forms of Aβ, which SSAO/VAP-1 endothelial cells induce on co-cultured neurons. Noteworthy, altogether is highly relevant as we have identified that an alteration from the vascular system is able to modify the levels of BDNF that are available in the neuronal environment, inducing further adverse changes in the parenchyma.

Recapitulating, we propose the following scenario **(figure 50)**. Under a persistent inflammatory state or in chronic diseases considered vascular risk factors for AD, SSAO/VAP-1 would be overexpressed. This overexpressed enzyme, via activity-independent mechanisms not yet described, would induce the alteration of the angioneurins secretion pattern, increasing inflammatory factors and reducing neurotrophic factors such as BDNF. Moreover, the SSAO/VAP-1 through its catalytic

activity, although in our hands we have not found changes in the presence of its endogenous substrate, would generate toxic metabolites (hydrogen peroxide and aldehydes) that would lead to a vascular damage. This vascular damage could involve inflammation (increasing even more the levels of SSAO/VAP-1 as an adhesion molecule), as well as vascular cell toxicity, BBB dysfunction and leakage, with the corresponding brain hypoperfusion. Altogether, the activity-independent alterations in the pattern of angioneurins release, along with the activity-dependent vascular damage (Unzeta *et al.*, 2007; Jiang, Richardson and Yu, 2008; Sun, Solé and Unzeta, 2014), would result in a sensitization of nearby neurons to any aversive stimulus like Aβ. In addition, increased levels of SSAO/VAP-1, both via activity-dependent and -independent, would also contribute to vascular aggregation of Aβ (Chen, Kazachkov and Yu, 2007), consequently boosting the toxic feedback loop that aggravates AD pathology through the earlier vascular damage (Solé, Miñano-Molina and Unzeta, 2015).

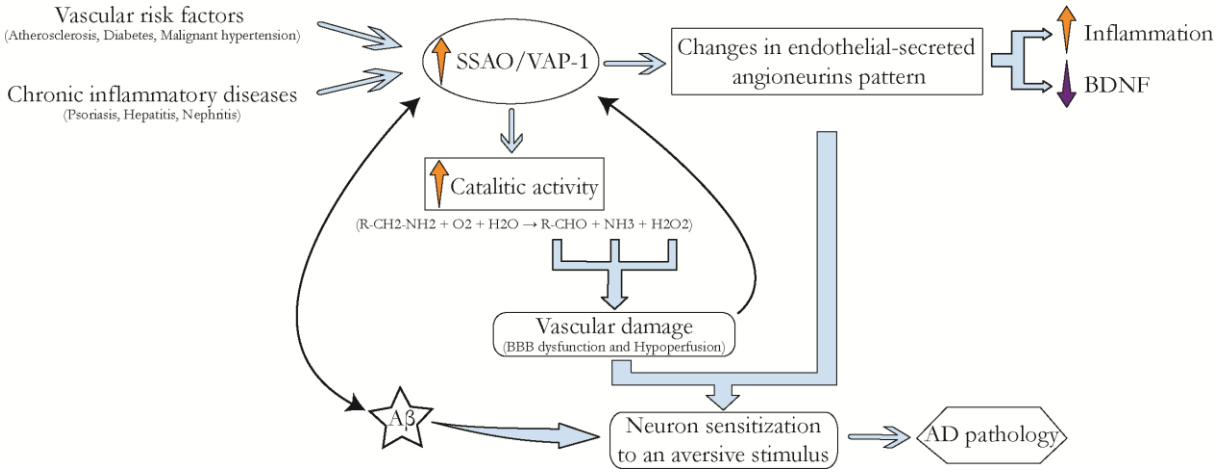

Figure 50: Graphical abstract summarizing the proposed links relating increase in SSAO/VAP-1 levels, due to vascular risk factors and/or inflammatory states, with AD pathology through NVU affectation. Pathologies associated with chronic inflammatory state can induce the overexpression of SSAO/VAP-1. This involves in one hand, the alteration of the pattern of endothelial-secreted angioneurins; enhancing several ones related with inflammation and decreasing others like BDNF. On the other hand, SSAO/VAP-1 overexpression implies an increase of its catalytic activity that can lead to a vascular damage in terms of release of cytotoxic products, BBB dysfunction and hypoperfusion. Combining both effects result in sensitizing nearby neurons in front of a toxic insult. Furthermore, increased levels of SSAO/VAP-1 also promote vascular aggregation of Aβ, consequently enhancing the toxic feedback loop that worse AD pathology through the initial vascular damage.

To further complete this scheme, more research is needed. Regarding previous publications about the association between BDNF depletion and tau phosphorylation, Aβ accumulation, neuroinflammation and neuronal apoptosis (Wang *et al.*, 2019), and specifically taking into account that Aβ disrupts BDNF signalling (Tanqueiro *et al.*, 2018), it would be interesting to assess the state BDNF/TrkB signalling pathway in neurons within mixed culture. In this sense, we performed preliminary immunoblots analyses. Although the obtained data showed that $A\beta_{1\text{-}40}D$+αBDNF-treated WT cells co-culture condition trended to reduce the amount of phosphorylated TrkB compared to $A\beta_{1\text{-}40}D$-treated WT cells, we could not observe the expected decrease in non-treated or $A\beta_{1\text{-}40}D$-treated SSAO/VAP-1 cells and neither the likely recovery in $A\beta_{1\text{-}40}D$+BDNF-treated SSAO/VAP-1 cells co-culture condition. These results, together with those obtained for the rest of the proteins analyzed

downstream the signaling pathway, were not statistically significant. One possible explanation for such results may be that the used samples were lysated later than required for this kind of studies. In order to study the activation of a signaling pathway, samples should be harvested sooner that we did from the moment that treatments were applied (Guo *et al.*, 2014; Kang *et al.*, 2017)). Therefore, new experiments must be performed but harvesting the cellular lysates at shorter times after treatments. Nevertheless, our results might be useful to get a preliminary view about the pathway at longer times. Additionally, it would be nice to extend our postulated scenario introducing tau protein and to determine which role might play.

Moreover, another element that would be exciting to be able to locate within the proposed scenario is the role of astrocytes. They are crucial components of the NVU and they have also been described to express BDNF and to secret it via exocytosis, in order to support nearby neurons and regulate their function (Hong *et al.*, 2016; De Pins *et al.*, 2019). According to this, astrocytes could be buffering the angioneurin's communication systems within our NVU *in vitro* model. We carried out exploratory experiments to measure GFAP protein levels in non-treated and treated co-culture conditions to assess if any of the experimental conditions increased astrocytic reactivity. Initially we might have speculated that, in response to SSAO/VAP-1 over-release of inflammatory-related angioneurins (Solé *et al.*, 2019), we might have found an increase in GFAP astrocytic levels. However, as we did not observe any difference, we decided to focus on the neuronal component of the mixed culture. Nevertheless, future projects might design more experiments to determine the involvement of astrocytes in our system.

Furthermore, related with the aforementioned endothelial-secreted angioneurins pattern (Solé *et al.*, 2019), in our hands we have determined the crucial role of BDNF in angioneurins communication within our NVU model. Nonetheless, there might be other signalling molecules present in the system that could be also affected by the SSAO/VAP-1. In order to assess whether alterations of other angioneurins can also induce modulating effects, coming experiments may address macroanalysis studies to determine the impact on NVU components of different angioneurins combinations to obtain a more complete picture of the angioneurin's communication system.

Collectively, our obtained results along with those that would be achieved from the suggested future experiments should be corroborated *in vivo*. Reviewing the aforementioned models where SSAO/VAP-1 has been previously described, the senescence accelerated mouse-prone 8 (SAMP8) has been considered a remarkable animal model (Liu, Liu and Shi, 2020). SAMP8 mice exhibit most features of pathogenesis of AD, including an abnormal expression of anti-aging factors (Zhou *et al.*, 2018), oxidative stress (Morley *et al.*, 2012), inflammation (Akiguchi *et al.*, 2017), Aβ deposits (Pallas *et al.*, 2008), tau hyperphosphorylation (Cheng, Zhou and Zhang, 2014), cognitive impairment (Cheng,

Zhou and Zhang, 2014) and neuronal loss (Li *et al.*, 2013). Besides, this transgenic mouse model also presents high levels of formaldehyde and high SSAO expressing levels, as well as increased SSAO enzymatic activity, in 3-month-old mice (Qiang *et al.*, 2014). A former publication investigated the cognitive function, CBF and BBB damage on SAMP8 animals (Zhang *et al.*, 2013). Their obtained results showed that the cognitive abilities of SAMP8 were damaged apparently even at 4 months of age. Moreover these animals presented an earlier and more severe impairment of CBF and BBB leakage compared with the senescence-accelerated mouse resistant-1 model. Also in this report, Zhang and colleagues determined the correlations between the cognitive function, CBF and BBB damage, but any kind of correlation was performed versus SSAO/VAP-1 levels. It may be interesting to apply techniques modifying SSAO/VAP-1 gene expression (such as silencing with shRNAs via viral vectors) and/or inhibiting its enzymatic activity to analyze the SSAO/VAP-1 specific contribution to those previously described alterations on SAMP8 mouse. Recently, the SAMP8 has been validated as a mouse model to study age-associated neuroinflammatory events (Fernández *et al.*, 2021). Nevertheless, in this report nothing has been described about the SSAO/VAP-1, so we could take advantage of these data to further corroborate our results obtained from this thesis. We may assess whether our findings are reproduced also in vivo and if they correlate, through statistical analysis, with alterations in CBF, inflammation and behavior. Additionally, more experiments may be suggested using human samples, for instance correlating SSAO/VAP-1 levels in plasma with the amount of BDNF. The correlation between peripheral and central BDNF is a currently discussed topic (Tarassova *et al.*, 2020). Maybe with such proposed experiments we could additionally collaborate in the discernment.

Noteworthy, our findings agree with previous proposals about the possibility to achieve great short and long-term improvement outcomes treating vascular dysfunction and inflammation at early stages in AD disease pathogenesis, or even in pre-symptomatic individuals (Govindpani *et al.*, 2019). Designing a potential therapeutic strategy based on regulating the SSAO/VAP-1 expression and/or inhibition or its angioneurins releasing pattern may result extremely powerful as it could be applied to a wide spectrum of diseases like AD, stroke and other inflammatory diseases.

From our results, which seem to be independent of SSAO/VAP-1 activity, we may not propose using inhibitors to block its enzymatic activity. However, it might be a useful strategy to modulate the other affectations inducing vascular damage, in which the SSAO/VAP-1 is implicated. For instance, the inhibitor known as PXS-4728 by Pharmaxis, could be a remarkable option as, although it was initially proposed for treating inflammation (Schilter *et al.*, 2015), it is currently being also studied for diabetic retinopathy and neuroinflammation. Furthermore, as reviewed by Salmi and Jalkanen, there are other small-molecule VAP-1 inhibitors that might be taken into account (Salmi and Jalkanen, 2019).

Regarding previous publications considering angioneurins as potential targets, several neurotrophins, such as NGF, BDNF and VEGF have been proposed as potential therapeutic agents for treating neurodegenerative disorders of the central nervous system (Steinman, Sun and Feng, 2021; Lin *et al.*, 2022). Particularly, several studies have found that BDNF produces neuroprotective effects against reactive oxygen species-induced cell death, highlighting its potential for treating neurodegenerative diseases (Chen *et al.*, 2017; Habtemariam, 2018). Furthermore, previous reports suggested that therapeutically increasing BDNF levels in brain regions important for memory and cognition may lead to improved clinical outcomes of AD patients (Blurton-Jones *et al.*, 2009; Xiang *et al.*, 2019). Consequently, the use of exogenous BDNF or stimulation of endogenous BDNF secretion have been proposed as promising approaches for treating AD.

Although the exogenous source of BDNF is a direct and effective strategy applied by some studies to compensate the pathological secreting levels (Arancibia *et al.*, 2008; Tapia-Arancibia *et al.*, 2008; Xu *et al.*, 2018), the main problem is that feasible delivery routes are limited due to the short half-life of BDNF (Poduslo and Curran, 1996). As a result, many intervention approaches have sought to restore BDNF levels endogenously either by indirectly enhancing its signalling and secretion in the brain (via physical exercise (Dao *et al.*, 2013; Wang and Holsinger, 2018; Belviranlı and Okudan, 2019; Jahangiri, Gholamnezhad and Hosseini, 2019), or directly promoting its endogenous production (via gene therapy (Nagahara *et al.*, 2018). According to our results, related with gene therapy, endothelial cells may be a remarkable target where to increase the expression and secretion of BDNF.

Undoubtedly a complex disease as AD would likely require a treatment involving the subtle modulation of multiple synergistic processes. Based on the results obtained in this thesis, we suggest a broader perspective considering the role of microvascular endothelial cells, specifically the involvement of SSAO/VAP-1 and/or vascular inflammation, on the disease to design new therapeutic strategies beyond the belief that eliminating plaques and/or Aβ alone will lead to a cure. Instead, Aβ might be seen as an important element of AD pathology that acts in combination with other mechanisms.

VIII. Conclusions

The data obtained from our NVU *in vitro* model reveal that SSAO/VAP-1 expression on microvascular endothelial cells implies a reduction in their release of BDNF. Consequently, this affects the communication between endothelium and neurons mediated by such angioneurin. Moreover, this impairment becomes critical for neurons, in front of an aversive stimulus, like soluble forms of Aβ. Altogether results in the decrease of the appropriate expression of GluA1 and PSD95, both relevantly involved in neuronal synaptic function.

This conclusion is drawn based on the following findings:

1. We have successfully established a new co-culture *in vitro* model to study the neurovascular unit.

2. We have determined that endothelial cells expressing SSAO/VAP-1 release lower levels of BDNF compared to WT endothelial cells.

3. We have observed that co-culturing neurons with SSAO/VAP-1-expressing endothelial cells results in a reduction in PSD95 and GluA1 synaptic protein levels.

4. We have described three neuronal subpopulation types, within the mixed culture from our NVU *in vitro* system, depending on their labeling intensity of several synaptic markers (GluA1, PSD95 and AKAP150).

5. We have found that co-culturing with Aβ-treated SSAO/VAP-1 endothelial cells induces a change in the expression pattern of GluA1 and PSD95; reducing the amount and the intensity of immunolabeled neurons classified as high intensity cells and increasing these same parameters in neurons classified as low intensity cells.

6. We have assessed that restoring the amount of BDNF from Aβ-treated SSAO/VAP-1 co-culture condition, to the WT levels, avoids the changes in the expression pattern described for GluA1 and PSD95, observed in the neuronal subpopulation types present within our *in vitro* model.

IX. References

'Alzheimer's association report' (2021). doi: 10.1002/alz.12328.

Abbott, N. J. et al. (2010) 'Structure and function of the blood-brain barrier', Neurobiology of disease. Neurobiol Dis, 37(1), pp. 13–25. doi: 10.1016/J.NBD.2009.07.030.

Abbott, N. J., Rönnbäck, L. and Hansson, E. (2006) 'Astrocyte-endothelial interactions at the blood-brain barrier', Nature reviews. Neuroscience. Nat Rev Neurosci, 7(1), pp. 41–53. doi: 10.1038/NRN1824.

Adams, R. H. and Eichmann, A. (2010) 'Axon guidance molecules in vascular patterning', Cold Spring Harbor perspectives in biology. Cold Spring Harb Perspect Biol, 2(5). doi: 10.1101/CSHPERSPECT.A001875.

Airas, L. et al. (2006) 'Elevated serum soluble vascular adhesion protein-1 (VAP-1) in patients with active relapsing remitting multiple sclerosis', Journal of neuroimmunology. J Neuroimmunol, 177(1–2), pp. 132–135. doi: 10.1016/J.JNEUROIM.2006.05.014.

Airas, L. et al. (2008) 'Vascular adhesion protein-1 in human ischaemic stroke', Neuropathology and applied neurobiology. Neuropathol Appl Neurobiol, 34(4), pp. 394–402. doi: 10.1111/J.1365-2990.2007.00911.X.

Akiguchi, I. et al. (2017) 'SAMP8 mice as a neuropathological model of accelerated brain aging and dementia: Toshio Takeda's legacy and future directions', Neuropathology : official journal of the Japanese Society of Neuropathology. Neuropathology, 37(4), pp. 293–305. doi: 10.1111/NEUP.12373.

Akiyama, H. et al. (2000) 'Inflammation and Alzheimer's disease', Neurobiology of aging. Neurobiol Aging, 21(3), pp. 383–421. doi: 10.1016/S0197-4580(00)00124-X.

Ali, M. et al. (2022) 'VEGF signalling causes stalls in brain capillaries and reduces cerebral blood flow in Alzheimer's mice', Brain : a journal of neurology. Brain, 145(4), pp. 1449–1463. doi: 10.1093/BRAIN/AWAB387.

Almeida, C. G. et al. (2005) 'Beta-amyloid accumulation in APP mutant neurons reduces PSD-95 and GluR1 in synapses', Neurobiology of disease. Neurobiol Dis, 20(2), pp. 187–198. doi: 10.1016/J.NBD.2005.02.008.

Altschul, S. F. et al. (1997) 'Gapped BLAST and PSI-BLAST: a new generation of protein database search programs', Nucleic Acids Research. Oxford Academic, 25(17), pp. 3389–3402. doi: 10.1093/NAR/25.17.3389.

Alzheimer Europe (2019) 'Dementia in Europe yearbook 2019: Estimating the prevalence of dementia in Europe.', Alzheimer Europe, p. 108. Available at: https://www.alzheimer-europe.org/sites/default/files/alzheimer_europe_dementia_in_europe_yearbook_2019.pdf.

Ambrose, C. T. (2012) 'Neuroangiogenesis: a vascular basis for Alzheimer's disease and cognitive decline during aging', Journal of Alzheimer's disease : JAD. J Alzheimers Dis, 32(3), pp. 773–788. doi: 10.3233/JAD-2012-120067.

András, I. E. et al. (2007) 'The NMDA and AMPA/KA receptors are involved in glutamate-induced alterations of occludin expression and phosphorylation in brain endothelial cells', Journal of Cerebral Blood Flow and Metabolism. SAGE PublicationsSage UK: London, England, 27(8), pp. 1431–1443. doi: 10.1038/sj.jcbfm.9600445.

Andreone, B. J., Lacoste, B. and Gu, C. (2015) 'Neuronal and vascular interactions', Annual review of neuroscience. Annu Rev Neurosci, 38, pp. 25–46. doi: 10.1146/ANNUREV-NEURO-071714-033835.

Andrés, N. et al. (2001) 'Tissue activity and cellular localization of human semicarbazide-sensitive amine oxidase', The journal of histochemistry and cytochemistry : official journal of the Histochemistry Society. J Histochem Cytochem, 49(2), pp. 209–217. doi: 10.1177/002215540104900208.

Arancibia, S. et al. (2008) 'Protective effect of BDNF against beta-amyloid induced neurotoxicity in vitro and in vivo in rats', Neurobiology of disease. Neurobiol Dis, 31(3), pp. 316–326. doi: 10.1016/J.NBD.2008.05.012.

Araque, A. et al. (1999) 'Tripartite synapses: glia, the unacknowledged partner', Trends in neurosciences. Trends Neurosci, 22(5), pp. 208–215. doi: 10.1016/S0166-2236(98)01349-6.

Arbor, S. (2017) 'Targeting amyloid precursor protein shuttling and processing - long before amyloid beta formation', Neural Regeneration Research. Medknow Publications, 12(2), pp. 207–209. doi: 10.4103/1673-5374.200800.

Armulik, A. et al. (2010) 'Pericytes regulate the blood–brain barrier', Nature 2010 468:7323. Nature Publishing Group, 468(7323), pp. 557–561. doi: 10.1038/nature09522.

Armulik, A., Genové, G. and Betsholtz, C. (2011) 'Pericytes: developmental, physiological, and pathological perspectives, problems, and promises', Developmental cell. Dev Cell, 21(2), pp. 193–215. doi: 10.1016/J.DEVCEL.2011.07.001.

Arriagada, P. V., Marzloff, K. and Hyman, B. T. (1992) 'Distribution of Alzheimer-type pathologic changes in nondemented elderly individuals matches the pattern in Alzheimer's disease', Neurology. Neurology, 42(9), pp. 1681–1688. doi: 10.1212/WNL.42.9.1681.

Ashby, M. C., Daw, M. I. and Isaac, J. T. R. (2008) 'AMPA Receptors', The Glutamate Receptors. Totowa, NJ: Humana Press, pp. 1–44. doi: 10.1007/978-1-59745-055-3_1.

Attems, J., Lintner, F. and Jellinger, K. A. (2004) 'Amyloid beta peptide 1-42 highly correlates with capillary cerebral amyloid angiopathy and Alzheimer disease pathology', Acta neuropathologica. Acta Neuropathol, 107(4), pp. 283–291. doi: 10.1007/S00401-004-0822-6.

Attneave, F., B., M. and Hebb, D. O. (1950) 'The Organization of Behavior; A Neuropsychological Theory', The American Journal of Psychology, 63(4), p. 633. doi: 10.2307/1418888.

Attwell, D. et al. (2010) 'Glial and neuronal control of brain blood flow', Nature 2010 468:7321. Nature Publishing Group, 468(7321), pp. 232–243. doi: 10.1038/nature09613.

Awasthi, S. and Boor, P. J. (1993) 'Semicarbazide protection from in vivo oxidant injury of vascular tissue by allylamine', Toxicology Letters. Elsevier, 66(2), pp. 157–163. doi: 10.1016/0378-4274(93)90090-K.

Azevedo, F. A. C. et al. (2009) 'Equal numbers of neuronal and nonneuronal cells make the human brain an isometrically scaled-up primate brain', The Journal of comparative neurology. J Comp Neurol, 513(5), pp. 532–541. doi: 10.1002/CNE.21974.

Bacakova, L. et al. (2018) 'The Role of Vascular Smooth Muscle Cells in the Physiology and Pathophysiology of Blood Vessels', Muscle Cell and Tissue - Current Status of Research Field. IntechOpen. doi: 10.5772/INTECHOPEN.77115.

Bahri, M. A. et al. (2017) 'Measuring brain synaptic vesicle protein 2A with positron emission tomography and [18F]UCB-H', Alzheimer's & Dementia : Translational Research & Clinical Interventions. Wiley-Blackwell, 3(4), p. 481. doi: 10.1016/J.TRCI.2017.08.004.

Baik, S. H. et al. (2014) 'Migration of neutrophils targeting amyloid plaques in Alzheimer's disease mouse model', Neurobiology of aging. Neurobiol Aging, 35(6), pp. 1286–1292. doi: 10.1016/J.NEUROBIOLAGING.2014.01.003.

Baik, S. H. et al. (2019) 'A Breakdown in Metabolic Reprogramming Causes Microglia Dysfunction in Alzheimer's Disease', Cell metabolism. Cell Metab, 30(3), pp. 493-507.e6. doi: 10.1016/J.CMET.2019.06.005.

Bailly, M. et al. (2015) 'Precuneus and Cingulate Cortex Atrophy and Hypometabolism in Patients with Alzheimer's Disease and Mild Cognitive Impairment: MRI and (18)F-FDG PET Quantitative Analysis Using FreeSurfer', BioMed research international. Biomed Res Int, 2015. doi: 10.1155/2015/583931.

Balabanov, R. and Dore-Duffy, P. (1998) 'Role of the CNS microvascular pericyte in the blood-brain barrier', Journal of Neuroscience Research, 53(6), pp. 637–644. doi: 10.1002/(SICI)1097-4547(19980915)53:6<637::AID-JNR1>3.0.CO;2-6.

Baloyannis, S. J. and Baloyannis, I. S. (2012) 'The vascular factor in Alzheimer's disease: a study in Golgi technique and electron microscopy', Journal of the neurological sciences. J Neurol Sci, 322(1–2), pp. 117–121. doi: 10.1016/J.JNS.2012.07.010.

Bao, W. et al. (2021) 'PET Neuroimaging of Alzheimer's Disease: Radiotracers and Their Utility in Clinical Research', Frontiers in aging neuroscience. Front Aging Neurosci, 13. doi: 10.3389/FNAGI.2021.624330.

Barde, Y. A., Edgar, D. and Thoenen, H. (1982) 'Purification of a new neurotrophic factor from mammalian brain', The EMBO journal. EMBO J, 1(5), pp. 549–553. doi: 10.1002/J.1460-2075.1982.TB01207.X.

Barres, B. A. (2003) 'What is a glial cell?', Glia. John Wiley & Sons, Ltd, 43(1), pp. 4–5. doi: 10.1002/GLIA.10252.

Barres, B. A. (2008) 'The mystery and magic of glia: a perspective on their roles in health and disease', Neuron. Neuron, 60(3), pp. 430–440. doi: 10.1016/J.NEURON.2008.10.013.

Basun, H. et al. (2008) 'Clinical and neuropathological features of the Arctic APP mutation causing early onset Alzheimer's disease', Archives of neurology. NIH Public Access, 65(4), p. 499. doi: 10.1001/ARCHNEUR.65.4.499.

Batool, S. et al. (2019) 'Synapse formation: from cellular and molecular mechanisms to neurodevelopmental and neurodegenerative disorders', Journal of neurophysiology. J Neurophysiol, 121(4), pp. 1381–1397. doi: 10.1152/JN.00833.2018.

Baumgart, M. et al. (2015) 'Summary of the evidence on modifiable risk factors for cognitive decline and dementia: A population-based perspective', Alzheimer's & dementia : the journal of the Alzheimer's Association. Alzheimers Dement, 11(6), pp. 718–726. doi: 10.1016/J.JALZ.2015.05.016.

Bélanger, M., Allaman, I. and Magistretti, P. J. (2011) 'Brain energy metabolism: focus on astrocyte-neuron metabolic cooperation', Cell metabolism. Cell Metab, 14(6), pp. 724–738. doi: 10.1016/J.CMET.2011.08.016.

Bell, A. H. et al. (2019) 'The Neurovascular Unit: Effects of Brain Insults During the Perinatal Period', Frontiers in Neuroscience. Frontiers Media SA, 13. doi: 10.3389/FNINS.2019.01452.

Belviranlı, M. and Okudan, N. (2019) 'Voluntary, involuntary and forced exercises almost equally reverse behavioral impairment by regulating hippocampal neurotrophic factors and oxidative stress in experimental Alzheimer's disease model', Behavioural brain research. Behav Brain Res, 364, pp. 245–255. doi: 10.1016/J.BBR.2019.02.030.

Bhattacharyya, S. et al. (2009) 'A critical role for PSD-95/AKAP interactions in endocytosis of synaptic AMPA receptors', Nature neuroscience. Nat Neurosci, 12(2), pp. 172–181. doi: 10.1038/NN.2249.

Biederer, T., Kaeser, P. S. and Blanpied, T. A. (2017) 'Transcellular Nanoalignment of Synaptic Function', Neuron. Neuron, 96(3), pp. 680–696. doi: 10.1016/J.NEURON.2017.10.006.

Bilbo, S. and Stevens, B. (2017) 'Microglia: The Brain's First Responders', Cerebrum: the Dana Forum on Brain Science. Dana Foundation, 2017. Available at: /pmc/articles/PMC6132046/ (Accessed: 11 June 2022).

Binder, D. K. and Scharfman, H. E. (2004) 'Brain-derived neurotrophic factor', Growth factors (Chur, Switzerland). Growth Factors, 22(3), pp. 123–131. doi: 10.1080/08977190410001723308.

Bliss, T. V. P. and Cooke, S. F. (2011) 'Long-term potentiation and long-term depression: a clinical perspective', Clinics (Sao Paulo, Brazil). Clinics (Sao Paulo), 66 Suppl 1(Suppl 1), pp. 3–17. doi: 10.1590/S1807-59322011001300002.

Blurton-Jones, M. et al. (2009) 'Neural stem cells improve cognition via BDNF in a transgenic model of Alzheimer disease', Proceedings of the National Academy of Sciences of the United States of America. Proc Natl Acad Sci U S A, 106(32), pp. 13594–13599. doi: 10.1073/PNAS.0901402106.

Bohlen und Halbach, O., Minichiello, L. and Unsicker, K. (2005) 'Haploinsufficiency for trkB and trkC receptors induces cell loss and accumulation of alpha-synuclein in the substantia nigra', FASEB journal : official publication of the Federation of American Societies for Experimental Biology. FASEB J, 19(12), pp. 1740–1742. doi: 10.1096/FJ.05-3845FJE.

Boillée, S. et al. (2006) 'Onset and progression in inherited ALS determined by motor neurons and microglia', Science (New York, N.Y.). Science, 312(5778), pp. 1389–1392. doi: 10.1126/SCIENCE.1123511.

Boomsma, F. et al. (1997) 'Plasma semicarbazide-sensitive amine oxidase is elevated in patients with congestive heart failure', Cardiovascular research. Cardiovasc Res, 33(2), pp. 387–391. doi: 10.1016/S0008-6363(96)00209-X.

Boomsma, F. et al. (1999) 'Circulating semicarbazide-sensitive amine oxidase is raised both in type I (insulin-dependent), in type II (non-insulin-dependent) diabetes mellitus and even in childhood type I diabetes at first clinical diagnosis', Diabetologia. Diabetologia, 42(2), pp. 233–237. doi: 10.1007/S001250051143.

Boomsma, F. et al. (2003) 'Plasma semicarbazide-sensitive amine oxidase in human (patho)physiology', Biochimica et Biophysica Acta (BBA) - Proteins and Proteomics. Elsevier, 1647(1–2), pp. 48–54. doi: 10.1016/S1570-9639(03)00047-5.

Boulouis, G. et al. (2016) 'Noncontrast Computed Tomography Hypodensities Predict Poor Outcome in Intracerebral Hemorrhage Patients', Stroke. Stroke, 47(10), pp. 2511–2516. doi: 10.1161/STROKEAHA.116.014425.

Braak, H. and Braak, E. (1991) 'Neuropathological stageing of Alzheimer-related changes', Acta neuropathologica. Acta Neuropathol, 82(4), pp. 239–259. doi: 10.1007/BF00308809.

Braschi, C. et al. (2021) 'Intranasal delivery of BDNF rescues memory deficits in AD11 mice and reduces brain microgliosis', Aging clinical and experimental research. Aging Clin Exp Res, 33(5), pp. 1223–1238. doi: 10.1007/S40520-020-01646-5.

Brown, R. C. et al. (2003) 'Protection against hypoxia-induced increase in blood-brain barrier permeability: Role of tight junction proteins and NFκB', Journal of Cell Science. doi: 10.1242/jcs.00264.

Bugiani, O. et al. (2010) 'Hereditary cerebral hemorrhage with amyloidosis associated with the E693K mutation of APP', Archives of neurology. Arch Neurol, 67(8), pp. 987–995. doi: 10.1001/ARCHNEUROL.2010.178.

Cai, Z. et al. (2017) 'Chronic Cerebral Hypoperfusion Promotes Amyloid-Beta Pathogenesis via Activating β/γ-Secretases', Neurochemical research. Neurochem Res, 42(12), pp. 3446–3455. doi: 10.1007/S11064-017-2391-9.

Cai, Z. et al. (2020) 'Synthesis and Preclinical Evaluation of an 18F-Labeled Synaptic Vesicle Glycoprotein 2A PET Imaging Probe: [18F]SynVesT-2', ACS Chemical Neuroscience. American Chemical Society, 11(4), pp. 592–603. doi: 10.1021/ACSCHEMNEURO.9B00618/SUPPL_FILE/CN9B00618_SI_001.PDF.

Caldeira, M. V. et al. (2007) 'Brain-derived neurotrophic factor regulates the expression and synaptic delivery of alpha-amino-3-hydroxy-5-methyl-4-isoxazole propionic acid receptor subunits in hippocampal neurons', The Journal of biological chemistry. J Biol Chem, 282(17), pp. 12619–12628. doi: 10.1074/JBC.M700607200.

Campion, D. et al. (2016) 'Alzheimer disease: modeling an Aβ-centered biological network', Molecular psychiatry. Mol Psychiatry, 21(7), pp. 861–871. doi: 10.1038/MP.2016.38.

Capsoni, S. et al. (2000) 'Alzheimer-like neurodegeneration in aged antinerve growth factor transgenic mice', Proceedings of the National Academy of Sciences of the United States of America. Proc Natl Acad Sci U S A, 97(12), pp. 6826–6831. doi: 10.1073/PNAS.97.12.6826.

Castillo, V. et al. (1998) 'Semicarbazide-sensitive amine oxidase (SSAO) from human and bovine cerebrovascular tissues: biochemical and immunohistological characterization', Neurochemistry international. Neurochem Int, 33(5), pp. 415–423. doi: 10.1016/S0197-0186(98)00045-X.

Cekanaviciute, E. and Buckwalter, M. S. (2016) 'Astrocytes: Integrative Regulators of Neuroinflammation in Stroke and Other Neurological Diseases', Neurotherapeutics : the journal of the American Society for Experimental NeuroTherapeutics. Neurotherapeutics, 13(4), pp. 685–701. doi: 10.1007/S13311-016-0477-8.

Chang, A. et al. (2002) 'Premyelinating oligodendrocytes in chronic lesions of multiple sclerosis', The New England journal of medicine. N Engl J Med, 346(3), pp. 165–173. doi: 10.1056/NEJMOA010994.

Chao, Y. X., He, B. P. and Tay, S. S. W. (2009) 'Mesenchymal stem cell transplantation attenuates blood brain barrier damage and neuroinflammation and protects dopaminergic neurons against MPTP toxicity in the substantia nigra in a model of Parkinson's disease', Journal of neuroimmunology. J Neuroimmunol, 216(1–2), pp. 39–50. doi: 10.1016/J.JNEUROIM.2009.09.003.

Charidimou, A. et al. (2017) 'Emerging concepts in sporadic cerebral amyloid angiopathy', Brain : a journal of neurology. Brain, 140(7), pp. 1829–1850. doi: 10.1093/BRAIN/AWX047.

Chen, C. J., Liao, S. L. and Kuo, J. S. (2000) 'Gliotoxic action of glutamate on cultured astrocytes', Journal of neurochemistry. J Neurochem, 75(4), pp. 1557–1565. doi: 10.1046/J.1471-4159.2000.0751557.X.

Chen, G. F. et al. (2017) 'Amyloid beta: structure, biology and structure-based therapeutic development', Acta pharmacologica Sinica. Acta Pharmacol Sin, 38(9), pp. 1205–1235. doi: 10.1038/APS.2017.28.

Chen, K., Kazachkov, M. and Yu, P. H. (2007) 'Effect of aldehydes derived from oxidative deamination and oxidative stress on β-amyloid aggregation; pathological implications to Alzheimer's disease', Journal of Neural Transmission 2007 114:6. Springer, 114(6), pp. 835–839. doi: 10.1007/S00702-007-0697-5.

Chen, M. K. et al. (2018) 'Assessing Synaptic Density in Alzheimer Disease With Synaptic Vesicle Glycoprotein 2A Positron Emission Tomographic Imaging', JAMA neurology. JAMA Neurol, 75(10), pp. 1215–1224. doi: 10.1001/JAMANEUROL.2018.1836.

Chen, S. Der et al. (2017) 'More Insight into BDNF against Neurodegeneration: Anti-Apoptosis, Anti-Oxidation, and Suppression of Autophagy', International Journal of Molecular Sciences. Multidisciplinary Digital Publishing Institute (MDPI), 18(3). doi: 10.3390/IJMS18030545.

Chen, X. et al. (2008) 'Caffeine protects against MPTP-induced blood-brain barrier dysfunction in mouse striatum', Journal of neurochemistry. J Neurochem, 107(4), pp. 1147–1157. doi: 10.1111/J.1471-4159.2008.05697.X.

Chen, X. et al. (2015) 'PSD-95 family MAGUKs are essential for anchoring AMPA and NMDA receptor complexes at the postsynaptic density', Proceedings of the National Academy of Sciences of the United States of America. Proc Natl Acad Sci U S A, 112(50), pp. E6983–E6992. doi: 10.1073/PNAS.1517045112.

Chen, Y., Fu, A. K. Y. and Ip, N. Y. (2019) 'Synaptic dysfunction in Alzheimer's disease: Mechanisms and therapeutic strategies', Pharmacology & therapeutics. Pharmacol Ther, 195, pp. 186–198. doi: 10.1016/J.PHARMTHERA.2018.11.006.

Cheng, X. rui, Zhou, W. xia and Zhang, Y. xiang (2014) 'The behavioral, pathological and therapeutic features of the senescence-accelerated mouse prone 8 strain as an Alzheimer's disease animal model', Ageing research reviews. Ageing Res Rev, 13(1), pp. 13–37. doi: 10.1016/J.ARR.2013.10.002.

Citri, A. and Malenka, R. C. (2007) 'Synaptic Plasticity: Multiple Forms, Functions, and Mechanisms', Neuropsychopharmacology 2008 33:1. Nature Publishing Group, 33(1), pp. 18–41. doi: 10.1038/sj.npp.1301559.

Citron, M. et al. (1992) 'Mutation of the beta-amyloid precursor protein in familial Alzheimer's disease increases beta-protein production', Nature. Nature, 360(6405), pp. 672–674. doi: 10.1038/360672A0.

Colledge, M. et al. (2000) 'Targeting of PKA to glutamate receptors through a MAGUK-AKAP complex', Neuron. Neuron, 27(1), pp. 107–119. doi: 10.1016/S0896-6273(00)00013-1.

Colucci-D'Amato, L., Perrone-Capano, C. and Di Porzio, U. (2003) 'Chronic activation of ERK and neurodegenerative diseases', BioEssays : news and reviews in molecular, cellular and developmental biology. Bioessays, 25(11), pp. 1085–1095. doi: 10.1002/BIES.10355.

Coluccio, M. L. et al. (2019) 'Microfluidic platforms for cell cultures and investigations', Microelectronic Engineering. Elsevier B.V., 208, pp. 14–28. doi: 10.1016/J.MEE.2019.01.004.

Cordonnier, C. and Van Der Flier, W. M. (2011) 'Brain microbleeds and Alzheimer's disease: innocent observation or key player?', Brain : a journal of neurology. Brain, 134(Pt 2), pp. 335–344. doi: 10.1093/BRAIN/AWQ321.

Cras, P. et al. (1998) 'Presenile Alzheimer dementia characterized by amyloid angiopathy and large amyloid core type senile plaques in the APP 692Ala→Gly mutation', Acta Neuropathologica, 96(3), pp. 253–260. doi: 10.1007/s004010050892.

Cruz Hernández, J. C. et al. (2019) 'Neutrophil adhesion in brain capillaries reduces cortical blood flow and impairs memory function in Alzheimer's disease mouse models', Nature neuroscience. Nat Neurosci, 22(3), pp. 413–420. doi: 10.1038/S41593-018-0329-4.

Cullen, K. M., Kócsi, Z. and Stone, J. (2005) 'Pericapillary haem-rich deposits: evidence for microhaemorrhages in aging human cerebral cortex', Journal of cerebral blood flow and metabolism : official journal of the International Society of Cerebral Blood Flow and Metabolism. J Cereb Blood Flow Metab, 25(12), pp. 1656–1667. doi: 10.1038/SJ.JCBFM.9600155.

Cunningham, E. L., McGuinness, B., Herron, B., & Passmore, A. P. (2015). 'Dementia', The Ulster medical journal. Ulster Med J, 84(2), 79–87.

Custodia, A. et al. (2022) 'Endothelial Progenitor Cells and Vascular Alterations in Alzheimer's Disease', Frontiers in aging neuroscience. Front Aging Neurosci, 13. doi: 10.3389/FNAGI.2021.811210.

Dacher, M. et al. (2013) 'A-kinase anchoring protein-calcineurin signaling in long-term depression of GABAergic synapses', The Journal of neuroscience : the official journal of the Society for Neuroscience. J Neurosci, 33(6), pp. 2650–2660. doi: 10.1523/JNEUROSCI.2037-12.2013.

Dao, A. T. et al. (2013) 'Treadmill exercise prevents learning and memory impairment in Alzheimer's disease-like pathology', Current Alzheimer research. Curr Alzheimer Res, 10(5), pp. 507–515. doi: 10.2174/1567205011310050006.

DaRocha-Souto, B. et al. (2012) 'Activation of glycogen synthase kinase-3 beta mediates β-amyloid induced neuritic damage in Alzheimer's disease', Neurobiology of disease. Neurobiol Dis, 45(1), pp. 425–437. doi: 10.1016/J.NBD.2011.09.002.

De La Torre, J. C. (2006) 'How do heart disease and stroke become risk factors for Alzheimer's disease?', Neurological research. Neurol Res, 28(6), pp. 637–644. doi: 10.1179/016164106X130362.

de la Torre, J. C. (2017) 'Are Major Dementias Triggered by Poor Blood Flow to the Brain? Theoretical Considerations', Journal of Alzheimer's disease : JAD. J Alzheimers Dis, 57(2), pp. 353–371. doi: 10.3233/JAD-161266.

De la Torre, J. C. and Mussivand, T. (1993) 'Can disturbed brain microcirculation cause Alzheimer's disease?', Neurological research. Neurol Res, 15(3), pp. 146–153. doi: 10.1080/01616412.1993.11740127.

De Pins, B. et al. (2019) 'Conditional BDNF delivery from astrocytes rescues memory deficits, spine density, and synaptic properties in the 5xFAD mouse model of alzheimer disease', Journal of Neuroscience. doi: 10.1523/JNEUROSCI.2121-18.2019.

De Pins, B. et al. (2019) 'Conditional BDNF Delivery from Astrocytes Rescues Memory Deficits, Spine Density, and Synaptic Properties in the 5xFAD Mouse Model of Alzheimer Disease', The Journal of neuroscience : the official journal of the Society for Neuroscience. J Neurosci, 39(13), pp. 2441–2458. doi: 10.1523/JNEUROSCI.2121-18.2019.

Del Mar Hernandez, M. et al. (2005) 'Human plasma semicarbazide sensitive amine oxidase (SSAO), beta-amyloid protein and aging', Neuroscience letters. Neurosci Lett, 384(1–2), pp. 183–187. doi: 10.1016/J.NEULET.2005.04.074.

Del Mar Hernandez, M. et al. (2005) 'Human plasma semicarbazide sensitive amine oxidase (SSAO), β-amyloid protein and aging', Neuroscience Letters. Elsevier Ireland Ltd, 384(1–2), pp. 183–187. doi: 10.1016/j.neulet.2005.04.074.

Dementia (no date). Available at: https://www.who.int/news-room/fact-sheets/detail/dementia (Accessed: 11 June 2022).

Deo, A. K. et al. (2014) 'Activity of P-Glycoprotein, a β-Amyloid Transporter at the Blood-Brain Barrier, Is Compromised in Patients with Mild Alzheimer Disease', Journal of nuclear medicine : official publication, Society of Nuclear Medicine. J Nucl Med, 55(7), pp. 1106–1111. doi: 10.2967/JNUMED.113.130161.

Dewar, D. et al. (1991) 'Glutamate metabotropic and AMPA binding sites are reduced in Alzheimer's disease: an autoradiographic study of the hippocampus', Brain Research. Elsevier, 553(1), pp. 58–64. doi: 10.1016/0006-8993(91)90230-S.

Di Lazzaro, V. et al. (2007) 'BDNF plasma levels in acute stroke', Neuroscience letters. Neurosci Lett, 422(2), pp. 128–130. doi: 10.1016/J.NEULET.2007.06.001.

Di, J. et al. (2016) 'Abnormal tau induces cognitive impairment through two different mechanisms: synaptic dysfunction and neuronal loss', Scientific reports. Sci Rep, 6. doi: 10.1038/SREP20833.

Doble, A. (1999) 'The role of excitotoxicity in neurodegenerative disease: implications for therapy', Pharmacology & therapeutics. Pharmacol Ther, 81(3), pp. 163–221. doi: 10.1016/S0163-7258(98)00042-4.

Donahue, J. E. et al. (2006) 'RAGE, LRP-1, and amyloid-beta protein in Alzheimer's disease', Acta neuropathologica. Acta Neuropathol, 112(4), pp. 405–415. doi: 10.1007/S00401-006-0115-3.

Dong, X. X., Wang, Y. and Qin, Z. H. (2009) 'Molecular mechanisms of excitotoxicity and their relevance to pathogenesis of neurodegenerative diseases', Acta Pharmacologica Sinica 2009 30:4. Nature Publishing Group, 30(4), pp. 379–387. doi: 10.1038/aps.2009.24.

Donovan, M. J. et al. (1995) 'Neurotrophin and Neurotrophin Receptors in Vascular Smooth Muscle Cells: Regulation of Expression in Response to Injury', The American Journal of

Pathology. American Society for Investigative Pathology, 147(2), p. 309. Available at: /pmc/articles/PMC1869811/?report=abstract (Accessed: 13 June 2022).

Dore, K. et al. (2021) 'PSD-95 protects synapses from β-amyloid', Cell Reports. ElsevierCompany., 35(9), p. 109194. doi: 10.1016/j.celrep.2021.109194.

Dowling, P. and Clynes, M. (2011) 'Conditioned media from cell lines: a complementary model to clinical specimens for the discovery of disease-specific biomarkers', Proteomics. Proteomics, 11(4), pp. 794–804. doi: 10.1002/PMIC.201000530.

Dugger, B. N. and Dickson, D. W. (2017) 'Pathology of Neurodegenerative Diseases', Cold Spring Harbor perspectives in biology. Cold Spring Harb Perspect Biol, 9(7). doi: 10.1101/CSHPERSPECT.A028035.

Duran-Vilaregut, J. et al. (2009) 'Blood-brain barrier disruption in the striatum of rats treated with 3-nitropropionic acid', Neurotoxicology. Neurotoxicology, 30(1), pp. 136–143. doi: 10.1016/J.NEURO.2008.10.007.

Edison, P., Donat, C. K. and Sastre, M. (2018) 'In vivo imaging of glial activation in alzheimer's disease', Frontiers in Neurology. Frontiers Media S.A., 9(AUG), p. 625. doi: 10.3389/FNEUR.2018.00625/BIBTEX.

Ehrlich, I. and Malinow, R. (2004) 'Postsynaptic density 95 controls AMPA receptor incorporation during long-term potentiation and experience-driven synaptic plasticity', The Journal of neuroscience : the official journal of the Society for Neuroscience. J Neurosci, 24(4), pp. 916–927. doi: 10.1523/JNEUROSCI.4733-03.2004.

Elbaz, B. and Popko, B. (2019) 'Molecular Control of Oligodendrocyte Development', Trends in neurosciences. Trends Neurosci, 42(4), pp. 263–277. doi: 10.1016/J.TINS.2019.01.002.

El-Husseini, A. E.-D. et al. (2000) 'PSD-95 involvement in maturation of excitatory synapses.', Science (New York, N.Y.). American Association for the Advancement of Science (AAAS), 290(5495), pp. 1364–1368. doi: 10.1126/science.290.5495.1364.

Espinera, A. R. et al. (2013) 'Citalopram enhances neurovascular regeneration and sensorimotor functional recovery after ischemic stroke in mice', Neuroscience. Neuroscience, 247, pp. 1–11. doi: 10.1016/J.NEUROSCIENCE.2013.04.011.

Estrada, S. et al. (2016) '[(11)C]UCB-A, a novel PET tracer for synaptic vesicle protein 2A', Nuclear medicine and biology. Nucl Med Biol, 43(6), pp. 325–332. doi: 10.1016/J.NUCMEDBIO.2016.03.004.

Esvald, E. E. et al. (2020) 'CREB Family Transcription Factors Are Major Mediators of BDNF Transcriptional Autoregulation in Cortical Neurons', The Journal of neuroscience : the official journal of the Society for Neuroscience. J Neurosci, 40(7), pp. 1405–1426. doi: 10.1523/JNEUROSCI.0367-19.2019.

Fairless, R., Bading, H. and Diem, R. (2021) 'Pathophysiological Ionotropic Glutamate Signalling in Neuroinflammatory Disease as a Therapeutic Target', Frontiers in Neuroscience. Frontiers Media S.A., 15, p. 1408. doi: 10.3389/FNINS.2021.741280/BIBTEX.

Feng, W. and Zhang, M. (2009) 'Organization and dynamics of PDZ-domain-related supramodules in the postsynaptic density', Nature reviews. Neuroscience. Nat Rev Neurosci, 10(2), pp. 87–99. doi: 10.1038/NRN2540.

Fernández, A. et al. (2021) 'Senescent accelerated prone 8 (SAMP8) mice as a model of age dependent neuroinflammation', Journal of Neuroinflammation 2021 18:1. BioMed Central, 18(1), pp. 1–20. doi: 10.1186/S12974-021-02104-3.

Ferrer, I. et al. (2002) 'Overexpression of semicarbazide sensitive amine oxidase in the cerebral blood vessels in patients with Alzheimer's disease and cerebral autosomal dominant arteriopathy with subcortical infarcts and leukoencephalopathy', Neuroscience Letters. Elsevier, 321(1–2), pp. 21–24. doi: 10.1016/S0304-3940(01)02465-X.

Ferrer, I. et al. (2002) 'Overexpression of semicarbazide sensitive amine oxidase in the cerebral blood vessels in patients with Alzheimer's disease and cerebral autosomal dominant arteriopathy with subcortical infarcts and leukoencephalopathy', Neuroscience letters. Neurosci Lett, 321(1–2), pp. 21–24. doi: 10.1016/S0304-3940(01)02465-X.

Fiala, M. et al. (2002) 'Cyclooxygenase-2-positive macrophages infiltrate the Alzheimer's disease brain and damage the blood-brain barrier', European journal of clinical investigation. Eur J Clin Invest, 32(5), pp. 360–371. doi: 10.1046/J.1365-2362.2002.00994.X.

Figueiredo, C. P. et al. (2013) 'Memantine Rescues Transient Cognitive Impairment Caused by High-Molecular-Weight Aβ Oligomers But Not the Persistent Impairment Induced by Low-Molecular-Weight Oligomers', The Journal of Neuroscience. Society for Neuroscience, 33(23), p. 9626. doi: 10.1523/JNEUROSCI.0482-13.2013.

Fillit, H. et al. (2008) 'Cardiovascular risk factors and dementia', The American journal of geriatric pharmacotherapy. Am J Geriatr Pharmacother, 6(2), pp. 100–118. doi: 10.1016/J.AMJOPHARM.2008.06.004.

Finkel, T. (1998) 'Oxygen radicals and signaling', Current opinion in cell biology. Curr Opin Cell Biol, 10(2), pp. 248–253. doi: 10.1016/S0955-0674(98)80147-6.

Finnema, S. J. et al. (2016) 'Imaging synaptic density in the living human brain', Science translational medicine. Sci Transl Med, 8(348). doi: 10.1126/SCITRANSLMED.AAF6667.

Flynn, K. C. (2013) 'The cytoskeleton and neurite initiation', Bioarchitecture. Taylor & Francis, 3(4), p. 86. doi: 10.4161/BIOA.26259.

Forner, S. et al. (2017) 'Synaptic Impairment in Alzheimer's Disease: A Dysregulated Symphony', Trends in neurosciences. Trends Neurosci, 40(6), pp. 347–357. doi: 10.1016/J.TINS.2017.04.002.

Francula-Zaninovic, S. and Nola, I. A. (2018) 'Management of Measurable Variable Cardiovascular Disease' Risk Factors', Current cardiology reviews. Curr Cardiol Rev, 14(3), pp. 153–163. doi: 10.2174/1573403X14666180222102312.

Franklin, R. J. M. and Ffrench-Constant, C. (2017) 'Regenerating CNS myelin - from mechanisms to experimental medicines', Nature reviews. Neuroscience. Nat Rev Neurosci, 18(12), pp. 753–769. doi: 10.1038/NRN.2017.136.

Franks, K. M., Stevens, C. F. and Sejnowski, T. J. (2003) 'Independent Sources of Quantal Variability at Single Glutamatergic Synapses', Journal of Neuroscience. Society for Neuroscience, 23(8), pp. 3186–3195. doi: 10.1523/JNEUROSCI.23-08-03186.2003.

Frenkel, D. (2020) 'Alzheimer's disease: A need for personalized therapeutic approaches', Drug development research. Drug Dev Res, 81(2), pp. 141–143. doi: 10.1002/DDR.21652.

Frost, B., Jacks, R. L. and Diamond, M. I. (2009) 'Propagation of tau misfolding from the outside to the inside of a cell', The Journal of biological chemistry. J Biol Chem, 284(19), pp. 12845–12852. doi: 10.1074/JBC.M808759200.

Fukumoto, K. et al. (2019) 'Activity-dependent brain-derived neurotrophic factor signaling is required for the antidepressant actions of (2 R,6 R)-hydroxynorketamine', Proceedings of the National Academy of Sciences of the United States of America. Proc Natl Acad Sci U S A, 116(1), pp. 297–302. doi: 10.1073/PNAS.1814709116.

Gaengel, K. et al. (2009) 'Endothelial-mural cell signaling in vascular development and angiogenesis', Arteriosclerosis, thrombosis, and vascular biology. Arterioscler Thromb Vasc Biol, 29(5), pp. 630–638. doi: 10.1161/ATVBAHA.107.161521.

Garaschuk, O. and Verkhratsky, A. (2019) 'GABAergic astrocytes in Alzheimer's disease', Aging (Albany NY). Impact Journals, LLC, 11(6), p. 1602. doi: 10.18632/AGING.101870.

Garpenstrand, H. et al. (1999) 'Elevated plasma semicarbazide-sensitive amine oxidase (SSAO) activity in Type 2 diabetes mellitus complicated by retinopathy', Diabetic Medicine. John Wiley & Sons, Ltd, 16(6), pp. 514–521. doi: 10.1046/J.1464-5491.1999.00103.X.

Garpenstrand, Håkan et al. (1999) 'Plasma semicarbazide-sensitive amine oxidase in stroke', European neurology. Eur Neurol, 41(1), pp. 20–23. doi: 10.1159/000007993.

Gezen-Ak, D. et al. (2013) 'BDNF, TNFα, HSP90, CFH, and IL-10 serum levels in patients with early or late onset Alzheimer's disease or mild cognitive impairment', Journal of Alzheimer's disease : JAD. J Alzheimers Dis, 37(1), pp. 185–195. doi: 10.3233/JAD-130497.

Ghatak, S. et al. (2019) 'Mechanisms of hyperexcitability in alzheimer's disease hiPSC-derived neurons and cerebral organoids vs. Isogenic control', eLife. eLife Sciences Publications Ltd, 8. doi: 10.7554/ELIFE.50333.

Ghosal, S. et al. (2018) 'Activity-Dependent Brain-Derived Neurotrophic Factor Release Is Required for the Rapid Antidepressant Actions of Scopolamine', Biological psychiatry. Biol Psychiatry, 83(1), pp. 29–37. doi: 10.1016/J.BIOPSYCH.2017.06.017.

Glenner, G. G. and Wong, C. W. (1984) 'Alzheimer's disease: initial report of the purification and characterization of a novel cerebrovascular amyloid protein', Biochemical and biophysical research communications. Biochem Biophys Res Commun, 120(3), pp. 885–890. doi: 10.1016/S0006-291X(84)80190-4.

Göktürk, C. et al. (2003) 'Overexpression of semicarbazide-sensitive amine oxidase in smooth muscle cells leads to an abnormal structure of the aortic elastic laminas', The American journal of pathology. Am J Pathol, 163(5), pp. 1921–1928. doi: 10.1016/S0002-9440(10)63550-X.

Govindpani, K. et al. (2019) 'Vascular Dysfunction in Alzheimer's Disease: A Prelude to the Pathological Process or a Consequence of It?', Journal of Clinical Medicine, 8(5), p. 651. doi: 10.3390/jcm8050651.

Grabowski, T. J. et al. (2001) 'Novel amyloid precursor protein mutation in an Iowa family with dementia and severe cerebral amyloid angiopathy', Annals of neurology. Ann Neurol, 49(6), pp. 697–705. doi: 10.1002/ANA.1009.

Grammas, P. and Ovase, R. (2001) 'Inflammatory factors are elevated in brain microvessels in Alzheimer's disease', Neurobiology of aging. Neurobiol Aging, 22(6), pp. 837–842. doi: 10.1016/S0197-4580(01)00276-7.

Greenberg, M. E. et al. (2009) 'Symposium: New Insights in the Biology of BDNF Synthesis and Release: Implications in CNS Function', The Journal of Neuroscience. Society for Neuroscience, 29(41), p. 12764. doi: 10.1523/JNEUROSCI.3566-09.2009.

Greenberg, S. M. et al. (2020) 'Cerebral amyloid angiopathy and Alzheimer disease - one peptide, two pathways', Nature reviews. Neurology. Nat Rev Neurol, 16(1), pp. 30–42. doi: 10.1038/S41582-019-0281-2.

Grönvall-Nordquist, J. L. E. et al. (2001) 'Follow-up of plasma semicarbazide-sensitive amine oxidase activity and retinopathy in Type 2 diabetes mellitus', Journal of diabetes and its complications. J Diabetes Complications, 15(5), pp. 250–256. doi: 10.1016/S1056-8727(01)00151-9.

Grundke-Iqbal, I., Iqbal, K., Quinlan, M., et al. (1986) 'Microtubule-associated protein tau. A component of Alzheimer paired helical filaments', Journal of Biological Chemistry. © 1986 ASBMB. Currently published by Elsevier Inc; originally published by American Society for Biochemistry and Molecular Biology., 261(13), pp. 6084–6089. doi: 10.1016/s0021-9258(17)38495-8.

Grundke-Iqbal, I., Iqbal, K., Tung, Y. C., et al. (1986) 'Abnormal phosphorylation of the microtubule-associated protein tau (tau) in Alzheimer cytoskeletal pathology', Proceedings of the National Academy of Sciences of the United States of America. Proc Natl Acad Sci U S A, 83(13), pp. 4913–4917. doi: 10.1073/PNAS.83.13.4913.

Gu, Z., Liu, W. and Yan, Z. (2009) '{beta}-Amyloid impairs AMPA receptor trafficking and function by reducing Ca2+/calmodulin-dependent protein kinase II synaptic distribution', The Journal of biological chemistry. J Biol Chem, 284(16), pp. 10639–10649. doi: 10.1074/JBC.M806508200.

Gubisne-Haberle, D. et al. (2004) 'Protein cross-linkage induced by formaldehyde derived from semicarbazide-sensitive amine oxidase-mediated deamination of methylamine', The Journal of pharmacology and experimental therapeutics. J Pharmacol Exp Ther, 310(3), pp. 1125–1132. doi: 10.1124/JPET.104.068601.

Gulley, R. L. and Reese, T. S. (1981) 'Cytoskeletal organization at the postsynaptic complex', The Journal of cell biology. J Cell Biol, 91(1), pp. 298–302. doi: 10.1083/JCB.91.1.298.

Gunawardana, C. G. et al. (2009) 'Comprehensive analysis of conditioned media from ovarian cancer cell lines identifies novel candidate markers of epithelial ovarian cancer', Journal of proteome research. J Proteome Res, 8(10), pp. 4705–4713. doi: 10.1021/PR900411G.

Guo, S. et al. (2008) 'Neuroprotection via matrix-trophic coupling between cerebral endothelial cells and neurons', Proceedings of the National Academy of Sciences of the United States of America. doi: 10.1073/pnas.0801105105.

Guo, W. et al. (2014) 'Neuronal activity alters BDNF-TrkB signaling kinetics and downstream functions', Journal of cell science. J Cell Sci, 127(Pt 10), pp. 2249–2260. doi: 10.1242/JCS.139964.

Gylys, K. H. et al. (2004) 'Synaptic changes in Alzheimer's disease: increased amyloid-beta and gliosis in surviving terminals is accompanied by decreased PSD-95 fluorescence', The American journal of pathology. Am J Pathol, 165(5), pp. 1809–1817. doi: 10.1016/S0002-9440(10)63436-0.

Haber, M., Zhou, L. and Murai, K. K. (2006) 'Cooperative Astrocyte and Dendritic Spine Dynamics at Hippocampal Excitatory Synapses', Journal of Neuroscience. Society for Neuroscience, 26(35), pp. 8881–8891. doi: 10.1523/JNEUROSCI.1302-06.2006.

Habtemariam, S. (2018) 'The brain-derived neurotrophic factor in neuronal plasticity and neuroregeneration: new pharmacological concepts for old and new drugs', Neural Regeneration Research. Wolters Kluwer -- Medknow Publications, 13(6), p. 983. doi: 10.4103/1673-5374.233438.

Haigh, J. J. et al. (2003) 'Cortical and retinal defects caused by dosage-dependent reductions in VEGF-A paracrine signaling', Developmental biology. Dev Biol, 262(2), pp. 225–241. doi: 10.1016/S0012-1606(03)00356-7.

Hall, C. N. et al. (2014) 'Capillary pericytes regulate cerebral blood flow in health and disease', Nature. Nature, 508(7494), pp. 55–60. doi: 10.1038/NATURE13165.

Hardy, J. A. and Higgins, G. A. (1992) 'Alzheimer's disease: the amyloid cascade hypothesis', Science (New York, N.Y.). Science, 256(5054), pp. 184–185. doi: 10.1126/SCIENCE.1566067.

Hardy, J. and Selkoe, D. J. (2002) 'The amyloid hypothesis of Alzheimer's disease: progress and problems on the road to therapeutics', Science (New York, N.Y.). Science, 297(5580), pp. 353–356. doi: 10.1126/SCIENCE.1072994.

Harraz, O. F. et al. (2018) 'Endothelial GqPCR activity controls capillary electrical signaling and brain blood flow through PIP2 depletion', Proceedings of the National Academy of Sciences of the United States of America. National Academy of Sciences, 115(15), pp. E3569–E3577. doi: 10.1073/PNAS.1800201115/SUPPL_FILE/PNAS.201800201SI.PDF.

Harris, K. D. and Shepherd, G. M. G. (2015) 'The neocortical circuit: themes and variations', Nature neuroscience. Nat Neurosci, 18(2), pp. 170–181. doi: 10.1038/NN.3917.

Harris, K. M. and Weinberg, R. J. (2012) 'Ultrastructure of synapses in the mammalian brain', Cold Spring Harbor perspectives in biology. Cold Spring Harb Perspect Biol, 4(5), p. 7. doi: 10.1101/CSHPERSPECT.A005587.

Herculano-Houzel, S., Mota, B. and Lent, R. (2006) 'Cellular scaling rules for rodent brains', Proceedings of the National Academy of Sciences of the United States of America. Proc Natl Acad Sci U S A, 103(32), pp. 12138–12143. doi: 10.1073/PNAS.0604911103.

Hernandez, M. et al. (2006) 'Soluble semicarbazide sensitive amine oxidase (SSAO) catalysis induces apoptosis in vascular smooth muscle cells', Biochimica et biophysica acta. Biochim Biophys Acta, 1763(2), pp. 164–173. doi: 10.1016/J.BBAMCR.2005.11.017.

Hernandez-Guillamon, M. et al. (2012) 'VAP-1/SSAO plasma activity and brain expression in human hemorrhagic stroke', Cerebrovascular diseases (Basel, Switzerland). Cerebrovasc Dis, 33(1), pp. 55–63. doi: 10.1159/000333370.

Herzig, M. C. et al. (2004) 'Abeta is targeted to the vasculature in a mouse model of hereditary cerebral hemorrhage with amyloidosis', Nature neuroscience. Nat Neurosci, 7(9), pp. 954–960. doi: 10.1038/NN1302.

Hill, R. A. et al. (2015) 'Regional Blood Flow in the Normal and Ischemic Brain Is Controlled by Arteriolar Smooth Muscle Cell Contractility and Not by Capillary Pericytes', Neuron. Neuron, 87(1), pp. 95–110. doi: 10.1016/J.NEURON.2015.06.001.

Hillen, A. E. J., Burbach, J. P. H. and Hol, E. M. (2018) 'Cell adhesion and matricellular support by astrocytes of the tripartite synapse', Progress in neurobiology. Prog Neurobiol, 165–167, pp. 66–86. doi: 10.1016/J.PNEUROBIO.2018.02.002.

Hol, E. M. et al. (2003) 'Neuronal expression of GFAP in patients with Alzheimer pathology and identification of novel GFAP splice forms', Molecular psychiatry. Mol Psychiatry, 8(9), pp. 786–796. doi: 10.1038/SJ.MP.4001379.

Hong, Y. et al. (2016) 'Mutant huntingtin impairs BDNF release from astrocytes by disrupting conversion of Rab3a-GTP into Rab3a-GDP', Journal of Neuroscience. doi: 10.1523/JNEUROSCI.0168-16.2016.

Hosmane, S. et al. (2010) 'Circular compartmentalized microfluidic platform: Study of axon–glia interactions', Lab on a Chip. The Royal Society of Chemistry, 10(6), pp. 741–747. doi: 10.1039/B918640A.

Howarth, C. (2014) 'The contribution of astrocytes to the regulation of cerebral blood flow', Frontiers in Neuroscience. Frontiers Research Foundation, 0(8 MAY), p. 103. doi: 10.3389/FNINS.2014.00103/BIBTEX.

Hsieh, H. et al. (2006) 'AMPAR removal underlies Abeta-induced synaptic depression and dendritic spine loss', Neuron. Neuron, 52(5), pp. 831–843. doi: 10.1016/J.NEURON.2006.10.035.

Huang, E. J. and Reichardt, L. F. (2003) 'Trk receptors: roles in neuronal signal transduction', Annual review of biochemistry. Annu Rev Biochem, 72, pp. 609–642. doi: 10.1146/ANNUREV.BIOCHEM.72.121801.161629.

Hughes, E. G. et al. (2018) 'Myelin remodeling through experience-dependent oligodendrogenesis in the adult somatosensory cortex', Nature neuroscience. Nat Neurosci, 21(5), pp. 696–706. doi: 10.1038/S41593-018-0121-5.

Hyman, B. T. et al. (2012) 'National Institute on Aging–Alzheimer's Association guidelines for the neuropathologic assessment of Alzheimer's disease', Alzheimer's & dementia : the journal of the Alzheimer's Association. NIH Public Access, 8(1), p. 1. doi: 10.1016/J.JALZ.2011.10.007.

Iadecola, C. (2004) 'Neurovascular regulation in the normal brain and in Alzheimer's disease', Nature reviews. Neuroscience. Nat Rev Neurosci, 5(5), pp. 347–360. doi: 10.1038/NRN1387.

Iadecola, C. (2010) 'The overlap between neurodegenerative and vascular factors in the pathogenesis of dementia', Acta neuropathologica. Acta Neuropathol, 120(3), pp. 287–296. doi: 10.1007/S00401-010-0718-6.

Iadecola, C. (2013) 'The pathobiology of vascular dementia', Neuron. Neuron, 80(4), pp. 844–866. doi: 10.1016/J.NEURON.2013.10.008.

Iadecola, C. (2017) 'The Neurovascular Unit Coming of Age: A Journey through Neurovascular Coupling in Health and Disease', Neuron, 96(1), pp. 17–42. doi: 10.1016/j.neuron.2017.07.030.

Iwata, E. et al. (1997) 'Different effects of oxidative stress on activation of transcription factors in primary cultured rat neuronal and glial cells', Brain research. Molecular brain research. Brain Res Mol Brain Res, 50(1–2), pp. 213–220. doi: 10.1016/S0169-328X(97)00190-3.

Iwatsubo, T. (2004) 'The gamma-secretase complex: machinery for intramembrane proteolysis', Current opinion in neurobiology. Curr Opin Neurobiol, 14(3), pp. 379–383. doi: 10.1016/J.CONB.2004.05.010.

Jack, C. R. et al. (2010) 'Hypothetical model of dynamic biomarkers of the Alzheimer's pathological cascade', The Lancet. Neurology. Lancet Neurol, 9(1), pp. 119–128. doi: 10.1016/S1474-4422(09)70299-6.

Jack, C. R. et al. (2011) 'Introduction to Revised Criteria for the Diagnosis of Alzheimer's Disease: National Institute on Aging and the Alzheimer Association Workgroups', Alzheimer's & dementia : the journal of the Alzheimer's Association. NIH Public Access, 7(3), p. 257. doi: 10.1016/J.JALZ.2011.03.004.

Jack, C. R. et al. (2019) 'Prevalence of Biologically vs Clinically Defined Alzheimer Spectrum Entities Using the National Institute on Aging-Alzheimer's Association Research Framework', JAMA neurology. JAMA Neurol, 76(10), pp. 1174–1183. doi: 10.1001/JAMANEUROL.2019.1971.

Jackson, J. et al. (2019) 'Targeting the synapse in Alzheimer's disease', Frontiers in Neuroscience. Frontiers Media S.A., 13(JUL), p. 735. doi: 10.3389/FNINS.2019.00735/BIBTEX.

Jahangiri, Z., Gholamnezhad, Z. and Hosseini, M. (2019) 'Neuroprotective effects of exercise in rodent models of memory deficit and Alzheimer's', Metabolic brain disease. Metab Brain Dis, 34(1), pp. 21–37. doi: 10.1007/S11011-018-0343-Y.

Jakobsson, E. et al. (2005) 'Structure of human semicarbazide-sensitive amine oxidase/vascular adhesion protein-1', Acta crystallographica. Section D, Biological crystallography. Acta Crystallogr D Biol Crystallogr, 61(Pt 11), pp. 1550–1562. doi: 10.1107/S0907444905028805.

Jalkanen, S. and Salmi, M. (2001) 'Cell surface monoamine oxidases: enzymes in search of a function', The EMBO Journal. John Wiley & Sons, Ltd, 20(15), pp. 3893–3901. doi: 10.1093/EMBOJ/20.15.3893.

Janeiro, M. H. et al. (2021) 'Biomarkers in Alzheimer's disease', Advances in Laboratory Medicine. Walter de Gruyter GmbH, 2(1), pp. 27–37. doi: 10.1515/ALMED-2020-0090/ASSET/GRAPHIC/J_ALMED-2020-0090_FIG_002.JPG.

Jankowsky, J. L. and Zheng, H. (2017) 'Practical considerations for choosing a mouse model of Alzheimer's disease', Molecular neurodegeneration. Mol Neurodegener, 12(1). doi: 10.1186/S13024-017-0231-7.

Jensen, S. K. and Yong, V. W. (2016) 'Activity-Dependent and Experience-Driven Myelination Provide New Directions for the Management of Multiple Sclerosis', Trends in neurosciences. Trends Neurosci, 39(6), pp. 356–365. doi: 10.1016/J.TINS.2016.04.003.

Jiang, Z. J., Richardson, J. S. and Yu, P. H. (2008) 'The contribution of cerebral vascular semicarbazide-sensitive amine oxidase to cerebral amyloid angiopathy in Alzheimer's disease', Neuropathology and applied neurobiology. Neuropathol Appl Neurobiol, 34(2), pp. 194–204. doi: 10.1111/J.1365-2990.2007.00886.X.

Jin (2020) 'Regulation of BDNF-TrkB Signaling and Potential Therapeutic Strategies for Parkinson's Disease', Journal of Clinical Medicine. doi: 10.3390/jcm9010257.

Jin, W. (2020) 'Regulation of BDNF-TrkB Signaling and Potential Therapeutic Strategies for Parkinson's Disease', Journal of clinical medicine. J Clin Med, 9(1). doi: 10.3390/JCM9010257.

Jo, S. et al. (2014) 'GABA from reactive astrocytes impairs memory in mouse models of Alzheimer's disease', Nature medicine. Nat Med, 20(8), pp. 886–896. doi: 10.1038/NM.3639.

Jung, Y. et al. (2020) 'BDNF-induced local translation of GluA1 is regulated by HNRNP A2/B1', Science Advances, 6(47). doi: 10.1126/sciadv.abd2163.

Kadry, H., Noorani, B. and Cucullo, L. (2020) 'A blood-brain barrier overview on structure, function, impairment, and biomarkers of integrity', Fluids and barriers of the CNS. Fluids Barriers CNS, 17(1). doi: 10.1186/S12987-020-00230-3.

Kahle, P. J. and De Strooper, B. (2003) 'Attack on amyloid', EMBO reports. EMBO Rep, 4(8), pp. 747–751. doi: 10.1038/SJ.EMBOR.EMBOR905.

Kallmann, B. A. et al. (2002) 'Characteristic gene expression profile of primary human cerebral endothelial cells', FASEB journal : official publication of the Federation of American Societies for Experimental Biology. FASEB J, 16(6), pp. 589–591. doi: 10.1096/FJ.01-0594FJE.

Kamino, K. et al. (1992) 'Linkage and mutational analysis of familial Alzheimer disease kindreds for the APP gene region', American Journal of Human Genetics. Elsevier, 51(5), p. 998. Available at: /pmc/articles/PMC1682859/?report=abstract (Accessed: 11 June 2022).

Kang, S. S. et al. (2017) 'TrkB neurotrophic activities are blocked by α-synuclein, triggering dopaminergic cell death in Parkinson's disease', Proceedings of the National Academy of Sciences of the United States of America. Proc Natl Acad Sci U S A, 114(40), pp. 10773–10778. doi: 10.1073/PNAS.1713969114.

Kapczinski, F. et al. (2008) 'Increased oxidative stress as a mechanism for decreased BDNF levels in acute manic episodes', Revista brasileira de psiquiatria (Sao Paulo, Brazil : 1999). Braz J Psychiatry, 30(3), pp. 243–245. doi: 10.1590/S1516-44462008000300011.

Karádi, I. et al. (2002) 'Serum semicarbazide-sensitive amine oxidase (SSAO) activity is an independent marker of carotid atherosclerosis.', Clinica Chimica Acta; International Journal of Clinical Chemistry, 323(1–2), pp. 139–146. doi: 10.1016/S0009-8981(02)00189-4.

Karve, I. P., Taylor, J. M. and Crack, P. J. (2016) 'The contribution of astrocytes and microglia to traumatic brain injury', British journal of pharmacology. Br J Pharmacol, 173(4), pp. 692–702. doi: 10.1111/BPH.13125.

Kasai, H. et al. (2010) 'Structural dynamics of dendritic spines in memory and cognition', Trends in neurosciences. Trends Neurosci, 33(3), pp. 121–129. doi: 10.1016/J.TINS.2010.01.001.

Keage, H. A. D. et al. (2009) 'Population studies of sporadic cerebral amyloid angiopathy and dementia: a systematic review', BMC neurology. BMC Neurol, 9. doi: 10.1186/1471-2377-9-3.

Kermani, P. and Hempstead, B. (2007) 'Brain-derived neurotrophic factor: a newly described mediator of angiogenesis', Trends in cardiovascular medicine. Trends Cardiovasc Med, 17(4), pp. 140–143. doi: 10.1016/J.TCM.2007.03.002.

Kessels, H. W. and Malinow, R. (2009) 'Synaptic AMPA receptor plasticity and behavior', Neuron. Neuron, 61(3), pp. 340–350. doi: 10.1016/J.NEURON.2009.01.015.

Kimelberg, H. K. (2004) 'Water homeostasis in the brain: basic concepts', Neuroscience. Neuroscience, 129(4), pp. 851–860. doi: 10.1016/J.NEUROSCIENCE.2004.07.033.

Kimelberg, H. K. (2010) 'Functions of mature mammalian astrocytes: a current view', The Neuroscientist : a review journal bringing neurobiology, neurology and psychiatry. Neuroscientist, 16(1), pp. 79–106. doi: 10.1177/1073858409342593.

Kimelberg, Harold K. (2004) 'The role of hypotheses in current research, illustrated by hypotheses on the possible role of astrocytes in energy metabolism and cerebral blood flow: From Newton to now', Journal of Cerebral Blood Flow and Metabolism. SAGE PublicationsSage UK: London, England, 24(11), pp. 1235–1239. doi: 10.1097/01.WCB.0000138668.10058.8C.

Kirabali, T. et al. (2020) 'Distinct changes in all major components of the neurovascular unit across different neuropathological stages of Alzheimer's disease', Brain Pathology. John Wiley & Sons, Ltd, 30(6), pp. 1056–1070. doi: 10.1111/BPA.12895.

Kirouac, L. et al. (2017) 'Activation of Ras-ERK Signaling and GSK-3 by Amyloid Precursor Protein and Amyloid Beta Facilitates Neurodegeneration in Alzheimer's Disease', eNeuro. eNeuro, 4(2). doi: 10.1523/ENEURO.0149-16.2017.

Kisler, K. et al. (2017) 'Cerebral blood flow regulation and neurovascular dysfunction in Alzheimer disease', Nature Reviews Neuroscience. Nature Publishing Group, 18(7), pp. 419–434. doi: 10.1038/nrn.2017.48.

Klementieva, O. et al. (2017) 'Pre-plaque conformational changes in Alzheimer's disease-linked Aβ and APP', Nature Communications 2017 8:1. Nature Publishing Group, 8(1), pp. 1–9. doi: 10.1038/ncomms14726.

Klinman, J. P. and Mu, D. (2003) 'QUINOENZYMES IN BIOLOGY', https://doi.org/10.1146/annurev.bi.63.070194.001503. Annual Reviews 4139 El Camino Way, P.O. Box 10139, Palo Alto, CA 94303-0139, USA , 63, pp. 299–344. doi: 10.1146/ANNUREV.BI.63.070194.001503.

Koffie, R. M. et al. (2009) 'Oligomeric amyloid beta associates with postsynaptic densities and correlates with excitatory synapse loss near senile plaques', Proceedings of the National Academy of Sciences of the United States of America. Proc Natl Acad Sci U S A, 106(10), pp. 4012–4017. doi: 10.1073/PNAS.0811698106.

Kommaddi, R. P. et al. (2018) 'Aβ mediates F-actin disassembly in dendritic spines leading to cognitive deficits in Alzheimer's disease', The Journal of neuroscience : the official journal of the Society for Neuroscience. J Neurosci, 38(5), pp. 1085–1099. doi: 10.1523/JNEUROSCI.2127-17.2017.

Kovacs, G. G. (2018) 'Cellular reactions of the central nervous system', Handbook of Clinical Neurology. Elsevier B.V., 145, pp. 13–23. doi: 10.1016/B978-0-12-802395-2.00003-1.

Kugler, E. C., Greenwood, J. and MacDonald, R. B. (2021) 'The "Neuro-Glial-Vascular" Unit: The Role of Glia in Neurovascular Unit Formation and Dysfunction', Frontiers in cell and developmental biology. Front Cell Dev Biol, 9. doi: 10.3389/FCELL.2021.732820.

Kumar-Singh, S. et al. (2002) 'Dense-Core Senile Plaques in the Flemish Variant of Alzheimer's Disease Are Vasocentric', The American Journal of Pathology. American Society for Investigative Pathology, 161(2), p. 507. doi: 10.1016/S0002-9440(10)64207-1.

Kunsch, C. and Medford, R. M. (1999) 'Oxidative stress as a regulator of gene expression in the vasculature', Circulation research. Circ Res, 85(8), pp. 753–766. doi: 10.1161/01.RES.85.8.753.

Kunze, R. and Marti, H. H. (2019) 'Angioneurins – Key regulators of blood–brain barrier integrity during hypoxic and ischemic brain injury', Progress in Neurobiology. Elsevier Ltd, 178. doi: 10.1016/j.pneurobio.2019.03.004.

Kurkijärvi, R. et al. (1998) 'Circulating Form of Human Vascular Adhesion Protein-1 (VAP-1): Increased Serum Levels in Inflammatory Liver Diseases', The Journal of Immunology, 161(3).

Kurmann, L. et al. (2021) 'Transcryptomic Analysis of Human Brain-Microvascular Endothelial Response to -Pericytes: Cell Orientation Defines Barrier Function', Cells. Cells, 10(4). doi: 10.3390/CELLS10040963.

Lacoste, B. et al. (2014) 'Sensory-related neural activity regulates the structure of vascular networks in the cerebral cortex', Neuron. Neuron, 83(5), pp. 1117–1130. doi: 10.1016/J.NEURON.2014.07.034.

Lalor, P. F. et al. (2007) 'Activation of vascular adhesion protein-1 on liver endothelium results in an NF-kappaB-dependent increase in lymphocyte adhesion', Hepatology (Baltimore, Md.). Hepatology, 45(2), pp. 465–474. doi: 10.1002/HEP.21497.

Landis, D. M. D. and Reese, T. S. (1983) 'Cytoplasmic organization in cerebellar dendritic spines', The Journal of cell biology. J Cell Biol, 97(4), pp. 1169–1178. doi: 10.1083/JCB.97.4.1169.

Langford, S. D., Trent, M. B. and Boor, P. J. (2002) 'Semicarbazide-sensitive amine oxidase and extracellular matrix deposition by smooth-muscle cells', Cardiovascular toxicology. Cardiovasc Toxicol, 2(2), pp. 141–150. doi: 10.1385/CT:2:2:141.

Lansdall, C. J. (2014) 'An effective treatment for Alzheimer's disease must consider both amyloid and tau', Bioscience Horizons: The International Journal of Student Research. Oxford Academic, 7, p. 2014. doi: 10.1093/BIOHORIZONS/HZU002.

Leal, G., Comprido, D. and Duarte, C. B. (2014) 'BDNF-induced local protein synthesis and synaptic plasticity', Neuropharmacology. Neuropharmacology, 76 Pt C(PART C), pp. 639–656. doi: 10.1016/J.NEUROPHARM.2013.04.005.

Lecrux, C. and Hamel, E. (2016) 'Neuronal networks and mediators of cortical neurovascular coupling responses in normal and altered brain states', Philosophical transactions of the Royal Society of London. Series B, Biological sciences. Philos Trans R Soc Lond B Biol Sci, 371(1705). doi: 10.1098/RSTB.2015.0350.

Lee, H. K. et al. (2010) 'Specific roles of AMPA receptor subunit GluR1 (GluA1) phosphorylation sites in regulating synaptic plasticity in the CA1 region of hippocampus', Journal of neurophysiology. J Neurophysiol, 103(1), pp. 479–489. doi: 10.1152/JN.00835.2009.

Lee, S. J., Seo, B. R. and Koh, J. Y. (2015) 'Metallothionein-3 modulates the amyloid β endocytosis of astrocytes through its effects on actin polymerization', Molecular Brain. BioMed Central Ltd., 8(1), pp. 1–12. doi: 10.1186/S13041-015-0173-3/FIGURES/6.

Lenhossek, M. V. (1893) 'Der Feinere Bau des Nervensystems', Lichte Neuester Forschung.

Lesné, S. et al. (2006) 'A specific amyloid-beta protein assembly in the brain impairs memory', Nature. Nature, 440(7082), pp. 352–357. doi: 10.1038/NATURE04533.

Leventhal, C. et al. (1999) 'Endothelial trophic support of neuronal production and recruitment from the adult mammalian subependyma', Molecular and cellular neurosciences. Mol Cell Neurosci, 13(6), pp. 450–464. doi: 10.1006/MCNE.1999.0762.

Levy, E. et al. (1990) 'Mutation of the Alzheimer's disease amyloid gene in hereditary cerebral hemorrhage, Dutch type', Science (New York, N.Y.). Science, 248(4959), pp. 1124–1126. doi: 10.1126/SCIENCE.2111584.

Lewinsohn, R. (1984) 'Mammalian monoamine-oxidizing enzymes, with special reference to benzylamine oxidase in human tissues.', Brazilian Journal of Medical and Biological Research = Revista Brasileira de Pesquisas Medicas e Biologicas, 17(3–4), pp. 223–256. Available at: https://europepmc.org/article/med/6442176 (Accessed: 12 June 2022).

Li, G. et al. (2013) 'Hippocampal neuron loss is correlated with cognitive deficits in SAMP8 mice', Neurological sciences : official journal of the Italian Neurological Society and of the Italian Society of Clinical Neurophysiology. Neurol Sci, 34(6), pp. 963–969. doi: 10.1007/S10072-012-1173-Z.

Li, H. et al. (2021) 'Vascular Adhesion Protein-1 (VAP-1)/Semicarbazide-Sensitive Amine Oxidase (SSAO): A Potential Therapeutic Target for Atherosclerotic Cardiovascular Diseases', Frontiers in pharmacology. Front Pharmacol, 12. doi: 10.3389/FPHAR.2021.679707.

Li, S. et al. (2019) 'Synthesis and in Vivo Evaluation of a Novel PET Radiotracer for Imaging of Synaptic Vesicle Glycoprotein 2A (SV2A) in Nonhuman Primates', ACS chemical neuroscience. ACS Chem Neurosci, 10(3), pp. 1544–1554. doi: 10.1021/ACSCHEMNEURO.8B00526.

Lian, H. and Zheng, H. (2016) 'Signaling pathways regulating neuron-glia interaction and their implications in Alzheimer's disease', Journal of neurochemistry. NIH Public Access, 136(3), p. 475. doi: 10.1111/JNC.13424.

Liddelow, S. A. (2019) 'Modern approaches to investigating non-neuronal aspects of Alzheimer's disease', The FASEB Journal. John Wiley & Sons, Ltd, 33(2), pp. 1528–1535. doi: 10.1096/FJ.201802592.

Liddelow, S. A. et al. (2017) 'Neurotoxic reactive astrocytes are induced by activated microglia', Nature. Nature, 541(7638), pp. 481–487. doi: 10.1038/NATURE21029.

Liem, R. K. H. and Messing, A. (2009) 'Dysfunctions of neuronal and glial intermediate filaments in disease', The Journal of Clinical Investigation. American Society for Clinical Investigation, 119(7), p. 1814. doi: 10.1172/JCI38003.

Lin, G.-B. et al. (2022) 'Protection of high-frequency low-intensity pulsed electric fields and brain-derived neurotrophic factor for SH-SY5Y cells against hydrogen peroxide-induced cell damage', bioRxiv. Cold Spring Harbor Laboratory, p. 2022.05.10.491265. doi: 10.1101/2022.05.10.491265.

Lisman, J. and Raghavachari, S. (2006) 'A unified model of the presynaptic and postsynaptic changes during LTP at CA1 synapses', Science's STKE : signal transduction knowledge environment. Sci STKE, 2006(356). doi: 10.1126/STKE.3562006RE11.

Liu, B., Liu, J. and Shi, J.-S. (2020) 'SAMP8 Mice as a Model of Age-Related Cognition Decline with Underlying Mechanisms in Alzheimer's Disease', Journal of Alzheimer's disease : JAD. J Alzheimers Dis, 75(2), pp. 385–395. doi: 10.3233/JAD-200063.

Livingston, G. et al. (2020) 'Dementia prevention, intervention, and care: 2020 report of the Lancet Commission', Lancet (London, England). Elsevier, 396(10248), p. 413. doi: 10.1016/S0140-6736(20)30367-6.

Lizcano, J. M. et al. (1990) 'Amine oxidase activities in bovine lung.', Journal of neural transmission. Supplementum. Springer, Vienna, 32, pp. 341–344. doi: 10.1007/978-3-7091-9113-2_46/COVER/.

Lizcano, J. M., Tipton, K. F. and Unzeta, M. (1998) 'Purification and characterization of membrane-bound semicarbazide-sensitive amine oxidase (SSAO) from bovine lung', The Biochemical journal. Biochem J, 331 (Pt 1)(Pt 1), pp. 69–78. doi: 10.1042/BJ3310069.

Lohmann, C. and Kessels, H. W. (2014) 'The developmental stages of synaptic plasticity', The Journal of Physiology. Wiley-Blackwell, 592(Pt 1), p. 13. doi: 10.1113/JPHYSIOL.2012.235119.

Lu, W. et al. (2009) 'Subunit composition of synaptic AMPA receptors revealed by a single-cell genetic approach', Neuron. Neuron, 62(2), pp. 254–268. doi: 10.1016/J.NEURON.2009.02.027.

Lucas, D. R. and Newhouse, J. P. (1957) 'The toxic effect of sodium L-glutamate on the inner layers of the retina', A.M.A. archives of ophthalmology. AMA Arch Ophthalmol, 58(2), pp. 193–201. doi: 10.1001/ARCHOPHT.1957.00940010205006.

Lyles, G. A. (1996) 'Mammalian plasma and tissue-bound semicarbazide-sensitive amine oxidases: biochemical, pharmacological and toxicological aspects', The international journal of biochemistry & cell biology. Int J Biochem Cell Biol, 28(3), pp. 259–274. doi: 10.1016/1357-2725(95)00130-1.

Lyles, G. A. and Singh, I. (1985) 'Vascular smooth muscle cells: a major source of the semicarbazide-sensitive amine oxidase of the rat aorta', The Journal of pharmacy and pharmacology. J Pharm Pharmacol, 37(9), pp. 637–643. doi: 10.1111/J.2042-7158.1985.TB05100.X.

Lynch, G. et al. (2008) 'The substrates of memory: Defects, treatments, and enhancement', European Journal of Pharmacology. Eur J Pharmacol, pp. 2–13. doi: 10.1016/j.ejphar.2007.11.082.

Lynch, M. A. (2004) 'Long-term potentiation and memory', Physiological reviews. Physiol Rev, 84(1), pp. 87–136. doi: 10.1152/PHYSREV.00014.2003.

Maat-Schieman, M. L. C. et al. (1996) 'Hereditary cerebral hemorrhage with amyloidosis-Dutch type (HCHWA-D): II--A review of histopathological aspects', Brain pathology (Zurich, Switzerland). Brain Pathol, 6(2), pp. 115–120. doi: 10.1111/J.1750-3639.1996.TB00794.X.

Macht, V. A. (2016) 'Neuro-immune interactions across development: A look at glutamate in the prefrontal cortex', Neuroscience and biobehavioral reviews. Neurosci Biobehav Rev, 71, pp. 267–280. doi: 10.1016/J.NEUBIOREV.2016.08.039.

Makin, S. (2018) 'The amyloid hypothesis on trial', Nature. Nature, 559(7715), pp. S4–S7. doi: 10.1038/D41586-018-05719-4.

Makita, T. et al. (2008) 'Endothelins are vascular-derived axonal guidance cues for developing sympathetic neurons', Nature. Nature, 452(7188), pp. 759–763. doi: 10.1038/NATURE06859.

Mandelkow, E. M. and Mandelkow, E. (2012) 'Biochemistry and cell biology of tau protein in neurofibrillary degeneration', Cold Spring Harbor perspectives in medicine. Cold Spring Harb Perspect Med, 2(7), pp. 1–25. doi: 10.1101/CSHPERSPECT.A006247.

Marchetti, L. and Engelhardt, B. (2020) 'Immune cell trafficking across the blood-brain barrier in the absence and presence of neuroinflammation', Vascular Biology. Bioscientifica Ltd., 2(1), p. H1. doi: 10.1530/VB-19-0033.

Marsh, J. and Alifragis, P. (2018) 'Synaptic dysfunction in Alzheimer's disease: the effects of amyloid beta on synaptic vesicle dynamics as a novel target for therapeutic intervention', Neural regeneration research. Neural Regen Res, 13(4), pp. 616–623. doi: 10.4103/1673-5374.230276.

Martella, G. et al. (2018) 'Synaptic Plasticity Changes: Hallmark for Neurological and Psychiatric Disorders', Neural Plasticity. Hindawi Limited, 2018. doi: 10.1155/2018/9230704.

Martinez-Lozada, Z. and Robinson, M. B. (2020) 'Reciprocal communication between astrocytes and endothelial cells is required for astrocytic glutamate transporter 1 (GLT-1) expression', Neurochemistry international. Neurochem Int, 139. doi: 10.1016/J.NEUINT.2020.104787.

Matejuk, A. and Ransohoff, R. M. (2020) 'Crosstalk Between Astrocytes and Microglia: An Overview', Frontiers in immunology. Front Immunol, 11. doi: 10.3389/FIMMU.2020.01416.

Mathys, K. C. et al. (2002) 'Semicarbazide-sensitive amine oxidase in aortic smooth muscle cells mediates synthesis of a methylglyoxal-AGE: implications for vascular complications in diabetes', Biochemical and biophysical research communications. Biochem Biophys Res Commun, 297(4), pp. 863–869. doi: 10.1016/S0006-291X(02)02293-3.

Matt, L. et al. (2018) 'α-Actinin Anchors PSD-95 at Postsynaptic Sites', Neuron, 97(5), pp. 1094-1109.e9. doi: 10.1016/j.neuron.2018.01.036.

Matthews, V. B. et al. (2009) 'Brain-derived neurotrophic factor is produced by skeletal muscle cells in response to contraction and enhances fat oxidation via activation of AMP-activated protein kinase', Diabetologia. Diabetologia, 52(7), pp. 1409–1418. doi: 10.1007/S00125-009-1364-1.

Mattson, M. P. (2008) 'Glutamate and neurotrophic factors in neuronal plasticity and disease', Annals of the New York Academy of Sciences. Ann N Y Acad Sci, 1144, pp. 97–112. doi: 10.1196/ANNALS.1418.005.

Matute, C. et al. (1997) 'Glutamate receptor-mediated toxicity in optic nerve oligodendrocytes', Proceedings of the National Academy of Sciences of the United States of America, 94(16), pp. 8830–8835. doi: 10.1073/pnas.94.16.8830.

Matyus, P. et al. (2004) 'Semicarbazide-sensitive amine oxidase: current status and perspectives', Current medicinal chemistry. Curr Med Chem, 11(10), pp. 1285–1298. doi: 10.2174/0929867043365305.

McKenzie, I. A. et al. (2014) 'Motor skill learning requires active central myelination', Science (New York, N.Y.). Science, 346(6207), pp. 318–322. doi: 10.1126/SCIENCE.1254960.

McKhann, G. et al. (1984) 'Clinical diagnosis of Alzheimer's disease: report of the NINCDS-ADRDA Work Group under the auspices of Department of Health and Human Services Task Force on Alzheimer's Disease', Neurology. Neurology, 34(7), pp. 939–944. doi: 10.1212/WNL.34.7.939.

Melchor, J. P., McVoy, L. and Van Nostrand, W. E. (2000) 'Charge alterations of E22 enhance the pathogenic properties of the amyloid beta-protein', Journal of neurochemistry. J Neurochem, 74(5), pp. 2209–2212. doi: 10.1046/J.1471-4159.2000.0742209.X.

Menaceur, C. et al. (2021) 'The Blood-Brain Barrier, an Evolving Concept Based on Technological Advances and Cell-Cell Communications', Cells. Cells, 11(1). doi: 10.3390/CELLS11010133.

Mercier, J. et al. (2014) 'Discovery of heterocyclic nonacetamide synaptic vesicle protein 2A (SV2A) ligands with single-digit nanomolar potency: opening avenues towards the first SV2A positron emission tomography (PET) ligands', ChemMedChem. ChemMedChem, 9(4), pp. 693–698. doi: 10.1002/CMDC.201300482.

Messaoudi, E. et al. (2002) 'Brain-Derived Neurotrophic Factor Triggers Transcription-Dependent, Late Phase Long-Term Potentiation In Vivo', The Journal of Neuroscience. Society for Neuroscience, 22(17), p. 7453. doi: 10.1523/JNEUROSCI.22-17-07453.2002.

Mészáros, Z. et al. (1999) 'Determination of human serum semicarbazide-sensitive amine oxidase activity: a possible clinical marker of atherosclerosis', European journal of drug metabolism and pharmacokinetics. Eur J Drug Metab Pharmacokinet, 24(4), pp. 299–302. doi: 10.1007/BF03190036.

Miller, D. L. et al. (1993) 'Peptide compositions of the cerebrovascular and senile plaque core amyloid deposits of Alzheimer's disease', Archives of biochemistry and biophysics. Arch Biochem Biophys, 301(1), pp. 41–52. doi: 10.1006/ABBI.1993.1112.

Miller, E. C. et al. (2014) 'Tau phosphorylation and tau mislocalization mediate soluble Aβ oligomer-induced AMPA glutamate receptor signaling deficits', The European journal of neuroscience. Eur J Neurosci, 39(7), pp. 1214–1224. doi: 10.1111/EJN.12507.

Miñano-Molina, A. J. et al. (2011) 'Soluble oligomers of amyloid-β peptide disrupt membrane trafficking of α-amino-3-hydroxy-5-methylisoxazole-4-propionic acid receptor contributing to early synapse dysfunction', The Journal of biological chemistry. J Biol Chem, 286(31), pp. 27311–27321. doi: 10.1074/JBC.M111.227504.

Miravalle, L. et al. (2000) 'Substitutions at codon 22 of Alzheimer's abeta peptide induce diverse conformational changes and apoptotic effects in human cerebral endothelial cells.', The Journal of Biological Chemistry, 275(35), pp. 27110–27116. doi: 10.1074/JBC.M003154200.

Mirra, S. S. et al. (1991) 'The Consortium to Establish a Registry for Alzheimer's Disease (CERAD). Part II. Standardization of the neuropathologic assessment of Alzheimer's disease', Neurology. Neurology, 41(4), pp. 479–486. doi: 10.1212/WNL.41.4.479.

Miyamoto, N. et al. (2015) 'Astrocytes Promote Oligodendrogenesis after White Matter Damage via Brain-Derived Neurotrophic Factor', The Journal of Neuroscience. Society for Neuroscience, 35(41), p. 14002. doi: 10.1523/JNEUROSCI.1592-15.2015.

Miyazaki, K. et al. (2011) 'Disruption of neurovascular unit prior to motor neuron degeneration in amyotrophic lateral sclerosis', Journal of neuroscience research. J Neurosci Res, 89(5), pp. 718–728. doi: 10.1002/JNR.22594.

Molyneaux, B. J. et al. (2007) 'Neuronal subtype specification in the cerebral cortex', Nature reviews. Neuroscience. Nat Rev Neurosci, 8(6), pp. 427–437. doi: 10.1038/NRN2151.

Monnier, A. et al. (2017) 'Brain-derived neurotrophic factor of the cerebral microvasculature: a forgotten and nitric oxide-dependent contributor of brain-derived neurotrophic factor in the brain', Acta Physiologica. doi: 10.1111/apha.12743.

Monro, O. R. et al. (2002) 'Substitution at codon 22 reduces clearance of Alzheimer's amyloid-beta peptide from the cerebrospinal fluid and prevents its transport from the central nervous system into blood', Neurobiology of aging. Neurobiol Aging, 23(3), pp. 405–412. doi: 10.1016/S0197-4580(01)00317-7.

Montagne, A., Zhao, Z. and Zlokovic, B. V. (2017) 'Alzheimer's disease: A matter of blood-brain barrier dysfunction?', The Journal of experimental medicine. J Exp Med, 214(11), pp. 3151–3169. doi: 10.1084/JEM.20171406.

Montine, T. J. et al. (2012) 'National Institute on Aging-Alzheimer's Association guidelines for the neuropathologic assessment of Alzheimer's disease: a practical approach', Acta Neuropathologica. NIH Public Access, 123(1), p. 1. doi: 10.1007/S00401-011-0910-3.

Morin, N. et al. (2001) 'Semicarbazide-Sensitive Amine Oxidase Substrates Stimulate Glucose Transport and Inhibit Lipolysis in Human Adipocytes', Journal of Pharmacology and Experimental Therapeutics, 297(2).

Morley, J. E. et al. (2012) 'The senescence accelerated mouse (SAMP8) as a model for oxidative stress and Alzheimer's disease', Biochimica et biophysica acta. Biochim Biophys Acta, 1822(5), pp. 650–656. doi: 10.1016/J.BBADIS.2011.11.015.

Nabulsi, N. B. et al. (2016) 'Synthesis and Preclinical Evaluation of 11C-UCB-J as a PET Tracer for Imaging the Synaptic Vesicle Glycoprotein 2A in the Brain', Journal of nuclear medicine : official publication, Society of Nuclear Medicine. J Nucl Med, 57(5), pp. 777–784. doi: 10.2967/JNUMED.115.168179.

Nagahara, A. H. et al. (2009) 'Neuroprotective effects of brain-derived neurotrophic factor in rodent and primate models of Alzheimer's disease', Nature medicine. Nat Med, 15(3), pp. 331–337. doi: 10.1038/NM.1912.

Nagahara, A. H. et al. (2018) 'MR-guided delivery of AAV2-BDNF into the entorhinal cortex of non-human primates', Gene therapy. Gene Ther, 25(2), pp. 104–114. doi: 10.1038/S41434-018-0010-2.

Naganawa, M. et al. (2021) 'First-in-Human Evaluation of 18 F-SynVesT-1, a Radioligand for PET Imaging of Synaptic Vesicle Glycoprotein 2A', Journal of nuclear medicine : official publication, Society of Nuclear Medicine. J Nucl Med, 62(4), pp. 561–567. doi: 10.2967/JNUMED.120.249144.

Nagele, R. G. et al. (2004) 'Contribution of glial cells to the development of amyloid plaques in Alzheimer's disease', Neurobiology of aging. Neurobiol Aging, 25(5), pp. 663–674. doi: 10.1016/J.NEUROBIOLAGING.2004.01.007.

Naha, N. (2021) 'Molecular Network for Management of Neurodegenerative Diseases and their Translational Importance using Animal Biotechnology as a Tool in Preclinical Studies', Advances in Animal Genomics. Academic Press, pp. 219–235. doi: 10.1016/B978-0-12-820595-2.00014-X.

Nair, D. et al. (2013) 'Super-resolution imaging reveals that AMPA receptors inside synapses are dynamically organized in nanodomains regulated by PSD95', Journal of Neuroscience, 33(32), pp. 13204–13224. doi: 10.1523/JNEUROSCI.2381-12.2013.

Nakagawa, S. et al. (2009) 'A new blood-brain barrier model using primary rat brain endothelial cells, pericytes and astrocytes', Neurochemistry international. Neurochem Int, 54(3–4), pp. 253–263. doi: 10.1016/J.NEUINT.2008.12.002.

Nakahashi, T. et al. (2000) 'Vascular endothelial cells synthesize and secrete brain-derived neurotrophic factor', FEBS letters. FEBS Lett, 470(2), pp. 113–117. doi: 10.1016/S0014-5793(00)01302-8.

Nakata, H. and Nakamura, S. (2007) 'Brain-derived neurotrophic factor regulates AMPA receptor trafficking to post-synaptic densities via IP3R and TRPC calcium signaling', FEBS letters. FEBS Lett, 581(10), pp. 2047–2054. doi: 10.1016/J.FEBSLET.2007.04.041.

Nation, D. A. et al. (2019) 'Blood-brain barrier breakdown is an early biomarker of human cognitive dysfunction', Nature medicine. Nat Med, 25(2), pp. 270–276. doi: 10.1038/S41591-018-0297-Y.

Navaratna, D. et al. (2011) 'Decreased Cerebrovascular Brain-Derived Neurotrophic Factor–Mediated Neuroprotection in the Diabetic Brain', Diabetes. American Diabetes Association, 60(6), p. 1789. doi: 10.2337/DB10-1371.

Nigam, S. M. et al. (2017) 'Exercise and BDNF reduce Aβ production by enhancing α-secretase processing of APP', Journal of neurochemistry. J Neurochem, 142(2), pp. 286–296. doi: 10.1111/JNC.14034.

Nikolopoulou, E. et al. (2017) 'Neural tube closure: cellular, molecular and biomechanical mechanisms', Development (Cambridge, England). Development, 144(4), pp. 552–566. doi: 10.1242/DEV.145904.

Nimmerjahn, A., Kirchhoff, F. and Helmchen, F. (2005) 'Resting microglial cells are highly dynamic surveillants of brain parenchyma in vivo', Science (New York, N.Y.). Science, 308(5726), pp. 1314–1318. doi: 10.1126/SCIENCE.1110647.

Nishida, H. and Okabe, S. (2007) 'Direct astrocytic contacts regulate local maturation of dendritic spines', The Journal of neuroscience : the official journal of the Society for Neuroscience. J Neurosci, 27(2), pp. 331–340. doi: 10.1523/JNEUROSCI.4466-06.2007.

Nitta, T. et al. (2003) 'Size-selective loosening of the blood-brain barrier in claudin-5-deficient mice', The Journal of cell biology. J Cell Biol, 161(3), pp. 653–660. doi: 10.1083/JCB.200302070.

Nizzari, M. et al. (2012) 'Amyloid-β protein precursor regulates phosphorylation and cellular compartmentalization of microtubule associated protein tau', Journal of Alzheimer's disease : JAD. J Alzheimers Dis, 29(1), pp. 211–227. doi: 10.3233/JAD-2011-101590.

Noda, K. et al. (2009) 'Vascular Adhesion Protein-1 Regulates Leukocyte Transmigration Rate in the Retina During Diabetes', Experimental eye research. NIH Public Access, 89(5), p. 774. doi: 10.1016/J.EXER.2009.07.010.

Noe, C. R. et al. (2020) 'Dysfunction of the Blood-Brain Barrier—A Key Step in Neurodegeneration and Dementia', Frontiers in Aging Neuroscience. Frontiers Media SA, 12, p. 24. doi: 10.3389/FNAGI.2020.00185.

Nortley, R. et al. (2019) 'Amyloid β oligomers constrict human capillaries in Alzheimer's disease via signaling to pericytes', Science (New York, N.Y.). Science, 365(6450). doi: 10.1126/SCIENCE.AAV9518.

Nunes, S. F. et al. (2010) 'Changes in the activities of semicarbazide-sensitive amine oxidase in inferior mesenteric artery segments and in serum of patients with type 2 diabetes', Acta diabetologica. Acta Diabetol, 47(2), pp. 179–182. doi: 10.1007/S00592-009-0174-8.

O'Brien, J. T. and Thomas, A. (2015) 'Vascular dementia', Lancet (London, England). Lancet, 386(10004), pp. 1698–1706. doi: 10.1016/S0140-6736(15)00463-8.

O'Sullivan, J. et al. (2004) 'Semicarbazide-Sensitive Amine Oxidases: Enzymes with Quite a Lot to Do', NeuroToxicology. Elsevier, 25(1–2), pp. 303–315. doi: 10.1016/S0161-813X(03)00117-7.

Obata, T. and Yamanaka, Y. (2000) 'Inhibition of monkey brain semicarbazide-sensitive amine oxidase by various antidepressants', Neuroscience letters. Neurosci Lett, 286(2), pp. 131–133. doi: 10.1016/S0304-3940(00)01087-9.

Obici, L. et al. (2005) 'A novel AbetaPP mutation exclusively associated with cerebral amyloid angiopathy', Annals of neurology. Ann Neurol, 58(4), pp. 639–644. doi: 10.1002/ANA.20571.

Oh, M. C. et al. (2006) 'Extrasynaptic membrane trafficking regulated by GluR1 serine 845 phosphorylation primes AMPA receptors for long-term potentiation', The Journal of biological chemistry. J Biol Chem, 281(2), pp. 752–758. doi: 10.1074/JBC.M509677200.

Okamoto, Y. et al. (2012) 'Cerebral hypoperfusion accelerates cerebral amyloid angiopathy and promotes cortical microinfarcts', Acta neuropathologica. Acta Neuropathol, 123(3), pp. 381–394. doi: 10.1007/S00401-011-0925-9.

Olsson, B. et al. (2016) 'CSF and blood biomarkers for the diagnosis of Alzheimer's disease: a systematic review and meta-analysis', The Lancet. Neurology. Lancet Neurol, 15(7), pp. 673–684. doi: 10.1016/S1474-4422(16)00070-3.

Olsson, F. et al. (2014) 'Characterization of intermediate steps in amyloid beta (Aβ) production under near-native conditions', The Journal of biological chemistry. J Biol Chem, 289(3), pp. 1540–1550. doi: 10.1074/JBC.M113.498246.

Pallas, M. et al. (2008) 'From aging to Alzheimer's disease: unveiling "the switch" with the senescence-accelerated mouse model (SAMP8)', Journal of Alzheimer's disease : JAD. J Alzheimers Dis, 15(4), pp. 615–624. doi: 10.3233/JAD-2008-15408.

Parfenova, H. et al. (2006) 'Glutamate induces oxidative stress and apoptosis in cerebral vascular endothelial cells: contributions of HO-1 and HO-2 to cytoprotection', American

journal of physiology. Cell physiology. Am J Physiol Cell Physiol, 290(5). doi: 10.1152/AJPCELL.00386.2005.

Park, H. and Poo, M. M. (2013) 'Neurotrophin regulation of neural circuit development and function', Nature reviews. Neuroscience. Nat Rev Neurosci, 14(1), pp. 7–23. doi: 10.1038/NRN3379.

Park, J. et al. (2012) 'Multi-compartment neuron-glia co-culture platform for localized CNS axon-glia interaction study', Lab on a Chip. doi: 10.1039/c2lc40303j.

Park, L. C. H., Zhang, H. and Gibson, G. E. (2001) 'Co-culture with astrocytes or microglia protects metabolically impaired neurons', in Mechanisms of Ageing and Development. doi: 10.1016/S0047-6374(01)00336-0.

Parpura, V. and Zorec, R. (2010) 'Gliotransmission: Exocytotic release from astrocytes', Brain research reviews. Brain Res Rev, 63(1–2), pp. 83–92. doi: 10.1016/J.BRAINRESREV.2009.11.008.

Parsons, M. P. et al. (2014) 'Bidirectional control of Postsynaptic Density-95 (PSD-95) clustering by Huntingtin', Journal of Biological Chemistry. American Society for Biochemistry and Molecular Biology, 289(6), pp. 3518–3528. doi: 10.1074/jbc.M113.513945.

Pearson, W. R. (2013) 'An Introduction to Sequence Similarity ("Homology") Searching', Current protocols in bioinformatics / editoral board, Andreas D. Baxevanis ... [et al.]. NIH Public Access, 0 3(SUPPL.42). doi: 10.1002/0471250953.BI0301S42.

Pedersen, F. N. et al. (2022) 'Diabetic Retinopathy Predicts Risk of Alzheimer's Disease: A Danish Registry-Based Nationwide Cohort Study', Journal of Alzheimer's disease : JAD. J Alzheimers Dis, 86(1), pp. 451–460. doi: 10.3233/JAD-215313.

Peng, S. et al. (2005) 'Precursor form of brain-derived neurotrophic factor and mature brain-derived neurotrophic factor are decreased in the pre-clinical stages of Alzheimer's disease', Journal of neurochemistry. J Neurochem, 93(6), pp. 1412–1421. doi: 10.1111/J.1471-4159.2005.03135.X.

Persidsky, Y. et al. (2006) 'Blood-brain barrier: structural components and function under physiologic and pathologic conditions', Journal of neuroimmune pharmacology : the official journal of the Society on NeuroImmune Pharmacology. J Neuroimmune Pharmacol, 1(3), pp. 223–236. doi: 10.1007/S11481-006-9025-3.

Poduslo, J. F. and Curran, G. L. (1996) 'Permeability at the blood-brain and blood-nerve barriers of the neurotrophic factors: NGF, CNTF, NT-3, BDNF', Brain research. Molecular brain research. Brain Res Mol Brain Res, 36(2), pp. 280–286. doi: 10.1016/0169-328X(95)00250-V.

Poon, W. W. et al. (2011) 'β-Amyloid impairs axonal BDNF retrograde trafficking', Neurobiology of Aging, 32(5), pp. 821–833. doi: 10.1016/J.NEUROBIOLAGING.2009.05.012.

Price, B. R. et al. (2018) 'An emerging role of astrocytes in vascular contributions to cognitive impairment and dementia', Journal of neurochemistry. J Neurochem, 144(5), pp. 644–650. doi: 10.1111/JNC.14273.

Qiang, M. et al. (2014) 'A novel mechanism for endogenous formaldehyde elevation in SAMP8 mouse', Journal of Alzheimer's disease : JAD. J Alzheimers Dis, 40(4), pp. 1039–1053. doi: 10.3233/JAD-131595.

Qu, L. et al. (2009) 'Synapse-to-synapse variation in mean synaptic vesicle size and its relationship with synaptic morphology and function', The Journal of comparative neurology. J Comp Neurol, 514(4), pp. 343–352. doi: 10.1002/CNE.22007.

Quesseveur, G. et al. (2013) 'BDNF overexpression in mouse hippocampal astrocytes promotes local neurogenesis and elicits anxiolytic-like activities', Translational psychiatry. Transl Psychiatry, 3(4). doi: 10.1038/TP.2013.30.

Quirié, A. et al. (2012) 'Comparative effect of treadmill exercise on mature BDNF production in control versus stroke rats', PloS one. PLoS One, 7(9). doi: 10.1371/JOURNAL.PONE.0044218.

Radka, S. F. et al. (1996) 'Presence of brain-derived neurotrophic factor in brain and human and rat but not mouse serum detected by a sensitive and specific immunoassay', Brain research. Brain Res, 709(1), pp. 122–130. doi: 10.1016/0006-8993(95)01321-0.

Ramonet, D. et al. (2003) 'Localization of monoamine oxidase A and B and semicarbazide-sensitive amine oxidase in human peripheral tissues', Inflammopharmacology. Inflammopharmacology, 11(2), pp. 111–117. doi: 10.1163/156856003765764272.

Ransohoff, R. M. (2016) 'How neuroinflammation contributes to neurodegeneration', Science (New York, N.Y.). Science, 353(6301), pp. 777–783. doi: 10.1126/SCIENCE.AAG2590.

Rauti, R. et al. (2020) 'BDNF impact on synaptic dynamics: extra or intracellular long-term release differently regulates cultured hippocampal synapses', Molecular Brain 2020 13:1. BioMed Central, 13(1), pp. 1–16. doi: 10.1186/S13041-020-00582-9.

Reed, M. J., Damodarasamy, M. and Banks, W. A. (2019) 'The extracellular matrix of the blood-brain barrier: structural and functional roles in health, aging, and Alzheimer's disease', Tissue barriers. Tissue Barriers, 7(4). doi: 10.1080/21688370.2019.1651157.

Reiner, A. and Levitz, J. (2018) 'Glutamatergic Signaling in the Central Nervous System: Ionotropic and Metabotropic Receptors in Concert', Neuron. Cell Press, 98(6), pp. 1080–1098. doi: 10.1016/J.NEURON.2018.05.018.

Reiss, A. B. et al. (2018) 'Amyloid toxicity in Alzheimer's disease', Reviews in the neurosciences. Rev Neurosci, 29(6), pp. 613–627. doi: 10.1515/REVNEURO-2017-0063.

Report, S. (2021) 'ALZHEIMER ' S DISEASE IN THE EU DURING AND ALZHEIMER ' S DISEASE IN THE EU DURING AND AFTER', (December).

Rhodius-Meester, H. F. M. et al. (2019) 'Survival in memory clinic cohort is short, even in young-onset dementia', Journal of neurology, neurosurgery, and psychiatry. J Neurol Neurosurg Psychiatry, 90(6), pp. 726–728. doi: 10.1136/JNNP-2018-318820.

Riss, T. L. et al. (2004) 'Cell Viability Assays', Assay Guidance Manual, (Md), pp. 1–25. Available at: http://www.ncbi.nlm.nih.gov/pubmed/23805433.

Robinet, C. and Pellerin, L. (2011) 'Brain-derived neurotrophic factor enhances the hippocampal expression of key postsynaptic proteins in vivo including the monocarboxylate transporter MCT2', Neuroscience. Pergamon, 192, pp. 155–163. doi: 10.1016/j.neuroscience.2011.06.059.

Robinson, R. A. S., Amin, B. and Guest, P. C. (2017) 'Multiplexing Biomarker Methods, Proteomics and Considerations for Alzheimer's Disease', Advances in experimental medicine and biology. Adv Exp Med Biol, 974, pp. 21–48. doi: 10.1007/978-3-319-52479-5_2.

Roher, A. E. et al. (1993) 'beta-Amyloid-(1-42) is a major component of cerebrovascular amyloid deposits: implications for the pathology of Alzheimer disease.', Proceedings of the National Academy of Sciences of the United States of America. National Academy of Sciences, 90(22), p. 10836. doi: 10.1073/PNAS.90.22.10836.

Roher, A. E. et al. (2012) 'Cerebral blood flow in Alzheimer's disease', Vascular Health and Risk Management. Dove Press, 8(1), p. 599. doi: 10.2147/VHRM.S34874.

Rosenfeld, R. D. et al. (1995) 'Purification and identification of brain-derived neurotrophic factor from human serum', Protein expression and purification. Protein Expr Purif, 6(4), pp. 465–471. doi: 10.1006/PREP.1995.1062.

Rossi, B. et al. (2021) 'Common Peripheral Immunity Mechanisms in Multiple Sclerosis and Alzheimer's Disease', Frontiers in immunology. Front Immunol, 12. doi: 10.3389/FIMMU.2021.639369.

Roth, M., Tomlinson, B. E. and Blessed, G. (1966) 'Correlation between Scores for Dementia and Counts of "Senile Plaques" in Cerebral Grey Matter of Elderly Subjects', Nature 1966 209:5018. Nature Publishing Group, 209(5018), pp. 109–110. doi: 10.1038/209109a0.

Russell, C. L. et al. (2012) 'Amyloid-β Acts as a Regulator of Neurotransmitter Release Disrupting the Interaction between Synaptophysin and VAMP2', PLOS ONE. Public Library of Science, 7(8), p. e43201. doi: 10.1371/JOURNAL.PONE.0043201.

Ryu, J. K. and McLarnon, J. G. (2009) 'A leaky blood-brain barrier, fibrinogen infiltration and microglial reactivity in inflamed Alzheimer's disease brain', Journal of cellular and molecular medicine. J Cell Mol Med, 13(9A), pp. 2911–2925. doi: 10.1111/J.1582-4934.2008.00434.X.

Sagare, A. P. et al. (2013) 'Pericyte loss influences Alzheimer-like neurodegeneration in mice', Nature communications. Nat Commun, 4. doi: 10.1038/NCOMMS3932.

Sagare, A. P., Bell, R. D. and Zlokovic, B. V. (2012) 'Neurovascular dysfunction and faulty amyloid β-peptide clearance in Alzheimer disease', Cold Spring Harbor perspectives in medicine. Cold Spring Harb Perspect Med, 2(10). doi: 10.1101/CSHPERSPECT.A011452.

Salmi, M. and Jalkanen, S. (1995) 'Different forms of human vascular adhesion protein-1 (VAP-1) in blood vessels in vivo and in cultured endothelial cells: implications for lymphocyte-endothelial cell adhesion models', European journal of immunology. Eur J Immunol, 25(10), pp. 2803–2812. doi: 10.1002/EJI.1830251014.

Salmi, M. and Jalkanen, S. (2005) 'Cell-surface enzymes in control of leukocyte trafficking', Nature reviews. Immunology. Nat Rev Immunol, 5(10), pp. 760–771. doi: 10.1038/NRI1705.

Salmi, M. and Jalkanen, S. (2019) 'Vascular Adhesion Protein-1: A Cell Surface Amine Oxidase in Translation', Antioxidants & redox signaling. Antioxid Redox Signal, 30(3), pp. 314–332. doi: 10.1089/ARS.2017.7418.

Salmi, M. et al. (2001) 'A cell surface amine oxidase directly controls lymphocyte migration', Immunity. Immunity, 14(3), pp. 265–276. doi: 10.1016/S1074-7613(01)00108-X.

Salmi, M., Kalimo, K. and Jalkanen, S. (1993) 'Induction and function of vascular adhesion protein-1 at sites of inflammation', The Journal of experimental medicine. J Exp Med, 178(6), pp. 2255–2260. doi: 10.1084/JEM.178.6.2255.

Sanderson, J. L. and Dell'Acqua, M. L. (2011) 'AKAP signaling complexes in regulation of excitatory synaptic plasticity', The Neuroscientist : a review journal bringing neurobiology, neurology and psychiatry. Neuroscientist, 17(3), pp. 321–336. doi: 10.1177/1073858410384740.

Sá-Pereira, I., Brites, D. and Brito, M. A. (2012) 'Neurovascular unit: a focus on pericytes', Molecular neurobiology. Mol Neurobiol, 45(2), pp. 327–347. doi: 10.1007/S12035-012-8244-2.

Sasi, M. et al. (2017) 'Neurobiology of local and intercellular BDNF signaling', Pflugers Archiv : European journal of physiology. Pflugers Arch, 469(5–6), pp. 593–610. doi: 10.1007/S00424-017-1964-4.

Scheff, S. W. et al. (2006) 'Hippocampal synaptic loss in early Alzheimer's disease and mild cognitive impairment', Neurobiology of aging. Neurobiol Aging, 27(10), pp. 1372–1384. doi: 10.1016/J.NEUROBIOLAGING.2005.09.012.

Scheffer, S. et al. (2021) 'Vascular Hypothesis of Alzheimer Disease: Topical Review of Mouse Models', Arteriosclerosis, thrombosis, and vascular biology. Arterioscler Thromb Vasc Biol, 41(4), pp. 1265–1283. doi: 10.1161/ATVBAHA.120.311911.

Schenk, D. et al. (1999) 'Immunization with amyloid-beta attenuates Alzheimer-disease-like pathology in the PDAPP mouse', Nature. Nature, 400(6740), pp. 173–177. doi: 10.1038/22124.

Schiera, G. et al. (2005) 'Permeability properties of a three-cell type in vitro model of blood-brain barrier', Journal of cellular and molecular medicine. J Cell Mol Med, 9(2), pp. 373–379. doi: 10.1111/J.1582-4934.2005.TB00362.X.

Schilter, H. C. et al. (2015) 'Effects of an anti-inflammatory VAP-1/SSAO inhibitor, PXS-4728A, on pulmonary neutrophil migration', Respiratory Research. BioMed Central Ltd., 16(1), pp. 1–14. doi: 10.1186/S12931-015-0200-Z/FIGURES/8.

Schousboe, A. et al. (2004) 'Role of astrocytic transport processes in glutamatergic and GABAergic neurotransmission', Neurochemistry international. Neurochem Int, 45(4), pp. 521–527. doi: 10.1016/J.NEUINT.2003.11.001.

Segarra, M., Aburto, M. R. and Acker-Palmer, A. (2021) 'Blood-Brain Barrier Dynamics to Maintain Brain Homeostasis', Trends in neurosciences. Trends Neurosci, 44(5), pp. 393–405. doi: 10.1016/J.TINS.2020.12.002.

Selkoe, D. J. and Hardy, J. (2016) 'The amyloid hypothesis of Alzheimer's disease at 25 years', EMBO molecular medicine. EMBO Mol Med, 8(6), pp. 595–608. doi: 10.15252/EMMM.201606210.

Sengillo, J. D. et al. (2013) 'Deficiency in mural vascular cells coincides with blood-brain barrier disruption in Alzheimer's disease', Brain pathology (Zurich, Switzerland). Brain Pathol, 23(3), pp. 303–310. doi: 10.1111/BPA.12004.

Serrano-Pozo, A. et al. (2011) 'Neuropathological alterations in Alzheimer disease', Cold Spring Harbor perspectives in medicine. Cold Spring Harb Perspect Med, 1(1). doi: 10.1101/CSHPERSPECT.A006189.

Shankar, G. M. et al. (2008) 'Amyloid-β protein dimers isolated directly from Alzheimer's brains impair synaptic plasticity and memory', Nature Medicine 2008 14:8. Nature Publishing Group, 14(8), pp. 837–842. doi: 10.1038/nm1782.

Shao, C. Y. et al. (2011) 'Postsynaptic degeneration as revealed by PSD-95 reduction occurs after advanced Aβ and tau pathology in transgenic mouse models of Alzheimer's disease', Acta neuropathologica. Acta Neuropathol, 122(3), pp. 285–292. doi: 10.1007/S00401-011-0843-X.

Sharp, C. D. et al. (2003) 'Glutamate causes a loss in human cerebral endothelial barrier integrity through activation of NMDA receptor', American Journal of Physiology - Heart and Circulatory Physiology. American Physiological Society, 285(6 54-6), pp. 2592–2598. doi: 10.1152/AJPHEART.00520.2003/ASSET/IMAGES/LARGE/H41232668005.JPEG.

Shi, M. et al. (2013) 'Glia co-culture with neurons in microfluidic platforms promotes the formation and stabilization of synaptic contacts', Lab on a chip. Lab Chip, 13(15), pp. 3008–3021. doi: 10.1039/C3LC50249J.

Silbereis, J. C. et al. (2016) 'The Cellular and Molecular Landscapes of the Developing Human Central Nervous System', Neuron. NIH Public Access, 89(2), p. 248. doi: 10.1016/J.NEURON.2015.12.008.

Šimić, G. et al. (1997) 'Volume and number of neurons of the human hippocampal formation in normal aging and Alzheimer's disease', Journal of Comparative Neurology, 379(4), pp. 482–494. doi: 10.1002/(SICI)1096-9861(19970324)379:4<482::AID-CNE2>3.0.CO;2-Z.

Smith, D. J. et al. (1998) 'Cloning of Vascular Adhesion Protein 1 Reveals a NovelMultifunctional Adhesion Molecule', The Journal of Experimental Medicine. The Rockefeller University Press, 188(1), p. 17. doi: 10.1084/JEM.188.1.17.

Sofroniew, M. V. (2009) 'Molecular dissection of reactive astrogliosis and glial scar formation', Trends in neurosciences. Trends Neurosci, 32(12), pp. 638–647. doi: 10.1016/J.TINS.2009.08.002.

Sofroniew, M. V. and Vinters, H. V. (2010) 'Astrocytes: biology and pathology', Acta neuropathologica. Acta Neuropathol, 119(1), pp. 7–35. doi: 10.1007/S00401-009-0619-8.

Solé, M. and Unzeta, M. (2011) 'Vascular cell lines expressing SSAO/VAP-1: a new experimental tool to study its involvement in vascular diseases', Biology of the cell. Biol Cell, 103(11), pp. 543–557. doi: 10.1042/BC20110049.

Solé, M. et al. (2019) 'Blood-brain barrier dysfunction underlying Alzheimer's disease is induced by an SSAO/VAP-1-dependent cerebrovascular activation with enhanced Aβ deposition', Biochimica et Biophysica Acta - Molecular Basis of Disease. Elsevier, 1865(9), pp. 2189–2202. doi: 10.1016/j.bbadis.2019.04.016.

Solé, M., Miñano-Molina, A. J. and Unzeta, M. (2015) 'A cross-talk between Aβ and endothelial SSAO/VAP-1 accelerates vascular damage and Aβ aggregation related to CAA-AD', Neurobiology of Aging. Elsevier Inc, 36(2), pp. 762–775. doi: 10.1016/j.neurobiolaging.2014.09.030.

Solé, M., Miñano-Molina, A. J. and Unzeta, M. (2015a) 'A cross-talk between Aβ and endothelial SSAO/VAP-1 accelerates vascular damage and Aβ aggregation related to CAA-AD', Neurobiology of Aging. Elsevier Inc, 36(2), pp. 762–775. doi: 10.1016/j.neurobiolaging.2014.09.030.

Solé, M., Miñano-Molina, A. J. and Unzeta, M. (2015b) 'Cross-talk between Aβ and endothelial SSAO/VAP-1 accelerates vascular damage and Aβ aggregation related to CAA-AD', Neurobiology of aging. Neurobiol Aging, 36(2), pp. 762–775. doi: 10.1016/J.NEUROBIOLAGING.2014.09.030.

Song, I. and Huganir, R. L. (2002) 'Regulation of AMPA receptors during synaptic plasticity', Trends in neurosciences. Trends Neurosci, 25(11), pp. 578–588. doi: 10.1016/S0166-2236(02)02270-1.

Steinman, J., Sun, H. S. and Feng, Z. P. (2021) 'Microvascular Alterations in Alzheimer's Disease', Frontiers in cellular neuroscience. Front Cell Neurosci, 14. doi: 10.3389/FNCEL.2020.618986.

Steinman, J., Sun, H. S. and Feng, Z. P. (2021a) 'Microvascular Alterations in Alzheimer's Disease', Frontiers in cellular neuroscience. Front Cell Neurosci, 14. doi: 10.3389/FNCEL.2020.618986.

Steinman, J., Sun, H. S. and Feng, Z. P. (2021b) 'Microvascular Alterations in Alzheimer's Disease', Frontiers in Cellular Neuroscience, 14(January). doi: 10.3389/fncel.2020.618986.

Stellwagen, D. and Malenka, R. C. (2006) 'Synaptic scaling mediated by glial TNF-alpha', Nature. Nature, 440(7087), pp. 1054–1059. doi: 10.1038/NATURE04671.

Stone, N. L., England, T. J. and O'Sullivan, S. E. (2019) 'A Novel Transwell Blood Brain Barrier Model Using Primary Human Cells', Frontiers in cellular neuroscience. Front Cell Neurosci, 13. doi: 10.3389/FNCEL.2019.00230.

Südhof, T. C. (2018) 'Towards an Understanding of Synapse Formation', Neuron. Neuron, 100(2), pp. 276–293. doi: 10.1016/J.NEURON.2018.09.040.

Sumi, T. and Harada, K. (2020) 'Mechanism underlying hippocampal long-term potentiation and depression based on competition between endocytosis and exocytosis of AMPA receptors', Scientific Reports 2020 10:1. Nature Publishing Group, 10(1), pp. 1–14. doi: 10.1038/s41598-020-71528-3.

Sun, P. et al. (2015) 'Protective effect of the multitarget compound DPH-4 on human SSAO/VAP-1-expressing hCMEC/D3 cells under oxygen-glucose deprivation conditions: An in vitro experimental model of cerebral ischaemia', British Journal of Pharmacology, 172(22), pp. 5390–5402. doi: 10.1111/bph.13328.

Sun, P., Solé, M. and Unzeta, M. (2014) 'Involvement of SSAO/VAP-1 in oxygen-glucose deprivation-mediated damage using the endothelial hSSAO/VAP-1-expressing cells as experimental model of cerebral ischemia', Cerebrovascular diseases (Basel, Switzerland). Cerebrovasc Dis, 37(3), pp. 171–180. doi: 10.1159/000357660.

Sweeney, M. D. et al. (2019) 'Blood-Brain Barrier: From Physiology to Disease and Back', Physiological reviews. Physiol Rev, 99(1), pp. 21–78. doi: 10.1152/PHYSREV.00050.2017.

Sweeney, M. D., Sagare, A. P. and Zlokovic, B. V. (2018) 'Blood–brain barrier breakdown in Alzheimer disease and other neurodegenerative disorders', Nature Reviews Neurology 2018 14:3. Nature Publishing Group, 14(3), pp. 133–150. doi: 10.1038/nrneurol.2017.188.

Swerdlow, R. H., Burns, J. M. and Khan, S. M. (2014) 'The Alzheimer's disease mitochondrial cascade hypothesis: progress and perspectives', Biochimica et biophysica acta. Biochim Biophys Acta, 1842(8), pp. 1219–1231. doi: 10.1016/J.BBADIS.2013.09.010.

Takami, M. et al. (2009) 'gamma-Secretase: successive tripeptide and tetrapeptide release from the transmembrane domain of beta-carboxyl terminal fragment', The Journal of neuroscience : the official journal of the Society for Neuroscience. J Neurosci, 29(41), pp. 13042–13052. doi: 10.1523/JNEUROSCI.2362-09.2009.

Takano, T. et al. (2006) 'Astrocyte-mediated control of cerebral blood flow', Nature neuroscience. Nat Neurosci, 9(2), pp. 260–267. doi: 10.1038/NN1623.

Tam, S. J. and Watts, R. J. (2010) 'Connecting vascular and nervous system development: angiogenesis and the blood-brain barrier', Annual review of neuroscience. Annu Rev Neurosci, 33, pp. 379–408. doi: 10.1146/ANNUREV-NEURO-060909-152829.

Tanaka, H., Sakaguchi, D. and Hirano, T. (2019) 'Amyloid-β oligomers suppress subunit-specific glutamate receptor increase during LTP', Alzheimer's & Dementia: Translational Research & Clinical Interventions. No longer published by Elsevier, 5, pp. 797–808. doi: 10.1016/J.TRCI.2019.10.003.

Tanqueiro, S. R. et al. (2018) 'Inhibition of NMDA receptors prevents the loss of BDNF function induced by amyloid β', Frontiers in Pharmacology. Frontiers Media S.A., 9(APR), p. 237. doi: 10.3389/FPHAR.2018.00237/BIBTEX.

Tao, C. L. et al. (2018) 'Differentiation and Characterization of Excitatory and Inhibitory Synapses by Cryo-electron Tomography and Correlative Microscopy', The Journal of neuroscience : the official journal of the Society for Neuroscience. J Neurosci, 38(6), pp. 1493–1510. doi: 10.1523/JNEUROSCI.1548-17.2017.

Tapia-Arancibia, L. et al. (2008) 'New insights into brain BDNF function in normal aging and Alzheimer disease', Brain research reviews. Brain Res Rev, 59(1), pp. 201–220. doi: 10.1016/J.BRAINRESREV.2008.07.007.

Tarassova, O. et al. (2020) 'Peripheral BDNF Response to Physical and Cognitive Exercise and Its Association With Cardiorespiratory Fitness in Healthy Older Adults', Frontiers in physiology. Front Physiol, 11. doi: 10.3389/FPHYS.2020.01080.

Tartaglia, N. et al. (2001) 'Protein Synthesis-dependent and -independent Regulation of Hippocampal Synapses by Brain-derived Neurotrophic Factor', Journal of Biological Chemistry. Elsevier, 276(40), pp. 37585–37593. doi: 10.1074/jbc.M101683200.

Terry, R. D. (1996) 'The Pathogenesis of Alzheimer Disease: An Alternative to the Amyloid Hypothesis', Journal of Neuropathology & Experimental Neurology. Oxford Academic, 55(10), pp. 1023–1025. doi: 10.1097/00005072-199655100-00001.

Texidó, L. et al. (2011) 'Amyloid β peptide oligomers directly activate NMDA receptors', Cell calcium. Cell Calcium, 49(3), pp. 184–190. doi: 10.1016/J.CECA.2011.02.001.

Thal, D. R. et al. (2002) 'Phases of A beta-deposition in the human brain and its relevance for the development of AD', Neurology. Neurology, 58(12), pp. 1791–1800. doi: 10.1212/WNL.58.12.1791.

Thoenen, H. (1995) 'Neurotrophins and neuronal plasticity', Science (New York, N.Y.). Science, 270(5236), pp. 593–598. doi: 10.1126/SCIENCE.270.5236.593.

Tipton, K. F. and Strolin, M. (2002) 'Amine Oxidases and the Metabolism of Xenobiotics', Enzyme Systems that Metabolise Drugs and Other Xenobiotics. John Wiley & Sons, Ltd, pp. 95–146. doi: 10.1002/0470846305.CH4.

Tong, L. et al. (2001) 'Effects of exercise on gene-expression profile in the rat hippocampus', Neurobiology of disease. Neurobiol Dis, 8(6), pp. 1046–1056. doi: 10.1006/NBDI.2001.0427.

Tong, L. et al. (2021) 'Imaging and optogenetic modulation of vascular mural cells in the live brain', Nature protocols. Nat Protoc, 16(1), pp. 472–496. doi: 10.1038/S41596-020-00425-W.

Traynelis, S. F. et al. (2010) 'Glutamate receptor ion channels: Structure, regulation, and function', Pharmacological Reviews, 62(3), pp. 405–496. doi: 10.1124/pr.109.002451.

Trejo-Lopez, J. A., Yachnis, A. T. and Prokop, S. (2022) 'Neuropathology of Alzheimer's Disease', Neurotherapeutics : the journal of the American Society for Experimental NeuroTherapeutics. Neurotherapeutics, 19(1), pp. 173–185. doi: 10.1007/S13311-021-01146-Y.

Tremblay, R., Lee, S. and Rudy, B. (2016) 'GABAergic interneurons in the neocortex: From cellular properties to circuits', Neuron. NIH Public Access, 91(2), p. 260. doi: 10.1016/J.NEURON.2016.06.033.

Tublin, J. M. et al. (2019) 'Getting to the Heart of Alzheimer Disease', Circulation research. Circ Res, 124(1), pp. 142–149. doi: 10.1161/CIRCRESAHA.118.313563.

U., D. S. et al. (2017) 'Human Co-culture Model of Neurons and Astrocytes to Test Acute Cytotoxicity of Neurotoxic Compounds', International Journal of Toxicology.

Ullah, K. et al. (2013) 'Arterial vascular cell line expressing SSAO: a new tool to study the pathophysiology of vascular amine oxidases', Journal of neural transmission (Vienna, Austria : 1996). J Neural Transm (Vienna), 120(6), pp. 1005–1013. doi: 10.1007/S00702-013-1015-Z.

Ullian, E. M. et al. (2001) 'Control of synapse number by glia', Science (New York, N.Y.). Science, 291(5504), pp. 657–661. doi: 10.1126/SCIENCE.291.5504.657.

Unzeta, M. et al. (2007) 'Semicarbazide-sensitive amine oxidase (SSAO) and its possible contribution to vascular damage in Alzheimer's disease', Journal of neural transmission (Vienna, Austria : 1996). J Neural Transm (Vienna), 114(6), pp. 857–862. doi: 10.1007/S00702-007-0701-0.

Unzeta, M. et al. (2007) 'Semicarbazide-sensitive amine oxidase (SSAO) and its possible contribution to vascular damage in Alzheimer's disease', Journal of Neural Transmission, 114(6), pp. 857–862. doi: 10.1007/S00702-007-0701-0.

Unzeta, M. et al. (2021) 'SSAO/VAP-1 in Cerebrovascular Disorders: A Potential Therapeutic Target for Stroke and Alzheimer's Disease', International journal of molecular sciences. Int J Mol Sci, 22(7). doi: 10.3390/IJMS22073365.

Unzeta, M. et al. (2021) SSAO / VAP-1 in Cerebrovascular Disorders : A Potential Therapeutic Target for Stroke and Alzheimer ' s Disease. doi: 10.3390/ijms22073365.

Valente, T. et al. (2012) 'Immunohistochemical study of semicarbazide-sensitive amine oxidase/vascular adhesion protein-1 in the hippocampal vasculature: pathological synergy of Alzheimer's disease and diabetes mellitus', Journal of neuroscience research. J Neurosci Res, 90(10), pp. 1989–1996. doi: 10.1002/JNR.23092.

Van De Haar, H. J. et al. (2016) 'Blood-Brain Barrier Leakage in Patients with Early Alzheimer Disease', Radiology. Radiology, 281(2), pp. 527–535. doi: 10.1148/RADIOL.2016152244.

van de Haar, H. J. et al. (2016) 'Neurovascular unit impairment in early Alzheimer's disease measured with magnetic resonance imaging', Neurobiology of aging. Neurobiol Aging, 45, pp. 190–196. doi: 10.1016/J.NEUROBIOLAGING.2016.06.006.

Van Essen, D. C., Donahue, C. J. and Glasser, M. F. (2018) 'Development and Evolution of Cerebral and Cerebellar Cortex', Brain, Behavior and Evolution. Karger Publishers, 91(3), pp. 158–169. doi: 10.1159/000489943.

Vellucci, S. V., Parrott, R. F. and Mimmack, M. L. (2001) 'Down-regulation of BDNF mRNA, with no effect on trkB or glucocorticoid receptor m RNAs, in the porcine hippocampus after acute dexamethasone treatment', Research in veterinary science. Res Vet Sci, 70(2), pp. 157–162. doi: 10.1053/RVSC.2001.0456.

Ventriglia, M. et al. (2013) 'Serum brain-derived neurotrophic factor levels in different neurological diseases', BioMed research international. Biomed Res Int, 2013. doi: 10.1155/2013/901082.

Verkhratsky, A. and Nedergaard, M. (2014) 'Astroglial cradle in the life of the synapse', Philosophical Transactions of the Royal Society B: Biological Sciences. The Royal Society, 369(1654). doi: 10.1098/RSTB.2013.0595.

Villemagne, V. L. et al. (2015) 'Tau imaging: early progress and future directions', The Lancet. Neurology. Lancet Neurol, 14(1), pp. 114–124. doi: 10.1016/S1474-4422(14)70252-2.

Vinters, H. V. (2015) 'Emerging concepts in alzheimer's disease', Annual Review of Pathology: Mechanisms of Disease. Annual Reviews Inc., 10, pp. 291–319. doi: 10.1146/annurev-pathol-020712-163927.

Vinuesa, A. et al. (2019) 'Early Exposure to a High-Fat Diet Impacts on Hippocampal Plasticity: Implication of Microglia-Derived Exosome-like Extracellular Vesicles', Molecular neurobiology. Mol Neurobiol, 56(7), pp. 5075–5094. doi: 10.1007/S12035-018-1435-8.

Virchow, R. (1858) 'Die Cellular pathologie', Ihrer Begründung auf Physiologische und Pathologische Gewebelehre.

Viswanathan, A. and Greenberg, S. M. (2011) 'Cerebral amyloid angiopathy in the elderly', Annals of neurology. Ann Neurol, 70(6), pp. 871–880. doi: 10.1002/ANA.22516.

von Bohlen und Halbach, O. and von Bohlen und Halbach, V. (2018) 'BDNF effects on dendritic spine morphology and hippocampal function', Cell and Tissue Research. Springer Verlag, pp. 729–741. doi: 10.1007/s00441-017-2782-x.

Vorbrodt, A. W. and Dobrogowska, D. H. (2003) 'Molecular anatomy of intercellular junctions in brain endothelial and epithelial barriers: electron microscopist's view', Brain research. Brain research reviews. Brain Res Brain Res Rev, 42(3), pp. 221–242. doi: 10.1016/S0165-0173(03)00177-2.

Walsh, D. M. and Selkoe, D. J. (2007) 'A beta oligomers - a decade of discovery', Journal of neurochemistry. J Neurochem, 101(5), pp. 1172–1184. doi: 10.1111/J.1471-4159.2006.04426.X.

Wang, J. Q. et al. (2005) 'Phosphorylation of AMPA receptors: mechanisms and synaptic plasticity', Molecular neurobiology. Mol Neurobiol, 32(3), pp. 237–249. doi: 10.1385/MN:32:3:237.

Wang, R. and Holsinger, R. M. D. (2018) 'Exercise-induced brain-derived neurotrophic factor expression: Therapeutic implications for Alzheimer's dementia', Ageing research reviews. Ageing Res Rev, 48, pp. 109–121. doi: 10.1016/J.ARR.2018.10.002.

Wang, R. and Reddy, P. H. (2017) 'Role of Glutamate and NMDA Receptors in Alzheimer's Disease', Journal of Alzheimer's disease : JAD. J Alzheimers Dis, 57(4), pp. 1041–1048. doi: 10.3233/JAD-160763.

Wang, S. H. et al. (2018) 'Inhibition of semicarbazide-sensitive amine oxidase reduces atherosclerosis in apolipoprotein E-deficient mice', Translational research : the journal of laboratory and clinical medicine. Transl Res, 197, pp. 12–31. doi: 10.1016/J.TRSL.2018.03.001.

Wang, T. et al. (2011) 'Neutralization of BDNF attenuates the in vitro protective effects of olfactory ensheathing cell-conditioned medium on scratch-insulted retinal ganglion cells', Cellular and molecular neurobiology. Cell Mol Neurobiol, 31(3), pp. 357–364. doi: 10.1007/S10571-010-9626-5.

Wang, Y.-W. et al. (2021) 'GluN2B-BDNF pathway in the cerebrospinal fluid-contacting nucleus mediates nerve injury-induced neuropathic pain in rats.', Sheng li xue bao : [Acta physiologica Sinica], 73(2), pp. 223–232. doi: 10.13294/j.aps.2020.0094.

Wang, Z. H. et al. (2019) 'Deficiency in BDNF/TrkB Neurotrophic Activity Stimulates δ-Secretase by Upregulating C/EBPβ in Alzheimer's Disease', Cell reports. Cell Rep, 28(3), pp. 655-669.e5. doi: 10.1016/J.CELREP.2019.06.054.

Watson, J. F., Ho, H. and Greger, I. H. (2017) 'Synaptic transmission and plasticity require AMPA receptor anchoring via its N-terminal domain', eLife, 6, pp. 1–20. doi: 10.7554/eLife.23024.

Wattendorff, A. R. et al. (1995) 'Hereditary cerebral haemorrhage with amyloidosis, Dutch type (HCHWA-D): clinicopathological studies.', Journal of Neurology, Neurosurgery, and Psychiatry. BMJ Publishing Group, 58(6), p. 699. doi: 10.1136/JNNP.58.6.699.

Weiss, H. G. et al. (2003) 'Plasma amine oxidase: a postulated cardiovascular risk factor in nondiabetic obese patients', Metabolism - Clinical and Experimental. Elsevier, 52(6), pp. 688–692. doi: 10.1016/S0026-0495(03)00028-3.

Weksler, B. B. et al. (2005) 'Blood-brain barrier-specific properties of a human adult brain endothelial cell line', FASEB Journal, 19(13), pp. 1872–1874. doi: 10.1096/fj.04-3458fje.

Weksler, B., Romero, I. A. and Couraud, P. O. (2013) 'The hCMEC/D3 cell line as a model of the human blood brain barrier', Fluids and Barriers of the CNS. Fluids and Barriers of the CNS, 10(1), pp. 1–10. doi: 10.1186/2045-8118-10-16.

Willis, C. L. (2011) 'Glia-induced reversible disruption of blood-brain barrier integrity and neuropathological response of the neurovascular unit', Toxicologic pathology. Toxicol Pathol, 39(1), pp. 172–185. doi: 10.1177/0192623310385830.

Willis, C. L. et al. (2004) 'Reversible disruption of tight junction complexes in the rat blood-brain barrier, following transitory focal astrocyte loss', Glia. Glia, 48(1), pp. 1–13. doi: 10.1002/GLIA.20049.

Winkler, E. A., Bell, R. D. and Zlokovic, B. V. (2011) 'Central nervous system pericytes in health and disease', Nature neuroscience. Nat Neurosci, 14(11), pp. 1398–1405. doi: 10.1038/NN.2946.

Wirths, O. and Bayer, T. A. (2012) 'Intraneuronal Aβ accumulation and neurodegeneration: Lessons from transgenic models', Life Sciences. Pergamon, 91(23–24), pp. 1148–1152. doi: 10.1016/J.LFS.2012.02.001.

Wood, J. G. et al. (1986) 'Neurofibrillary tangles of Alzheimer disease share antigenic determinants with the axonal microtubule-associated protein tau (tau)', Proceedings of the National Academy of Sciences of the United States of America. Proc Natl Acad Sci U S A, 83(11), pp. 4040–4043. doi: 10.1073/PNAS.83.11.4040.

Worzfeld, T. and Schwaninger, M. (2016) 'Apicobasal polarity of brain endothelial cells', Journal of Cerebral Blood Flow & Metabolism. SAGE Publications, 36(2), p. 340. doi: 10.1177/0271678X15608644.

Wu, A., Ying, Z. and Gomez-Pinilla, F. (2004) 'The interplay between oxidative stress and brain-derived neurotrophic factor modulates the outcome of a saturated fat diet on synaptic plasticity and cognition', The European journal of neuroscience. Eur J Neurosci, 19(7), pp. 1699–1707. doi: 10.1111/J.1460-9568.2004.03246.X.

Xiang, J. et al. (2019) 'Delta-secretase-cleaved Tau antagonizes TrkB neurotrophic signalings, mediating Alzheimer's disease pathologies', Proceedings of the National Academy of Sciences of the United States of America. Proc Natl Acad Sci U S A, 116(18), pp. 9094–9102. doi: 10.1073/PNAS.1901348116.

Xiao, L. et al. (2016) 'Rapid production of new oligodendrocytes is required in the earliest stages of motor-skill learning', Nature neuroscience. Nat Neurosci, 19(9), pp. 1210–1217. doi: 10.1038/NN.4351.

Xu, A. H. et al. (2018) 'Exogenous brain-derived neurotrophic factor attenuates cognitive impairment induced by okadaic acid in a rat model of Alzheimer's disease', Neural Regeneration Research. Wolters Kluwer -- Medknow Publications, 13(12), p. 2173. doi: 10.4103/1673-5374.241471.

Xue, Q. et al. (2013) 'A novel brain neurovascular unit model with neurons, astrocytes and microvascular endothelial cells of rat', International Journal of Biological Sciences. doi: 10.7150/ijbs.5115.

Xue, Q. et al. (2013) 'A novel brain neurovascular unit model with neurons, astrocytes and microvascular endothelial cells of rat', International journal of biological sciences. Int J Biol Sci, 9(2), pp. 174–189. doi: 10.7150/IJBS.5115.

Yamazaki, Y. and Kanekiyo, T. (2017) 'Blood-Brain Barrier Dysfunction and the Pathogenesis of Alzheimer's Disease', International journal of molecular sciences. Int J Mol Sci, 18(9). doi: 10.3390/IJMS18091965.

Yates, P. A. et al. (2014) 'Incidence of cerebral microbleeds in preclinical Alzheimer disease', Neurology. Neurology, 82(14), pp. 1266–1273. doi: 10.1212/WNL.0000000000000285.

Yoshii, A. and Constantine-Paton, M. (2014) 'Postsynaptic localization of PSD-95 is regulated by all three pathways downstream of TrkB signaling', Frontiers in Synaptic Neuroscience. Frontiers Research Foundation, 6(MAR). doi: 10.3389/fnsyn.2014.00006.

Yoshii, A. et al. (2011) 'TrkB and protein kinase Mζ regulate synaptic localization of PSD-95 in developing cortex', The Journal of neuroscience : the official journal of the Society for Neuroscience. J Neurosci, 31(33), pp. 11894–11904. doi: 10.1523/JNEUROSCI.2190-11.2011.

Yoshioka, A. et al. (1995) 'Alpha-amino-3-hydroxy-5-methyl-4-isoxazolepropionate (AMPA) receptors mediate excitotoxicity in the oligodendroglial lineage', Journal of neurochemistry. J Neurochem, 64(6), pp. 2442–2448. doi: 10.1046/J.1471-4159.1995.64062442.X.

Yu, P. H. and Zuo, D. M. (1993) 'Oxidative deamination of methylamine by semicarbazide-sensitive amine oxidase leads to cytotoxic damage in endothelial cells. Possible consequences for diabetes', Diabetes. Diabetes, 42(4), pp. 594–603. doi: 10.2337/DIAB.42.4.594.

Yu, P. H. et al. (2003) 'Physiological and pathological implications of semicarbazide-sensitive amine oxidase', Biochimica et biophysica acta. Biochim Biophys Acta, 1647(1–2), pp. 193–199. doi: 10.1016/S1570-9639(03)00101-8.

Yurchenco, P. and Patton, B. (2009) 'Developmental and pathogenic mechanisms of basement membrane assembly', Current pharmaceutical design. Curr Pharm Des, 15(12), pp. 1277–1294. doi: 10.2174/138161209787846766.

Zaccaro, M. C. et al. (2001) 'p75 Co-receptors regulate ligand-dependent and ligand-independent Trk receptor activation, in part by altering Trk docking subdomains', The Journal of biological chemistry. J Biol Chem, 276(33), pp. 31023–31029. doi: 10.1074/JBC.M104630200.

Zacchigna, S., Lambrechts, D. and Carmeliet, P. (2008) 'Neurovascular signalling defects in neurodegeneration', Nature Reviews Neuroscience. Nat Rev Neurosci, pp. 169–181. doi: 10.1038/nrn2336.

Zagrebelsky, M. and Korte, M. (2014) 'Form follows function: BDNF and its involvement in sculpting the function and structure of synapses', Neuropharmacology. Neuropharmacology, 76 Pt C(PART C), pp. 628–638. doi: 10.1016/J.NEUROPHARM.2013.05.029.

Zarekiani, P. et al. (2022) 'The neurovascular unit in leukodystrophies: towards solving the puzzle', Fluids and Barriers of the CNS. BioMed Central Ltd, 19(1), pp. 1–19. doi: 10.1186/S12987-022-00316-0/FIGURES/1.

Zenaro, E. et al. (2015) 'Neutrophils promote Alzheimer's disease-like pathology and cognitive decline via LFA-1 integrin', Nature medicine. Nat Med, 21(8), pp. 880–886. doi: 10.1038/NM.3913.

Zeng, H. and Sanes, J. R. (2017) 'Neuronal cell-type classification: challenges, opportunities and the path forward', Nature reviews. Neuroscience. Nat Rev Neurosci, 18(9), pp. 530–546. doi: 10.1038/NRN.2017.85.

Zhang, H. et al. (2021) 'Cerebral blood flow in mild cognitive impairment and Alzheimer's disease: A systematic review and meta-analysis', Ageing research reviews. Ageing Res Rev, 71. doi: 10.1016/J.ARR.2021.101450.

Zhang, L. Y. et al. (2020) 'Microglia exacerbate white matter injury via complement C3/C3aR pathway after hypoperfusion', Theranostics. Theranostics, 10(1), pp. 74–90. doi: 10.7150/THNO.35841.

Zhang, X. et al. (2013) 'Age-related alteration in cerebral blood flow and energy failure is correlated with cognitive impairment in the senescence-accelerated prone mouse strain 8 (SAMP8)', Neurological sciences : official journal of the Italian Neurological Society and of the Italian Society of Clinical Neurophysiology. Neurol Sci, 34(11), pp. 1917–1924. doi: 10.1007/S10072-013-1407-8.

Zhang, Y. et al. (2021) 'Endothelial cell-derived SSAO can increase MLC 20 phosphorylation in VSMCs'. doi: 10.1515/biol-2021-0114.

Zhang, Z. et al. (2017) 'BDNF regulates the expression and secretion of VEGF from osteoblasts via the TrkB/ERK1/2 signaling pathway during fracture healing', Molecular medicine reports. Mol Med Rep, 15(3), pp. 1362–1367. doi: 10.3892/MMR.2017.6110.

Zhao, C. et al. (2007) 'TNF-alpha knockout and minocycline treatment attenuates blood-brain barrier leakage in MPTP-treated mice', Neurobiology of disease. Neurobiol Dis, 26(1), pp. 36–46. doi: 10.1016/J.NBD.2006.11.012.

Zhao, Z. et al. (2015) 'Establishment and Dysfunction of the Blood-Brain Barrier', Cell. Cell, 163(5), pp. 1064–1078. doi: 10.1016/J.CELL.2015.10.067.

Zhong, Z. et al. (2008) 'ALS-causing SOD1 mutants generate vascular changes prior to motor neuron degeneration', Nature neuroscience. Nat Neurosci, 11(4), pp. 420–422. doi: 10.1038/NN2073.

Zhou, H. J. et al. (2018) 'Lentivirus-mediated klotho up-regulation improves aging-related memory deficits and oxidative stress in senescence-accelerated mouse prone-8 mice', Life sciences. Life Sci, 200, pp. 56–62. doi: 10.1016/J.LFS.2018.03.027.

Zhu, J., Shang, Y. and Zhang, M. (2016) 'Mechanistic basis of MAGUK-organized complexes in synaptic development and signalling', Nature reviews. Neuroscience. Nat Rev Neurosci, 17(4), pp. 209–223. doi: 10.1038/NRN.2016.18.

Zhu, M. et al. (2022) 'Regulation of inflammation by VEGF/BDNF signaling in mouse retinal Müller glial cells exposed to high glucose', Cell and tissue research. Cell Tissue Res, 388(3), pp. 521–533. doi: 10.1007/S00441-022-03622-Z.

Ziegenhorn, A. A. et al. (2007) 'Serum neurotrophins--a study on the time course and influencing factors in a large old age sample', Neurobiology of aging. Neurobiol Aging, 28(9), pp. 1436–1445. doi: 10.1016/J.NEUROBIOLAGING.2006.06.011.

Zlokovic, B. V. (2005) 'Neurovascular mechanisms of Alzheimer's neurodegeneration', Trends in neurosciences. Trends Neurosci, 28(4), pp. 202–208. doi: 10.1016/J.TINS.2005.02.001.

Zlokovic, B. V. (2008) 'The blood-brain barrier in health and chronic neurodegenerative disorders', Neuron. Neuron, 57(2), pp. 178–201. doi: 10.1016/J.NEURON.2008.01.003.

Zlokovic, B. V. (2011) 'Neurovascular pathways to neurodegeneration in Alzheimer's disease and other disorders', Nature Reviews Neuroscience 2011 12:12. Nature Publishing Group, 12(12), pp. 723–738. doi: 10.1038/nrn3114.

Zonta, M. et al. (2002) 'Neuron-to-astrocyte signaling is central to the dynamic control of brain microcirculation', Nature Neuroscience 2002 6:1. Nature Publishing Group, 6(1), pp. 43–50. doi: 10.1038/nn980.

X. Annex: contribution to previous publications

1.- Solé, Montse, María Esteban-Lopez, Biel Taltavull, Cristina Fábregas, Rut Fadó, Núria Casals, Jose Rodríguez-Álvarez, Alfredo J. Miñano-Molina, and Mercedes Unzeta. 2019. "Blood-Brain Barrier Dysfunction Underlying Alzheimer's Disease Is Induced by an SSAO/VAP-1-Dependent Cerebrovascular Activation with Enhanced Aβ Deposition." ***Biochimica et Biophysica Acta - Molecular Basis of Disease*** **1865 (9): 2189–2202. https://doi.org/10.1016/j.bbadis.2019.04.016**

BBA - Molecular Basis of Disease 1865 (2019) 2189–2202

Contents lists available at ScienceDirect

BBA - Molecular Basis of Disease

journal homepage: www.elsevier.com/locate/bbadis

Blood-brain barrier dysfunction underlying Alzheimer's disease is induced by an SSAO/VAP-1-dependent cerebrovascular activation with enhanced Aβ deposition

Montse Solé[a,*,1], María Esteban-Lopez[a], Biel Taltavull[a], Cristina Fábregas[a], Rut Fadó[b], Núria Casals[b,c], Jose Rodríguez-Álvarez[a,d,e], Alfredo J. Miñano-Molina[a,d], Mercedes Unzeta[a,*]

[a] Biochemistry and Molecular Biology Department, Institute of Neurosciences (INc), Universitat Autònoma de Barcelona (UAB), Bellaterra, Barcelona, Spain
[b] Basic Sciences Department, Facultat de Medicina i Ciències de la Salut, Universitat Internacional de Catalunya (UIC), Sant Cugat del Vallès, Spain
[c] Centro de Investigación Biomédica en Red de Fisiopatología de la Obesidad y la Nutrición (CIBEROBN), Santiago de Compostela, Spain
[d] Centro de Investigación Biomédica en Red sobre Enfermedades Neurodegenerativas (CIBERNED), Madrid, Spain
[e] Dominick P. Purpura Department of Neuroscience, Albert Einstein College of Medicine, New York, NY 10461, USA

ARTICLE INFO

Keywords:
Alzheimer's disease (AD)
Angioneurins
Blood-brain barrier (BBB)
Neurovascular unit (NVU)
Semicarbazide-sensitive amine oxidase (SSAO/VAP-1)

ABSTRACT

Dysfunctions of the vascular system directly contribute to the onset and progression of Alzheimer's disease (AD). The blood-brain barrier (BBB) shows signs of malfunction at early stages of the disease. When Abeta peptide (Aβ) is deposited on brain vessels, it induces vascular degeneration by producing reactive oxygen species and promoting inflammation. These molecular processes are also related to an excessive SSAO/VAP-1 (semicarbazide-sensitive amine oxidase) enzymatic activity, observed in plasma and in cerebrovascular tissue of AD patients. We studied the contribution of vascular SSAO/VAP-1 to the BBB dysfunction in AD using in vitro BBB models. Our results show that SSAO/VAP-1 expression is associated to endothelial activation by altering the release of pro-inflammatory and pro-angiogenic angioneurins, most highly IL-6, IL-8 and VEGF. It is also related to a BBB structure alteration, with a decrease in tight-junction proteins such as zona occludens or claudin-5. Moreover, the BBB function reveals increased permeability and leukocyte adhesion in cells expressing SSAO/VAP-1, as well as an enhancement of the vascular Aβ deposition induced by mechanisms both dependent and independent of the enzymatic activity of SSAO/VAP-1. These results reveal an interesting role of vascular SSAO/VAP-1 in BBB dysfunction related to AD progression, opening a new window in the search of alternative therapeutic targets for fighting AD.

1. Introduction

Besides the two main pathological hallmarks of Alzheimer's disease (AD), which include extraneuronal β-amyloid (Aβ) plaques and neurofibrillary tangles, other traits are also present in AD, such as cerebral amyloid angiopathy (CAA), inflammation and cerebral hypoperfusion. Literature supports nowadays that the cerebrovasculature importantly contributes to the onset and progression of AD [1–6], postulating the existence of a strong link between vascular damage and this pathology. This link is evidenced for instance, by the fact that a high percentage of patients having suffered stroke subsequently develop AD [7], or by the increased blood-brain barrier (BBB) permeability found in mild cognitive impairment (MCI) patients [8].

Hypoperfusion/hypoxia is thought to play an important role in AD pathogenesis [9], as being responsible of vascular activation [2] and angiogenesis induction [10]. Factors responsible of angiogenesis are found upregulated in brain microvessels of AD patients [11] and in transgenic mouse models of AD [12]. However, despite the pro-angiogenic factors release observed in the AD brain, they are not correlated with increased vascularity. Therefore, no shut off feedback signals are generated, and endothelial cells become irreversibly activated [2]. AD microvessels release a wide variety of bioactive, neurotoxic and inflammatory factors promoting vascular activation and angiogenesis, including interleukins, tumor necrosis factor alpha (TNF-α), vascular

* Corresponding authors at: Biochemistry and Molecular Biology Department, Institute of Neurosciences, Universitat Autònoma de Barcelona, 08193 Bellaterra, Barcelona, Spain.
E-mail addresses: spmontse2@gmail.com (M. Solé), mercedes.unzeta@uab.es (M. Unzeta).
[1] Present address: Neurovascular Research Laboratory, Vall d'Hebron Research Institute, Universitat Autònoma de Barcelona. Passeig Vall d'Hebron, 119-129, 08035 Barcelona, Spain.

https://doi.org/10.1016/j.bbadis.2019.04.016
Received 20 November 2018; Received in revised form 3 March 2019; Accepted 26 April 2019
Available online 30 April 2019
0925-4439/

endothelial growth factor (VEGF) and matrix metalloproteinases (MMPs) [2,13]. These mediators are known as angioneurins, a terminus including angiogenic factors released at the nervous system as well as neurotrophic factors with angiogenic properties [14]. Their release has deleterious consequences for the neuronal health and brain homeostasis, affecting the neurovascular unit (NVU) function [15]. The NVU, integrated by neurons, astrocytes, brain endothelium, pericytes, vascular smooth muscle cells and microglia, constitutes a functional unit able to maintain the homeostasis of the brain's microenvironment, controlling the exchange of molecules across the BBB, regulating blood flow, supplying trophic support and maintaining the immune surveillance of brain cells [16]. Therefore, the study of neurovascular crosstalk and its alterations is important to understand the molecular basis of AD.

BBB dysfunction associated to the AD pathogenesis has been shown in transgenic mouse models, in which BBB integrity is already compromised before developing amyloid plaques and cognitive impairment [17,18]. Oxidative stress is also increased in brain blood vessels in the APP23 mouse model before the emergence of amyloid plaques or CAA [19], which may contribute to this loss of the BBB integrity, but also to the vascular activation itself. Among different reactive oxygen species, hydrogen peroxide (H_2O_2) is one of the most important endothelium-derived modulators of vascular function involved in the AD pathophysiology, as it is able to interact with multiple signaling systems [20]. In the same line, the BBB in AD seems to be more vulnerable to inflammation, becoming leaky in AD brains of transgenic mouse models and therefore allowing peripheral inflammation spreading into the brain [21]. Thus, a cerebrovascular system dysfunction displaying angioneurins release, oxidative stress, inflammation and BBB leakage seems to be strongly related with the AD pathogenesis, and prompts to a pharmacological intervention aimed to reduce vascular activation in order to improve cognitive function underlying this pathology [15,22]. However, the molecular mechanisms responsible of these vascular alterations, and therefore, the potential therapeutic targets, are still not well established.

In this regard, the increased overexpression of the vascular-adhesion protein (VAP-1), a homodimeric glycoprotein with semicarbazide-sensitive amine oxidase (SSAO, E.C 1.4.3.21) enzymatic activity, found in cerebrovascular tissue of AD patients, may turn it into a good candidate.

SSAO/VAP-1 appears overexpressed in cerebrovasculature from AD patients [23], and released into blood plasma in AD [24], cerebral ischemia [25–27] and other pathologies displaying inflammation [28–30]. As an enzyme, it generates H_2O_2, aldehydes and ammonia as metabolic products, which are able to induce cellular damage when overproduced [31,32], but it is also able to modulate the expression of other adhesion molecules [33,34] and to enhance Aβ aggregation [35,36]. SSAO/VAP-1 behaves also as an adhesion protein, binding leukocytes through its enzymatic activity [37,38], and allowing their infiltration through the BBB into the brain parenchyma, enhancing cell damage and brain inflammation. Therefore, it is believed that the increased SSAO/VAP-1 levels may contribute to the physiopathology of these diseases, and specifically of AD.

In the context of AD pathology, the main objectives of this study were to assess whether the overexpression and/or activity of SSAO/VAP-1 in human microvascular brain endothelial cells are involved in endothelial activation, through the modification of angioneurins release, altering the BBB function, hence elucidating the role of SSAO/VAP-1 in the BBB dysfunction. Furthermore, we decided to confirm whether SSAO/VAP-1 is able to modify vascular Aβ deposition, altering BBB permeability and leukocyte adhesion using a NVU experimental model.

2. Materials and methods

If not otherwise indicated, reagents were purchased from Sigma Aldrich, Madrid, Spain.

2.1. Cell lines

The hCMEC/D3 cell line (human cerebral microvascular endothelial cells) was obtained from Dr. Couraud's laboratory in Paris, France [39,40]. The hCMEC/D3 cell line expressing human SSAO/VAP-1 (hCMEC/D3 hSSAO/VAP-1) was generated as described previously [41]. Considering that the proportion of vessels in brain is around 1% [42], this cell line shows SSAO/VAP-1 activity levels comparable to those observed in human brain tissue [26,41]. By contrast, non-transfected wild type (WT) hCMEC/D3 cells do not express SSAO/VAP-1, as previously demonstrated [41]. The hCMEC/D3 cells were cultured as recommended, on 150 μg/mL collagen type 1 (Rat Tail, Corning, NY, USA)-coated plates in EBM-2 (Lonza, Barcelona, Spain) medium supplemented with 5% FBS (Fetal Bovine Serum, Life Technologies, Madrid, Spain), 1.4 μM Hydrocortisone, 5 μg/mL Ascorbic Acid, 1% Chemically Defined Lipid Concentrate (Life Technologies, Madrid, Spain), 1 mM HEPES (Life Technologies, Madrid, Spain) and 1 ng/mL human bFGF (Fibroblast Growth Factor-basic), 100 U/mL penicillin and 100 μg/mL streptomycin. Cells expressing hSSAO/VAP-1 were maintained in media containing 100 μg/mL geneticin (G418, Life Technologies, Madrid, Spain) to ensure DNA maintenance. THP-1 monocytic cells were obtained from the American Type Culture Collection (ATCC, Barcelona, Spain) and grown in RPMI 1640 medium (Life Technologies) supplemented with 10% FBS. All cells were maintained at 37 °C, in a humidified atmosphere containing 5% CO_2.

2.2. BBB - neurovascular unit model

To mimic a NVU environment, hCMEC/D3 cells were co-cultured with mouse mixed neuron-glia primary cultures. hCMEC/D3 cells were seeded at 2×10^5 cells/mL in collagen and fibronectin-coated 12-well Transwell inserts (Transwell polyester membrane inserts, pore size 0.4 μM, Corning, NY, USA) and allowed to grow for 3 days in vitro (DIV). At 3th DIV, hCMEC/D3 were starved in FBS, ascorbic acid and bFGF-free EBM-2 media. At 4th DIV, endothelial cells were put in co-culture by joining hCMEC/D3-containing inserts with 12-well plates containing 12th DIV neuron-glia cultures. Mouse mixed neuron-glia primary cultures were performed as described in [43], with some modifications: E14.5–15.5 C57BL/6 mice were used; cells were seeded on poly-D-lysine-coated plates in BME media (Invitrogen) supplemented with 5% horse serum (HS), 5% FBS, 10 mM glucose and 2 mM Glutamax; at 7 DIV, media was changed by BME supplemented with 10% HS and 10 μM cytosine arabinoside; at 12 DIV, half of the media was changed by BME with 5% HS. After 1 DIV in co-culture, endothelial cells were treated according to each type of experiment.

2.3. Cell treatments

For conditioned media treatments, media from WT and SSAO/VAP-1-expressing cells were collected after 4 days in culture under starvation conditions. This media was used to treat endothelial cells: at day 1, media from each cell type was completely changed by conditioned media from the other cell type (i.e. media from WT cells was added to hSSAO/VAP-1-expressing cells); then, half of this media was replaced by new conditioned media each 24 h until day 4.

For treatment with compounds or blocking antibodies, cells were starved for 24 h and then treatments were added. SSAO inhibitors semicarbazide (Sc), BTT 2079 and BTT 2089 were added 30 min before SSAO substrate (methylamine, MA) addition, and AβD ($Aβ_{1–40}$ peptide containing the Dutch mutation, Bachem AG, Hauptstrasse, Switzerland) was introduced 15 min after MA. Specific SSAO inhibitors BTT 2079 and BTT 2089 were provided by Dr. Smith (Biotie Therapies, Turku, Finland). Aβ was pretreated with 1,1,1,3,3,3-hexa-fluoro-2-propanol (HFIP), aliquoted, evaporated and stored at −80 °C until its use, being then dissolved in sterile phosphate-buffered saline (PBS) containing 0.1% ammonium hydroxide. Anti interleukin 6 blocking antibody (IL-6;

MAB206-100, R&D Systems, Minneapolis, USA) or a control antibody (MAB002, R&D Systems) were added at 5 μg/μL for 48 h.

2.4. Luminex assays

Media to analyze the different angioneurins of interest were obtained from inserts containing non-treated hCMEC/D3 endothelial cells expressing or not the hSSAO/VAP-1 (hSSAO/VAP-1 hCMEC/D3 vs wild type – WT cells), after 3 days of co-culture with mixed cultures. Media were kept aliquoted at −80 °C until used. Magnetic milliplex kits (Merck-Millipore, Madrid, Spain) containing detection antibodies for the following molecules were used: vascular endothelial growth factor 1 (VEGF-1); interleukins 1β, 6 and 8 (IL-1β, IL-6, IL-8); tumor necrosis factor alpha (TNF-α); fibroblast growth factor 2 (FGF-2); soluble vascular cell adhesion molecule 1 (sVCAM-1); soluble inducible cell adhesion molecule 1 (sICAM-1); nerve growth factor (NGF); E and P-selectins (E-sel, P-sel), transforming growth factor beta 1 (TGF-β1) and insulin growth factor 1 (IGF-1). Angioneurins were detected by Milliplex MAP Human Magnetic Bead Panels following the manufacturer instructions. Quantification was performed with a Magpix analytical test instrument xPONENT (Luminex, Austin, TX, USA) and xPONENT 4.2 software (Luminex), with support of the technical staff in the INc (Neurosciences Institute, UAB, Barcelona).

2.5. Western blot analysis

Equal amounts of protein (20 μg per lane), determined by the Bradford method (Bio-Rad, Barcelona, Spain) were separated by SDS-PAGE and transferred onto nitrocellulose membranes. For Aβ detection, 12% bistris/bicine polyacrylamide gels were used as previously described [44] and proteins were transferred onto polyvinylidene fluoride membranes (PVDF; GE Healthcare, Barcelona, Spain). After blocking with tris-buffered saline with 0.1% Triton X-100 (TBST) plus 5% non-fat dry milk (10% non-fat dry milk and 0.1% bovine serum albumin for Aβ gels) for 1 h, they were incubated overnight at 4 °C with the corresponding primary antibody: VCAM-1 (1:000) (3540-S; Epitomics, Burlingame, CA, USA); ICAM-1 (1:1000) (GTX100-450; GeneTex, Barcelona, Spain); Zona Occludens 1 (ZO-1, 1:1000) (40-2200; Life Technologies); Glyceraldehyde 3-phosphate dehydrogenase (GAPDH, 1:20,000) (ADI-CSA-335; Enzo Life Sciences, New York, NT, USA); Claudin-5 (1:500) (sc-374221; Santa Cruz Biotechnology, Dallas, TX USA); VE-Cadherin (1:500) (sc-9989; Santa Cruz Biotechnology); Signal transducer and activator of transcription 3 (STAT3, 1:1000) (sc-8019; Santa Cruz Biotechnology); phospho-STAT3 (p-STAT3, 1:1000) (sc-8059; Santa Cruz Biotechnology); Matrix Metalloproteinase 2 (MMP-2, 1:1000) (ab37150; Abcam, Bristol, UK); Matrix Metalloproteinase 9 (MMP-9, 1:1000) (ab7299; Abcam); Tissue Inhibitor of Metalloproteinases (TIMP-1, 1:2000) (ab38978; Abcam); Low density lipoprotein receptor-related protein 1 (LRP-1, 1:10,000) (2703-S; Epitomics); VEGF Receptor 2 (VEGFR2, 1:1000) (1672479S; Cell Signaling Technology, Danvers, MA, USA); phospho-VEGFR2 (pVEGFR2, 1:1000) (1674991T; Cell Signaling Technology); Cleaved Caspase-3 (1:1000) (9661; Cell Signaling Technology); Bax (1:1000) (2772; Cell Signaling Technology); Bcl-2 (1:1000) (610538; BD Biosciences, San Jose, CA, USA); Amyloid precursor protein (APP, 1:1000) (antibody generated by the 20.1 hybrydoma cell line, a kind gift from Dr. W.E. Van Nostrand, NY USA); SSAO (1:1000) [45]; beta actin (β-actin, 1:10,000) (A1978; Sigma). Secondary HRP (horseradish peroxidase)-conjugated antibodies used were anti-mouse IgG (1:2000) (P0161; Dako, Madrid, Spain) and anti-rabbit IgG (1:2000) (554021; BD Biosciences). Blots were developed using ECL® Chemiluminiscent detection reagents and High Performance Chemiluminiscence Films (GE Healthcare). The ImageJ software (National Institutes of Health, USA) was used to quantify the Western blot signals.

2.6. Immunocytofluorescence

Cells were grown on collagen-I-coated glass coverslips and fixed in methanol-acetic acid (3:1) at −20 °C for 20 min at the indicated times after reaching confluence. After permeabilization with PBS containing 0.2% Triton X-100 (PBST) for 30 min, cells were blocked with PBST containing 0.2% gelatin, 20 mM glycine and 5% FBS for 20 min. Then, cells were incubated with primary antibodies (ZO-1, 1:100, 1874–30, Life Technologies; APP, 1:500) in blocking solution with 3% FBS overnight at 4 °C with the addition of 30 min at room temperature. After washing with PBS, secondary antibody (Alexa Fluor 568 goat anti-rabbit IgG, 1:1000, Life Technologies) was added in the same buffer as the primary antibody for 1 h at room temperature, and cell nuclei were contrasted with Hoechst 33258 (1:1000). Coverslips were mounted on slides with Mowiol mounting media. Images were taken using the Zeiss LSM700 confocal microscope at the microscopy facility of the INc in UAB.

2.7. Cell viability

For the determination of cell viability by 3-(4,5-dimethylthiazol-2-yl)2,5-diphenyl-tetrazolium bromide (MTT) reduction assay, MTT solution (0.5 mg/mL, final concentration) was added to the cells 1 h before the end of treatments. The medium was then replaced by dimethyl sulfoxide to dissolve the formazan blue precipitate formed, which was quantified at 560 and 620 nm in a microplate reader (Synergy HT and data analysis software KC4, Bio-Tek Instruments Inc., Winooski, VT, USA).

For the Lactate-deshidrogenase (LDH) activity assay, TOX-7 (Sigma-Aldrich) kit was used following manufacturer's instructions. Seventy-five μL of media from each well was used for the assay, performed in 96-well plates, and incubated for 1 h in the dark with LDH assay mixture. Then, absorbance was read at 490 nm, and it was subtracted the value of reading the plate at 690 nm.

2.8. Dextran assay for cell permeability determination

After 3 days of co-culture with mixed cultures or the corresponding treatments, 500 μL of DMEM medium (Invitrogen, Madrid, Spain) containing 2 mg/mL 70 kDa Fluorescein isothiocyanate-dextran were added replacing the insert culture media. The permeable filter inserts were then changed to 12-well plates containing pre-warmed DMEM and sequentially transported to new wells at 5 min intervals for 30 min. Cells were maintained at 37 °C during the process. At the end, the fluorescence of each well (lower chamber of the inserts) was measured (485 nm and 520 nm ex/em) and apparent permeability coefficients (Pe; cm/s) were calculated from curves slopes (fitted using linear regression) obtained by plotting cumulative volume cleared against time, for all experimental conditions. Non-treated cells (NT), or WT cells for comparing basal conditions were used as controls, and differences in permeability coefficients were expressed as % of control.

2.9. Transendothelial electrical resistance

Transendothelial electrical resistance (TEER) of endothelial cells seeded on inserts was measured at 0, 6, 24, 48 and 72 h after the co-culture establishment with mixed cultures. TEER measurements were recorded using a STX2 probe with EVOM2 (World Precision Instruments, Sarasota, USA). In each experiment, the average of three different readings was used for each insert.

2.10. Adhesion assays

For adhesion assays, hCMEC/D3 cells were seeded on 24-well plates. THP-1 monocytes were labelled with 1 μM Calcein-AM for 30 min, and then added to endothelial cells (2.5×10^5 THP-1 cells per

well). After 30 min incubation at 37 °C, unbound monocytes were removed by turning over the plates onto absorbent paper, carefully adding FBS-free RPMI 1640 medium to the plates with an auto-pipette, and repeating the washing for three times. The fluorescence intensity was measured using a microplate reader ($\lambda_{ex}/\lambda_{em}$: 495/530 nm) (Synergy HT and data analysis software KC4; Bio-Tek Instruments Inc.). Micrographs were taken using a Nikon Eclipse TE 2000-E inverted fluorescence microscope and a Hamamatsu C-4742-80-12AG camera and Metamorph® Imaging System software.

2.11. MMPs activity

For the measurement of MMP-2 and MMP-9 activity, it was used the fluorimetric assay SensoLyte ® 520 MMP-2 Assay Kit (Anaspec, AS-71151), according to the manufacturer's instructions. Briefly, cells were lysed in the recommended buffer and kept at −80 °C until their use. First, dose and time curves were performed to determine the best conditions for the incubation with the substrate. Then, equal amounts of protein were incubated at 37 °C for 90 min and the cleavage of a FRET peptide that releases the fluorescent 5-FAM from its quencher QXL520 was measured at ex/em 490/520 nm with the fluorescence microplate reader. The concentration of this substrate for each sample was obtained by interpolation into a reference standard concentration curve. Data were normalized for each experiment to the values obtained in the WT cells and presented as percentage of change in MMPs activity versus WT cells.

2.12. Statistical analysis

Results are given as mean ± SEM of independent experiments. Statistical analyses were performed by one-way ANOVA tests followed by a Newman-Keuls or Bonferroni multiple comparison tests when comparing > 2 conditions; statistical differences between 2 conditions were evaluated by unpaired Student's *t*-test. A two-way ANOVA test was performed when the influence of 2 independent variables on one independent variable were analyzed. A $p < 0.05$ was considered to be statistically significant, according to the following significance levels: $^{***}p < 0.001$, $^{**}p < 0.01$ and $^{*}p < 0.05$. Statistical analyses and graphic representations were obtained with Graph-Pad Prism 6.0 software (San Diego, CA, USA).

3. Results

3.1. The expression of SSAO/VAP-1 induces brain endothelial activation towards a pro-inflammatory phenotype

Previous work in our laboratory showed that an increase in SSAO/VAP-1 was related to endothelial dysfunction and AD [36,46]. In one hand human umbilical vein endothelial cells (HUVECs) expressing SSAO/VAP-1 showed enhanced cell toxicity in the presence of Aβ in vitro [36], while on the other hand, we observed increased SSAO/VAP-1 in brain vessels from AD patients [46]. Thus, in the present work we decided to study whether the expression of SSAO/VAP-1 in human brain endothelial cells was able to alter the release of a group of angioneurins that have been associated to AD or to endothelial dysfunction throughout bibliography (Table 1). Their basal release was quantified in culture media obtained from human cerebral microvascular endothelial cells expressing or not the hSSAO/VAP-1 [41], after being co-cultured with neuron-glia mixed cultures to generate a NVU environment (Fig. 1).

Results showed that the release of trophic factors VEGF, TGFβ-1 and NGF is significantly higher in endothelial cells expressing hSSAO/VAP-1, while they display a non-significant reduced trend to release FGF-2 compared to WT cells, that do not express the protein (Fig. 1A). No changes were detected in IGF-1, whose levels were similar to those measured in cell culture media (Fig. 1A and Suppl Fig. 1). On the other hand, regarding the release of molecules related with inflammatory processes, it was observed that cells expressing hSSAO/VAP-1 release significantly higher amounts of IL-6 and IL-8 (Fig. 1B). IL-1β and TNF-α were also analyzed but they were not detected. Moreover, hSSAO/VAP-1-expressing cells release significantly higher levels of the soluble form of the adhesion protein VCAM1 (sVCAM-1) (Fig. 1C). A trend in the same line was observed in case of soluble ICAM-1 (sICAM-1), and E and P-selectins were not detected. The membrane-bound forms of both VCAM-1 and ICAM-1 are significantly increased in cells expressing hSSAO/VAP-1 as well (Fig. 1D). Similar results were obtained in angioneurins released from endothelial cells without being co-cultured with neuron-glia mixed cultures (data not shown) suggesting that changes in angioneurins release induced by SSAO/VAP-1 expression is cell autonomous, and not influenced by the neurovascular context. Treatments with MA and/or AβD did not induce significant changes compared to the basal levels in each cell type (Suppl Fig. 1).

3.2. Human brain endothelial cells expressing hSSAO/VAP-1 show increased basal blood-brain barrier permeability

An endothelial pro-inflammatory phenotype may be associated to the alteration of the BBB permeability in order to allow the pass of peripheral inflammatory cells through the barrier [74]. As our cells showed an increased release of pro-inflammatory angioneurins, when BBB function of endothelial cells expressing hSSAO/VAP-1 was studied, it was observed that they show an increased basal permeability to 70 kDa Dextran (Fig. 2A), as well as decreased TEER (Ω/cm^2) throughout time (Fig. 2B). A two-way ANOVA of time and genotype (WT or hSSAO/VAP-1) on TEER revealed significant main effect of time [$F(4, 20) = 2.936$, $p < 0.05^{*}$] and genotype [$F(1, 20) = 10.96$, $p < 0.01^{**}$], with non-significant time x genotype interaction [$F(4, 20) = 1.268$, $p = 0.32$]. In addition, hSSAO/VAP-1-expressing endothelial cells display an increased ability to bind leukocytes compared to WT cells, as indicated by a significantly higher THP-1 adhesion in basal conditions (Fig. 2C). These functional alterations may be related to the decreased expression of the tight junction-related proteins ZO-1 and claudin-5 (Fig. 2D), and the adherens junction-related protein VE-cadherin (Fig. 2E) in endothelial cells expressing hSSAO/VAP-1. In the same line, immunofluorescence images obtained by confocal microscopy of ZO-1 (red) revealed a ZO-1 location compatible with that of tight junctions only in WT cells, while it was completely delocalized in hSSAO/VAP-1-expressing cells, analyzed at different time points (Fig. 2F). Matrix MMP-2 and MMP-9, proteins involved in extracellular matrix stability and degradation in inflammatory conditions, were also evaluated. MMP-2 protein was increased in hSSAO/VAP-1 cells, while MMP-9 was not changed between both cell types (Suppl Fig. 2A). However, the overall gelatinase activity levels were higher in WT cells (Suppl Fig. 2B), which could be explained by an increase of the endogenous MMP inhibitor TIMP-1 in hSSAO/VAP-1-expressing cells (Suppl Fig. 2C).

3.3. The angioneurins secreted by hSSAO/VAP-1-expressing human brain endothelial cells are able to activate their own signaling pathways and contribute to disturbing BBB functions

Next, we aimed to determine whether the higher levels of the angioneurins released by hSSAO/VAP-1-expressing cells are able to induce changes in endothelial cell signaling, and therefore could be responsible of the functional alterations found in these cells. To this end, we analyzed the basal activation status of the molecular pathways activated by VEGF, IL-8 and IL-6 related to BBB permeability, as they showed the greatest increases in hSSAO/VAP-1-expressing cells (see Fig. 1). Because it has been reported that IL-8-induced endothelial permeability requires the transactivation of VEGFR-2 through the IL-8 receptor CXCL8 activation [54], both VEGF and IL-8 action on BBB were studied by determining the VEGFR2 phosphorylation levels at

Table 1
Angioneurins released by endothelial cells, neurons and glia, selected as candidates tested in our study due to their potential involvement in AD. All cell types (endothelial cells, ECs; neurons and glia, N + G) express receptors for all the angioneurins listed in the table. "+++" means that the molecule is mostly expressed by this cell/s type/s over the other/s, while "+" means that is expressed at lower levels and "−" means that no expression has been found.

	EXPRESSION		Functions in AD		Described in	References
	ECs	N + G	ECs	N + G	AD patients	
VEGF (Vascular endothelial growth factor)	+++	+	Angiogenesis, vascular permeability and dilation, cell migration, proliferation, differentiation and survival	Neurogenesis, neuronal and glial survival, neuronal proliferation, neuronal and glial migration, axon growth and dendritic arborization	Increased in CSF	[1,14,47,48]
TGF-β (Transforming growth factor)	+	+++	Angiogenesis, VEGF induction and maintenance of the BBB integrity	Neuroprotection, glial scar and microglia activation	Increased in plasma and CSF. Decreased in serum	[1,14,47,49,50]
NGF/pro-NGF (Nerve growth factor)	+	+++	Angiogenesis, cell survival, proliferation, migration and VEGF induction	Neuroprotection, neuronal survival	Increased in serum and CSF	[14,47]
FGF-2 (Fibroblast growth factor)	+	+	Angiogenesis, cell proliferation, VEGF induction and maintenance of the BBB integrity	Neuroprotection, neuronal survival, synaptic stimulation and glial differentiation	Not changed	[14,47]
IGF-1 (Insulin like growth factor)	+	+	Angiogenesis, survival, migration, proliferation and inflammatory responses	Neuronal/glial growth and survival, neuronal differentiation, migration, cytoskeletal assembly, synaptic formations and myelinic production/maintenance	Increased in plasma	[14,47,51,52]
TNF-α (Tumor Necrosis Factor)	+	+++	Blood vessels remodeling, adhesion molecules and cytokines induction	Neurotoxicity, dysregulation of synaptic transmission, inhibition of synaptic plasticity, and microglia activation	Increased in plasma/serum and CSF	[1,14,47,50,53]
IL-6 (Interleukin 6)	+	+	Angiogenesis, adhesion molecules upregulation	Neurogenesis, neuroprotection, gliogenesis, neuronal and glial differentiation and proliferation.	Increased in plasma/serum and CSF	[1,47,50,53]
IL-8 (Interleukin 8)	+	+	Unknown	Unknown	Increased in plasma/serum	[1,53,54]
IL-1β (Interleukin 1β)	+	+++	IL-6 and TNF-α induction, early initiation of the inflammatory response, adhesion molecules upregulation	IL-6 and TNF-α induction, neuroinflammation, neurotoxicity, microglia and astrocyte activation and differentiation	Increased in plasma/serum	[1,47,50,53,55]
ICAM-1/CD54 (intercellular adhesion molecule)	+	−[a]	Angiogenesis, proinflammatory cytokines induction, transendothelial migration of leukocytes	Proinflammatory cytokines induction	Increased in plasma/serum	[47,56,57,58]
VCAM-1/CD106 (vascular cell adhesion molecule)	+	−[a]	Inhibition of cell extravasation, alteration of TJs morphology	Proinflammatory cytokines induction	Increased in plasma	[47,58,59,60]
ELAM-1/CD62E or *E*-selectin (endothelial leucocyte adhesion molecule)	+	−	Chronic inflammation	Unknown	Not changed	[47,58,61]
LRP-1 (low density lipoprotein receptor-related protein 1)	++	++	Efflux of brain Aβ, opening of BBB, MMPs induction	Cell signaling, calcium entrance regulation, Aβ production and clearance	Decreased (controversy)	[62–68]
RAGE (receptor for advanced glycation endproducts)	++	+	Influx of Aβ into brain, oxidative stress, increase of proinflammatory cytokines	Oxidative stress and inflammation, Ab production increase, neurotoxicity and synaptic loss	Increased in brain tissue	[69–72]

[a] Some authors found VCAM-1 and ICAM-1 expression in neurons [73], but there is no recent data about it.

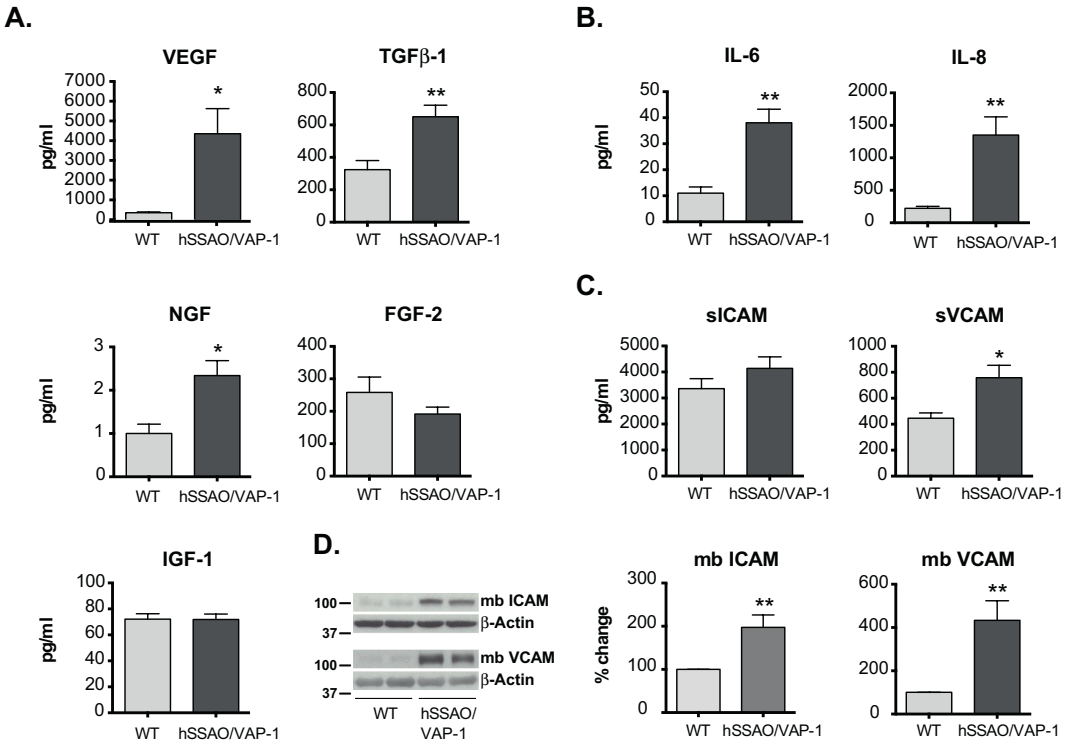

Fig. 1. The secretion of angioneurins is altered in hSSAO/VAP-1-expressing hCMEC/D3 cells. (A) Levels of trophic factors VEGF, TGFβ-1, NGF, FGF-2 and IGF-1, (B) pro-inflammatory interleukins IL-6 and IL-8, and (C) soluble vascular adhesion proteins sICAM and sVCAM quantified by Luminex in the media of WT and hSSAO/VAP-1-expressing hCMEC/D3 cells co-cultured for 3 days with mouse brain mixed primary cultures. (D) Membrane-bound forms of VCAM-1 and ICAM-1 determined by Western blot in cell lysates after 3 days in confluence. Beta actin was used as loading control. Data is expressed as mean ± SEM of quantifications (pg/mL) in A-C, or of percentage change vs WT in D, obtained from at least 4 independent experiments. $^{*}p < 0.05$, $^{**}p < 0.01$.

tyrosine 951, a major autophosphorylation site located in the kinase insert domain, indicator of receptor activation [75] and related with vascular permeability [76]. Results revealed almost no VEGFR2 phosphorylation in WT endothelial cells (Fig. 3A). Surprisingly, VEGFR2 expression was drastically reduced in hSSAO/VAP-1-expressing cells. On the other hand, IL-6 action was evidenced by the activation of the STAT3 pathway, since increased levels of pSTAT3 were observed in hSSAO/VAP-1-expressing cells compared to WT cells (Fig. 3B).

To confirm the involvement of these over-released angioneurins in the activation of these molecular pathways, it was collected conditioned media from WT and hSSAO/VAP-1-expressing endothelial cells after 4 days in culture. Then, WT cells were treated for 4 days in the presence of hSSAO/VAP-1 conditioned media, and hSSAO/VAP-1-expressing cells were cultured in WT-conditioned media. During the treatments, half of the media was replaced by new conditioned media every 24 h to maintain the levels of angioneurins similar to those of the conditioned medias. Results showed that media from hSSAO/VAP-1 cells induces a decrease in VEGFR2 expression (Fig. 3C) and an increase in pSTAT3 levels in WT cells (Fig. 3D). However, media from WT cells is not able to restore VEGFR2 expression or to decrease STAT3 activation levels.

Then, to explore whether the differential release of angioneurins observed in both cells is the responsible of the BBB disturbances detected in hSSAO/VAP-1-expressing cells, tight junction proteins were determined by Western blot after treatments with conditioned media (Fig. 3E). In line with that previously observed, WT cells treated with hSSAO/VAP-1-conditioned media showed a decreased amount of claudin-5, while WT-conditioned media in hSSAO/VAP-1-expressing cells did not modify its expression. Surprisingly, neither ZO-1, nor VE-cadherin amounts were modified in WT or in hSSAO/VAP-1-expressing cells by conditioned media treatments (Suppl Fig. 3). Permeability to 70-kDa dextran was also determined in cells after treatment with conditioned media as a BBB functional parameter (Fig. 3F). Results showed a small increase in Pe in WT cells treated with hSSAO/VAP-1-conditioned media, but not reaching the high Pe values observed in hSSAO/VAP-1-expressing cells in basal conditions. In addition, IL-6 blocking antibody prevented this Pe increase induced by hSSAO/VAP-1 conditioned media on WT cells. Again, no changes were observed in hSSAO/VAP-1-expressing cells in the presence of WT-conditioned media. To confirm the STAT3 pathway modulation by conditioned media from hSSAO/VAP-1 cells, STAT3 phosphorylation was evaluated by Western blot after conditioned media and IL-6 blocking antibody treatments (Fig. 3G). Results confirmed the increase of pSTAT3 in WT cells treated with hSSAO/VAP-1-conditioned media, and its prevention by the blocking of IL-6 as well as the decrease of pSTAT3 in hSSAO/VAP-1 cells treated with the IL-6 blocking antibody. The control antibody did not induce any change in Pe or STAT3 phosphorylation.

3.4. Endothelial cells expressing hSSAO/VAP-1 show a positive feedback loop with AβD, enhancing its vascular deposition and inducing BBB function alterations and cytotoxicity

Alterations observed in BBB between WT and hSSAO/VAP-1-expressing cells were only partially explained by the differential release of proteins from both endothelial cells. Thus, we then explored other possible alterations in BBB affected by the presence of SSAO/VAP-1, focused on the AD context. Mainly $A\beta_{40}$ is deposited on cerebral blood vessels inducing Cerebral Amyloid Angiopathy (CAA), although $A\beta_{42}$ can be also deposited in small capillaries [77,78]. Endothelial cells were therefore first treated with $A\beta_{40}$ containing the Dutch mutation (AβD), a vasculotropic form of Aβ, and its deposition on endothelial cells was measured. It was observed by Western blot that higher amounts of AβD were deposited on endothelial cells expressing hSSAO/VAP-1 (Fig. 4A). To explore whether this AβD deposition was dependent on SSAO/VAP-

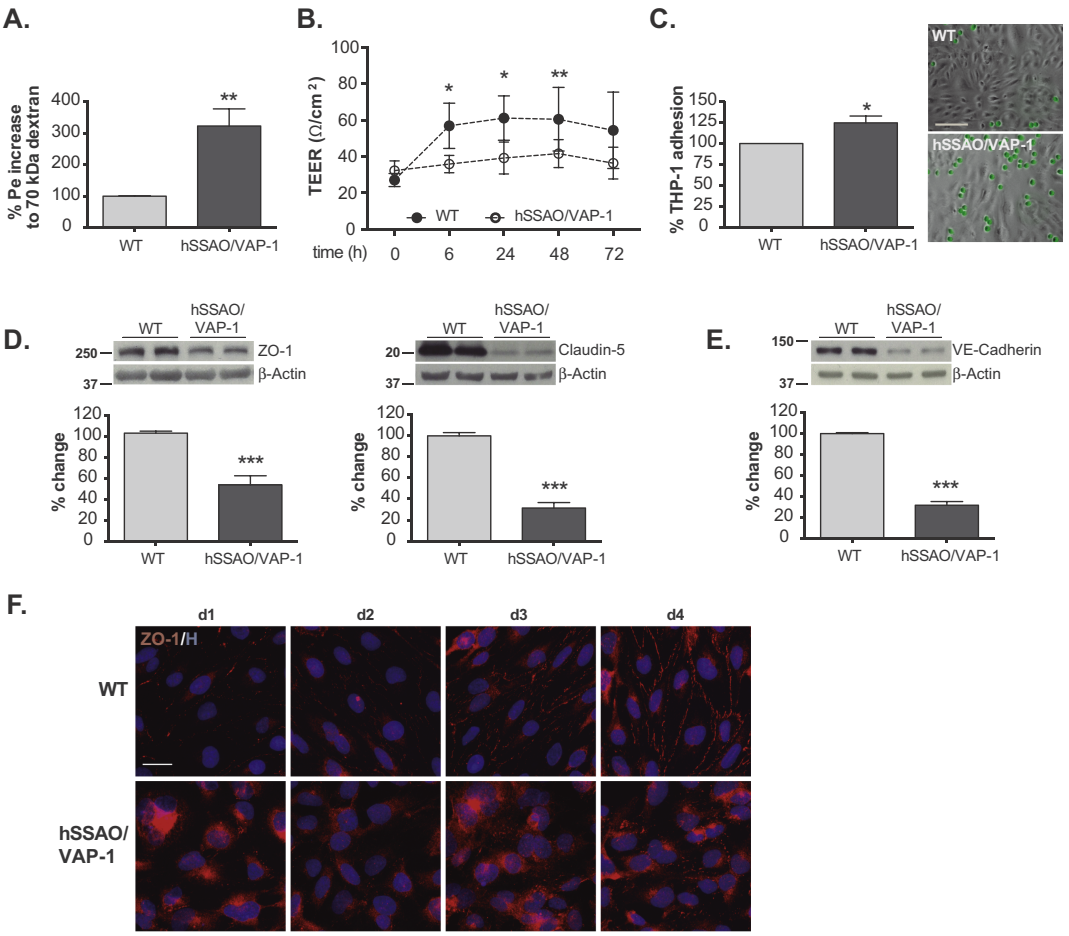

Fig. 2. hSSAO/VAP-1-expressing hCMEC/D3 cells display an increased basal BBB permeability and leukocyte adhesion. (A) BBB functionality analyzed by trans-cellular permeability assay measuring the crossing of 70 kDa FITC-Dextran through transwell-seeded endothelial cell monolayers co-cultured for 3 days with mouse brain primary cultures, and (B) TEER measured by an EVOM2 epithelial voltohmmeter in the same cells at different times (0, 6, 24, 48 and 72 h) from the co-culture beginning. Data are expressed as mean ± SEM of percentage in permeability increase and Ω/cm^2, respectively, from at least 3 independent experiments. (C) Basal endothelial inflammatory function by leukocyte-adhesion assay using Calcein-AM-labelled THP1 leukocytes in WT and hSSAO/VAP-1-expressing cells. Representative images show THP1 leukocytes (green) adhesion on endothelial cell monolayers. Scale bar: 100 μM. (D) BBB structure of hCMEC/D3 cells after 3 days confluence in culture, studied by Western blot determination of the tight junctions-related proteins ZO-1 and claudin 5, and (E) the adherens junctions-related protein VE-cadherin levels. Results are expressed as mean ± SEM of at least 3 independent experiments. Beta-actin was used as loading control. Representative images are shown for each graph. (F) ZO-1 cell distribution determined by immunofluorescence and confocal microscopy at days 1, 2, 3 and 4 post-confluence; ZO-1, red; Hoechst (H), blue. Scale bar: 20 μM. $*p < 0.05$, $**p < 0.01$ and $***p < 0.001$. In B, * indicates differences vs time 0.

1 enzymatic activity, the same experiment was performed adding MA as SSAO substrate, and BTT 2079 as SSAO specific inhibitor. Results showed that, besides the higher deposition on cells expressing hSSAO/VAP-1, AβD deposition was also enhanced in the presence of MA only in hSSAO/VAP-1-expressing cells (Fig. 4B). The addition of the SSAO inhibitor BTT 2079 restored AβD deposition levels to the basal ones in these cells, while neither MA, nor inhibitor addition modified AβD deposition on WT cells. This effect was confirmed by immunofluorescence analysis (Fig. 4C). Same experiments were performed using $Aβ_{42}$, but no significant differences in $Aβ_{42}$ deposition were found between WT and hSSAO/VAP-1-expressing cells and only a trend was observed among different treatments (Suppl Fig. 4A). To explore possible differences in other proteins involved in Aβ processing or transport, the basal levels of APP, receptor for advanced glycation end-products (RAGE) and LRP-1 were determined (Suppl Fig. 4B). While APP and RAGE were not different between WT and hSSAO/VAP-1 cells, LRP-1 was highly expressed by the latter, although treatments with MA and/or AbD did not induce significant changes of LRP-1 in any of the cell types (Suppl Fig. 4C).

On the other hand, it was also studied a possible effect of AβD presence on SSAO/VAP-1 enzymatic activity and protein levels. AβD treatment of hSSAO/VAP-1-expressing cells induced an increase in the SSAO enzymatic activity (Fig. 4D), which was not significant at the protein levels (Fig. 4E). Similar results were observed with $Aβ_{42}$, but at lower concentrations compared to AβD (Suppl Fig. 4D–E).

Then, BBB function was first explored by Pe determination in WT and hSSAO/VAP-1-expressing endothelial cells treated with MA, AβD and BTT. Besides the basal higher Pe already observed in hSSAO/VAP-1-expressing cells compared to WT cells, AβD but not MA induced a significant Pe increase in hSSAO/VAP-1-expressing cells (Fig. 5A). The addition of the specific SSAO inhibitor BTT 2079 tended to decrease Pe, but this effect was not statistically significant. Interestingly, Pe was not modified in WT cells by any of these treatments. The leukocyte adhesion was also measured under same conditions (Fig. 5B,C). Both MA and AβD treatments induced an increase in leukocyte adhesion to hSSAO/VAP-1-expressing cells, an effect that was enhanced by the co-treatment with both compounds. The presence of each of two different SSAO specific inhibitors, BTT 2019 and BTT 2089, was able to partially reduce leukocyte adhesion. In WT cells, all treatments containing AβD increased leukocyte adhesion with no differences by the addition of MA or SSAO inhibitors.

In addition to these functional disturbances of the BBB, the

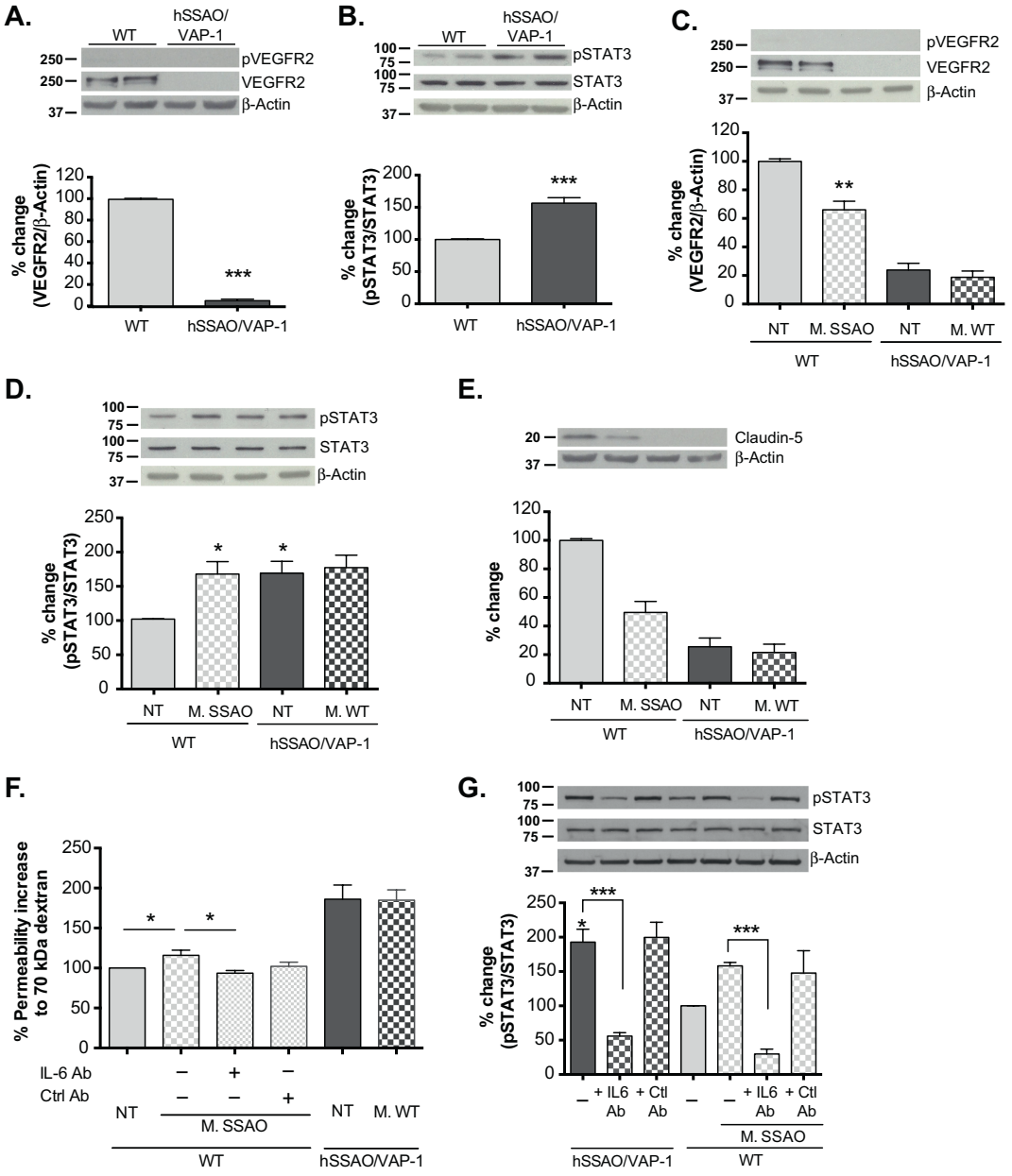

Fig. 3. Secreted angioneurins alter VEGF and IL-6 signaling pathways and contribute to the BBB leakage. (A) Basal activation status of IL-8/VEGF and (B) IL-6 molecular pathways through pVEGFR2/VEGFR2 and pSTAT3/STAT3 determination by Western blot. For VEGFR2, only the total form was quantified and represented in the graphs, as its phosphorylation form was almost non-detected. Beta actin and the total form of STAT3 were used as loading controls. (C) Effect of 4 days-conditioned media from WT and hSSAO/VAP-1-expressing cells on VEGFR2 and (D) STAT3 activation in hSSAO/VAP-1 and WT cells, respectively, analyzed by Western blot. Initial media was changed by conditioned media at day 1, and half of this media was replaced by new conditioned media each 24 h until day 4. (E) Effects of conditioned media on the tight junction protein claudin-5, analyzed by Western blot. (F) Permeability to 70 kDa FITC-Dextran of the endothelial cell monolayers in presence of conditioned media and IL-6 blocking or control antibodies (added at 5 μg/mL). (G) Effect of IL-6 blocking antibody or a control antibody on the phosphorylation status of STAT3. Data in graphs is represented as mean ± SEM of percentage change from at least 3 independent experiments. $^{*}p < 0.05$, $^{**}p < 0.01$ and $^{***}p < 0.001$ vs WT NT or as indicated.

treatment of hSSAO/VAP-1-expressing cells with MA and AβD induced cytotoxicity, determined by MTT reduction (Fig. 6A), by LDH activity in media of these cells (Fig. 6B) and by the increase of the active fragment of caspase-3 (Fig. 6C) without alterations in the total caspase-3, as an indicator of apoptotic cell death induction. This cell death was not mediated by the mitochondrial cell death pathway, as indicated the absence of changes in the Bax/Bcl-2 ratio (Fig. 6D). Under these conditions, the presence of an SSAO inhibitor partly prevented the cell death induced by MA and AβD. Cytotoxicity was also evaluated treating with $Aβ_{42}$, and results showed a higher $Aβ_{42}$ cytotoxicity compared to AβD, with no additive effect due to MA treatment, and no recovery using the SSAO inhibitors in the MTT assay. However, caspase-3 activation was significantly higher in $Aβ_{42}$-MA co-treatment, and differently from AβD, the Bax/Bcl-2 ratio was significantly higher when treating with $Aβ_{42}$ and co-treating with MA. SSAO inhibitors did not induce significant recoveries when treating with $Aβ_{42}$ (Suppl. Fig. 5). The optimal treatment conditions with MA, AβD and $Aβ_{42}$ were tested previously (Suppl. Fig. 6). Thus, AβD and $Aβ_{42}$ effects were different, being the former more related to the SSAO/VAP-1 actions.

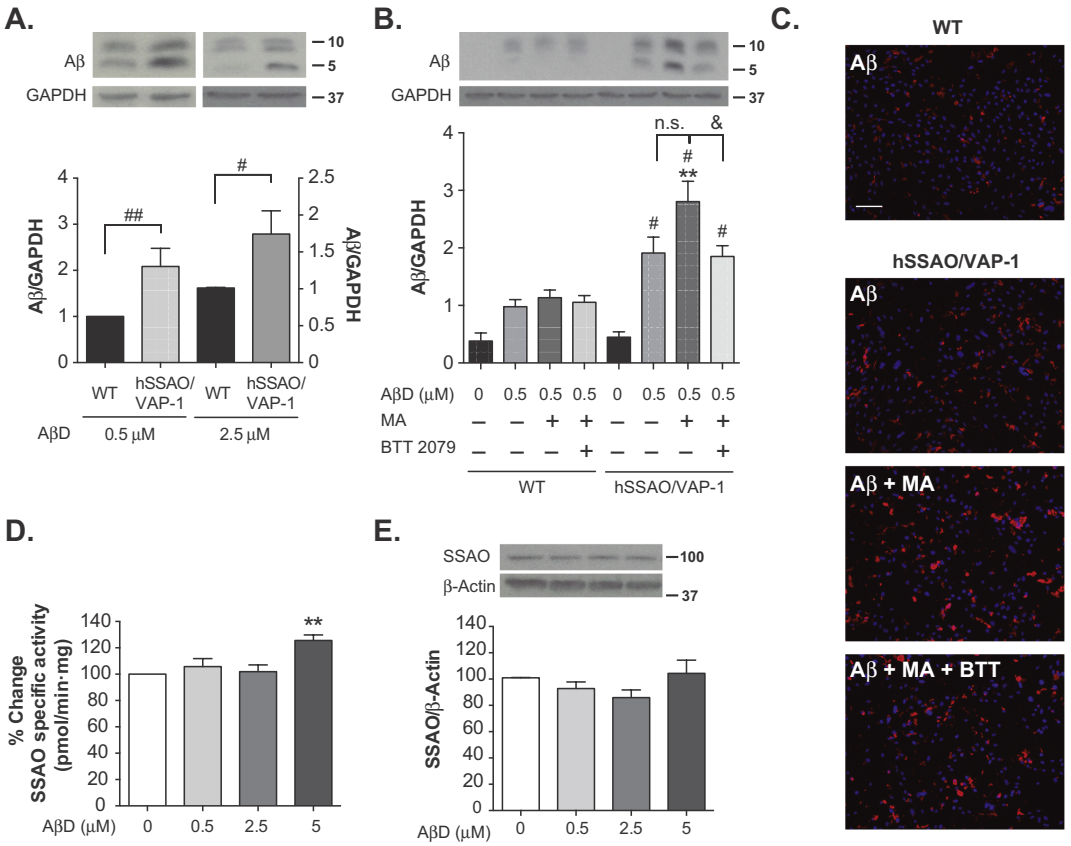

Fig. 4. Positive feedback loop between AβD aggregation and SSAO/VAP-1. (A) Basal AβD deposition on WT and hSSAO/VAP-1-expressing hCMEC/D3 cells determined by tris/bicine Western blots after 48 h of AβD treatment (0.5 and 2.5 μM). (B) AβD deposition on cells after 48 h treatment with AβD (0.5 μM), the SSAO substrate MA (1 mM) and its specific inhibitor BTT2079 (10 μM, added as 30 min pre-treatment), measured by Western blot or (C) by Aβ immunofluorescence (red). Cell nuclei were stained with Hoechst (blue); scale bar: 100 μM. (D) SSAO specific activity and (E) protein levels were measured in hCMEC/D3 hSSAO/VAP-1-expressing cells in the presence of different concentrations (0.5, 2.5 and 5 μM) of AβD for 48 h. SSAO enzymatic activity (pmol/min·mg of protein) was determined with the radiometric method using ^{14}C-benzylamine as substrate. Protein levels were analyzed by Western blot, using β-Actin or GAPDH as loading controls. Representative Western blot images are shown for each quantification graph. Data in graphs is expressed as mean ± SEM of at least 3 independent experiments. $^{**}p < 0.01$ vs non-treated cells; $^{\#}p < 0.05$ and $^{\#\#}p < 0.01$ vs same treatment in WT cells; $^{\&}p < 0.05$ as indicated.

4. Discussion

A cerebral endothelial vascular activation occurs in AD, altering the brain homeostasis and inducing the expression of interleukins (IL-1β, IL-6, IL-8), TNF-α, VEGF and MMPs, among others [2,11,13]. SSAO/VAP-1 is also increased in plasma [24] and cerebrovascular tissue [23] of AD patients. In this regard, we have found that in our cells expressing hSSAO/VAP-1, several of these angioneurins related to inflammation (IL-6, IL-8, ICAM, VCAM) or the trophic factors VEGF, TGF-β1 and NGF were over released. VEGF regulates vessel growth in healthy and diseased tissues [79]; it is a hypoxia-inducible protein, with angiogenic behavior and vascular permeability-enhancing properties, and in AD it appears overexpressed and co-localized with Aβ plaques [80]. These data together with its increase in our vascular cells expressing hSSAO/VAP-1 corroborates the idea that cerebrovascular dysfunction plays an important role in the neurodegenerative cascade, with a possible induction through SSAO/VAP-1 actions. TGF-β1 is also increased in AD, and it is responsible of other inflammatory factors and interleukins release, contributing as well to the inflammatory process linked to this neurodegenerative disorder [81]. The TGF-β1 increase was observed in our hSSAO/VAP-1-expressing human brain endothelial cells and it was also correlated with the levels of IL-6, IL-8, VCAM and ICAM-1. NGF is a neurotrophin required to promote neuron survival pathways, and it is found normally decreased in AD [82]. Its increase in our hSSAO/VAP-1-expressing cells could be related with a compensatory signal, although other trophic factors (FGF-2, IGF-1) were not significantly modified. NGF increase could be also related with a pro-NGF increase observed in AD brains, which has been shown to induce apoptosis in neuronal cell cultures [83]. Unfortunately, our analysis method does not discriminate between NGF and pro-NGF, so we cannot confirm this possibility. In the same line, NGF is able to modify the lipid composition of neuronal membranes, therefore potentiating Aβ accumulation and cytotoxicity on these cells [84]. Whether this effect also occurs in our vascular cells, or if it could be involved in the crosstalk between Aβ aggregation and SSAO/VAP-1 effects needs to be addressed in the future, as well as the significance of this change for the neurovascular unit function.

The alterations of the angioneurins release or the reduced levels of BBB-related proteins observed in brain endothelial hSSAO/VAP-1-expressing cells, suggests that this multifunctional enzyme could be involved in protein expression regulation. Although we have not identified the molecular inductor of the structural and functional changes observed in these cells, it has been described that the products resulting from SSAO/VAP-1 enzymatic activity are able to induce E and P-selectins expression and release in HUVEC cells [33], an effect that we have not observed in our brain endothelial cells. However, it cannot be ruled out that, since SSAO/VAP-1 is also a pro-inflammatory protein, its expression could be related to structural changes in endothelial cells that in turn, would promote a differential protein expression pattern leading to endothelial activation. Alternatively, the enzymatic metabolism of other unknown substrates could modify the protein expression, and explain the differences observed in hSSAO/VAP-1-expressing cells, such as a higher expression of VCAM-1, ICAM-1, and LRP-1 or a

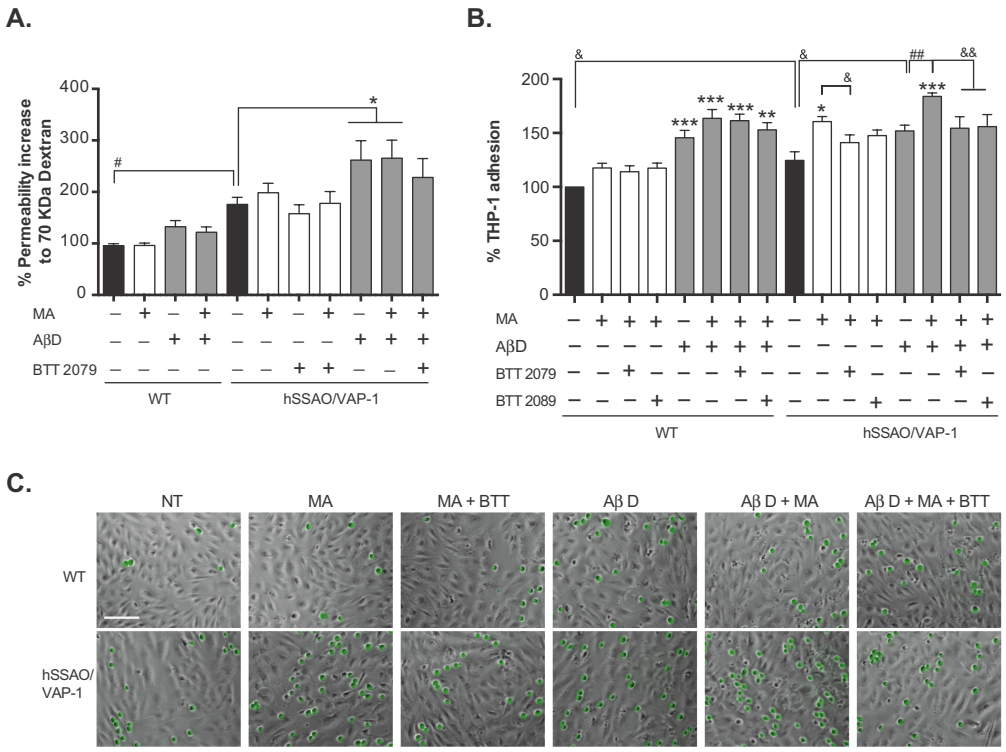

Fig. 5. The AβD-SSAO feedback induces alteration of the BBB function. (A) Endothelial permeability to 70 kDa FITC-Dextran measured in WT and hSSAO/VAP-1-expressing cells treated for 48 h with AβD (5 μM), MA (1 mM) and BTT2079 (10 μM). (B,C) Endothelial leukocyte adhesion to WT and hSSAO/VAP-1-expressing cells was measured in the same conditions, adding also the inhibitor BTT2089 (1 μM). (C) Representative images showing calcein-AM-labelled THP-1 leukocytes (green) attached to endothelial cell monolayers in the same treatment conditions, using BTT2079 as inhibitor. Scale bar: 100 μM. Data in graphs are expressed as mean ± SEM of percentage difference vs non-treated cells from at least 3 independent experiments. $^{*}p < 0.05$, $^{**}p < 0.01$ and $^{***}p < 0.001$ vs non-treated cells; $^{\#}p < 0.05$ and $^{\#\#\#}p < 0.001$ vs as indicated, by one-way ANOVA and the addition of Newman-Keuls multiple comparison test. $^{\&}p < 0.05$ and $^{\&\&}p < 0.01$ vs WT, NT or as indicated, by Student's *t*-test.

reduced expression of the junctional proteins VE-cadherin, claudin-5 and ZO-1. The molecular inductor of these differences, or if it is directly SSAO/VAP-1, needs further studies. On the other hand, although increased MMPs have been found in AD associated to the BBB leakage [85], the MMP-2 protein increase observed in hSSAO/VAP-1 cells seems not to be relevant for the changes observed in these cells, because the overall MMP activity was found to be lower in them. Other MMPs not analyzed in this work could be altered in hSSAO/VAP-1-expressing cells explaining this result, as the substrate used here for measuring MMPs activity can be metabolized by other MMPs besides MMP-2. In addition, the lower MMPs activity found could be related with the MMPs/TIMPs ratio, as TIMP-1 was found significantly increased in hSSAO/VAP-1-expressing cells. Interestingly, this MMPs inhibitor increase has been recently identified as a possible blood biomarker for AD [86]. Whether these changes are relevant for the endothelial activation and BBB opening phenotype observed in hSSAO/VAP-1-expressing cells, or if they are related with hSSAO/VAP-1 protein expression remains to be elucidated. In particular, MMP-2 observed changes could be related with the increase in SSAO/VAP-1 expression, as MMP-2 has been related with the SSAO/VAP-1 shedding [87].

Analyzing the functionality of brain endothelial cells expressing hSSAO/VAP-1, the observed pro-inflammatory phenotype of these cells correlated with a slight increase in basal leukocyte adhesion and with a higher permeability of the BBB formed by these cells. A dysfunctional BBB is found in AD, and it has been associated to a deficient clearance of Aβ [88] and to the contribution to an early cognitive impairment [74]. BBB tightness is controlled by transmembrane tight junction proteins that seal the paracellular gap (Claudins and Cadherins) and fix the transmembrane proteins to the actin cytoskeleton (ZO-1) [89,90]. The lack of TEER increase and ZO-1 positioning at tight junctions along different time points suggests that hSSAO/VAP-1 expressing endothelial cells are not able to close the BBB and therefore form a functional BBB. These functional BBB disturbances may be probably explained by the decrease in the expression of claudin-5, VE-cadherin and ZO-1 in hSSAO/VAP-1-expressing cells. All these effects make sense because as an adhesion protein, SSAO/VAP-1 will promote leukocyte binding and transmigration through the endothelium, by which the BBB will need to be opened, mediated by these changes.

When evaluating the role of the over released angioneurins in these functional BBB alterations, we found that these alterations could not be explained only by the differential release of proteins between both cell types, because the secreted media did not mimic all the changes previously found in cells expressing hSSAO/VAP-1. With the conditioned media treatments, we observed the decrease in claudin-5 but not changes in VE-cadherin or ZO-1, indicating differences in the stimulus regulating these proteins. Consequently, only a slight increase in permeability was observed after treatment with conditioned media, much less evident than that of endothelial cells expressing hSSAO/VAP-1. We first attributed these changes to the most altered angioneurins, VEGF, IL-8 and IL-6, and thus we checked that their signaling pathways were consequently altered in hSSAO/VAP-1-expressing cells. VEGF and IL-8 signaling would converge in activating VEGFR2 molecular pathway in order to promote an endothelial permeability increase, as described by others [54]. However, in our cells we found a drastic reduction in the expression of VEGFR2. These results correlate with the findings that VEGF levels were found increased in plasma from AD patients, while plasma and mRNA levels of its receptors VEGFR1 and VEGFR2 were decreased in these patients [91]. Several harmful stimuli have been shown to reduce VEGFR2 expression, as oxidized low-density lipoproteins or methylglyoxal [92–94]. Interestingly, methylglyoxal is one of the metabolic products of the enzymatic activity of SSAO/VAP-1, when metabolizing aminoacetone. Although we have not observed significant differences in the release of angioneurins when treating with methylamine as SSAO substrate, we cannot rule out that other endogenous substrates could contribute to these alterations. IL-6 was the other signaling pathway analyzed as possible responsible of these BBB alterations, and in this regard, the STAT3 pathway was consequently more activated in endothelial cells expressing SSAO/VAP-1. The dependence of these changes on IL-6-activated STAT3 pathway was confirmed through the addition of an IL-6 blocking antibody, which abolished the permeability changes induced by hSSAO/VAP-1 conditioned media on WT cells. IL-6 is a major inflammatory interleukin, and its

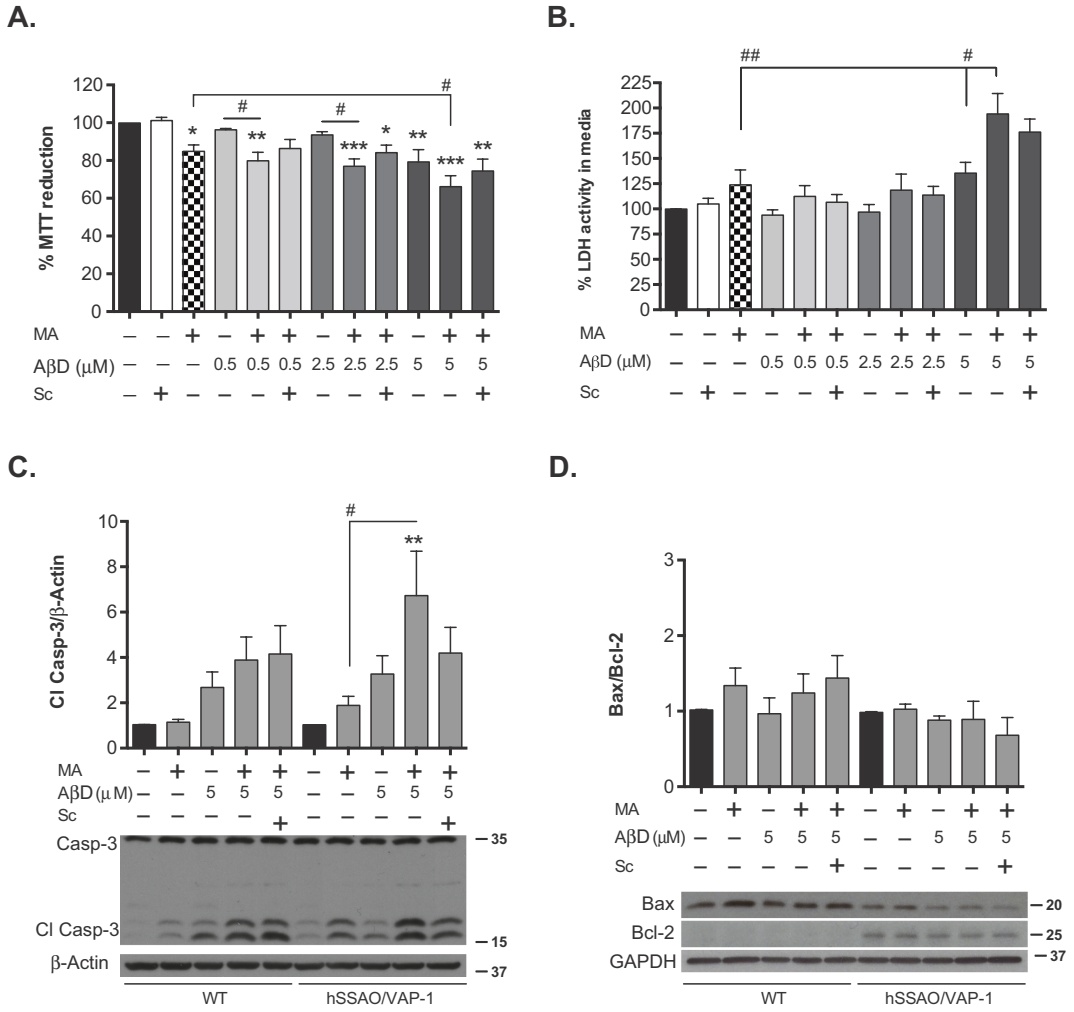

Fig. 6. The AβD-SSAO feedback induces endothelial cell toxicity. Cell viability was determined by (A) MTT reduction or (B) LDH activity in the media in hCMEC/D3 cells expressing hSSAO/VAP-1 treated for 48 h with increasing concentrations of AβD (0.5, 2.5 and 5 μM), MA (3 mM) and the SSAO inhibitor semicarbazide (Sc, 1 mM). (C) Determination of the appearance of the cleaved caspase-3 fragment (Cl Casp-3) and Bax/Bcl-2 ratio (D) in cell lysates, analyzed by Western blot, under same treatments using 5 μM AβD. GAPDH was used as loading control. Representative images are shown for each protein analyzed. Data in graphs is expressed as fold change and represented by mean ± SEM values obtained from at least 3 independent experiments. $^{*}p < 0.05$, $^{**}p < 0.01$ and $^{***}p < 0.001$ vs non-treated cells; $^{\#}p < 0.05$ and $^{\#\#}p < 0.01$ as indicated, by one-way ANOVA and the addition of Newman-Keuls multiple comparison test.

increase has been found in AD, together with other cytokines [95], but although it is associated to dementia, it is not specific for AD, albeit it clearly affects BBB function [96].

Although we cannot rule out the participation of other soluble molecules not analyzed in this work, the results obtained with conditioned media experiments indicate that the dysfunctional alterations found in these cells cannot be completely explained by differential secretion patterns. In addition, the results also indicate that the differential secreted proteins can affect the surrounding microenvironment, and suggest that SSAO/VAP-1 expression could alter the neurovascular unit function through these released factors. For instance, it has been described that VEGF can directly affect the glutamatergic synaptic function, and the silencing of VEGFR in neural cells impairs synaptic plasticity [97]. Whether these endothelial-secreted molecules are able to reach the parenchyma and if they can mediate these or other effects under AD conditions in neural cells is currently being studied in our model.

Despite it has been described that SSAO/VAP-1 is overexpressed in CAA-AD patients, colocalizing with Aβ deposits [23,98], the exact contribution of this enzyme to this pathology and the mechanisms involved are not completely understood. The association of a BBB dysfunction, which according to our results could be promoted by SSAO/VAP-1 expression, with the impairment of Aβ clearance, prompted us to study the relationship between SSAO/VAP-1 and Aβ in these brain microvascular endothelial cells. By treating cells with the vasculotropic AβD, we observed that AβD was highly deposited on hSSAO/VAP-1-expressing. This effect observed was both dependent and independent of the SSAO enzymatic activity using MA as substrate. Similar results were previously observed in HUVEC cells [36], and on the other hand, it has been described the potential of the SSAO metabolic products to induce Aβ aggregation [35,99]. Besides the clear contribution of SSAO/VAP-1 to the AβD deposition, the increased expression of LRP-1 in hSSAO/VAP-1-expressing cells, which binds Aβ, could also contribute to the enhanced Aβ deposition on these cells. In this regard, the results presented in this work seem to be in controversy with the general observation of the LRP-1 decrease found in AD tissue, including ours [98]. The main hypothesis on the LRP-1 role in AD is based on the fact that the LRP-1 decrease promotes Aβ accumulation, initiating therefore the pathology. However, other authors have found LRP-1 increased (reviewed in [100]), and interestingly, Sagare and collegues [101] observed an increase of oxidized sLRP-1 in the plasma of MCI individuals, which showed low affinity for Aβ, suggesting an impairment of Aβ clearance from the brain at this early stage of AD. In this context, we have observed the SSAO/VAP-1 increase and LRP-1 decrease in AD

tissue when Aβ is already deposited on blood vessels, but it is not known what occurs before this point with these two proteins. Considering our in vitro model, we do not have an established AD situation, because our initiating point is only an increased SSAO/VAP-1 expression, so it is not surprising that we do not observe an LRP-1 decrease; by contrast, the LRP-1 increase may be due to other stimulus in our model, and could also be related to the BBB breakdown observed, an LRP-1 role suggested by others [102,103]. Similarly, we previously observed a RAGE increase in human AD tissue, while we do not observe changes in our in vitro model; in this sense, others and us hypothesize that this increase could be attributed to the increased AGEs levels detected in these patients, which is not present in our cell culture model. Obviously, the use of this or other models has limitations, because they are not able to consider all the players involved in the pathological process. In addition, AD is a multifactorial disease with probably several deregulations acting at the same time, and the molecular changes responsible of the initiation of the pathology, before the initial Aβ aggregation, are not fully understood yet. Thus, we are testing the SSAO/VAP-1 increase, which can be present in any inflammatory condition, as one of the alterations leading to the AD initiation and progression. In this regard, our model can be useful for this objective, although it may not consider other molecular players, as other models do not consider SSAO/VAP-1.

A slight increase in SSAO activity was observed after treating cells with AβD, indicating a crosstalk between these two molecules. This relationship was also evidenced at the BBB functional level, since results obtained after treatments with AβD and SSAO substrates and/or inhibitors revealed that SSAO/VAP-1 presence amplifies the effect of AβD on the BBB dysfunction, clearly affecting its permeability. The additive toxicity of AβD and MA treatments was also evidenced by the cell viability tests. However, the enzymatic SSAO activity is more related to the leukocyte adhesion process, with a small additive effect of the AβD treatment but a clear reduction in leukocyte adhesion in the presence of SSAO specific inhibitors.

In some of the parameters previously analyzed we did not obtain the same responses using AβD or $Aβ_{42}$. For instance, $Aβ_{42}$ deposition was less modulated by SSAO/VAP-1 than AβD, changes in SSAO activity and cell viability were induced at lower $Aβ_{42}$ concentrations than AβD, and the cell death induced by $Aβ_{42}$ and MA was dependent on the mitochondrial apoptotic pathway while it was not by AβD and MA. We think that these differential effects could be related to the higher deposition rate of $Aβ_{42}$ (3 times higher than AβD according to our Western blot experiments), which does not allow a modulation of its deposition procedure while the slower AβD aggregation rate does.

5. Conclusions

Our results indicate that the presence of SSAO/VAP-1 in human brain microvessels induces an endothelial activation status towards a pro-inflammatory phenotype, accompanied by BBB leakage and leukocyte adhesion. The molecular mechanisms regulating these phenotypic changes are not known, but they could be related to the activation of signaling pathways by the products generated during SSAO enzymatic activity or by structural modifications provoked by the SSAO/VAP-1 presence. Leukocyte adhesion and AβD deposition on endothelial cells are enhanced by SSAO enzymatic activity, indicating that SSAO/VAP-1 inhibition could report beneficial effects in the treatment of the AD progression. However, SSAO/VAP-1 also affects leukocyte adhesion, AβD deposition, as well as BBB permeability, by enzymatic activity-independent mechanisms. The pro inflammatory molecules over released by cells expressing hSSAO/VAP-1 could have consequences in the surrounding microenvironment, therefore affecting other neighboring cells in the brain and thus, the neurovascular unit function. These aspects should be evaluated in further experiments in order to determine the scope of these alterations in neurons and glia under AD conditions, where SSAO/VAP-1 is overexpressed.

Funding

This work was supported by grants from Ministerio de Economía y Competitividad (SAF2014-59697-R, SAF2017-89271-R), CIBERNED (CB06/05/0042), Fundació La Marató de TV3 (2014-3610) and Generalitat de Catalunya (SGR2009-1231 and SGR2014-0984). CF is supported by a grant from the Departament de Bioquímica i Biologia Molecular, in UAB.

Transparency document

The Transparency document associated with this article can be found, in online version.

Acknowledgements

We gratefully acknowledge Dr. Couraud (Institut Cochin, Paris, France), Dr. Babette Weksler (Weill Cornell Medical College, New York, NY) and Dr. Ignacio Romero (Open University, Milton Keynes, UK) for kindly providing the hCMEC/D3 cell line. We thank Dr. W. E. Van Nostrand (Stony Brook University, Stony Brook, NY, USA) for his kind gift of the hybridoma cell line producing the mouse anti-APP 20.1 antibody. We also acknowledge Dr. D. Smith (Biotie Therapeutics, Turku, Finland) for providing the SSAO inhibitors BTT 2079 and BTT 2089. Our gratefulness is also to our colleagues from the microscope and histology facilities in the Institut de Neurociències of Universitat Autònoma de Barcelona (Barcelona, Spain).

Author's contributions

MS, MEL, BT, CF and AJMM performed the experiments. MS, AJMM and MU designed the experiments. MS and MU supervised the experiments and were responsible for writing the manuscript. RF, AJMM, NC and JRA contributed to the project design and manuscript writing. MU and JRA provided funding.

Declaration of conflicting interests

The authors declare no competing financial interests.

Appendix A. Supplementary data

Supplementary data to this article can be found online at https://doi.org/10.1016/j.bbadis.2019.04.016.

References

[1] B.V. Zlokovic, Neurovascular pathways to neurodegeneration in Alzheimer's disease and other disorders, Nat. Rev. Neurosci. 12 (2011) 723–738.
[2] P. Grammas, Neurovascular dysfunction, inflammation and endothelial activation: implications for the pathogenesis of Alzheimer's disease, J. Neuroinflammation 8 (2011) 26.
[3] H.M. Snyder, R.A. Corriveau, S. Craft, J.E. Faber, S.M. Greenberg, D. Knopman, B.T. Lamb, T.J. Montine, M. Nedergaard, C.B. Schaffer, J.A. Schneider, C. Wellington, D.M. Wilcock, G.J. Zipfel, B. Zlolovic, L.J. Bain, F. Bosetti, Z.S. Galis, W. Koroshetz, M.C. Carrillo, Vascular contributions to cognitive impairment and dementia including Alzheimer's disease, Alzheimers Dement. 11 (2015) 710–717.
[4] R.F. Gottesman, A.L. Schneider, Y. Zhou, J. Coresh, E. Green, N. Gupta, D.S. Knopman, A. Minz, A. Rahmim, A.R. Sharrett, L.E. Wagenknecht, D.F. Wong, T.H. Mosley, Association between midlife vascular risk factors and estimated brain amyloid deposition, JAMA 317 (2017) 1443–1450.
[5] C. Iadecola, The neurovascular unit coming of age: a journey through neurovascular coupling in health and disease, Neuron 96 (2017) 17–42.
[6] M.D. Sweeney, Z. Zhao, A. Montagne, A.R. Nelson, B.V. Zlokovic, Blood-brain barrier: from physiology to disease and back, Physiol. Rev. 99 (2019) 21–78.
[7] J. Zhou, J.T. Yu, H.F. Wang, X.F. Meng, C.C. Tan, J. Wang, C. Wang, L. Tan, Association between stroke and Alzheimer's disease: systematic review and meta-analysis, J. Alzheimers Dis. 43 (2015) 479–489.
[8] A. Montagne, S.R. Barnes, M.D. Sweeney, M.R. Halliday, A.P. Sagare, Z. Shao, A.W. Toga, R.E. Jacobs, C.Y. Liu, L. Amezcua, M.G. Harrington, H.C. Chui, M. Law,

B.V. Zlokovic, Blood-brain barrier breakdown in the aging human hippocampus, Neuron 85 (2015) 296–302.
[9] C. Peers, M.L. Dallas, H.E. Boycott, J.L. Scragg, H.A. Pearson, J.P. Boyle, Hypoxia and neurodegeneration, Ann. N. Y. Acad. Sci. 1177 (2009) 169–177.
[10] A.H. Vagnucc Jr., W.W. Li, Alzheimer's disease and angiogenesis, Lancet 361 (2003) 605–608.
[11] L. Thirumangalakudi, P.G. Samany, A. Owoso, B. Wiskar, P. Grammas, Angiogenic proteins are expressed by brain blood vessels in Alzheimer's disease, J. Alzheimers Dis. 10 (2006) 111–118.
[12] C. Schultheiss, B. Blechert, F.C. Gaertner, E. Drecoll, J. Mueller, G.F. Weber, A. Drzezga, M. Essler, In vivo characterization of endothelial cell activation in a transgenic mouse model of Alzheimer's disease, Angiogenesis 9 (2006) 59–65.
[13] P. Grammas, R. Ovase, Inflammatory factors are elevated in brain microvessels in Alzheimer's disease, Neurobiol. Aging 22 (2001) 837–842.
[14] S. Zacchigna, D. Lambrechts, P. Carmeliet, Neurovascular signalling defects in neurodegeneration, Nat. Rev. Neurosci. 9 (2008) 169–181.
[15] P. Grammas, J. Martinez, A. Sanchez, X. Yin, J. Riley, D. Gay, K. Desobry, D. Tripathy, J. Luo, M. Evola, A. Young, A new paradigm for the treatment of Alzheimer's disease: targeting vascular activation, J. Alzheimers Dis. 40 (2014) 619–630.
[16] C. Iadecola, The overlap between neurodegenerative and vascular factors in the pathogenesis of dementia, Acta Neuropathol. 120 (2010) 287–296.
[17] M. Ujiie, D.L. Dickstein, D.A. Carlow, W.A. Jefferies, Blood-brain barrier permeability precedes senile plaque formation in an Alzheimer's disease model, Microcirculation 10 (2003) 463–470.
[18] A. Montagne, Z. Zhao, B.V. Zlokovic, Alzheimer's disease: a matter of blood-brain barrier dysfunction? J. Exp. Med. 214 (2017) 3151–3169.
[19] S. Takeda, N. Sato, D. Takeuchi, H. Kurinami, M. Shinohara, K. Niisato, M. Kano, T. Ogihara, H. Rakugi, R. Morishita, Angiotensin receptor blocker prevented beta-amyloid-induced cognitive impairment associated with recovery of neurovascular coupling, Hypertension 54 (2009) 1345–1352.
[20] G. Aliev, M.A. Smith, D. Sevdov, M.L. Neal, B.T. Lamb, A. Nunomura, E.K. Gasimov, H.V. Vinters, G. Perry, J.C. LaManna, R.P. Friedland, The role of oxidative stress in the pathophysiology of cerebrovascular lesions in Alzheimer's disease, Brain Pathol. 12 (2002) 21–35.
[21] S. Takeda, N. Sato, K. Ikimura, H. Nishino, H. Rakugi, R. Morishita, Increased blood-brain barrier vulnerability to systemic inflammation in an Alzheimer disease mouse model, Neurobiol. Aging 34 (2013) 2064–2070.
[22] B.I.Rini. Sunitinib, Expert. Opin. Pharmacother. 8 (2007) 2359–2369.
[23] I. Ferrer, J.M. Lizcano, M. Hernández, M. Unzeta, Overexpression of semicarbazide sensitive amine oxidase in the cerebral blood vessels in patients with Alzheimer's disease and cerebral autosomal dominant arteriopathy with subcortical infarcts and leukoencephalopathy, Neurosci. Lett. 321 (2002) 21–24.
[24] M. del Mar Hernandez, M. Esteban, P. Szabo, M. Boada, M. Unzeta, Human plasma semicarbazide sensitive amine oxidase (SSAO), beta-amyloid protein and aging, Neurosci. Lett. 384 (2005) 183–187.
[25] L. Airas, P.J. Lindsberg, M.L. Karjalainen-Lindsberg, I. Mononen, K. Kotisaari, D.J. Smith, S. Jalkanen, Vascular adhesion protein-1 in human ischaemic stroke, Neuropathol. Appl. Neurobiol. 34 (2008) 394–402.
[26] M. Hernandez-Guillamon, L. Garcia-Bonilla, M. Solé, V. Sosti, M. Parés, M. Campos, A. Ortega-Aznar, C. Domínguez, M. Rubiera, M. Ribó, M. Quintana, C.A. Molina, J. Álvarez-Sabín, A. Rosell, M. Unzeta, J. Montaner, Plasma VAP-1/SSAO activity predicts intracranial hemorrhages and adverse neurological outcome after tissue plasminogen activator treatment in stroke, Stroke 41 (2010) 1528–1535.
[27] M. Hernandez-Guillamon, M. Solé, P. Delgado, L. García-Bonilla, D. Giralt, C. Boada, A. Penalba, S. García, A. Flores, M. Ribó, J. Álvarez-Sabín, A. Ortega-Aznar, M. Unzeta, J. Montaner, VAP-1/SSAO plasma activity and brain expression in human hemorrhagic stroke, Cerebrovasc. Dis. 33 (2012) 55–63.
[28] R. Kurkijärvi, D.H. Adams, R. Leino, T. Möttönen, S. Jalkanen, M. Salmi, Circulating form of human vascular adhesion protein-1 (VAP-1): increased serum levels in inflammatory liver diseases, J. Immunol. 161 (1998) 1549–1557.
[29] F. Boomsma, U.M. Bhaggoe, A.M. van der Houwen, A.H. van den Meiracker, Plasma semicarbazide-sensitive amine oxidase in human (patho)physiology, Biochim. Biophys. Acta 1647 (2003) 48–54.
[30] R. Pannecoeck, D. Serruys, L. Benmeridja, J.R. Delanghe, N. van Geel, R. Speeckaert, M.M. Speeckaert, Vascular adhesion protein-1: role in human pathology and application as a biomarker, Crit. Rev. Clin. Lab. Sci. 52 (2015) 284–300.
[31] P.H. Yu, Y.L. Deng, Endogenous formaldehyde as a potential factor of vulnerability of atherosclerosis: involvement of semicarbazide-sensitive amine oxidase-mediated methylamine turnover, Atherosclerosis 140 (1998) 357–363.
[32] M. Solé, M. Hernandez-Guillamon, M. Boada, M. Unzeta, p53 phosphorylation is involved in vascular cell death induced by the catalytic activity of membrane-bound SSAO/VAP-1, Biochim. Biophys. Acta 1783 (2008) 1085–1094.
[33] S. Jalkanen, M. Karikoski, N. Mercier, K. Koskinen, T. Henttinen, K. Elima, K. Salmivirta, M. Salmi, The oxidase activity of vascular adhesion protein-1 (VAP-1) induces endothelial E- and P-selectins and leukocyte binding, Blood 110 (2007) 1864–1870.
[34] P.F. Lalor, P.J. Sun, C.J. Weston, A. Martin-Santos, M.J. Wakelam, D.H. Adams, Activation of vascular adhesion protein-1 on liver endothelium results in an NF-kappaB-dependent increase in lymphocyte adhesion, Hepatology 45 (2007) 465–474.
[35] K. Chen, J. Maley, P.H. Yu, Potential implications of endogenous aldehydes in beta-amyloid misfolding, oligomerization and fibrillogenesis, J. Neurochem. 99 (2006) 1413–1424.
[36] M. Solé, A.J. Miñano-Molina, M. Unzeta, A cross-talk between Aβ and endothelial SSAO/VAP-1 accelerates vascular damage and Aβ aggregation related to CAA-AD, Neurobiol. Aging 36 (2015) 762–775.
[37] D.J. Smith, M. Salmi, P. Bono, J. Hellman, T. Leu, S. Jalkanen, Cloning of vascular adhesion protein 1 reveals a novel multifunctional adhesion molecule, J. Exp. Med. 188 (1998) 17–27.
[38] S. Jalkanen, M. Salmi, VAP-1 and CD73, endothelial cell surface enzymes in leukocyte extravasation, Arterioscler. Thromb. Vasc. Biol. 28 (2008) 18–26.
[39] B.B. Weksler, E.A. Subileau, N. Perrier, P. Charneau, K. Holloway, M. Leveque, H. Tricoire-Leignel, A. Nicotra, S. Bourdoulous, P. Turowski, D.K. Male, F. Roux, J. Greenwood, I.A. Romero, P.O. Couraud, Blood-brain barrier-specific properties of a human adult brain endothelial cell line, FASEB J. 19 (2005) 1872–1874.
[40] B. Weksler, I.A. Romero, P.O. Couraud, The hCMEC/D3 cell line as a model of the human blood brain barrier, Fluids Barriers CNS 10 (2013) 16.
[41] P. Sun, G. Esteban, T. Inokuchi, J. Marco-Contelles, B.B. Weksler, I.A. Romero, P.O. Couraud, M. Unzeta, M. Solé, Protective effect of the multitarget compound DPH-4 on human SSAO/VAP-1-expressing hCMEC/D3 cells under oxygen–glucose deprivation conditions: an *in vitro* experimental model of cerebral ischaemia, Br. J. Pharmacol. 172 (2015) 5390–5402.
[42] H.J. Ball, B. McParland, C. Driussi, N.H. Hunt, Isolating vessels from the mouse brain using laser capture microdissection, Brain Res Brain Res Protoc 9 (2002) 113–206.
[43] C. Malagelada, X. Xifro, A. Miñano, J. Sabria, J. Rodriguez-Alvarez, Contribution of caspase-mediated apoptosis to the cell death caused by oxygen-glucose deprivation in cortical cell cultures, Neurobiol. Dis. 20 (2005) 27–37.
[44] J. Wiltfang, A. Smirnov, B. Schnierstein, G. Kelemen, U. Matthies, H.W. Klafki, M. Staufenbiel, G. Hüther, E. Rüther, J. Kornhuber, Improved electrophoretic separation and immunoblotting of beta-amyloid (a beta) peptides 1-40, 1-42, and 1-43, Electrophoresis 18 (1997) 527–532.
[45] J.M. Lizcano, K.F. Tipton, M. Unzeta, Purification and characterization of membrane-bound semicarbazide-sensitive amine oxidase (SSAO) from bovine lung, Biochem. J. 331 (1998) 69–78.
[46] M. Unzeta, M. Solé, M. Boada, M. Hernández, Semicarbazide-sensitive amine oxidase (SSAO) and its possible contribution to vascular damage in Alzheimer's disease, J. Neural Transm. 114 (2007) 857–862.
[47] L. Olson, C. Humpel, Growth factors and cytokines/chemokines as surrogate biomarkers in cerebrospinal fluid and blood for diagnosing Alzheimer's disease and mild cognitive impairment, Exp. Gerontol. 45 (2010) 41–46.
[48] P. Carmeliet, C. Ruiz de Almodovar, VEGF ligands and receptors: implications in neurodevelopment and neurodegeneration, Cell. Mol. Life Sci. 70 (2013) 1763–1778.
[49] K.P. Doyle, E. Cekanaviciute, L.E. Mamer, M.S. Buckwalter, TGFb signaling in the brain increases with aging and signals to astrocytes and innate immune cells in the weeks after stroke, J Neuroinflam 7 (2010) 62.
[50] A. Fuster-Matanzo, M. Llorens-Martín, F. Hernández, J. Avila, Role of neuroinflammation in adult neurogenesis and Alzheimer's disease: therapeutic approaches, Mediat. Inflamm. (2013) 1–9.
[51] H.S. Suh, M.L. Zhao, L. Derico, N. Choi, S.C. Lee, Insulin-like growth factor 1 and 2 (IGF1, IGF2) expression in human microglia: differential regulation by inflammatory mediators, J Neuroinflam 10 (2013) 37.
[52] L.A. Bach, Endothelial cells and the IGF system, J. Mol. Endocrinol. 54 (2015) R1–13.
[53] M. Erta, A. Quintana, J. Hidalgo, Interleukin-6, a major cytokine in the central nervous system, Int. J. Biol. Sci. 8 (2012) 1254–1266.
[54] M.L. Petreaca, M. Yao, Y. Liu, K. Defea, M. Martins-Green, Transactivation of vascular endothelial growth factor receptor-2 by interleukin-8 (IL-8/CXCL8) is required for IL-8/CXCL8-induced endothelial permeability, Mol. Biol. Cell 18 (2007) 5014–5023.
[55] S.S. Shaftel, W.S. Griffin, M.K. O'Banion, The role of interleukin-1 in neuroinflammation and Alzheimer disease: an evolving perspective, J Neuroinflamm 5 (2008) 7.
[56] S.J. Lee, K. Drabik, N.J. Van Wagoner, S. Lee, C. Choi, Y. Dong, E.N. Benveniste, ICAM-1-induced expression of proinflammatory cytokines in astrocytes: involvement of extracellular signal-regulated kinase and p38 mitogen-activated protein kinase pathways, J. Immunol. 165 (2000) 4658–4666.
[57] P. Turowski, P. Adamson, J. Greenwood, Pharmacological targeting of ICAM-1 signaling in brain endothelial cells: potential for treating neuroinflammation, Cell. Mol. Neurobiol. 25 (2005) 153–170.
[58] M. Ewers, M.M. Mielke, H. Hampel, Blood-based biomarkers of microvascular pathology in Alzheimer's disease, Exp Geront 45 (2010) 75–79.
[59] B.A. Kallmann, V. Hummel, T. Lindenlaub, K. Ruprecht, K.V. Toyka, P. Rieckmann, Cytokine-induced modulation of cellular adhesion to human cerebral endothelial cells is mediated by soluble vascular cell adhesion molecule-1, Brain 123 (2000) 687–697.
[60] A. Haarmann, E. Nowak, A. Deib, S. van der Pol, C.M. Monoranu, G. Kooij, N. Müller, P. van der Valk, G. Stoll, H.E. De Vries, F.Berberich-Siebelt.M. Buttamann, Soluble VCAM-1 impairs human brain endothelial barrier integrity via integrin a-4-transduced outside-in signaling, Acta Neuropathol. 129 (2015) 639–652.
[61] G. Zuliani, M. Cavalieri, M. Galvani, A. Passaro, M.R. Munari, C. Bosi, A. Zurlo, R. Fellin, Markers of endotelial dysfunction in older subjects with late onset Alzheimer's disease or vascular dementia, J. Neurol. Sci. 272 (2008) 164–170.
[62] R. Deane, Z. Wu, A. Sagare, J. Davis, S. Du Yan, K. Hamm, F. Xu, M. Parisi, B. LaRue, H.W. Hu, P. Spijkers, H. Guo, X. Song, P.J. Lenting, W.E. Van Nostrand, B.V. Zlokovic, LRP/amyloid beta-peptide interaction mediates differential brain efflux of Abeta isoforms, Neuron 43 (2004) 333–344.

[63] Y. Zhao, D. Li, J. Zhao, J. Song, Y. Zhao, The role of the low-density lipoprotein receptor-related protein 1 (LRP-1) in regulating blood-brain barrier integrity, Rev. Neurosci. 27 (2016) 623–634.
[64] X. Wang, S.R. Lee, K. Arai, S.R. Lee, K. Truji, G.W. Rebeck, E.H. Lo, Lipoprotein receptor-mediated induction of matrix metalloproteinase by tissue plasminogen activator, Nat. Med. 9 (2003) 1313–1317.
[65] U. Beffert, P.C. Stolt, J. Herz, Functions of lipoprotein receptors in neurons, J. Lipid Res. 45 (2004) 403–409.
[66] Z. Qiu, D.K. Strickland, B.T. Hyman, G.W. Rebeck, Alpha 2-macroglobulin exposure reduces calcium responses to N-methyl-D-aspartate via low density lipoprotein receptor-related protein in cultured hippocampal neurons, J. Biol. Chem. 277 (2002) 14458–14466.
[67] T. Kanekiyo, J.R. Cirrito, C.C. Liu, M. Shinohara, J. Li, D.R. Schuler, M. Shinohara, D.M. Holtzman, G. Bu, Neuronal clearance of amyloid-b by endocytic receptor LRP-1, J. Neurosci. 33 (2013) 19276–19283.
[68] M. Shinohara, M. Tachibana, T. Kanekiyo, G. Bu, Role of LRP1 in the pathogenesis of Alzheimer's disease: evidence from clinical and preclinical studies, J. Lipid Res. 58 (2017) 1267–1281.
[69] Z. Cai, N. Liu, C. Wang, B. Qin, Y. Zhou, M. Xiao, L. Chang, L.J. Yan, B. Zhao, Role of RAGE in Alzheimer's disease, Cell. Mol. Neurobiol. 36 (2016) 483–495.
[70] D. Walker, L.F. Lue, G. Paul, A. Patel, M.N. Sabbagh, Receptor for advanced glycation endproduct modulators: a new therapeutic target in Alzheimer's disease, Expert Opin. Investig. Drugs 24 (2015) 393–399.
[71] R. Deane, S. Du Yan, R.K. Submamaryan, B. LaRue, S. Jovanovic, E. Hogg, D. Welch, L. Manness, C. Lin, J. Yu, H. Zhu, J. Ghiso, B. Frangione, A. Stern, A.M. Schmidt, D.L. Armstrong, B. Arnold, B. Liliensiek, P. Nawroth, F. Hofman, M. Kindy, D. Stern, B. Zlokovic, RAGE mediates amyloid-beta peptide transport across the blood-brain barrier and accumulation in brain, Nat. Med. 9 (2003) 907–913.
[72] O. Arancio, H.P. Zhang, X. Chen, C. Lin, F. Trinchese, D. Puzzo, S. Liu, A. Hegde, S.F. Yan, A. Stem, J.S. Luddy, L.F. Lue, D.G. Walker, A. Roher, M. Buttini, L. Mucke, W. Li, A.M. Schmidt, M. Kindy, P.A. Hyslop, D.M. Stern, S.S. Du Yan, RAGE potentiates Abeta-induced perturbation of neuronal function in transgenic mice, EMBO J. 23 (2004) 4096–4105.
[73] H.H. Birdsall, C. Lane, M.N. Ramser, D.C. Anderson, Induction of VCAM-1 and ICAM-1 on human neural cells and mechanisms of mononuclear leukocyte adherence, J. Immunol. 148 (1992) 2717–2723.
[74] E. Zenaro, G. Piacentino, G. Constantin, The blood-brain barrier in Alzheimer's disease, Neurobiol. Dis. 107 (2017) 41–56.
[75] M. Dougher-Vermazen, J.D. Hulmes, P. Böhlen, B.I. Terman, Biological activity and phosphorylation sites of the bacterially expressed cytosolic domain of the KDR VEGF-receptor, Biochem. Biophys. Res. Commun. 205 (1994) 728–738.
[76] Z. Sun, X. Li, S. Massena, S. Kutschera, N. Padhan, L. Gualandi, V. Sundvold-Gjerstad, K. Gustafsson, W.W. Choy, G. Zhang, M. Quach, L. Jansson, M. Philipson, M.R. Abid, A. Spurkland, L. Claesson-Welsh, VEGFR2 induces c-Src signaling and vascular permeability in vivo via the adaptor protein TSAd, J. Exp. Med. 209 (2012) 1363–1377.
[77] M.C. Herzig, D.T. Winkler, P. Burgermeister, M. Pfeifer, E. Kohler, S.D. Schmidt, S. Danner, D. Abramowski, C. Struchler-Pierrat, K. Burki, S.G. Van Duinen, M.L. Maat-Shiemann, M. Staufenbiel, P.M. Mathews, M. Jucker, Abeta is targeted to the vasculature in a mouse model of hereditary herebral hemorrhage with amyloidosis, Nat. Neurosci. 7 (2004) 954–960.
[78] R. Natte, H. Yamaguchi, M.L. Maat-Schieman, F.A. Prins, P. Neeskens, R.A. Roos, S.G. van Duinen, Ultrastructural evidence of early non-fibrillar Abeta42 in the capillary basement membrane of patients with hereditary cerebral hemorrhage with amyloidosis, Dutch type, Acta Neuropathol. 98 (1999) 577–582.
[79] P. Carmeliet, Mechanisms of angiogenesis and arteriogenesis, Nat. Med. 6 (2000) 389–395.
[80] S.P. Yang, D.G. Bae, H.J. Kang, B.J. Gwag, Y.S. Gho, C.B. Chae, Co-accumulation of vascular endothelial growth factor with beta-amyloid in the brain of patients with Alzheimer's disease, Neurobiol. Aging 25 (2004) 283–290.
[81] P. Grammas, R. Ovase, Cerebrovascular transforming growth factor-beta contributes to inflammation in the Alzheimer's disease brain, Am. J. Pathol. 160 (2002) 1583–1587.
[82] R. Schliebs, T. Arendt, The cholinergic system in aging and neuronal degeneration, Behav. Brain Res. 221 (2011) 555–563.
[83] P. Podlesniy, A. Kichev, C. Pedraza, J. Saurat, M. Encinas, B. Perez, I. Ferrer, C. Espinet, Pro-NGF from Alzheimer's disease and normal human brain displays distinctive abilities to induce processin and nuclear translocation of intracellular domain of p75NTR and apoptosis, Am. J. Pathol. 169 (2006) 119–131.
[84] C.J. Xu, J.L. Wang, W.L. Jin, The emergint therapeutic role of NGF in Alzheimer's disease, Neurochem. Res. 41 (2016) 1211–1218.
[85] X.X. Wang, M.S. Tan, J.T. Yu, L. Tan, Matrix metalloproteinases and their multiple roles in Alzheimer's disease, Biomed. Res. Int. 2014 (2014) 908636.
[86] F. Yao, K. Zhang, Y. Zhang, Y. Guo, A. Li, S. Xiao, Q. Liu, L. Shen, J. Ni, Identification of blood biomarkers for Alzheimer's disease through compuntational prediction and experimental validation, Front. Neurol. 9 (2018) 1158.
[87] P. Sun, M. Solé, M. Unzeta, Involvement of SSAO/VAP-1 in oxygen-glucose deprivation-mediated damage using the endothelial hSSAO/VAP-1-expressing cells as an experimental model of cerebral ischemia, Cerebrovascular Dis 37 (2014) 171–180.
[88] B.V. Zlokovic, Neurovascular mechanisms of Alzheimer's neurodegeneration, Trends Neurosci. 28 (2005) 202–208.
[89] N. Ahmed Khan, R. Siddiqui, The neuropathogenesis of Acanthamoeba encephalitis: barriers to overcome, J Cell Sci Ther (2011) 001 S3.
[90] E.E. Benarroch, Blood-brain barrier: recent developments and clinical correlations, Neurology 78 (2012) 1268–1276.
[91] S.J. Cho, M.H. Park, C. Han, K. Yoon, Y.H. Koh, VEGFR2 alteration in Alzheimer's disease, Sci. Rep. 7 (2017) 17713.
[92] M. Zhang, L. Jiang, Oxidized low-density lipoprotein decreases VEGFR2 expression in HUVECs and impairs angiogenesis, Exp Ther Med 12 (2016) 3742–3748.
[93] F. Jin, N. Hagemann, U. Brockmeier, S.T. Schäfer, A. Zechariah, D.M. Hermann, LDL attenuates VEGF-induced angiogènesis via mechanisms involving VEGFR2 internalization and degradation following endosome-trans-Golgi network trafficking, Angiogenesis 16 (2013) 625–637.
[94] H. Liu, S. Yu, H. Zhang, J. Xu, Angiogenesis impairment in diabetis: role of methylglyoxal-induced receptor for advanced glycation endproducts, autophagy and vascular endothelial growth factor receptor 2, PLoS One 7 (2012) e46720.
[95] W. Swardfager, K. Lanctôt, L. Rothenburg, A. Wong, J. Cappell, N. Herrmann, A meta-analysis of cytokines in Alzheimer's disease, Biol. Psychiatry 68 (2010) 930–941.
[96] S.K.L. Darweesh, F.J. Wolters, M.A. Ikram, F. De Wolf, D. Bos, A. Hofman, Inflammatory markers and the risk of dementia and Alzheimer's disease: a meta-analysis, Alzheimers Dement. (2018) S1552–5260 30068-2.
[97] P. de Rossi, E. Harde, J.P. Dupuis, L. Martin, N. Chounlamountri, M. Bardin, C. Watrin, C. Benetollo, K. Pernet-Gallay, H.J. Luhmann, J. Honnorat, G. Malleret, L. Groc, A. Acker-Palmer, P.A. Salin, C. Meissirel, A critical role for VEGF and VEGFR2 in NMDA receptor synaptic function and fear-related behavior, Mol. Psychiatry 21 (2016) 1768–1780.
[98] T. Valente, A. Gella, M. Solé, N. Durany, M. Unzeta, Immunohistochemical study of semicarbazide-sensitive amine oxidase/vascular adhesion protein-1 in the hippocampal vasculature: pathological synergy of Alzheimer's disease and diabetes mellitus, J. Neurosci. Res. 90 (2012) 1989–1996.
[99] K. Chen, M. Kazachkov, P.H. Yu, Effect of aldehydes derived from oxidative deamination and oxidative stress on beta-amyloid aggregation; pathological implications to Alzheimer's disease, J. Neural Transm. (Vienna) 114 (2007) 835–839.
[100] M. Shinohara, M. Tachibana, T. Kanekiyo, G. Bu, Role of LRP1 in the pathogenesis of Alzheimer's disease: evidence from clinical and preclinical studies, Thematic review series: ApoE and Lipid Homeostasis in Alzheimer's disease, J Lipid Res 58 (2017) 1267–1281.
[101] A.P. Sagare, R. Deane, H. Zetterberg, A. Wallin, K. Blennow, B.V. Zlokovic, Impaired lipoprotein receptor-mediated peripheral binding of plasma amyloid-β is an early biomarker for mild cognitive impairment preceding Alzheimer's disease, J. Alzheimers Dis. 24 (2011) 25–34.
[102] M. Yepes, M. Sandkvist, E.G. Moore, T.H. Bugge, D.K. Strickland, D.A. Lawrence, Tissue-type plasminogen activator induces opening of the blood-brain barrier via the LDL receptor-related protein, J. Clin. Invest. 112 (2003) 1533–1540.
[103] Y. Zhao, D. Li, J. Song, Y. Zhao, The role of the low-density lipoprotein receptor-related protein 1 (LRP-1) in regulating blood-brain barrier integrity, Rev. Neurosci. 27 (2016) 623–634.

2.- Siedlecki-Wullich, Dolores, Judit Català-Solsona, Cristina Fábregas, Isabel Hernández, Jordi Clarimon, Alberto Lleó, Merce Boada, Carlos A. Saura, José Rodríguez-Álvarez, and Alfredo J. Miñano-Molina. 2019. "Altered MicroRNAs Related to Synaptic Function as Potential Plasma Biomarkers for Alzheimer's Disease." ***Alzheimer's Research and Therapy*** **11 (1): 1–11. https://doi.org/10.1186/s13195-019-0501-4**

Siedlecki-Wullich et al. Alzheimer's Research & Therapy (2019) 11:46
https://doi.org/10.1186/s13195-019-0501-4

Alzheimer's Research & Therapy

RESEARCH Open Access

Altered microRNAs related to synaptic function as potential plasma biomarkers for Alzheimer's disease

Dolores Siedlecki-Wullich[1,2], Judit Català-Solsona[1,2], Cristina Fábregas[1,2], Isabel Hernández[3], Jordi Clarimon[2,4], Alberto Lleó[2,4], Merce Boada[2,3], Carlos A. Saura[1,2], José Rodríguez-Álvarez[1,2,5*] and Alfredo J. Miñano-Molina[1,2*]

Abstract

Background: Several evidences suggest that failure of synaptic function occurs at preclinical stages of Alzheimer's disease (AD) preceding neuronal loss and the classical AD pathological hallmarks. Nowadays, there is an urgent need to identify reliable biomarkers that could be obtained with non-invasive methods to improve AD diagnosis at early stages. Here, we have examined plasma levels of a group of miRNAs related to synaptic proteins in a cohort composed of cognitive healthy controls (HC), mild cognitive impairment (MCI) and AD subjects.

Methods: Plasma and brain levels of miRNAs were analysed in two different cohorts including 38 HC, 26 MCI, 56 AD dementia patients and 27 frontotemporal dementia (FTD) patients. D'Agostino and Pearson and Shapiro-Wilk tests were used to evaluate data normality. miRNA levels between groups were compared using a two-sided nonparametric Mann-Whitney test and sensitivity and specificity was determined by receiver operating characteristic curve analysis.

Results: Significant upregulation of miR-92a-3p, miR-181c-5p and miR-210-3p was found in the plasma of both MCI and AD subjects. MCI patients that progress to AD showed higher plasma levels of these miRNAs. By contrast, no changes in miR-92a-3p, miR-181c-5p or miR-210-3p levels were observed in plasma obtained from a cohort of FTD.

Conclusion: Our study shows that plasma miR-92a-3p, miR-181c-5p and miR-210-3p constitute a specific molecular signature potentially useful as a potential biomarker for AD.

Keywords: Alzheimer's disease, Mild cognitive impairment, Synapses, miRNAs, Plasma, Human, Biomarker, Frontotemporal dementia

Background

It is estimated that more than 40 million people worldwide are affected by Alzheimer's disease (AD) and it is expected that about 100 million could be affected by 2050. Unfortunately, there is no treatment to prevent or even reverse AD, making the finding of new therapeutic breakthroughs a huge challenge for our societies [1]. During the last decade, much effort has been devoted to the establishment of early AD biomarkers that could help to implement appropriate personalised care programmes before the onset of neurodegeneration and dementia. Moreover, effective early AD biomarkers could improve the design of clinical trials and help to reverse the continuous failures in the search of disease-modifying agents for AD obtained in the last years [2–4].

The best AD biomarkers achieved to date are based on neuroimaging methods (Aβ in the brain or hippocampal atrophy) or by the detection in the cerebrospinal fluid (CSF) of total tau, phospho-tau and $A\beta_{42}$ [5–8]. Recently, a specific roadmap has been suggested to validate these neuroimaging- and CSF-derived biomarkers [9]. Unfortunately, all these potential biomarkers could not

* Correspondence: jose.rodriguez@uab.cat; alfredo.minano@uab.cat
[1]Institut de Neurociències and Dpt. Bioquímica i Biología Molecular, Universitat Autònoma de Barcelona, 08193 Cerdanyola del Vallès, Spain
Full list of author information is available at the end of the article

be used in routine clinical screening due to their invasiveness and economic limitations.

On the other hand, several evidences indicate that cognitive impairment observed in early stages of AD could be explained by alterations in synaptic function that precedes neurodegeneration [10]. Furthermore, some reports have shown that deregulation of synaptic proteins could be related to early cognitive dysfunction in experimental models of AD [11–14]. Thus, changes in the regulatory mechanisms involved in the expression of synaptic proteins could be valuable for assessing prognosis and the rate of cognitive decline in AD.

MicroRNAs (miRNAs) are small non-coding RNAs that play a significant role in local control of mRNA translation. In fact, a single miRNA could regulate the local expression of multiple proteins. Several studies have shown that some miRNAs control the formation, maturation and function of synapses [15] and alteration in their levels could underlie synaptic dysfunction in pathological states [16]. Notably, a number of specific miRNAs are misregulated in AD, including miRNAs implicated in the regulation of key genes involved in AD, such as APP or BACE1, or neuronal function such as glutamate receptors [17–20]. Extensive interest has been focused on identifying changes in specific miRNAs that could be used as AD biomarkers [21–25]. miRNAs can be found in the blood where they are transported in different structures that protect them from degradation [26, 27]. Since blood collection is an easy and non-invasive procedure, the identification of blood-based miRNA biomarkers for AD has drawn attention during the last years [28]. Altered levels of certain miRNAs in plasma of AD patients have been previously reported [21, 25, 29–32]; however, few data exist about changes in plasma levels of miRNAs that are related to synaptic protein function in AD [33]. In the present study, we have analysed several miRNAs related to synaptic proteins in plasma samples from mild cognitive impairment (MCI) and AD subjects. We have also monitored plasma samples from frontotemporal dementia (FTD) patients to verify the specificity of the obtained results. Our data suggest that miR-92a-3p, miR-181c-5p and miR-2 10-3p are potential and specific plasma biomarkers for AD.

Methods

Subjects

Plasma samples analysed in this study were obtained from two different cohorts. The first cohort provided by Fundació ACE (Barcelona, Spain) includes 14 HC, 26 MCI and 56 AD dementia patients. The second cohort was recruited at the Memory Unit of the Hospital Sant Pau (Barcelona, Spain) and consists of 24 HC and 27 FTD patients. Participants were clinically diagnosed by neurologists and classified according to internationally accepted diagnostic criteria [34]. Specifically, MCI subjects fulfilled Petersen's diagnostic criteria [35], and their neuropsychological assessment was done by the previously validated NBACE battery tests [36]. FTD participants include 19 patients with possible or probable behavioural variant [37] and 6 with semantic variant of primary progressive aphasia [38]. Two patients with FTD were additionally diagnosed with concomitant ALS according to El Escorial criteria [39]. Demographic and clinical characteristics of cohorts 1 and 2 are summarised in Table 1. Brain tissue samples were provided by 3 different Spanish centres: Fundación Cien, Hospital Clinic-IDIBAPS and Hospital Universitario Fundación Alcorcón. Demographic and clinical characteristics of the subjects are listed in Additional file 1: Table S1. Brain tissue from entorhinal cortex ($n = 13$), hippocampus ($n = 49$) and cerebellum ($n = 30$) was analysed.

Sample processing, RNA extraction and reverse transcription

Blood samples were collected in EDTA-containing tubes, as recommended [40]. After 20 min centrifugation (2500×*g*), plasma was separated, aliquoted and stored at − 80 °C until use. Plasma samples were thawed on ice for RNA extraction, and hemolysis of each sample was analysed at the time measuring absorbance at 414/375 nm (414/375 ratio > 1.4 were considered hemolysed) [41]. RNA was isolated from 200 μL of plasma, using the miRNeasy RNA isolation kit (Qiagen) following the manufacturer's indications. Two microlitres of RNA was reverse-transcribed to cDNA using TaqMan™ Advanced miRNA cDNA Synthesis Kit (Thermo Fisher Scientific).

Table 1 The expression levels of miRNAs related to synaptic proteins

Cohort 1				Cohort 2	
	HC	MCI	AD	HC	FTD
Cohort size	14	26	56	24	27
Men/women	7/7	10/16	15/41	11/13	17/10
Age (years)	68.29 ± 8.99	72.0 ± 8.49	77.77 ± 6.69	67.03 ± 5.05	68.87 ± 7.48
GDS	2.07 ± 0.26	3.15 ± 0.37	4.64 ± 1.02	1 ± 0	3.76 ± 0.99
MMSE	29.21 ± 1.05	26.92 ± 2.22	16.05 ± 7.23	28.5 ± 1.69	25.5 ± 3.76

All data are shown as mean ± SD

HC cognitively healthy controls, *MCI* mild cognitive impairment, *AD* Alzheimer's disease, *FTD* frontotemporal dementia, *MMSE* Mini-Mental State Examination, *GDS* Global Deterioration Scale

Postmortem brains were quickly homogenated in dry ice to prevent thawing, and RNA was isolated from 20 to 50 mg of tissue from each brain area using *miR*Vana miRNA Isolation Kit (Thermo Fisher Scientific) following the manufacturer's instructions. RNA quality was evaluated using the Agilent 2100 bioanalyzer. Samples with RNA integrity number (RIN) under 4 were excluded [40, 42]. Ten nanogrammes of RNA were reverse-transcribed to cDNA using TaqMan™ MicroRNA Reverse Transcription Kit (Thermo Fisher Scientific).

miRNAs quantification by RT-qPCR

Quantitative real-time PCR (RT-qPCR) was performed from 5 μL of 1/10 diluted cDNA (plasma samples) using TaqMan Fast Advanced Master Mix and TaqMan Advanced miRNA Assays (Thermo Fisher Scientific) or from 1.33 μL of cDNA (tissue samples) using TaqMan™ Universal Master Mix II, with UNG. Applied Biosystems 7500 Fast instrument was used for amplification. Samples were run in duplicate, and internal control samples were repeated in every plate to avoid batch effects. Raw Ct data acquired using the 7500 Software v2.0.6 (Applied Biosystems) was exported to LinRegPCR software to calculate the amplification efficiency for each reaction. Reactions with amplification efficiency below 1.6 were discarded. Ct values and average efficiencies obtained from LinRegPCR were used to analyse miRNA levels by the comparative ΔΔCt method [43]. To date, there is no consensus on the use of particular reference genes for miRNA level normalisation in AD studies. Therefore, in this study, the stability of some described reference genes was evaluated using the NormFinder algorithm [44]. hsa-miR-191-5p and hsa-miR-484 were identified as the most stable reference genes along with all plasma samples. In addition, hsa-miR-191-5p and hsa-miR-484 showed higher correlation than other candidates (Spearman's correlation coefficient $r = 0.89$; $P < 0.0001$). U18 and RNU48 were selected for tissue data normalisation. miRNA levels were normalised versus the geometric mean of selected reference genes, to compensate abundance differences between miRNAs and prevent statistical outliers [45].

Western blotting

Human brain tissue was lysed in ice with cold RIPA buffer (50 mM Tris base pH 7.4, 150 mM NaCl, 2 mM EDTA, 1% NP40, 0.5% Triton X-100, 0.1% SDS, 1 mM Na_3VO_4, 25 mM NaF, 1 mM PMSF, 1/100 protease inhibitors and 1/100 phosphatases inhibitors cocktail), sonicated and centrifuged. The supernatant was recovered, and concentration was determined by BCA assay. An equal amount of protein was loaded in 10–12% polyacrylamide gels and separated by electrophoresis under denaturing conditions (SDS-PAGE). Proteins were then transferred to nitrocellulose membrane (GE Healthcare), and membranes were further incubated with blocking solution (10% dry milk, 0.1% BSA, pH 7.4) for 1 h and washed with phosphate buffer saline-Tween (PBT-T). Next, membranes were incubated with primary antibodies (anti-NPTX1 (1:1000, BD), anti-NPTXR (1:500, Santa Cruz) and anti-b-actin (1:5000, Sigma) overnight at 4 °C. After washing membranes with PBT-T, they were incubated at room temperature for 1 h with secondary peroxidase-coupled antibodies (mouse or rabbit as needed) prepared in blocking solution. After repeated washes, proteins were detected by chemoluminescence reaction using ECL Western Blotting reagent (GE Healthcare). Immunoblots were analysed by densitometry using ImageJ (National Institutes of Health, Bethesda, MD), and protein levels were corrected for corresponding loading control.

Statistical analysis

Ct values were normalised versus the Ct mean of the control group and log2 transformed. D'Agostino and Pearson and Shapiro-Wilk tests were used to evaluate data normality. miRNA levels from controls, and patients were compared using a two-sided nonparametric Mann-Whitney test. Bonferroni correction was applied for multiple comparisons when needed. Non-parametric Spearmen's rank correlation test was used to determine the correlation between miRNA expression levels and age. P values < 0.05 were considered statistically significant. ROC curve analysis under a nonparametric approach was used to obtain the area under de curve (AUC) to evaluate sensitivity and specificity of each miRNA as a predictive biomarker. Logistic regression was applied to evaluate biomarker combination by ROC curve analysis. Statistical analysis was performed using GraphPad Prism software v6.01 (GraphPad Software Inc., CA, USA) and MedCalc (v17.9.7).

Results

Upregulation of miR-92a, miR-181c and miR-210 in plasma of MCI and AD patients

The expression levels of miRNAs related to synaptic proteins, miR-92a-3p, miR-181c-5p, miR-210-3p and miR-584-5p (Additional file 1: Table S2), were analysed by RT-qPCR in the plasma of a cohort consisting of 14 HC, 26 MCI and 56 sporadic AD subjects (Table 1). We found a significant increase in the levels of miR-92a-3p, miR-181c-5p and miR-210-3p in plasma from AD patients when compared with HC (Fig. 1a; miR-92a-3p: $P = 0.0442$, log2 fold change = 0.52; miR-181c-5p: $P = 0.0024$, log2 fold change = 0.67; miR-210-3p: $P = 0.0006$, log2 fold change = 0.60). A significant increase was also observed in MCI plasma samples for miR-181c-5p ($P = 0.0004$, log2 fold change = 0.80) and miR-210-3p ($P =$

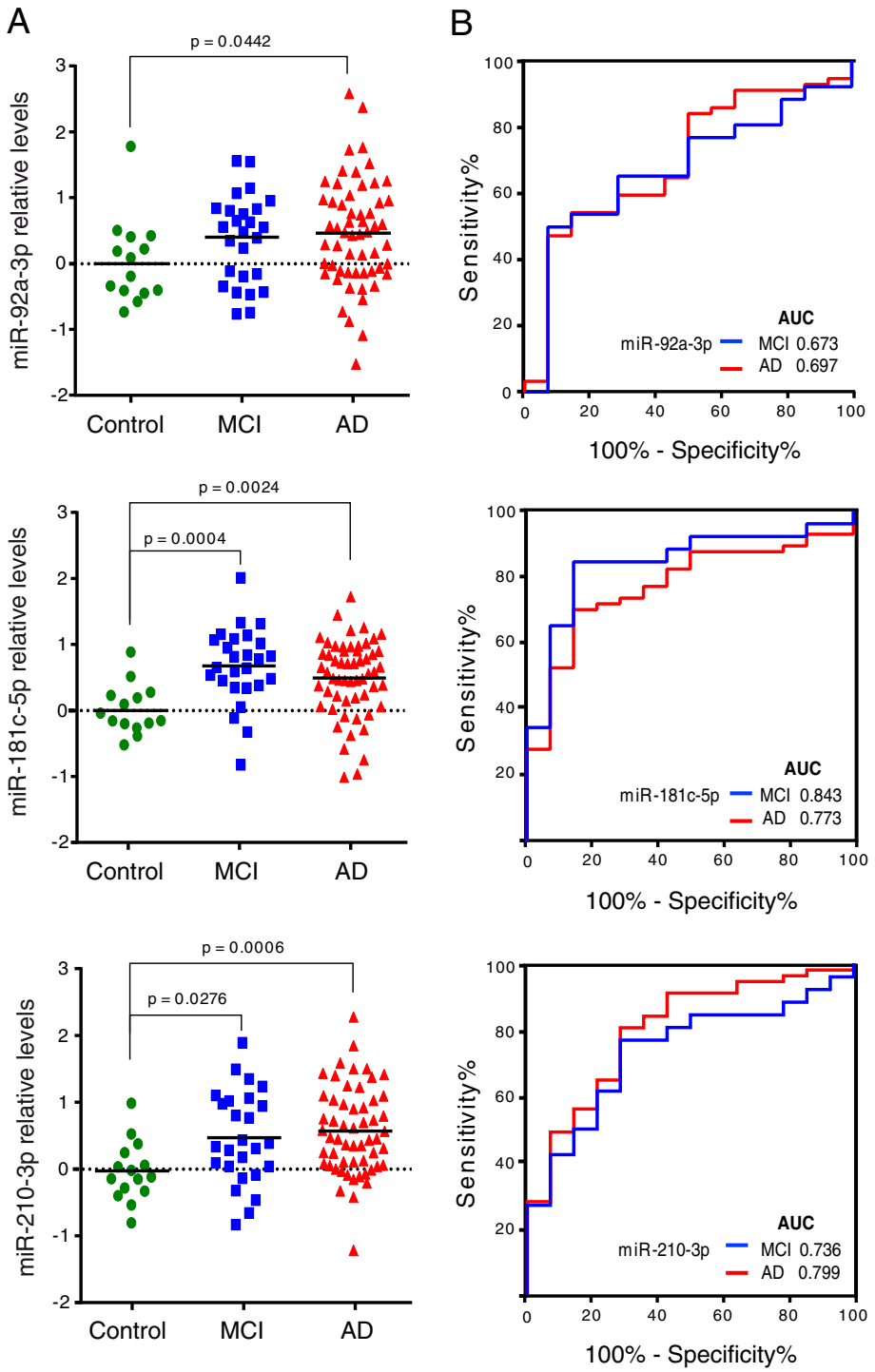

Fig. 1 Circulating miRNA levels at different stages of AD pathology compared with cognitively normal controls (**a**). Log2 transformed data were normalised versus the geometric mean of miR-191-5p and miR-484 levels. Statistical significance was evaluated by the Mann-Whitney *U* test followed by the Bonferroni correction for multiple comparisons. *P* values < 0.05 were considered statistically significant. **b** Receiver operating characteristic (ROC) curve analysis was performed to distinguish MCI (blue) and AD (red) cases from healthy controls. The area under the curve (AUC) is shown for each miRNA and stage

0.0276, log2 fold change = 0.49) whereas an increasing trend was observed for miR-92a-3p ($P = 0.0798$, log2 fold change = 0.55). By contrast, no apparent changes were observed in miR-584-5p expression levels between HC and MCI or AD subjects (data not shown). Statistical correlation analysis revealed that those changes were not due to the increasing age in the MCI and AD groups (Additional file 1: Figure S2). Also, no differences between sexes were observed in HC, MCI and AD groups (Additional file 1: Figure S3).

Next, ROC curve analysis was performed to evaluate the diagnostic potential of miR-92a-3p, miR-181c-5p and miR-210-3p (Fig. 1b). The values obtained for miR-92a-3p, miR-181c-5p and miR-210-3p when HC were compared with MCI subjects were as follows: AUC values of 0.67, 0.84 and 0.74, respectively; 50.00%, 84.62% and 76.92% of sensitivity, respectively; and 92.86%, 85.71% and 71.43% of specificity, respectively (Table 2). AUC values for miR-92a-3p, miR-181c-5p and miR-210-3p when AD subjects were compared to HC were 0.70, 0.77 and 0.80, respectively. Whereas miR-92a-3p has 47.37% of sensitivity and 92.86% of specificity, miR-181c-5p has 70.18% of sensitivity and 85.71% of specificity and miR-210-3p has 80.70% of sensitivity and 71.43% of specificity (Table 3). ROC curve analysis using logistic regression for miR-92a-3p, miR-181c-5p and miR-210-3p combination yielded a better diagnostic value for MCI and AD, suggesting that these miRNAs together could be used as a molecular signature for early diagnosis of MCI and/or AD. We determined an AUC value of 0.893, a sensitivity of 84.62% and a specificity of 85.71% for distinguishing MCI from HC (Fig. 2a and Table 2). This molecular miRNA signature provided an AUC value of 0.855, a sensitivity of 92.86% and a specificity of 71.43% when AD samples were compared to HC (Fig. 2b and Table 3).

We also looked for eventual sex-dependent differences in the diagnostic potential of the examined miRNAs (Fig. 2). We found a slightly better diagnostic value for men than for women to distinguish MCI from HC subjects (Table 2): (a) the AUC values for women and men are 0.82 and 0.96 respectively; (b) 87.50% sensitivity for women and 100% for men; and (c) 71.43% and 85.71% specificity for women and men, respectively. On the other hand, the values obtained when comparing AD with HC subjects indicated a better diagnostic specificity and a lower sensitivity for men than for women (Table 3): (a) the AUC values for women and men are 0.82 and 0.94; (b) 90.24% and 75.00% sensitivity for women and men; and (c) 71.43% and 100% specificity for women and men, respectively.

In order to provide further support to the value of our molecular miRNA signature as a molecular biomarker for early AD diagnosis, we have followed up 19 of the 26 MCI subjects for 1 to 12 years (Additional file 1: Table S3). Three subjects diagnosed as MCI (11.5%; P4, P8 and P22) showed no cognitive impairment after 1 (P4 and P22) or 4 (P8) years, and another two (P14 and P18) were still diagnosed as MCI after 3 and 11 years. The rest of the cases, all developed dementia being AD the most prominent. Only one patient progressed to FTD (P7) and another to vascular dementia (P11; Additional file 1: Table S3). Interestingly, we have observed that all the MCI patients that progressed to AD have higher values of the miRNA signature compared to the MCI patients that did not evolve to AD (Fig. 3).

Expression levels of miR-92a, miR-181c and miR-210 in AD brains

To investigate whether the observed changes in miR-92a-3p, miR-181c-5p and miR-210-3p levels were associated to changes in the brain, we measured their levels in the entorhinal cortex, hippocampus and cerebellum from cognitively normal controls (Braak I/II) and early (Braak III/IV) and late (Braak V/VI) AD patients (Additional file 1: Table S1 and Additional file 1: Figure S1). We found that

Table 2 Individual and signature miRNAs performance characteristics in predicting MCI stage. Signature miRNA performance characteristics in women and men

miRNA/signature	AUC	Sensitivity %	Specificity %	Youden Index J	*P* value
miR-92a-3p	0.673	50.00	92.86	0.428	0.0563
miR-181c-5p	0.843	84.62	85.71	0.703	< 0.0001
miR-210-3p	0.736	76.92	71.43	0.483	0.0038
miR-92a-3p/miR-210-3p	0.731	73.08	71.43	0.445	0.0050
miR-92a-3p/miR-181c-5p	0.838	84.62	78.57	0.632	< 0.0001
miR-181c-5p/miR-210-3p	0.865	88.46	78.57	0.670	< 0.0001
miR-92a-3p/miR-181c-5p/ miR-210-3p	0.893	84.62	85.71	0.703	< 0.0001
Women	0.821	87.50	71.43	0.589	0.0005
Men	0.957	100.0	85.71	0.857	< 0.0001

AUC area under the curve

Table 3 Individual and signature miRNAs performance characteristics in predicting AD. Signature miRNAs performance characteristics in women and men

miRNA/signature	AUC	Sensitivity %	Specificity %	Youden Index J	*P* value
miR-92a-3p	0.697	47.37	92.86	0.402	0.0124
miR-181c-5p	0.773	70.18	85.71	0.559	< 0.0001
miR-210-3p	0.799	80.70	71.43	0.521	< 0.0001
miR-92a-3p/miR-210-3p	0.807	87.72	64.29	0.520	< 0.0001
miR-92a-3p/miR-181c-5p	0.787	84.21	71.43	0.556	0.0001
miR-181c-5p/miR-210-3p	0.853	84.21	78.57	0.628	< 0.0001
miR-92a-3p/miR-181c-5p/ miR-210-3p	0.855	92.86	71.43	0.644	< 0.0001
Women	0.815	90.24	71.43	0.617	0.0009
Men	0.938	75.0	100.0	0.750	< 0.0001

AUC area under the curve

miR-92a-3p, miR-181c-5p and miR-210-3p levels are slightly increased in the entorhinal cortex at early and late AD compared to HC. However, it only reached statistical significance in the case of miR-92a-3p when compared to late AD (Braak V-VI; Additional file 1: Figure S1A), probably due to the small number of samples analysed in this region. A similar trend was observed for miR-92a-3p and miR-181c-5p in the hippocampus (Additional file 1: Figure S1B). No significant changes of miR-210-3p in the hippocampus or in miR92a-3p, miR-181c-5p and miR-210-3p in the cerebellum were observed at any disease stage (Additional file 1: Figure S1B, C). Thus, although there is an overall trend to increase in the hippocampus and entorhinal cortex, it is not possible to conclude that miRNA changes observed in plasma are related to those observed in the brain since they lack global statistical significance. miR-181c-5p has neuronal pentraxin 1 (NPTX1) and neuronal pentraxin receptor (NPTXR) as potential targets. Since miR-181c-5p is increased in the entorhinal cortex, we next examined the protein levels of NPTX1 and NPTXR wanted to check whether this increase coincided with a change in the levels of these proteins. As shown in Additional file 1: Figure S3, we observed a decrease in NPTX1 and NPTXR although it did not reach statistical significance likely due to the low number of samples.

Expression levels of miR92a, miR181c and miR210 are not affected in FTD patients

In order to determine whether the changes observed in miR-92a-3p, miR-181c-5p and miR-210-3p in plasma were specific of MCI and AD subjects, we decided to analyse plasma samples from a cohort of FTD patients. None of the abovementioned miRNAs were altered in FTD (Fig. 4) suggesting that the changes observed could be specific for MCI and AD subjects.

Discussion

The search of blood-based biomarkers for early detection of AD has gained increasing attention during the last decade due to the non-invasiveness of the procedure and its low economical costs when compared to the use of CSF or neuroimaging techniques, which would potentially allow their use in routine tests worldwide. Among the diversity of molecules and factors that could be analysed in blood-derived samples, miRNAs represent one of the most promising approaches to identify peripheral AD biomarkers [7, 17, 20, 46] since they are relatively abundant and highly stable in blood.

Several reports have performed miRNAs profiling in brain and CSF that have identified numerous miRNAs as potential biomarkers to detect AD [46–49]. Whereas some studies have focused on miRNAs regulating specific AD-related proteins, little attention has been devoted to miRNAs involved in the regulation of synaptic proteins. In the present study, we have analysed plasma levels of specific miRNAs related to the regulation of synaptic proteins, especially glutamatergic synapses, in HC, MCI and AD patients. Thus, this work complements other reports that have suggested the potential of miRNAs as biomarkers for AD.

From the different miRNAs analysed, we have observed a significant increase in miR-92a-3p, miR-181c-5p and miR-210-3p plasma levels in MCI and AD. Moreover, an increase in the levels of these three miRNAs was observed in AD entorhinal cortex. However, only miR-92a-3p changes reached statistical significance probably due to the low number of available samples used. No significant changes in hippocampal levels were observed for miR-181c-5p and miR-210-3p. Hence, our data adds on many previous reports indicating that miRNA changes between brain and CSF/plasma samples do not necessarily run in parallel [22].

Among other targets, miR181c-5p and miR-210-3p have neuronal pentraxin 1 (NPTX1) and neuronal

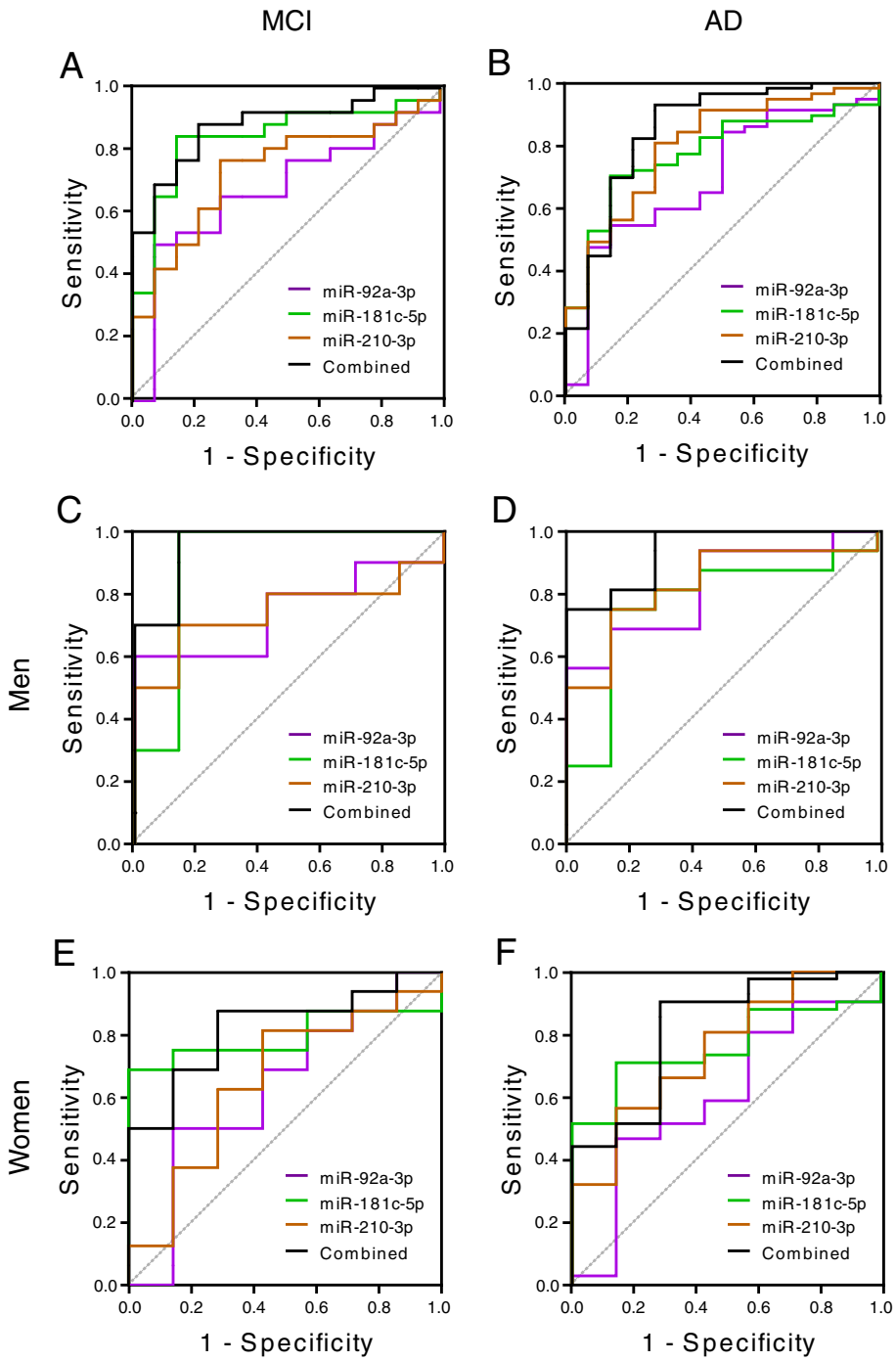

Fig. 2 miRNAs were combined to reach the best predictive value. ROC curve analysis for MCI (**a**) and AD (**b**) cases are shown. Values for men (**c**, **d**) and women (**e**, **f**) are represented separately

pentraxin receptor (NPTXR) as potential targets. Indeed, it has been described that miR-210-3p regulates the expression of NPTX1 and NPTXR [50]. These proteins are involved in the recruitment and clustering of AMPA receptors in postsynaptic terminals, organising and modelling the activity of glutamatergic synapses in the hippocampus affecting their synaptic plasticity [51, 52]. Thus, an increase of these miRNAs would reduce the levels of NPTX1 and NPTXR and could contribute to the glutamatergic synaptic dysfunction and early cognitive impairment present in AD prior to neurodegeneration. In fact, the increase in miR-181c-5p coincided with a decrease in NPTX1 and NPTXR protein in the entorhinal cortex.

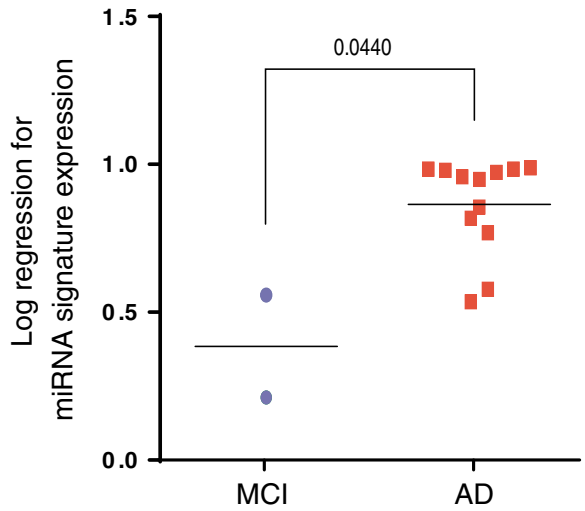

Fig. 3 MCI patients were separated according to follow-up diagnosis. From 26 patients diagnosed as MCI in the first place, 2 remained stable and 12 have progressed to AD (see Additional file 1: Table S3). miRNA expression levels were combined using log regression approach. Mean of miRNA signature values for each group is shown. Statistical significance was evaluated by the Mann-Whitney *U* test. *P* values < 0.05 were considered statistically significant

Based on the observed increase in miR-92a-3p, miR-181c-5p and miR-210-3p, we propose that these miRNAs constitute a molecular signature that could be used as a biomarker for MCI and AD. The AUC values of this molecular signature are similar (0.893 accuracy, 84.6% sensitivity and 85.71% sensitivity) to the ones obtained in other studies that have proposed either a 12-miRNA signature that distinguishes MCI with 0.842 accuracy, 81.1% specificity and 87.7% sensitivity in blood [29] or a 9-miRNAs serum signature for AD cases identification with an AUC value of 0.978, 93.4% sensitivity and 98.8% of specificity [53]. Our results are the first that described an alteration of miR-92a-3p and miR-210-3p levels in biological fluids from AD patients. Only a previous report showed that soluble Aβ secreted from 7PA2 cells produced an increase in miR-210 levels in a mature primary culture of cortical neurons [54] and another study by Cogswell and co-workers reported that the levels of miR-92 were enhanced in AD hippocampus [47]. On the other hand, the observed increase in miR-181c-5p in plasma of MCI and AD subjects is challenged by previous reports reporting opposite observations. For instance, a decrease in miR-181c levels was reported in serum [20, 30, 53] and CSF [47] from AD patients. The causes of these discrepancies are currently unclear.

We were able to follow up for several years the evolution of the MCI patients included in our study, and we observed that the signature values in the plasma of the MCI patients that progressed to AD were significantly higher than the values found in the MCI patients that did not progress to dementia. Thus, plasma levels of miR-92a-3p, miR-181c-5p and miR-210-3p could not only be used as a biomarker signature for MCI and AD but might also indicate whether a patient with MCI will progress to AD. To our knowledge, this is the first study in which miRNAs levels in MCI patients are associated with the diagnosis of AD. However, we are aware that due to the low number of MCI patients that did not progress to AD, further studies with more samples should be done before we can conclude that plasma levels of miR-92a-3p, miR-181c-5p and miR-210-3p are a good prognostic signature for the progression from MCI to AD.

Several studies have shown that AD-associated changes in miRNAs expression are also found in other types of dementia such as frontotemporal dementia or dementia with Lewy bodies [55]. Thus, those miRNAs could not be considered as eventual specific biomarkers

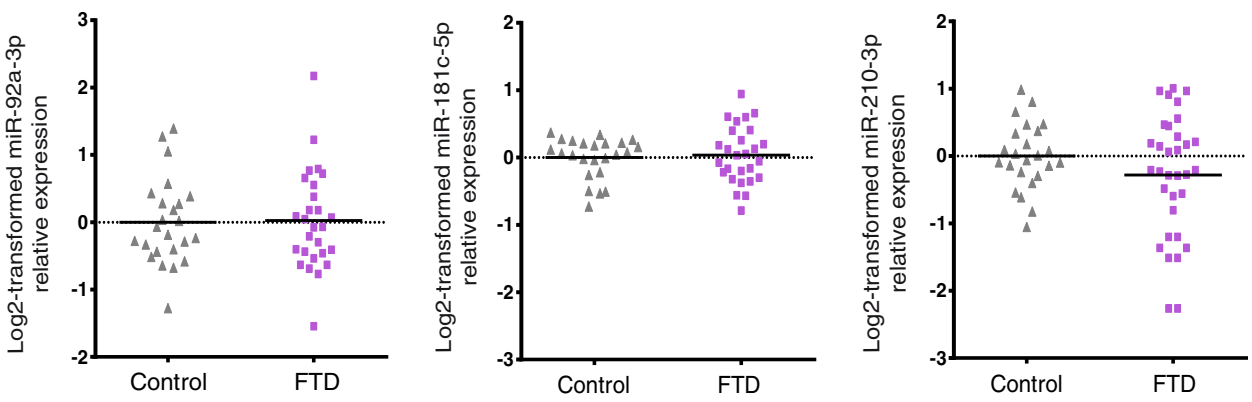

Fig. 4 Plasma miRNA levels in FTD compared to cognitively normal controls. Log2 transformed data were normalised versus the geometric mean of miR-191-5p and miR-484 levels. Statistical significance was evaluated by the Mann-Whitney *U* test. *P* values < 0.05 were considered statistically significant

for AD. For example, some reports have shown that miR-132 levels are downregulated in AD [46, 49, 56] and similar results were obtained in other neurodegenerative diseases [19, 55, 57], suggesting that the alteration of this miRNA is linked to common pathological mechanisms in neurodegenerative diseases. In order to know whether this coincidence was also observed with miR-92a-3p, miR-181c-5p and miR-210-3p levels, we analysed their levels in plasma samples from a cohort of FTD patients. The results obtained indicate that no changes exist in our molecular miRNA signature between HC and FTD samples, suggesting that the increase in miR-92a-3p, miR-181c-5p and miR-210-3p levels could be specific for AD.

The existence of sex differences in AD is well established. Not only in the prevalence but also in the severity of the disease progression, being suggested that women could be more susceptible than men to the neuropathological cascade of AD [58]. Thus, it has become more necessary to introduce the effects of sex in the studies [59]. We have analysed whether differences exist between men and women and we did not find significant differences between sexes neither in the levels of the miRNAs nor in their value as a molecular signature. Only a slightly higher AUC was obtained in men to predict MCI (0.957 vs 0.821) or AD (0.938 vs 0.815) compared to women. Thus, data from the studied cohort supports that our miRNA signature would be equally effective as a biomarker for AD in both men and women.

In summary, this study provides data supporting that a plasma miRNA signature composed of miR-92a-3p, miR-181c-5p and miR-210-3p could be useful as a non-invasive clinical biomarker for diagnosis of AD that could be used for improving current clinical trials and in future therapeutic strategies. Moreover, the levels of these miRNAs in MCI patients could predict the progression to AD dementia. Further studies are needed to assess whether changes in this miRNA signature correlates with known AD biomarkers. Likewise, obtaining additional data from other MCI and AD cohorts would be necessary to fully validate the data presented in this study and to establish this miRNA signature as a reliable biomarker for early stages of AD.

Conclusions

Deficits in synaptic function are likely to be involved in the development of AD in its preclinical stages. Here, we have analysed the levels of specific miRNAs related to synaptic proteins finding that the levels of miR-92a-3p, miR-181c-5p and miR-210-3p are deregulated in plasma from MCI and AD subjects while no changes are observed in plasma from FTD patients. Moreover, the analysis combining these three miRNAs yielded high diagnosis accuracy for distinguishing both MCI and AD subjects from healthy controls and could also predict MCI progress to AD. Thus, we propose plasma levels of miR-92a-3p, miR-181c-5p and miR-210-3p as a molecular signature to be used as a novel biomarker for AD.

Additional file

Additional file 1: Figure S1. miRNA levels in human entorhinal cortex (A), hippocampus (B) and cerebellum (C) at different stages of AD pathology compared with cognitively healthy controls. **Figure S2.** Correlation plots for plasma miRNAs expression levels vs age. **Figure S3.** Circulating miRNAs levels comparison between sexes. **Figure S4.** NPTX1 and NPTXR protein levels in AD human entorhinal cortex. **Table S1.** Tissue samples information. **Table S2.** Validated miRNA-target interactions for candidate miRNAs based on miRWalk2.0 database. Only selected synaptic-related targets are shown. **Table S3.** Follow-up of MCI patients. (PDF 1295 kb)

Abbreviations

AD: Alzheimer's disease; AUC: Area under the curve; CSF: Cerebrospinal fluid; FTD: Frontotemporal dementia; HC: Healthy controls; MCI: Mild cognitive impairment; miRNAs: MicroRNAs; NPTX1: Neuronal pentraxin 1; NPTXR: Neuronal pentraxin receptor; ROC: Receiver operating characteristic; RT-qPCR: Quantitative real-time PCR

Acknowledgements

"Not applicable"

Funding

This work was supported by grants from Ministerio de Ciencia, Innovación y Universidades (SAF2014-59697-R; SAF2017-89271-R), Fundació La Marató TV3 (TV3-2014-3610), CIBERNED (CB06/05/0042 and PI2017/01) and Generalitat de Catalunya (SGR2014-0984 and SGR2017-749) to JRA and by the Department de Salut de la Generalitat de Catalunya, Pla Estratègic de Recerca I Innovació en Salut (SLT002/16/00408) to AL. DSW was supported by the Fundació La Marató TV3. JCS is a recipient of a Ph.D. Fellowship from the Ministerio de Ciencia, Innovación y Universidades. CF is a recipient of a Ph.D. Fellowship from the Department of Biochemistry and Molecular Biology of the Universitat Autònoma de Barcelona.

Availability of data and materials

The datasets used and/or analysed during the current study is available from the corresponding authors on reasonable request.

Authors' contributions

JRA and AJMM conceived and designed the study. DSW performed the experiments. IH, MB and AL participated in the clinical diagnosis of subjects and the collection of serum. DSW, JCS and CF analysed the data. DSW, JRA and AJMM wrote the manuscript. CAS, JC and AL gave critical opinion and revised the written manuscript. All authors read and approved the final manuscript.

Ethics approval and consent to participate

All patients or their relatives gave written consent for plasma extraction and inclusion in the experimental cohorts. All clinical investigations were conducted according to the principles expressed in the Declaration of Helsinki, carried out according to the international Good Laboratory Practice (GLP) and Good Clinical Practice (GCP) standards and approved by the institution ethics committee.
Human brain tissue was provided by the Brain Bank of the Fundación CIEN, the BioBank of the Hospital Clinic-IDIBAPS and the Hospital Universitario Fundación Alcorcón following the guidelines of Spanish legislation.

Consent for publication

"Not applicable"

Competing interests

The authors declare that they have no potential competing interests.

Publisher's Note

Author details
[1]Institut de Neurociències and Dpt. Bioquímica i Biología Molecular, Universitat Autònoma de Barcelona, 08193 Cerdanyola del Vallès, Spain. [2]Centro de Investigación Biomédica en Red sobre Enfermedades Neurodegenerativas (CIBERNED), Madrid, Spain. [3]Research Center and Memory Clinic, Fundació ACE, Institut Català de Neurociències Aplicades, Universitat Internacional de Catalunya, Barcelona, Spain. [4]Memory Unit, Department of Neurology, Institut d'Investigacions Biomèdiques Sant Pau - Hospital de Sant Pau, Universitat Autònoma de Barcelona, Barcelona, Spain. [5]Dominick P. Purpura Department of Neuroscience, Albert Einstein College of Medicine, New York, NY 10461, USA.

Received: 13 February 2019 Accepted: 28 April 2019
Published online: 15 May 2019

References

1. Polanco JC, Li C, Bodea LG, Martinez-Marmol R, Meunier FA, Götz J. Amyloid-β and tau complexity-towards improved biomarkers and targeted therapies. Nat Rev Neurol. 2018;14:22–39.
2. Honig LS, Vellas B, Woodward M, Boada M, Bullock R, Borrie M, et al. Trial of solanezumab for mild dementia due to Alzheimer's disease. N Engl J Med. 2018;378:321–30.
3. Egan MF, Kost J, Tariot PN, Aisen PS, Cummings JL, Vellas B, et al. Randomized trial of Verubecestat for mild-to-moderate Alzheimer's disease. N Engl J Med. 2018;378:1691–703.
4. Lleó A, Cavedo E, Parnetti L, Vanderstichele H, Herukka SK, Andreasen N, et al. Cerebrospinal fluid biomarkers in trials for Alzheimer and Parkinson diseases. Nat Rev Neurol. 2015;11:41–55.
5. Blennow K, Mattsson N, Schöll M, Hansson O, Zetterberg H, et al. Amyloid biomarkers in Alzheimer's disease. Trends Pharmacol Sci. 2015;36:297–309.
6. Zetterberg H. Tau in biofluids - relation to pathology, imaging and clinical features. Neuropathol Appl Neurobiol. 2015;43:194–9.
7. Jack CR Jr, Knopman DS, Jagust WJ, Petersen RC, Weiner MW, Aisen PS, et al. Tracking pathophysiological processes in Alzheimer's disease: an updated hypothetical model of dynamic biomarkers. Lancet Neurol. 2013;12:207–16.
8. Kadmiri NE, Said N, Slassi I, Moutawakil BE, Nadifi S, et al. Biomarkers for Alzheimer disease: classical and novel candidate's review. Neuroscience. 2018;370:181–90.
9. Frisoni GB, Boccardi M, Barkhof F, Blennow K, Cappa S, Chiotis K, et al. Strategic roadmap for an early diagnosis of Alzheimer's disease based on biomarkers. Lancet Neurol. 2017;16:661–76.
10. Forner S, Baglietto-Vargas D, Martini AC, Trujillo-Estrada L, LaFerla FM. Synaptic impairment in Alzheimer's disease: a dysregulated symphony. Trends Neurosci. 2017;40:347–57.
11. Miñano-Molina AJ, España J, Martin E, Barneda-Zahonero B, Fado R, Sole M, et al. Soluble oligomers of amyloid-beta peptide disrupt membrane trafficking of alpha-amino-3-hydroxy-5-methylisoxazole-4-propionic acid receptor contributing to early synapse dysfunction. J Biol Chem. 2011;286:27311–21.
12. Roselli F, Hutzler P, Wegerich Y, Livrea P, Almeida OFX. Disassembly of shank and Homer synaptic clusters is driven by soluble β-amyloid$_{1-40}$ through divergent NMDAR-dependent signalling pathways. PLoS One. 2009;4:e6011. https://doi.org/10.1371/journal.pone.0006011.
13. Reddy PH, Mani G, Park BS, Jacques J, Murdoch G, Whetsell W Jr, et al. Differential loss of synaptic proteins in Alzheimer's disease: implications for synaptic dysfunction. J Alzheimers Dis. 2005;7:103–17.
14. Casaletto KB, Elahi FM, Bettcher BM, Neuhaus J, Bendlin BB, Asthana S, et al. Neurogranin, a synaptic protein, is associated with memory independent of Alzheimer biomarkers. Neurology. 2017;89:1782–8.
15. Schratt G. microRNAs at the synapse. Nat Rev Neurosci. 2009;10:842–9.
16. Im HI, Kenny PJ. MicroRNAs in neuronal function and dysfunction. Trends Neurosci. 2012;35:325–34.
17. Lau P, Bossers K, Janky R, Salta E, Frigerio CS, Barbash S, et al. Alteration of the microRNA network during the progression of Alzheimer's disease. EMBO Mol Med. 2013;5:1613–34.
18. Hébert SS, Horré K, Nicolaï L, Bergmans B, Papadopoulou AS, Delacourte A, et al. MicroRNA regulation of Alzheimer's amyloid precursor protein expression. Neurobiol Dis. 2009;33:422–8.
19. Nelson PT, Wang WX. MiR-107 is reduced in Alzheimer's disease brain neocortex: validation study. J Alzheimers Dis. 2010;21:75–9.
20. Salta E, De Strooper B. microRNA-132: a key noncoding RNA operating in the cellular phase of Alzheimer's disease. FASEB J. 2017;31:424–33.
21. Geekiyanage H, Jicha GA, Nelson PT, Chan C. Blood serum miRNA: non-invasive biomarkers for Alzheimer disease. Exp Neurol. 2012;235:491–6.
22. Sala-Frigerio C, Pau P, Salta E, Tournoy J, Bossers K, Vandenberghe R, et al. Reduced expression of hsa-miR-27a-3p in CSF of patients with Alzheimer disease. Neurology. 2013;81:2103–6.
23. Müller M, Kuiperij HB, Claassen JA, Küsters B, Verbeek MM. MicroRNAs in Alzheimer's disease: differential expression in hippocampus and cell-free cerebrospinal fluid. Neurobiol Aging. 2014;35:152–8.
24. Denk J, Boelmans K, Siegismund C, Lassner D, Arlt S, Jahn H. MicroRNA profiling of CSF reveals potential biomarkers to detect Alzheimer's disease. PLoS One. 2015;10(5):e0126423.
25. Hara N, Kikuchi M, Miyashita A, Hatsuta H, Saito Y, Kasuga K, et al. Serum microRNA miR-501-3p as a potential biomarker related to the progression of Alzheimer's disease. Acta Neuropathol Commun. 2017;5:10. https://doi.org/10.1186/s40478-017-0414-z.
26. Kalani A, Tyagi A, Tyagi N. Exosomes: mediators of neurodegeneration, neuroprotection and therapeutics. Mol Neurobiol. 2014;49:590–600.
27. Riancho J, Vazquez-Higuera JL, Pozueta A, Lage C, Kazimierczak M, Bravo M, et al. MicroRNA profile in patients with Alzheimer's disease: analysis of miR-9-5p and miR-598 in raw and exosome enriched cerebrospinal fluid samples. J Alzheimers Dis. 2017;57:483–91.
28. Zetterberg H, Blennow K. From cerebrospinal fluid to blood: the third wave of fluid biomarkers for Alzheimer's disease. J Alzheimers Dis. 2018;64:S271–9.
29. Sheinerman KS, Tsivinsky VG, Abdullah L, Crawford F, Umansky SR. Plasma microRNA biomarkers for detection of mild cognitive impairment: biomarker validation study. Aging. 2013;5:925–38.
30. Leidinger P, Backes C, Deutscher S, Schmitt K, Mueller SC, Frese KA. Blood based 12-miRNA signature of Alzheimer disease patients. Genome Biol. 2013;14:R78.
31. Tan L, Yu JT, Tan MS, Liu QY, Wang HF, Zhang W. Genome-wide serum microRNA expression profiling identifies serum biomarkers for Alzheimer's disease. J Alzheimers Dis. 2014;40:1017–27.
32. Nagaraj S, Laskowska-Kaszub K, Debski KJ, Wojsiat J, Dabrowski M, Gabryelewicz T, et al. Profile of 6 microRNA in blood plasma distinguish early stage Alzheimer's disease patients from non-demented subjects. Oncotarget. 2017;8:16122–43.
33. Cosín-Tomás M, Antonell A, Lladó A, Alcolea D, Fortea J, Ezquerra M, Lleó A, et al. Plasma miR-34a-5p and miR-545-3p as early biomarkers of Alzheimer's disease: potential and limitations. Mol Neurobiol. 2017;54:5550–62.
34. Illán-Gala I, Alcolea D, Montal V, Dols-Icardo O, Muñoz L, de Luna N, et al. CSF sAPPβ, YKL-40, and NfL along the ALS-FTD spectrum. Neurology. 2018;91:e1619–28.
35. Petersen RC, Smith GE, Waring SC, Ivnik RJ, Tangalos EG, Kokmen E. Mild cognitive impairment: clinical characterization and outcome. Arch Neurol. 1999;56:303–8.
36. Espinosa A, Alegret M, Valero S, Vinyes-Junque G, Hernandez I, Mauleon A, et al. A longitudinal follow-up of 550 mild cognitive impairment patients: evidence for large conversion to dementia rates and detection of major risk factors involved. J Alzheimers Dis. 2013;34:769–80.
37. Rascovsky K, Hodges JR, Knopman D, Mendez MF, Kramer JH, Neuhaus J, et al. Sensitivity of revised diagnostic criteria for the behavioural variant of frontotemporal dementia. Brain. 2011;134:2456–77.
38. Gorno-Tempini ML, Hillis AE, Weintraub S, Kertesz A, Mendez M, Cappa SF, et al. Classification of primary progressive aphasia and its variants. Neurology. 2011;15:1006–14.
39. Brooks BR, Miller RG, Swash M, Munsat TL. El Escorial revisited: revised criteria for the diagnosis of amyotrophic lateral sclerosis. Amyotroph Lateral Scler Other Motor Neuron Disord. 2000;1(5):293–9.
40. Moldovan L, Batte KE, Trgovcich J, Wisler J, Marsh CB, Piper M. Methodological challenges in utilizing miRNAs as circulating biomarkers. J Cell Mol Med. 2014;18:371–90.
41. Fortunato O, Boeri M, Verri C, Conte D, Mensah M, Suatoni P, Pastorino U, et al. Assessment of circulating microRNAs in plasma of lung cancer patients. Molecules. 2014;19:3038–54.
42. Vennemann M, Koppelkamm A. Postmortem mRNA profiling II: practical considerations. Forensic Sci Int. 2010;203:76–82.
43. Pfaffl MW. A new mathematical model for relative quantification in real-time RT-PCR. Nucleic Acids Res. 2001;29:45e–45.

44. Andersen CL, Jensen JL, Ørntoft TF. Normalization of real-time quantitative reverse transcription-PCR data: a model-based variance estimation approach to identify genes suited for normalization, applied to bladder and color cancer data sets. Cancer Res. 2004;64:5245–50.
45. Vandesompele J, De Preter K, Pattyn F, Poppe B, Van Roy N, De Paepe A, et al. Accurate normalization of real-time quantitative RT-PCR data by geometric averaging of multiple internal control genes. Genome Biol. 2002; 3:34–1.
46. Cogswell JP, Ward J, Taylor IA, Waters M, She Y, Cannon B, et al. Identification of miRNA changes in Alzheimer's disease brain and CSF yields putative biomarkers and insights into disease pathways. J Alzheimers Dis. 2008;14:27–41.
47. Nunez-Iglesias J, Liu CC, Morgan TE, Finch CE, Zhou XJ. Joint genome-wide profiling of miRNA and mRNA expression in Alzheimer's disease cortex reveals altered miRNA regulation. PLoS One. 2010;5:e8898.
48. Wiedrick JT, Phillips JI, Lusardi TA, McFarland TJ, Lind B, Sandau US, et al. Validation of microRNA biomarkers dor Alzheimer disease in human cerebrospinal fluid. J Alzheimers Dis. 2019;67:875-91.
49. Pichler S, Gu W, Hartl D, Gasparoni G, Leidinger P, Keller A, et al. The miRNome of Alzheimer's disease: consistent down regulation of the miR-132/212 cluster. Neurobiol Aging. 2016;167:e1–167 e10.
50. Pulkkinen K, Malm T, Turunen M, Koistinaho J, Ylä-Herttuala S. Hypoxia induces microRNA miR-210 in vitro and in vivo ephrin-A3 and neuronal pentraxin 1 are potentially regulated by miR-210. Have as a predicted target. FEBS Lett. 2008;582:2397–401.
51. Pelkey KA, Barksdale E, Craig MT, Yuan X, Sukumaran M, Vargish GA, et al. Pentraxins coordinante excitatory synapse maturation and circuit integration of parvalbumin interneurons. Neuron. 2015;85:1257–72.
52. Lee SJ, Wei M, Zhang C, Maxeiner S, Pak C, Calado Boteho S, et al. Presynaptic neuronal pentraxin receptor organizes excitatory and inhibitory synapses. J Neurosci. 2017;37:1062–80.
53. Guo R, Fan G, Zhang J, Wu C, Du Y, Ye H, et al. A 9-microRNA signature in serum serves as a noninvasive biomarker in early diagnosis of Alzheimer's disease. J Alzheimers Dis. 2017;60:1365–77.
54. Li JJ, Dolios G, Wang R, Liao FF. Soluble beta-amyloid peptides, but not insoluble fibrils, have specific effect on neuronal microRNA expression. PLoS One. 2014;9:e90770.
55. Hébert SS, Wang WX, Zhu Q, Nelson PT. A study of small RNAs from cerebral neocortex of pathology-verified Alzheimer's disease, dementia with Lewy bodies, hippocampal sclerosis, frontotemporal lobar dementia, and non-demented human controls. J Alzheimers Dis. 2013;35:335–48.
56. Zhu QB, Unmehopa U, Bossers K, Hu YT, Verwer R, Balesar R, et al. Micro-RNA-132 and early growth response-1 in nucleus basalts of Meynert during the course of Alzheimer's disease. Brain. 2016;139:908–21.
57. Chen-Plotkin AS, Unger TL, Gallagher MD, Bill E, Kwong LK, Volpicelli-Daley L, et al. TMEM106B, the risk gene for frontotemporal dementia, is regulated by the microRNA-132/212 cluster and affects progranulin pathways. J Neurosci. 2012;32:11213–27.
58. Sinforiani E, Citterio A, Zucchella C, Bono G, Corbetta S, Merlo P, et al. Impact of gender differences on the outcome of Alzheimer's disease. Dementia. 2010;30:147–54.
59. Mazure CM, Swendsen J. Sex differences in Alzheimer's disease and other dementias. Lancet Neurol. 2016;15:451–2.

3.- Cheng, Wenwen, Dolores Siedlecki-Wullich, Judit Català-Solsona, Cristina Fábregas, Rut Fadó, Núria Casals, Montse Solé, et al. 2020. "Proteasomal-Mediated Degradation of Akap150 Accompanies Ampar Endocytosis during Cltd." ***ENeuro*** **7 (2): 1–19. https://doi.org/10.1523/ENEURO.0218-19.2020**

eNeuro

Research Article: New Research

Neuronal Excitability

Proteasomal-Mediated Degradation of AKAP150 Accompanies AMPAR Endocytosis during cLTD

Wenwen Cheng,[1,2] Dolores Siedlecki-Wullich,[1,2] Judit Català-Solsona,[1,2] Cristina Fábregas,[1,2] Rut Fadó,[3] Núria Casals,[3,4] Montse Solé,[1,5] Mercedes Unzeta,[1] Carlos A. Saura,[1,2] José Rodríguez-Alvarez,[1,2,6] and Alfredo J. Miñano-Molina[1,2]

https://doi.org/10.1523/ENEURO.0218-19.2020

[1]Institut de Neurociències and Dpt. Bioquímica i Biologia Molecular, Universitat Autònoma de Barcelona, Cerdanyola del Vallès 08193, Spain, [2]Centro de Investigación Biomédica en Red sobre Enfermedades Neurodegenerativas (CIBERNED), Madrid 28031, Spain, [3]Basic Sciences Department, Facultat de Medicina i Ciències de la Salut, Universitat Internacional de Catalunya (UIC), Sant Cugat del Vallès 08195, Spain, [4]Centro de Investigación Biomédica en Red de Fisiopatología de la Obesidad y la Nutrición (CIBEROBN), Instituto de Salud Carlos III, Madrid E-28029, Spain, [5]Neurovascular Research Laboratory, Vall d'Hebron Institute of Research, Universitat Autònoma de Barcelona, Barcelona 08035, Spain, and [6]Dominick P. Purpura Department of Neuroscience, Albert Einstein College of Medicine, New York, NY 10461

Abstract

The number and function of synaptic AMPA receptors (AMPARs) tightly regulates excitatory synaptic transmission. Current evidence suggests that AMPARs are inserted into the postsynaptic membrane during long-term potentiation (LTP) and are removed from the membrane during long-term depression (LTD). Dephosphorylation of GluA1 at Ser-845 and enhanced endocytosis are critical events in the modulation of LTD. Moreover, changes in scaffold proteins from the postsynaptic density (PSD) could be also related to AMPAR regulation in LTD. In the present study we analyzed the effect of chemical LTD (cLTD) on A-kinase anchoring protein (AKAP)150 and AMPARs levels in mouse-cultured neurons. We show that cLTD induces AKAP150 protein degradation via proteasome, coinciding with GluA1 dephosphorylation at Ser-845 and endocytosis of GluA1-containing AMPARs. Pharmacological inhibition of proteasome activity, but not phosphatase calcineurin (CaN), reverted cLTD-induced AKAP150 protein degradation. Importantly, AKAP150 silencing induced dephosphorylation of GluA1 Ser-845 and GluA1-AMPARs endocytosis while AKAP150 overexpression blocked cLTD-mediated GluA1-AMPARs endocytosis. Our results provide direct evidence that cLTD-induced AKAP150 degradation by the proteasome contributes to synaptic AMPARs endocytosis.

Key words: AKAP150; AMPAR; LTD; LTP; plasticity; trafficking

Significance Statement

Multiple evidences have shown that changes in glutamatergic synaptic AMPA receptors (AMPARs) modulate excitatory synaptic plasticity, playing a fundamental role in learning and memory-related processes such as long-term potentiation (LTP) or long-term depression (LTD). AMPARs are inserted in the synapses during LTP and removed during LTD although the mechanisms involved in synaptic AMPARs dynamics are not fully understood. Here, we show that chemical LTD (cLTD)-dependent proteasome degradation of A-kinase anchoring protein (AKAP)150, a scaffold protein from the postsynaptic density (PSD), is related to synaptic AMPARs removal during cLTD whereas restored AKAP150 levels blocks cLTD-mediated endocytosis of AMPARs. Thus, our findings expand our understanding of the regulatory role of AKAP150 on AMPARs dynamics at glutamatergic synapses.

Introduction

NMDA receptor-dependent long-term potentiation (LTP) and long-term depression (LTD) in excitatory hippocampal synapses are believed to play a fundamental role in learning and memory. Several reports have shown that changes in synaptic AMPA receptor (AMPAR) number, properties or subunits composition are involved in LTP and LTD (Huganir and Nicoll, 2013). It is now well established that LTP involves the modulation of AMPARs that are already present at the synapse and/or the rapid recruitment of new AMPARs from extrasynaptic sites to the synapse (Benke et al., 1998; Park et al., 2004; Makino and Malinow, 2009; Petrini et al., 2009). On the other hand, removal of synaptic AMPARs from synapses and even their degradation, seem to be fundamental issues for LTD (Beattie et al., 2000; Ehlers 2000; Lee et al., 2000).

It has been described that membrane insertion of GluA1-containing AMPARs is regulated by cAMP-dependent protein kinase (PKA), Ca^{2+}/calmodulin-dependent protein kinase II (CaMKII), and protein kinase C (PKC) phosphorylation of Ser-845, Ser-831, and Ser-818, respectively (Mammen et al., 1997; Song and Huganir, 2002; Esteban et al., 2003; Boehm et al., 2006). Among them, PKA-mediated phosphorylation of Ser-845 seems to be essential for new AMPARs recruitment to extrasynaptic sites and was proposed to represent a necessary event for the establishment of LTP (Esteban et al., 2003; Makino and Malinow, 2009; Lee et al., 2010). Activity-dependent AMPAR exocytosis at extrasynaptic sites during LTP also depends on the binding of complexin to a postsynaptic unique SNARE complex (Ahmad et al., 2012; Jurado et al., 2013). However, extrasynaptic AMPARs delivery and lateral diffusion to the synapse are necessary but not sufficient for LTP because AMPARs reaching the synapse are not necessarily retained (Ehlers et al., 2007; Petrini et al., 2009). Synaptic retention of AMPARs occurs mainly through binding with transmembrane AMPAR regulatory proteins (TARPs) and PDZ-containing scaffolding proteins present in the postsynaptic density (PSD) such as Stargazin or PSD95 (Ehrlich and Malinow, 2004; Kim and Sheng, 2004; Elias et al., 2006; Opazo et al., 2010).

In contrast to LTP, removal of synaptic AMPARs during LTD seems to be mediated by clathrin-dependent endocytosis (Beattie et al., 2000; Man et al., 2000) followed by activation of degradation or recycling pathways (Ehlers 2000). LTD triggered by NMDA receptor activation is Ca^{2+}-dependent and requires the activation of phosphatases that dephosphorylate AMPARs and their associated proteins to promote the destabilization of synaptic AMPARs, lateral diffusion to extrasynaptic sites and endocytosis (Mulkey et al., 1994; Lee et al., 1998, 2000; Tomita et al., 2004). For instance, dephosphorylation of GluA1 Ser-845 by PP2B (calcineurin; CaN) is necessary for LTD-mediated synaptic AMPARs removal (Oh et al., 2006; Lee et al., 2010). Since PKA-mediated phosphorylation of Ser-845 is needed for LTP priming, fine-tuning of PKA/CaN activity is determinant for the insertion or removal of synaptic AMPARs during LTP/LTD. On the other hand, CaMKII is also emerging as an additional requirement for LTD, reducing synaptic location of GluA1-containing AMPAR and thus, producing synaptic depression (Lu et al., 2010; Coultrap et al., 2014).

A-kinase anchoring protein 79 (AKAP79; in human) or AKAP150 (the rodent homolog) is a postsynaptic scaffold protein that anchors PKA, PKC, and CaN to the PSD, regulating AMPAR phosphorylation, trafficking and activity associated with LTP and LTD (Tavalin et al., 2002; Smith et al., 2006; Lu et al., 2007, 2008; Tavalin, 2008; Jurado et al., 2010; Sanderson et al., 2012). AKAP79/150 is linked to both AMPAR and NMDAR by additional binding to the membrane-associated guanylate kinase (MAGUK) scaffold proteins SAP97 and PSD95 (Colledge et al., 2000; Bhattacharyya et al., 2009; Robertson et al., 2009). All of them are S-palmitoylated in an activity-dependent manner controlling their targeting to dendritic spines and regulating trafficking, spine enlargement and synaptic function (Fukata and Fukata, 2010; Keith et al., 2012; Purkey et al., 2018). Recently, it has been reported that LTD induces removal of synaptic AKAP79/150 via CaMKII (Woolfrey et al., 2018) contributing, together with the regulation of PKA/CaN, to synaptic GluA1-AMPARs removal. Thus, antagonistic regulation of PKA, CaN and CaMKII activities together with the cycling of AKAP79/150 in and out the synapses are major molecular mechanisms controlling synaptic AMPARs. However, it is still unknown whether degradation of AKAP79/150 is triggered by LTD and whether it could be associated to AMPARs endocytosis.

Received June 6, 2019; accepted March 2, 2020; First published March 16, 2020.

The authors declare no competing financial interests.

Author contributions: J.R.-A. and A.J.M.-M. designed research; W.C., D.S.-W., J.C.-S., C.F., and A.J.M.-M. performed research; R.F., N.C., M.S., and M. U. contributed unpublished reagents/analytic tools; W.C., D.S.-W., C.A.S., J. R.-A., and A.J.M.-M. analyzed data; J.R.-A. and A.J.M.-M. wrote the paper.

This work was partially supported by grants from Ministerio de Economia y Competitividad (SAF2014-59697-R, SAF2017-89271-R, and SAF2017-83813-C3-3-R), the Centro de Investigación Biomédica en Red sobre Enfermedades Neurodegenerativas Grant CB06/05/0042, the Centro de Investigación Biomédica en Red de Fisiopatología de la Obesidad y la Nutrición Grant CB06/03/0001, Fundació La Marató de TV3 Grants 2014-3610 and 201627.30.31, and Generalitat de Catalunya Grants SGR2009-1231 and SGR2014-0984 (to J.R.-A. and N.C.). W.C. was a recipient of a PhD fellowship from the China Scholarship Council. J.C.-S. is supported by a FPU (Formación del Profesorado Universitario) fellowship from Ministerio de Economía y Competitividad. C.F. is supported by a PIF (Personal Investigador en Formación) fellowship from Unitat de Bioquímica, Departament de Bioquímica I Biologia Molecular, in UAB (Universitat Autònoma de Barcelona). UC Davis/National Institutes of Health (NIH) NeuroMabs Facility provided the SAP97 monoclonal antibody supported by NIH Grant U24NS050606 and maintained by the Department of Neurobiology, Physiology, and Behavior, College of Biological Sciences, University of California, Davis, CA 95616.

Acknowledgements: We thank Dr. John D. Scott (Howard Hughes Medical Institute investigator, University of Washington, Seattle) for kindly providing pcDNA3-AKAP150 construct. We also thank Helena Montón and Núria Barba for their unvaluable technical assistance at Servei de Microscopia, Universitat Autònoma de Barcelona.

Correspondence should be addressed to Alfredo J. Miñano-Molina at alfredo.minano@uab.cat or José Rodriguez-Alvarez at jose.rodriguez@uab.cat

https://doi.org/10.1523/ENEURO.0218-19.2020

In the present study, we show that AKAP150 is targeted to the ubiquitin-proteasome system (UPS) and degraded under chemical LTD (cLTD) conditions. Interestingly, pharmacological inhibition of proteasome restores basal AKAP150 levels and blocks AKAP150 removal from synapses. This degradation of AKAP150 goes in parallel with LTD-mediated GluA1 dephosphorylation at Ser-845 and GluA1-AMPARs endocytosis. Indeed, maintaining AKAP150 levels blocks LTD-mediated GluA1-AMPARs endocytosis.

Materials and Methods

Cell culture, transfection, and transduction

Dissociated hippocampal cultures were prepared from newborn C57BL/6J wild-type mice as previously described (Ahmad et al., 2012). Briefly, hippocampi were isolated and incubated with a digestion solution containing papain (10 U/ml; Worthington) and DNase I (300–450 Kunitz/ml; Sigma) for 30 min at 37°C. A papain inactivation solution containing fetal bovine serum and bovine serum albumin was then applied. Tissue was triturated and cells were plated on poly-D-lysine (0.01 mg/ml in 0.1 M borate buffer, pH 8.4; both from Sigma)-coated 24-well plates with 12-mm coverslip (Paul Marienfeld) at a density of 75,000 cells per cover slip (for imaging studies) or from 300,000 to 900,000 cells per 35- to 60-mm dishes, respectively (for Western blotting). Wells contained Neurobasal-A media (Thermo Fisher Scientific) supplemented with B-27 (Thermo Fisher Scientific) and GlutaMAX (Thermo Fisher Scientific). Glial growth was inhibited by 5-fluorodeoxyuridine (FDUR) at 3 days in vitro (DIV). Neurons were maintained in a humidified incubator at 37°C with 5% CO_2, and half medium was replaced with fresh medium every week until use at 17–21 DIV. All animal procedures were performed in accordance with Universitat Autònoma de Barcelona animal care committee's regulations. When necessary, neurons were transduced with lentivirus [2–3 transducing units (TU)] on day 7 in culture and assayed as indicated in results. Direct counting of GFP-positive cells was used to monitor the efficiency of infection in each experiment. The percentage of infected cells reached at least 75%. Overexpression or down-regulation of AKAP was assessed by immunoblotting and immunocytochemistry.

HEK293T cells were maintained in DMEM supplemented with 10% fetal bovine serum and 1× pen/strep (Thermo Fisher Scientific). Cells at 90% confluence were passaged every 6 d using 1× Trypsin-EDTA solution (T3924-Sigma) replacing the media every 3 d. HEK293T cells were transfected using the calcium phosphate method with 20 μg plasmid DNA.

Plasmids and lentivirus production

AKAP150 was cloned by PCR from pcDNA3-AKAP150 vector (kindly provided by J. D. Scott; Howard Hughes Medical Institute, University of Washington, Seattle) and inserted into the lentiviral vector pWPI-IRES-GFP at the PmeI site for lentiviral overexpression experiments. pWPI vector was a gift from Didier Trono (Addgene plasmid #12 254). For RNAi interference experiments, a shAKAP150 construct was generated using the Thermo Fisher Scientific RNAi designer webtool (https://rnaidesigner.thermofisher.com/rnaiexpress/) using specific oligonucleotides against mouse AKAP150 (NM_001101471.1) indicated by capital letter as follows: RNAi, forward, 5'-agatctcccGGAAAGTGCTTTCA TTCAAAGttcaagagaCTTTGAATGAAAGCACTTTCC ttttta-3′ and reverse, 5'-aagcttaaaaaGGAAAGTGCTTTCATTCAAAG tctcttgaaTTTGAATGAAAGCACTTTCCgggg-3′. Oligonulceotides were purchased at Thermo Fisher Scientific and cloned between BglII and HindIII sites of the pSUPER.retro.puro vector (OligoEngine), under the control of the DNA Pol III promoter of H1 (Brummelkamp et al., 2002). Lentiviral constructs were achieved by digestion at the EcoRI-ClaI sites to replace H1 promoter in the lentiviral vector pLVTHM with H1-short hairpin RNA cassette from pSUPER. pLVTHM-H1-RNAi was used for lentiviral knockdown experiments. pLVTHM vector was a gift from Didier Trono (Addgene plasmid #12247). Lentiviruses were produced in HEK293T cells using calcium phosphate transfection of a 20 μg of pLVTHM-shAKAP150 or 20 μg of pWPI-AKAP150 (for AKAP down-regulation or over-expression, respectively), together with 15 μg of psPax2 and 6 μg of pMD2.G (gifts from Didier Trono, Addgene, #12260 and #12259, respectively); 24, 36, and 48 h after transfection, lentivirus-containing media were harvested, filtered with 0.45 μm filter units and centrifuged at 25,000 rpm for 2 h at 4°C. Pelleted viruses were resuspended in ice-cold PBS buffer by shaking at 175 rpm overnight at 4°C. Lentiviruses were aliquoted and stored at −80°C until use. Biological titers of the viral preparations expressed as a number of TUs per milliliter were determined by infecting HEK293T cells with serial dilutions. After 48 h, the percentage of GFP-positive cells was detected by flow cytometry (Cytomics FC 500, Beckman Coulter) and analyzed with RXT software.

Cell stimulation and lysate preparation

cLTD was induced as previously described (Oh et al., 2006). Cultures were first incubated in ACSF for 30 min at room temperature: 125 mM NaCl, 2.5 mM KCl, 1 mM $MgCl_2$, 2 mM $CaCl_2$, 33 mM D-glucose, and 25 mM HEPES (pH 7.3), followed by stimulation with 50 μM NMDA in ACSF (no $MgCl_2$) for 5 min. After NMDA treatment, neurons were replaced in regular ACSF and then subjected to the corresponding procedure at indicated time points. Cultures were then washed with ice-cold PBS once and lysed in cold 1% NP-40 homogenization buffer (20 mM Tris, pH 7.5, 150 mM NaCl, 5 mM EDTA, 1 mM PMSF, 1 mM Na_2VO_4, and 1× Sigma protease inhibitor and phosphatase inhibitor cocktails). When indicated, cultures were pre-treated or post-treated with BAPTA-AM (20 μM), FK506 (10 μM), MG132 (10 μM), or MK801 (10 μM; all from Tocris) and were present until cells were lysed. cLTP was induced as previously described (Otmakhov et al., 2004) by application of forskolin (50 μM) and rolipram (0.1 μM; both from Tocris), 60 min before or after cLTD. Cells were lysed 60 min after cLTP or cLTD treatment. Lysates were centrifuged at 12,000 × g for 10 min at 4°C and protein in the supernatant was quantified by Bradford method assay

kit (Bio-Rad Laboratories). The intensity of the cLTD protocol may vary depending on the cultures.

Surface biotinylation

Treated cells were transferred to ice-cold PBS-Ca^{2+}-Mg^{2+} buffer (pH 7.4; 1 mM $CaCl_2$; 0.1 mM $MgCl_2$), followed by biotinylation in 1 mg/ml of biotin (EZ-Link Sulfo-NHS-SS-Biotin; Thermo Fisher Scientific) for 30 min with slow agitation. Free biotin was quenched by wash (3×) in cold PBS-Ca^{2+}-Mg^{2+} + glycine 0.1 M. Cell cultures were immediately lysed in cold 1% Triton X-100 homogenization buffer (150 µl/35 mm well; two well per condition; 50 mM NaCl, 10 mM EDTA, 10 mM EGTA, 1 mM Na_3VO_4, 50 mM NaF, 25 mM NaPPi, 1 mM β-glycerphosphate, 1 mM phenylmethylsulfonyl fluoride, 1× protease inhibitor cocktail, 1× phosphatase inhibitor cocktail, and 50 mM HEPES; pH 7.5). Cell lysates were centrifuged at 10,000 × *g* for 20 min to pellet insoluble fraction. A total of 75 µl of the supernatant were mixed and heated with 25 µl of 4× SDS sample buffer to determine total fraction of GluA1 (surface plus internal). Biotinylated surface proteins in the remaining supernatant (225 µl) were pulled-down with 40 µl of 50% avidin-agarose beads (ImmunoPure Immobilized Avidin; Thermo Fisher Scientific) overnight at 4°C. The beads were pelleted and 75 µl of the supernatant (internal fraction) were mixed and heated with 25 µl of 4× SDS sample buffer. The beads were then rinsed three times with 1% Triton X-100 homogenization buffer and heated in 100 µl of 2× SDS sample buffer (surface fraction). Equal volumes of total and biotinylated fractions were subjected to 10% SDS-PAGE, probed by immunoblot for total GluA1 levels and normalized to GAPDH.

Immunoprecipitation

Neurons were washed in ice-cold PBS 1× and immediately lysed in cold immunoprecipitation buffer (200 µl × 60 mm plate; four plates per condition; 0.1% SDS, 1% Triton X-100, 1 mM EDTA, 1 mM EGTA, 50 mM NaF, 5 mM NaPPi, 10 mM N-ethylmaleimide, 1 × protease inhibitor cocktail, and 1 × phosphatase inhibitor cocktail). Homogenates from cultures were centrifuged at 16,000 × *g* for 10 min at 4°C and the protein in the supernatant was quantified by BCA protein assay kit (Bio-Rad Laboratories); 50 µg of protein from each supernatant were mixed and heated with 4× SDS sample buffer to keep total homogenate fraction (1 µg/µl). The remaining supernatants were immunoprecipitated with 5 µg of either rabbit anti-AKAP150 (clone R-300; sc-10 765; RRID: AB_2289482, Santa Cruz Biotechnology) or control rabbit IgG (011-000-003; RRID: AB_2337118; Jackson ImmunoResearch) antibodies overnight at 4°C, with gentle rocking. Immune complexes were precipitated for 1 h at 4°C using 40 µl protein G Sepharose beads (GE Healthcare Life Sciences). The beads were pelleted, washed and denatured in 100 µl of 2× SDS sample buffer, and 20 µl were loaded on an SDS-PAGE gel for immunoblotting.

Immunoblotting

Samples were separated on 7.5% or 10% SDS-PAGE and transferred onto Hybond-C Extra, Nitrocellulose membranes (GE Healthcare Life Sciences). Blots were blocked at room temperature for 1 h with 10% dry milk, 0.1% BSA (fraction V), pH 7.4 in PBS and incubated at 4° C overnight with primary antibody in PBS 0.1% BSA, pH 7.4. Primary antibodies were: anti-phospho-Ser-845-GluA1 (1:1000; clone EPR2148; 04–1073; RRID: AB_1977219; Merck-Millipore), anti-GluA1 (1:1000; AB1504; RRID: AB_2113602; Merck-Millipore), anti-AKAP150 (1:1000; 07–210; RRID: AB_310430; Merck-Millipore), anti-PSD95 (1:1000; clone 6G6-1C9; ab2723; RRID: AB_303248; Abcam), anti-SAP97 (1:1000; clone K64/15; 75–030; RRID: AB_2091920; UC Davis/NIH NeuroMab), anti-Ubiquitin (1:5000; U5379; RRID: AB_477667), anti-β-tubulin (1:20,000; clone 5H1; 556321; RRID: AB_396360; BD Biosciences), anti-β-actin (1:20,000; clone AC-74; A2228; RRID: AB_476697; Sigma), and anti-GAPDH (1:40 000; clone 6C5; AM4300; RRID: AB_437392; Thermo Fisher Scientific). After washing, blots were incubated with horseradish peroxidase-conjugated secondary antibodies, goat anti-mouse or goat anti-rabbit (554002 and 554021; RRID: AB_395198 and RRID: 395213, respectively; BD Biosciences), diluted in blocking buffer, and developed using the ECL Western Blotting Detection Reagents (GE Healthcare Life Sciences). Semi-quantitative analysis of immunoblots was performed by densitometry using ImageJ 2.0v (https://imageJ.nih.gov/ij/) and protein levels were corrected for corresponding loading control.

Immunocytochemistry

Neuronal cultures on coverslips were washed with ice-cold 1× PBS, fixed with ice-cold 4% paraformaldehyde with 4% sucrose in 1× PBS for 15 min at 4°C and then permeabilized with 0.1% Triton X-100 for 20 min at room temperature. For surface GluA1-containing AMPARs detection, no permeabilization was done. Afterwards, plates were washed twice with PBS, blocked with 2% normal Goat serum (Sigma) in 1× PBS (blocking buffer) for 1 h at 37°C and then incubated for 1 h at 37°C with specific antibodies detecting AKAP150 (1:200; clone N-19; sc-6446; RRID: AB_2225903 and 1:200; clone R-300; sc-10 765; AB_2289482, Santa Cruz Biotechnology), PSD95 (1:1000; clone 6G6-1C9; ab2723; RRID: AB_303248; Abcam), GluA1 (1:1000; AB1504; RRID: AB_2113602; Merck-Millipore), GFP (1:1000; ab13970; RRID: 300798; Abcam), and VGLUT1 (1:500; AB5905; RRID: 2301751; Merck-Millipore). Surface GluA1-containing AMPARs were measured using a rabbit polyclonal antibody directed against the N terminus of the GluA1 subunit (1:30; PC246; RRID: 564636; Merck-Millipore). Neurons were washed with warmed PBS-MC-sucrose (PBS 1×, 0.5 mM $CaCl_2$, 1 mM $MgCl_2$, 4% sucrose) and incubated with N-term-GluA1 antibody in PBS-MC-sucrose at 37°C for 5 min. Cells were then washed with ice-cold PBS-MC and fixed with ice-cold 4% paraformaldehyde with 4% sucrose in 1× PBS for 15 min at 4°C. Next, plates were washed twice with ice-cold PBS-MC, blocked for 1 h, and incubated with Alexa Flour-conjugated secondary antibody (1:300) in blocking buffer for 1 h, both at room temperature. Cells were washed, postfixed with methanol at −20°C for 1 min, blocked, and incubated with specific antibodies

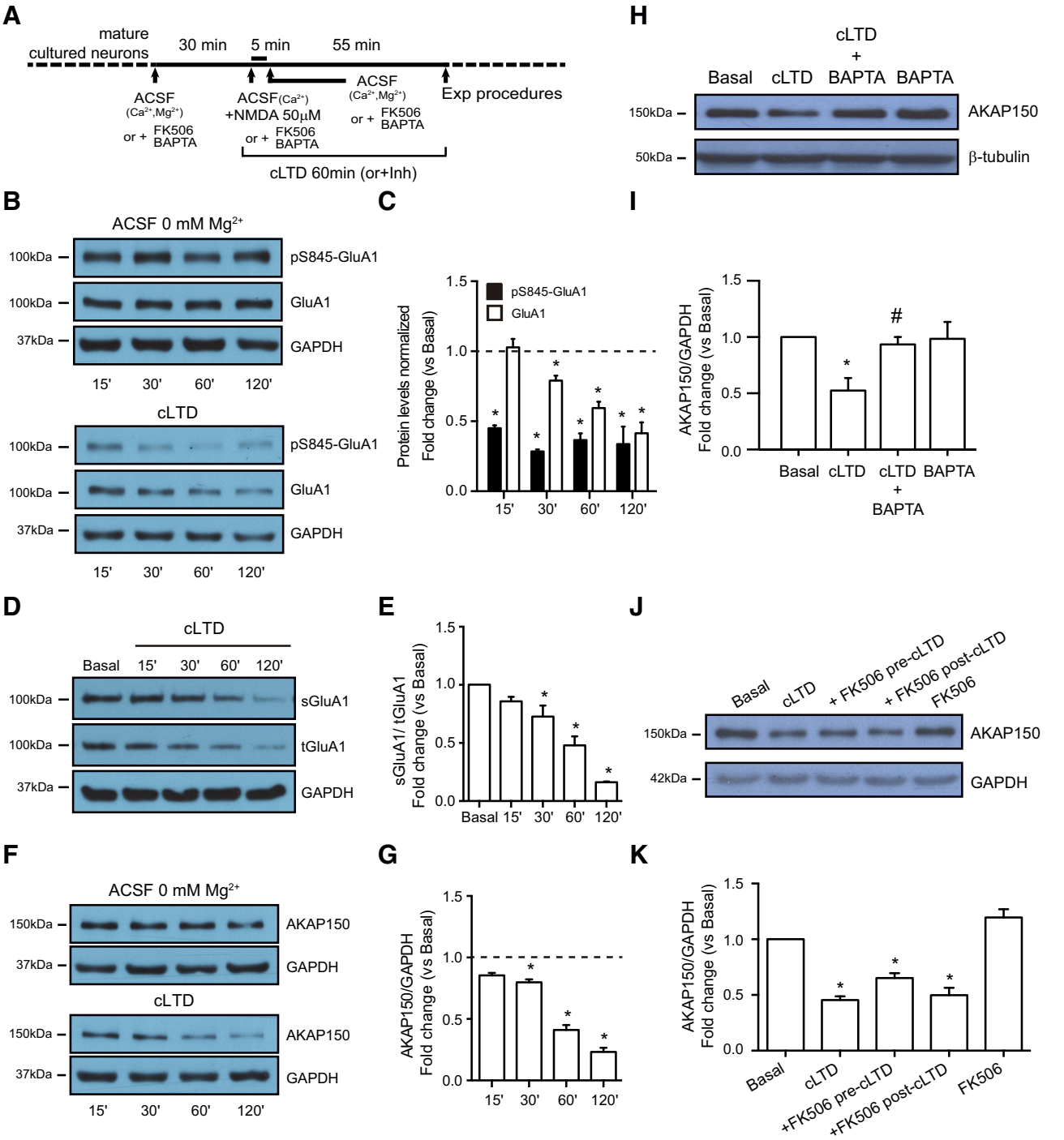

Figure 1. cLTD reduces AKAP150. ***A***, Cultured neurons were incubated in ACSF buffer for 30 min to equilibrate cells before 50 μM NMDA treatment for 5 min (cLTD). Cells were lysed after cLTD induction at indicated times (or 60 min if no time is indicated) in the presence or absence of inhibitors, antagonists, or cell-permeable Ca^{2+} chelators as indicated in the experimental design scheme. ***B***, Representative blot images showing reduced levels of Ser-845 GluA1 and GluA1 after treatment (cLTD) compared with cells in ACSF buffer. Ser-845 GluA1 levels (pS845-GluA1; ~110-kDa band, top panel) were related to total GluA1 (GluA1; ~110-kDa band, middle panel). GAPDH was used as a loading control (~36-kDa band, bottom panel). ***C***, Quantification of pS845-GluA1 and GluA1 changes in response to NMDA stimulation compared with basal condition ($n = 5$–17, $*p < 0.0001$ vs basal). ***D***, Representative blot images showing reduced levels of surface GluA1 after treatment (sGluA1; ~110-kDa band, top panel) related to total GluA1 (tGluA1; ~110-kDa band, middle panel). GAPDH was used as a loading control (~36-kDa band, bottom panel). ***E***, Quantification of surface GluA1 changes in response to cLTD compared with basal condition ($n = 6$, $*p = 0.0310$ for 30 min and $*p < 0.0001$ for 60 min and 120 min vs basal). ***F***, Representative blot images showing reduced levels of AKAP150 after cLTD (~150-kDa band, top panel) related to GAPDH (bottom panel). ***G***, Quantification of AKAP150 changes in response to cLTD compared with baseline ($n = 5$–20,

continued

$*p = 0.0021$ for 30 min and $*p < 0.0001$ for 60 min and 120 min vs basal). ***H***, ***J***, Representative blot images showing the effect of the presence of Ca^{2+} chelator BAPTA (***H***; 20 μM) or Ca^{2+}-dependent phosphatase CaN inhibitor FK506 (***J***; 10 μM) on AKAP150 protein levels after cLTD (top panel) related to β-tubulin (~51-kDa band, bottom panel) or GAPDH (bottom panel) used as a loading control. ***I***, ***K***, Quantification of AKAP150 changes in response to cLTD in presence of BAPTA (***I***) or FK506 (***K***) compared with cLTD treatment ($n = 3$ in BAPTA experiments, $*p = 0.0187$ vs basal and $\#p = 0.0377$ vs cLTD, $n = 3$–10 in FK506 pre-cLTD, $*p < 0.0001$ vs basal and FK506 post-cLTD experiments, $*p = 0.0073$ vs basal). Bar represent mean ± SEM.

against desired protein. Overall, primary antibodies were detected after washing with 1× PBS by incubation (1 h at 37°C) with Alexa Fluor-conjugated secondary antibodies (1:500 or 1:1000; A405, A488, A568 and/or A633; Thermo Fisher Scientific) in blocking buffer. Cells were washed in 1× PBS and when necessary, treated with HOECHST 33258 for nuclei staining (1:10,000 in PBS; H3569; Thermo Fisher Scientific). Following, coverslips were washed with 1× PBS, and mounted on glass slides on Fluoromount-G as an anti-quenching reagent (Southern Biotech).

Confocal imaging and analysis

Confocal z-stacks were acquired on a Zeiss LSM700 confocal microscope using the 63×/1.40 NA oil objective or Olympus FV3000 confocal microscope using the 60×/1.5 NA oil High Resolution objective. Sequential frame acquisition was set to acquire an average of 10 planes per stack at 16 bits and a minimum of 1024 × 1024 resolution. Channel gain settings were optically adjusted to minimize saturation of punctae and were maintained across experimental groups. Unmodified images were used for all analyses that were done blind and linear scaling was applied on images only for presentation purposes using ImageJ software. Fluorescent signal on the single planes from a stack, quantification of punctae number and punctae integrated fluorescence intensity over area measurements were performed with ImageJ software. Untreated and treated cells from the same culture preparation were always compared. For each experimental group an average of > 200 μm dendrite was quantified for 8–12 images per experiment in duplicate and repeated for a total of three or four independent experiments.

Statistical analysis

Statistical analysis was performed with Prism 6.0 (GraphPad Software). One-way ANOVA with Bonferroni's multiple comparison *post hoc* test or unpaired Student's *t* test was used for mean comparisons between experimental conditions as required. Differences were considered significant when $p < 0.05$. Depending on the type of experiment the number of samples used for statistical analyses, *n* refers to the accumulated number of dendrites, punctae, or independent cultures assayed per group (as indicated in figure legend) being always three or more independent biological replicates. Data in bar graphs are reported as mean ± SEM.

Results

cLTD triggers a decrease in Ser-845 GluA1 phosphorylation, GluA1 protein levels, GluA1-AMPAR surface expression, and AKAP150 degradation

First, we analyzed different cLTD paradigms used in the literature, changing NMDA dose and time of NMDAR stimulation, to observe the characteristics features of Ser-845-GluA1 dephosphorylation and decrease of GluA1-AMPARs levels (Kamal et al., 1999; Oh et al., 2006; Bhattacharyya et al., 2009; Li et al., 2010; Keith et al., 2012; Shehata et al., 2012; Bacaj et al., 2015; Yap et al., 2017). Since consistent results (data not shown) were observed when hippocampal cultures were treated with 50 μM NMDA for 5 min in 0 mM Mg^2, we decided to use these conditions in our experiments. Western blot analysis revealed a time-dependent decrease of Ser-845 GluA1 phosphorylation in hippocampal cultured neurons after cLTD induction [50 μM for 5 min; cLTD (Fig. 1*A–C*); cLTD: 0.449 ± 0.020 for 15 min, 0.283 ± 0.014 for 30 min, 0.365 ± 0.047 for 60 min, and 0.335 ± 0.125 for 120 min; $*p < 0.0001$, respectively, vs basal) in accordance to previously reported data (Beattie et al., 2000; Ehlers 2000; He et al., 2011). Moreover, significant time-dependent changes were also found in GluA1 total levels after NMDA stimulus (cLTD: 0.791 ± 0.034 for 30 min; $*p = 0.0189$, 0.594 ± 0.045 for 60 min and 0.415 ± 0.077 for 120 min; $*p < 0.0001$, respectively, vs basal) as previously reported (Fernández-Monreal et al., 2012). A reduction in surface GluA1-containing AMPARs after NMDA application was also observed by biotinylation and Western blot analyses. The surface reduction in GluA1-containing AMPARs was also time-dependent starting with 30-min NMDA application (Fig. 1*D*,*E*; 0.726 ± 0.095 for 30 min; $*p = 0.0310$, 0.478 ± 0.077 for 60 min and 0.161 ± 0.005 for 120 min; $*p < 0.0001$, respectively, vs basal). Previous reports showed that cLTD causes a redistribution of the scaffolding protein AKAP150 away from synapses (Gomez et al., 2002). However, it has not been reported whether this redistribution is also associated to changes in total AKAP150 levels. Our results indicate that cLTD significantly reduces AKAP150 levels in a time-dependent manner, as shown in the immunoblot analysis (Fig. 1*F*,*G*; cLTD: 0.799 ± 0.024 for 30 min; $*p = 0.0021$, 0.410 ± 0.041 for 60 min, 0.232 ± 0.034 for 120 min; $*p < 0.0001$ vs basal). As expected, application of Ca^{2+} chelator BAPTA-AM blocked cLTD-mediated AKAP150 levels decrease (Fig. 1*H*,*I*; cLTD: 0.525 ± 0.111; cLTD + BAPTA: 0.935 ± 0.066; $*p = 0.0187$ vs basal, $\#p = 0.0377$ vs cLTD).

Moreover, the phosphatase CaN has been described to form a complex with AKAP150 that is required for cLTD (Jurado et al., 2010) and to play a major role in AMPAR endocytosis by dephosphorylation of GluA1 Ser-845 (Oh et al., 2006; Lee et al., 2010). Therefore, we examined whether CaN activity is necessary for cLTD NMDA-dependent AKAP150 degradation. Pharmacological inhibition of CaN with FK506 after or during cLTD induction did not prevent the degradation of AKAP150 (Fig. 1*J*,*K*; cLTD: 0.454 ± 0.034; cLTD + FK506 post-cLTD: 0.652 ± 0.043;

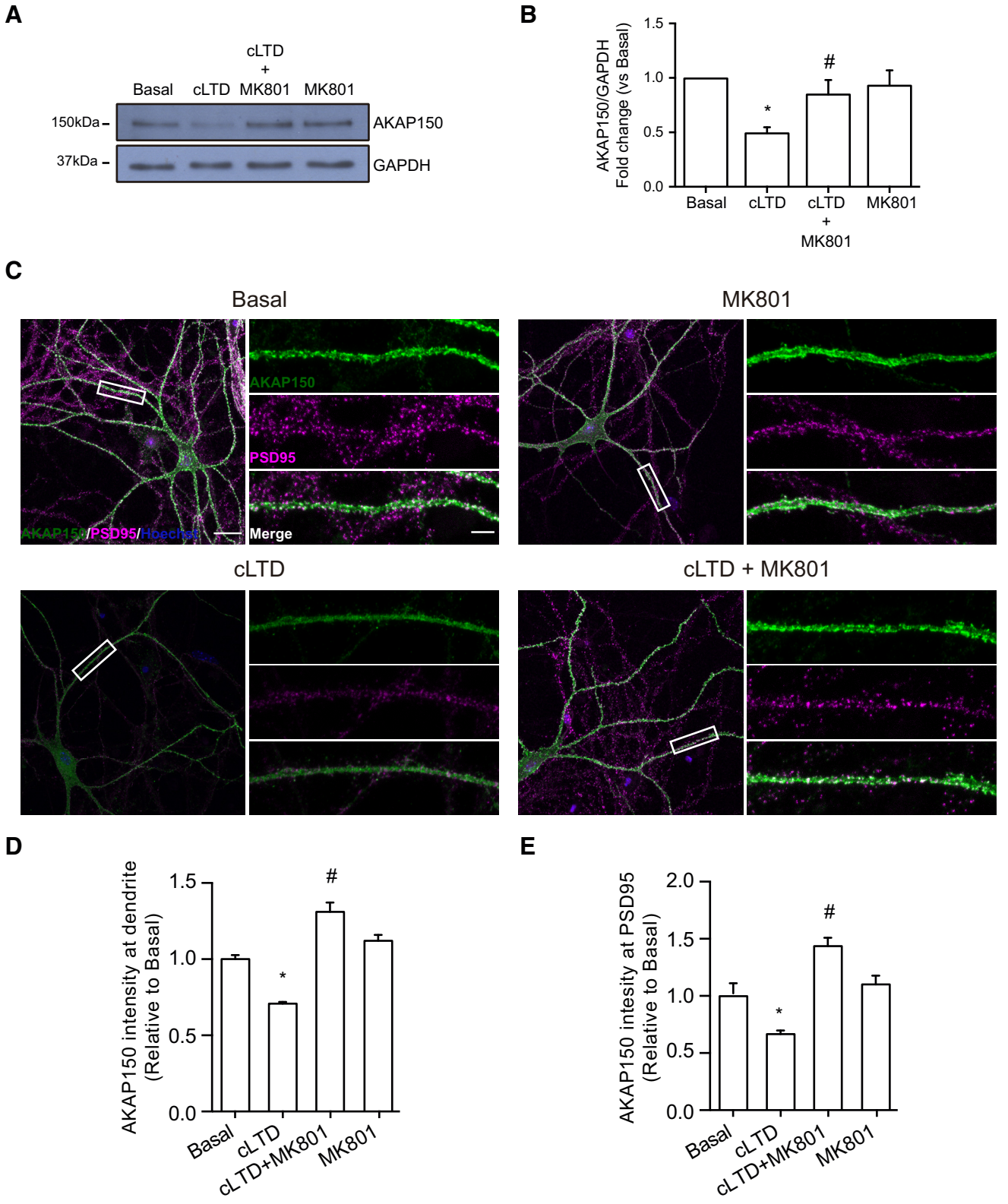

Figure 2. cLTD-mediated reduction of AKAP150 requires calcium influx through NMDA receptors. ***A***, Representative blot images showing the effect of NMDAR antagonist MK801 (10 μM) on AKAP150 protein levels after cLTD (top panel) related to GAPDH (bottom panel) used as a loading control. ***B***, Quantification of AKAP150 changes in response to NMDA stimulation in presence of MK801 compared with cLTD ($n = 4$, $*p = 0.0036$ vs basal and $\#p = 0.0395$ vs cLTD). ***C***, Representative confocal images of primary neurons showing AKAP150 (green), postsynaptic marker PSD95 (magenta) and nuclei (blue) staining. Separated color panels for individual marker from the boxed regions have been magnified for dendrite clarity (right panels). Lower right panels show the merge

continued

for AKAP150 (green)/PSD95 (magenta), where cLTD reduced dendritic and synaptic intensity in AKAP150 staining. The presence of MK801 (10 μM) blocks this reduction. ***D***, Quantification of AKAP150 intensity at dendrites. cLTD reduced AKAP150 dendritic intensity and the presence of MK801 avoids this reduction ($n > 15$ dendrites of different neurons from four independent cultures, $*p < 0.0001$ vs basal; $\#p < 0.0001$ vs cLTD). ***E***, Quantification of AKAP150 intensity at the PSD95. cLTD reduction of synaptic AKAP150 intensity was blocked by MK801 ($n > 50$ puncta from >15 dendrites from four independent cultures, $*p = 0.0150$ vs basal; $\#p < 0.0001$ vs cLTD). Scale bars = 20 μm (***C***, left panels) and 5 μm (***C***, right panels). Bars represent mean ± SEM.

$*p = 0.0073$ vs basal; cLTD + FK506 pre-cLTD: 0.499 ± 0.066; $*p < 0.0001$ vs basal). These results confirm that although CaN mediates cLTD-dependent AKAP150 redistribution away from the synapse (Smith et al., 2006), it is not involved in cLTD-dependent AKAP150 degradation.

Ubiquitin-proteasome system mediates cLTD-dependent AKAP150 degradation

After our finding that cLTD produced a decrease in AKAP150 levels we wondered whether this effect was mediated by proteasome activation. The reduction in AKAP150 levels was blocked by pretreatment with the NMDA antagonist MK801 (Fig. 2*A*,*B*; cLTD + MK801: 0.847 ± 0.133; $\#p = 0.0395$ vs cLTD) and also by the specific inhibition of proteasome activity with MG132 (Fig. 3*A*,*B*; cLTD + MG132: 1.228 ± 0.184; $\#p = 0.0014$ vs cLTD). Since cLTD-induced NMDAR activation causes a persistent loss of synaptic AKAP150 in cultured neurons (Smith et al., 2006), we analyzed whether changes in AKAP150 levels go beyond synapse relocation and whether its degradation is participating on AKAP150 removal from synapses. We assessed AKAP150 levels by confocal microscopy pretreating neurons with both MK801 and MG132. We observed a significant reduction in AKAP150 immunoreactivity at dendrites after cLTD that was blocked by MK801 and MG132 application (Figs. 2*C*,*D*, 3*E*,*F*; cLTD: 0.504 ± 0.042; $*p < 0.0001$; cLTD + MK801: 1.31 ± 0.061; $\#p < 0.0001$ vs cLTD; cLTD + MG132: 1.140 ± 0.0471; $\#p < 0.0001$ vs cLTD). Moreover, we analyzed AKAP150 levels at PSD95 clusters and we observed that both MK801 and MG132 were able to maintain AKAP150 at synapses after cLTD (Figs. 2*C*,*E*, 3*E*,*G*; cLTD: 0.666 ± 0.031; $*p = 0.0150$; cLTD + MK801: 1.435 ± 0.073; $\#p < 0.0001$ vs cLTD; cLTD + MG132: 1.239 ± 0.086; $\#p < 0.0001$ vs cLTD). Previous work by Colledge et al., (2003) indicated that cLTD treatment of cultured neurons induces proteasomal degradation of PSD95, leading its decreased synaptic clustering and contributing to the removal of synaptic AKAP150 and AMPARs (Colledge et al., 2003; Smith et al., 2006). Therefore, we analyzed PSD95 levels after cLTD by Western blotting and we observed that protein levels were reduced and treatment with MG132 was able to restore them (Fig. 3*C*,*D*; cLTD + MG132: 1.001 ± 0.078; $\#p = 0.0091$ vs cLTD). We also quantified both PSD95 cluster intensity and punctae number after cLTD treatment of cultured hippocampal neurons. Consistent with previously reported data (Colledge et al., 2003; Smith et al., 2006; Bhattacharyya et al., 2009), we observed a significant decrease in PSD95 cluster intensity after 1 h of treatment (Fig. 3*E*,*H*; cLTD: 0.659 ± 0.011; $*p = 0.0005$ vs basal) that was not observed in the presence of MG132 (Fig. 3*E*,*H*; cLTD + MG132: 1.088 ± 0.013; $\#p = 0.0002$ vs cLTD). However, we did not observe changes in PSD95 punctae number at dendrites after cLTD treatment (Fig. 3*I*; basal: 17.164 ± 2.002 punctae vs cLTD: 14.929 ± 2.428 punctae per 10 μm). Our data in cultured neurons suggest that not only redistribution of AKAP150 but also its degradation may play a role in the early stages of LTD. To determine whether cLTD-mediated AKAP150 decrease required AKAP150 ubiquitination, we check ubiquitination levels after cLTD induction in the presence of MG132 in cultured neurons. Surprisingly, we observed less ubiquitin-conjugated pattern after cLTD induction in whole lysate compared with basal levels (Fig. 4*A*,*B*; cLTD: 0.666 ± 0.066; $*p = 0.0355$), despite we expected an increase in ubiquitination levels since inhibition of ubiquitination attenuates NMDA-dependent cLTD (Citri et al., 2009). Proteasome inhibition with MG132 restored ubiquitination levels (Fig. 4*A*,*B*; cLTD+MG132: 1.039 ± 0.079; $\#p = 0.0183$ vs cLTD), suggesting that cLTD could be inducing rapid protein degradation via ubiquitin-proteasome system. Previous studies surveying substrates of ubiquitin ligation in the PSD identified AKAP150 as a highly ubiquitinated protein under basal conditions which is highly regulated by synaptic activity (Ehlers 2003; Jia et al., 2008). Accordingly, while cLTD reduced AKAP150 levels (Fig. 4*C*; cLTD: 0.614 ± 0.059; $*p = 0.0121$ vs basal), pull-down results showed a significant increase in total ubiquitin conjugated-AKAP150 observed in AKAP150 shift when overexposed (Fig. 4*C*,*D*; cLTD: 1.813 ± 0.125; $*p = 0.0026$ vs basal). These results suggest that synaptic AKAP150 degradation by ubiquitin-proteasome system could be an important factor in cLTD-induced synapse regulation. It is known that AKAP150 participates in the regulation of LTP processes and even it expression is upregulated in this conditions (Génin et al., 2003; Sanderson and Dell'Acqua, 2011). Since our results show that cLTD induce AKAP150 degradation, we studied whether LTP could restore AKAP150 levels in our neuronal cultures. For this purpose we used a chemical stimulation protocol of forskolin and rolipram (Fig. 5*A*; cLTP; 50 μM /0.1 μM) that results in LTP (Grey and Burrell, 2008) and produces and increase in both GluA1 phosphorylation at Ser-845 and cell surface GluA1 levels (Fig. 5*B*,*C*; cLTD: 0.418 ± 0.085; $*p < 0.0001$; cLTP 1.325 ± 0.041; $*p = 0.0009$ vs basal; Oh et al., 2006; Miñano-Molina et al., 2011). When cLTP was induced in cultured neurons after cLTD no reversion of cLTD-mediated effects on AKAP150 levels was observed by immunoblotting (Fig. 5*D*,*E*; cLTD: 0.545 ± 0.049; cLTD + cLTP: 0.400 ± 0.052; $*p < 0.0001$ vs basal) or by immunocytochemistry (Fig. 5*F*,*G*; cLTD: 0.444 ± 0.046; $*p = 0.0004$ vs basal; cLTD + cLTP: 0.467 ± 0.065; $\#p = 0.0017$ vs basal). Similarly, AKAP150 was not observed even when we tried to favor AKAP150 retention at the synapses by inducing cLTP before cLTD

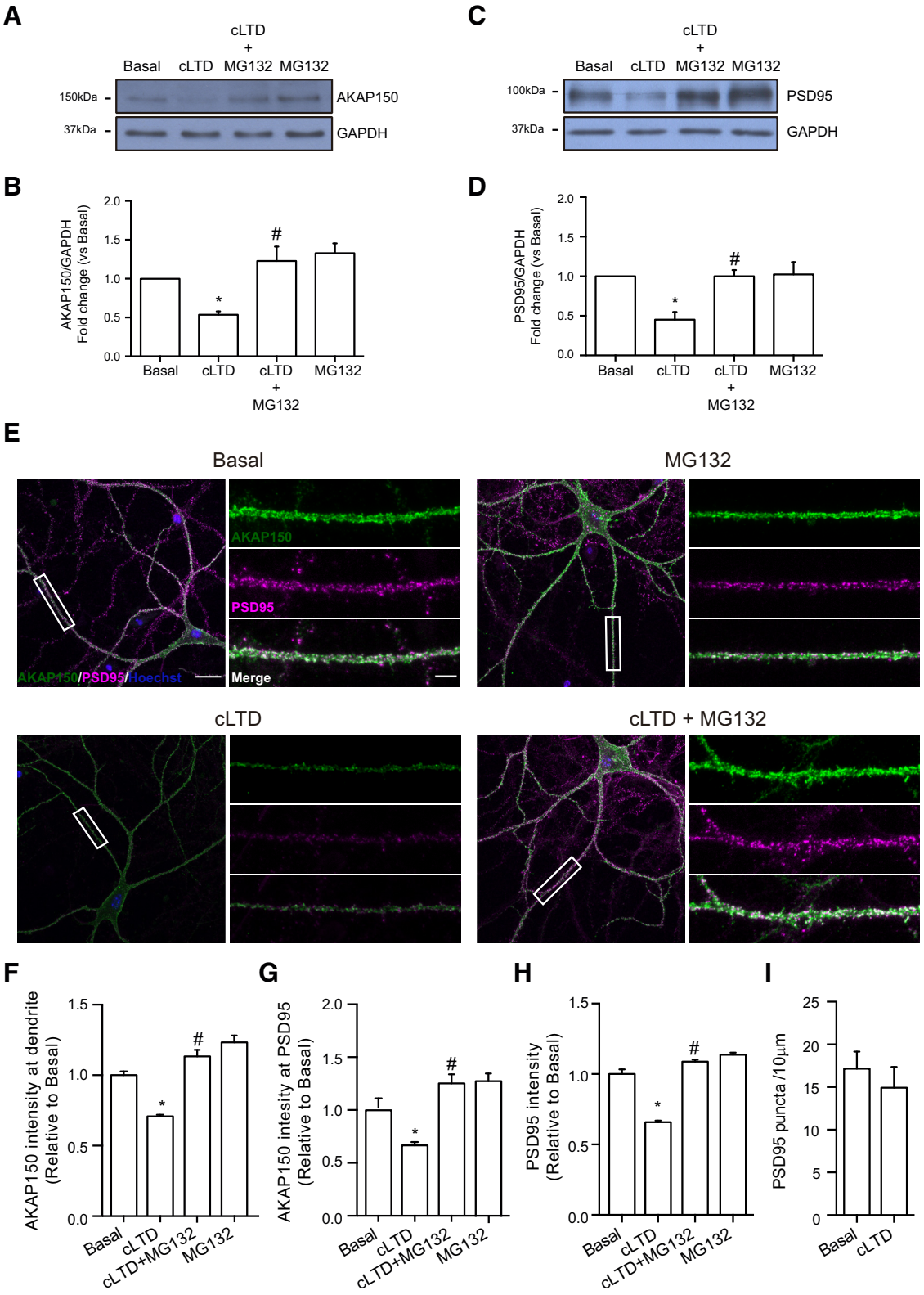

Figure 3. cLTD-mediated reduction of AKAP150 requires proteasome activity. ***A***, Representative blot images showing the effect of proteasome inhibitor MG132 (10 μM) on AKAP150 protein levels after cLTD (top panel) related to GAPDH (bottom panel) used as loading control. ***B***, Quantification of AKAP150 changes in response to NMDA stimulation in presence of MG132 compared with cLTD (for $n = 4$, $*p = 0.0125$ vs basal and $\#p = 0.0014$ vs cLTD). ***C***, Representative blot images showing the effect of proteasome inhibitor MG132 (10 μM) on PSD95 protein levels after cLTD (top panel) related to GAPDH (bottom panel) used as loading control. ***D***, Quantification of PSD95 changes in response to NMDA stimulation in presence of MG132 compared with cLTD (for $n = 3$,

continued
$*p = 0.0092$ vs basal and $\#p = 0.0091$ vs cLTD). ***E***, Representative confocal images of primary neurons showing AKAP150 (green), postsynaptic marker PSD95 (magenta) and nuclei (blue) staining. Separated color panels for individual marker from the boxed regions have been magnified for dendrite clarity (right panels). Lower right panels show the merge for AKAP150 (green)/PSD95 (magenta), where cLTD reduced dendritic and synaptic intensity in AKAP150 staining. The presence of MG132 (10 μM) blocks this reduction. ***F***, Quantification of AKAP150 intensity at dendrites. cLTD reduced AKAP150 dendritic intensity and the presence of MG132 avoids this reduction ($n > 15$ dendrites of different neurons from four independent cultures, $*p < 0.0001$ vs basal; $\#p < 0.0001$ vs cLTD). ***G***, Quantification of AKAP150 intensity at the PSD95. cLTD reduction of synaptic AKAP150 intensity was blocked by MG132 ($n > 50$ puncta from >15 dendrites from four independent cultures, $*p = 0.0150$ vs basal; $\#p < 0.0001$ vs cLTD). ***H***, Quantification of PSD95 intensity at dendrites. cLTD reduction of PSD95 intensity was blocked by MG132 ($n > 15$ dendrites of different neurons from four independent cultures, $*p = 0.0005$ vs basal; $\#p = 0.0002$ vs cLTD). ***I***, Quantification of PSD95 puncta at dendrites normalized to basal. There is no difference in puncta number between basal and cLTD conditions ($n > 50$ puncta from >15 dendrites from four independent cultures). Scale bars = 20 μm (***A***, left panels) and 5 μm (***A***, right panels). Bars represent mean ± SEM.

(Fig. 5*D*,*E*; cLTP: 0.869 ± 0.051; cLTP + cLTD: 0.245 ± 0.044; $*p < 0.0001$ vs basal).

Endogenous AKAP150 knock-down triggers dephosphorylation and endocytosis of AMPARs

Synaptic distribution of AKAP150 is a key factor for synaptic expression of AMPARs (Tavalin et al., 2002). Previous reports have shown that removal of AKAP150 from synapses, toward the cytosol in dendritic shafts or soma, elicits synaptic AMPARs endocytosis (Bhattacharyya et al., 2009; Keith et al., 2012). In this context, we explored AKAP150 silencing effect on AMPAR. Using shRNA-mediated acute knock-down of endogenous AKAP150 (shAKAP150), we were able to effectively reduce AKAP150 expression in cultured neurons (Fig. 6*A*). Interestingly, whereas cLTD produces the degradation of AKAP150 (Fig. 1*F*,*G*), PSD95 (Fig. 3*C*,*D*), and SAP97 (data not shown), knock-down of endogenous AKAP150 did not induce significant changes in PSD95 or SAP97 levels (Fig. 6*B*,*C*; shAKAP150: 1.070 ± 0.112 and 0.873 ± 0.145, respectively). However, AKAP150 silencing decreased S845-GluA1 phosphorylation and GluA1 total levels (Fig. 6*D*,*E*; shAKAP150: 0.327 ± 0.101; $*p = 0.0057$ and 0.516 ± 0.073; $\#p = 0.0070$, respectively, vs Ø). Consistent with the results observed by immunoblotting, AKAP150 knock-down reduced both synaptic and dendritic GluA1 levels (Fig. 6*H*,*I*; shAKAP150: 0.432 ± 0.088; $*p < 0.0001$ and 0.445 ± 0.023; $\#p < 0.0001$, respectively), followed by a decrease in surface GluA1 expression (Fig. 7*A*,*B*; shAKAP150: 0.401 ± 0.109; $*p < 0.0001$ vs basal). Next, we wanted to test whether this reduction in surface GluA1 by AKAP150 silencing could occlude further AMPAR removal after cLTD induction. We induced cLTD in AKAP150-silenced neurons and surface GluA1 levels were analyzed. We observed that after cLTD in shAKAP150 conditions, further reduction of GluA1 surface levels was observed (Fig. 6*J*,*K*; shAKAP150: 0.472 ± 0.115; $*p = 0.0141$, cLTD: 0.287 ± 0.081; $*p = 0.0030$ and shAKAP150 + cLTD: 0.152 ± 0.053; $*p = 0.0012$ vs basal). These results clearly show that silencing endogenous AKAP150 decreases Ser-845 phosphorylation, GluA1 levels and consequently reduces GluA1-containing AMPARs recruitment to synapses and surface expression. Remaining levels of AKAP150, under shAKAP150 conditions, seem to be enough to partially keep anchored AMPAR to the membrane and, after cLTD, its degradation still contribute to increase GuA1 internalization (Fig. 6*J*,*L*; shAKAP150: 0.279 ± 0.018; $*p = 0.0003$, cLTD: 0.517 ± 0.070; $*p = 0.0080$ and shAKAP150 + cLTD: 0.131 ± 0.027; $*p < 0.0001$ vs basal).

Overexpression of AKAP150 blocks cLTD-mediated AMPARs endocytosis

Above results show that a decrease in AKAP150 endogenous levels either by cLTD induction, shRNA-mediated knock-down or both, triggers GluA1-containing AMPARs endocytosis. Therefore, we studied whether overexpression of AKAP150 was able to rescue AMPARs endocytosis produced after cLTD. According to previous studies showing that AKAP150 overexpression somehow increases basal AMPAR surface expression (Bhattacharyya et al., 2009), neurons overexpressing AKAP150 showed a slight no significant increase in Ser-845 phosphorylation without affecting GluA1 total levels (Fig. 6*F*,*G*; ovAKAP150: 1.180 ± 0.047 and 0.963 ± 0.125, respectively). However, AKAP150 overexpression did elevate surface GluA1 labeling (~24%) compared with basal (Fig. 7*A*,*B*; ovAKAP150: 1.274 ± 0.098; $\#p = 0.0419$). When cLTD was induced in AKAP150 overexpressing neurons, surface GluA1 levels remained unchanged (Fig. 7*C*,*D* and *E*,*F*; ovAKAP150+ cLTD: 0.996 ± 0.112; $\#p = 0.0185$ vs cLTD and ovAKAP150+ cLTD: 0.893 ± 0.125; $\#p = 0.0016$ vs cLTD).

Discussion

It is well known that modulation of AMPAR function and membrane trafficking, in and out the synapses, is a major contributor to synaptic plasticity processes, such as LTP or LTD, that are believed to underlie learning and memory (Huganir and Nicoll, 2013). Whereas LTP has been associated to the insertion of AMPARs in the postsynaptic membrane, the synaptic AMPARs endocytosis drives NMDA-dependent LTD (Lledo et al., 1998; Carroll et al., 1999; Takumi et al., 1999; Shi et al., 2001). It has been previously described that the phosphorylated state of AMPARs modulates their insertion or removal from synaptic membranes (Lee et al., 1998, 2000, 2003, 2010; Chung et al., 2000; Esteban et al., 2003; Boehm et al., 2006; Oh et al., 2006; Delgado et al., 2007; Lu et al., 2010; Coultrap et al., 2014). Among AMPARs subunits, it is believed that GluA1 trafficking in and out the synapse depends on neuronal activity, while GluA2 subunit seems to be constitutively regulated in a neuronal activity-

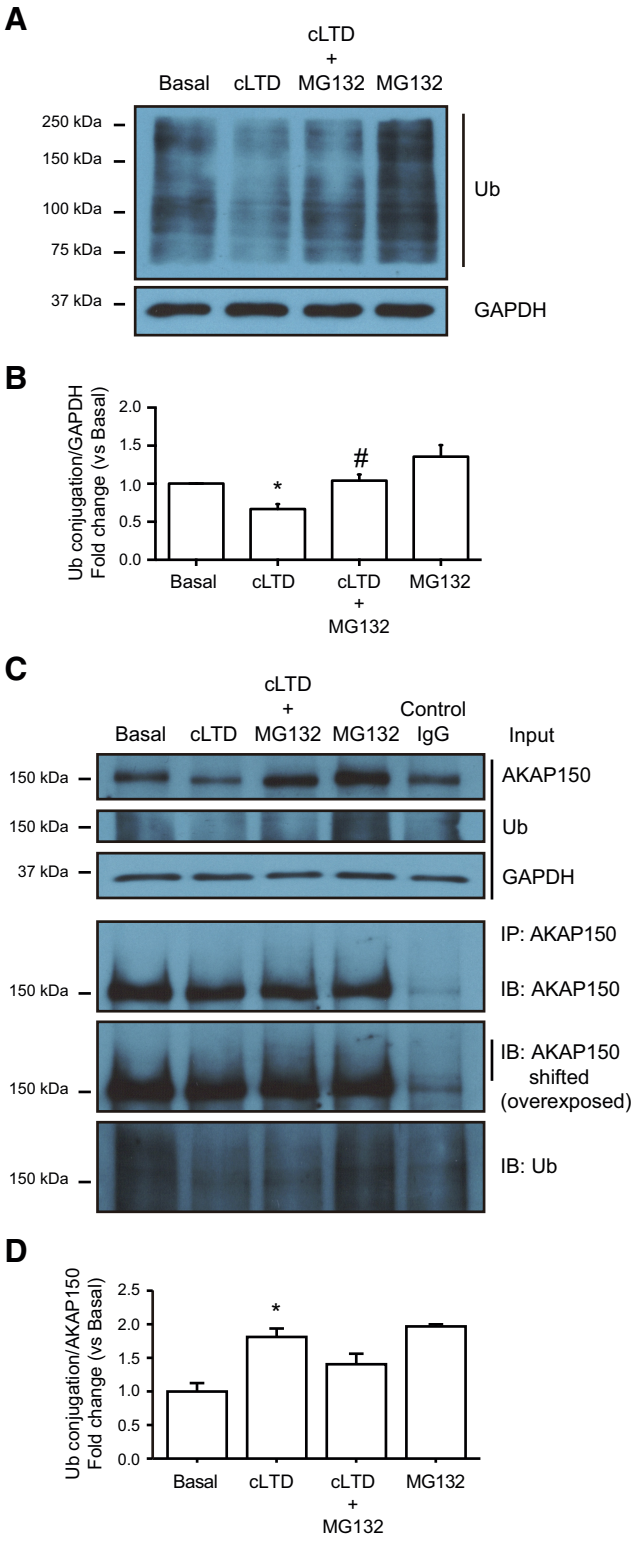

Figure 4. cLTD-mediated AKAP150 degradation requires AKAP150 ubiquitination. ***A***, Representative blot images showing the ubiquitination (Ub) of high molecular weight protein after cLTD (top panel) related to GAPDH (bottom panel) used as a loading control. ***B***, Quantification of total ubiquitination signal in response to cLTD in presence of MG132 (10 μM) compared with cLTD ($n = 6$, $*p = 0.0355$ vs basal and $\#p = 0.0183$ vs cLTD). ***C***, Representative blot images showing an increase in AKAP150 ubiquitination after cLTD. Lysates from neurons after cLTD were immunoprecipitated with anti-AKAP150 or control rabbit IgG (control IgG) and blotted with anti-AKAP150 and anti-ubiquitin (Ub). The three top panels show representative blot images (input) for AKAP150 and 150-kDa ubiquitinated proteins (Ub) related to GAPDH (bottom panel of three) used as a loading control. The three bottom panels show representative blot images of immunoprecipitated Ub-AKAP150 protein (IP:AKAP150; including overexposed panel to observe AKAP150-shifted) and total ubiquitination levels (Ub). ***D***, Quantification of ubiquitinated-AKAP150 levels related to total AKAP150 signal in response to cLTD compared with basal ($n = 3$ for each group, $*p = 0.0026$ vs basal). Bars represent mean ± SEM.

independent manner (Passafaro et al., 2001; Shi et al., 2001). Phosphorylation status of GluA1 on Ser-845 seems to determine synaptic localization of GluA1 AMPARs during LTP or LTD processes. In this way, PKA-mediated Ser-845 phosphorylation facilitates AMPARs trafficking to the synapses favoring LTP (Oh et al., 2006; Makino et al., 2011) whereas Ser-845 dephosphorylation by CaN has been shown to promote AMPARs endocytosis associated to hippocampal LTD (Mulkey et al., 1994; Beattie et al., 2000; Lee et al., 2000).

Several studies have reported that the scaffolding protein AKAP79/150 has a prominent role in the reciprocal modulation of PKA and CaN activities at the synapse and therefore in the regulation of AMPARs cycling in and out the synapses during LTP and LTD (Tavalin et al., 2002; Lu et al., 2008; Jurado et al., 2010). AKAP79/150 forms a complex with PKA and CaN (Bauman et al., 2004; Jurado et al., 2010) that binds the MAGUK scaffold proteins PSD95 and SAP97, linking the AKAP79/150 complex to AMPARs (Colledge et al., 2000; Bhattacharyya et al., 2009; Robertson et al., 2009). Thus, a disruption in the interaction between these proteins in the PSD could lead to an alteration in plasticity of glutamatergic synapses. For instance, PSD95 knock-down by shRNA or inhibition of PSD95 binding to AKAP150, blocks NMDA-dependent LTD endocytosis of synaptic AMPARs in cultured neurons (Bhattacharyya et al., 2009). In the present work, we studied the eventual changes in AKAP150 levels caused by cLTD and whether these changes are involved in synaptic AMPARs endocytosis triggered by cLTD in neuronal cultures.

Previous results suggested that during LTD, AKAP79/150, together with PKA, translocate away from PSD95 and synaptic spines (Gomez et al., 2002; Smith et al., 2006). This translocation is believed to favor CaN activity promoting the dephosphorylation of postsynaptic substrates, such as GluA1 and leading to synaptic AMPARs endocytosis (Smith et al., 2006). Our results show that besides AKAP79/150 redistribution away from the synapses, cLTD produces an additional and significant proteasome-dependent decrease in total AKAP150 levels that it is accompanied by a reduction in surface and total GluA1 levels. Furthermore, our data also show that the addition of shAKAP150 does not blocks NMDA-dependent LTD endocytosis of synaptic AMPAR, indicating a differential role of AKAP150, PSD95, and its interaction on AMPAR

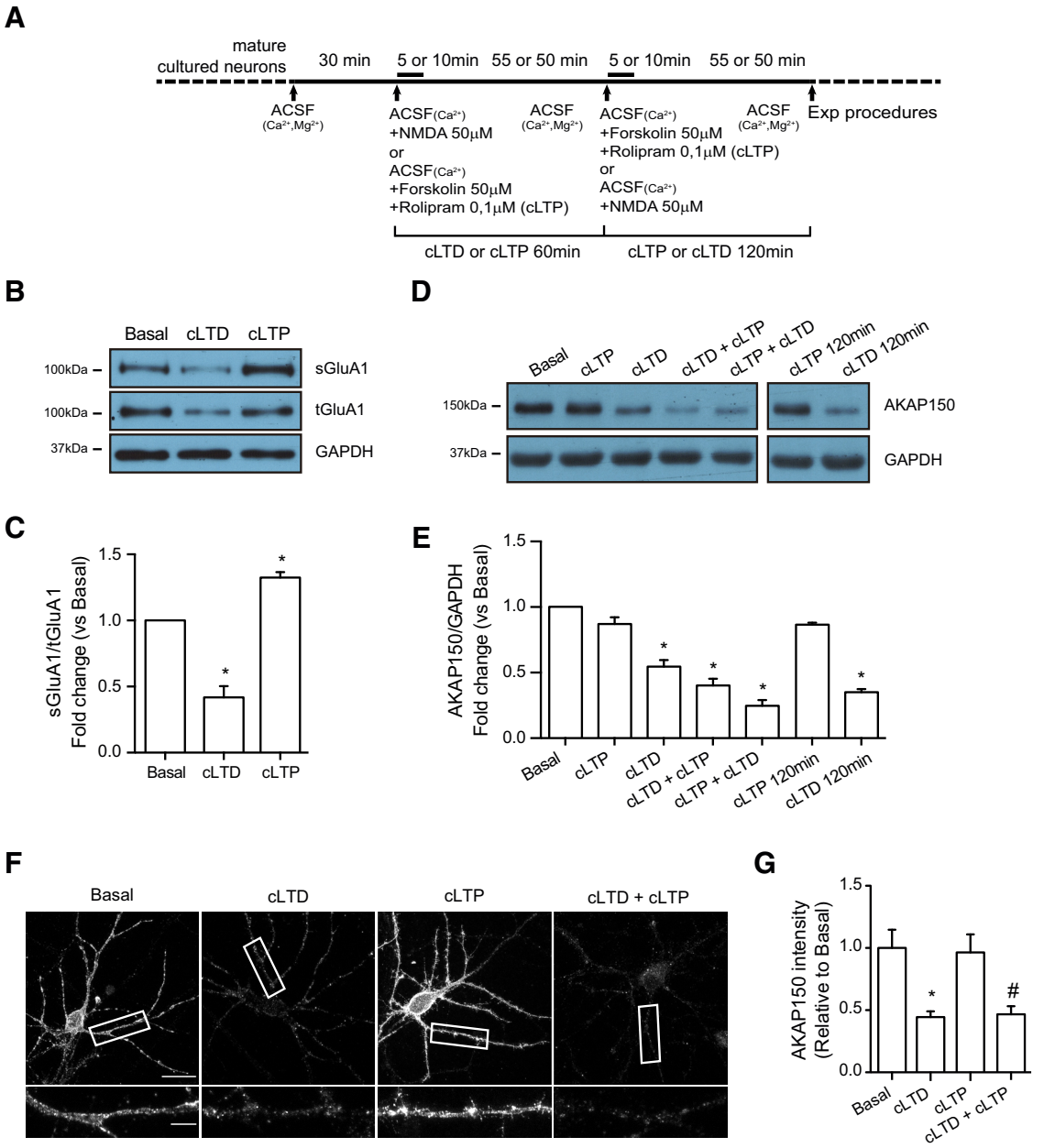

Figure 5. cLTP neither rescue nor prevents cLTD-mediated reduction of AKAP150 levels. ***A***, Hippocampal neurons were cultured during 17–21 DIV. cLTP was induced with forskolin/rolipram (50 μM/0.1 μM) for 60 min (10-min stimulation plus 50-min incubation in ACSF buffer) before or after cLTD as indicated in experimental design scheme. ***B***, Representative blot images showing increased levels of surface GluA1 after cLTP treatment (sGluA1; ~110-kDa band, top panel) related to total GluA1 (tGluA1; ~110-kDa band, middle panel). GAPDH was used as a loading control (~36-kDa band, bottom panel). ***C***, Quantification of surface GluA1 changes in response to cLTD and cLTP compared with basal condition ($n = 4$–9, $*p < 0.0001$ for cLTD and $*p = 0.0009$ for cLTP vs basal). ***D***, Representative blot images showing levels of AKAP150 in response to cLTP before and after cLTD treatment (top panel) and GAPDH (bottom panel) as a loading control. ***E***, Quantification of AKAP150 changes in response to cLTP before and after cLTD treatment compared with basal ($n = 3$–9, $*p < 0.0001$ vs basal). ***F***, Dendritic staining for AKAP150 after cLTD with or without cLTP. Representative confocal images showing AKAP150 (gray). Separated panels from the boxed regions have been magnified for dendrite clarity (bottom panels). cLTD reduced AKAP150 staining. The presence of cLTP (50 μM; 0.1 μM) does not rescue AKAP150 levels. ***G***, Quantification of AKAP150 intensity at dendrites normalized to basal condition. cLTD reduced AKAP150 dendritic intensity and cLTP induction does not prevent this reduction ($n > 25$ dendrites of different neurons from three independent cultures, $*p = 0.0004$ vs basal; $\#p = 0.0017$ vs basal). Scale bars = 20 μm (***F***, top panels) and 5 μm (***F***, bottom panels). Bars represent mean ± SEM.

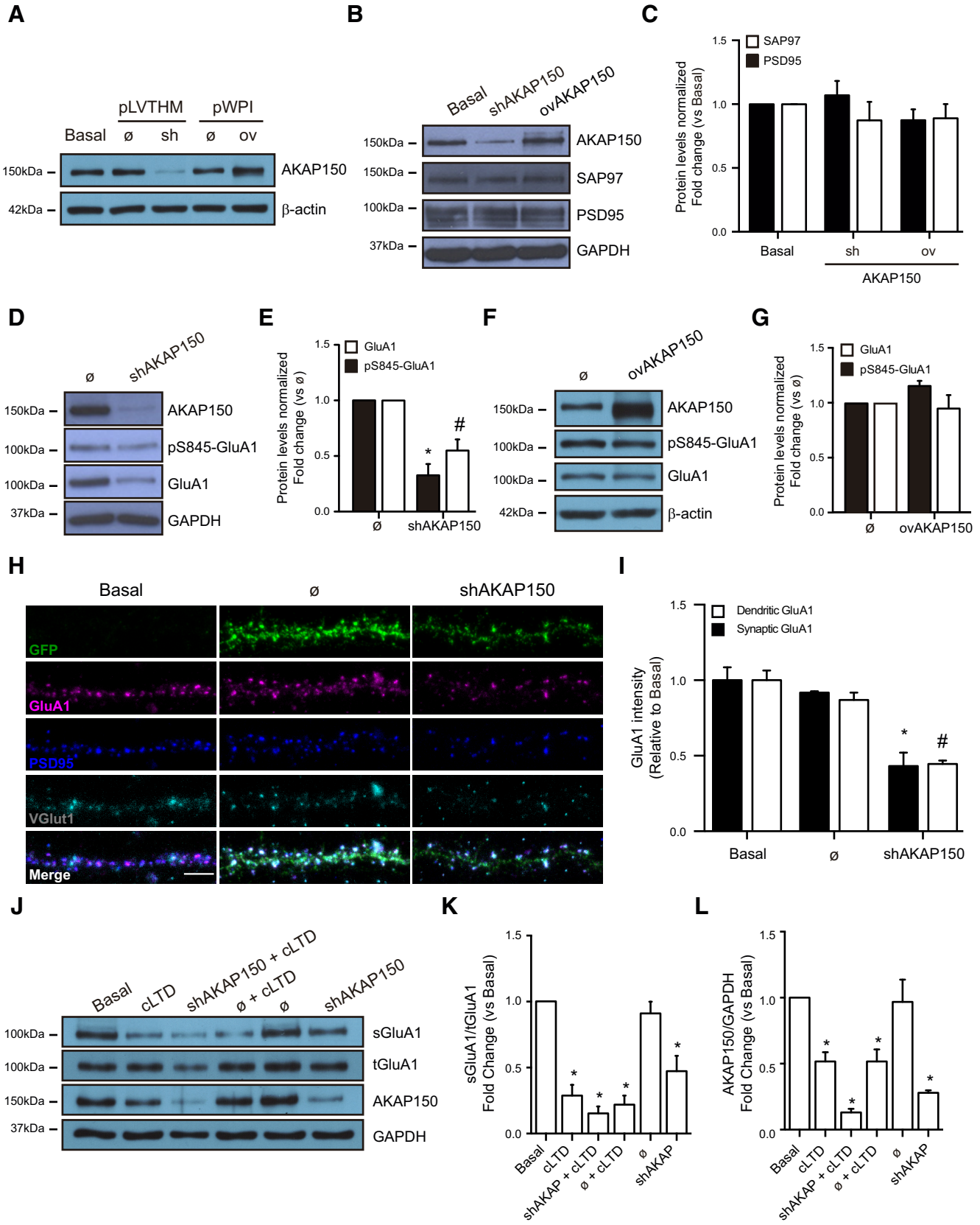

Figure 6. Silencing endogenous AKAP150 reduces AMPARs-GluA1 subunit levels. ***A***, AKAP150 was silenced (sh or shAKAP150) or overexpressed (ov or ovAKAP150) in neuronal cultures after transduction with lentiviral vectors. Representative blot images showing the efficiency of shAKAP150 or ovAKAP150 transduction in primary neurons. Empty lentiviral vector (Ø; pLVTHM or pWPI) was used

continued

as a control. ***B***, Silencing AKAP150 does not affect related scaffold proteins like PSD95 (~95-kDa band) or SAP97 (~140-kDa band). Representative blot images showing levels of AKAP150 (top panel; as a control of silencing or overexpressing), PSD95 and SAP97 when endogenous AKAP150 was knocked down (shAKAP150) or overexpressed (ovAKAP150). GAPDH (bottom panel) was used as a loading control. ***C***, Quantification of PSD95 or SAP97 levels when AKAP150 was silenced (shAKAP150) or overexpressed (overAKAP150) normalized to basal ($n = 4$). ***D***, Endogenous AKAP150 silencing reduces S845-GluA1 phosphorylation and total GluA1 protein. Representative blot images showing AKAP150 levels (top panel; as a control of silencing), phosphorylated GluA1 (pS845-GluA1), total GluA1 and GAPDH (bottom panel; loading control). ***E***, Quantification in pS845-GluA1 and GluA1 levels in response to AKAP150 knock-down compared with basal ($n = 3$, $*p = 0.0057$ vs basal; $\#p = 0.0070$ vs basal). ***F***, AKAP150 overexpression does not modify S845-GluA1 phosphorylation and total GluA1 protein levels. Representative blot images showing AKAP150 (top panel; as a control of overexpression), phosphorylated GluA1 (pS845-GluA1), total GluA1 and GAPDH (bottom panel; loading control) levels. ***G***, Quantification of pS845-GluA1 and GluA1 in response to AKAP150 overexpression compared with basal ($n > 3$). ***H***, Representative confocal images of dendrites show GluA1 (magenta), presynaptic VGlut1 (gray), and postsynaptic PSD95 (blue) levels after knocking down AKAP150 compared with basal condition (Ø; empty vector). GFP expression (green) is used as a control of transduction. Down-regulation of endogenous AKAP150 reduced dendritic and synaptic GluA1 intensity. Bottom panels in ***H*** show the merge for GFP/GluA1/PSD95/VGlut1. ***I***, Quantification of GluA1 (GluA1) intensity normalized to basal. AKAP150 knock-down expression reduced dendritic (o) and synaptic (ν) GluA1 ($n > 30$ dendrites of different neurons from five independent cultures, $*p < 0.0001$ vs basal; $\#p < 0.0001$ vs basal). ***J***, Surface GluA1 levels on cLTD in presence of shAKAP150. Representative blot images showing decreased levels of surface GluA1 after cLTD in presence of shAKAP150 (sGluA1; ~110-kDa band, top panel) related to total GluA1 (tGluA1; ~110-kDa band, middle panel). GAPDH was used as a loading control (~36-kDa band, bottom panel). ***K***, Quantification of surface GluA1 changes in response to cLTD in presence of shAKAP150 compared with basal condition ($n = 3$, $*p = 0.0030$ for cLTD, $*p = 0.0012$ for shAKAP150+cLTD, $*p = 0.0018$ for empty+cLTD and $*p = 0.0141$ for shAKAP150 vs basal). ***L***, Quantification of AKAP150 in response to cLTD in presence of shAKAP150 compared with basal condition ($n = 3$, $*p = 0.0080$ for cLTD, $*p < 0.0001$ for shAKAP150+cLTD, $*p = 0.0080$ for empty+cLTD and $*p = 0.0003$ for shAKAP150 vs basal). Scale bars = 5 μm. Bars represent mean ± SEM.

endocytosis in LTD (Bhattacharyya et al., 2009). Moreover, the maintenance of AKAP150 levels by overexpression is sufficient to prevent GluA1-AMPARs endocytosis associated to cLTD in cultured neurons. A causative relationship between AKAP150 levels decrease and AMPARs endocytosis is also supported by our data using shAKAP150 together with AKAP150 overexpression; whereas AKAP150 silencing produced the expected dephosphorylation of GluA1 Ser-845 and the endocytosis of GluA1-AMPARs, overexpression of AKAP150 increased GluA1 Ser-845 phosphorylation and surface GluA1 levels. Precisely, overexpression of AKAP150 not only drives more AMPAR to the membrane but can also block cLTD-mediated GluA1-AMPARs endocytosis, indicating that the presence of AKAP150 is increasing retention/stabilization at synaptic locations. Further work remains to be done to address whether changes in AKAP150 could, and how, also affect other scaffolding proteins. Moreover, since LTD triggers AKAP150 degradation, AKAP150 plays an important role regulating LTP processes (Sanderson and Dell'Acqua, 2011) and LTP is associated with up-regulation of AKAP150 gene expression (Génin et al., 2003), we postulate that AKAP150 degradation would impair subsequent LTP. This is supported by our data showing that cLTD prevent cLTP induction due to a failure in normal AKAP150 levels recovery. Surprisingly, prior cLTP induction as a strategy to retain AKAP150 levels and block cLTD effect on GluA1-AMPAR was unproductive according to our data. It is possible that cLTP induction 1 h before cLTD is not enough to protect AKAP150 from cLTD. However, from our images it seems that there may be more AKAP150 concentrated at the plasma membrane after cLTP induction, with bigger and more intense clusters than in basal conditions in agreement with the notion that LTP recruits more AKAP150 to the plasma membrane (Purkey et al., 2018). Additional experiments are needed to explore this possibility at different time points. Based on these data, we propose that cLTD has a double effect on AKAP79/150 that is responsible for AMPARs dephosphorylation and endocytosis: a translocation of AKAP79/150 out of the synapses that precedes its synaptic or extra-synaptic degradation by proteasome (Fig. 8). Since, cLTD would prevent cLTP induction depending on AKAP150 levels, it is feasible to hypothesize that the intensity of cLTD stimulus could determine the extent of AKAP150 degradation and the recovery time necessary for cLTP induction, although additional experiments are needed.

Our results indicating that AKAP150 levels influence surface expression and phosphorylation of AMPARs, support previous reports showing that the expression levels of other components of the PSD complex regulate synaptic distribution and function of AMPARs. For instance, it has been described that overexpression of PSD95 in cultured neurons increases synaptic AMPARs delivery (El-Husseini et al., 2000). By contrast, shRNA-mediated knock-down of PSD95 decreases synaptic AMPARs and enhances LTD (Elias et al., 2006; Schlüter et al., 2006; Ehrlich et al., 2007; Bhattacharyya et al., 2009). Similar results have been observed with SAP97 (Rumbaugh et al., 2003; Schlüter et al., 2006; Howard et al., 2010). Interestingly, we have also observed that PSD95 and SAP97 (unpublished data) levels decrease after cLTD induction. However, shRNA-mediated silencing of endogenous AKAP150 did not change PSD95 and SAP97 levels in cultured neurons, suggesting that although cLTD triggers a coordinated down-regulation of these proteins, an indirect cross-regulation mechanism may occur between them.

It has been reported a key role of CaN in the modulation of AMPARs trafficking in and out the synapses mediated by its capacity to dephosphorylate AMPARs and other proteins in the PSD (Smith et al., 2006; Jurado et al.,

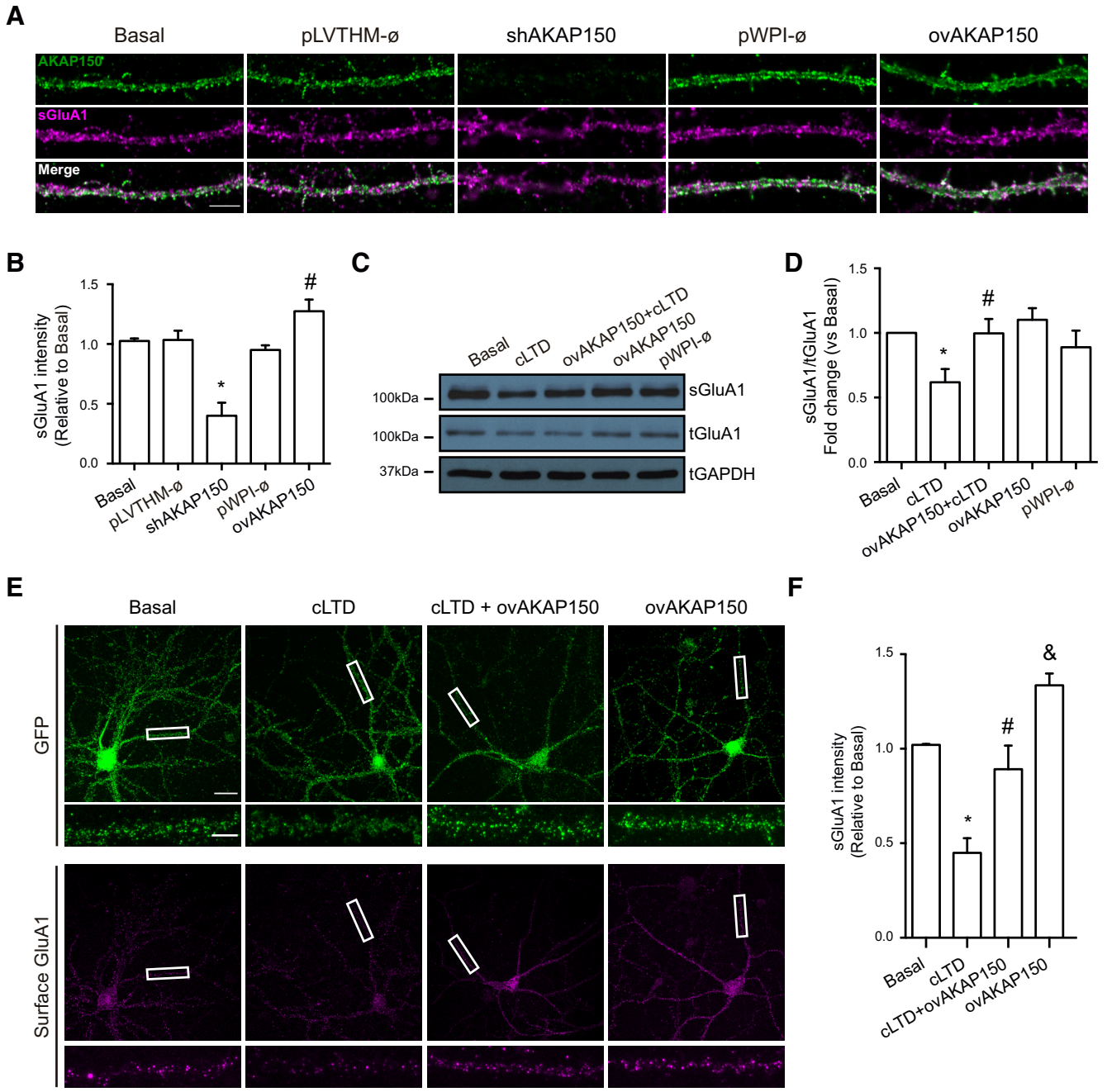

Figure 7. Overexpression of AKAP150 blocked cLTD-mediated GluA1-AMPARs endocytosis. ***A***, Representative confocal images of dendrites showing AKAP150 silencing (shAKAP150) and overexpressing (ovAKAP150) effect on surface GluA1 expression. AKAP150 (green) and surface GluA1 (magenta). Bottom panels, Merge for AKAP150/sGluA1. Knocking down endogenous AKAP150 reduced and AKAP150 overexpression increased surface GluA1 intensity. Empty lentiviral vector (Ø; pLVTHM or pWPI) was used as a control. Scale bar = 5 μm. ***B***, Quantification of surface GluA1 intensity (sGluA1) after silencing or overexpressing AKAP150 ($n > 12$ dendrites of different neurons from four independent cultures, $*p < 0.0001$, $\#p = 0.0419$ vs basal). ***C***, cLTD was induced in primary neurons overexpressing AKAP150 and surface proteins were biotinylated and pulled-down. Representative blot images show surface GluA1 (top panel; sGluA1), total GluA1 (middle panel; tGluA1) and GAPDH levels (bottom panel; loading control). ***D***, Quantification of surface GluA1 intensity (sGluA1) in response to cLTD without or with overexpression of AKAP150 compared with basal ($n = 6$, $*p = 0.0173$ vs basal; $\#p = 0.0185$ vs cLTD). ***E***, Representative confocal images show surface GluA1 and GFP staining on primary neurons overexpressing AKAP150 after cLTD induction. Separated panels from the boxed regions have been magnified for dendrite clarity (bottom panels). AKAP150 overexpression prevents cLTD-dependent surface GluA1 reduction compared with control cells expressing GFP. ***F***, Quantification of surface GluA1 intensity (sGluA1) in response to cLTD without or with overexpression of AKAP150 ($n = 10$ dendrites from 10 independent cultures, $*p < 0.0001$ vs basal; $\#p = 0.0016$ vs cLTD; $\&p = 0.0285$ vs basal). Scale bars = 20 μm (top panels) and 5 μm (bottom panels). Bars represent mean ± SEM.

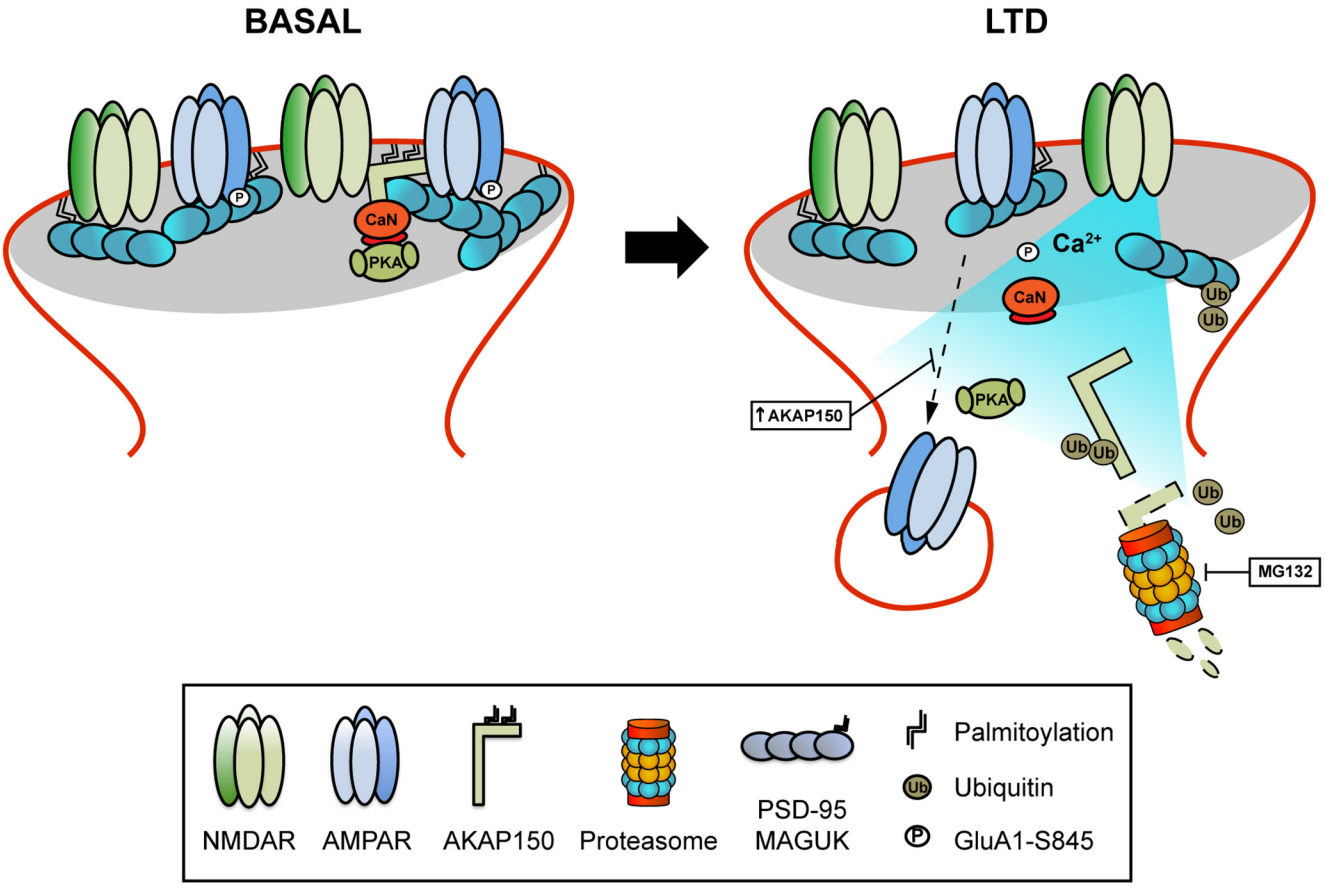

Figure 8. Model for LTD-mediated AKAP150 degradation through the proteasome system. Under basal conditions, a pool of palmitoylated AKAP150 is anchoring and regulating PKA and CaN function in dendritic spines. After LTD induction, a weak and extended Ca^{2+} influx depalmitoylate and remove AKAP150 from spines. This removal promotes CaN-mediated dephosphorylation and consequent endocytosis of GluA1-AMPARs. During this process AKAP150 is ubiquitinated and degraded via proteasome. The presence of 20S proteasome inhibitor MG132 blocks not only LTD-mediated AKAP150 degradation but also its removal from spines. Maintenance of AKAP150 levels is sufficient to prevent LTD-induced GluA1-AMPARs endocytosis suggesting that AKAP150 degradation by the proteasome could be an important factor in the regulation of surface GluA1-AMPARs at spines.

2010). Here, we have reported that CaN activation is not necessary for cLTD-mediated AKAP150 degradation by proteasome. Therefore, CaN would be able to favor cLTD by enhancing synaptic AMPARs endocytosis but it would not participate in the induction of AKAP79/150 degradation. In this context, It has been described that activity-dependent palmitoylation of AKAP79/150 is necessary for synaptic targeting of AKAP79/150 and cLTP induction (Keith et al., 2012). In addition, cLTD activates CaMKII regulating depalmitoylation and synaptic removal of AKAP79/150 (Woolfrey et al., 2018) being feasibly a prerequisite for posterior degradation in the proteasome.

At present, the mechanism through which cLTD induces proteasome-dependent AKAP150 degradation is unknown. However, It is well known that AKAP150 is highly ubiquitinated and can be regulated by ubiquitin-proteasome system depending on synaptic activity (Ehlers 2003; Jia et al., 2008). Moreover, it has recently been described that Nedd4 ubiquitinates (Schwarz et al., 2010; Lin et al., 2011) and USP46 deubiquitinates (Huo et al., 2015) AMPARs. Some controversy exists about the role of cLTD on ubiquitination-proteasome system and synaptic function. Previous data from Citri and colleagues showed that cLTD-mediated AMPAR endocytosis requires ubiquitination but not proteasomal degradation (Citri et al., 2009), while our results suggest that both ubiquitin and proteasome processes are involved in cLTD-mediated AKAP150 degradation. AKAP150 seems to be part of a complex of synaptic proteins regulated by proteasome system in the molecular mechanisms of LTD. Here, we also find involved PSD95 and GluA1 (data not shown) in proteasomal-mediated degradation indicating that it could be a more general effect on synaptic proteins. Furthermore, restoration of AKAP150 levels by overexpression was able to rescue cLTD-dependent GluA1-AMPAR endocytosis. This finding highlights the importance of AKAP150 levels in excitatory synapses along with their interaction to other scaffolding proteins through the MAGUK binding domain (Robertson et al., 2009). Nevertheless, further work should be addressed interfering selectively with AKAP150 cLTD-induced ubiquitination and to prevent aspects of LTD expression or whether

Nedd4 and/or USP46 proteins also regulate AKAP79/150 ubiquitination and their activities under cLTD condition to further support an AKAP150-degradation centric model in control of AMPAR endocytosis in LTD.

In summary, consistent with previous results describing AKAP79/150 translocation away from synapses in cLTD (Gomez et al., 2002; Smith et al., 2006; Woolfrey et al., 2018), our data show that proteasome-dependent AKAP150 degradation in cLTD could be an important mechanism in the regulation of surface GluA1-AMPARs at excitatory synapses (Fig. 8).

References

Ahmad M, Polepalli JS, Goswami D, Yang X, Kaeser-Woo YJ, Südhof TC, Malenka RC (2012) Postsynaptic complexin controls AMPA receptor exocytosis during LTP. Neuron 73:260–267.

Bacaj T, Ahmad M, Jurado S, Malenka RC, Südhof TC (2015) Synaptic function of rab11fip5: selective requirement for hippocampal long-term depression. J Neurosci 35:7460–7474.

Bauman AL, Goehring AS, Scott JD (2004) Orchestration of synaptic plasticity through AKAP signaling complexes. Neuropharmacology 46:299–310.

Beattie EC, Carroll RC, Yu X, Morishita W, Yasuda H, von Zastrow M, Malenka RC (2000) Regulation of AMPA receptor endocytosis by a signaling mechanism shared with LTD. Nat Neurosci 3:1291–1300.

Benke TA, Lüthi A, Isaac JT, Collingridge GL (1998) Modulation of AMPA receptor unitary conductance by synaptic activity. Nature 393:793–797.

Bhattacharyya S, Biou V, Xu W, Schlüter O, Malenka RC (2009) A critical role for PSD-95/AKAP interactions in endocytosis of synaptic AMPA receptors. Nat Neurosci 12:172–181.

Boehm J, Kang MG, Johnson RC, Esteban J, Huganir RL, Malinow R (2006) Synaptic incorporation of AMPA receptors during LTP is controlled by a PKC phosphorylation site on glur1. Neuron 51:213–225.

Brummelkamp TR, Bernards R, Agami R (2002) A system for stable expression of short interfering rnas in mammalian cells. Science 296:550–553.

Carroll RC, Lissin DV, von Zastrow M, Nicoll RA, Malenka RC (1999) Rapid redistribution of glutamate receptors contributes to long-term depression in hippocampal cultures. Nat Neurosci 2:454–460.

Chung HJ, Xia J, Scannevin RH, Zhang X, Huganir RL (2000) Phosphorylation of the AMPA receptor subunit glur2 differentially regulates its interaction with PDZ domain-containing proteins. J Neurosci 20:7258–7267.

Citri A, Soler-Llavina G, Bhattacharyya S, Malenka RC (2009) N-methyl-D-aspartate receptor- and metabotropic glutamate receptor-dependent long-term depression are differentially regulated by the ubiquitin-proteasome system. Eur J Neurosci 30:1443–1450.

Colledge M, Dean RA, Scott GK, Langeberg LK, Huganir RL, Scott JD (2000) Targeting of PKA to glutamate receptors through a MAGUK-AKAP complex. Neuron 27:107–119.

Colledge M, Snyder EM, Crozier RA, Soderling JA, Jin Y, Langeberg LK, Lu H, Bear MF, Scott JD (2003) Ubiquitination regulates PSD-95 degradation and AMPA receptor surface expression. Neuron 40:595–607.

Coultrap SJ, Freund RK, O'Leary H, Sanderson JL, Roche KW, Dell'Acqua ML, Bayer KU (2014) Autonomous camkii mediates both LTP and LTD using a mechanism for differential substrate site selection. Cell Rep 6:431–437.

Delgado JY, Coba M, Anderson CNG, Thompson KR, Gray EE, Heusner CL, Martin KC, Grant SGN, O'Dell TJ (2007) NMDA receptor activation dephosphorylates AMPA receptor glutamate receptor 1 subunits at threonine 840. J Neurosci 27:13210–13221.

Ehlers MD (2000) Reinsertion or degradation of AMPA receptors determined by activity-dependent endocytic sorting. Neuron 28:511–525.

Ehlers MD (2003) Activity level controls postsynaptic composition and signaling via the ubiquitin-proteasome system. Nat Neurosci 6:231–242.

Ehlers MD, Heine M, Groc L, Lee MC, Choquet D (2007) Diffusional trapping of glur1 AMPA receptors by input-specific synaptic activity. Neuron 54:447–460.

Ehrlich I, Malinow R (2004) Postsynaptic density 95 controls AMPA receptor incorporation during long-term potentiation and experience-driven synaptic plasticity. J Neurosci 24:916–927.

Ehrlich I, Klein M, Rumpel S, Malinow R (2007) PSD-95 is required for activity-driven synapse stabilization. Proc Natl Acad Sci USA 104:4176–4181.

El-Husseini AE, Schnell E, Chetkovich DM, Nicoll RA, Bredt DS (2000) PSD-95 involvement in maturation of excitatory synapses. Science 290:1364–1368.

Elias GM, Funke L, Stein V, Grant SG, Bredt DS, Nicoll RA (2006) Synapse-specific and developmentally regulated targeting of AMPA receptors by a family of MAGUK scaffolding proteins. Neuron 52:307–320.

Esteban JA, Shi SH, Wilson C, Nuriya M, Huganir RL, Malinow R (2003) PKA phosphorylation of AMPA receptor subunits controls synaptic trafficking underlying plasticity. Nat Neurosci 6:136–143.]

Fernández-Monreal M, Brown TC, Royo M, Esteban JA (2012) The balance between receptor recycling and trafficking toward lysosomes determines synaptic strength during long-term depression. J Neurosci 32:13200–13205.

Fukata Y, Fukata M (2010) Protein palmitoylation in neuronal development and synaptic plasticity. Nat Rev Neurosci 11:161–175.

Génin A, French P, Doyère V, Davis S, Errington ML, Maroun M, Stean T, Truchet B, Webber M, Wills T, Richter-Levin G, Sanger G, Hunt SP, Mallet J, Laroche S, Bliss TVP, O'Connor V (2003) LTP but not seizure is associated with up-regulation of AKAP-150. Eur J Neurosci 17:331–340.

Gomez LL, Alam S, Smith KE, Horne E, Dell'Acqua ML (2002) Regulation of a-kinase anchoring protein 79/150-camp-dependent protein kinase postsynaptic targeting by NMDA receptor activation of calcineurin and remodeling of dendritic actin. J Neurosci 22:7027–7044.

Grey KB, Burrell BD (2008) Forskolin induces NMDA receptor-dependent potentiation at a central synapse in the leech. J Neurophysiol 99:2719–2724.

He K, Lee A, Song L, Kanold PO, Lee HK (2011) AMPA receptor subunit glur1 (glua1) serine-845 site is involved in synaptic depression but not in spine shrinkage associated with chemical long-term depression. J Neurophysiol 105:1897–1907.

Howard MA, Elias GM, Elias LA, Swat W, Nicoll RA (2010) The role of SAP97 in synaptic glutamate receptor dynamics. Proc Natl Acad Sci USA 107:3805–3810.

Huganir RL, Nicoll RA (2013) AMPARs and synaptic plasticity: the last 25 years. Neuron 80:704–717.

Huo Y, Khatri N, Hou Q, Gilbert J, Wang G, Man HY (2015) The deubiquitinating enzyme USP46 regulates AMPA receptor ubiquitination and trafficking. J Neurochem 134:1067–1080.

Jia JM, Chen Q, Zhou Y, Miao S, Zheng J, Zhang C, Xiong ZQ (2008) Brain-derived neurotrophic factor-tropomyosin-related kinase B signaling contributes to activity-dependent changes in synaptic proteins. J Biol Chem 283:21242–21250.

Jurado S, Biou V, Malenka RC (2010) A calcineurin/AKAP complex is required for NMDA receptor-dependent long-term depression. Nat Neurosci 13:1053–1055.

Jurado S, Goswami D, Zhang Y, Molina AJ, Südhof TC, Malenka RC (2013) LTP requires a unique postsynaptic SNARE fusion machinery. Neuron 77:542–558.

Kamal A, Ramakers GM, Urban IJ, De Graan PN, Gispen WH (1999) Chemical LTD in the CA1 field of the hippocampus from young and mature rats. Eur J Neurosci 11:3512–3516.

Keith DJ, Sanderson JL, Gibson ES, Woolfrey KM, Robertson HR, Olszewski K, Kang R, El-Husseini A, Dell'acqua ML (2012) Palmitoylation of a-kinase anchoring protein 79/150 regulates dendritic endosomal targeting and synaptic plasticity mechanisms. J Neurosci 32:7119–7136.

Kim E, Sheng M (2004) PDZ domain proteins of synapses. Nat Rev Neurosci 5:771–781.

Lee HK, Kameyama K, Huganir RL, Bear MF (1998) NMDA induces long-term synaptic depression and dephosphorylation of the glur1 subunit of AMPA receptors in hippocampus. Neuron 21:1151–1162.

Lee HK, Barbarosie M, Kameyama K, Bear MF, Huganir RL (2000) Regulation of distinct AMPA receptor phosphorylation sites during bidirectional synaptic plasticity. Nature 405:955–959.

Lee HK, Takamiya K, Han JS, Man H, Kim CH, Rumbaugh G, Yu S, Ding L, He C, Petralia RS, Wenthold RJ, Gallagher M, Huganir RL (2003) Phosphorylation of the AMPA receptor glur1 subunit is required for synaptic plasticity and retention of spatial memory. Cell 112:631–643.

Lee HK, Takamiya K, He K, Song L, Huganir RL (2010) Specific roles of AMPA receptor subunit glur1 (glua1) phosphorylation sites in regulating synaptic plasticity in the CA1 region of hippocampus. J Neurophysiol 103:479–489.

Li Z, Jo J, Jia JM, Lo SC, Whitcomb DJ, Jiao S, Cho K, Sheng M (2010) Caspase-3 activation via mitochondria is required for long-term depression and AMPA receptor internalization. Cell 141:859–871.

Lin A, Hou Q, Jarzylo L, Amato S, Gilbert J, Shang F, Man HY (2011) Nedd4-mediated AMPA receptor ubiquitination regulates receptor turnover and trafficking. J Neurochem 119:27–39.

Lledo PM, Zhang X, Südhof TC, Malenka RC, Nicoll RA (1998) Postsynaptic membrane fusion and long-term potentiation. Science 279:399–403.

Lu W, Isozaki K, Roche KW, Nicoll RA (2010) Synaptic targeting of AMPA receptors is regulated by a camkii site in the first intracellular loop of glua1. Proc Natl Acad Sci USA 107:22266–22271.

Lu Y, Allen M, Halt AR, Weisenhaus M, Dallapiazza RF, Hall DD, Usachev YM, McKnight GS, Hell JW (2007) Age-dependent requirement of akap150-anchored PKA and glur2-lacking AMPA receptors in LTP. EMBO J 26:4879–4890.

Lu Y, Zhang M, Lim IA, Hall DD, Allen M, Medvedeva Y, McKnight GS, Usachev YM, Hell JW (2008) AKAP150-anchored PKA activity is important for LTD during its induction phase. J Physiol 586:4155–4164.

Makino H, Malinow R (2009) AMPA receptor incorporation into synapses during LTP: the role of lateral movement and exocytosis. Neuron 64:381–390.

Makino Y, Johnson RC, Yu Y, Takamiya K, Huganir RL (2011) Enhanced synaptic plasticity in mice with phosphomimetic mutation of the glua1 AMPA receptor. Proc Natl Acad Sci USA 108:8450–8455.

Mammen AL, Kameyama K, Roche KW, Huganir RL (1997) Phosphorylation of the alpha-amino-3-hydroxy-5-methylisoxazole4-propionic acid receptor glur1 subunit by calcium/calmodulin-dependent kinase II. J Biol Chem 272:32528–32533.

Man HY, Lin JW, Ju WH, Ahmadian G, Liu L, Becker LE, Sheng M, Wang YT (2000) Regulation of AMPA receptor-mediated synaptic transmission by clathrin-dependent receptor internalization. Neuron 25:649–662.

Miñano-Molina AJ, España J, Martín E, Barneda-Zahonero B, Fadó R, Solé M, Trullás R, Saura CA, Rodríguez-Alvarez J (2011) Soluble oligomers of amyloid-β peptide disrupt membrane trafficking of α-amino-3-hydroxy-5-methylisoxazole-4-propionic acid receptor contributing to early synapse dysfunction. J Biol Chem 286:27311–27321.

Mulkey RM, Endo S, Shenolikar S, Malenka RC (1994) Involvement of a calcineurin/inhibitor-1 phosphatase cascade in hippocampal long-term depression. Nature 369:486–488.

Oh MC, Derkach VA, Guire ES, Soderling TR (2006) Extrasynaptic membrane trafficking regulated by glur1 serine 845 phosphorylation primes AMPA receptors for long-term potentiation. J Biol Chem 281:752–758.

Opazo P, Labrecque S, Tigaret CM, Frouin A, Wiseman PW, De Koninck P, Choquet D (2010) CaMKII triggers the diffusional trapping of surface ampars through phosphorylation of stargazin. Neuron 67:239–252.

Otmakhov N, Khibnik L, Otmakhova N, Carpenter S, Riahi S, Asrican B, Lisman J (2004) Forskolin-induced LTP in the CA1 hippocampal region is NMDA receptor dependent. J Neurophysiol 91:1955–1962.

Park M, Penick EC, Edwards JG, Kauer JA, Ehlers MD (2004) Recycling endosomes supply AMPA receptors for LTP. Science 305:1972–1975.

Passafaro M, Piëch V, Sheng M (2001) Subunit-specific temporal and spatial patterns of AMPA receptor exocytosis in hippocampal neurons. Nat Neurosci 4:917–926.

Petrini EM, Lu J, Cognet L, Lounis B, Ehlers MD, Choquet D (2009) Endocytic trafficking and recycling maintain a pool of mobile surface AMPA receptors required for synaptic potentiation. Neuron 63:92–105.

Purkey AM, Woolfrey KM, Crosby KC, Stich DG, Chick WS, Aoto J, Dell'Acqua ML (2018) AKAP150 palmitoylation regulates synaptic incorporation of ca2+-permeable AMPA receptors to control LTP. Cell Rep 25:974–987.e4.

Robertson HR, Gibson ES, Benke TA, Dell'Acqua ML (2009) Regulation of postsynaptic structure and function by an a-kinase anchoring protein-membrane-associated guanylate kinase scaffolding complex. J Neurosci 29:7929–7943.

Rumbaugh G, Sia GM, Garner CC, Huganir RL (2003) Synapse-associated protein-97 isoform-specific regulation of surface AMPA receptors and synaptic function in cultured neurons. J Neurosci 23:4567–4576.

Sanderson JL, Dell'Acqua ML (2011) AKAP signaling complexes in regulation of excitatory synaptic plasticity. Neuroscientist 17:321–336.

Sanderson JL, Gorski JA, Gibson ES, Lam P, Freund RK, Chick WS, Dell'Acqua ML (2012) AKAP150-anchored calcineurin regulates synaptic plasticity by limiting synaptic incorporation of ca2+-permeable AMPA receptors. J Neurosci 32:15036–15052.

Schlüter OM, Xu W, Malenka RC (2006) Alternative n-terminal domains of PSD-95 and SAP97 govern activity-dependent regulation of synaptic AMPA receptor function. Neuron 51:99–111.

Schwarz LA, Hall BJ, Patrick GN (2010) Activity-dependent ubiquitination of glua1 mediates a distinct AMPA receptor endocytosis and sorting pathway. J Neurosci 30:16718–16729.

Shehata M, Matsumura H, Okubo-Suzuki R, Ohkawa N, Inokuchi K (2012) Neuronal stimulation induces autophagy in hippocampal neurons that is involved in AMPA receptor degradation after chemical long-term depression. J Neurosci 32:10413–10422.

Shi S, Hayashi Y, Esteban JA, Malinow R (2001) Subunit-specific rules governing AMPA receptor trafficking to synapses in hippocampal pyramidal neurons. Cell 105:331–343.

Smith KE, Gibson ES, Dell'Acqua ML (2006) CAMP-dependent protein kinase postsynaptic localization regulated by NMDA receptor activation through translocation of an a-kinase anchoring protein scaffold protein. J Neurosci 26:2391–2402.

Song I, Huganir RL (2002) Regulation of AMPA receptors during synaptic plasticity. Trends Neurosci 25:578–588.

Takumi Y, Matsubara A, Rinvik E, Ottersen OP (1999) The arrangement of glutamate receptors in excitatory synapses. Ann NY Acad Sci 868:474–482.

Tavalin SJ (2008) AKAP79 selectively enhances protein kinase C regulation of glur1 at a ca2+-calmodulin-dependent protein kinase II/protein kinase C site. J Biol Chem 283:11445–11452.

Tavalin SJ, Colledge M, Hell JW, Langeberg LK, Huganir RL, Scott JD (2002) Regulation of glur1 by the a-kinase anchoring protein 79 (AKAP79) signaling complex shares properties with long-term depression. J Neurosci 22:3044–3051.

Tomita S, Fukata M, Nicoll RA, Bredt DS (2004) Dynamic interaction of stargazin-like tarps with cycling AMPA receptors at synapses. Science 303:1508–1511.
Woolfrey KM, O'Leary H, Goodell DJ, Robertson HR, Horne EA, Coultrap SJ, Dell'Acqua ML, Bayer KU (2018) CaMKII regulates the depalmitoylation and synaptic removal of the scaffold protein AKAP79/150 to mediate structural long-term depression. J Biol Chem 293:1551–1567.
Yap KA, Shetty MS, Garcia-Alvarez G, Lu B, Alagappan D, Oh-Hora M, Sajikumar S, Fivaz M (2017) STIM2 regulates AMPA receptor trafficking and plasticity at hippocampal synapses. Neurobiol Learn Mem 138:54–61.